UNIVERSITÀ DI PARMA

UNIVERSITA' DEGLI STUDI DI PARMA

DOTTORATO DI RICERCA IN

"*Scienze Chimiche*"

CICLO XXXVIII°

Selective construction of complex molecular architectures through the activation of C-C π-bonds

Coordinatore:

Chiar.mo Prof. Giovanni Maestri

Tutore:

Chiar.mo Prof. Giovanni Maestri

Dottorando: Gabriele Scarica

Anni Accademici 2022/2023 – 2024/2025

Contents

General Introduction

General Introduction for Photocatalysis

Chemists have drawn profound inspiration from nature, particularly in the development of photochemistry. Beginning with the pioneering work of Ciamician, which laid the foundation for much of modern photochemistry, the natural process of photosynthesis has driven generations of chemists to explore light-mediated chemical transformations (Figure 1). [1-3]

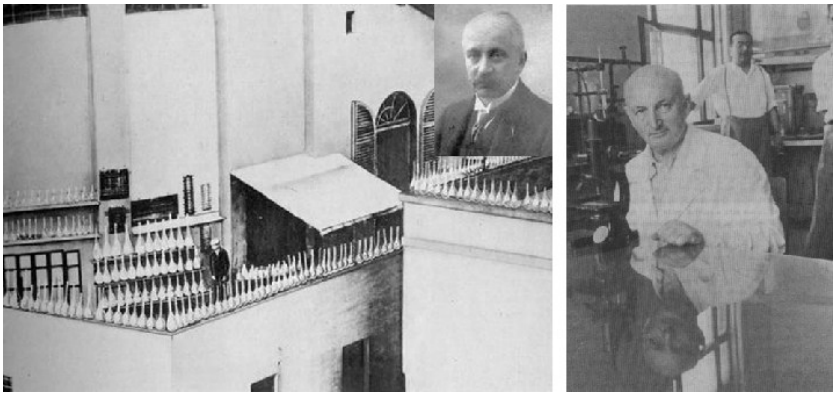

Figure 1: Ciamician in his rooftop laboratory in Bologna in 1886.

Ciamician's work was outstanding thanks to the sensational results obtained, which were impossible to imagine according to the knowledge of the time.[4] Nevertheless, even if these reactions uncovered entirely new and complementary pathways offering alternatives to traditional processes that rely purely on thermal energy, these needed weeks or months to get to completion. The introduction of the concept of photocatalysts[5] has emerged as a cornerstone in the advancement of the field. These are defined as substances capable of absorbing light and transferring energy to non-absorbing substrates, triggering multiple reaction manifolds with both efficiency and selectivity. The ability to induce chemical reactivity in molecules that would otherwise remain inert has made photocatalysis an indispensable tool in modern organic chemistry, but until the 2000's this concept remained something hard to investigate, and that's the reason why reactions promoted by visible light arose with the use of metal catalysts.[6-7] Many of the most employed photocatalysts are polypyridyl iridium-based complexes. (Figure 2).

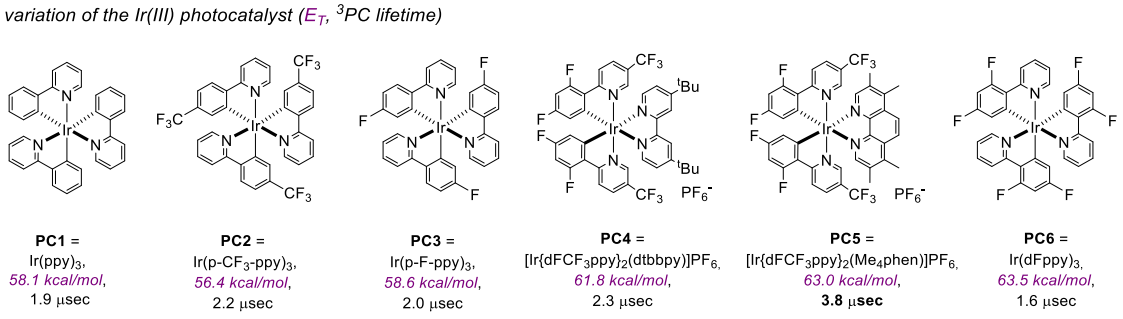

Figure 2: Commonly employed Iridium-based photocatalysts in photochemistry.

These metal photocatalysts stood out among other candidates because, even if expensive, they offer the possibility to tune their properties by changing both bipyridyl and phenyl-pyridyl ligands. For example, both the triplet energy and triplet lifetime can be tuned. These are key parameters in determining whether a specific substrate can be activated. Specifically, triplet energy is the energy of a molecule in an electronically excited state, where two electrons have parallel spins, while the triplet lifetime refers to the average time a molecule remains in its electronically excited triplet state after photoexcitation, before relaxing back to the ground state. This feature has uncovered entirely new reaction pathways offering alternatives to traditional processes that rely purely on thermal energy or UV activation, which has always been problematic because of the narrow reaction scope and the low selectivity associated with it (Figure 3).[8-9] Once this concept has been realized, this has allowed researchers to embrace more sustainable and energy-efficient approaches.

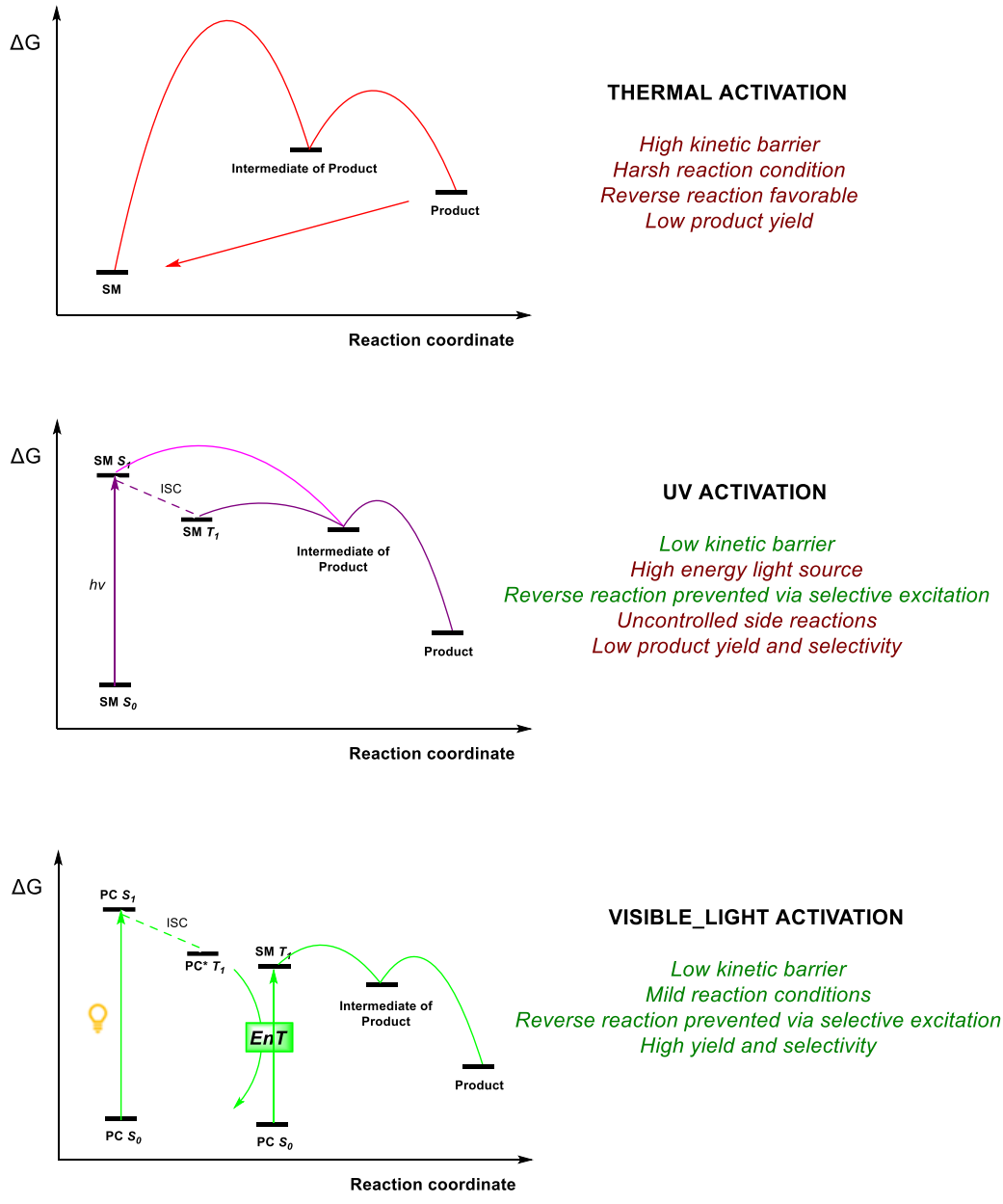

Figure 3: Differences between thermal, UV and visible-light activation.

This method relies on visible-light activation, also referred to as photochemical activation, and exploits the absorption of photons, in the visible range, by photoactive species. The process selectively promotes the molecule to an electronically excited state, which is characterized by a very different reactivity compared to that associated with the ground state. Crucially, this excitation is often selective because it involves only the chromophores that absorb light in that specific range of irradiation. This feature enables precise control over the selectivity of the reaction. Moreover, visible light activation allows the development of novel and highly selective transformations under mild conditions.[10-11]

The energy transfer (EnT) process has proven to be a highly valuable tool in photocatalysis, allowing access to energetic triplet states that can overcome otherwise unaccessible energy barriers (Figure 4).

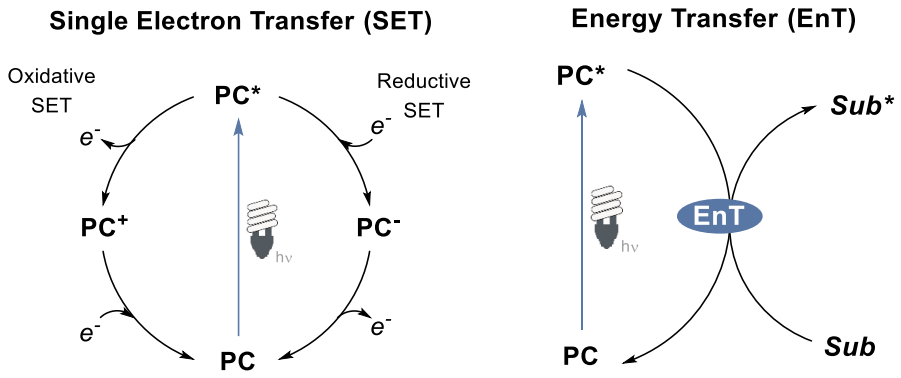

Figure 4: Possible Photocatalytic mechanisms.

Contrarily, in the single-electron transfer mechanism (SET), the excited photocatalyst either donates or accepts a single electron to or from a substrate. This process changes the oxidation state of the molecules involved and leads to the formation of a reactive radical intermediate, which is then able to react and form the desired product. On the other hand, energy transfer does not require a redox step: the excited photocatalyst transfers its energy of excitation to a substrate, bringing that molecule to an excited electronic state without altering its charge.[16]

Going a bit deeper with this concept, the absorption of an energetic photon, typically in a specific part of the visible-light spectrum, by a photocatalyst, populates the singlet excited state of the latter as described in Figure 5. Then, the subsequent intersystem crossing (ISC) allows the state transition into a triplet state. This one (T_1) is characterized by significantly enhanced lifetime compared to S_1, ranging from nanoseconds to microseconds. This feature is essential for an efficient bimolecular quenching event to finally occur, although radiative processes can happen from both the T_1 and the S_1 states. In fact, the former could also undergo an EnT to a ground-state acceptor, commonly referred to as the substrate.

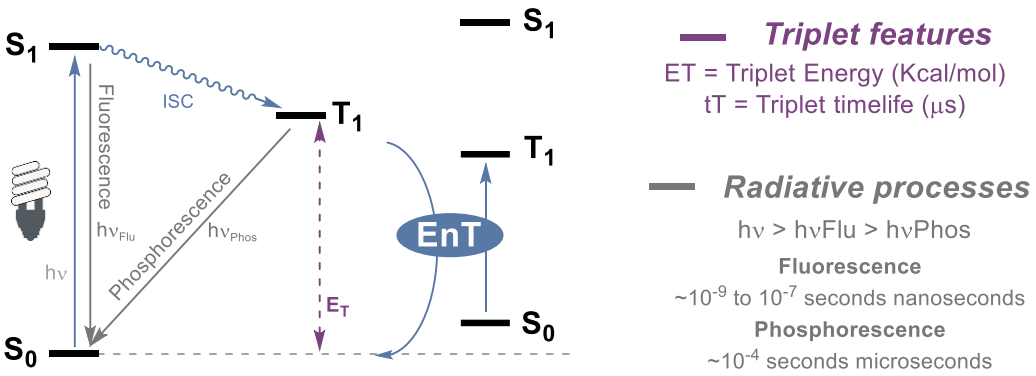

Figure 5: Jablonski diagram illustrating energy transfer activation of a general substrate.

From a molecular perspective, we can categorize three distinct types of EnT mechanisms: primitive energy transfer via an emission-absorption process; the Förster resonance energy transfer; and the Dexter energy transfer (Figure 6). [18-19]

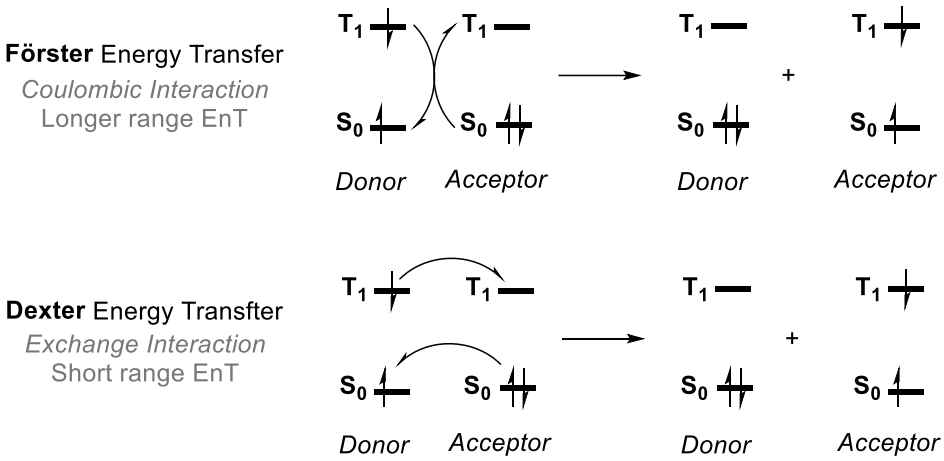

Figure 6: Energy transfer mechanisms.

The first one, primitive energy transfer, occurs through a simple emission-absorption process between two species with suitably overlapping spectral bands. The Förster resonance energy transfer operates instead via a radiation-free, non-radiative mechanism, relying on the close spatial proximity between the donor and acceptor molecules. However, in this paragraph, I decided to mainly focus on Dexter-type energy transfer, because it is the one involved in synthetic photocatalysis. Notably, this energy transfer mechanism involves a more intricate two-electron exchange process, in which the donor transfers an electron from its singly occupied molecular orbital (SOMO) to the lowest unoccupied molecular orbital (LUMO) of the acceptor, while simultaneously receiving an electron from the highest occupied molecular orbital (HOMO) of the acceptor. This exchange facilitates the population of the T_1 state of the acceptor while simultaneously regenerating the ground state of the donor. At the molecular level, the Dexter energy transfer mechanism requires a degree of orbital

overlap between the donor and the acceptor, implying that a molecular proximity for the process to occur is somehow needed. In solution, this one is often achieved through the diffusion-driven formation of a transient, solvent-shared encounter complex. The Dexter-type energy transfer can take place within this supramolecular entity, whose subsequent dissociation liberates the activated acceptor, which can potentially engage in a chemical reaction. EnT is inherently a dual electron transfer process, whose efficiency is governed by a combination of several fundamental factors. Three primary parameters play a crucial role in determining the overall dynamics of the process: (a) The thermodynamic driving force serves as a critical determinant, as it reflects the free energy difference between the initial and final states of the system; (b) The reorganization energy barrier represented by the structural and solvation changes required for the electrons to successfully transfer from the donor to the acceptor; (c) The electronic overlap between the wavefunctions of the donor and the acceptor states is essential for an efficient electron transfer.[20]

Most of the time, the feasibility of EnT events for synthetic applications is often assessed by focusing primarily on the first factor (a). Indeed, the driving force can be initially evaluated by comparing the triplet energies of both the donor and the acceptor. This preliminary evaluation can be carried out experimentally by collecting phosphorescence spectra or through computational methods that rely on high-quality quantum-mechanical models, which have proved to afford very reliable values at relatively reasonable computational costs. Finally, since the efficiency of the EnT depends on the compatibility of the two components, when the triplet energy of the acceptor is higher than that of the donor, the energy transfer will be either highly inefficient or outright not possible.

An additional persistent and critical challenge in EnT catalysis is the selection of an appropriate sensitizer. The conventional approach involves screening a range of catalysts to optimize the reactivity. However, performing Stern–Volmer luminescence quenching studies can be useful and reliable. This methodology is highly effective for determining whether a photocatalyst interacts with a substrate, regardless of whether the mechanism involves single-electron transfer (SET) or energy transfer (EnT). Experimentally, the process involves measuring the emission intensity of the excited photocatalyst (I_0), followed by incremental additions of the substrate referred to as the quencher [Q], with the resulting emission intensities (I) recorded after each addition. These data are then analyzed to produce a Stern–Volmer plot, where I_0/I is plotted against [Q]. A linear relationship with a positive slope indicates quenching between the photocatalyst and the substrate, and the slope corresponds to the Stern–Volmer constant (K_{SV}), based on the equation: $I_0/I = 1 + K_{SV}[Q]$.

Conversely, if the line remains flat and K_{SV} is close to zero, it suggests there is no significant interaction, meaning that the substrate does not quench the photocatalyst. An interesting example of a straight line is described by Figure 7, in which it has been reported the positive quenching of an allenamide substrate **1a** with a general Ir-based photocatalyst.

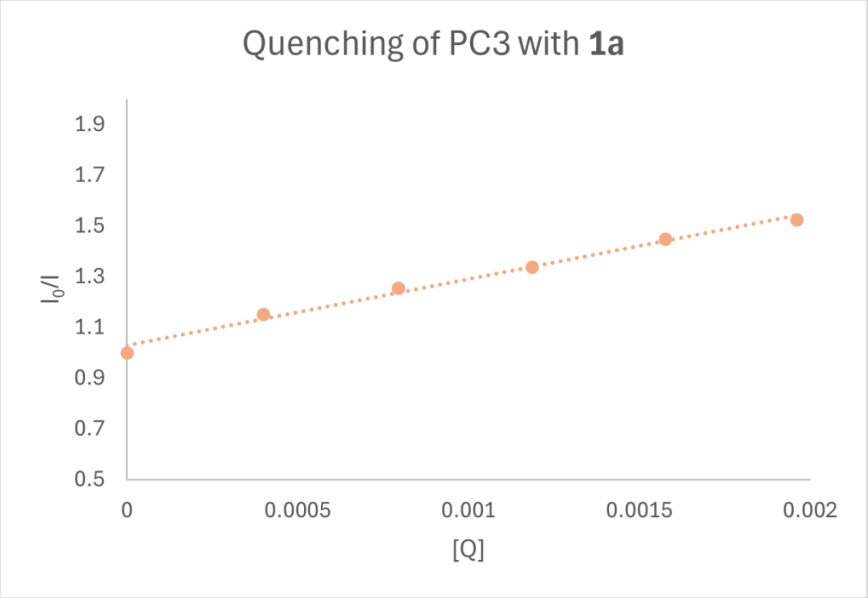

Figure 7: General appearance of a positive interaction in a Stern-Volmer plot.

Beyond these luminescence quenching studies, mechanistic investigations, including DFT calculations, can further elucidate the suitability of a sensitizer.[21-22] Usually, even if it's very resource-intensive, mechanistic investigations give the most reliable and accurate data.

Finally, EnT reactions are also highly sensitive to the number of absorbed photons. Consequently, the irradiation intensity plays a crucial role in determining the reaction efficiency: insufficient light limits the reaction rate, while excessive irradiation can lead to side and undesired effects. Therefore, optimizing light intensity is crucial to maximizing the yield, selectivity, and stability of the system.

Temperature control is another critical aspect of photochemical reactions since it can affect reaction rates and selectivity. Additionally, reactor dimensions must be considered, as changes in reactor size can influence photon flux and, consequently, the reaction rate.

Full understanding of these parameters is crucial for designing optimized reaction conditions that maximize photocatalytic efficiencies. Usually, these are all important factors that are investigated in an optimization phase before passing on to generalizing the reaction. In this optimization phase, a major limitation emerges in EnT-driven catalysis. This one is associated with the necessity of conducting reactions under an oxygen-free atmosphere because triplet oxygen, in its ground state, is a powerful quencher thanks to its narrow triplet energy. Therefore, unless the reacting species are able to quench the excited photocatalyst more rapidly than dioxygen, an inert atmosphere, typically argon or nitrogen, realized through freeze-pump-thaw cycles is required, even if these procedures are sometimes cumbersome for the setup of the reaction itself.

References

[1] G. Ciamician, *Science*, **1912**, 36, 385–394.

[2] V. Balzani, A. Credi, M. Venturi, *ChemSusChem*, **2008**, 1, 26–58.

[3] F. E. Osterloh, *ACS Energy Lett.,* **2017**, 2, 445–453.

[4] G. Buchi, C. G. Inman, E. S. Lipinsky, *J. Am. Chem. Soc.,* **1954**, 76, 4327-4331.

[5] N. Serpone, A. V. Emeline, S. Horikoshi, V. N. Kuznetsov, V. K. Ryabchuk, *Photochem. Photobiol. Sci.,* **2012**, 11, 1121-1150.

[6] D. A. Nicewicz, D. W. C. MacMillan, *Science*, **2008**, 322, 77-80.

[7] M. A. Ischay, M. E. Anzovino, J. Du, T. P. Yoon, *J. Am. Chem.Soc.*, **2008**, 130, 12886-12887.

[8] G. L. Lackner, K. W. Quasdorf, L. E. Overman, *John Wiley & Sons, Ltd*, **2018**, 1, 283–297.

[9] N. Hoffmann, *Chem. Rev.,* **2008**, 108, 1052–1103.

[10] P. Ji, K. Duan, M. Li, Z. Wang, X. Meng, Y. Zhang, W. Wang, *Chem. Soc. Rev.,* **2024**, 53, 6600-6624.

[11] Y. Z. Cheng, Z. Feng, X. Zhang, S. L. You, *Chem. Soc. Rev.,* **2022**, 51, 2145-2170.

[12] J. Twilton, C. Le, P. Zhang, M. H. Shaw, R. W. Evans, D. W. C. MacMillan, *Nat. Rev. Chem.,* **2017**, 1, 52-71.

[13] M. Akita, P. Ceroni, C. R. J. Stephenson, G. Masson, *J. Org. Chem.,* **2023**, 88, 6281–6283.

[14] F. Mueller, J. Mattay, *Chem. Rev.,* **1993**, 93, 99–117.

[15] M. H. Shaw, J. Twilton, D. W. C. MacMillan, *J. Org. Chem.,* **2016**, 81, 6898–6926.

[16] S. Dutta, J. E. Erchinger, F. Strieth-Kalthoff, R. Kleinmans, F. Glorius, *Chem. Soc. Rev*., **2024**, 53, 1068-1080.

[17] J. W. Verhoeven, *Pure Appl. Chem.,* **1996**, 68, 2223–2286.

[18] T. Förster, *Annalen der Physik*, **1948**, 437, 55–75.

[19] D. L. Dexter, *J. Chem. Phys.,* **1953**, 21, 836–850.

[20] F. Strieth-Kalthoff, M. J. James, M. Teders, L. Pitzer, F. Glorius, *Chem. Soc. Rev.* **2018**, 47, 7190–7202.

[21] L. Buzzetti, G. E. M. Crisenza, P. Melchiorre, *Angew. Chem. Int. Ed.*, **2019**, 58, 3730.

[22] F. Juliá, *ACS Catal.,* **2025**, 15, 4665–4680.

Introduction to Dearomatizations

Aromatic compounds are one of the most available feedstocks in the world, with a production of over 100 million tons per year.[1] Their use in the synthesis of polymers, solvents, as well as in the fuel field has tempted chemists to expand their use also for other synthetic transformations. In fact, their ability to be chromophores, to be easy to install and for their inertness has generated great interest also from a synthetic point of view. The last peculiarity that made them so important is the commercial availability of a myriad of aromatics with different functional groups, differently oriented.[2]

These ones can be added onto a molecular scaffold in several ways, from metal-catalyzed couplings to nucleophilic substitution of benzyl halides. However, aromatics can also undergo reactions on their scaffold, being the starting point of the synthesis. The most common reaction is the electrophilic aromatic substitution (SEAr). With the latest, one or more hydrogens can be changed with different and interesting functional groups, maintaining the aromaticity of the system (Figure 8).

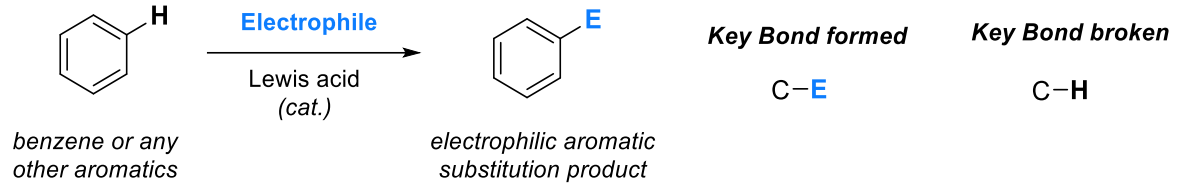

Figure 8: Electrophilic aromatic substitution.

However, instead of preserving the aromatic π-system, dearomatizing reactions redirect that reactivity to form new bonds that disrupt the ring, enabling the synthesis of complex and highly functionalized cyclic structures that would be challenging to access through traditional aromatic substitution.[3] In detail, this one is a typology of reactions that significantly increase the complexity of the system, moving from a planar 2D scaffold, common to aromatic systems, to an alicyclic 3D structure, starting from cheap and readily available feedstocks. This reaction allowed chemists to access molecules that are otherwise difficult to obtain via classical transformations. This is something different to achieve with respect to the previously mentioned SeAr reaction.

However, dearomatization reactions are connected to one important challenge, which is the usual high stabilization energy of generic aromatic compounds.[4] This feature is a result of the extensive delocalization of π-electrons within a planar, cyclic, fully conjugated ring system. (Figure 9)

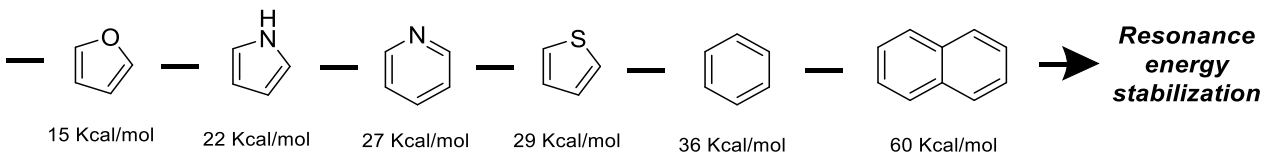

Figure 9: Resonance energy stabilization of the most common aromatics.

This issue is connected to overcoming high energetic barriers, usually by exploiting harsh reaction conditions. Once again, this can result in low functional group tolerance and poor environmentally sustainable procedures. Moreover, low selectivity generally leads to the formation of inseparable mixtures of products.

Nevertheless, if we look at the advances in recent years, growing interest has been associated with this reactivity.[5-6]. As illustrated in Figure 10, the number of publications referencing “dearomatization” has grown exponentially, with a marked increase over the past decade. For instance, in 2023, there were 415 publications on the topic, compared to just 134 in 2013.

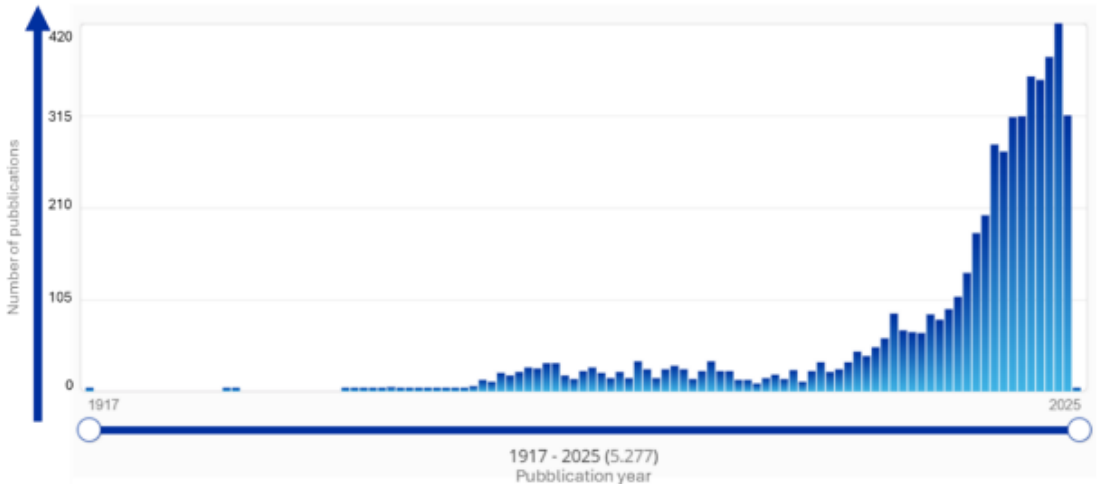

Figure 10: Recent growth of publications relative to ‘dearomatization’. Data from scifinder-n.cas.org.

Over the years, various strategies have been developed to achieve dearomatization, each offering different modes of reactivity and selectivity. One of the first examples came in 1944, when Arthur J. Birch developed a protocol for the reduction of aromatic compounds into cyclohexadienes (Figure 11).[7]

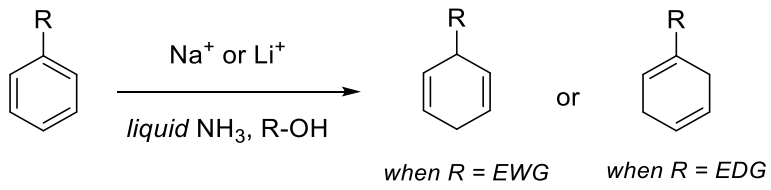

Figure 11: Birch reduction and regiochemistry.

This reactivity is also known as the Birch reduction, and it is recognized as a classical reductive dearomatization in which aromatic rings are converted into 1,4-cyclohexadienes through the action of alkali metals (e.g., Na or Li) in liquid ammonia, typically paired with an alcohol as a proton source. The reaction proceeds via single-electron transfer steps and leads to the loss of aromaticity. The reduction shows a clear

pattern of regioselectivity influenced by the nature of the substituents on the aromatic ring. Electron-withdrawing groups (EWGs) tend to direct the reduction to the ortho and para positions relative to themselves, whereas electron-donating groups (EDGs) typically guide the reaction toward the meta positions. This behavior enables a controlled and predictable transformation of simple aromatic compounds into non-aromatic, functionally diverse cyclic intermediates.

More recently, in 2007, Xi and coworkers described a highly efficient and selective intramolecular nucleophilic addition of the butadienyllithium to the aromatic ring, resulting in a dearomatization of phenyl rings via an ipso attack (Figure 12).[8]

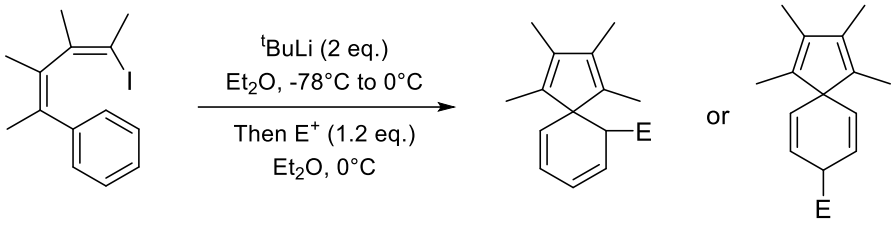

Figure 12: Example of nucleophilic dearomatization.

Performing dearomatization through nucleophilic addition is a valuable synthetic strategy that enables the transformation of aromatic systems by introducing a nucleophile into an activated or electronically biased arene. The result is that the aromaticity is disrupted. Here, the halogen-lithium exchange was performed at -78 °C, even if to induce dearomatization, the reaction was then allowed to reach 0 °C. Then, the carbanion was trapped with an electrophile (usually an aldehyde or a ketone) to achieve the final product. Authors declare that regiochemistry is dictated primarily by the aromatic substrate and by the nature of the electrophile.

Another possible class of dearomatization is the one mediated by Samarium(II) diiodide (SmI_2).[9] This one is a radical-based transformation that proceeds via single-electron transfer (SET) from SmI_2 to an aromatic substrate. This reduction generates a radical anion, which can undergo intramolecular or intermolecular reactions, leading once again to the loss of aromaticity. The resulting non-aromatic products are valuable building blocks for constructing complex molecules, as reported in the work by Reißig's group in 2007 (Figure 13).[10]

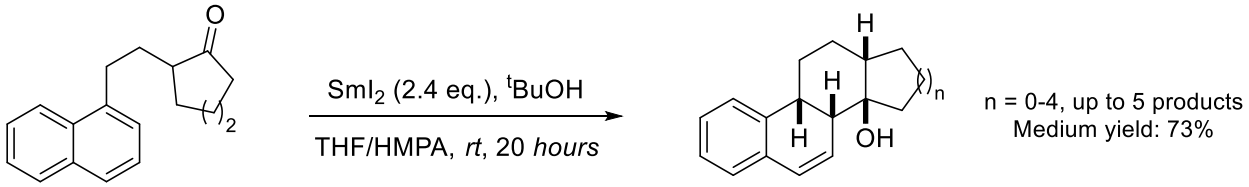

Figure 13: Diasteroselective cyclization mediated by Samarium diiodide.

Here, four contiguous stereogenic centers are generated by an induced cyclization of naphthyl-substituted aryl ketones mediated by samarium diiodide. The reaction outcome was reported to be highly dependent on the steric interactions between the alkoxy-samarium and the arene motifs. The resulting tetracyclic compound resembles human steroid-like cholesterol and estradiol, and for this reason, attracted a lot of attention.

Dearomatization is also induced thanks to the use of a transition metal to mediate the transformation. In literature, it is reported that complexes based on Cr and Mn can induce nucleophilic substitution on the arene through a η^6 coordination, eventually trapping an electrophile to have a double substitution or a proton to re-aromatize.[11-12] However, Harman and co-workers in 1998 exploited a different complexation using Os.[13] It is reported that these complexes prefer a η^2 coordination of the arene, increasing the nucleophilicity of the system and enabling new electrophilic substitutions. Moreover, this method allows a single coordination to one double bond out of three, and as a matter of fact, it can also result as a "protecting agent" for that bond. The authors applied this concept to an original Diels-Alder cyclization with electron-poor dienophiles and the electron-rich diene derived after the activation of the benzene ring with an Osmium complex, as reported in Figure 14

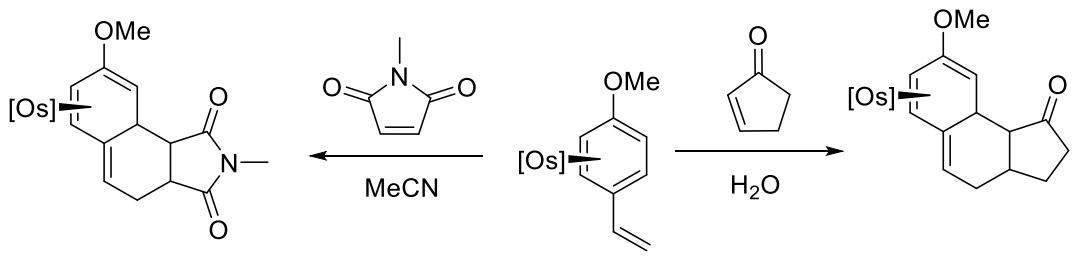

Figure 14: Application of Os-mediated activation with Diels-Alder cyclization.

Historically, what marked a turning point in the development of dearomative methodologies was the studies conducted by Egbert Havinga.[14] He was a prominent Dutch organic chemist and professor at Leiden University, known for his significant contributions to the study of photochemistry. From one of his lectures, he said that the aromatic nucleus is well-known for its rigidity in the ground state, but this one can become an extremely flexible and extrovert acrobat when being doped with a light quantum.

This statement brought us to imagine that what was once considered inert in its ground state can now be activated using light. Because of that, the advent of photocatalysis has enabled the development of many efficient dearomative strategies.

One of the first UV-activated photocycloadditions involving an arene moiety came in 1977 when Yamada and co-workers reported the intermolecular [2+2] cycloaddition between anisole and acrylonitrile derivatives (Figure 15).[15]

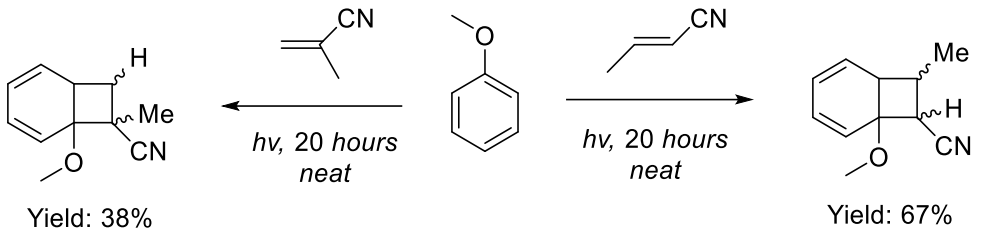

Figure 15: Dearomative [2+2] between anisole and acylonitrile derivatives (through UV activation).

Here, the cycloaddition reaction between anisole and methacrylonitrile proceeded with moderate yield (38%), under photochemical conditions employing a low-pressure mercury arc lamp as the irradiation source over a period of 20 hours. Interestingly, when crotononitrile was used as the cycloaddition partner under identical conditions, the yield significantly improved to 67%, highlighting a notable substrate effect on the efficiency of the cycloaddition process.

In the same report, the investigation has been extended to include a series of dimethoxybenzene derivatives as possible alternative aromatic substrates. However, in all the cases, the photochemical reaction failed to provide the desired cycloadducts, instead leading to complex mixtures of undefined side products. A single exception was observed with meta-dimethoxybenzene in combination with crotononitrile, which afforded the expected cycloaddition product, albeit in a relatively low yield.

In 1992, Gilbert and coworkers observed the [2+2] intramolecular cycloaddition of substituted anisoles with an alkene moiety (Figure 16).[16]

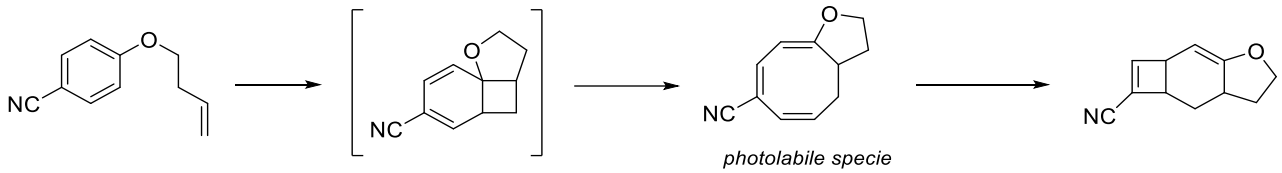

Figure 16: Intramolecular [2+2] of electron-poor anisoles with an alkene moiety.

The authors evaluated the effect of an electron-withdrawing substituent in the reported cyclization. They tested both cyano and methoxycarbonyl groups, in ortho, meta and para positions. The ortho and para-cyano isomers underwent the photocycloaddition in high yields, whereas the meta-cyano isomer reacted inefficiently; therefore, the regiochemistry plays a crucial role in determining the outcome of the process. The resulting structure was a fascinating eight-member cycle triene derived from a ring expansion, defined by a high photolability and, because of that, easily converted to a more stable 4-oxatricyclo- [7.2.0.$0^{3,7}$] undeca-2,10-diene.

More recently, an example from You in 2019 presented how intramolecular dearomative cycloaddition can be applied to heterocyclic compounds such as indoles (Figure 17).[17-18]

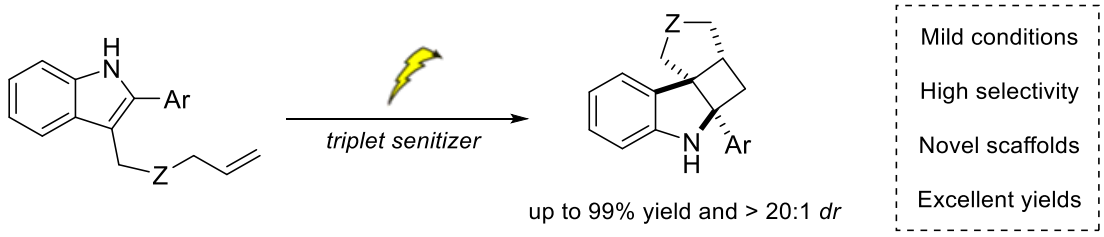

Figure 17: Intramolecular dearomative [2+2] of indoles by You.

The highly strained cyclobutane-fused angular tetracyclic spiroindolines featured in the product, typically unattainable under thermal conditions, were accessed in high yields (up to 99%) with excellent diastereoselectivity (>20:1 dr) under mild conditions. The method was also compatible with diverse functional groups and amenable to flexible transformations.

Based on these findings, in our group, we recently reported a light-mediated [2+2] dearomatization strategy for simple and benzo-fused heteroaromatics (Figure 18).[19]

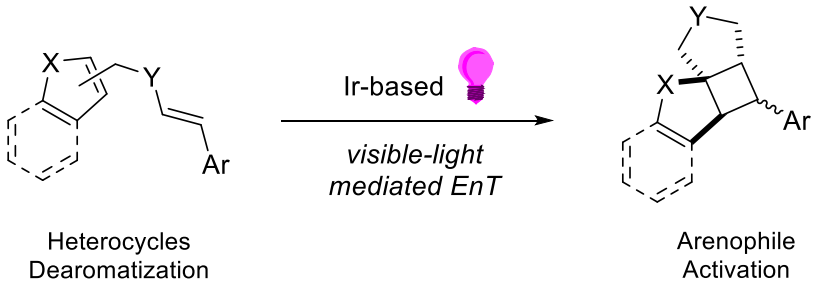

Figure 18: [2+2] dearomatization of heteroarenes with alkenes.

Compared to other cases where the activation of heteroarenes has been achieved through the introduction of conjugated auxochromes, such as carbonyl or phenyl groups, this [2+2] dearomative cycloaddition of simple heteroarenes remains significantly underexplored. In this context, reactivity is driven by the selective activation of the arenophile partner, rather than by functionalization of the heteroarene itself.

References

[1] C. J. Huck, D. Sarlah, *Chem*., **2020**, 6, 1589-1603.

[2] T. J. Ritchie, S. J. F. Macdonald, *Drug Discovery Today*, **2009**, 14, 1011-1020.

[3] T. P. Gonçalves, I. Dutta, K. W. Huang, *Chem. Commun.*, **2021**, 57, 3070-3082.

[4] M. Okumora, D. Sarlah, *Synlett*, **2018**, 29, 845-855.

[5] S. P. Roche, J. A. Porco Jr, *Angew. Chem. Int. Ed.,* **2011**, 50, 4068-4093.

[6] W. C. Wertjes, E. H. Southgate, D. Sarlah, *Chem. Soc. Rev.*, **2018**, 47, 7996-8017.

[7] A. J. Birch, *J. Chem. Soc.*, **1944**, 430-436.

[8] L. Liu, Z. Wang, F. Zhao, Z. Xi, *J. Org. Chem.,* **2007**, 72, 3484–3491.

[9] C. U. Dinesh, H. U. Reißig, *Angew. Chem. Int. Ed.,* **1999**, 38, 789-791.

[10] F. Aulenta, M. Berndt, I. Brüdgam, H. Hartl, S. Sörgel, H. U. Reißig, *Chem. Eur.,* **2007**, 13, 6047-6062.

[11] M. F. Semmelhack, G. R. Clark, J. L. Garcia, J. J. Harrison, Y. Theetaranonth, W. Wulff, A. Yamashita, *Tetrahedron*, **1981**, 23, 3957-3965.

[12] A. R. Pape, K. P. Kaliappan, E. P. Kundig, *Chem. Rev.,* **2000**, 100, 2917–2940.

[13] S. P. Kolis, M. D. Chordia, R. Liu, M. E. Kopach, W. D. Harman, *J. Am. Chem. Soc.,* **1998**, 120, 2218–2226.

[14] E. Havinga, R. O. De Jongh, M. E. Kronenberg*, Helv. Chem. Acta,* **1967**, 50, 2550-2560.

[15] M. Ohashi, Y. Tanaka, S. Yamada, *Tetrahedron Lett.,* **1977**, 41, 3629-3632.

[16] S. Y. Al-Qaradawi, K. B. Cosstick, A. Gilbert, *J. Chem. Soc., Perkin Trans. 1,* **1992**, 1145-1148.

[17] M. Zhu, C. Zheng, X. Zhang, S. L. You, *J. Am. Chem. Soc.,* **2019**, 141, 2636-2644.

[18] Q. Ding, X. Zhou, R. Fan, *Org. Biomol. Chem.*, **2014**, 12, 4807-4815.

[19] M. Chiminelli, C. Galbardi, R. Maggi, F. Bigi, L. Capaldo, N. Della Cà, R. Viscardi, L. Marchiò, G. Maestri, M. Lanzi. *Org. Lett.,* **2025**, 27, 8909–8914.

Crossed [2+2] cycloadditions

Another important class of reactions that will be explored is cycloaddition. This class of transformation has been defined by IUPAC[1] as “a reaction in which two or more unsaturated molecules (or parts of the same molecule) combine with the formation of a cyclic adduct in which there is a net reduction of the bond multiplicity”. It comes with the definition that this type of chemical reaction is undoubtedly one of the best strategies to increase bond saturation in a product, a parameter associated with the Fsp^3 factor and with the consequent clinical success of the molecule. The reaction allows the formation of multiple C-C bonds in only one synthetic step with complete atom economy.[2] Cycloadditions have thus proven to be extremely useful reactions in organic chemistry, with applications in the total synthesis field of bioactive molecules.[3-5] Their main advantages are the potential excellent regio- and diastereoselectivities and the possibility to achieve complete atom economy. Additionally, this reaction is associated with a reduced amount of waste, which demonstrates that it could also be interesting in regard to the principles of green chemistry.

Two classes have been identified: an intramolecular variant that enabled the rapid construction of congested bicyclic scaffolds[6] and the intermolecular variant that instead allowed the construction of interesting cyclobutane rings, usually difficult to achieve in any other way (Figure 19).[7]

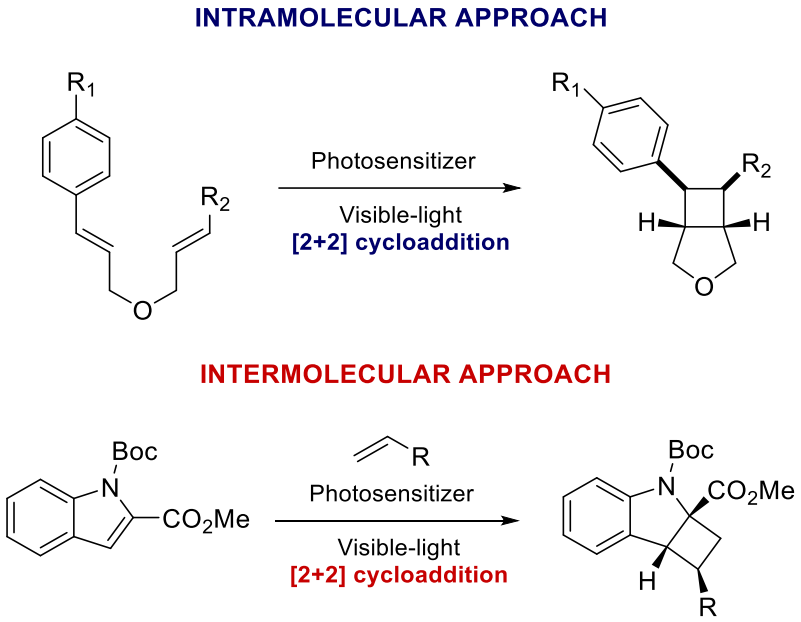

Figure 19: Examples of [2+2] intermolecular and intramolecular photocycloaddition.

However, to lay the foundation for this kind of reactivity, it is necessary to give a general overview of the topic. The first feature to underline is the general incompatibility of [2+2] cycloaddition reaction from a thermodynamic point of view. The [2+2] cycloaddition is symmetry forbidden because the interaction of the HOMO and LUMO of the two π systems inevitably leads to a mismatch in orbital symmetry. This is the reason why most of the [2+2] cycloadditions known are photocatalyzed.[8-9] Therefore, a stepwise mechanism occurs under certain

conditions: the use of a sensitizer promotes an energy transfer to one π partner as represented in Figure 20, now able to interact with a second ground-state π system in a concerted fashion.

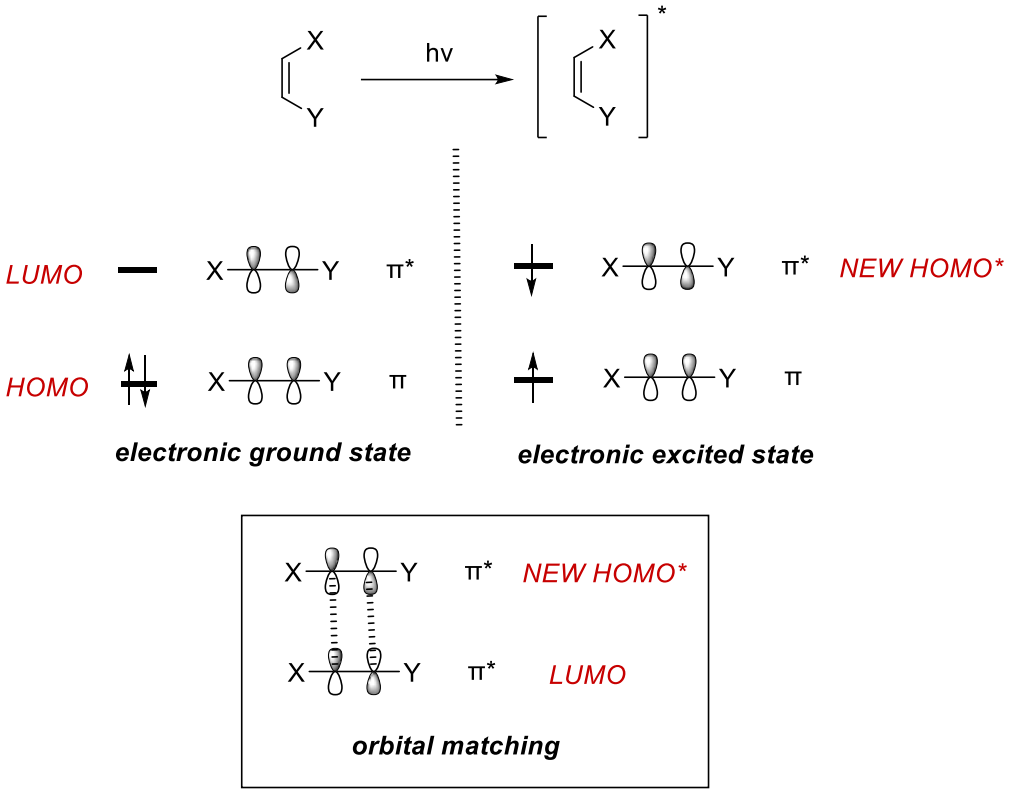

Figure 20: Orbital interactions explain why thermal [2+2] cycloadditions are typically symmetry-forbidden for simple alkenes but allowed photochemically.

A 1,n diene can react in two different [2+2] cycloaddition modes. Taking two tethered olefinic fragments connected by a linker, a straight cycloaddition would pair the “proximal” carbon of one olefinic fragment with the ‘proximal’ carbon of the other olefinic fragment. In contrast, a crossed cycloaddition instead pairs the ‘distal’ carbon with the ‘proximal’ carbon of the other olefinic fragment, thereby creating a bridged bicyclic structure rather than a fused ring. The result is often a bridged bicycle or similar motif, depending on the tether geometry and on the nature of the olefinic partners involved. The intramolecular enone-alkene cycloaddition reported in Figure 21 is a clear example. In fact, it has been demonstrated that a tether with three atoms leads preferentially to the straight product, establishing a five-membered ring, while if the tether contains only two atoms, a possible four-membered ring formation is avoided, and the reaction proceeds to the formation of a ‘bent’ product. [10-11]

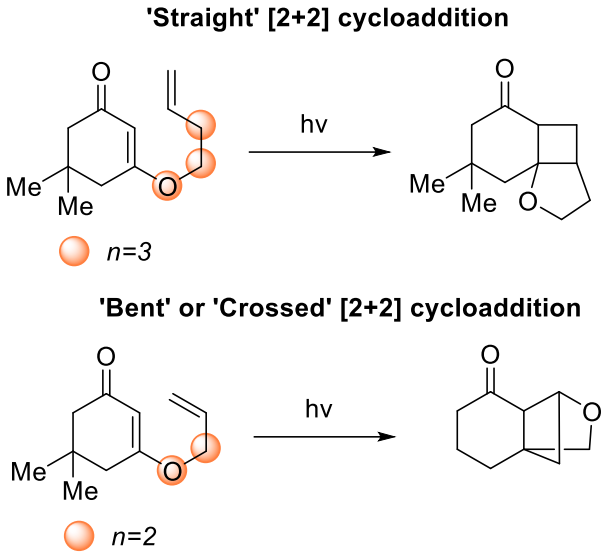

Figure 21: Enone-alkene straight vs crossed [2+2] cycloaddition.

A similar but more elegant example of a crossed intramolecular [2+2] photocycloaddition of tethered alkenoxycyclohexenones is reported by Bach and co-workers in 2022.[12] This reaction reinforces the previous concept explained, in which it has been remarked that the nature of the olefinic partner interferes with the final product obtained. Here, the authors proposed a way in which they can achieve stereocontrol on the reaction by adding a chiral catalyst, as reported in Figure 22.

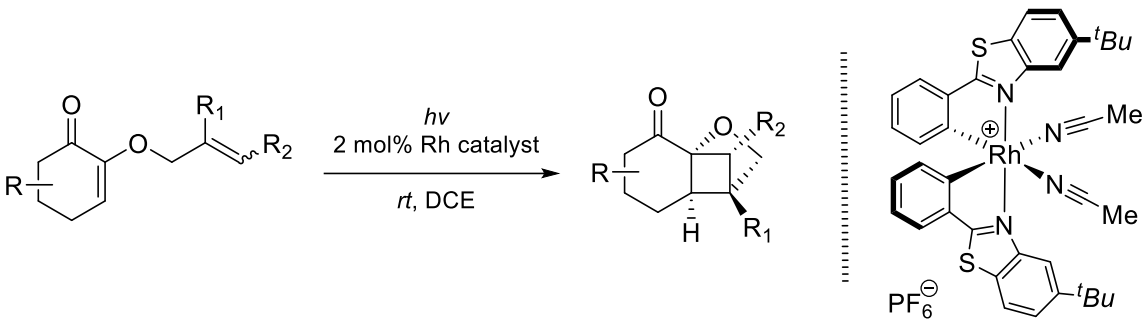

Figure 22: Intramolecular crossed [2+2] photocycloaddition of various substituted 2-(2′-alkenyloxy)cyclohex-2-enones to bridged tricyclic products.

In this case, the crossed reaction pathway was identified as the most rewarding reactivity because it enables the establishment of a bonding that is very difficult to attain in a thermal reaction. Because of that, the authors have decided to study in deep this kind of transformation with respect to the classical straight one.

In general, in bent systems, the energetic barrier to get connectivity may be higher due to the low ideal orbital alignment or the competition of a linear approach.

The reactivity of straight vs crossed [2+2] cycloadditions depends on a delicate balance of three main factors:

- **Geometry and length**: If the tether forces the π systems into proximity in a particular orientation, it may facilitate a crossed connectivity in the final product.
- **Orbital overlap**: The quality of π–π overlap in the transition state it's very important.
- **Steric and substituent effects**: Bulky substituents may sterically favor one approach instead of the straight one.

One of the first works that highlights the importance of these factors in determining a clear pathway between a 'bent' cyclization instead of a 'straight' one is the enantioselective intramolecular [2+2] photocycloaddition reported by Harms and coworkers in 2000.[13] As reported by Figure 23, the authors here focus their attention on the use of a quinolone derivative that contains a terminal alkene. When this one is irradiated with UV light, this substrate can selectively undergo intramolecular crossed [2+2] cycloadditions, forming a fused/bridged cyclobutane product with high diastereoselectivity.

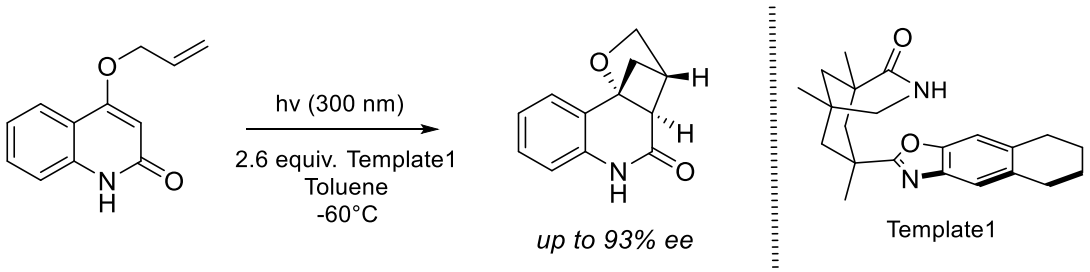

Figure 23: Enantioselective Intramolecular [2+2]-Photocycloaddition Reactions in solution.

The main challenge was to achieve enantioselectivity in this reaction, which led the authors to introduce a chiral lactam-based host molecule (Template1) that binds the substrate through hydrogen bonding and finally leads to high enantiomeric excesses, up to 93% ee. In this case, the length of the alkenyl side chain as well as the geometry restrictions due to the presence of a δ-lactam functional group are the parameters responsible for the observed cyclization.

Another important work worth noting is the one from Kwon's group in 2017.[14] Here, they triggered an intramolecular crossed [2+2] cycloaddition of dienones promoted through sensitization of an Iridium(III) catalyst, to form bridged bicycloheptanones (Figure 24).

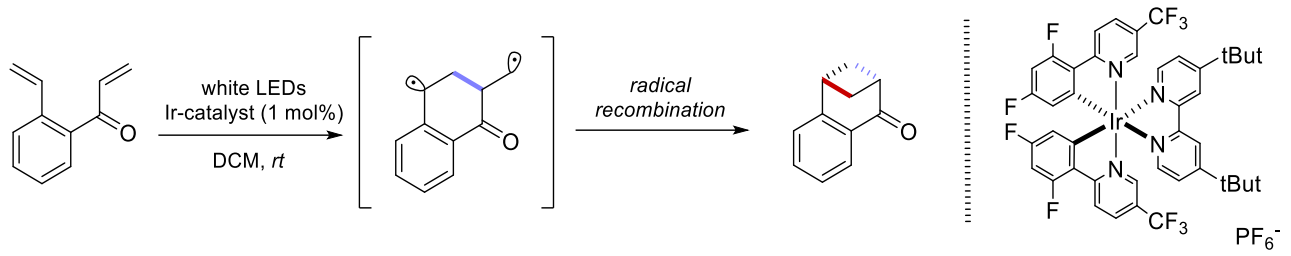

Figure 24: Intramolecular Crossed [2+2] Photocycloaddition through Visible Light-induced EnT.

The excellent regioselectivity observed in this reaction is certainly an advance in the construction of this kind of bridged bicyclic structure. Additionally, this one is considered the first example of an exclusive crossed [2+2] cycloaddition promoted by visible light. The reaction presents full atom economy, and it can be performed using simple photochemical equipment under mild conditions.

More recently, in 2024, Li's group reported another similar work regarding a visible light-driven intramolecular 'crossed' and 'straight' catalyst-free [2+2] cycloaddition.[15] In this work, they utilized bis(cinnamoyl)ketenedithioacetals that, when irradiated with visible light, performed an intramolecular [2+2] cycloaddition, without the addition of any catalyst, to give easily separable mixtures of bridged, when a crossed cycloaddition happens, and fused, when a straight cycloaddition happens, interesting bicyclic products (Figure 25).

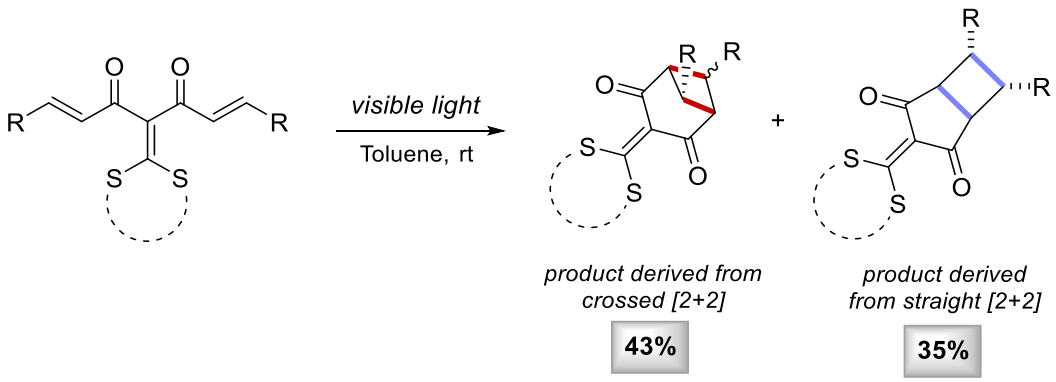

Figure 25: Visible-light-driven, catalyst-free intramolecular crossed and straight [2+2] cycloaddition.

Here, the formation of both crossed and straight [2+2] cycloaddition products in this visible-light-driven, catalyst-free reaction can be rationalized by a combination of structural and energetic factors. The flexible tether allows the reactive conjugated system to adopt multiple conformations, enabling different orbital overlaps in the transition state. Reported computational studies reveal that both cyclization pathways are energetically accessible, with relatively low and comparable activation barriers that justify the presence of both products with comparable yields. Additionally, steric and electronic effects from substituents do not strongly disfavor either pathway, allowing both products to form.

All the examples highlight the importance of achieving control over this reactivity. This topic holds for wide future application in modern chemistry, thanks to the fact that the cycloaddition reaction is a type of reactivity known and very effective in the synthesis of a myriad of interesting products.

References

[1] Cycloaddition' in IUPAC Compendium of Chemical Terminology, 3rd ed. *International Union of Pure and Applied Chemistry*; **2006**.

[2] B. M. Trost, *Science*, **1991**, 254, 1471-1477.

[3] K.C. Nicolaou, S. A. Snyder, T. Montagnon, G. Vassilikogiannakis, *Angew. Chem. Int. Ed.,* **2002**, 41, 1668-1698.

[4] J. Zhu, H. Bienaymé, *Chem. Rev.,* **2005**, 105, 547-587.

[5] K. C. Nicolaou, T. Montagnon, P. S. Baran, Y. L. Zhong, *Chem. Soc. Rev.,* **2002**, 31, 67-79.

[6] T. Zhang, Y. Zhang, S. Das, *ChemCatChem*, **2020**, 12, 6173-6185.

[7] M. S. Oderinde**,** A. Ramirez, T. G. Murali Dhar, L. A. M. Cornelius, C. Jorge, D. Aulakh, B. Sandhu, J. Pawluczyk, A. A. Sarjeant, N. A. Meanwell, A. Mathur, J. Kempson, *J. Org. Chem.,* **2021**, 86, 1730–1747.

[8] J. Kagan, B. E. Firth, *J. Org. Chem.,* **1974**, 39, 3145–3147.

[9] F. D. Lewis, T. I. Ho, R. J. DeVoe, *J. Org. Chem.,* **1980**, 45, 5283–5286.

[10] Y. Tamura, Y. Kita, H. Ishibashi, M. Ikeda, *J. Chem. Soc. D*., **1971**, 19, 1167-1167.

[11] R. M. Coates, P. D. Senter, W. R. Baker, *J. Org. Chem.,* **1982**, 47, 3597–3607.

[12] T. Rigotti, D. P. Schwinger, R. Graβl, C. Jandl, T. Bach, *Chem. Sci.,* **2022**, 13, 2378-2384.

[13] T. Bach, H. Bergmann, K. Harms, *Angew. Chem. Int. Ed.,* **2000**, 39, 2302-2304.

[14] J. Zaho, J. L. Brosmer, Q, Tang, Z. Yang, K. N. Houk, P. L. Diaconescu, O. Kwon*, J. Am. Chem. Soc.,* **2017**, 139, 9807–9810.

[15] Y. Sang, X. Zohu, C. Jin, L. Pang, Q. Liu, H. Yuan, Y. Li, *Org. Chem. Front.,* **2024**,11, 3478-3484.

Hydrogen Atom Transfer (HAT)

One of the key aspects that will be thoroughly examined is the implementation of Hydrogen Atom Transfer (HAT) within photocatalytic methodologies. This reactivity offers unique opportunities in organic synthesis, enabling the activation of C-H bonds in most cases, but also Si-H or S-H bonds, permitting the synthesis of important products.[1] This typology of reaction lies as one of the most important chemical and biological processes in modern chemistry. Generally, if we want to detail this process, a HAT transformation involves the concerted transfer of a hydrogen atom from a donor (A-H) to an acceptor radical (B•), delivering B–H and the radical A• (Figure 26).[2-4]

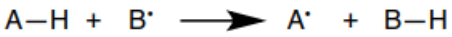

Figure 26: Model HAT reactivity between an acceptor and a donor.

In detail, a synthetic route based on HAT must be judiciously planned, starting with choosing the proper hydrogen abstractor (B). The newly formed B−H bond has to be stronger than the A−H bond to cleave, to provide the driving force for the overall process. This thermodynamic driving force is probably the dominant factor for a HAT reaction and can be approximated by the difference in bond dissociation energies of the A–H bond being cleaved and the new bond (B-H) being formed, but it's not the only parameter to be considered. This simple "driving force" is particularly useful in the approaching phase, comparing candidate donor–acceptor pairs. When the bond formed with the acceptor is stronger than the bond broken in the donor, the transformation is thermodynamically favorable. Conversely, if this condition is not met, the reaction is either unlikely to occur or significantly disfavored due to thermodynamic constraints. In such cases, it is advisable to reconsider the strategy and explore alternative coupling partners.[5]

During recent years, various reaction models have been constructed in an attempt to completely predict these reactivity events. However, even though these models are highly precise, real systems strongly diverge from ideal models in several important aspects. In this paragraph, some of them will be overviewed by trying to have a complete vision of the complexity of such reactivity, proposing some interesting examples.

Behind the homolytic cleavage and the consequent release of the product, numerous other non-negligible factors contribute. Among all of them, the most important are the bond strength, polar effects, strain release, steric/torsional effects, and hyperconjugative effects (Figure 27).[6]

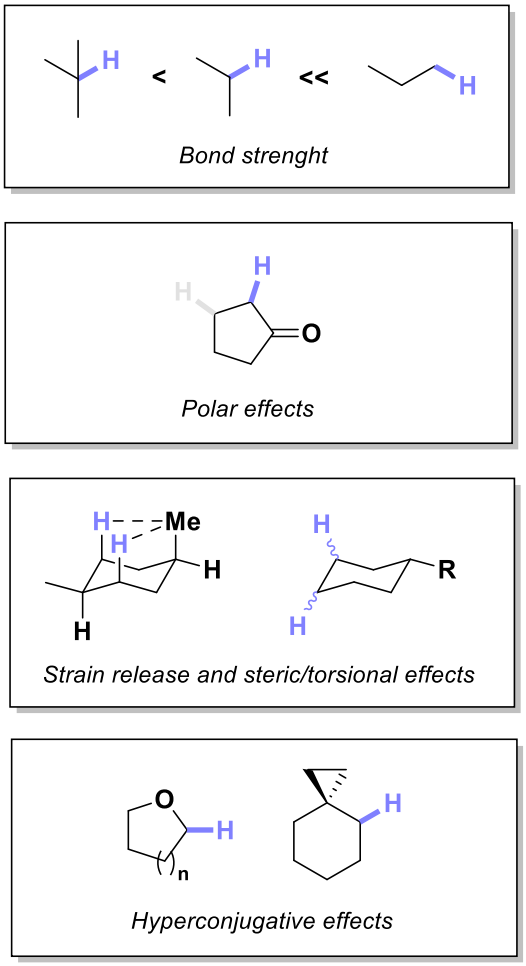

Figure 27: Main factors operating in the selective HAT-based C−H functionalization in organic compounds.

Apart from the first one, in which the relative stability of the generated organoradical drives the cleavage of a tertiary C−H bond over that of a secondary or a primary C−H bond, taking the case of hydrocarbons as reference, the most important factors to put under analysis are the polar and the electrostatic factors. In fact, the interaction between the radical acceptor and the hydrogen donor can be influenced by a simple electrostatic polarization.[7-8] For instance, an acceptor with a strongly electron-withdrawing substituent may better stabilize the incipient negative charge accompanying proton transfer. Similarly, hydrogen-bonding networks or secondary coordination sphere interactions can also prepolarize or preorganize the donor–acceptor pair, lowering activation barriers. This concept is well illustrated in Figure 28 and can be summarized by saying that, despite being uncharged species, radicals can have nucleophilic or electrophilic behaviors.[9-11]

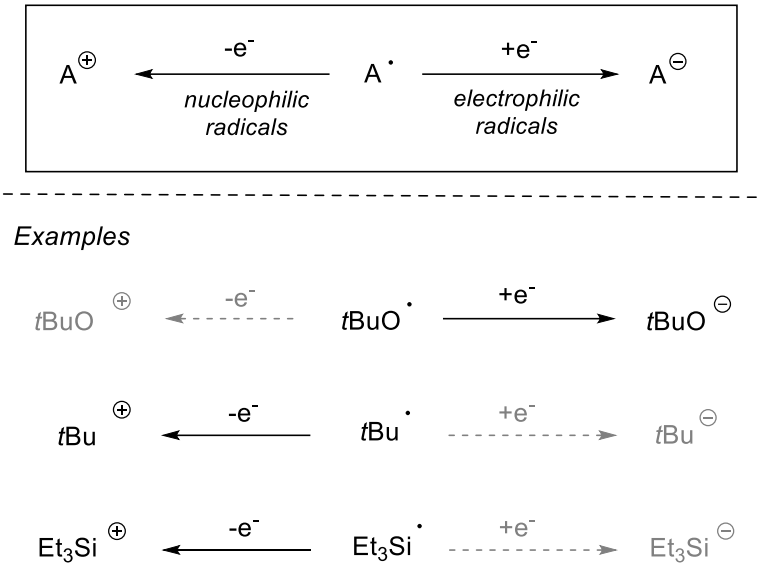

Figure 28: Effect of radical 'philicities' on HAT sequences.

As reported by Figure 28, the polarity matching principle applies: HAT reactions are more favorable when the acceptor is electronically complementary (e.g., an electrophilic hydrogen abstractor for a nucleophilic bond). This concept is at the basis of polarity-reversal catalysis (PRC), which is characterized by a replacement of a single-step abstraction, due to slow and unfavorable polar effects, with a two-step process in which intermediates are instead polarity-matched. The principle is generalized in Figure 29. An example is then applied, which regards control reactivity and selectivity in radical-chain reactions for the functionalization of an ester carbonyl group.[12]

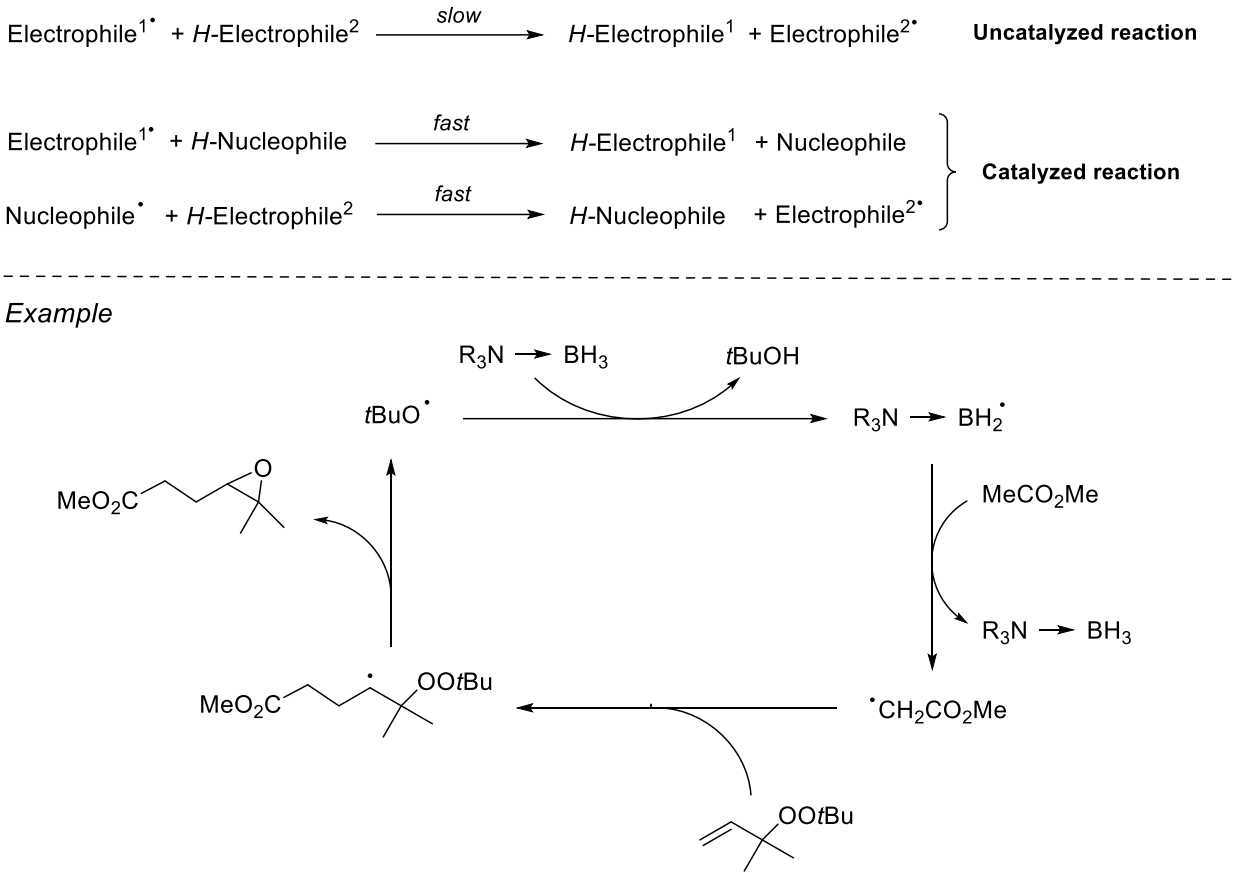

Figure 29: Use of a borane-based catalyst to unlock epoxypropilation reaction via 'PRC'.

It has been observed that in the presence of a borane-based catalyst, methyl acetate, dimethyl malonate, triethyl methanetricarboxylate and ethyl cyanoacetate all react with allylic tert-butyl peroxides at 30°C in benzene to give products resulting from 2,3-epoxypropylation. In the absence of the amine–borane, such epoxypropylation reactions are sluggish and require a much higher temperature to happen.

Trialkylsilanes represent another example worth noting, as they generally exhibit low efficiency in mediating homolytic reductions of functional groups through hydrogen atom transfer (HAT) (Figure 30).

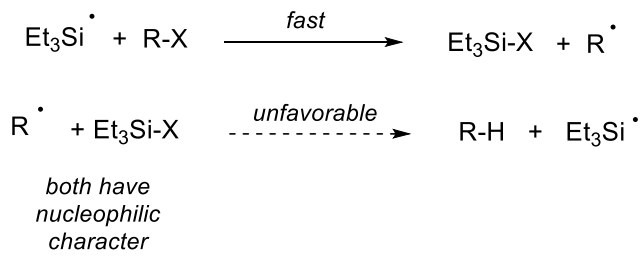

Figure 30: Example of matching reactant polarities for favorable reactivity.

In 1991, Roberts and co-workers disclosed that polar factors are unfavorable for the reaction involving a nucleophilic alkyl radical while abstracting an electron-rich hydrogen atom.[13] Because of that, they have proposed that this reaction should be subject to polarity reversal catalysis (PRC) by thiols, which are more electrophilic radicals, proposing a replacement of a single-step process with a cycle of two reactions, as reported in Figure 31.

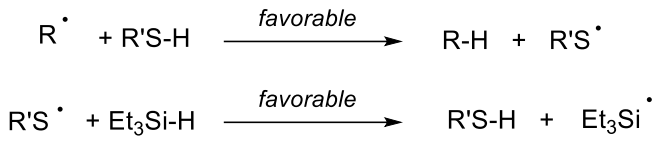

Figure 31: Thyls radical brings favorable charge transfer interactions in the transition state.

Another important feature is the steric hindrance near the donor or around the radical acceptor. This feature can inevitably slow or facilitate HAT events because the distances between a potential donor and a potential acceptor strongly influence the outcome.[14] The shorter transfer distances typically favor lower barriers, while constrained geometries may force a more distorted pathway or higher reorganization costs, which lead to reactions that are slow or unable to happen.

An important example is reported in the regio- and stereoselective decatungstate photocatalyzed alkylation of alkenes by alkylcyclohexanes, by Albini and co-workers (Figure 32).[15]

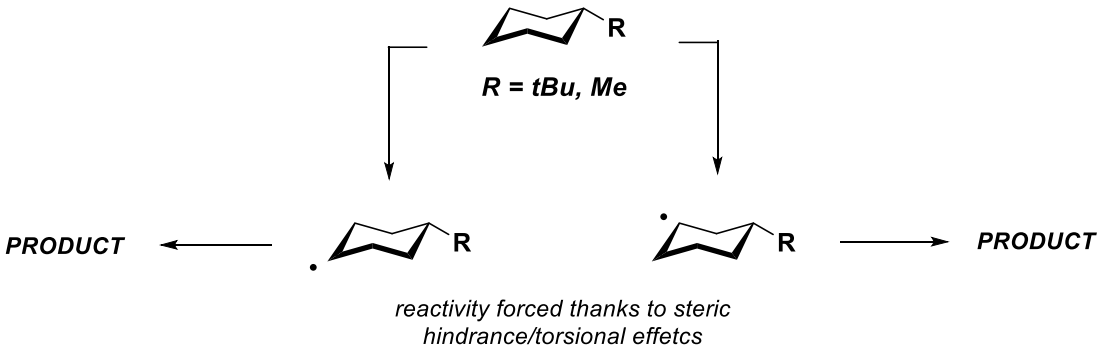

Figure 32: Selective C-H activation at positions 3 and 4 of substituted cyclohexanes.

Here, the data demonstrates a remarkable steric effect, illustrating that an alkyl substituent on cyclohexanes directs the hydrogen-abstraction step, while not hindering the trapping of the resulting radical by electrophilic alkenes. In fact, the geometry of the molecule forces the activation toward precise reaction sites (precisely positions 3 and 4) due to simple steric/torsional effects.

Bietti and co-workers have also reported a similar investigation. In this case, the site selectivity of 5-amino-1-pentanol has been studied (Figure 33).[16]

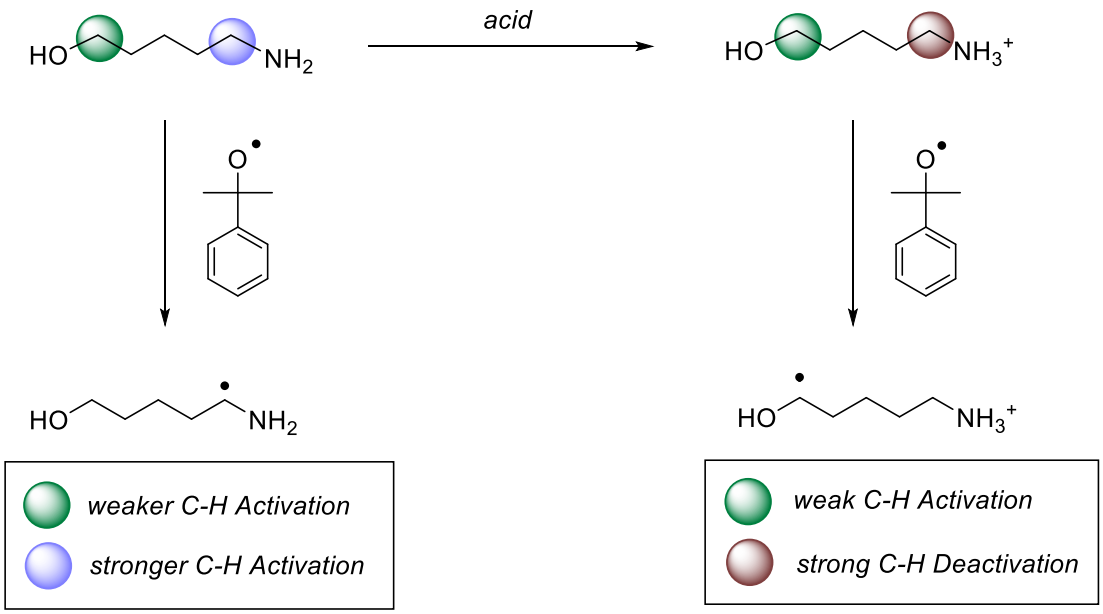

Figure 33: Protonation of the amino group strongly deactivates the proximal and remote methylene groups toward HAT.

Here, the reactivity can be drastically changed through protonation of bifunctional substrates that bear a strongly activating NH_2 group, with HAT that shifts then to the C–H bonds that are adjacent to the OH group.

Another common substrate-dependent effect influencing HAT reactions is associated with electron-donating functional groups, particularly heteroatoms such as oxygen and nitrogen. These atoms can activate adjacent C–H bonds through hyperconjugation. This effect is typically observed in compounds like ethers, acetals, alcohols, amines, and amides, in which the presence of the heteroatom lowers the bond dissociation energy (BDE) of neighboring C–H bonds and stabilizes the resulting radical intermediate via hyperconjugative interactions. This trend will be further exemplified in later chapters, because it plays a key role in explaining the reactivity of allenamides (Figure 34).

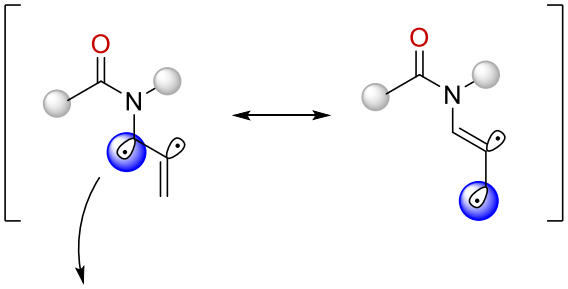

More stable radical due to the presence of nitrogen and its lone pair that stabilize

Figure 34: Stabilization of radicals in activated allenamide substrates.

Usually, to unravel the mechanistic details of HAT events, chemists take advantage of a variety of experimental techniques, such as determining kinetic isotope effects, performing the reaction with H vs D, and then

determining the ratio between the two relative constants (k_H/k_D).[17] Then, if possible, spectroscopic and time-resolved methods like laser flash photolysis, transient absorption, and pulse radiolysis can directly monitor radical formation and decay pathways. These techniques are usually expensive, but they can clearly define HAT processes. In the next chapters, computational modeling and DFT calculations will be used primarily to elucidate the reaction mechanism involving HAT events. These methods can help in mapping reaction coordinates, estimate the presence of transition states, and predict their relative energy.

The growing interest in photocatalyzed HAT processes is justified by their increasing relevance in synthetic chemistry and their occurrence in several natural processes.[18] In this thesis, the interest will be focused on synthetic radical functionalization. HAT is a powerful tool to create carbon-centered radicals from C–H bonds, enabling subsequent functionalization and triggering the release of interesting products difficult to achieve through any other synthetic pathway.

References

[1] L. Capaldo, D. Ravelli, M. Fagnoni, *Chem. Rev.,* **2022**, 122, 1875–1924.

[2] J. F. Hartwig, M. A. Larsen, *ACS Cent. Sci.,* **2016**, 2, 281– 292.

[3] R. Ludwig, Chem. Phys. Chem., **2007**, 8, 2539-2539.

[4] W. Lai, C. Li, H. Chen, S. Shaik, *Angew. Chem., Int. Ed.*, **2012**, 51, 5556– 5578.

[5] J. M. Mayer, *Acc. Chem. Res.*, **2011**, 44, 36–46

[6] J. M. Mayer, *Annual Review of Physical Chemistry*, **2004**, 55, 363-390.

[7] B. P. Roberts, *Chem. Soc. Rev.,* **1999**, 28, 25–35.

[8] M. Salamone, F. Basili, M. Bietti, *J. Org. Chem.*, **2015**, 80, 3643–3650.

[9] H. Fisher, L. Radom, *Angew. Chem. Int. Ed.,* **2001**, 40, 1340-1371.

[10] K. Héberger, A. Lopata, J. C. Jászberényi, *J. Phys. Org. Chem.,* **2000**, 13, 151-156.

[11] F. V. Vleeschouwer, V. Van Speybroeck, M. Waroquier, P. Geerlings, F. De Proft, *Org. Lett.*, **2007**, 9, 2721–2724.

[12] H. S. Dang, B. P. Roberts, *J. Chem. Soc., Perkin Trans. 1*, **1993**, 8, 891-898.

[13] S. J. Cole, J. N. Kirwan, B. P. Roberts, C. R. Willis, *J. Chem. Soc, Perkin Trans. 1,* **1991**, 1, 103-112.

[14] M. Salamone, T. Martin, M. Milan, M. Costas, M. Bietti, *J. Org. Chem.,* **2017**, 82, 13542– 13549.

[15] D. Dondi, D. Ravelli, M. Fagnoni, M. Mella, A. Molinari, A. Maldotti, A. Albini, Chem. Eur. J., **2009**, 15, 7949-7957.

[16] M. Salamone, G. Carboni, M. Bietti, *J. Org. Chem.,* **2016**, 81, 9269–9278.

[17] T. Ishimoto, M. Tachikawa, H. Tokiwa, U. Nagashima, *Chemical Physics*, **2005**, 314, 231–237.

[18] M. Dutra, J. A. Amaya, S. McElhenney, O. M. Manley, T. M. Makris, V. Rassolov, S. Garashchuk, *J. Phys. Chem. B,* **2022**, 126, 3493–3504.

Chapter 1:

'Visible-Light Promoted Intermolecular para-Cycloadditions of Allenamides on Naphthalene'

From this chapter:

M. Chiminelli, G. Scarica, D. Balestri, L. Marchiò, N. Della Ca', G. Maestri. The visible light-promoted intermolecular para-cycloadditions of allenamides on naphthalene, *Tetrahedron Chem.*, **2023**, 8, 100053. DOI:10.1016/j.tchem.2023.100053.

Introduction

Dearomative cycloaddition reactions can proceed through activation at the ortho, meta, or para positions of aromatic substrates, leading to distinct structural and mechanistic outcomes. However, reactions occurring at the ortho position are often hindered by pronounced steric congestion and unfavorable transition-state geometries, whereas meta-selective processes remain intrinsically challenging due to limited electronic communication between the reactive centers and the site of activation.[1] On the other hand, para-selective processes offer higher regioselectivity and synthetic control, but in the literature, there are just a few examples reported.[2-3] The cause of that is related to the activation of the benzene ring, which is recognized as a very challenging transformation in modern chemistry. Nevertheless, even if it has been intensively studied over the last 60 years, this topic maintains high interest.

The methodologies reported present high scope limitations, which are often associated with the necessity of harsh conditions as reported by the works of Himbert and Vanderwal, respectively in 1986 and 2013, where they performed the transformation at high reaction temperatures (Scheme 1).[4-5]

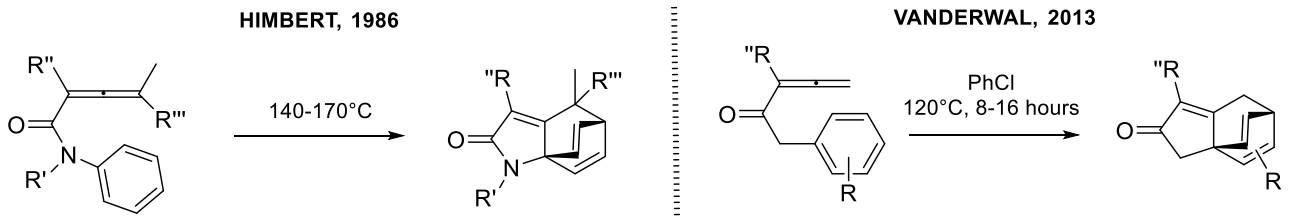

Scheme 1: Studies on allene/arene cycloaddition.

However, in 2023, our group developed a synthetic way to perform an intramolecular para-cycloaddition on simple aromatics, which arises as a great element of novelty around this topic because, for the first time, mild conditions and high tolerance towards different functional groups were achieved.[6]

Taking inspiration from this one, we wondered about dearomatizing naphthalene in an intermolecular fashion. The naphthalene bicycle has a notably lower aromatic stabilization than benzene. As shown in Scheme 2, the dearomatization of a single ring significantly reduces the stability of the system. However, in the case of naphthalene, disruption of one ring leaves a second aromatic ring that can stabilize the resulting product.

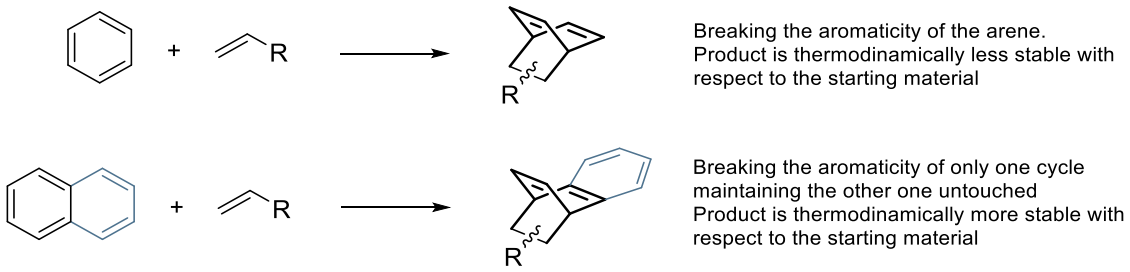

Scheme 2: Differentiation in dearomatizing simple arene or naphthalene.

This is the reason why the dearomatization of naphthalene is usually more developed with respect to the benzene one. Nevertheless, the most recent examples will be examined about this topic.

In 2022, Brown and Maji reported two independent works regarding the dearomative para-cycloaddition of alkenes on naphthalene derivatives (Scheme 3).[7-8]

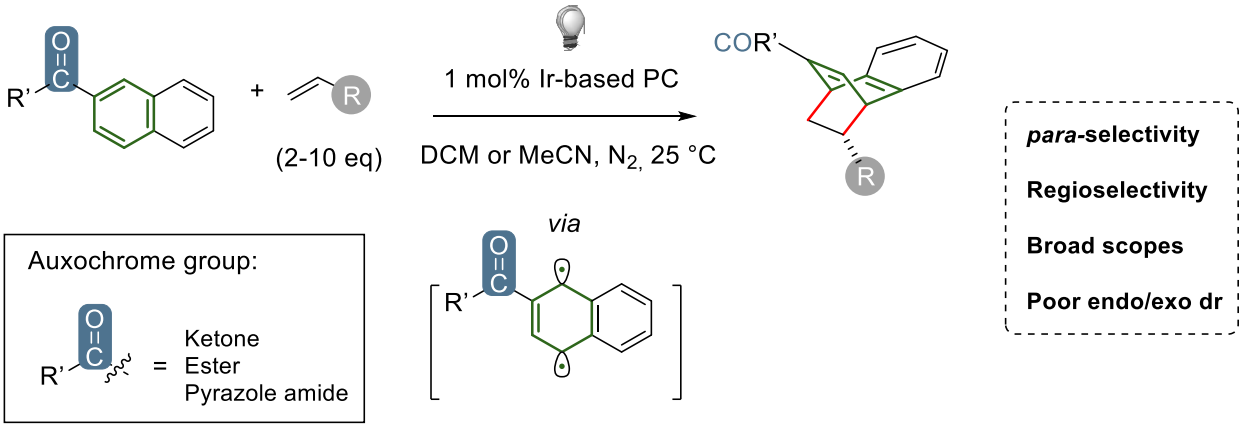

Scheme 3: Intermolecular dearomative para-cycloaddition on naphthalenes bearing an auxochrome group.

The reaction starts with the sensitization of the naphthalene derivative by energy transfer to form a biradical intermediate. Once formed, this one can trap an alkene to obtain the bridged polycycle. The presence of the carbonyl group conjugated to the naphthalene core is necessary to increase the conjugation of the system, lowering the E_T of the naphthalene unit. With this methodology, the authors had the opportunity to synthesize a wide scope of products with high regioselectivity. However, a mixture of two diastereomers (endo/exo) with poor diastereoselectivity was obtained.

Both these works exhibit several common features with Glorius's innovative dearomatization of bicyclic aza-arenes with alkenes (Scheme 4). Here, the methodology allows the sensitization of quinolines, (iso)quinolines, and quinazolines. It's important to understand the mechanism of activation, because these species are scarcely applied in cycloaddition reactions due to the inherently low reactivity of the aromatic system and selectivity challenges, by enabling the reaction of one of the two rings.[9]

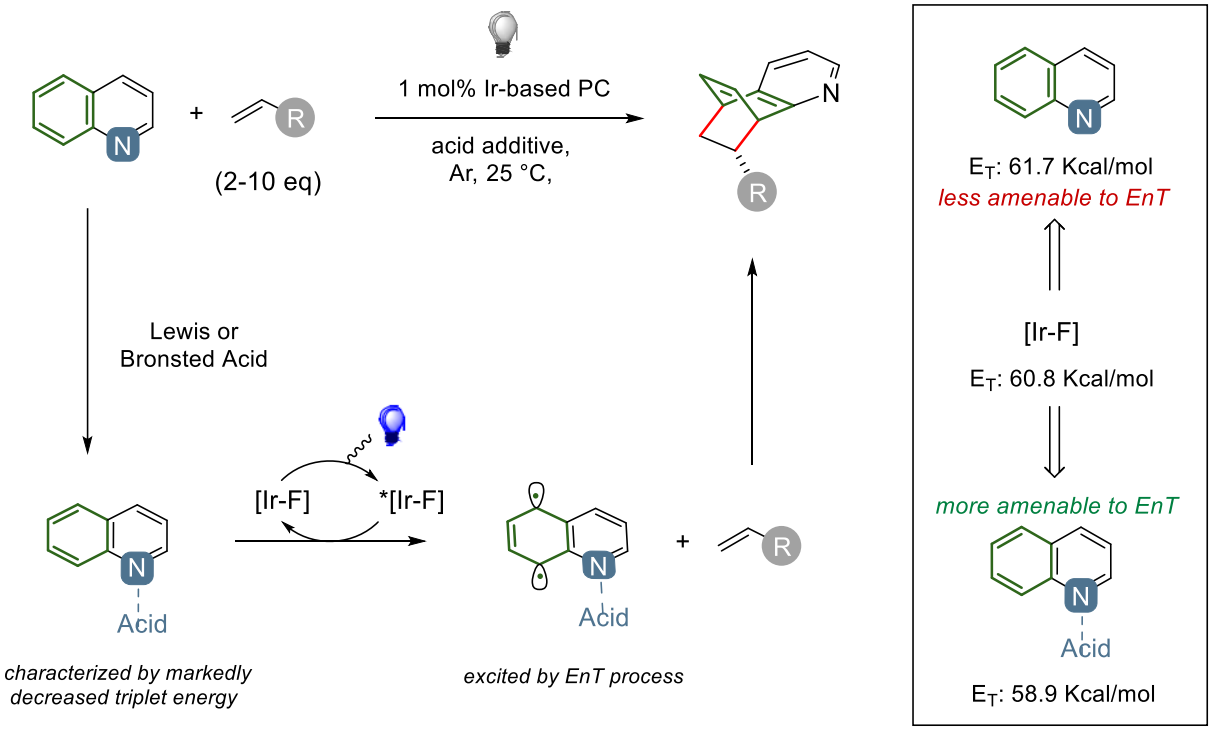

Scheme 4: Intermolecular dearomative para-cycloaddition on naphthalene derivatives through quinolonium cation sensitization.

The great difference in the strategy reported is relative to the addition of a Lewis or Bronsted acid, which can form an in-situ intermediate that can lower the E_T of the quinoline. The Iridium photocatalyst used (Ir[*d*F(CF_3)ppy]$_2$[dtbbpy]){PF_6}) is unable to activate the quinoline itself due to the high E_T, so the formation of the salt is mandatory to lower the E_T and to trigger the formation of a biradical that can react with the alkene and consequently deliver the structure reported in Scheme 4.

Here, not only is the reaction very selective due to the functionalization of the carbocyclic ring of the heterocycle, but it is important to note the high para-selectivity achieved. However, although a broad substrate scope has been reported, these methodologies remain inherently restricted to systems containing a sensitizable moiety, since the transformation proceeds through activation of the arene rather than the arenophile. This strategy has been far more extensively explored in the current literature compared to the opposite approach.

In 2023, Brown and coworkers overcame the limitation of a poor endo/exo dr encountered in their last work by building a new and more efficient intermolecular para-cycloaddition on a diverse naphthalene derivative (Scheme 5).[10]

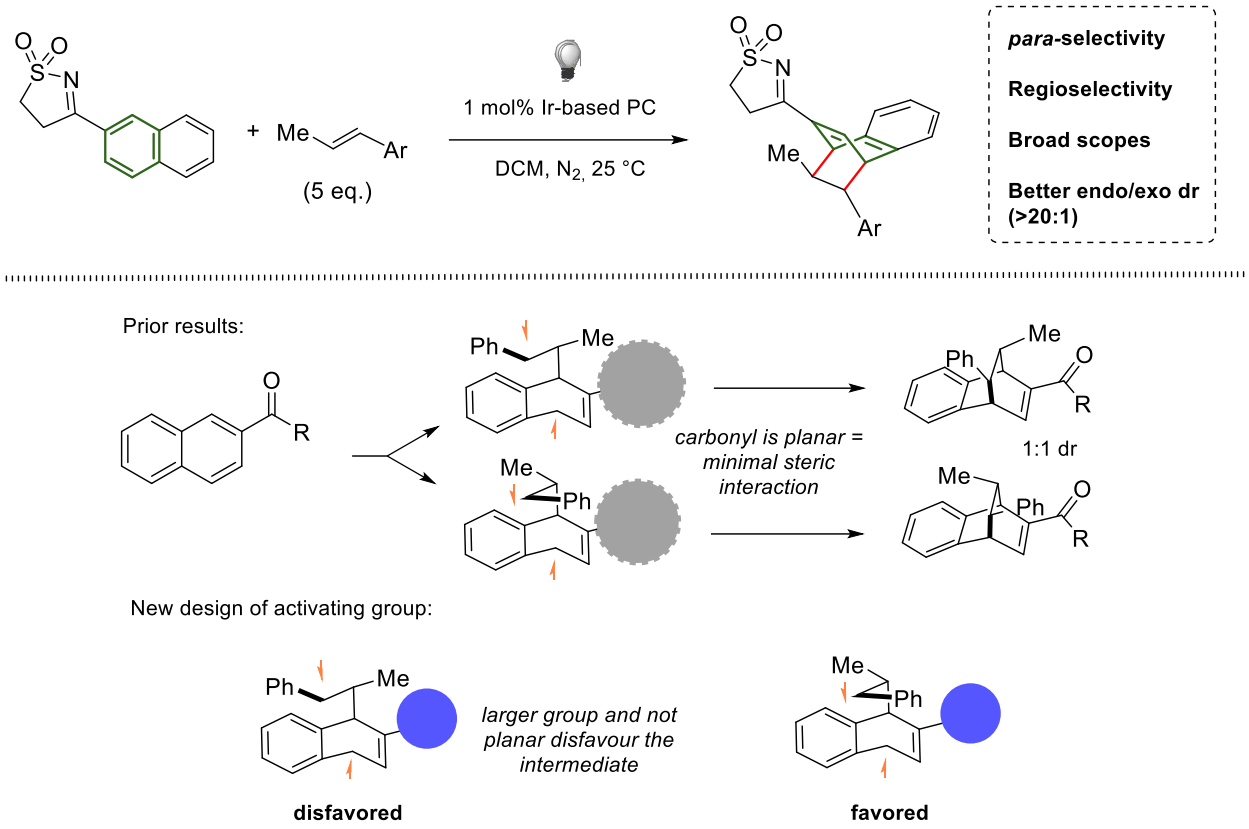

Scheme 5: Intermolecular dearomative para-cycloaddition on naphthalene derivatives with increased endo selectivity.

Here, the authors opted to use a sulfonylimine as an auxochrome group, justifying this choice by suggesting that the steric hindrance of this newly introduced substituent prevents one of the possible attacks to the alkene resulting then in a highly diasteroselective reaction with reported endo/exo dr of 20:1. Unfortunately, this strategy was limited by the use of disubstituted styrenes, otherwise the most favored reaction involved would have been the [2+2] cycloaddition between the sulfonylimine and the alkene (aza Paternò-Buchi reaction).

In 2016, Sarlah and co-workers presented a brilliant dearomative dihydroxylation with arenophiles (Scheme 6).[11]

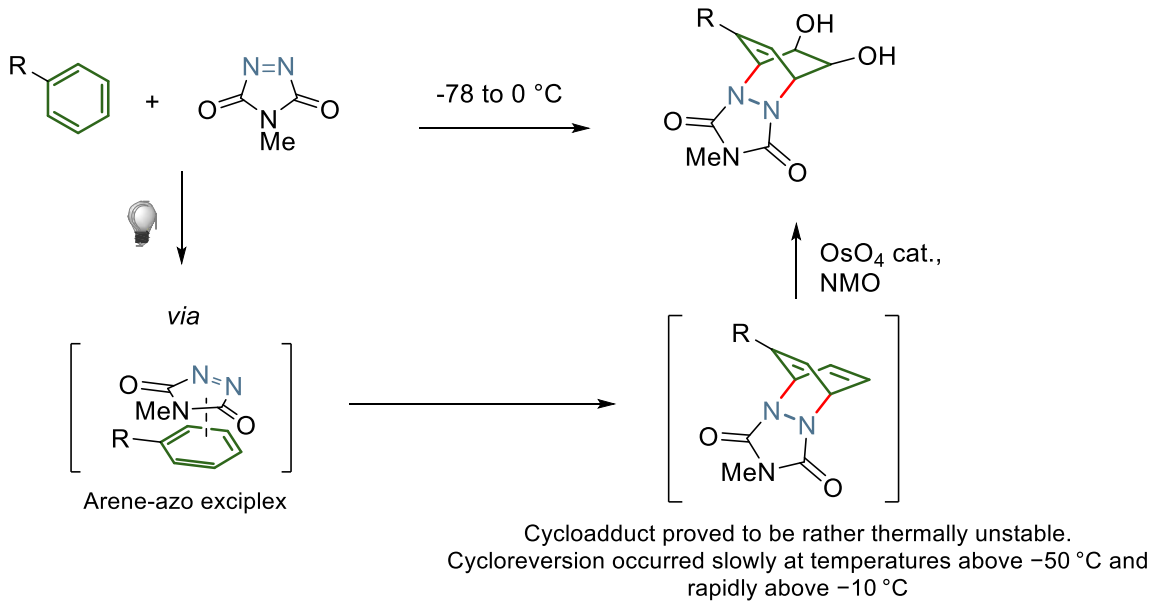

Scheme 6: Sarlah intermolecular dearomative dihydroxylation with arenophiles.

Upon irradiation with visible light, the authors discovered the formation of an exciplex between a generic arene and the excited 4-methyl-1,2,4-triazoline-3,5-dione. This intermediate brings to the desired cycloaddition product with optimal yields despite the complexity of the transformation. However, the challenging operational conditions required for this transformation should be noted. The reaction is conducted at −78 °C to prevent cycloreversion events that may occur already at −50 °C. This transformation also requires the use of OsO_4, a catalyst necessary for the dihydroxylation step, which affords a more stable and isolable product.

To conclude, one of the last works worth noting is the one from Matsunaga and co-workers disclosed in 2023, taking inspiration from the latest reported work from Sarlah. Here they decided instead to test the dearomatization on substituted naphthalenes and benzenes (Scheme 7).[12]

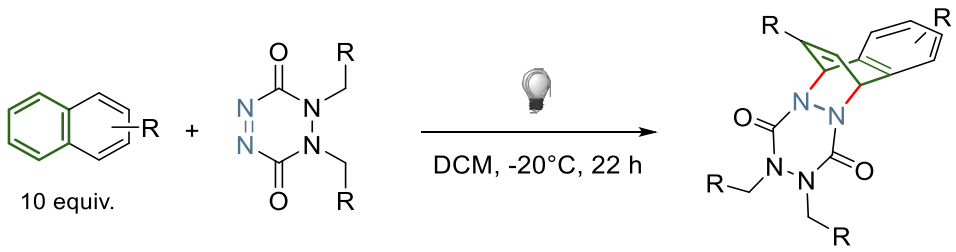

Scheme 7: Dearomatization with substituted naphthalenes and benzenes.

With respect to Sarlah's work, the authors in this case propose that the product of the transformation presents some variations. For example, it has been demonstrated that a much more stable cycloadduct forms and that it is also possible to crystallize it. Moreover, the fact that this transformation does not require osmium-based

reagents and can be carried out at higher temperatures makes it particularly interesting and distinguishes it from previous studies, giving it a character of novelty.

Nevertheless, despite the more extensive investigation into naphthalene dearomatization and the few reported examples in the literature, significant limitations remain, particularly in achieving efficient intermolecular dearomatization of simple naphthalene.

Results and discussions

In this chapter, a new kind of dearomative para-cycloaddition of allenamides on naphthalene in an intermolecular fashion is presented (Scheme 1).

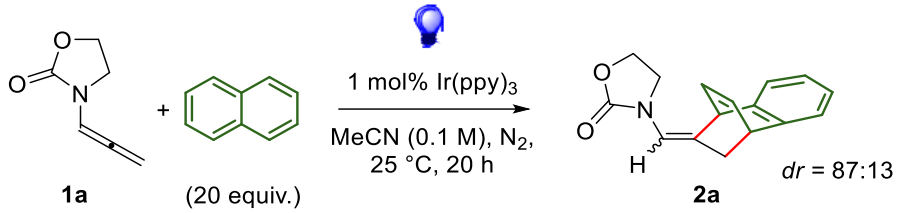

Scheme 1: General reaction of the newly discovered intermolecular dearomatization of simple naphthalenes.

The product observed has a [2.2.2]-bicyclooctene core that has a higher Fsp^3 character than the one observed in the starting material. These structures are particularly interesting for the alicyclic scaffold of the product, difficult to achieve through any other synthetic procedure. As reported in the paragraph before, most of the examples must tailor the naphthalene moiety with different auxochrome substituents, lowering the E_T and thus enabling reactivity. On the other hand, the novelty of this method lies in the functionalization of simple naphthalene using various allenamide partners with different substituents.

Therefore, once the optimal conditions were established, a series of modifications to the reaction were explored, as reported in Table 1.

Entry	Deviation from optimal	**2a** conversion [%][b]	**2a** yield [%][b]
1	-	>99	87
2	in DMF	>99	79
3	in Acetone	>99	78
4	in DCM	>99	58
5	in Toluene	>99	79
6	with $Ir(p\text{-}F\text{-}ppy)_3$	>99	75
7	with $Ir(p\text{-}CF_3\text{-}ppy)_3$	>99	78
8	using 10 equiv, of Naphthalene	93	69
9	using 5 equiv. of Naphthalene	80	60
10	using 2 equiv. of Naphthalene	65	47

11	w/o sensitizer	0	0
12	w/o light	0	0

Table 1: [a] Reaction conditions: 0.15 mmol of **1a** (0.1 M in MeCN), 3 mmol of Naphthalene (20 equiv.), 1 mol % of sensitizer, reaction irradiated for a total of 20 hours with blue LEDS at 25°C; [b] ^{1}H-NMR yield calculated using 1,3,5-trimethoxybenzene as internal standard.

Here are reported just some of the most important examples regarding this transformation. The best outcome was achieved mixing **1a** (0.15 mmol, 0.1 M in acetonitrile) with 20 equiv. of naphthalene in the presence of 1 mol% of the sensitizer, which in our case was $Ir(ppy)_3$. The solution was transferred to a standard 5-mm NMR tube to optimize the surface/volume ratio, then degassed via freeze-pump-thaw, kept at a temperature of 25 °C, and irradiated with blue LEDs for around 20 hours. Full conversion of the substrate was achieved checking with thin layer chromatography, and the desired product was obtained with 87% yield, as determined by ^{1}H-NMR (entry 1). Slightly lower results were obtained with other solvents, with their polarity having minimal impact on process efficiency, except for chlorinated solvents, which were less effective (entries 2–5). Various Ir-based photosensitizers have been used, but none outperformed $Ir(ppy)_3$ (entries 6–7). The molar excess of the arene was also examined. Reducing its amount resulted in a slight decrease in yield (entries 8–10). Finally, routine control experiments highlighted the crucial roles of both the sensitizer and light in the model reaction (entries 11–12).

The product was always obtained as a mixture of two diastereomers easily separable via silica gel chromatography, with the major one presenting the double bond in the E configuration. Here it is important to underline that the main advantage of this dearomatization is the use of very mild operating conditions,

At this point, with the best conditions in hand, we evaluated the generality of the method (Scheme 2).

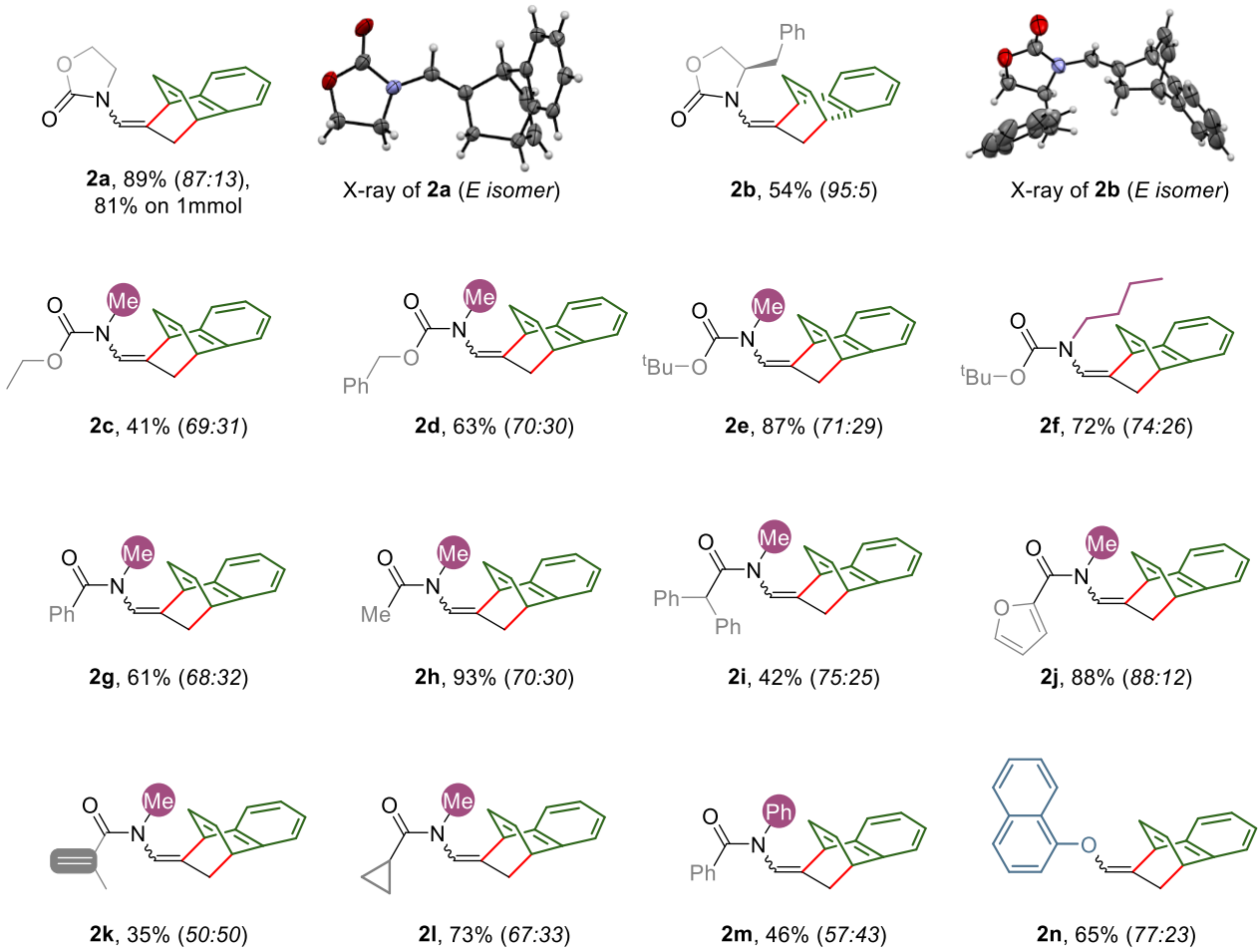

Scheme 2: Scope of dearomatization of simple allenamides.

The model reaction can be scaled up to 1 mmol without a significant efficiency loss. In the model substrate, the cyclic carbamate unit can be decorated by additional groups, as witnessed by product **2b** that was derived from L-phenylalanine. The product was isolated in a lower yield compared to the model but with higher diastereoselectivity, indicating that the chiral information of the substrate can be efficiently transferred to the stereocenters generated by the naphthalene dearomatization. Then we decided to test various linear carbamates, and all of them turned out to be good candidates to be converted into the corresponding products (**2c-f**), with the best result arising from the Boc-protected derivatives. Moreover, the reaction was shown not to be limited to carbamates, as amides were found to be productive as well (**2g-m**).

Between these last experiments, the worst results were achieved employing substrates that present relatively acidic protons (**2i**) and in the presence of an additional terminal C–C double bond, as observed with product **2k**. On the contrary, excellent yields were observed using an acyl- and a furoyl-protected allenamide (**2h** and **2j**, respectively). Finally, we moved from allenamides and employed allenyl ether **1n** to afford dearomatized product **2n**. This last product is very interesting because there are few reports in the literature regarding the sensitization of allenols. This result can open the way for further studies on this chemistry.

The limitations of this reactivity are the activation of sulfonyl allenamides and allenoates. These substrates were expected to broaden the scope of the products, but when subjected to the reaction conditions, they proved to be completely unreactive. Limitations also emerged with the arene partner. The method seems to be unsuitable for the dearomatization of monocyclic heteroarenes and bicyclic heteroarenes such as benzofurans and indoles. On the other hand, the attempted dearomatization of (iso)quinolines led to a complex mixture in which both the carbo- and the hetero-cyclic ring were unselectively difunctionalized by the allenamide partner.

We then decided to prepare a 1,6-enallene (**3a**), wondering whether it would have been possible to selectively trigger an additional cyclization within the same sequence (Scheme 3).

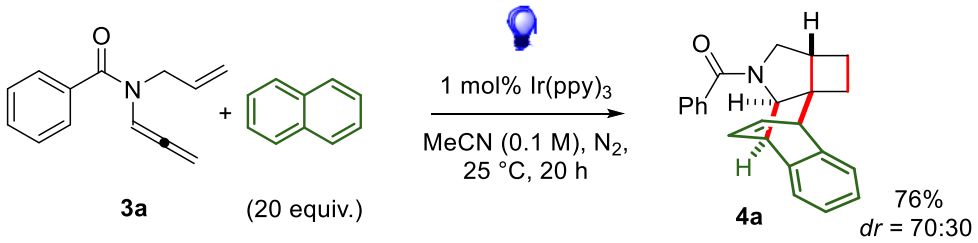

Scheme 3: Dearomative para cycloaddition of enallenes.

As expected, this reaction proceeded smoothly under the optimized reaction conditions reported in Table 1 in only 8 hours, with complete conversion and an isolated yield of 76% in product **4a**, that, after MS, ^{1}H-NMR analysis and XRD resolution analysis showed the new structure corresponding to a congested, fused/bridged tetracycle, which results from the formation of 4 new C-C bonds in one step. Furthermore, this product is obtained as a mixture of only two diastereomers out of the 16 possible ones. The cascade also led to the direct conversion of the central sp-hybridized carbon of the allene into a synthetically challenging doubly spiro carbon, which is shared among three different rings.

Intrigued by this original sequence, we decided to widen the scope by maintaining the 1,6 enallene core and examining different substitutions of the alkenyl side chain (Scheme 4).

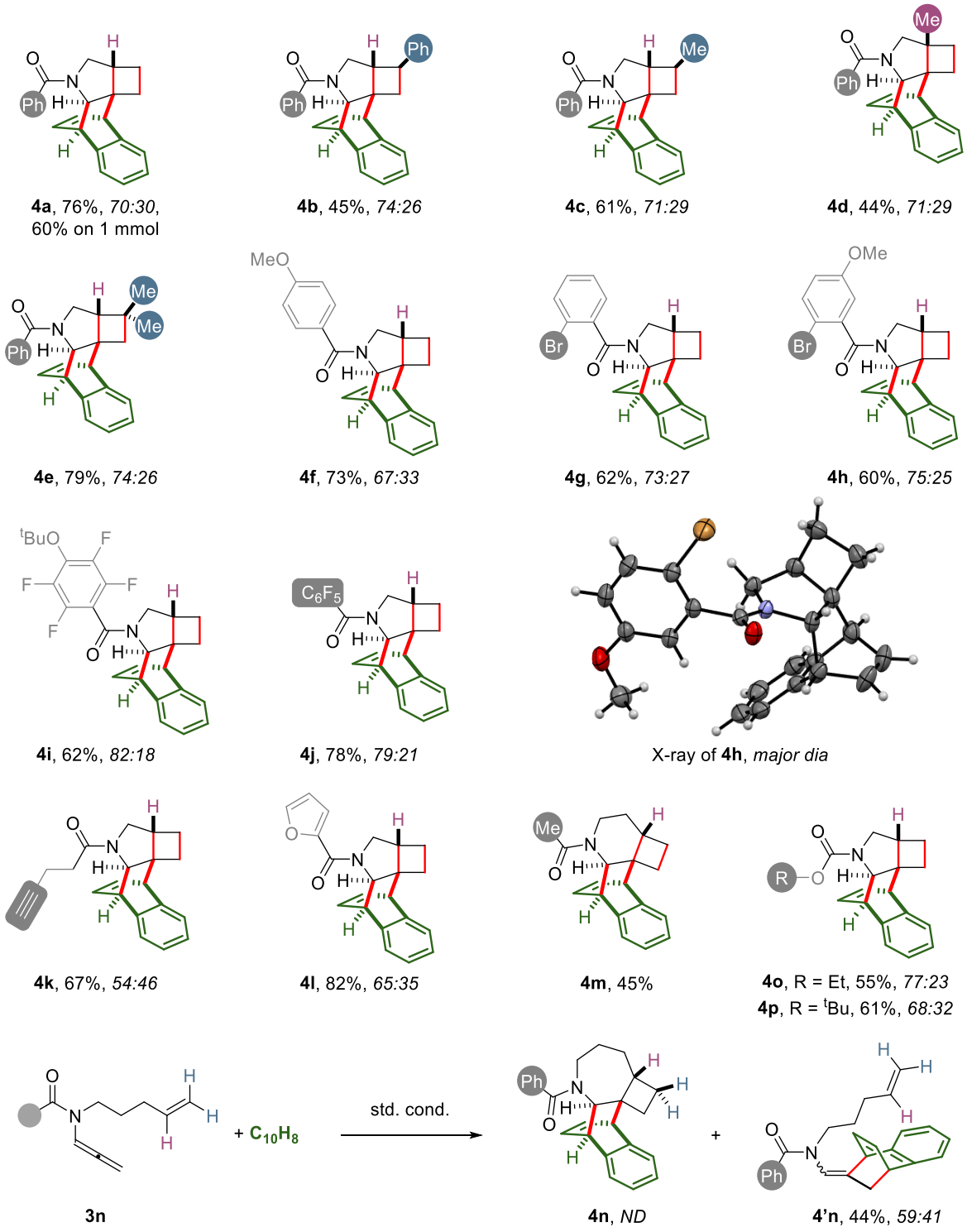

Scheme 4: Scope of dearomatization of 1,6 enallenes.

Gratifyingly, various substituted olefins were well tolerated, affording the corresponding products in moderate to good yields (**4b-e**, 44–79%, Scheme 4). The substitution of the acyl group was then tested. Various aryl rings, regardless of their stereo-electronic properties, were well tolerated by the method as identified by examples **4f-l**, with yields ranging from 60 to 82%. This method also allows the positioning of a piperidine central ring in a synthetically useful yield (**4m**). Then, inspired by the possibility of accommodating a ring larger

than a 5-member one, we examined a further elongation of the tether between the insaturation and the allene moiety. Unfortunately, in this case, the desired product could not be achieved, probably due to the relatively slower rate of the radical 7-exo-trig annulation. On the other hand, we observed the product of intermolecular dearomatization with a moderate yield. Finally, we tested if the amido group of the substrate could be replaced by a carbamate one, with excellent results in isolating the products **4o-p**.

Regarding the limitations, no traces of polycycle were observed when we tested sulfonylallenamides as starting materials. These reactions led to the formation of complex, inseparable mixtures and this could be due to a competitive sulfonyl β-scission upon the initial sensitization, which could hinder the desired process.[13]

Clarifying the potential mechanism, when a general 1,6 enallene is involved, upon the initial sensitization of the cumulated double-bond, this undergoes a fast intramolecular 5-exo-trig cyclization with the alkene partner. This step would become more favorable with an intermediate like **I,** because in this case, it would give an attack on a tertiary carbon by the radical. On the contrary, the corresponding 6-endo-trig cyclization can become competitive in the presence of terminal disubstituted alkenes as radical acceptors. This hypothesis was supported by testing a related substrate bearing an α-styrene pendant (**4q**) as reported by Scheme 5. In fact, a complex mixture of products that contained just traces of the desired polycycle was observed, likely because the corresponding radical 6-endo-trig became too fast in this case.

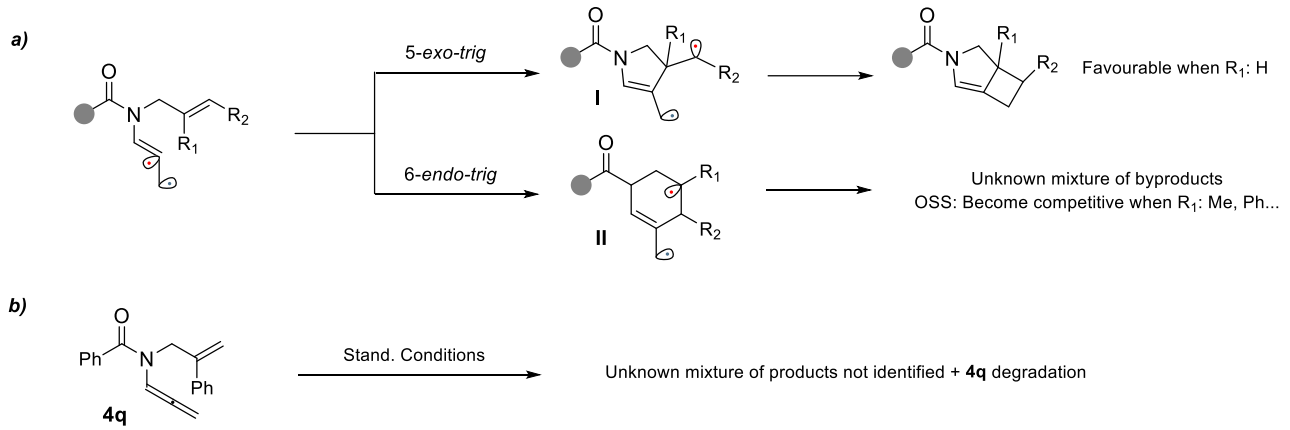

Scheme 5: a) Representation of the two possible reactive pathways of the starting material. b) Represented attempt on one substrate with R_1 bearing a phenyl substituent.

In order to get insights into the reaction mechanism, we initially carried out Stern-Volmer experiments on substrates **1g** and **3a**, demonstrating that they quench the luminescence of the photocatalyst, deriving the corresponding Stern–Volmer plots (Scheme 6).

.

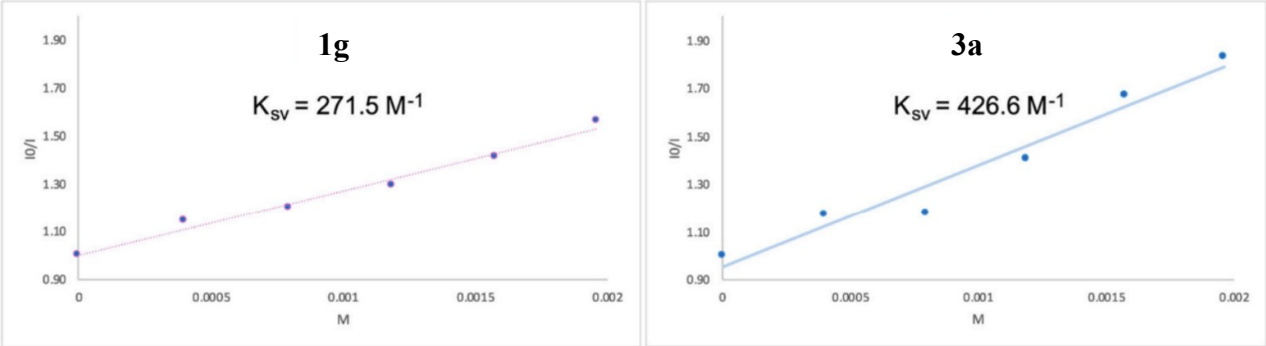

Scheme 6: Stern-Volmer analysis of the substrates **1g** and **3a**.

From the plots, the resulting quenching constants confirm that both substrates were activated by the Ir photocatalyst.

To further corroborate this hypothesis, additional support for the proposed mechanism was obtained by examining a model reaction involving **1a** and 1-methoxynaphthalene. Although the reaction could generate several regioisomeric dearomatized products, we hypothesized that functionalization of the more substituted aryl ring would be favored due to the enhanced stability of the resulting radical intermediate. The reaction produced an 85% combined yield of dearomatized products, with preparative TLC affording **2o** and **2o'** in a 20:80 ratio. This study holds significance as it provides further evidence that the cumulated system acts as the starting reactive site in the cascade process. (Scheme 7).

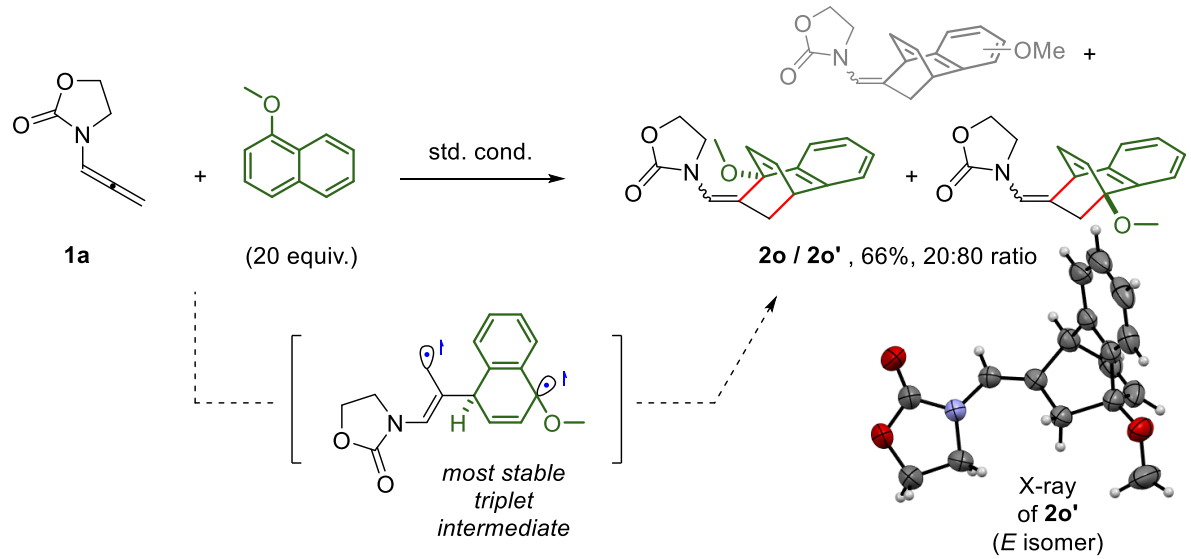

Scheme 7: Additional support for the proposed mechanism of dearomative cycloaddition of naphthalene with simple allenamides.

To conclude, as reported in Scheme 8, the entire process is thought to commence with the excitation of the Iridium catalyst, which subsequently forms a triplet biradical intermediate **I**. This biradical then undergoes radical addition to the naphthalene, giving rise to intermediate **II**. Although this step disrupts aromaticity, the destabilization is mitigated by resonance stabilization involving allylic or benzylic motifs. Following intersystem crossing (ISC), radical recombination takes place. Notably, the less hindered terminal carbon of the original allene is the preferred site for this recombination, leading to the formation of a [4+2] para cycloaddition product.

The cascade on 3a involves a slightly different mechanism. After triplet sensitization, intramolecular radical cyclization leads to a [3.2.0] bicyclic enamine **III.** Then this intermediate can undergo a second energy transfer, resulting in radical species **IV**. Subsequently, intermolecular dearomatization of the naphthalene partner occurs, giving rise to the final product.[14]

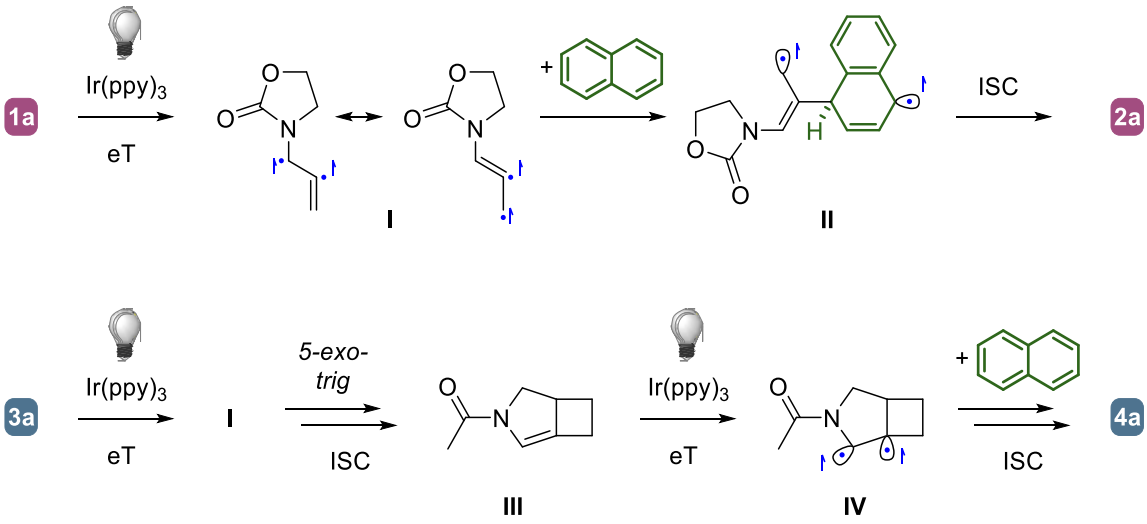

Scheme 8: Illustrated mechanistic hypothesis for the discussed cyclization.

Conclusions

In summary, a new method to dearomatize naphthalene in an intermolecular fashion, using allenamides as an arenophiles, has been developed. The reaction allows the synthesis of a [2.2.2]-bicyclooctene unit that has a potential biorelevant 3D alicyclic scaffold, starting from sp^2 -rich compounds. Moreover, with more complicated substrates such as enallenamides, we obtained a complex congested fused/bridged tetracycle with the formation of 4 new C-C bonds in one step. With this cascade, we established up to six contiguous stereocenters, significantly increasing the Fsp^3 of the product with respect to the starting materials used. The reactions are both performed in very mild conditions, with a cheap and simple setup. These demonstrated to tolerate several functional groups and have a complete atom economy. Simple allenamides are converted to the corresponding product in 24 hours with satisfactory yields, while enallenes gave product **4** with excellent selectivity.

References

[1] A. Palai, P. Rai, B. Maji, *Chem. Sci.,* **2023**, 14, 12004-12025.

[2] K. Kishikawa, S. Akimoto, S. Kohmoto, M. Yamamoto, K. Yamada, *J. Chem. Soc., Perkin Trans. 1*, **1997**, 77-84.

[3] B. D. Bryce-Smith, B. E. Foulger, A. Gilbert, *J. Chem. Soc., Chem. Commun.*, **1972**, 664-665.

[4] G. Himbert, L. Henn, *Angew. Chem. Int. Ed. Engl.*, **1982**, 21, 620-629.

[5] Y. Schmidt, J. K. Lam, H. V. Pham, K. N. Houk, C. D. Vanderwal, *J. Am. Chem. Soc.*, **2013**, 135, 7339-7348.

[6] M. Chiminelli, A. Serafino, D. Ruggeri, L. Marchiò, F. Bigi, R. Maggi, M. Malacria, G. Maestri, *Angew. Chem. Int. Ed.,* **2023**, 62, e202216817.

[7] P. Rai, K. Maji, S. K. Jana, B. Maji, *Chem. Sci.*, **2022**, 13, 12503-12510.

[8] W. Wang, Y. Cai, R. Guo, M. K. Brown, *Chem. Sci.*, **2022**, 13, 13582-13587.

[9] J. Ma, S. Chen, P. Bellotti, R. Guo, F. Schäfer, A. Heusler, X. Zhang, C. Daniliuc, M. Kevin Brown, K. N. Houk, F. Glorius, *Science*, **2021**, 371, 1338-1345.

[10] W. Wang, M. K. Brown, *Angew. Chem. Int. Ed.*, **2023**, 62, e202305622.

[11] E. H. Southgate, J. Pospech, J. Fu, D. R. Holycross, D. Sarlah, *Nat. Chem.,* **2016**, 8, 922-928.

[12] K. Ikeda, R. Kojima, K. Kawai, T. Murakami, T. Kikuchi, M. Kojima, T. Yoshino, S. Matsunaga, *J. Am. Chem. Soc.,* **2023**, 145, 16, 9326–9333.

[13] J. Kim, M. Kim, J. Jeong, S. Hong, *J. Am. Chem. Soc.,* **2023**, 145, 14510–14518.

[14] W. Yao, E. A. Bazan-Bergamino, N. Y. Ngai, *Chem. Cat. Chem.,* **2022**, 14, e202101292.

Experimental Section

General remarks

All chemicals for which it is not reported the syntheses hereafter were purchased from commercial sources and used as received. Solvents were dried by passing through alumina columns using an Inert® system and were stored under nitrogen. Present visible-light promoted reactions did not require the use of dry solvents but the presence of molecular oxygen exerts a negative effect on their rate. Chromatographic purifications were performed under gradient using a Combiflash® system and prepacked disposable silica cartridges or through isocratic flash chromatography using commercial 60 Å silica gel. All reactions that required heating were performed with the use of high-vacuum grade silicon oil. Reactions promoted by visible light were performed into standard 5 mm NMR tubes, surrounded by a commercial strip of 300 household leds (12V, 17W). These were put at a distance of ca 10 cm and emitted blue light (chip SMD5630-300 ip65). The tubes were inside an oil bath fitted with a thermometer to monitor the temperature. Cooling was ensured by two fans recovered by outdated PCs to avoid reproducibility issues. During summertime, solutions are kept at 25 °C through the addition of a transparent rubber spire inside the silicon oil bath. The spire is linked to a chiller that keeps pumping a cooled water/ethylene glycol solution to maintain the desired temperature. ^{1}H and ^{13}C NMR spectra were recorded at 300 K on a Bruker 400 MHz or a Jeol 600 MHz spectrometers using residual non-deuterated solvents as internal standards (7.26 ppm for ^{1}H NMR and 77.00 ppm for ^{13}C-NMR for $CDCl_3$, 2.05 ppm for ^{1}H NMR and 29.84 ppm for ^{13}C NMR for acetone-d6). ^{19}F-NMR spectra were recorded in $CDCl_3$ at 298 K on a Jeol 600 spectrometer fitted with a BBFO probehead at 564 MHz. The terms m, s, d, t, q and quint represent multiplet, singlet, doublet, triplet, quadruplet and quintuplet respectively, and the term brs means a broad signal. Reported assignments were based on decoupling, COSY, NOESY, HSQC and HMBC correlation experiments. Mass analyses were recorded on an Infusion Water Acquity Ultra Performance LC HO6UPS-823M instrument equipped with a SQ detector (Electrospray source); high-resolution mass analyses were recorded on a LTQ ORBITRAP XL Thermo Mass Spectrometer (Electrospray source). CCDC 2297940-2297943 contain the supplementary crystallographic data for compounds **2a**, **2b**, **4h** and **2o'**, respectively. These data can be obtained free of charge via www.ccdc.cam.ac.uk/data_request/cif. Single crystal Data were collected with a Bruker D8 diffractometer equipped with a PhotonII area detector, using a CuKα or a MoKα microfocus 4 radiation source. The data collection strategy covered the sphere of reciprocal space. Absorption corrections were applied using the program SADABS. The structure was solved with the SHELXT code. Fourier analysis and refinement were performed by the full-matrix least-squares methods based on F2 using SHELXL-2014 as implemented in Olex2. All the non-H atoms were refined with anisotropic displacement parameters.

Optimization experiments for simple allenes

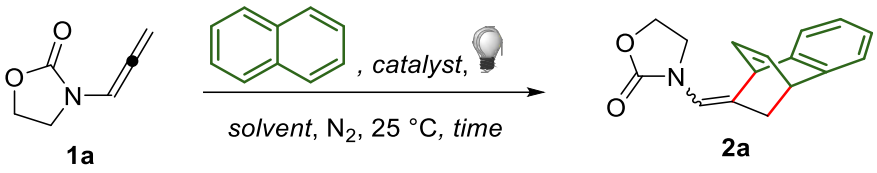

1a **2a**

A vial was charged with allene **1a** (12.5 mg, 0.1 mmol, 1.0 equiv.) and the desired iridium catalyst (1 mol%). The mixture was dissolved in the freshly distilled desired solvent. The solution was then transferred into an NMR tube capped with a rubber septum and directly irradiated. Once achieved full conversion of SM, monitored by TLC analysis, the solvent was removed, 1,3,5-Trimethoxybenzene (5.65 mg, 0.033 mmol) was added as internal standard and ^{1}H NMR of the crude measured.

Initial evaluation of the effect of different sensitizers in white light

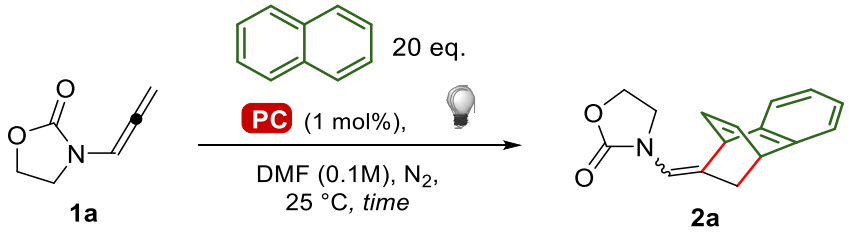

1a **2a**

Entry	Catalyst (1 mol%)	Time (h)	Conversion of **1a** [%][a]	Yield of **2a** [%][a]
1	$Ir(ppy)_3$	40	76	58
2	$Ru(bpy)_3Cl_2$	40	19	0
3	$(Ir[dF(CF3)ppy]_2(bpy))PF_6$	40	39	19
4	$(Ir[dF(CF3)ppy]_2(dtbbpy))PF_6$	40	63	43
5	$Ir(p\text{-}F\text{-}ppy)_3$	40	93	70
6	$[Ir(dtbbpy)(ppy)_2]PF_6$	40	25	0
7	$Ir(p\text{-}CF_3\text{-}ppy)_3$	40	86	65
8	$Ir(p\text{-}tBu\text{-}ppy)_3$	40	59	35
9	2,4,6-Triphenylpyrylium tetrafluoroborate[b]	40	>99	0
10	Thioxanthen-9-one[b]	40	21	0
11	Eosin Y[b]	40	20	0
12	$Ir(ppy)_3$[c]	40	>99	77

Table S1a. [a] by ^{1}H NMR using 1,3,5-Trimethoxybenzene as internal standard. [b] 10 mol%. [C] Tested in blue light for 40 hours. Best result was highlighted in pale orange.

Different Ir(III) photocatalysts were initially tested using white LEDs irradiation in function of their properties. All of them gave modest results in terms of yield but for a 40 hours time reaction we were never able to observe complete conversion of the starting material 1a. This led us to try photocatalyst of different nature such as the

$Ru(bpy)_3Cl_2$ reported in entry 2 or organic sensitizer reported in entries 9-11. Unfortunately, all these attempts turned out to be ineffective for the desired transformation. Little conversion of the starting material was observed but the dearomatization product was never observed either in traces. In the end, entry 12 turned out to be the most important experiment because changing the light of the LEDs brought us to complete conversion in 40 hours' time but most importantly a high yield. Because of this result we decided to investigate more deeply this class of photocatalyst in better reaction conditions.

Initial evaluation on the effect of different sensitizers in blue light

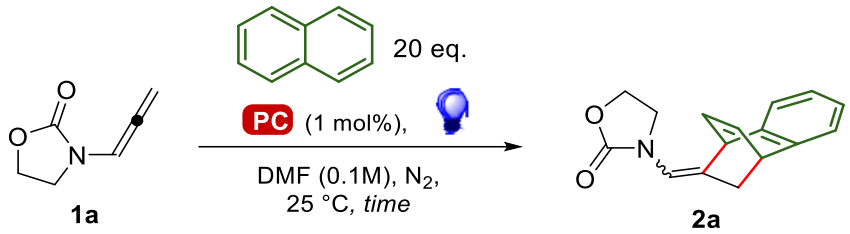

Entry	Catalyst (1 mol%)	Time (h)	Conversion of **1a** [%][a]	Yield of **2a** [%][a]
13	$Ir(ppy)_3$	20	>99	79
14	$Ir(p\text{-}F\text{-}ppy)_3$	20	>99	75
15	$Ir(p\text{-}CF_3\text{-}ppy)_3$	20	>99	78

Table S1b. [a] by ^1H NMR using 1,3,5-Trimethoxybenzene as internal standard. Best result was highlighted in pale orange.

Three different Ir(III) photocatalysts were initially tested using blue LEDs irradiation. In this case, the different photocatalysts tried in these conditions show a slight differentiation. As a matter of fact, we decided to keep $Ir(ppy)_3$ as the photocatalyst of the reaction which was the cheapest one and the one that reported the best results. Probably the nature of the sensitizer for this reactivity has a tiny effect on the reaction outcome.

Initial evaluation of the effect of the solvent

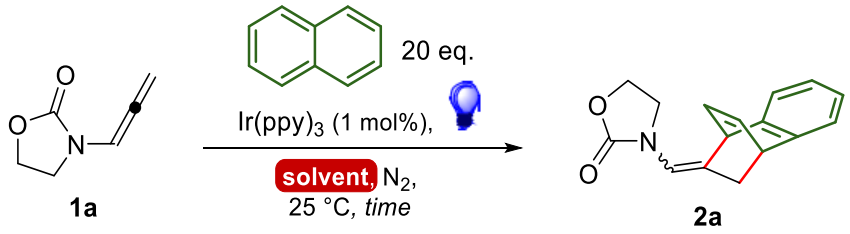

Entry	Solvent (0.1 M)	Time (h)	Conversion of **1a** [%][a]	Yield of **2a** [%][a]
13	DMF	20	>99	79
16	DCM	20	>99	58
17	MeOH	20	NP is insoluble	
18	Acetone	20	>99	78

19	MeCN	20	>99	87
20	Toluene	20	>99	79
21[d]	Toluene	20	0	0
22	THF	20	>99	70
23	MeCN-Tol 1:1	20	>99	81

Table S1c. [a] by ^{1}H NMR using 1,3,5-Trimethoxybenzene as internal standard. [d] Absence of the additive. Best result was highlighted in pale orange.

Several different solvents characterized by different nature in terms of polarity and dieletric constant were tested and presented in **Table S1c**. Overall, the polarity of the medium and the rate of conversion of **1a** and the yield of **2a**, show a discrete correlation. Entry 19 demonstrates that using an aprotic and polar solvent such as MeCN, the best results were identified with a yield of 87%. A mixture of solvents composed by MeCN and Toluene in 1:1 ratio was tested to enhance the effect of both solvents, but unfortunately, this time we couldn't further increase the yield. Entry 21 then demonstrates that the presence of the additive is obviously fundamental to the reaction end. Particularly interesting is the case of THF where we observed a faster conversion in respect to the other entries reported, but coupled with a lower yield. Because of that, we decided to keep toluene as the solvent for the rest of the optimization effort, because in this initial part, we were more interested in reaching higher yields rather than lower reaction rate time.

Evaluation of the effect of different additive concentrations

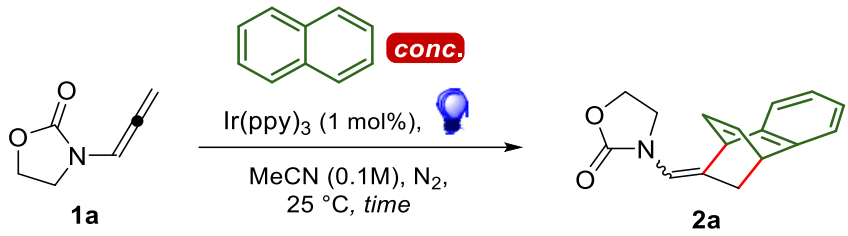

	Additive equiv.	Time (h)	Conversion of **1a**[a] [%]	Yield of **2a**[a] [%]
19	20	20	>99	87
24	10	20	93	69
25	5	20	80	60
26	2	20	65	47

Table S1d. [a] by ^{1}H NMR using 1,3,5-Trimethoxybenzene as internal standard. Best result was highlighted in pale orange.

In this case, three different additive concentrations were tested. The reason behind that is the possibility to achieve a more attractive dearomatization without the necessity of using a high excess of the additive. However, it's already clear from the result reported by entries 24 that a decrease to 10 equivalents of naphthalene leads to incomplete conversion of the reaction in 20 hours' time and a decrease in the yield observed through ^{1}H NMR internal standard. When 5 equivalents were tried, worse results were obtained as

reported by entry 25 and 26. This behavior suggested us that a reduced concentration of the additive in the reaction media is not favorable and that is the reason why we kept 20 equivalents even if it's a major excess.

Blank experiments

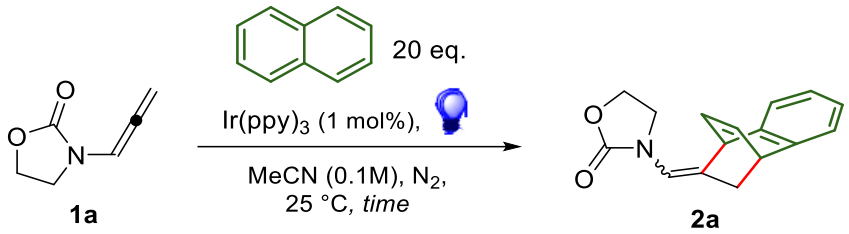

Entry	Variation	Time (h)	Conversion of **1a**[a] [%]	Yield of **2a**[a] [%]
27	No **PC**	20	--	--
28	No light	20	--	--

Table S1e. [a] by ^{1}H NMR using 1,3,5-Trimethoxybenzene as internal standard.

The reaction was finally tested without the photocatalyst and then without light. In both cases, no product formation was observed. This confirms that both components are essential for the reaction to proceed. The lack of reactivity is consistent with the proposed photocatalytic mechanism.

Optimization experiments enallenes

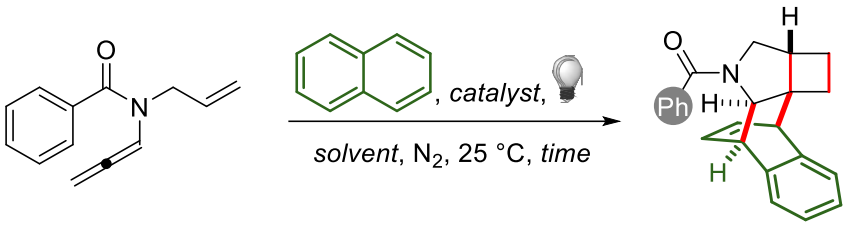

3a **4a**

A vial was charged with allene (19.9 mg, 0.1 mmol, 1.0 equiv.) and the desired iridium catalyst (1 mol%). The mixture was dissolved in the freshly distilled desired solvent. The solution was then transferred into an NMR tube capped with a rubber septum and directly irradiated. Once full conversion of SM was achieved, monitored by TLC analysis, the solvent was removed. 1,3,5-Trimethoxybenzene (5.65 mg, 0.033 mmol) was added as an internal standard, and ^{1}H NMR of the crude was measured.

Evaluation of the effect of different additive concentrations

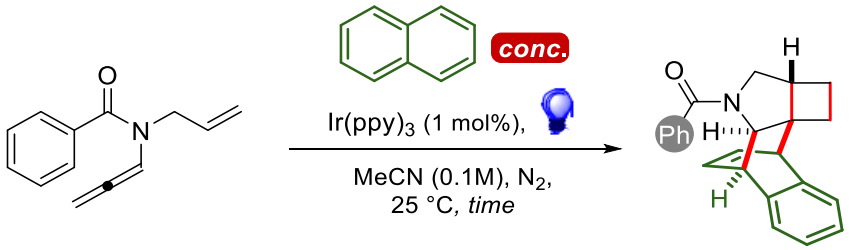

3a **4a**

	Additive equiv.	Time (h)	Conversion of **1a**[a] [%]	Yield of **2a**[a] [%]
29	20	18	>99	76
30	10	18	>99	63
31	5	18	>99	56
32	2	18	>99	35

Table S1f. [a] by ^{1}H NMR using 1,3,5-Trimethoxybenzene as internal standard. Best result was highlighted in pale orange.

We didn't perform another entire optimization for the enallenes substrate because we kept the datas observed for the classical intermolecular dearomatization of naphthalene observed with the cyclic carbamate **1a**. However, since the reaction is faster in respect to the first one, we decided to test once again different naphthalene concentrations always to test the possibility to use a smaller excess of the arene involved in the reaction. The entries reported in Table 1Sf demonstrate that in 18 hours' time independently from the excess of additive use we always get the complete conversion of the substrate. Nonetheless, we preferred to maintain the same reaction conditions as the first part for a more comfortable scope and because the yields obtained once again demonstrate that using a large excess brings better results.

Stern-Volmer quenching studies

The measurements of fluorescence emissions were carried out with a FLS1000 Edinburgh fluorometer, equipped with automatic polarizers. Emissions have been collected by exciting samples with a Xenon lamp at 375 nm and the luminescence was measured at 527 nm. Fluorescence spectra are corrected for the excitation intensity and detector sensitivity.

Stern – Vollmer quenching studies were carried out using a $5*10^{-5}$ M solution of $Ir(ppy)_3$ [PC1] in acetonitrile and variable concentrations of both **1g** and **3a** from 0 to 2 mM. 2.5 mL of PC1's solution was transferred in a 3.5 mL quartz cuvette and degassed twice for 5 minutes (with a 30 second break in between) before collecting the first spectra. Then, after each addition of quenching, the samples were degassed for 3 minutes and spectra were quickly recorded. *Note: $Ir(ppy)_3$ emission is highly sensitive to the presence of oxygen, more than other common photocatalysts.*

A linear Stern – Vollmer plot was obtained at varying concentrations of both **1g** and **3a**, and K_{SV} constants were extracted according to the equation $I_0/I = 1 + K_{SV}[Q]$. There are slight differences between the values of the two constants, that are consistent with previous data collected in our group with similar allenamides[1]. However, these values are not sufficient to explain such a large difference in reaction rate, which is more reasonably imputable to the fast intramolecular step involved in the cyclization of enallenes **3**.

Comprehensive table of Stern – Volmer constants

QUENCHER	**K_{SV}**	**R^2**
1g	271,5 M^{-1}	0.98
3a	426.6 M^{-1}	0.95

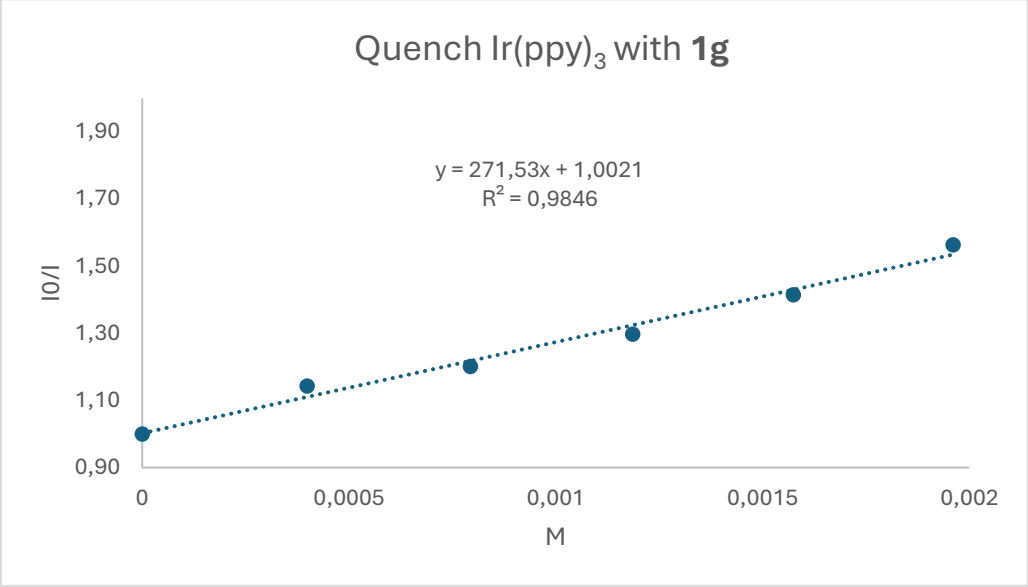

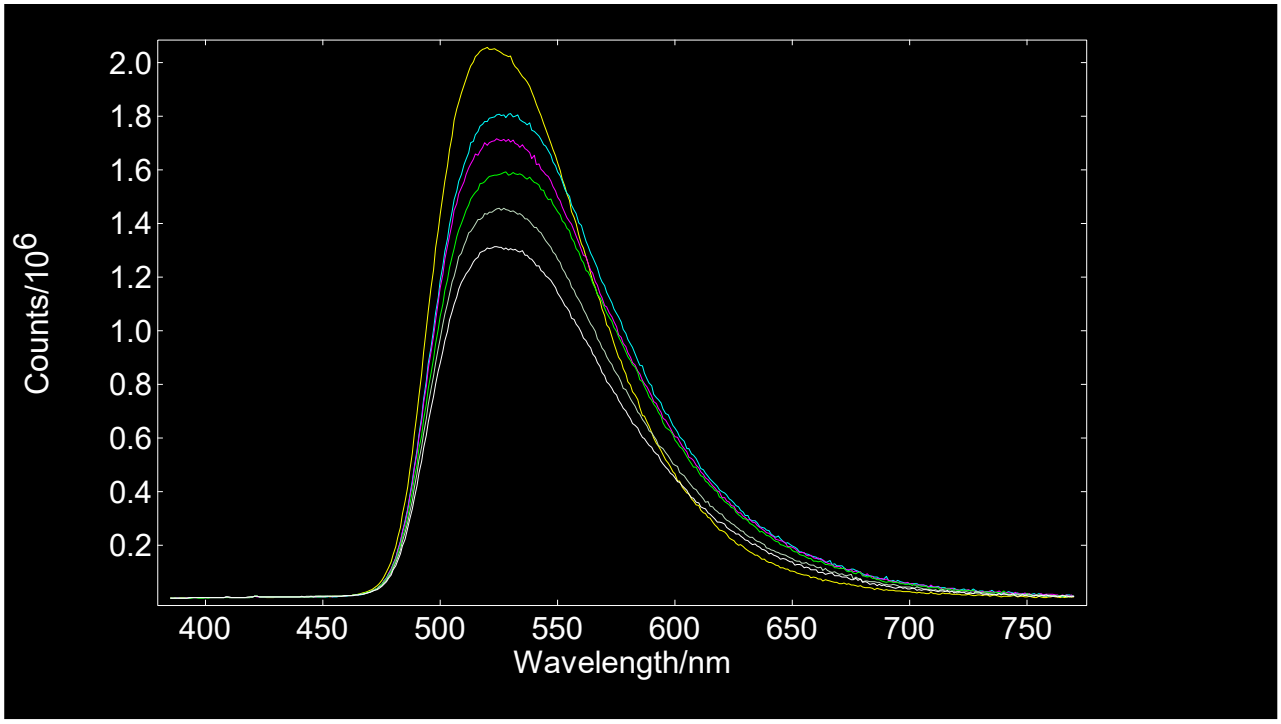

Figure 1: Measured emissions for quench of $Ir(ppy)_3$ with **1g**.

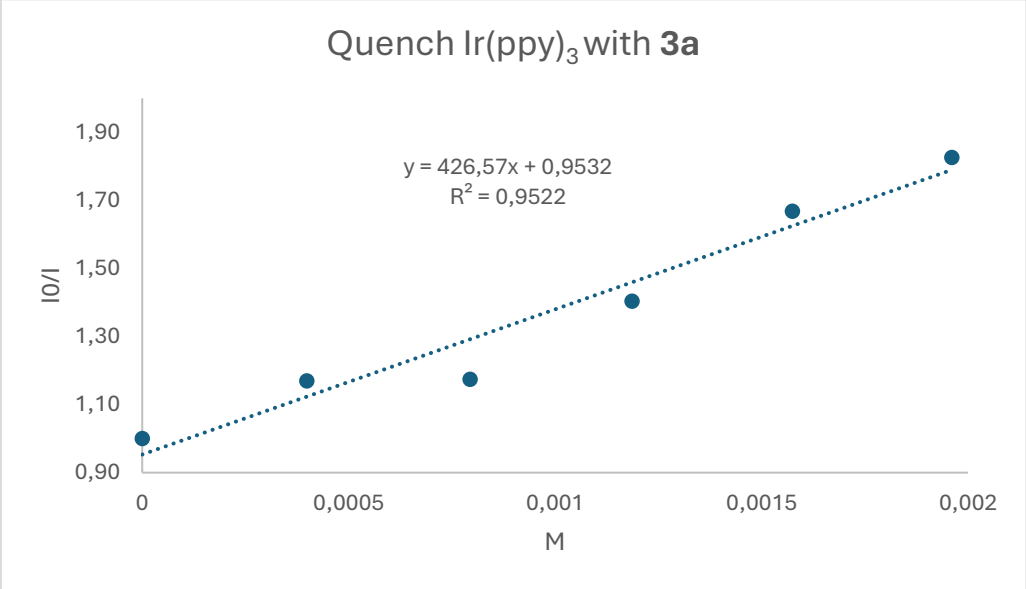

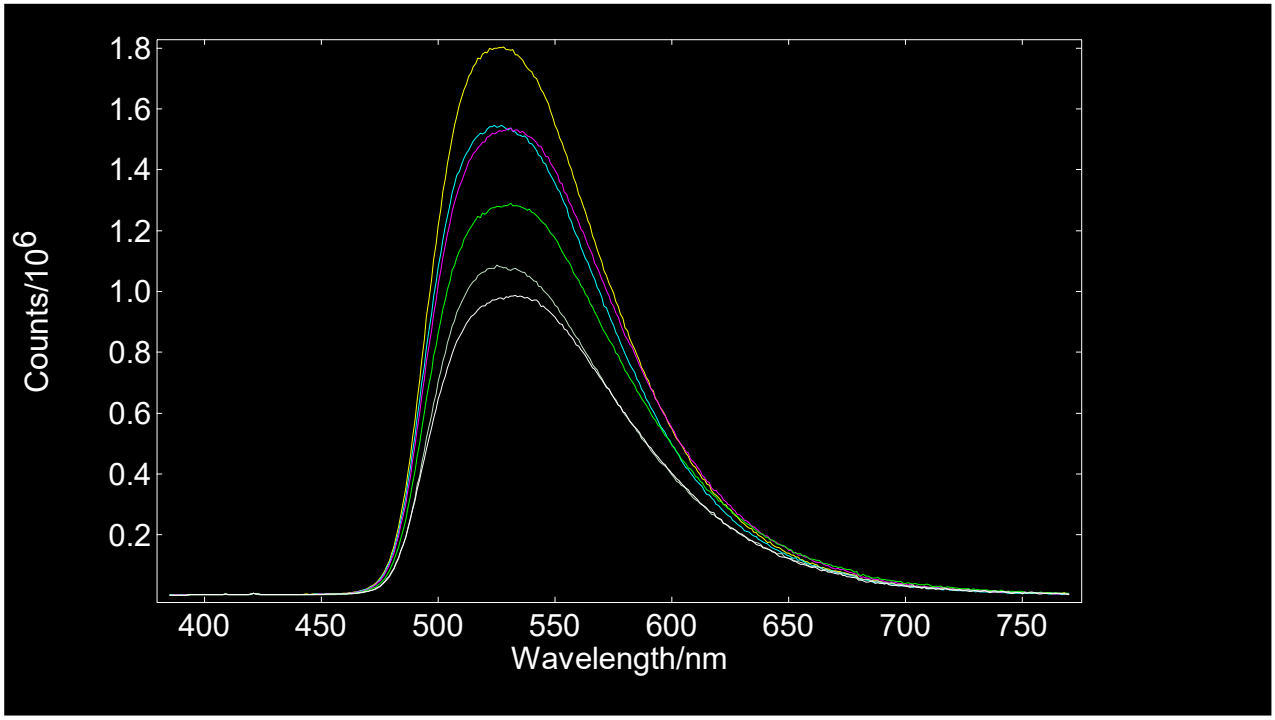

Figure 2: Measured emissions for quench of $Ir(ppy)_3$ with **3a.**

Unsuccessful Substrates

The following substrates did not afford the desired products. Moreover, the aromatic compounds in the bottom could not dearomatize with model allene **1a**.

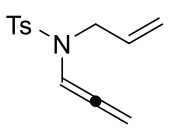

DEC

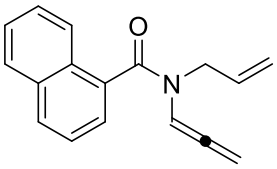

DEC + SR

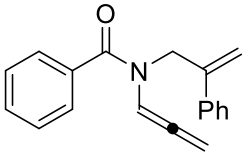

DEC + SR

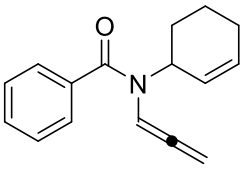

SR

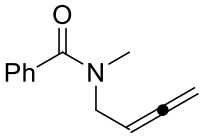

RSM

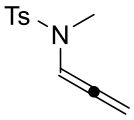

RSM

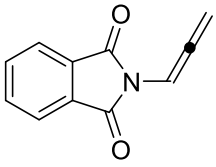

RSM

RSM: recovery of starting material
DEC: decomposition
SR: side reaction, intramolecular cyclization

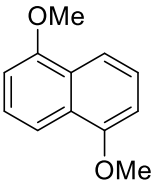

INSOLUBLE

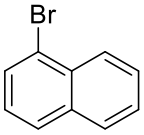

DEC

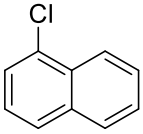

RSM + DEC

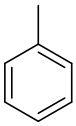

RSM

RSM

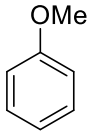

RSM

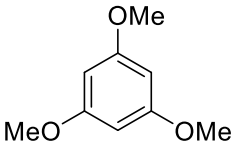

RSM

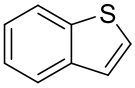

RSM

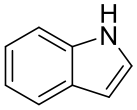

RSM

Synthesis of substrates

Synthesis of secondary amines

Synthesis of N-(prop-2-yn-1-yl)butan-1-amine

In a round bottom flask equipped with a magnetic stirring bar, propargyl bromide (1 equiv.) was added at 0 °C to *n*-butylamine (6 equiv.) and the resulting solution was stirred for 18 h at room temperature. After complete conversion as monitored by TLC, the mixture was quenched with a saturated $NaHCO_3$ solution and extracted with Et_2O (3 times). The combined organic phase was washed with brine, dried over Na_2SO_4 and concentrated under reduced pressure. The crude was finally purified by chromatography on silica gel (*n*-hexane/EtOAc gradient) to afford the desired product (Yield = 50%).

Synthesis of N-(prop-2-yn-1-yl)prop-2-en-1-amine

In a round bottom flask equipped with a magnetic stirring bar, propargyl bromide (1 equiv.) was added at 0 °C to allylamine (6 equiv.) and the resulting solution was stirred for 4 h at room temperature. When the solution turn to red, it was quenched with a saturated $NaHCO_3$ solution and extracted with Et_2O (3 times). The combined organic phase was washed with brine, dried over Na_2SO_4 and concentrated. The vacuum was kept at 500 psi and the bath was at 35 °C. The crude was used for the next step without purification, with a slight excess of amine.

Synthesis of N-(prop-2-yn-1-yl)but-3-en-1-amine

In a round bottom flask equipped with a magnetic stirring bar, omoallyl bromide (1 equiv.) was added at 0 °C to propargylamine (6 equiv.) and the resulting solution was stirred for 4 h at room temperature. When the solution turn to red, it was quenched with a saturated $NaHCO_3$ solution and extracted with Et_2O (3 times). The combined organic phase was washed with brine, dried over Na_2SO_4 and concentrated. The vacuum was kept at 500 psi and the bath was at 35 °C. The crude was used for the next step without purification, with a slight excess of amine.

N-Derivatization of primary amines

Representative procedure for the preparation of primary benzamides/carbamates

In a round bottom flask equipped with a magnetic stirring bar, primary amine (1 equiv.), DMAP (0.02 equiv.) and TEA (1 equiv.) were dissolved in DCM (0.25 M). The solution was cooled to 0 °C and chloride (1 equiv.) was then added. The mixture was stirred at room temperature until completion, monitoring the process by TLC. The solution was then quenched with saturated NH_4Cl solution and diluted with DCM. The organic phase was then washed with brine, dried over Na_2SO_4 and concentrated under reduced pressure. The crude was finally purified by chromatography on silica gel (*n*-hexane/EtOAc gradient) to afford the desired products.

OSS: BOC_2O was used for **1e**.

Synthesis of propargyl amides/carbamates

Representative procedure for the preparation of propargyl amides/carbamates *via* secondary amines

In a 25 mL round bottom flask equipped with a magnetic stirring bar, the desired acid was dissolved in DCM (0.6 M) and a catalytic amount of DMF (3 drops) was added. The solution was then cooled to 0 °C and oxalyl chloride (1.5 equiv) was added. The solution was stirred for 1 h at room temperature. Then, the mixture was concentrated under reduced pressure to afford the acyl chloride, that was added to a solution of DMAP (0.02 equiv.), TEA (1 equiv.) and the desired secondary amine (1 equiv.) in DCM (0.25 M) at 0 °C. The mixture was stirred for 18 h at room temperature. After complete conversion as monitored by TLC, the solution was diluted with DCM and washed with saturated NH_4Cl solution, followed by a saturated $NaHCO_3$ one. The aqueous layers were extracted with DCM (3 times), and the combined organic phase was finally washed with brine, dried over Na_2SO_4 and concentrated under reduced pressure. The crude was finally purified by chromatography on silica gel (*n*-hexane/EtOAc gradient) to afford the desired products.

Alkynyl amides precursors of **1f, 3g, 3i, 3m, 3o** were directly prepared from commercially available alkyl-, aryl-chlorides or chloroformate, BOC_2O was used for **3p**.

Representative procedure for the preparation of propargyl amides/carbamates *via* nucleophilic substitution (GP-1)

To a solution of primary amide/carbamate (1 equiv.) in DMF (0.6 M) at 0° C, NaH (60% in paraffine oil, 1.3 equiv.) was slowly added and the mixture was stirred for 1 h. The desired alkyl halide (1.5 equiv.) was then slowly added, and the reaction was stirred at room temperature for 18 h. After complete conversion as monitored by TLC, the mixture was quenched with a saturated NH_4Cl solution and extracted with EtOAc (3 times). The combined organic layers were washed with brine (3 times), dried over Na_2SO_4 and concentrated under reduced pressure. The crude was purified by chromatography on silica gel (*n*-hexane/EtOAc gradient) to afford the desired products.

Synthesis of 3-(prop-2-yn-1-yl)oxazolidin-2-one

To a solution of oxazolidin-2-one (1 equiv.) in DMF (0.6 M) at 0° C, NaH (60% in paraffine oil, 1.3 equiv.) was slowly added and the mixture was stirred for 1 h. Propargyl bromide (1.5 equiv.) was then slowly added, and the reaction was stirred at room temperature for 18 h. After complete conversion as monitored by TLC, the mixture was quenched with a saturated NH_4Cl solution and extracted with EtOAc (3 times). The combined organic layers were washed with brine (3 times), dried over Na_2SO_4 and concentrated under reduced pressure. The crude was purified by chromatography on silica gel (*n*-hexane/EtOAc gradient) to afford the desired product (Yield = 77%).

Representative procedure for the propargylation of amides *via* nucleophilic substitution

To a solution of primary amide (1 equiv.) in DMF (0.6 M) at 0° C, NaH (60% in paraffine oil, 1.3 equiv.) was slowly added and the mixture was stirred for 1 h. Propargyl bromide (1.5 equiv.) was then slowly added, and the reaction was stirred at room temperature for 18 h. After complete conversion as monitored by TLC, the mixture was quenched with a saturated NH_4Cl solution and extracted with EtOAc (3 times). The combined organic layers were washed with brine (3 times), dried over Na_2SO_4 and concentrated under reduced pressure. The crude was purified by chromatography on silica gel (*n*-hexane/EtOAc gradient) to afford the desired product.

Preparation of precursors of 1b, 1n

Synthetic route to afford (S)-4-benzyl-3-(propa-1,2-dien-1-yl)oxazolidin-2-one (precursor of 1b)

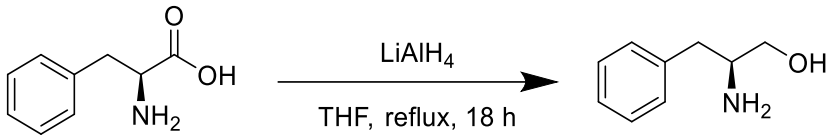

A Schlenk-type flask under nitrogen was charged with $LiAlH_4$ (2 equiv.) in THF (0.33 M). L-Phenylalanine (1 equiv.) was added at 0 °C to the mixture, that was stirred for 1 h at the same temperature. Then, the reaction was refluxed for 18 h. After complete conversion as monitored by TLC, the temperature was decreased to 0 °C and the reaction was quenched with NaOH (2M). After filtration on Celite®, the solution was diluted with EtOAc and washed twice with brine. The combined organic layers were dried over Na_2SO_4 and concentrated under reduced pressure. The crude was purified by chromatography on silica gel (DCM/MeOH gradient) to afford the desired aminoalcohol (Yield = 74%).

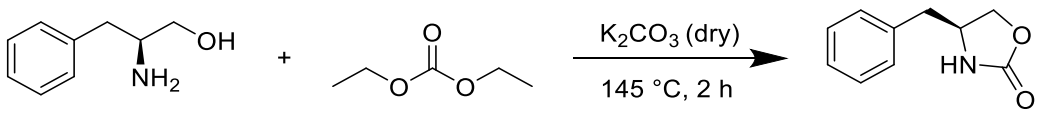

A distillation apparatus was charged with aminoalcohol (1 equiv.), diethyl carbonate (2 equiv.) and dry K_2CO_3 (0.9 equiv.). The mixture was heated to 145 °C and stirred. Meanwhile, coproduct ethanol was collected in another flask and was used to monitor the reaction. After 2 h, when ethanol stopped to collect, the mixture was cooled to room temperature and potassium carbonate was filtered off. The solution was then diluted with DCM and washed twice with brine. The combined organic layers were dried over Na_2SO_4 and concentrated under reduced pressure. The crude was purified by chromatography on silica gel (*n*-hexane/EtOAc gradient) to afford (S)-4-benzyloxazolidin-2-one (Yield = 90%).

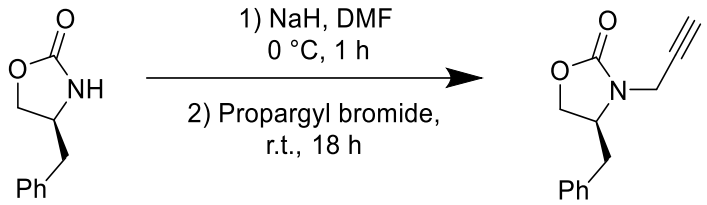

To a solution of (S)-4-benzyloxazolidin-2-one (1 equiv.) in DMF (0.6 M) at 0° C, NaH (60% in paraffine oil, 1.5 equiv.) was slowly added and the mixture was stirred for 1 h. Propargyl bromide (4 equiv.) was then slowly added, and the reaction was stirred at room temperature for 18 h. After complete conversion as monitored by TLC, the mixture was quenched with a saturated NH_4Cl solution and extracted with EtOAc (3 times). The combined organic layers were washed with brine (3 times), dried over Na_2SO_4 and concentrated under reduced pressure. The crude was purified by chromatography on silica gel (*n*-hexane/EtOAc gradient) to afford (S)-4-benzyl-3-(propa-1,2-dien-1-yl)oxazolidin-2-one (Yield = 78%).

Synthesis of 1-(prop-2-yn-1-yloxy)naphthalene (precursor of 1n)

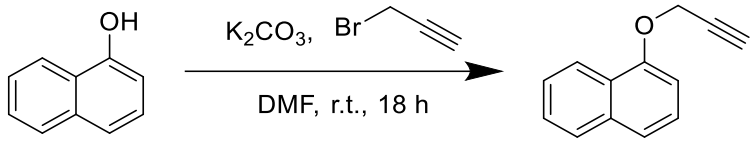

In a round bottom flask were added 1-naphthol (1.2 equiv.) and potassium carbonate (1.6 equiv.) in DMF (0.66 M). The mixture was stirred at room temperature for 1 h, then propargyl bromide (1 equiv.) was slowly added and the mixture was reacted for 18 h. After complete conversion as monitored by TLC, potassium carbonate was filtered off and the solution was quenched with a saturated NH_4Cl solution and extracted with EtOAc (3 times). The combined organic layers were washed with brine (3 times), dried over Na_2SO_4 and concentrated under reduced pressure. The crude was purified by chromatography on silica gel (*n*-hexane/EtOAc gradient) to afford the desired product (Yield = 95%)

General procedure for the synthesis of allenamides (GP-2):

The desired propargyl amide/carbamate (1 equiv.) and THF (0.20 M) were sequentially added to a Schlenk tube equipped with a magnetic stirring bar. ^{t}BuOK (0.2 equiv.) was added and the resulting mixture was stirred at room temperature for 10 minutes. After complete conversion as monitored by TLC, 5 ml of a saturated NH_4Cl solution were added. The mixture was extracted with EtOAc (3 x 15 ml), the organic layers separated and dried over Na_2SO_4. The solution was concentrated under reduced pressure and the crude purified by chromatography on silica gel (*n*-hexane/EtOAc gradient) to afford the corresponding allene.

Note: sometimes the isomerization is not quantitative with 0.2 equiv. of ^{t}BuOK. Other portions of base were added.

Characterization of substrates

3-(propa-1,2-dien-1-yl)oxazolidin-2-one

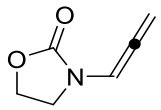

Allene **1a** was prepared following general procedure **GP-2** from the corresponding propargyl carbamate (179.0 mg, 1.43 mmol). White solid (108.4 mg, 61% yield). **^{1}H NMR** (400 MHz, $CDCl_3$) δ 6.86 (t, *J* = 6.4 Hz, 1H), 5.42 (d, *J* = 6.3 Hz, 2H), 4.45 – 4.37 (m, 2H), 3.63 – 3.56 (m, 2H). **^{13}C NMR** (101 MHz, $CDCl_3$) δ 201.4, 155.3, 97.0, 87.9, 62.3, 43.1. **ESI-MS** calcd for $C_6H_7NNaO_2$ $[M+Na]^+$, 148.04 found 148.16.

(S)-4-benzyl-3-(propa-1,2-dien-1-yl)oxazolidin-2-one

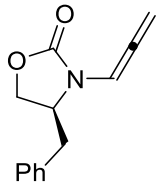

Allene **1b** was prepared following general procedure **GP-2** from the corresponding propargyl carbamate (215.2 mg, 1 mmol). Pale yellow oil (194.4 mg, 90% yield). **^{1}H NMR** (400 MHz, $CDCl_3$) δ 7.38 – 7.26 (m, 3H), 7.22 – 7.15 (m, 2H), 6.93 (t, *J* = 6.5 Hz, 1H), 5.63 – 5.49 (m, 2H), 4.29 – 4.23 (m, 1H), 4.20 – 4.09 (m, 2H), 3.28 (dd, *J* = 13.7, 3.2 Hz, 1H), 2.76 (dd, *J* = 13.7, 8.9 Hz, 1H). **^{13}C NMR** (101 MHz, $CDCl_3$) δ 201.7, 155.0, 135.4, 129.3, 128.9, 127.3, 96.0, 87.9, 66.7, 55.6, 37.2. **ESI-MS** calcd for $C_{13}H_{13}NNaO_2$ $[M+Na]^+$ 238.24, found 238.59.

Ethyl methyl(propa-1,2-dien-1-yl)carbamate

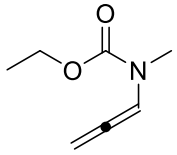

Allene **1c** was prepared following general procedure **GP-2** from the corresponding propargyl carbamate (114.4 mg, 0.81 mmol). *Note: it was necessary add 1% TEA to the eluent to prevent the degradation of the product during the separation.* Pale yellow oil (59.7 mg, 52% yield). Two rotamers are observed due to the dynamic rotation of the carbamate. **^{1}H NMR** (400 MHz, $CDCl_3$) δ 7.26 – 7.02 (m, 1H RotA, 1H RotB), 5.36 (s, 2H RotA, 2H RotB), 4.19 (q, *J* = 7.1 Hz, 2H RotA, 2H RotB), 3.00 – 2.88 (m, 3H RotA, 3H RotB), 1.28 (t, *J* = 7.1 Hz, 3H RotA, 3H RotB). **^{13}C NMR** (101 MHz, $CDCl_3$) δ 201.7, 200.7, 154.1, 101.6, 101.0, 87.3, 86.7, 62.12, 62.05, 31.8, 31.6, 14.6. **ESI-MS** calcd for $C_7H_{12}NO_2$ $[M+H]^+$ 142.18, found 142.35.

Benzyl methyl(propa-1,2-dien-1-yl)carbamate

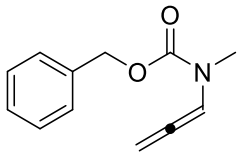

Allene **1d** was prepared following general procedure **GP-2** from the corresponding propargyl carbamate (168.2 mg, 0.83 mmol). Pale yellow oil (140.0 mg, 83% yield). Two rotamers are observed due to the dynamic rotation of the carbamate. **^{1}H NMR** (400 MHz, $CDCl_3$) δ 7.41 – 7.30 (m, 5H RotA, 5H RotB), 7.27 – 7.21 (m, 1H RotB), 7.12 (t, *J* = 6.4 Hz, 1H RotA), 5.42 – 5.34 (m, 2H RotA, 2H RotB), 5.20 (s, 2H RotA, 2H RotB), 3.01 – 2.94 (m, 3H RotA, 3H RotB). **^{13}C NMR** (101 MHz, $CDCl_3$) δ 201.7, 200.8, 154.0, 153.9, 136.3, 136.2, 128.6, 128.2, 128.1, 101.6, 101.0, 87.5, 86.9, 67.8, 67.7, 32.1, 31.8. **ESI-MS** calcd for $C_{12}H_{13}KNO_2$ $[M+K]^+$ 242.34, found 242.42.

Tert-butyl methyl(propa-1,2-dien-1-yl)carbamate

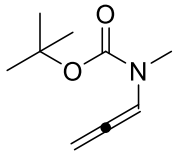

Allene **1e** was prepared following general procedure **GP-2** from the corresponding propargyl carbamate (165.0 mg, 0.98 mmol). *Note: it was necessary add 1% TEA to the eluent to prevent the degradation of the product during the separation.* Yellow oil (135.4 mg, 81% yield). Two rotamers are observed due to the dynamic rotation of the carbamate. **^{1}H NMR** (400 MHz, $CDCl_3$) δ 7.19 (s, 1H RotB), 7.02 (s, 1H RotA), 5.33 (s, 2H RotA, 2H RotB), 2.88 (s, 3H RotA, 3H RotB), 1.47 (s, 9H RotA, 9H RotB). **^{13}C NMR** (101 MHz, $CDCl_3$) δ 201.8, 200.7, 153.1, 153.0, 101.5, 101.4, 87.0, 86.4, 80.9, 80.8, 31.9, 31.3, 28.3. **ESI-MS** calcd for $C_9H_{16}NO_2$ $[M+H]^+$ 170.22, found 169.98.

Tert-butyl butyl(propa-1,2-dien-1-yl)carbamate

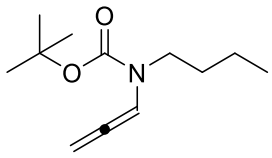

Allene **1f** was prepared following general procedure **GP-2** from the corresponding propargyl carbamate (190.3 mg, 0.9 mmol). Pale yellow oil (98.3 mg, 52% yield). Two rotamers are observed due to the dynamic rotation of the carbamate. **^{1}H NMR** (400 MHz, $CDCl_3$) δ 7.11 (s, 1H RotA), 6.95 (s, 1H RotB), 5.29 (d, *J* = 5.7 Hz, 2H RotA, 2H RotB), 3.37 – 3.24 (m, 2H RotA, 2H RotB), 1.53 – 1.39 (m, 11H RotA, 11H RotB), 1.27 (h, *J* = 7.4 Hz, 2H RotA, 2H RotB), 0.88 (t, *J* = 7.4 Hz, 3H RotA, 3H RotB). **^{13}C NMR** (101 MHz, $CDCl_3$) δ 201.7, 200.5,

153.0, 152.6, 100.4, 100.3, 86.6, 86.0, 80.7, 80.6, 44.7, 44.4, 30.0, 29.6, 28.3, 19.9, 19.8, 13.9. **ESI-MS** calcd for $C_{12}H_{22}NO_2$ $[M+H]^+$ 212.16, found 212.88.

N-methyl-N-(propa-1,2-dien-1-yl)benzamide

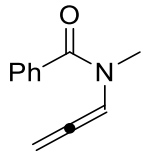

Allene **1g** was prepared following general procedure **GP-2** from the corresponding propargyl amide (173.7 mg, 1 mmol). Pale yellow oil (104.2 mg, 60% yield). Two rotamers are observed due to the dynamic rotation of the amide. **^{1}H NMR** (400 MHz, $CDCl_3$) δ 7.71 (brs, 1H RotB), 7.54 – 7.40 (m, 5H RotA, 5H RotB), 6.76 (brs, 1H RotA), 5.49 – 5.34 (m, 2H RotA, 2H RotB), 3.24 – 2.95 (m, 3H RotA, 3H RotB). **^{13}C NMR** (101 MHz, $CDCl_3$) δ 202.8, 200.0, 169.6, 164.4, 135.3, 134.9, 130.2, 128.5, 127.9, 127.4, 103.4, 100.0, 87.0, 35.8, 31.4. **ESI-MS** calcd for $C_{11}H_{12}NO$ $[M+H]^+$ 174.23, found 174.48. *(Partial decomposition was observed during the acquisition of NMR spectra).*

N-methyl-N-(propa-1,2-dien-1-yl)acetamide

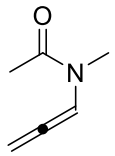

Allene **1h** was prepared following general procedure **GP-2** from the corresponding propargyl amide (182.3 mg, 1.64 mmol). Pale yellow oil (97.1 mg, 53% yield). Two rotamers are observed due to the dynamic rotation of the amide. **^{1}H NMR** (400 MHz, $CDCl_3$) δ 7.53 (t, *J* = 6.4 Hz, 1H RotB), 6.76 (t, *J* = 6.2 Hz, 1H RotA), 5.39 – 5.36 (m, 2H RotA, 2H RotB), 3.02 (s, 3H RotA), 2.96 (s, 3H RotB), 2.19 – 2.15 (m, 3H RotA, 3H RotB). **^{13}C NMR** (101 MHz, $CDCl_3$) δ 202.3, 200.9, 168.8, 168.5, 102.0, 99.5, 87.1, 86.7, 33.6, 30.7, 22.2, 21.5. **ESI-MS** calcd for $C_6H_{10}NO$ $[M+H]^+$ 112.15, found 112.39.

N-methyl-2,2-diphenyl-N-(propa-1,2-dien-1-yl)acetamide

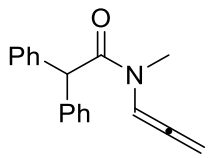

Allene **1i** was prepared following general procedure **GP-2** from the corresponding propargyl amide (269.3 mg, 1 mmol). White solid (152.9 mg, 57% yield). Two rotamers are observed due to the dynamic rotation of the amide. **^{1}H NMR** (400 MHz, $CDCl_3$) δ 7.68 (t, *J* = 6.4 Hz, 1H RotA), 7.37 – 7.26 (m, 10H RotA, 10H RotB), 6.90

(t, *J* = 6.2 Hz, 1H RotB), 5.41 – 5.31 (m, 3H RotA, 3H RotB), 3.07 (s, 3H RotA, 3H RotB). **^{13}C NMR** (101 MHz, $CDCl_3$) δ 202.5, 201.2, 170.1, 170.0, 139.0, 138.9, 129.0, 128.7, 127.2, 101.3, 100.2, 87.3, 86.6, 55.6, 55.1, 33.2, 31.8. **ESI-MS** calcd for $C_{18}H_{18}NO$ $[M+H]^+$ 264.14, found 264.21.

N-methyl-N-(propa-1,2-dien-1-yl)furan-2-carboxamide

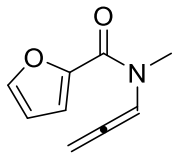

Allene **1j** was prepared following general procedure **GP-2** from the corresponding propargyl amide (163.1 mg, 1 mmol). Yellow pale oil (144.7 mg, 88% yield). **^{1}H NMR** (400 MHz, $CDCl_3$) δ 7.53 (d, *J* = 1.7 Hz, 1H), 7.47 – 7.45 (m, 1H), 7.06 (d, *J* = 3.5 Hz, 1H), 6.49 (dd, *J* = 3.5, 1.8 Hz, 1H), 5.42 (d, *J* = 6.3 Hz, 2H), 3.19 (s, 3H). **^{13}C NMR** (101 MHz, $CDCl_3$) δ 202.5, 201.1, 158.1, 147.2, 144.6, 117.5, 111.4, 102.2, 100.7, 87.2, 34.1, 32.1. **ESI-MS** calcd for $C_9H_{10}NO_2$ $[M+H]^+$ 164.07, found 164.17.

N-methyl-N-(propa-1,2-dien-1-yl)methacrylamide

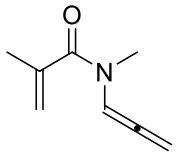

Enallene **1k** was prepared following general procedure **GP-2** from the corresponding enyne (159.1 mg, 1.16 mmol). Pale yellow liquid (75.2 mg, 47% yield). **^{1}H NMR** (400 MHz, $CDCl_3$) δ 7.55 (s, 1H RotB), 7.01 (s, 1H RotA), 5.39 (d, *J* = 6.3 Hz, 2H RotA, 2H RotB), 5.31 (d, *J* = 6.5 Hz, 1H RotA, 1H RotB), 5.15 (s, 1H RotA, 1H RotB), 3.03 (s, 3H RotA, 3H RotB), 1.98 (t, *J* = 1.4 Hz, 3H RotA, 3H RotB). **^{13}C NMR** (101 MHz, $CDCl_3$) δ 202.6, 200.1, 170.5, 139.7, 117.7, 116.8, 102.7, 99.3, 86.7, 34.7, 30.5, 20.3. **ESI-MS** calcd for $C_8H_{12}NO$ $[M+H]^+$ 138.09, found 138.55.

N-methyl-N-(propa-1,2-dien-1-yl)cyclopropanecarboxamide

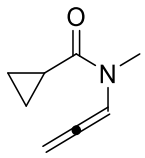

Allene **1l** was prepared following general procedure **GP-2** from the corresponding propargyl amide (148.3 mg, 1.08 mmol). Yellow oil (74.8 mg, 51% yield). Two rotamers are observed due to the dynamic rotation of the amide. **^{1}H NMR** (400 MHz, $CDCl_3$) δ 7.57 (t, *J* = 6.4 Hz, 1H RotA), 7.17 (t, *J* = 6.2 Hz, 1H RotB), 5.55 – 5.23 (m, 2H RotA, 2H RotB), 3.21 (s, 3H RotA), 3.01 (s, 3H RotB), 1.84 (tt, *J* = 8.2, 4.8 Hz, 1H RotA, 1H RotB), 1.05

(h, *J* = 4.2 Hz, 2H RotA, 2H RotB), 0.85 (dt, *J* = 8.0, 3.4 Hz, 2H RotA, 2H RotB). **^{13}C NMR** (101 MHz, $CDCl_3$) δ 202.2, 201.5, 171.9, 171.8, 101.5, 100.2, 87.0, 86.6, 32.9, 31.5, 11.9, 11.5, 8.3, 7.9. **ESI-MS** calcd for $C_8H_{12}NO$ $[M+H]^+$ 138.09, found 138.00.

N-phenyl-N-(propa-1,2-dien-1-yl)benzamide

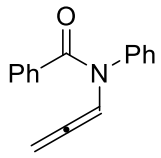

Allene **1m** was prepared following general procedure **GP-2** from the corresponding propargyl amide (235.3 mg, 1 mmol). Pale orange solid (108.4 mg, 70% yield). **^{1}H NMR** (400 MHz, $CDCl_3$) δ 7.68 (t, *J* = 6.4 Hz, 1H), 7.44 – 7.32 (m, 2H), 7.38 – 7.10 (m, 6H), 7.11 (dd, *J* = 7.4, 1.8 Hz, 2H), 5.10 (d, *J* = 6.3 Hz, 2H). **^{13}C NMR** (101 MHz, $CDCl_3$) δ 202.7, 168.5, 140.3, 135.1, 130.0, 128.85, 128.82, 128.5, 127.8, 127.5, 102.0, 86.8. **ESI-MS** calcd for $C_{16}H_{14}NO$ $[M+H]^+$ 236.11, found 236.23.

1-(propa-1,2-dien-1-yloxy)naphthalene

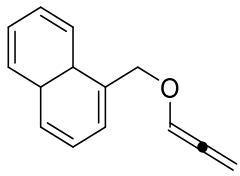

Allene **1n** was prepared following general procedure **GP-2** from the corresponding propargyl naphthol (182.2 mg, 1 mmol). Pale yellow solid (111.7 mg, 61% yield). **^{1}H NMR** (400 MHz, $CDCl_3$) δ 8.35 – 8.28 (m, 1H), 7.89 – 7.83 (m, 1H), 7.61 – 7.50 (m, 3H), 7.43 (t, *J* = 7.9 Hz, 1H), 7.14 (d, *J* = 6.6 Hz, 1H), 7.05 (t, *J* = 5.9 Hz, 1H), 5.52 (d, *J* = 5.9 Hz, 2H). Spectroscopic data are consistent with those reported in literature[2].

N-allyl-N-(propa-1,2-dien-1-yl)benzamide

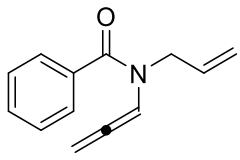

Enallene **3a** was prepared following general procedure **GP-2** from the corresponding enyne (199.3 mg, 1 mmol). Pale yellow oil (143.6 mg, 72% yield). Two rotamers are observed due to the dynamic rotation of the amide. **^{1}H NMR** (400 MHz, $CDCl_3$) δ 7.67 – 7.31 (m, 5H RotA, 6H RotB), 6.65 (s, 1H RotA), 5.94 – 5.65 (m, 1H RotA, 1H RotB), 5.39 – 5.03 (m, 4H RotA, 4H RotB), 4.34 – 3.88 (m, 2H RotA, 2H RotB). **^{13}C NMR** (101 MHz, $CDCl_3$) δ 202.9, 200.3, 169.9, 169.1, 135.3, 134.9, 132.8, 132.5, 130.3, 128.4, 128.0, 126.8, 117.2, 102.2, 98.5, 87.0, 49.9, 46.5. **ESI-MS** calcd for $C_{13}H_{14}NO$ $[M+H]^+$ 200.11, found 200.43.

N-cinnamyl-N-(propa-1,2-dien-1-yl)benzamide

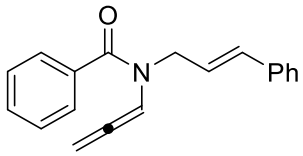

Enallene **3b** was prepared following general procedure **GP-2** from the corresponding enyne (319 mg, 1.16 mmol). Yellow viscous oil (216.6 mg, 68% yield). Two rotamers are observed due to the dynamic rotation of the amide. **^{1}H NMR** (400 MHz, $CDCl_3$) δ 7.78 – 7.11 (m, 10H RotA, 11H RotB), 6.79 – 6.05 (m, 3H RotA, 2H RotB), 5.48 – 5.36 (m, 2H RotA, 2H RotB), 4.56 – 4.11 (m, 2H RotA, 2H RotB). **^{13}C NMR** (101 MHz, $CDCl_3$) δ 203.0, 200.4, 170.0, 169.2, 136.8, 135.4, 134.8, 133.4, 132.3, 130.4, 128.6, 128.5, 128.1, 127.7, 127.0, 126.5, 126.4, 124.1, 102.2, 98.6, 87.1, 49.7, 46.3. **ESI-MS** calcd for $C_{19}H_{17}NNaO$ $[M+Na]^+$ 298.12, found 297.82.

(E)-N-(but-2-en-1-yl)-N-(propa-1,2-dien-1-yl)benzamide

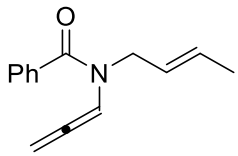

Enallene **3c** was prepared following general procedure **GP-2** from the corresponding enyne (255.4 mg, 1 mmol). Yellow oil (178.0 mg, 70% yield). **^{1}H NMR** (400 MHz, $CDCl_3$) δ 7.50 – 7.37 (m, 5H), 6.63 (s, 1H), 5.70 – 5.32 (m, 4H), 4.06 (m, 2H), 1.69 (d, *J* = 6.0 Hz, 3H). **^{13}C NMR** (101 MHz, $CDCl_3$) δ 203.1, 200.4, 169.7, 169.0, 135.0, 130.2, 129.2, 128.4, 128.4, 128.0, 126.9, 125.2, 102.1, 98.4, 86.8, 49.4, 46.0, 17.8. **ESI-MS** calcd for $C_{14}H_{16}NO$ $[M+H]^+$ 214.12, found 213.97.

N-(2-methylallyl)-N-(propa-1,2-dien-1-yl)benzamide

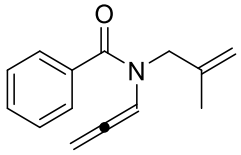

Enallene **3d** was prepared following general procedure **GP-2** from the corresponding enyne (170.6 mg, 0.8 mmol). Pale yellow oil (140.3 mg, 82% yield). Two rotamers are observed due to the dynamic rotation of the amide. **^{1}H NMR** (400 MHz, $CDCl_3$) δ 7.70 – 7.31 (m, 5H RotA, 6H RotB), 6.67 (brs, 1H RotA), 5.30 (s, 2H RotA, 2H RotB), 4.96 – 4.78 (m, 2H RotA, 2H RotB), 4.24 (s, 2H RotA), 3.86 (s, 2H RotB), 1.84 – 1.51 (m, 3H RotA, 3H RotB). **^{13}C NMR** (101 MHz, $CDCl_3$) δ 202.9, 200.4, 170.0, 169.2, 139.9, 135.3, 135.0, 130.2, 128.5, 128.4, 127.9, 126.7, 111.0, 102.3, 98.8, 86.8, 53.1, 49.4, 20.2. **ESI-MS** calcd for $C_{14}H_{16}NO$ $[M+H]^+$ 214.12, found 214.06. *(Partial decomposition was observed during the acquisition of NMR spectra).*

N-(3-methylbut-2-en-1-yl)-N-(propa-1,2-dien-1-yl)benzamide

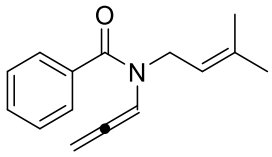

Enallene **3e** was prepared following general procedure **GP-2** from the corresponding enyne (181.8 mg, 0.8 mmol). Orange oil (103 mg, 57% yield). Two rotamers are observed due to the dynamic rotation of the amide. **^{1}H NMR** (400 MHz, $CDCl_3$) δ 7.63 – 7.31 (m, 5H RotA, 6H RotB), 6.62 (s, 1H RotA), 5.41 – 5.07 (m, 3H RotA, 3H RotB), 4.35 – 3.83 (m, 2H RotA, 2H RotB), 1.89 – 1.12 (m, 6H RotA, 6H RotB). **^{13}C NMR** (101 MHz, $CDCl_3$) δ 202.7, 200.1, 169.7, 169.1, 135.5, 135.2, 134.7, 130.1, 128.4, 128.0, 127.0, 119.7, 102.2, 98.5, 86.5, 46.3, 42.7, 25.8, 18.2. **ESI-MS** calcd for $C_{15}H_{18}NO$ $[M+H]^+$ 228.14, found 228.66.

N-allyl-4-methoxy-N-(propa-1,2-dien-1-yl)benzamide

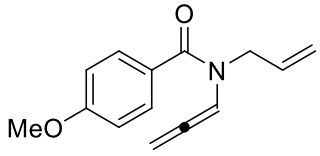

Enallene **3f** was prepared following general procedure **GP-2** from the corresponding enyne (183.4 mg, 0.8 mmol). Pale yellow oil (127.6 mg, 87% yield). **^{1}H NMR** (400 MHz, $CDCl_3$) δ 7.51 (d, *J* = 8.6 Hz, 2H), 6.91 (d, *J* = 8.7 Hz, 2H), 6.87 – 6.64 (m, 1H), 5.84 (brs, 1H), 5.34 (d, *J* = 6.3 Hz, 2H), 5.26 – 5.14 (m, 2H), 4.20 (brs, 2H), 3.83 (s, 3H). **^{13}C NMR** (101 MHz, $CDCl_3$) δ 200.5, 161.3, 132.8, 130.0, 117.1, 113.7, 102.4, 86.9, 55.4, 46.9. **ESI-MS** calcd for $C_{14}H_{16}NO_2$ $[M+H]^+$ 230.12, found 229.84.

N-allyl-2-bromo-N-(propa-1,2-dien-1-yl)benzamide

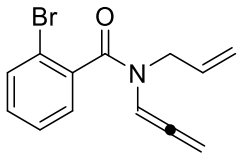

Enallene **3g** was prepared following general procedure **GP-2** from the corresponding enyne (236.4 mg, 0.85 mmol). Pale yellow viscous oil (149.1 mg, 63% yield). Two rotamers are observed due to the dynamic rotation of the amide. **^{1}H NMR** (400 MHz, $CDCl_3$) δ 7.67 – 7.58 (m, 1H RotA, 2H RotB), 7.44 – 7.25 (m, 3H RotA, 3H RotB), 6.34 (t, J = 6.3 Hz, 1H RotA), 5.98 – 5.85 (m, 1H RotA), 5.73 – 5.62 (m, 1H RotB), 5.46 – 5.22 (m, 4H RotA, 2H RotB), 5.16 – 5.09 (m, 1H RotB), 5.03 – 4.95 (m, 1H RotB), 4.46 – 4.17 (m, 2H RotA), 3.99 – 3.77 (m, 2H RotB). **^{13}C NMR** (101 MHz, $CDCl_3$) δ 202.9, 200.6, 167.3, 166.8, 137.3, 137.0, 133.0, 132.8, 132.2, 132.0, 130.8, 130.6, 128.4, 128.0, 127.8, 127.4, 119.5, 119.2, 117.6, 117.4, 100.9, 97.8, 87.4, 87.2, 49.4, 46.0. **ESI-MS** calcd for $C_{13}H_{13}BrNO$ $[M+H]^+$ 278.02, found 277.80.

N-allyl-2-bromo-5-methoxy-N-(propa-1,2-dien-1-yl)benzamide

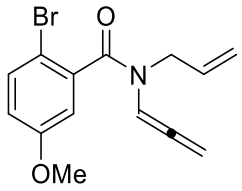

Enallene **3h** was prepared following general procedure **GP-2** from the corresponding enyne (277.4 mg, 0.9 mmol). Pale yellow viscous oil (185.6 mg, 67% yield). Two rotamers are observed due to the dynamic rotation of the amide. **^{1}H NMR** (400 MHz, $CDCl_3$) δ 7.60 (t, *J* = 6.5 Hz, 1H RotB), 7.49 – 7.41 (m, 1H RotA, 1H RotB), 6.86 – 6.75 (m, 2H RotA, 2H RotB), 6.35 (t, *J* = 6.3 Hz, 1H RotA), 5.96 – 5.82 (m, 1H RotA), 5.75 – 5.61 (m, 1H RotB), 5.43 – 5.26 (m, 3H RotA, 2H RotB), 5.25 – 5.19 (m, 1H RotA), 5.14 – 5.09 (m, 1H RotB), 5.03 – 4.96 (m, 1H RotB), 4.43 – 4.15 (m, 2H RotA), 3.99 – 3.72 (m, 3H RotA, 5H RotB). **^{13}C NMR** (101 MHz, $CDCl_3$) δ 202.9, 200.6, 167.1, 166.6, 159.2, 158.8, 137.9, 137.6, 133.8, 133.7, 132.4, 132.0, 117.7, 117.3, 117.2, 117.0, 113.4, 113.3, 109.6, 109.3, 100.9, 97.7, 87.4, 87.3, 55.7, 55.6, 49.5, 45.9. **ESI-MS** calcd for $C_{14}H_{15}BrNO_2$ $[M+H]^+$ 308.03, found 307.85.

N-allyl-4-(tert-butoxy)-2,3,5,6-tetrafluoro-N-(propa-1,2-dien-1-yl)benzamide

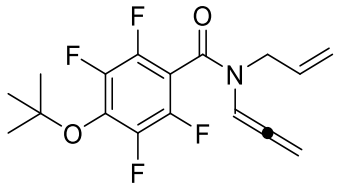

Enallene **3i** was prepared following general procedure **GP-2** from the corresponding enyne (289.2 mg, 1 mmol). *Note: The correspondent allene was obtained in mixture with allene **3j** as a consequence of the base excess performing the isomerization.* Yellow pale oil (128.8 mg, 45% yield). Two rotamers are observed due to the dynamic rotation of the amide. **^{1}H NMR** (600 MHz, $CDCl_3$) δ 7.53 (t, *J* = 6.5 Hz, 1H RotB), 6.39 (t, *J* = 6.3 Hz, 1H RotA), 5.82 (ddt, *J* = 17.3, 10.5, 5.3 Hz, 1H RotA), 5.67 – 5.52 (m, 1H RotB), 5.43 (d, *J* = 6.5 Hz, 2H RotB), 5.34 (d, *J* = 6.3 Hz, 2H RotA), 5.24 (t, *J* = 1.6 Hz, 1H RotA), 5.24 – 5.20 (m, 1H RotA), 5.10 (dq, *J* = 10.3, 1.4 Hz, 1H RotB), 4.95 (d, *J* = 17.2 Hz, 1H RotB), 4.30 (dd, *J* = 5.4, 1.7 Hz, 2H RotA), 3.93 (d, *J* = 5.3 Hz, 2H RotB), 1.40 (s, 9H RotA), 1.39 (s, 9H RotB). **^{13}C NMR** (151 MHz, $CDCl_3$) δ 202.8, 201.3, 158.0, 157.6, 144.8 – 144.2 (m), 144.1 – 143.6 (m), 143.1 – 142.3 (m), 142.5 – 141.8 (m), 136.0 (t, *J* = 13.5 Hz), 135.8 (t, *J* = 13.5 Hz), 131.7, 131.3, 117.8, 117.5, 110.5 (t, *J* = 21.3 Hz), 110.1 (t, *J* = 21.0 Hz), 100.0, 98.0, 88.1, 87.6, 86.2, 49.7, 46.8, 28.5. **^{19}F NMR** (565 MHz, CDCl3) δ -142.2 (dp, *J* = 18.2, 5.8 Hz, 2F RotA, 2F RotB), -146.4 – -151.4 (m, 2F RotA, 2F RotB). **ESI-MS** calcd for $C_{17}H_{17}F_4NNaO_2$ $[M+Na]^+$ 365.90, found 366.10.

N-allyl-2,3,4,5,6-pentafluoro-N-(propa-1,2-dien-1-yl)benzamide

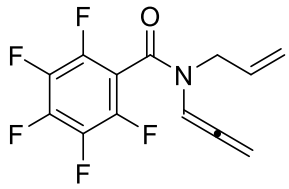

Enallene **3j** was prepared following general procedure **GP-2** from the corresponding enyne (289.2 mg, 1 mmol). *Note: The correspondent allene was obtained in mixture with allene **3i**.* Yellow pale oil (122.2 mg, 42% yield). Two rotamers are observed due to the dynamic rotation of the amide. **^{1}H NMR** (600 MHz, $CDCl_3$) δ 7.52 – 7.50 (m, 1H RotB), 6.33 (t, *J* = 6.3 Hz, 1H RotA), 5.81 (ddt, *J* = 17.5, 10.6, 5.4 Hz, 1H RotA), 5.64 (ddt, *J* = 17.2, 10.5, 5.3 Hz, 1H RotB), 5.44 (d, *J* = 6.5 Hz, 2H RotB), 5.35 (d, *J* = 6.2 Hz, 2H RotA), 5.23 (dt, *J* = 3.7, 1.4 Hz, 1H RotA), 5.22 – 5.20 (m, 1H RotA), 5.13 (dq, *J* = 10.5, 1.4 Hz, 1H RotB), 5.00 (dt, *J* = 17.2, 1.8 Hz, 1H RotB), 4.29 (dt, *J* = 5.4, 1.7 Hz, 2H RotA), 3.93 – 3.92 (m, 2H RotB). **^{13}C NMR** (151 MHz, $CDCl_3$) δ 202.7, 201.5, 156.9, 156.5, 144.3 – 143.7 (m), 143.5 – 142.9 (m), 142.6 – 142.0 (m), 141.8 – 140.9 (m), 139.0 – 138.3 (m), 137.7 – 136.8 (m), 131.5, 131.1, 117.9, 117.7, 112.5 – 109.3 (m), 99.6, 97.9, 88.2, 87.7, 49.6, 47.0. **^{19}F NMR** (565 MHz, $CDCl_3$) δ -135.1 – -142.1 (m, 2F RotA, 2F RotB), -150.9 (tt, *J* = 20.6, 3.0 Hz, 1F RotA), -151.2 (tt, *J* = 20.6, 2.7 Hz, 1F RotB), -159.5 (dddd, *J* = 26.0, 20.6, 11.6, 5.1 Hz, 2F RotA, 2F RotB). **ESI-MS** calcd for $C_{13}H_9F_5NO$ $[M+H]^+$ 290.05, found 289.05.

N-allyl-N-(propa-1,2-dien-1-yl)pent-4-ynamide

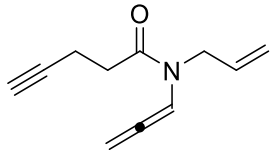

Enallene **3k** was prepared following general procedure **GP-2** from the corresponding enyne (196.3 mg, 1.12 mmol). Yellow oil (61,9 mg, 32% yield). Two rotamers are observed due to the dynamic rotation of the amide. **^{1}H NMR** (400 MHz, $CDCl_3$) δ 7.54 (t, *J* = 6.4 Hz, 1H Rot A), 6.72 (t, *J* = 6.3 Hz, 1H Rot B), 5.77 (dddd, *J* = 19.2, 11.1, 9.6, 5.2 Hz, 1H RotA, 1H RotB), 5.38 (dd, *J* = 6.4, 1.9 Hz, 2H RotA, 2H RotB), 5.23 – 5.11 (m, 2H RotA, 2H RotB), 4.15 – 4.04 (m, 2H RotA, 2H RotB), 2.73 – 2.54 (m, 4H RotA, 4H RotB), 1.99 (dt, *J* = 4.9, 2.6 Hz, 1H RotA, 1H RotB). **^{13}C NMR** (101 MHz, $CDCl_3$) δ 202.1, 201.5, 169.3, 168.6, 132.5, 132.0, 117.1, 116.5, 99.6, 98.7, 87.3, 86.8, 83.2, 68.9, 68.9, 47.7, 46.6, 32.7, 32.6, 14.3. **ESI-MS** calcd for $C_{11}H_{14}NO$ $[M+H]^+$ 176.11, found 176.43.

N-allyl-N-(propa-1,2-dien-1-yl)furan-2-carboxamide

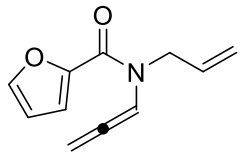

Enallene **3l** was prepared following general procedure **GP-2** from the corresponding enyne (189.2 mg, 1 mmol). Orange oil (104.8 mg, 55% yield). **^{1}H NMR** (400 MHz, $CDCl_3$) δ 7.60 – 7.31 (m, 2H), 7.11 (dd, *J* = 3.5, 0.8 Hz, 1H), 6.49 (dd, *J* = 3.5, 1.8 Hz, 1H), 5.87 (ddt, *J* = 17.1, 10.4, 5.2 Hz, 1H), 5.39 (d, *J* = 6.4 Hz, 2H), 5.22 – 5.17 (m, 1H), 5.17 (t, *J* = 1.7 Hz, 1H), 4.30 (s, 2H). ^{13}C NMR (101 MHz, $CDCl_3$) δ 201.6, 157.8, 147.0, 144.71, 132.7, 117.5, 117.1, 111.5, 100.8, 99.7, 87.2, 48.5, 47.8. **ESI-MS** calcd for $C_{11}H_{12}NO_2$ $[M+H]^+$ 190.09, found 189.95.

N-(but-3-en-1-yl)-N-(propa-1,2-dien-1-yl)acetamide

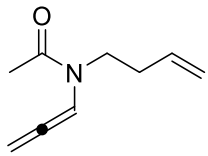

Enallene **3m** was prepared following general procedure **GP-2** from the corresponding enyne (158.6 mg, 1.05 mmol). Pale yellow oil (78.9 mg, 50% yield). Two rotamers are observed due to the dynamic rotation of the amide. **^{1}H NMR** (400 MHz, $CDCl_3$) δ 7.50 (t, *J* = 6.5 Hz, 1H RotB), 6.69 (t, *J* = 6.2 Hz, 1H RotA), 5.82 – 5.70 (m, 1H RotA, 1H RotB), 5.41 – 5.37 (m, 2H RotA, 2H RotB), 5.16 – 4.97 (m, 2H RotA, 2H RotB), 3.59 – 3.54 (m, 2H RotA), 3.50 – 3.44 (m, 2H RotB), 2.39 – 2.23 (m, 2H RotA, 2H RotB), 2.21 – 2.16 (m, 3H RotA, 3H RotB). **^{13}C NMR** (101 MHz, $CDCl_3$) δ 202.1, 200.9, 168.5, 168.2, 135.2, 134.0, 117.6, 116.5, 100.9, 98.0, 86.8, 86.5, 46.1, 43.1, 32.5, 31.7, 21.9, 21.8. **ESI-MS** calcd for $C_9H_{14}NO$ $[M+H]^+$ 152.11, found 151.78.

N-(pent-4-en-1-yl)-N-(propa-1,2-dien-1-yl)benzamide

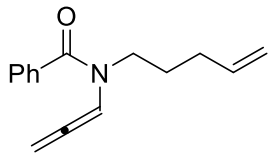

Enallene **3n** was directly obtained following general procedure **GP-1** from the corresponding propargyl amide (478.1 mg, 3 mmol). *Note: It is well known in literature that sometimes, performing the alkylation reaction with NaH, you can directly obtain allene in mixture with the correspondent enyne.* Pale yellow oil (235.2 mg, 34% yield). Two rotamers are observed due to the dynamic rotation of the amide. **^{1}H NMR** (400 MHz, $CDCl_3$) δ 7.49 – 7.34 (m, 5H RotA, 5H RotB), 6.62 (s, 1H RotA, 1H RotB), 5.81 (ddt, *J* = 16.6, 10.4, 6.2 Hz, 1H RotA, 1H

RotB), 5.31 (d, *J* = 6.2 Hz, 2H RotA. 2H RotB), 5.06 – 4.80 (m, 2H RotA, 2H RotB), 3.65 (t, *J* = 7.6 Hz, 2H Rot A), 3.34 – 3.32 (m, 2H Rot B), 2.21 – 1.60 (m, 4H RotA, 4H RotB). **^{13}C NMR** (101 MHz, $CDCl_3$) δ 202.5, 199.9, 169.6, 169.1, 137.9, 137.1, 135.6, 135.2, 130.2, 129.8, 128.5, 127.9, 126.7, 115.3, 115.0, 102.4, 98.3, 86.7, 47.2, 44.0, 31.1, 30.7, 27.3, 26.4. **ESI-MS** calcd for $C_{15}H_{18}NO$ $[M+H]^+$ 228.13, found 228.24.

Ethyl allyl(propa-1,2-dien-1-yl)carbamate

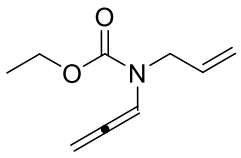

Enallene **3o** was prepared following general procedure **GP-2** from the corresponding enyne (142.1 mg, 0.85 mmol). Yellow pale oil (115.6 mg, 81% yield). Two rotamers are observed due to the dynamic rotation of the carbamate. **^{1}H NMR** (600 MHz, $CDCl_3$) δ 7.14 (t, *J* = 6.2 Hz, 1H RotA), 6.98 (t, *J* = 6.5 Hz, 1H RotB), 5.74 – 5.71 (m, 1H RotA, 1H RotB), 5.30 (s, 2H RotA, 1H RotB), 5.09 (s, 2H RotA, 2H RotB), 4.17 (q, *J* = 7.1 Hz, 2H RotA, 2H RotB), 3.99 – 3.92 (m, 2H RotA, 2H RotB), 1.25 (dt, *J* = 12.9, 6.8 Hz, 3H RotA, 3H RotB). **^{13}C NMR** (151 MHz, $CDCl_3$) δ 201.8, 200.9, 153.9, 153.7, 132.9, 116.8, 116.5, 100.4, 99.9, 87.4, 86.9, 62.2, 47.1, 14.6. **ESI-MS** calcd for $C_9H_{14}NO_2$ $[M+H]^+$ 168.14, found 168.10.

Tert-butyl allyl(propa-1,2-dien-1-yl)carbamate

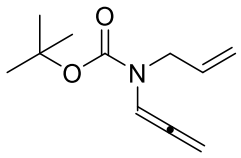

Enallene **3p** was prepared following general procedure **GP-2** from the corresponding enyne (128.9 mg, 0.66 mmol). White liquid (73.9 mg, 57% yield). Two rotamers are observed due to the dynamic rotation of the carbamate. **^{1}H NMR** (400 MHz, $CDCl_3$) δ 7.22 – 6.94 (m, 1H RotA, 1H RotB), 5.85 – 5.71 (m, 1H RotA, 1H RotB), 5.39 – 5.28 (m, 2H RotA, 2H RotB), 5.19 – 5.07 (m, 2H RotA, 2H RotB), 4.04 – 3.88 (m, 2H RotA, 2H RotB), 1.50 (s, 3H RotA, 3H RotB). **^{13}C NMR** (101 MHz, $CDCl_3$) δ 201.7, 200.8, 152.8, 133.1, 116.2, 100.2, 87.1, 86.6, 81.0, 47.4, 46.8, 28.3. **ESI-MS** calcd for $C_{11}H_{18}NO_2$ $[M+H]^+$ 196.13, found 195.87. *(Partial decomposition was observed during the acquisition of NMR spectra).*

Synthesis and characterization of products

Photocatalytic reactions [GP-3A]:

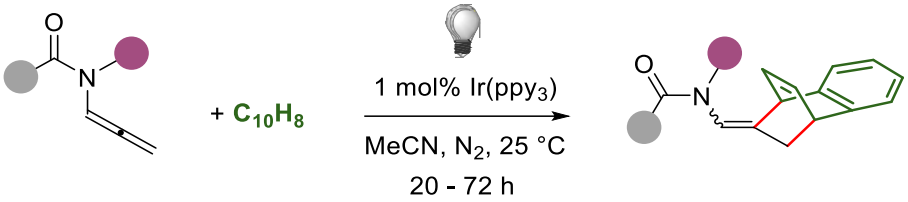

A vial was charged with substrate **1** (1 equiv., 0.15 mmol), $Ir(ppy)_3$ (1 mol%), naphthalene (20 equiv.), and dry ACN (0.1 M). The solution was transferred into an NMR tube capped with a rubber septum, degassed by freeze-pump-thaw (3 times) and the tube was placed in an oil bath kept at 25 °C by means of a chiller. The tube was irradiated with a blue LED strip for 20 – 72 h. Conversion was monitored by TLC and the mixture was then concentrated in vacuo. The residue was purified by chromatography on silica gel; the catalyst and the excess of naphthalene were removed, and could be recovered, using toluene as eluent prior to the separation of desired products (*n*-hexane/EtOAc, under gradient).

Photocatalytic reactions [GP-3B]:

A vial was charged with substrate **1** (1 equiv., 0.15 mmol), $Ir(ppy)_3$ (1 mol%), naphthalene (20 equiv.), and dry ACN (0.1 M). The solution was transferred into an NMR tube capped with a rubber septum, degassed by freeze-pump-thaw (3 times) and the tube was placed in an oil bath kept at 25 °C by means of a chiller. The tube was irradiated with a blue LED strip for 8-24 h. Conversion was monitored by TLC and the mixture was then concentrated in vacuo. The residue was purified by chromatography on silica gel; the catalyst and the excess of naphthalene were removed, and could be recovered, using toluene as eluent prior to the separation of desired products (*n*-hexane/EtOAc, under gradient).

3-((1,4-dihydro-1,4-ethanonaphthalen-9-ylidene)methyl)oxazolidin-2-one

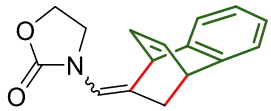

Product **2a** was obtained as a mixture of diastereomers (87:13) following general procedure **GP3-A** from the corresponding allene (18.8 mg, 0.15 mmol; 150.0 mg, 1.2 mmol). White solid (34 mg, 89% yield; 245.2 mg, 81%). The reaction required 20 h of irradiation to fully consume the starting material.

Product **2a** was further purified by crystallization to obtain single crystals of the *E*- isomer. The relative structure was confirmed with selective NOE experiments. **^{1}H NMR** (400 MHz, Acetone-*d*6) δ 7.28 – 7.20 (m, 2H), 7.12 – 7.04 (m, 2H), 6.66 – 6.54 (m, 2H), 6.46 (t, *J* = 2.4 Hz, 1H), 4.45 – 4.41 (m, 1H), 4.36 – 4.25 (m, 2H), 4.17 – 4.12 (m, 1H), 3.96 – 3.83 (m, 2H), 2.51 (dt, *J* = 15.2, 2.6 Hz, 1H), 2.33 (dt, *J* = 15.2, 2.5 Hz, 1H). **^{13}C NMR** (101 MHz, Acetone-*d*6) δ 156.2, 143.7, 143.0, 135.2, 134.5, 125.3, 125.1, 123.1, 122.7, 122.6, 117.5, 62.0, 49.0, 44.5, 41.0, 31.7. **ESI-HRMS** calcd for $C_{16}H_{16}NO_2$ $[M+H]^+$ 254.1176, found 254.1180.

(4S)-4-benzyl-3-((1,4-dihydro-1,4-ethanonaphthalen-9-ylidene)methyl)oxazolidin-2-one

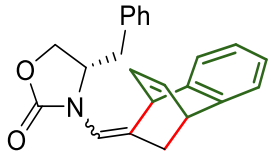

Product **2b** was obtained as a mixture of diastereomers (95:5) following general procedure **GP-3A** from the corresponding allene (32.4 mg, 0.15 mmol). White solid (35.6 mg, 54% yield). The reaction required 40 h of irradiation to fully consume the starting material.

Product **2b** was further purified by crystallization to obtain single crystals of the *E*- isomer. **^{1}H NMR** (400 MHz, $CDCl_3$) δ 7.33 – 7.21 (m, 5H), 7.17 – 7.10 (m, 2H), 7.02 – 6.96 (m, 2H), 6.69 – 6.57 (m, 2H), 6.30 (t, *J* = 2.3 Hz, 1H), 4.46 (dd, *J* = 5.9, 1.7 Hz, 1H), 4.23 – 4.06 (m, 4H), 2.81 (dd, *J* = 13.8, 3.2 Hz, 1H), 2.52 (dd, *J* = 13.8, 8.7 Hz, 1H), 2.43 (dt, *J* = 15.3, 2.6 Hz, 1H), 2.23 (dt, *J* = 15.4, 2.5 Hz, 1H). **^{13}C NMR** (101 MHz, $CDCl_3$) δ 156.0, 143.8, 141.8, 135.3, 134.7, 131.7, 129.1, 128.9, 127.2, 125.7, 125.6, 123.0, 122.8, 115.1, 66.2, 57.1, 49.0, 41.1, 37.8, 33.2. **ESI-HRMS** calcd for $C_{23}H_{22}NO_2$ $[M+H]^+$ 344.1645, found 344.1652.

Ethyl ((1,4-dihydro-1,4-ethanonaphthalen-9-ylidene)methyl)(methyl)carbamate

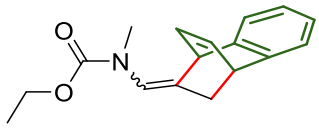

Product **2c** was obtained as a mixture of diastereomers (69:31) following general procedure **GP-3A** from the corresponding allene (21.2 mg, 0.15 mmol). Pale yellow solid (16.4 mg, 41% yield). The reaction required 20 h of irradiation to fully consume the starting material. Two rotamers are observed due to the dynamic rotation

of the carbamate. **^{1}H NMR** was taken at 273K to decrease the dynamic rotation and increase spectral resolution. **^{1}H NMR** (400 MHz, $CDCl_3$) δ 7.25 – 7.05 (m, Dia1, 4H RotA, 4H RotB; Dia2, 4H RotA, 4H RotB), 6.67 – 6.48 (m, Dia1, 2H RotA, 3H RotB; Dia2, 2H RotA, 2H RotB), 6.38 (s, Dia1, 1H RotA), 5.93 (s, Dia2, 1H RotB), 5.82 (s, Dia2, 1H RotA), 4.68 – 4.64 (m, Dia2, 1H RotA, 1H RotB), 4.38 – 4.30 (m, Dia1, 1H RotA, 1H RotB), 4.24 – 4.01 (m, Dia1, 3H RotA, 3H RotB; Dia2, 3H RotA, 3H RotB), 3.12 (s, Dia2, 3H RotA, 3H RotB), 2.96 (s, Dia1, 3H RotA, 3H RotB), 2.42 – 2.28 (m, Dia1, 1H RotA, 1H RotB; Dia2, 1H RotA, 1H RotB), 2.25 – 2.13 (m, Dia1, 1H RotA, 1H RotB; Dia2, 1H RotA, 1H RotB), 1.36 – 1.15 (m, Dia1, 3H RotA, 3H RotB; Dia2, 3H RotA, 3H RotB). **^{13}C NMR** (101 MHz, $CDCl_3$) δ 156.3, 155.4, 144.1, 143.8, 142.5, 141.3, 136.4, 135.5, 134.4, 133.3, 130.1, 125.6, 125.5, 125.4, 123.1, 123.0, 122.8, 122.7, 121.7, 120.6, 61.7, 61.6, 48.9, 44.0, 41.2, 40.8, 37.5, 34.9, 33.0, 32.5, 14.8, 14.6. **ESI-HRMS** calcd for $C_{17}H_{20}NO_2$ $[M+H]^+$ 270.1489, found 270.1486.

Benzyl ((1,4-dihydro-1,4-ethanonaphthalen-9-ylidene)methyl)(methyl)carbamate

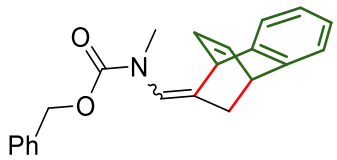

Product **2d** was obtained as a mixture of diastereomers (70:30) following general procedure **GP-3A** from the corresponding allene (30.5 mg, 0.15 mmol). Transparent oil (31.3 mg, 63% yield). The reaction required 24 h of irradiation to fully consume the starting material. Two rotamers are observed due to the dynamic rotation of the carbamate. **^{1}H NMR** (400 MHz, $CDCl_3$) δ 7.50 – 7.10 (m, Dia1, 9H RotA, 9H RotB; Dia2 9H RotA, 9H RotB), 6.68 – 6.32 (m, Dia1, 3H RotA, 3H RotB; Dia2, 2H RotA, 2H RotB), 5.92 – 5.86 (m, Dia2, 1H RotA, 1H RotB), 5.39 – 5.11 (m, Dia1, 2H RotA, 2H RotB), 4.69 (dd, Dia2, *J* = 6.1, 1.4 Hz, 1H RotA, 1H RotB), 4.42 – 4.34 (m, Dia1, 1H RotA, 1H RotB), 4.12 – 4.06 (m, Dia1, 1H RotA, 1H RotB; Dia2, 1H RotA, 1H RotB), 3.19 (s, Dia2, 3H RotA, 3H RotA), 3.16 (s, Dia1, 3H RotB), 3.02 (s, Dia1, 3H RotA), 2.48 – 2.12 (m, Dia1, 2H RotA, 2H RotB; Dia2, 2H RotA, 2H RotB). **^{13}C NMR** (101 MHz, $CDCl_3$) δ 162.8, 156.1, 155.3, 144.1, 142.3, 141.2, 136.9, 136.6, 136.4, 135.7, 134.3, 133.3, 132.5, 128.8, 128.5, 127.9, 127.6, 125.7, 125.6, 125.5, 123.2, 123.0, 122.9, 122.8, 122.5, 121.5, 120.5, 68.9, 67.2, 49.0, 48.6, 44.0, 41.1, 40.8, 37.6, 35.2, 33.0, 32.4. **ESI-HRMS** calcd for $C_{22}H_{22}NO_2$ $[M+H]^+$ 332.1651, found 332.1646.

Tert-butyl ((1,4-dihydro-1,4-ethanonaphthalen-9-ylidene)methyl)(methyl)carbamate

Product **2e** was obtained as a mixture of diastereomers (71:29) following general procedure **GP-3A** from the corresponding allene (24.5 mg, 0.15 mmol). Pale yellow solid (38.8 mg, 87% yield). The reaction required 24 h of irradiation to fully consume the starting material. Two rotamers are observed due to the dynamic rotation of the carbamate. **^{1}H NMR** was taken at 273K to decrease the dynamic rotation and increase spectral resolution. **^{1}H NMR** (600 MHz, $CDCl_3$) δ 7.26 – 7.04 (m, Dia1, 4H RotA, 4H RotB; Dia2, 4H RotA, 4H RotB),

6.66 – 6.49 (m, Dia1, 2H RotA, 3H RotB; Dia2, 2H RotA, 2H RotB), 6.27 (s, Dia1, 1H RotA), 5.92 (s, Dia2, 1H RotB), 5.81 (s, Dia2, 1H RotA), 4.71 – 4.61 (m, Dia2, 1H RotA, 1H RotB), 4.36 – 4.27 (m, Dia1, 1H RotA, 1H RotB), 4.12 – 4.00 (m, Dia1, 1H RotA, 1H RotB; Dia2, 1H RotA, 1H RotB), 3.08 (s, Dia2, 3H RotA, 3H RotB), 2.91 (s, Dia1, 3H RotA, 3H RotB), 2.41 – 2.11 (m, Dia1, 2H RotA, 2H RotB; Dia2, 2H RotA, 2H RotB), 1.57 – 1.29 (m, Dia1, 9H RotA, 9H RotB; Dia2, 9H RotA, 9H RotB). **^{13}C NMR** (101 MHz, $CDCl_3$) δ 155.5, 154.4, 144.2, 143.8, 142.6, 141.5, 136.3, 135.4, 134.3, 133.4, 130.1, 125.6, 125.5, 125.3, 123.1, 123.0, 122.8, 122.7, 122.2, 121.4, 80.0, 79.9, 48.9, 44.0, 41.2, 40.8, 36.9, 34.9, 34.4, 33.0, 32.4, 29.7, 28.4, 28.3. **ESI-HRMS** calcd for $C_{19}H_{23}NNaO_2$ $[M+Na]^+$ 320.1621, found 320.1620.

Tert-butyl butyl((1,4-dihydro-1,4-ethanonaphthalen-9-ylidene)methyl)carbamate

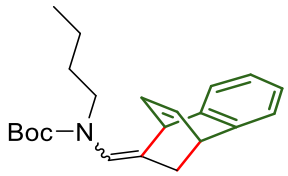

Product **2f** was obtained as a mixture of diastereomers (74:26) following general procedure **GP-3A** from the corresponding allene (31.7 mg, 0.15 mmol). Pale yellow solid (36.5 mg, 72% yield). The reaction required 24 h of irradiation to fully consume the starting material.

Product **2f** was further purified to obtain diastereomers **E**. Two rotamers are observed due to the dynamic rotation of the carbamate. **^{1}H NMR** was taken at 273K to decrease the dynamic rotation and increase spectral resolution. **^{1}H NMR** (600 MHz, $CDCl_3$) δ 7.23 – 7.05 (m, 4H RotA, 4H RotB), 6.57 (s, 2H RotA, 2H RotB), 6.26 (s, 1H RotB), 5.98 (s, 1H RotA), 4.35 – 4.32 (m, 1H RotA, 1H RotB), 4.10 – 4.04 (m, 1H RotA, 1H RotB), 3.30 – 3.14 (m, 2H RotA, 2H RotB), 2.31 – 2.04 (m, 2H RotA, 2H RotB), 1.47 – 1.15 (m, 13H RotA, 13H RotB), 0.84 (t, *J* = 7.3 Hz, 3H RotA, 3H RotB). **^{13}C NMR** (101 MHz, $CDCl_3$) δ 154.2, 143.9, 142.5, 135.6, 134.0, 125.4, 125.3, 122.8, 122.6, 120.4, 79.5, 48.8, 46.9, 41.2, 32.6, 29.72, 29.68, 28.5, 28.2, 19.9, 13.8. **ESI-HRMS** calcd for $C_{22}H_{30}NO_2$ $[M+H]^+$ 340.2271, found 340.2276.

N-((1,4-dihydro-1,4-ethanonaphthalen-9-ylidene)methyl)-N-methylbenzamide

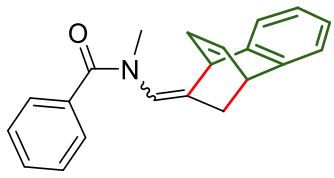

Product **2g** was obtained as a mixture of diastereomers (68:32) following general procedure **GP-3A** from the corresponding allene (26.1 mg, 0.15 mmol). White solid (27.6 mg, 61% yield). *Note: **2g** was isolated with traces of a third inseparable product.* The reaction required 40 h of irradiation to fully consume the starting material. **^{1}H NMR** was taken at 273K to decrease the dynamic rotation and increase spectral resolution. **^{1}H NMR** (400 MHz, $CDCl_3$) δ 7.55 (d, *J* = 7.1 Hz, 1H Dia1), 7.46 – 7.04 (m, 8H Dia1, 9H Dia2), 6.58 – 6.43 (m, 2H Dia1, 2H

Dia2), 6.19 (s, 1H Dia1), 5.89 (s, 1H Dia2), 4.61 (d, *J* = 6.1 Hz, 1H Dia2), 4.23 (d, *J* = 6.0 Hz, 1H Dia1), 4.10 – 4.05 (m, 1H Dia1), 4.01 – 3.96 (m, 1H Dia2), 3.27 (s, 3H Dia2), 3.13 (s, 3H Dia1), 2.26 – 2.01 (m, 2H Dia1, 2H Dia2). **^{13}C NMR** (101 MHz, $CDCl_3$) δ 171.0, 170.5, 143.8, 143.3, 141.2, 140.6, 136.9, 136.7, 136.1, 136.0, 135.8, 133.3, 130.0, 129.9, 128.6, 128.1, 127.7, 127.6, 125.8, 125.7, 125.6, 125.5, 124.6, 123.2, 123.03, 123.00, 122.92, 122.88, 48.2, 43.8, 40.8, 40.6, 36.9, 34.8, 33.3, 32.7. **ESI-HRMS** calcd for $C_{21}H_{20}NO$ $[M+H]^+$ 302.1539, found 302.1544.

N-((1,4-dihydro-1,4-ethanonaphthalen-9-ylidene)methyl)-N-methylacetamide

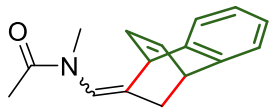

Product **2h** was obtained as a mixture of diastereomers (70:30) following general procedure **GP-3A** from the corresponding allene (22.2 mg, 0.2 mmol). White viscous oil (44.6 mg, 93% yield). The reaction required 44 h of irradiation to fully consume the starting material.

Product **2h** was further purified to obtain diastereomer **E**. **^{1}H NMR** (400 MHz, $CDCl_3$) δ 7.26 – 7.09 (m, 4H), 6.67 – 6.56 (m, 2H), 6.25 (s, 1H), 4.42 – 4.38 (m, 1H), 4.15 – 4.09 (m, 1H), 2.91 (s, 3H), 2.26 (dt, *J* = 16.0, 2.6 Hz, 1H), 2.13 – 2.06 (m, 1H), 1.89 (s, 3H). **^{13}C NMR** (101 MHz, $CDCl_3$) δ 170.8, 143.6, 141.4, 139.2, 136.3, 133.6, 125.8, 125.7, 123.0, 122.97, 122.9, 48.1, 40.8, 33.9, 32.4, 21.8. **ESI-HRMS** calcd for $C_{16}H_{17}NNaO$ $[M+Na]^+$ 262.1202, found 262.1207.

N-((1,4-dihydro-1,4-ethanonaphthalen-9-ylidene)methyl)-N-methyl-2,2-diphenylacetamide

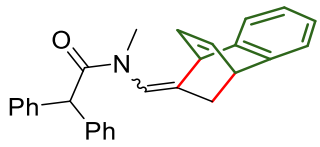

Product **2i** was obtained as a mixture of diastereomers (75:25) following general procedure **GP-3A** from the corresponding allene (40.4 mg, 0.15 mmol). Colorless oil (25.0 mg, 42% yield). The reaction required 24 h of irradiation to fully consume the starting material.

Product **2i** was further purified to obtain diastereomer **E**. **^{1}H NMR** (400 MHz, $CDCl_3$) δ 7.33 – 7.07 (m, 12H), 6.98 – 6.93 (m, 2H), 6.61 (dq, *J* = 7.6, 5.8 Hz, 2H), 6.23 (t, *J* = 2.4 Hz, 1H), 4.98 (s, 1H), 4.42 (dd, *J* = 5.6, 1.9 Hz, 1H), 4.01 (dd, *J* = 5.5, 2.6 Hz, 1H), 2.96 (s, 3H), 2.05 (dt, *J* = 16.1, 2.6 Hz, 1H), 1.78 (dt, *J* = 16.1, 2.5 Hz, 1H). **^{13}C NMR** (101 MHz, $CDCl_3$) δ 172.1, 143.6, 142.1, 141.2, 139.7, 139.1, 136.6, 133.2, 128.8, 128.4, 126.8, 126.7, 125.9, 125.8, 123.2, 123.0, 122.4, 54.7, 47.9, 40.7, 34.3, 32.1. **ESI-HRMS** calcd for $C_{28}H_{26}NO$ $[M+H]^+$ 392.2014, found 392.2020.

N-((1,4-dihydro-1,4-ethanonaphthalen-9-ylidene)methyl)-N-methylfuran-2-carboxamide

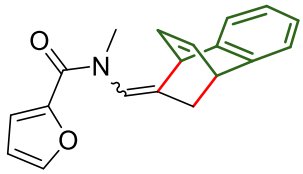

Product **2j** was obtained as a mixture of diastereomers (88:12) following general procedure **GP-3A** from the corresponding allene (24.5 mg, 0.15 mmol). Yellow oil (38.5 mg, 88% yield). The reaction required 48 h of irradiation to fully consume the starting material.

Product **2j** was further purified to obtain diastereomer **E**. **^{1}H NMR** (400 MHz, $CDCl_3$) δ 7.45 (s, 1H), 7.23 (d, *J* = 7.1 Hz, 1H), 7.13 (ddd, *J* = 7.2, 5.0, 3.7 Hz, 1H), 7.07 (d, *J* = 4.4 Hz, 3H), 6.70 – 6.69 (m, 1H), 6.63 (ddd, *J* = 7.4, 6.0, 1.3 Hz, 2H), 6.32 (dd, *J* = 8.3, 5.2 Hz, 3H), 6.07 (t, *J* = 2.0 Hz, 1H), 4.66 (dd, *J* = 6.1, 1.3 Hz, 1H), 4.09 (dq, *J* = 6.0, 2.4 Hz, 2H), 2.39 (dt, *J* = 15.3, 2.4 Hz, 2H), 2.25 (dt, *J* = 15.3, 2.3 Hz, 2H). **^{13}C NMR** (101 MHz, $CDCl_3$) δ 159.9, 147.3, 144.4, 143.7, 140.5, 139.1, 136.7, 132.8, 125.8, 125.7, 123.3, 123.0, 122.0, 116.6, 111.0, 43.8, 40.7, 37.0, 33.3. **ESI-HRMS** calcd for $C_{19}H_{18}NO_2$ $[M+H]^+$ 292.1338, found 292.1342.

N-((1,4-dihydro-1,4-ethanonaphthalen-9-ylidene)methyl)-N-methylmethacrylamide

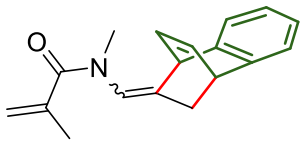

Product **2k** was obtained as a mixture of diastereomers (50:50) following general procedure **GP-3A** from the corresponding allene (20.5 mg, 0.15 mmol). Transparent oil (14.6 mg, 35% yield). The reaction required 56 h of irradiation to fully consume the starting material. **^{1}H NMR** (400 MHz, $CDCl_3$) δ 7.27 – 7.06 (m, Dia1, 4H; Dia2, 4H), 6.69 – 6.47 (m, Dia1, 2H; Dia2, 2H), 6.32 (s, Dia1, 1H), 5.93 (t, Dia2, *J* = 1.9 Hz, 1H), 5.18 (d, Dia1, *J* = 4.3 Hz, 1H; d, Dia2, *J* = 4.3 Hz, 1H), 5.10 (d, Dia1, *J* = 3.4 Hz, 1H), 5.01 (s, Dia2, 1H), 4.64 (d, Dia1, *J* = 6.1 Hz, 1H), 4.34 (d, Dia2, *J* = 5.7 Hz, 1H), 4.18 – 4.03 (m, Dia1, 1H; m, Dia2, 1H), 3.17 (s, Dia1, 3H), 3.00 (s, Dia2, 3H), 2.37 – 2.25 (m, Dia1, 1H ; m, Dia2, 1H), 2.25 – 2.11 (m, Dia1, 1H; m, Dia2, 1H), 1.90 (s, Dia1, 3H), 1.79 (s, Dia2, 3H) **^{13}C NMR** (101 MHz, $CDCl_3$) δ 172.5, 171.9, 143.9, 143.5, 141.6, 141.0, 140.7, 137.4, 137.0, 136.0, 134.8, 133.6, 132.7, 125.9, 125.7, 125.6, 123.7, 123.2, 123.1, 122.9, 122.4, 118.4, 117.8, 48.4, 43.8, 41.0, 40.7, 36.5, 34.2, 33.2, 32.6, 20.1, 19.8. **ESI-HRMS** calcd for $C_{18}H_{20}NO$ $[M+H]^+$ 266.1545, found 266.1544.

N-((1,4-dihydro-1,4-ethanonaphthalen-9-ylidene)methyl)-N-methylcyclopropanecarboxamide

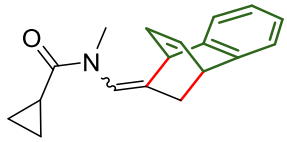

Product **2l** was obtained as a mixture of diastereomers (67:33) following general procedure **GP-3A** from the corresponding allene (20.6 mg, 0.15 mmol). Yellow oil (29.1 mg, 73% yield). The reaction required 48 h of irradiation to fully consume the starting material. Two rotamers are observed due to the dynamic rotation of the amide. **^{1}H NMR** (400 MHz, Acetone-*d6*) δ 7.31 – 7.21 (m, Dia1, 2H RotA, 2H RotB; Dia2, 2H RotA, 2H RotB), 7.15 – 7.06 (m, Dia1, 2H RotA, 2H RotB; Dia2, 2H RotA, 2H RotB), 6.73 – 6.57 (m, Dia 1, 2H RotA, 2H RotB; Dia2, 2H RotA, 2H RotB), 6.44 (t, Dia1, *J* = 2.4 Hz, 1H RotA, 1H RotB), 6.06 (t, Dia2, *J* = 1.9 Hz, 1H RotA, 1H RotB), 4.72 (dd, Dia2, *J* = 6.0, 1.4 Hz, 1H RotA, 1H RotB), 4.58 (dd, Dia1, *J* = 5.9, 1.7 Hz, 1H RotA, 1H RotB), 4.19 – 4.14 (m, Dia1, 1H RotA, 1H RotB; Dia2, 1H RotA, 1H RotB), 2.99 (s, Dia2, 3H RotA, 3H RotB), 2.83 (s, Dia1, 3H RotA; Dia2, 3H RotA), 2.44 (t, Dia2, *J* = 2.4 Hz, 1H RotB), 2.40 (t, Dia2, *J* = 2.4 Hz, 1H RotA), 2.36 (t, Dia1, *J* = 2.7 Hz, 1H RotB), 2.32 (t, Dia1, *J* = 2.7 Hz, 1H RotA), 2.24 (t, Dia2, *J* = 2.4 Hz, 1H RotA), 2.20 (t, Dia2, *J* = 2.3 Hz, 1H RotB), 2.15 (t, Dia1, *J* = 2.6 Hz, 1H RotA), 2.12 – 2.10 (m, Dia1, 1H RotB), 1.76 (tt, Dia2, *J* = 7.9, 4.6 Hz, 1H RotA, 1H RotB), 1.65 (tt, Dia1, *J* = 7.9, 4.7 Hz, 1H RotA, 1H RotB), 1.11 – 0.99 (m, Dia2 2H RotA), 0.94 – 0.51 (m, Dia1, 3H RotA, 3H RotB; Dia2, 2HRotA, 4H RotB), 0.49 – 0.38 (m, Dia1, 1H RotA, 1H RotB) **^{13}C NMR** (101 MHz, Acetone-*d6*) δ 172.6, 172.0, 144.3, 144.0, 142.0, 141.1, 140.0, 139.7, 136.9, 136.2, 133.6, 133.0, 125.6, 125.4, 123.3, 123.0, 122.9, 122.6, 121.5, 47.8, 43.8, 40.7, 40.6, 34.6, 33.0, 32.2, 11.3, 11.0, 8.6, 7.3, 7.2, 6.7. **ESI-HRMS** calcd for $C_{18}H_{20}NO$ $[M+H]^+$ 266.1545, found 266.1547.

N-((1,4-dihydro-1,4-ethanonaphthalen-9-ylidene)methyl)-N-phenylbenzamide

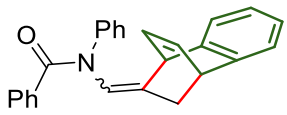

Product **2m** was obtained as a mixture of diastereomers (57:43) following general procedure **GP-3A** from the corresponding allene (35.3 mg, 0.15 mmol). White solid (25.4 mg, 46% yield, 73% conversion). The reaction was irradiated for 72h. **^{1}H NMR** (400 MHz, $CDCl_3$) δ 7.56 (dd, *J* = 6.2, 2.6 Hz, Dia1, 1H; Dia 2, 1H), 7.37 – 7.00 (m, Dia1, 12H; Dia2, 12H), 6.69 (d, *J* = 7.1 Hz, Dia1, 1H; Dia2, 1H), 6.56 – 6.50 (m, Dia 1, 2H; Dia2, 2H), 6.17 – 6.16 (m, Dia1, 1H; Dia2, 1H), 4.50 (dd, *J* = 6.1, 1.3 Hz, Dia 2, 1H), 4.42 (d, *J* = 5.8 Hz, Dia1, 1H), 4.01 (dq, *J* = 6.8, 2.3 Hz, Dia2 1H), 3.91 – 3.90 (m, Dia 1 1H), 2.45 – 2.30 (m, Dia2, 1H), 2.25 – 2.20 (m, Dia 1, 1H), 1.69 – 1.63 (m, Dia1, 1H; Dia2, 1H). **^{13}C NMR** (101 MHz, $CDCl_3$) δ 170.4, 169.6, 144.0, 143.6, 143.2, 141.8, 141.7, 140.2, 136.6, 136.0, 136.0, 135.9, 133.5, 132.6, 130.3, 130.0, 129.1, 129.0, 128.8, 128.8, 127.9, 127.7, 127.1, 127.0, 126.4, 126.4, 126.2, 126.0, 125.6, 125.5, 125.4, 125.4, 123.6, 123.0, 122.8, 122.7, 121.6, 48.9, 43.8, 41.0, 40.6, 33.8, 32.9. **ESI-HRMS** calcd for $C_{26}H_{22}NO$ $[M+H]^+$ 364.1736, found 364.1744.

9-((naphthalen-1-yloxy)methylene)-1,4-dihydro-1,4-ethanonaphthalene

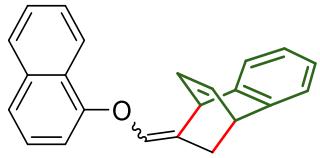

Product **2n** was obtained as a mixture of diastereomers (77:23) following general procedure **GP-3A** from the corresponding allene (27.3 mg, 0.15 mmol). *Note: it was necessary add 1% TEA to the eluent to prevent the degradation of the product during the separation.* White solid (30 mg, 65% yield). The reaction required 28 h of irradiation to fully consume the starting material. **^{1}H NMR** (400 MHz, Acetone-*d*6) δ 8.44 – 8.38 (m, 1H Dia2), 8.22 – 8.16 (m, 1H Dia1), 7.95 – 7.84 (m, 1H Dia1, 1H Dia2), 7.63 – 7.46 (m, 3H Dia1, 3H Dia2), 7.39 (t, *J* = 8.0 Hz, 1H Dia1, 1H Dia2), 7.31 – 7.23 (m, 2H Dia1, 2H Dia2), 7.15 – 7.06 (m, 2H Dia1, 2H Dia2), 7.01 – 6.91 (m, 2H Dia1, 1H Dia2), 6.71 – 6.62 (m, 2H Dia1, 2H Dia2), 6.56 – 6.53 (m, 1H Dia2), 5.22 – 5.18 (m, 1H Dia2), 4.63 – 4.55 (m, 1H Dia1), 4.24 – 4.15 (m, 1H Dia1, 1H Dia2), 2.55 – 2.42 (m, 1H Dia1, 1H Dia2), 2.38 – 2.24 (m, 1H Dia1, 1H Dia2). **^{13}C NMR** (101 MHz, Acetone-*d*6) δ 153.5, 153.1, 144.4, 144.2, 143.0, 142.3, 136.2, 136.1, 134.83, 134.76, 134.3, 134.1, 133.8, 133.1, 127.6, 127.5, 126.6, 126.5, 125.93, 125.86, 125.6, 125.5, 125.34, 125.32, 125.2, 124.4, 123.9, 123.0, 122.9, 122.6, 121.7, 121.6, 121.54, 121.53, 107.7, 107.6, 44.9, 41.7, 40.8, 40.7, 31.2, 31.0. **ESI-HRMS** calcd for $C_{23}H_{18}NaO$ $[M+Na]^+$ 333.1250, found 333.1252.

3-((1-methoxy-1,4-dihydro-1,4-ethanonaphthalen-9-ylidene)methyl)oxazolidin-2-one

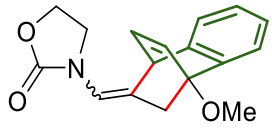

Product **2o'** was obtained as a mixture of diastereomers (91:9) following a modified general procedure **GP-3A** from the corresponding allene (19.4 mg, 0.15 mmol). *Note: O_2 was removed by bubbling N_2 in the solution because freeze-pump-thaw broke the NMR tube.* White solid (22.9 mg, 53% yield). The reaction required 42 h of irradiation to fully consume the starting material.

Product **2o'** was further purified by crystallization to obtain single crystals of the *E*- isomer. **^{1}H NMR** (400 MHz, CDCl3) δ 7.41 (d, *J* = 8.6 Hz, 1H), 7.22 – 7.10 (m, 3H), 6.68 (d, *J* = 8.2 Hz, 1H), 6.62 – 6.57 (m, 1H), 6.50 – 6.47 (m, 1H), 4.37 – 4.22 (m, 3H), 3.91 – 3.65 (m, 5H), 2.70 (dd, *J* = 14.0, 2.2 Hz, 1H), 2.32 (dd, *J* = 14.0, 2.1 Hz, 1H). **^{13}C NMR** (101 MHz, $CDCl_3$) δ 156.5, 142.9, 140.2, 134.3, 133.1, 126.0, 125.5, 122.5, 122.3, 119.8, 117.3, 82.9, 62.1, 53.6, 48.7, 44.7, 36.8. **ESI-HRMS** calcd for $C_{17}H_{18}NO_3$ $[M+H]^+$ 284.1281, found 284.1290.

(1,2,2a,3,5,10-hexahydro-5,10-ethenobenzo[f]cyclobuta[c]indol-4(4aH)-yl)(phenyl)methanone

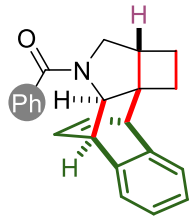

Product **4a** was obtained as a mixture of diastereomers (70:30) following general procedure **GP-3B** from the corresponding enallene (29.6 mg, 0.15 mmol; 239.3 mg). White oil (37.4 mg, 76% yield; 235.4 mg, 60%). Two rotamers are observed due to the dynamic rotation of the amide. *Note: For model product **4a**, assignments of B rotamer resonances were made with a series of selective NOE experiments.* **^{1}H NMR** (400 MHz, $CDCl_3$) δ 7.66 – 6.95 (m, Dia1, 9H RotA, 9H RotB; Dia2, 9H RotA, 9H RotB), 6.70 – 6.54 (m, Dia1, 2H RotA; Dia2, 2H RotA; 1H RotB), 6.53 – 6.48 (m, 1H RotB), 6.36 (t, *J* = 6.8 Hz, 1H RotB), 6.15 (t, *J* = 6.3 Hz, 1H RotB), 4.75 – 4.70 (m, Dia2, 1H RotA), 4.66 – 4.58 (m, Dia1, 2H RotA), 4.43 (d, *J* = 3.2 Hz, Dia2, 1H RotA), 4.09 (d, *J* = 3.3 Hz, Dia1, RotB), 3.92 – 3.81 (m, Dia1, 1H RotA, 1H RotB; Dia2, 1H RotA, 3H RotB), 3.67 (dd, *J* = 10.9, 5.8 Hz, Dia2, 1H RotA), 3.60 – 3.52 (m, Dia1, 1H RotB; Dia2, 2H RotB), 3.47 (d, *J* = 12.3 Hz, Dia1, 1H RotB), 3.26 (d, *J* = 10.9 Hz, Dia2, 1H RotA), 2.77 (d, *J* = 11.0 Hz, Dia1, 1H RotA; Dia2, 1H RotB), 2.66 (q, *J* = 7.2 Hz, Dia2, 1H RotA), 2.36 – 1.71 (m, Dia1, 5H RotA, 5H RotB; Dia2, 2H RotA, 2H RotB), 1.65 – 1.47 (m, Dia1, 1H RotA, 1H RotB; Dia2, 2H RotA, 2H RotB). **^{13}C NMR** (101 MHz, $CDCl_3$) δ 171.0, 170.8, 170.0, 169.7, 141.5, 141.2, 141.1, 140.7, 140.5, 140.3, 138.6, 138.0, 137.4, 137.3, 136.1, 135.3, 134.8, 134.6, 134.3, 134.1, 133.9, 133.3, 132.1, 129.8, 129.7, 128.8, 128.7, 128.25, 128.15, 127.2, 127.0, 126.7, 126.6, 126.4, 126.04, 125.96, 125.89, 125.73, 125.67, 125.61, 125.57, 125.48, 124.8, 124.7, 124.5, 123.94, 123.89, 123.7, 123.5, 122.9, 122.8, 73.3, 72.2, 71.5, 70.0, 58.6, 57.5, 56.8, 56.7, 55.9, 55.6, 55.1, 53.8, 51.1, 51.0, 50.7, 46.6, 46.4, 44.29, 44.27, 42.7, 42.0, 41.0, 40.5, 31.9, 31.0, 21.6, 21.1, 21.0, 20.4. **ESI-HRMS** calcd for $C_{23}H_{22}NO$ $[M+H]^+$ 328.1696, found 328.1690.

Phenyl(2-phenyl-1,2,2a,3,5,10-hexahydro-5,10-ethenobenzo[f]cyclobuta[c]indol-4(4aH)-yl)methanone

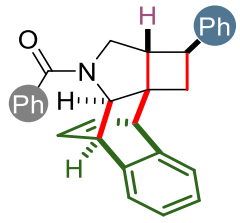

Product **4b** was obtained as a mixture of diastereomers (74:26) following general procedure **GP-3B** from the corresponding enallene (41.9 mg, 0.15 mmol). White solid (27.3 mg, 45% yield). Two rotamers are observed due to the dynamic rotation of the amide. **^{1}H NMR** (400 MHz, $CDCl_3$) δ 7.70 – 6.98 (m, Dia1, 14H RotA, 14H RotB; Dia2, 14H RotA, 14H RotB), 6.74 – 6.55 (m, Dia1, 2H RotA; Dia2, 2H RotA; 2H RotB), 6.42 (t, *J* = 6.7 Hz, 1H RotB), 6.24 – 6.18 (m, 1H RotB), 4.82 – 4.76 (m, Dia2, 1H RotA), 4.74 – 4.65 (m, Dia1, 2H RotA), 4.53 (d, *J* = 3.2 Hz, Dia2, 1H RotA), 4.20 (d, *J* = 3.3 Hz, 1H RotB), 4.13 (d, *J* = 12.4 Hz, Dia2, 1H RotB), 4.02 (d, *J* = 3.1 Hz, 1H RotB), 3.97 – 3.84 (m, Dia1, 1H RotA; Dia2, 1H RotA; 2H RotB), 3.80 (dd, *J* = 11.0, 5.6 Hz, Dia2,

1H RotA), 3.74 – 3.58 (m, 4H RotB), 3.48 (d, *J* = 11.0 Hz, Dia2, 1H RotA), 3.33 – 3.21 (m, 2H RotB), 3.14 – 2.95 (m, Dia1, 2H RotA; Dia2, 1H RotA), 2.85 – 2.72 (m, Dia2, 1H RotA, 1H RotB), 2.64 – 2.50 (m, Dia1, 1H RotA; 1H RotB), 2.44 – 2.07 (m, Dia1, 2H RotA; Dia2, 2H RotA; 4H RotB), 1.93 (dd, *J* = 11.1, 5.4 Hz, Dia1, 1H RotA), 1.85 (dd, *J* = 12.5, 5.6 Hz, Dia1, 1H RotB). **^{13}C NMR** (101 MHz, $CDCl_3$) δ 171.0, 170.8, 170.0, 169.7, 144.1, 143.9, 141.4, 141.0, 140.9, 140.4, 140.3, 138.6, 137.8, 137.2, 137.1, 135.1, 134.9, 134.5, 134.3, 134.2, 133.4, 132.5, 130.0, 129.9, 128.9, 128.8, 128.6, 128.5, 128.45, 128.42, 128.3, 128.24, 128.16, 127.2, 127.0, 126.7, 126.6, 126.4, 126.32, 126.29, 126.26, 126.22, 126.16, 126.1, 126.0, 125.9, 125.8, 125.7, 124.9, 124.8, 124.7, 124.01, 123.96, 123.8, 123.7, 72.8, 71.7, 71.2, 69.6, 58.2, 56.4, 55.2, 53.9, 53.5, 53.1, 52.1, 51.3, 51.02, 50.98, 50.8, 50.64, 50.61, 50.2, 49.7, 49.2, 46.6, 46.3, 44.28, 44.27, 39.5, 38.9, 38.8, 38.7, 38.4, 38.1. **ESI-HRMS** calcd for $C_{29}H_{26}NO$ $[M+H]^+$ 404.2009, found 404.2004.

(2-methyl-1,2,2a,3,5,10-hexahydro-5,10-ethenobenzo[f]cyclobuta[c]indol-4(4aH)-yl)(phenyl)methanone

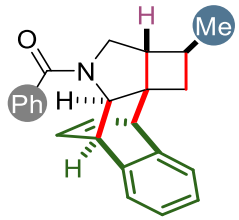

Product **4c** was obtained as a mixture of diastereomers (71:29) following general procedure **GP-3B** from the corresponding allene (38.3 mg, 0.15 mmol). Yellow oil (35.3 mg, 61% yield). Two rotamers are observed due to the dynamic rotation of the amide. **^{1}H NMR** (400 MHz, $CDCl_3$) δ 7.64 – 7.04 (m, Dia1, 9H RotA, 9H RotB; Dia2, 9H RotA, 9H RotB), 6.75 – 6.49 (m, Dia1, 2H RotA, 2H RotB; Dia2, 2H RotA, 1H RotB), 6.24 (t, Dia2, *J* = 1.7 Hz, 1H RotB), 4.73 – 4.70 (m, Dia2, 1H RotA, 1H RotB), 4.63 – 4.60 (m, Dia1, 1H RotA, 1H RotB), 4.53 – 4.52 (m, Dia1, 1H RotA, 1H RotB), 4.36 – 4.32 (m, Dia2, 1H RotA, 1H RotB), 3.93 – 3.79 (m, Dia1, 1H RotA, 1H RotB; Dia2,1H RotA, 1H RotB), 3.67 (dd, Dia2, *J* = 10.9, 5.8 Hz, 1H RotB), 3.38 (d, Dia2, *J* = 11.4 Hz, 1H RotB), 3.29 (d, Dia2, *J* = 10.8 Hz, 1H RotA), 2.91 (d, Dia1, *J* = 11.6 Hz, 1H RotB), 2.80 (d, Dia1, *J* = 10.9 Hz, 1H RotA), 2.47 – 2.13 (m, Dia1, 1H RotA, 1H RotB; Dia2, 1H RotA, 1H RotB), 1.93 – 1.54 (m, Dia1, 5H RotA, 4H RotB; Dia2, 3H RotA, 3H RotB), 1.02 (d, Dia1, *J* = 6.5 Hz, 3H RotB), 0.98 (d, Dia2, *J* = 6.6 Hz, 3H RotA), 0.87 (dd, Dia2, *J* = 7.3, 1.4 Hz, 3H RotA, 3H RotB). **^{13}C NMR** (101 MHz, $CDCl_3$) δ 169.9, 169.6, 169.3, 166.2, 141.7, 141.2, 141.0, 140.4, 140.2, 138.2, 137.6, 137.5, 137.3, 134.6, 134.4, 134.4, 134.2, 134.0, 133.9, 133.6, 133.3, 130.2, 129.8, 129.7, 129.6, 128.8, 128.7, 128.4, 128.2, 128.2, 128.1, 127.7, 127.2, 127.0, 126.8, 126.6, 125.9, 125.8, 125.8, 125.6, 125.5, 125.4, 124.8, 124.6, 124.5, 123.9, 123.9, 123.7, 116.6, 73.1, 71.6, 71.3, 69.7, 58.0, 56.2, 54.4, 54.3, 52.9, 52.9, 52.0, 51.9, 52.0, 51.3, 51.1, 50.7, 50.7, 50.1, 44.4, 44.2, 44.0, 43.2, 39.5, 38.6, 38.4, 29.0, 24.8, 24.5, 21.2, 21.0, 15.4, 15.1, 12.0. **ESI-HRMS** calcd for $C_{24}H_{24}NO$ $[M+H]^+$ 342.1858, found 342.1861.

(2a-methyl-1,2,2a,3,5,10-hexahydro-5,10-ethenobenzo[f]cyclobuta[c]indol-4(4aH) yl)(phenyl)methanone

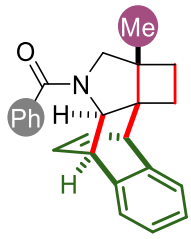

Product **4d** was obtained as a mixture of diastereomers (71:29) following general procedure **GP-3B** from the corresponding enallene (32.0 mg, 0.15 mmol). White solid (22.3 mg, 44% yield). Two rotamers are observed due to the dynamic rotation of the amide. **^{1}H NMR** (400 MHz, $CDCl_3$) δ 7.62 – 6.93 (m, Dia1, 9H RotA, 9H RotB; Dia2, 9H RotA, 9H RotB), 6.70 – 6.50 (m, Dia1, 2H RotA, 1H RotB; Dia2, 2H RotA, 1H RotB), 6.33 (t, *J* = 6.8 Hz, Dia1, 1H RotB), 6.18 – 6.10 (m, Dia2, 1H RotB), 4.78 – 4.63 (m, Dia1, 1H RotA; Dia2, 2H RotA), 4.51 – 4.46 (m, Dia1, 1H RotA), 4.20 (brs, Dia2, 1H RotB), 3.98 (brs, Dia1, 1H RotB), 3.93 – 3.85 (m, Dia1, 1H RotB; Dia2, 1H RotA), 3.83 – 3.74 (m, Dia1, 1H RotA, 1H RotB), 3.58 – 3.48 (m, Dia1, 1H RotB), 3.34 (d, *J* = 10.6 Hz, Dia1, 1H RotA), 3.30 – 3.18 (m, Dia1, 1H RotA, 1H RotB), 2.83 (d, *J* = 10.8 Hz, Dia2, 1H RotA), 2.15 (q, *J* = 10.2 Hz, Dia2, 1H RotA), 2.03 – 1.64 (m, Dia1, 2H RotA, 2H RotB; Dia2, 4H RotA, 4H RotB), 1.58 – 1.20 (m, Dia1, 5H RotA, 5H RotB; Dia2, 3H RotB), 1.07 (s, Dia2, 3H RotA). **^{13}C NMR** (101 MHz, $CDCl_3$) δ 170.6, 169.7, 169.6, 141.7, 141.3, 141.2, 141.1, 140.9, 137.6, 137.4, 137.3, 134.8, 134.7, 134.4, 134.2, 133.9, 132.1, 129.8, 129.7, 128.8, 128.7, 128.24, 128.15, 127.2, 127.0, 126.7, 126.6, 125.8, 125.7, 125.6, 125.53, 125.49, 124.9, 124.8, 124.6, 123.9, 123.7, 123.6, 74.4, 72.9, 71.4, 64.3, 62.7, 61.1, 58.8, 57.0, 55.2, 47.9, 47.8, 47.0, 46.90, 46.86, 46.6, 45.5, 44.4, 44.0, 29.6, 28.9, 27.89, 27.86, 27.3, 19.1, 18.7, 16.7. **ESI-HRMS** calcd for $C_{24}H_{24}NO$ $[M+H]^+$ 342.1852, found 342.1860.

(2,2-dimethyl-1,2,2a,3,5,10-hexahydro-5,10-ethenobenzo[f]cyclobuta[c]indol-4(4aH) yl)(phenyl)methanone

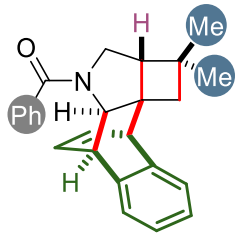

Product **4e** was obtained as a mixture of diastereomers (74:26) following general procedure **GP-3B** from the corresponding enallene (34.5 mg, 0.15 mmol). Pale yellow viscous oil (42.0 mg, 79% yield). Two rotamers are observed due to the dynamic rotation of the amide. **^{1}H NMR** (400 MHz, $CDCl_3$) δ 7.62 – 6.95 (m, Dia1, 9H RotA, 9H RotB; Dia2, 9H RotA, 9H RotB), 6.73 – 6.49 (m, Dia1, 2H RotA; Dia2, 2H RotA; 2H RotB), 6.35 (t, *J* = 6.8 Hz, 1H RotB), 6.14 (t, *J* = 7.0 Hz, 1H RotB), 4.70 (brs, Dia2, 1H RotA), 4.62 (q, *J* = 3.4 Hz, Dia1, 1H RotA), 4.49 (d, *J* = 3.3 Hz, Dia1, 1H RotA), 4.33 – 4.28 (m, Dia2, 1H RotA), 4.05 – 3.99 (m, 2H RotB), 3.89 – 3.76 (m, Dia1, 1H RotA; Dia2, 1H RotA; 1H RotB), 3.65 – 3.47 (m, Dia2, 1H RotA; 3H RotB), 3.38 (d, *J* = 11.5

Hz, Dia2, 1H RotA), 2.91 (d, *J* = 11.4 Hz, Dia1, 1H RotA), 2.36 (d, *J* = 7.4 Hz, 1H RotB), 2.26 (d, *J* = 7.0 Hz, Dia2, 1H RotA), 2.05 – 1.70 (m, Dia1, 4H RotA; Dia2, 1H RotA), 1.57 – 1.48 (m, Dia2, 1H RotA; 2H RotB), 1.23 (s, 3H RotB), 1.18 (s, 3H RotB), 1.12 – 1.01 (m, Dia1, 3H RotA; Dia2, 6H RotA), 0.85 (s, Dia1, 3H RotA, 3H RotB). **^{13}C NMR** (101 MHz, $CDCl_3$) δ 170.1, 169.74, 169.67, 169.3, 141.6, 141.4, 141.24, 141.19, 141.15, 140.7, 140.2, 138.5, 138.0, 137.7, 137.6, 136.1, 135.9, 135.2, 134.9, 134.30, 134.27, 133.7, 133.5, 131.8, 129.73, 129.69, 129.6, 128.8, 128.7, 128.3, 128.2, 126.8, 126.6, 126.5, 126.45, 126.39, 125.9, 125.75, 125.71, 125.65, 125.59, 125.5, 125.4, 124.85, 124.76, 124.5, 124.05, 123.97, 123.8, 123.5, 122.84, 122.76, 74.3, 73.3, 72.7, 71.2, 54.6, 53.1, 51.9, 51.55, 51.52, 51.47, 50.94, 50.88, 50.2, 49.8, 49.7, 49.1, 46.5, 46.35, 46.28, 46.0, 45.8, 45.6, 44.3, 32.5, 32.44, 32.38, 31.3, 31.1, 30.9, 30.8, 23.5, 23.2, 22.8, 22.6. **ESI-HRMS** calcd for $C_{25}H_{26}NO$ $[M+H]^+$ 356.2009, found 356.2010.

(1,2,2a,3,5,10-hexahydro-5,10-ethenobenzo[f]cyclobuta[c]indol-4(4aH)-yl)(4-methoxyphenyl)methanone

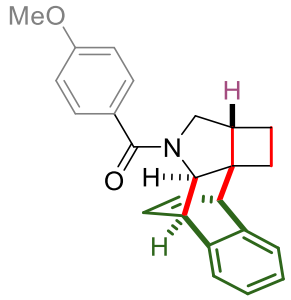

Product **4f** was obtained as a mixture of diastereomers (67:33) following general procedure **GP-3B** from the corresponding enallene (34.6 mg, 0.15 mmol). White solid (39.2 mg, 73% yield). Two rotamers are observed due to the dynamic rotation of the amide. *Note: small traces of resonances due to the minor rotamers of products are not assigned.* **^{1}H NMR** (400 MHz, $CDCl_3$) δ 7.63 – 7.49 (m, Dia2, 2H RotA; 2H RotB), 7.37 – 6.89 (m, Dia1, 6H RotA; Dia2, 6H RotA; 6H RotB), 6.83 (d, *J* = 8.7 Hz, Dia1, 2H RotA), 6.67 – 6.52 (m, Dia1, 2H RotA, 2H RotB; Dia2, 2H RotA, 2H RotB), 4.70 – 4.61 (m, Dia1, 1H RotA; Dia2, 1H RotA), 4.57 (q, *J* = 3.4 Hz, Dia1, 1H RotA), 4.48 – 4.43 (m, Dia2, 1H RotA), 3.93 – 3.77 (m, Dia1, 4H RotA, 3H RotB; Dia2, 4H RotA, 3H RotB), 3.72 (dd, *J* = 10.7, 5.9 Hz, Dia2, 1H RotA), 3.34 (d, *J* = 10.8 Hz, Dia2, 1H RotA), 2.84 (d, *J* = 10.9 Hz, Dia1, 1H RotA), 2.67 (q, *J* = 6.8 Hz, Dia2, 1H RotA), 2.31 – 2.21 (m, Dia1, 1H RotA), 2.19 – 1.81 (m, Dia1, 4H RotA; Dia2, 2H RotA), 1.63 – 1.47 (m, Dia1, 1H RotA, 1H RotB; Dia2, 2H RotA, 2H RotB). **^{13}C NMR** (101 MHz, $CDCl_3$) δ 170.6, 169.6, 169.4, 160.8, 160.7, 141.5, 141.2, 141.1, 140.4, 135.2, 134.9, 134.5, 134.2, 134.1, 134.0, 133.3, 129.6, 129.5, 129.3, 129.1, 128.5, 126.4, 125.9, 125.8, 125.6, 125.5, 124.8, 124.7, 124.5, 123.9, 123.7, 114.0, 113.9, 113.4, 113.3, 72.3, 71.6, 70.0, 58.7, 56.9, 56.8, 55.7, 55.4, 55.3, 54.9, 54.1, 51.1, 50.7, 46.3, 44.4, 42.8, 42.2, 40.4, 31.1, 21.1, 20.4. **ESI-HRMS** calcd for $C_{24}H_{24}NO_2$ $[M+H]^+$ 358.1802, found 358.1808.

(2-bromophenyl)(1,2,2a,3,5,10-hexahydro-5,10-ethenobenzo[f]cyclobuta[c]indol-4(4aH)-yl)methanone

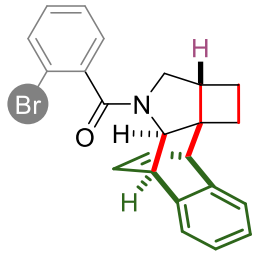

Product **4g** was obtained as a mixture of diastereomers (73:27) following general procedure **GP-3B** from the corresponding enallene (42.2 mg, 0.15 mmol). White solid (37.9 mg, 62% yield). Two rotamers are observed due to the dynamic rotation of the amide.

Product **4g** was further purified to obtain major diastereomer. **^{1}H NMR** (400 MHz, $CDCl_3$) δ 7.71 – 7.43 (m, 1H RotA, 2H RotB), 7.38 – 6.87 (m, 7H RotA, 6H RotB), 6.65 – 6.43 (m, 2H RotA, 1H RotB), 6.18 – 6.11 (m, 1H RotB), 4.80 – 4.64 (m, 1H RotA), 4.54 – 4.47 (m, 1H RotA), 3.89 – 3.73 (m, 1H RotA, 2H RotB), 3.68 – 3.57 (m, 2H RotB), 2.61 – 2.47 (m, 1H RotA), 2.36 – 1.40 (m, 6H RotA, 6H RotB). **^{13}C NMR** (101 MHz, $CDCl_3$) δ 168.0, 167.6, 141.2, 140.0, 139.5, 134.8, 134.4, 133.9, 132.7, 130.4, 130.0, 127.7, 127.6, 127.4, 126.3, 126.1, 125.9, 124.7, 123.9, 69.8, 56.1, 55.7, 50.6, 43.8, 41.4, 40.7, 30.9, 20.9, 20.4. **ESI-HRMS** calcd for $C_{23}H_{21}BrNO$ $[M+H]^+$ 406.0801, found 406.0805.

(2-bromo-5-methoxyphenyl)(1,2,2a,3,5,10-hexahydro-5,10-ethenobenzo[f]cyclobuta[c]indol-4(4aH)-yl)methanone

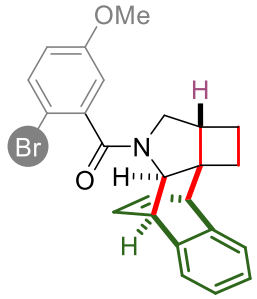

Product **4h** was obtained as a mixture of diastereomers (75:25) following general procedure **GP-3B** from the corresponding enallene (46.3 mg, 0.15 mmol). White solid (39 mg, 60% yield). Two rotamers are observed due to the dynamic rotation of the amide.

Product **4h** was further purified by crystallization to obtain single crystals of the major isomer. **^{1}H NMR** (400 MHz, $CDCl_3$) δ 7.52 (brs, 1H RotB), 7.38 – 7.05 (m, 5H RotA, 4H RotB), 6.89 (dd, *J* = 8.9, 3.0 Hz, 1H RotB), 6.70 (dd, *J* = 8.8, 3.0 Hz, 1H RotA), 6.64 – 6.44 (m, 3H RotA, 2H RotB), 6.18 (t, *J* = 6.9 Hz, 1H RotB), 4.75 (s, 1H RotA, 1H RotB), 4.53 – 4.45 (m, 1H RotA), 3.95 – 3.71 (m, 4H RotA, 6H RotB), 2.63 – 2.49 (m, 1H RotA), 2.35 – 1.40 (m, 6H RotA, 6H RotB). **^{13}C NMR** (101 MHz, $CDCl_3$) δ 167.7, 167.4, 159.1, 158.9, 141.2, 140.9, 140.2, 134.8, 134.5, 133.8, 133.5, 126.3, 126.1, 125.9, 125.7, 124.6, 124.0, 116.2, 112.7, 69.6, 56.1, 55.8, 55.5, 50.6, 43.7, 41.4, 30.8, 20.9, 20.4. **ESI-HRMS** calcd for $C_{24}H_{23}BrNO_2$ $[M+H]^+$ 436.0907, found 436.0902.

(4-(tert-butoxy)-2,3,5,6-tetrafluorophenyl)(1,2,2a,3,5,10-hexahydro-5,10-ethenobenzo[f]cyclobuta[c]indol-4(4aH)-yl)methanone

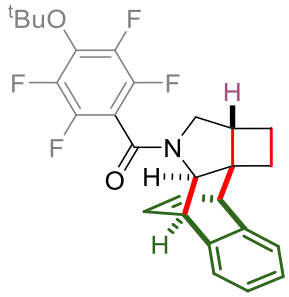

Product **4i** was obtained as a mixture of diastereomers (82:18) following general procedure **GP-3B** from the corresponding allene (51.5 mg, 0.15 mmol). White solid (43.5 mg, 62% yield). Two rotamers are observed due to the dynamic rotation of the amide. **^{1}H NMR** (400 MHz, $CDCl_3$) δ 7.37 – 7.35 (m, Dia2, 1H RotA, 1H RotB), 7.27 – 7.27 (m, Dia 1, 1H RotA, 1H RotB), 7.21 – 7.13 (m, Dia 1, 3H RotA, 3H RotB; Dia2, 3H RotA, 3H RotB), 6.61 (qt, Dia 1, *J* = 7.8, 3.9 Hz, 2H RotA, 1H RotB; Dia2, *J* = 7.8, 3.9 Hz, 1H RotA, 1H RotB), 6.55 – 6.50 (m, Dia2, 1H RotA), 6.35 (ddd, Dia2 *J* = 7.5, 6.0, 1.5 Hz, 1H RotB), 6.25 (ddd, Dia 1 *J* = 7.7, 6.2, 1.4 Hz, 1H RotB), 4.83 (ddd, Dia2, *J* = 5.4, 3.1, 1.6 Hz, 1H RotA, 1H RotB), 4.68 (ddd, Dia 1, *J* = 5.5, 3.2, 1.8 Hz, 1H RotA, 1H RotB), 4.51 (d, Dia 1, *J* = 3.3 Hz, 1H RotA), 4.31 (d, Dia1 *J* = 3.2 Hz, 1H RotB), 3.88 (ddd, Dia1, *J* = 11.0, 5.8, 1.8 Hz, 1H RotA, 1H RotB), 3.77 (d, Dia2, *J* = 3.3 Hz, 1H RotA), 3.69 (t, Dia2, *J* = 4.1 Hz, 1H RotB), 3.65 – 3.62 (m, Dia2, 1H RotA), 3.59 – 3.52 (m, Dia2, 1HRotA, 3H RotB), 3.15 (d, Dia2 *J* = 10.6 Hz, 1H RotA), 2.79 (q, Dia2, *J* = 7.5 Hz, 1H RotB), 2.69 (m, Dia1 ,1H RotA, 1H RotB; Dia2 ,1H RotA), 2.38 – 2.31 (m, Dia1, 1H RotB), 2.26 (td, Dia1, *J* = 8.4, 5.6 Hz, 1H RotA), 2.20 – 2.15 (m, Dia1, 1H RotA, 1H RotB; Dia2, 1H RotA, 1H RotB), 2.10 – 1.96 (m, Dia1, 2H RotA, 2H RotB; Dia2, 2H RotA, 2H RotB), 1.72 – 1.58 (m, Dia1, 2H RotA, 2H RotB; Dia2, 1H RotA, 1H RotB), 1.49 (s, Dia2, 9H RotA), 1.44 (s, Dia 1, 9H RotB), 1.40 (s, Dia1, 9H RotA), 1.37 (s, Dia2, 9H RotB). **^{13}C NMR** (101 MHz, $CDCl_3$) δ 158.4, 158.1, 145.0 – 144.5 (m), 144.3 – 143.9 (m), 143.7 – 143.3 (m), 142.8, 142.5 – 142.0 (m), 141.9 – 141.4 (m), 141.3, 140.8, 140.6, 140.5, 139.2, 138.0, 136.5, 135.2, 134.6, 133.9, 133.6, 132.8, 132.7, 126.6, 126.1, 125.9, 125.3, 125.2, 124.2, 124.0, 123.8, 123.7, 112.7 (t, *J* = 21.4 Hz), 86.1, 85.8, 85.7, 85.4, 73.0, 72.0, 71.5, 70.5, 56.9, 56.5, 55.6, 55.3, 53.6, 50.8, 50.5, 50.4, 43.7, 43.5, 41.7, 41.1, 40.8, 40.5, 30.9, 30.8, 28.4, 28.4, 21.3, 21.2, 20.6, 20.4. **^{19}F NMR** (565 MHz, CDCl3) δ -142.4 (ddd, *J* = 23.5, 9.6, 5.1 Hz), -142.6 (ddd, *J* = 23.6, 9.8, 5.3 Hz), -143.0 (ddd, *J* = 23.5, 10.2, 4.8 Hz), -143.1 (ddd, *J* = 23.7, 9.4, 5.0 Hz), -143.3 (ddd, *J* = 23.6, 9.9, 4.8 Hz), -143.6 (ddd, *J* = 23.6, 9.8, 4.9 Hz), -143.8 (ddd, *J* = 24.1, 9.7, 5.2 Hz), -144.5 (ddd, *J* = 23.5, 9.8, 4.9 Hz), -148.5 (dd, *J* = 23.3, 9.7 Hz), -149.3 (dd, *J* = 23.9, 9.6 Hz), -149.5 (dd, *J* = 23.4, 9.6 Hz), -149.8 (dt, *J* = 23.2, 11.3 Hz), -150.0 (dd, *J* = 23.7, 9.9 Hz), -151.0 (dd, *J* = 23.9, 9.1 Hz). **ESI-HRMS** calcd for $C_{27}H_{25}F_4NO_2$ $[M+H]^+$ 472.1900, found 472.1904.

(1,2,2a,3,5,10-hexahydro-5,10-ethenobenzo[f]cyclobuta[c]indol-4(4aH)-yl)(perfluorophenyl)methanone

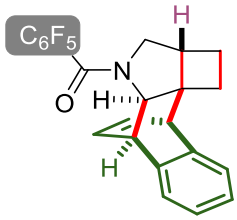

Product **4j** was obtained as a mixture of diastereomers (79:21) following general procedure **GP-3B** from the corresponding allene (43.4 mg, 0.15 mmol). White solid (48.8 mg, 78% yield). Two rotamers are observed due to the dynamic rotation of the amide. **^{1}H NMR** (400 MHz, $CDCl_3$) δ 7.36 – 7.34 (m, Dia2, 1H RotA, 1H RotB), 7.27 – 7.25 (m, Dia1 1H RotA, 1H RotB), 7.22 – 710 (m, Dia 1, 3H RotA, 3H RotB; Dia2 3H RotA, 3H RotB), 6.65 – 6.57 (m, Dia1, 2H RotA, 1H RotB; Dia2, 1H RotA, 1H RotB), 6.51 (dd, Dia2 *J* = 7.7, 5.8 Hz, 1H RotA), 6.43 (ddd, Dia 2, *J* = 7.6, 6.0, 1.6 Hz, 1H RotB), 6.30 (ddd, Dia1 *J* = 7.7, 6.1, 1.4 Hz, 1H RotB), 4.81 (ddd, Dia2 *J* = 5.4, 3.2, 1.6 Hz, 1H RotA, 1H RotB), 4.67 (ddd, Dia1 *J* = 5.6, 3.4, 1.5 Hz, 1H RotA, 1H RotB), 4.50 (d, Dia 1, *J* = 3.2 Hz, 1H RotA), 4.30 (d, Dia1, *J* = 3.2 Hz, 1H RotB), 3.89 (ddd, Dia 1 *J* = 11.6, 5.9, 1.6 Hz, 1H RotA, 1H RotB), 3.74 (d, Dia2 *J* = 3.3 Hz, 1H RotA), 3.68 – 3.66 (m, Dia2, 1H RotB), 3.65 – 3.62 (m, Dia2, 1H RotA), 3.56 – 3519 (m, Dia 2, 1H RotA, 3H RotB), 3.12 (d, Dia2, *J* = 10.5 Hz, 1H RotA), 2.82 – 2.77 (m, Dia2, 1H RotB), 2.72 – 2.64 (m, Dia1 ,1H RotA, 1H RotB; Dia2 ,1H RotA), 2.36 (td, Dia1, *J* = 8.1, 5.5 Hz, 1H RotB), 2.27 (td, Dia 1, *J* = 8.5, 5.6 Hz, 1H RotA), 2.22 – 2.16 (m, Dia1, 1H RotA, 1H RotB; Dia2, 1H RotA, 1H RotB), 2.10 – 1.92 (m, Dia1, 2H RotA, 2H RotB; Dia2, 2H RotA, 2H RotB), 1.70 – 1.58 (m, Dia1, 2H RotA, 2H RotB; Dia2, 1H RotA, 1H RotB). **^{13}C NMR** (101 MHz, $CDCl_3$) δ 157.2, 157.0, 144.5 – 142.4 (m), 141.9 – 141.4 (m), 141.2, 140.7, 140.4, 139.1, 139.0 – 138.5 (m), 137.8, 136.8, 136.7 – 136.1 (m), 135.3, 134.7, 133.8, 133.5, 132.7, 132.2, 131.9, 131.6, 126.7, 126.4, 126.0, 125.9, 125.8, 125.2, 125.2, 124.6, 124.2, 124.0, 123.8, 123.7, 113.2 – 111.8 (m), 73.1, 72.0, 71.6, 70.6, 56.9, 56.6, 55.6, 55.3, 50.4, 47.4, 47.1, 43.6, 43.5, 41.0, 31.6, 30.9, 30.8, 29.7, 21.2, 20.5, 20.4. **^{19}F NMR** (565 MHz, $CDCl_3$) δ -140.0 (dt, *J* = 23.9, 6.7 Hz), -140.1 – -140.2 (m), -140.5 (d, *J* = 25.1 Hz), -140.7 (ddd, *J* = 23.6, 8.9, 4.5 Hz), -141.0 (ddd, *J* = 23.1, 9.1, 4.5 Hz), -141.2 (ddd, *J* = 23.3, 9.1, 4.7 Hz), -141.5 (ddd, *J* = 23.5, 9.0, 4.9 Hz), -141.8 (dt, *J* = 23.5, 7.0 Hz), -142.3 (ddd, *J* = 23.6, 9.1, 4.6 Hz), -151.2 (t, *J* = 21.4 Hz), -151.5 (t, *J* = 20.7 Hz), -152.2 (t, *J* = 20.5 Hz), -152.5 (t, *J* = 20.5 Hz), -158.5 (ddd, *J* = 23.1, 20.6, 8.9 Hz), -159.1 (ddd, *J* = 23.7, 20.7, 8.7 Hz), -159.5 (ddd, *J* = 23.3, 20.4, 8.9 Hz), -159.7 (td, *J* = 22.0, 8.3 Hz), -159.7 – -160.0 (m), -161.4 (ddd, *J* = 24.0, 21.4, 8.2 Hz). **ESI-HRMS** calcd for $C_{23}H_{16}F_5NO$ $[M+H]^+$ 418.1230, found 418.1235.

1-(1,2,2a,3,5,10-hexahydro-5,10-ethenobenzo[f]cyclobuta[c]indol-4(4aH)-yl)pent-4-yn-1-one (Dia 1)

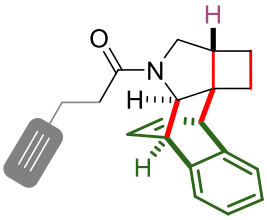

Product **4k** (Dia 1) was obtained as a single diastereomer following general procedure **GB-3B** from the corresponding allene (26.3 mg, 0.15 mmol). Transparent oil (16.5 mg, 36% yield). Two rotamers are observed due to the dynamic rotation of the amide. **^{1}H NMR** (600 MHz, $CDCl_3$) δ 7.26 – 7.04 (m, 4H RotA, 4H RotB), 6.61 (ddd, *J* = 7.7, 6.1, 1.5 Hz, 1H RotB), 6.53 (ddd, *J* = 7.7, 6.1, 1.6 Hz, 1H RotA), 6.38 – 6.35 (m, 1H RotA, 1H RotB), 4.67 (ddd, *J* = 5.5, 3.1, 1.6 Hz, 1H RotA), 4.17 (ddd, *J* = 5.9, 3.0, 1.5 Hz, 1H RotB), 4.09 (d, *J* = 3.1 Hz, 1H RotA), 3.88 (dd, *J* = 6.1, 1.4 Hz, 1H RotB), 3.85 – 3.82 (m, 1H RotA, 2H RotB), 3.49 (dd, *J* = 10.2, 6.0 Hz, 1H RotA), 3.40 (d, *J* = 10.2 Hz, 1H RotA), 3.31 (dd, *J* = 12.0, 6.0 Hz, 1H RotB), 2.76 – 2.42 (m, 5H RotA, 5H RotB), 2.09 – 1.94 (m, 3H RotA, 3H RotB), 1.60 – 1.50 (m, 2H RotA, 2H RotB). **^{13}C NMR** (151 MHz, $CDCl_3$) δ 169.9, 141.5, 141.2, 135.6, 134.4, 133.8, 132.2, 126.1, 125.9, 125.8, 125.6, 124.5, 124.2, 123.8, 83.7, 72.2, 71.8, 69.0, 68.7, 56.0, 51.1, 47.2, 43.9, 42.0, 41.1, 34.3, 33.3, 30.8, 21.6, 21.4, 15.0, 14.4. **ESI-HRMS** calcd for $C_{21}H_{21}NNaO$ $[M+Na]^+$ 326.1521, found 326.1523.

1-(1,2,2a,3,5,10-hexahydro-5,10-ethenobenzo[f]cyclobuta[c]indol-4(4aH)-yl)pent-4-yn-1-one (Dia 2)

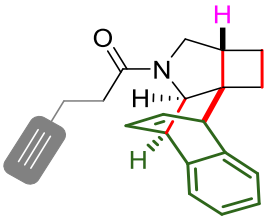

Product **4k'** (Dia 2) was obtained as a single diastereomer following general procedure **GP-3B** from the corresponding allene (26.3 mg, 0.15 mmol). Transparent oil (14.7 mg, 31% yield). Two rotamers are observed due to the dynamic rotation of the amide. **^{1}H NMR** (600 MHz, $CDCl_3$) δ 7.16 – 7.05 (m, 4H RotA, 4H RotB), 6.60 – 6.47 (m, 2H RotA, RotB), 4.56 (ddd, *J* = 6.2, 3.3, 1.4 Hz, 1H RotA), 4.28 (d, *J* = 3.2 Hz, 1H RotA), 4.08 (ddd, *J* = 6.2, 3.2, 1.2 Hz, 1H RotB), 4.03 (d, *J* = 3.1 Hz, 1H RotB), 3.83 (dd, *J* = 6.0, 1.4 Hz, 1H RotB), 3.79 (dd, *J* = 5.8, 1.5 Hz, 1H RotA), 3.41 (d, *J* = 12.2 Hz, 1H RotB), 2.94 (d, *J* = 10.3 Hz, 1H RotA), 2.81 – 2.62 (m, 4H RotB), 2.55 – 2.45 (m, 2H RotA), 2.35 (ddd, *J* = 15.3, 8.3, 6.8 Hz, 1H RotA), 2.25 (td, *J* = 8.1, 5.5 Hz, 1H RotA), 2.20 – 2.07 (m, 2H RotA, Rot B), 2.03 (t, *J* = 2.6 Hz, 1H RotB), 1.99 – 1.93 (m, 3H RotA, 2H RotB), 1.68 (dd, *J* = 10.4, 5.7 Hz, 1H RotA, 1H RotB), 1.56 – 1.48 (m, 1H RotA, 1H RotB). **^{13}C NMR** (151 MHz, $CDCl_3$) δ 169.7, 141.0, 140.0, 135.1, 134.3, 134.1, 133.4, 126.4, 126.2, 126.0, 125.7, 125.1, 124.8, 124.0, 123.8, 83.7, 71.3, 70.6, 69.0, 68.7, 54.9, 54.3, 50.8, 43.7, 41.4, 40.5, 34.0, 33.3, 30.9, 20.9, 20.7, 15.0, 14.3. **ESI-HRMS** calcd for $C_{21}H_{21}NNaO$ $[M+Na]^+$ 326.1521, found 326.1523.

Furan-2-yl(1,2,2a,3,5,10-hexahydro-5,10-ethenobenzo[f]cyclobuta[c]indol-4(4aH)-yl)methanone

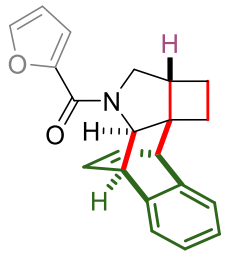

Product **4l** was obtained as a mixture of diastereomers (65:35) following general procedure **GP-3B** from the corresponding allene (28.4 mg, 0.15 mmol). Pale yellow oil (39.0 mg, 82% yield). Two rotamers are observed due to the dynamic rotation of the amide. **^{1}H NMR** (400 MHz, $CDCl_3$) δ 7.64 – 7.61 (m, 2H RotB), 7.53 (t, Dia2, *J* = 1.2 Hz, 1H RotA), 7.43 (d, Dia2, *J* = 1.6 Hz, 1H RotA), 7.34 – 7.08 (m, Dia1, 5H RotA, 6HRotB; Dia2 5H RotA, 5H RotB), 6.81 (d, Dia 1, *J* = 3.4 Hz, 1H RotA), 6.62 – 6.42 (m, Dia1, 3H RotA, 3H RotB; Dia2, 3H RotA, 3H RotB), 4.75 (d, Dia 2, *J* = 3.1 Hz, 1H RotB), 4.72 (ddd, Dia2 = 5.4, 3.2, 1.6 Hz, 1H RotA), 4.62 – 4.58 (m, Dia1, 2H RotA, 2H RotB; Dia2, 1H RotB), 4.42 (d, Dia2 *J* = 3.1 Hz, 1H RotA), 4.07 – 4.02 (m, 1H RotB), 3.99 – 3.96 (m, 1H RotB), 3.91 – 3.84 (m, Dia 1, 1H RotA; Dia2, 3H RotA; 1H RotB), 3.56 (dd, *J* = 12.5, 6.1 Hz, 1H RotB), 3.49 (d, *J* = 12.5 Hz, 1H RotB), 3.42 (d, Dia1, *J* = 11.1 Hz, 1H RotA), 2.82 – 2.68 (m, Dia2, 1H RotA, 1H RotB), 2.38 – 2.33 (m, Dia 1, 1H RotA, 1H RotB), 2.27 – 1.94 (m, Dia 1, 3H RotA, 2H RotB; Dia2, 1H RotA, 1H RotB), 1.77 – 1.71 (m, 1H RotB), 1.68 – 1.55 (m, Dia2, 1H RotA, 1H RotB). **^{13}C NMR** (101 MHz, $CDCl_3$) δ 158.5, 158.3, 149.1, 148.9, 148.4, 144.1, 144.1, 144.0, 143.8, 141.6, 141.4, 141.0, 140.0, 135.4, 134.9, 134.4, 134.1, 133.9, 133.6, 132.3, 126.3, 126.0, 125.7, 125.6, 125.0, 124.9, 124.6, 124.1, 123.8, 123.7, 123.6, 117.1, 116.9, 116.1, 115.6, 111.8, 111.7, 111.4, 111.1, 72.5, 71.9, 71.2, 57.8, 57.0, 56.9, 56.3, 55.4, 54.7, 54.6, 53.9, 51.0, 50.8, 50.7, 47.5, 43.9, 43.9, 42.7, 42.0, 40.1, 39.6, 31.2, 31.0, 30.9, 30.8, 21.5, 21.4, 20.8, 20.7. **ESI-HRMS** calcd for $C_{21}H_{20}NO_2$ $[M+H]^+$ 356.1053, found 356.1058.

1-(2,2a,3,4,6,11-hexahydro-1H-6,11-ethenobenzo[g]cyclobuta[d]quinolin-5(5aH)-yl)ethan-1-one

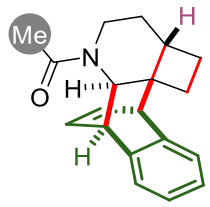

Product **4m** was obtained as a single diastereomer following general procedure **GP-3B** from the corresponding enallene (23.0 mg, 0.15 mmol). White solid (18.8 mg, 45% yield). Two rotamers are observed due to the dynamic rotation of the amide. **^{1}H NMR** (400 MHz, $CDCl_3$) δ 7.28 – 7.04 (m, 4H RotA, 4H RotB), 6.65 – 6.55 (m, 2H RotA, 2H RotB), 4.24 – 4.11 (m, 1H RotA, 1H RotB), 4.04 – 3.93 (m, 2H RotA, 1H RotB), 3.86 – 3.79 (m, 1H RotB), 3.47 (s, 1H RotB), 3.22 – 3.13 (m, 1H RotA), 2.46 – 2.24 (m, 1H RotA, 4H RotB), 2.19 – 2.04 (m, 4H RotA, 1H RotB), 1.98 – 1.82 (m, 2H RotA, 2H RotB), 1.61 – 1.45 (m, 2H RotA, 2H RotB), 1.25 – 0.97 (m, 2H RotA, 1H RotB), 0.70 – 0.59 (m, 1H RotB). **^{13}C NMR** (101 MHz, $CDCl_3$) δ 170.4, 169.9, 142.6, 142.2, 141.0, 139.5, 135.5, 134.9, 133.8, 133.2, 125.9, 125.6, 125.2, 125.1, 124.88, 124.85, 124.5, 64.9, 61.2, 50.4,

50.2, 48.9, 46.0, 42.2, 41.2, 40.9, 38.4, 38.2, 36.4, 31.9, 31.7, 29.1, 28.4, 23.4, 23.2, 22.9, 21.8. **ESI-HRMS** calcd for $C_{19}H_{22}NO$ $[M+H]^+$ 280.1696, found 280.1700.

N-((1,4-dihydro-1,4-ethanonaphthalen-9-ylidene)methyl)-N-(pent-4-en-1-yl)benzamide

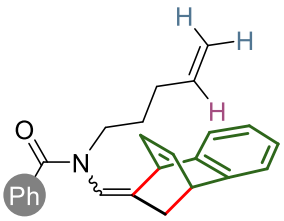

Product **4'n** was obtained as a mixture of diastereomers (59:41) following general procedure **GP-3B** from the corresponding allene (34.0 mg, 0.15 mmol). Pale yellow oil (23.5 mg, 44% yield). The reaction required 72 h of irradiation to fully consume the starting material. **^{1}H NMR** (400 MHz, $CDCl_3$) δ 7.64 – 7.55 (m, Dia1, 1H; m, Dia2, 1H), 7.31 (d, Dia1, *J* = 8.4 Hz, 2H; d, Dia2, *J* = 8.4 Hz, 2H), 7.24 – 7.03 (m, Dia1, 6H; m, Dia2, 6H), 6.51 – 6.32 (m, Dia1, 2H; m, Dia2, 2H), 6.12 (s, Dia1, 1H), 5.89 – 5.75 (m, Dia1, 1H; m, Dia2, 1H), 5.70 (t, Dia2, *J* = 6.7 Hz, 1H), 5.11 – 4.92 (m, Dia1, 2H; m, Dia2, 2H), 4.44 (d, Dia2, *J* = 6.0 Hz, 1H), 4.23 (d, Dia1, *J* = 5.9 Hz, 1H), 3.94 (d, Dia1, *J* = 16.5 Hz, 1H; d, Dia2, *J* = 16.5 Hz, 1H), 3.86 – 3.75 (m, Dia2, 1H), 3.59 – 3.39 (m, Dia1, 2H; Dia2, 1H), 2.20 – 1.96 (m, Dia1, 4H; m, Dia2, 4H), 1.91 – 1.56 (m, Dia1, 2H; m, Dia2, 2H). **^{13}C NMR** (101 MHz, $CDCl_3$) δ 170.2, 170.0, 143.9, 143.2, 140.5, 138.1, 137.9, 136.4, 136.2, 136.1, 135.8, 135.0, 133.1, 132.0, 130.0, 129.7, 128.8, 128.6, 127.9, 127.6, 125.7, 125.5, 125.5, 125.5, 123.4, 122.9, 122.8, 121.2, 115.0, 48.4, 48.3, 46.8, 43.7, 40.7, 40.5, 33.5, 32.9, 31.3, 31.2, 26.7, 26.6. **ESI-HRMS** calcd for $C_{25}H_{26}NO$ $[M+H]^+$ 356.2014, found 356.2020.

Ethyl 1,2,2a,3,5,10-hexahydro-5,10-ethenobenzo[f]cyclobuta[c]indole-4(4aH)-carboxylate

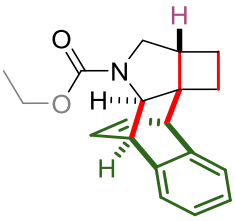

Product **4o** was obtained as a mixture of diastereomers (77:23) following general procedure **GP-3B** from the corresponding allene (25.1 mg, 0.15 mmol). White solid (24.5 mg, 55% yield).

Product **4o** was further purified to obtain diastereomer **E**. Two rotamers are observed due to the dynamic rotation of the carbamate. **^{1}H NMR** (600 MHz, Acetone-*d6*) δ 7.25 – 7.22 (m, 1H RotA, 1H RotB), 7.14 – 7.07 (m, 3H RotA, 3H RotB), 6.60 (ddd, *J* = 7.5, 5.8, 1.4 Hz, 1H RotA, 1H RotB), 6.50 (ddd, *J* = 7.7, 6.1, 1.5 Hz, 1H RotA, 1H RotB), 4.46 (ddd, *J* = 6.2, 3.3, 1.4 Hz, 1H RotA), 4.35 – 4.24 (m, 2H RotB), 4.13 – 3.99 (m, 3H RotA, 2H RotB), 3.94 (dt, *J* = 5.8, 1.7 Hz, 1H RotA, RotB), 3.02 (dd, *J* = 14.8, 10.9 Hz, 1H RotA, 1H RotB), 2.27 – 2.17 (m, 2H RotA, 2H RotB), 2.00 – 1.94 (m, 2H RotA, 2H RotB), 1.61 – 1.54 (m, 2H RotA, 2H RotB), 1.36 (t,

J = 7.1 Hz, 3H RotB), 1.17 (t, *J* = 7.1 Hz, 3H RotA). **^{13}C NMR** (151 MHz, Acetone-*d6*) δ 154.3, 154.1, 141.2, 141.2, 140.1, 139.9, 134.7, 134.6, 133.6, 133.6, 125.7, 125.6, 125.5, 125.5, 124.7, 124.6, 123.9, 70.8, 70.1, 60.3, 60.0, 56.4, 55.2, 53.6, 53.3, 50.5, 45.8, 44.3, 41.3, 40.6, 30.5, 20.7, 20.6, 14.4, 14.2. **ESI-HRMS** calcd for $C_{19}H_{21}NO_2$ $[M+H]^+$ 296.1651, found 296.1657.

Tert-butyl 1,2,2a,3,5,10-hexahydro-5,10-ethenobenzo[f]cyclobuta[c]indole-4(4aH)-carboxylate

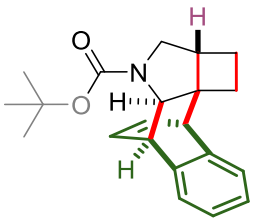

Product **4p** was obtained as a mixture of diastereomers (68:32) following general procedure **GP-3B** from the corresponding enallene (29.9 mg, 0.15 mmol). White viscous oil (29.8 mg, 61% yield). Two rotamers are observed due to the dynamic rotation of the carbamate.

Product **4p** was further purified to obtain major diastereomer. **^{1}H NMR** (400 MHz, $CDCl_3$) δ 7.16 – 7.05 (m, 4H RotA, 4H RotB), 6.58 – 6.51 (m, 2H RotA), 6.49 – 6.43 (m, 2H RotB), 4.56 – 4.52 (m, 1H RotA), 4.30 – 4.26 (m, 1H RotB), 4.04 (d, *J* = 3.3 Hz, 1H RotA), 3.91 (d, *J* = 3.2 Hz, 1H RotB), 3.80 – 3.76 (m, 1H RotA, 1H RotB), 3.06 (d, *J* = 11.2 Hz, 1H RotB), 2.94 (d, *J* = 11.1 Hz, 1H RotA), 2.22 – 1.91 (m, 4H RotA, 4H RotB), 1.64 – 1.53 (m, 2H RotA, 11H RotB), 1.43 (s, 9H RotA). **^{13}C NMR** (101 MHz, $CDCl_3$) δ 154.6, 154.2, 141.1, 140.8, 140.2, 139.6, 134.7, 134.3, 134.1, 133.7, 126.1, 125.8, 125.7, 125.5, 124.9, 124.8, 123.75, 123.68, 79.4, 79.0, 70.4, 70.3, 56.4, 55.4, 53.9, 53.5, 50.9, 45.8, 44.2, 41.3, 40.7, 31.0, 30.9, 28.8, 28.5, 21.0, 20.9. **ESI-HRMS** calcd for $C_{21}H_{25}NNaO_2$ $[M+Na]^+$ 346.1778, found 346.1771.

Chapter 2:

'Synthesis of Strained Heterocycles from Allenamides via Energy-Transfer Relay'

From this chapter:

Manuscript in preparation

Introduction

In Chapter 1, a new method to dearomatize naphthalene in an intermolecular fashion using allenamides as an arenophiles has been presented. The reaction allowed the synthesis of [2.2.2]-bicyclooctene units starting from sp^2-rich compounds.[1] However, when the scope of this transformation was studied, specifically with enallenamide **1a**, a product different from the expected one was isolated under the optimized conditions. After careful investigation, a 'crossed' [2+2] cycloaddition product was hypothesized (Scheme 1).

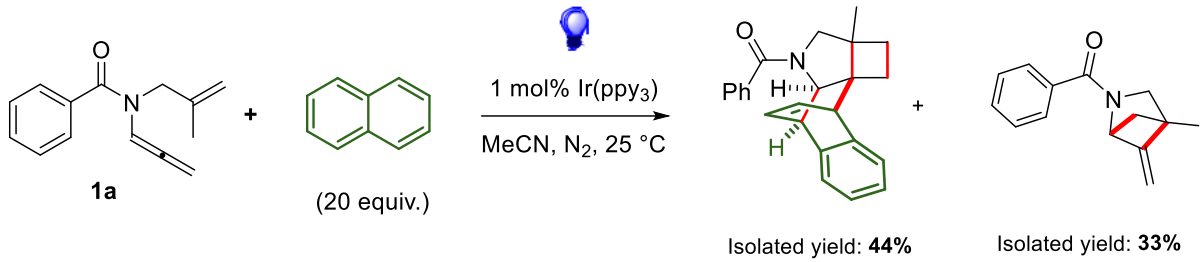

Scheme 1: Case scenario of substrate **1a**: mixture of products obtained.

The nature of the product was confirmed through XRD analysis. In literature, it is well known that these Csp^3-rich, three-dimensional ring systems are valuable scaffolds in modern medicinal chemistry.[2] These saturated, conformationally restricted architectures appear to serve as important bio-isosteres of benzene[3] and structural replacements that preserve biological activity, offering multiple advantages over traditional flat and aromatic systems.[4] The increased three-dimensionality enhances the overall physicochemical profile of drug candidates, improving properties such as metabolic stability, aqueous solubility and, as a consequence of that also membrane permeability in human tissues. Additionally, their more complex spatial arrangement can improve the selectivity and specificity of ligand–target interactions, helping to reduce off-target effects thanks to the possibility of having a design in/out-of-plane of substituents, adjusting the molecular shape as well as tuning the receptor/ligand complementarity.[5] As a matter of fact, these molecules are becoming increasingly important for pharmaceutical development, as reported in Scheme 2, and new ways to obtain them through strategies featuring complete atom economy are always worth noticing.

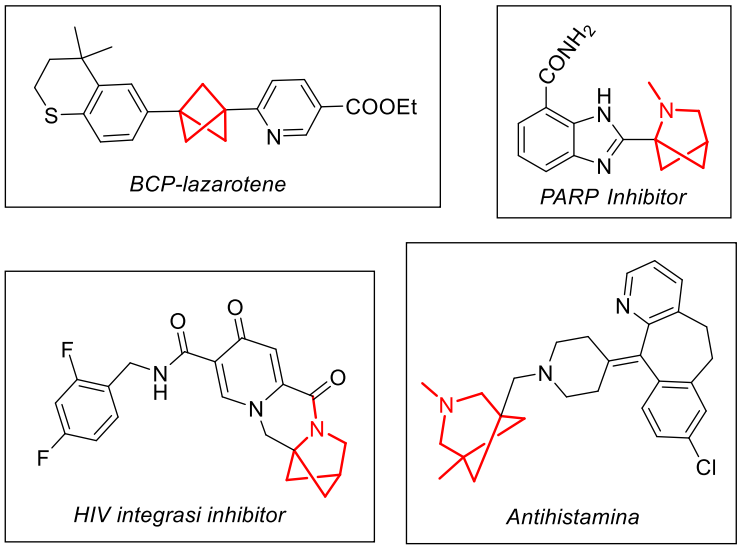

Scheme 2: Examples of the activity of different three-dimensional ring systems in medicinal chemistry.

While these molecules are undoubtedly attractive for pharmaceutical applications, an equally important aspect lies in how they are synthesized. Only a few methods for the construction of these molecules have been reported in the literature, and each of them presents specific limitations or challenges. Among the possible synthetic strategies, the intramolecular [2+2] cyclization of enallenes represents a particularly attractive approach. For this reason, it is important to examine in detail the potential [2+2] cyclization pathways available to a generic enallene. Depending on the geometry, the tether length, and the chemical nature of the starting material, four distinct products can be envisioned, as reported in Scheme 3.[6]

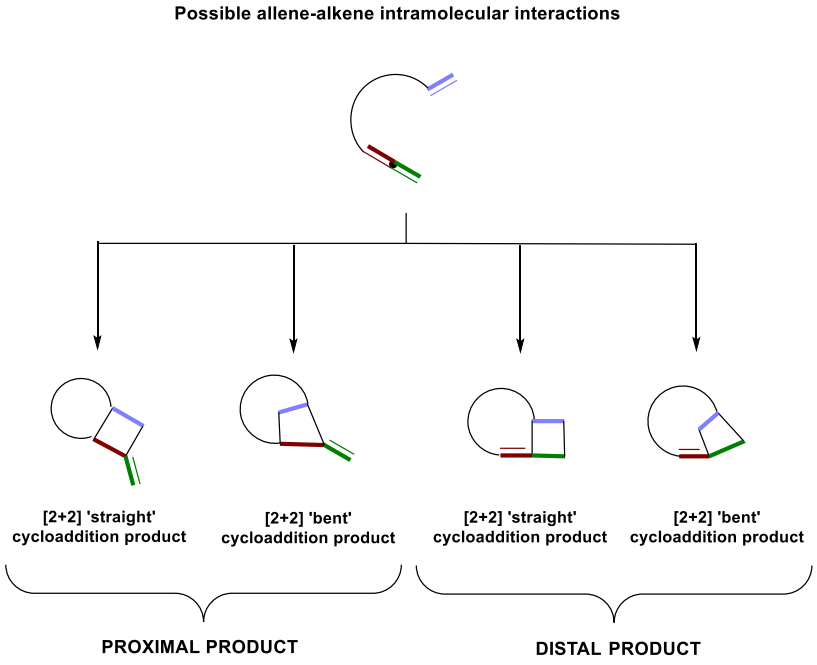

Scheme 3: Possible intramolecular reaction pathways for an enallene specie.

More specifically, it is possible to distinguish between 2 classes of products for a cycloaddition of an enallene. The first one is a proximal product where the internal double bond of the allene is involved in the transformation, and the second one is a distal product in which the external double bond is involved instead. Between these two classes, in both cases, two possible products can be hypothesized: a straight and a bent one.

Pioneering works by Padwa's group have shown a thermal intramolecular [2+2] cycloaddition regarding the formation of a distal product.[7] Starting from a non-activated allene, several α-tethered allenyl sulfones afforded the products in excellent yields with complete stereospecificity. The initial rate-determining carbon-carbon bond formation occurs between the central allene carbon and the proximal alkene carbon atom. Evidently, the straight product is favored because the 1,6-exo-trig cyclization is faster than the 1,7-endo-trig one (Scheme 4).

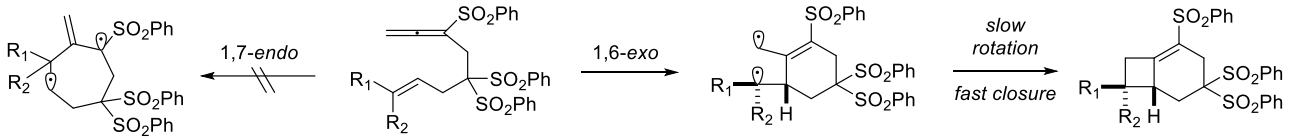

Scheme 4: Stereospecificity of the [2+2] cycloaddition of allenyl sulfones.

For a proximal approach instead, a remarkable example was reported by Carreira in 1994, involving the straight photocycloaddition of tert-butyl-substituted allenes with enones to give products in excellent yields and up to 99% of asymmetric induction (Scheme 5).[8]

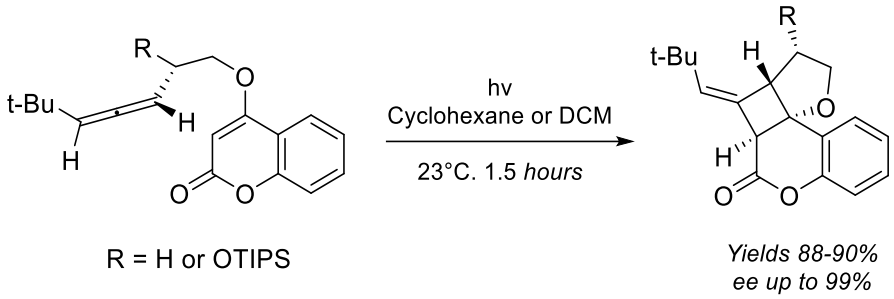

Scheme 5: Diastereoselective [2+2] photocycloaddition of allenic coumarins.

Another important work comes from Hiemstra in 2006, in which they examined another straight [2+2] photocycloaddition.[9] The reaction proceeded, leading to a single product in a moderate yield. The exclusive formation of one compound emphasizes the great preference for five-membered ring formation in the intramolecular [2+2] cycloaddition (Scheme 6).

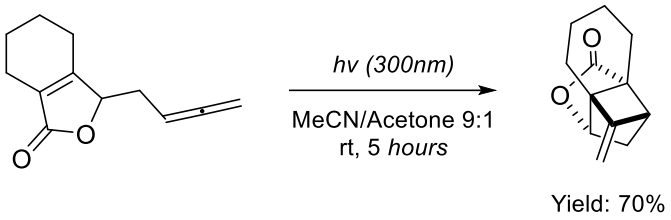

Scheme 6: Examination of the intramolecular [2+2] photocycloaddition by Hiemstra.

From the literature, it's clear that a reaction pathway in which an activated allene reacts with an alkene, giving a proximal or a distal product through a 'crossed' [2+2] cycloaddition is missing.

Interestingly, the byproduct described in Scheme 1 represents a significant example of a crossed [2+2] proximal cycloadduct. This observation highlights the relevance of further optimizing the developed transformation.

Similar products were already reported in the literature through the use of different reagents. The first reports go back to 1988 by Clardy and co-workers when they achieved the formation of the 2-azabicyclo[2.1.1]hexane skeleton through a [2+2] cycloaddition of appropriate protected amino acid derivatives under the influence of UV light (Scheme 7).[10]

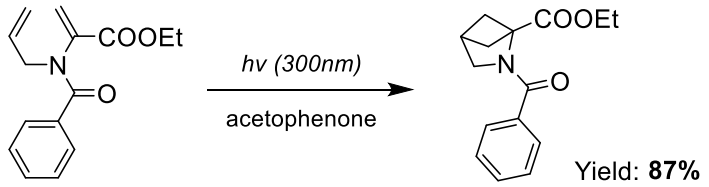

Scheme 7: First report for the synthesis of 2-azabicycles[2.1.1]hexanes by Clardy in 1988.

This elegant photocatalyzed transformation occurred in brief reaction times with high yields, but the use of highly conjugated systems, necessary for the reaction to occur, as well as the need to perform the reaction using low wavelengths, is something that inevitably introduces limitations, such as the stability of some useful functional groups.

Later, in 1996 and in 1998, respectively, De Kimpe reported a way to synthesize this scaffold via 3-(chloromethyl)cyclobutanone, while Yuan and co-workers developed a novel synthesis directly from pyridine.[11-12] These synthetic ways presented some criticalities, such as low selectivity and a high number of synthetic steps that affected the final yield. However, these reactions are an inspiration for more modern approaches.

In fact, more recently, Leitch's group in 2022 reported an interesting synthetic way (Scheme 8).[13]

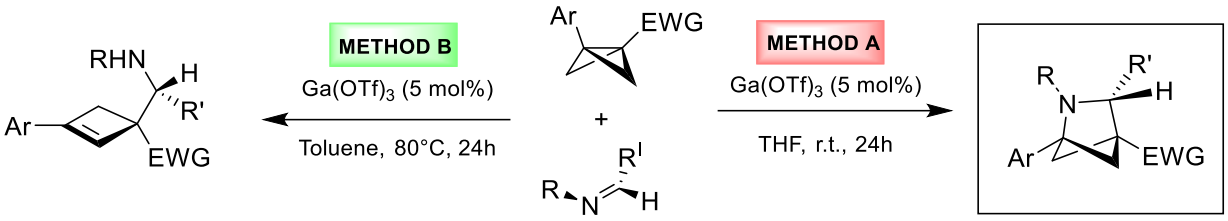

Scheme 8: Leitch's approach for getting interesting 2-azabicycles[2.1.1]hexanes.

The development of two divergent and complementary Lewis acid-catalyzed additions of bicyclobutanes to imines was described. It is reported that *N*-arylimines can undergo formal (3+2) cycloaddition with bicyclobutanes, exploiting their steric tension, to yield azabicyclo[2.1.1]hexanes in a single step. Under similar reaction conditions, the same can undergo an addition/elimination sequence to generate cyclobutenyl methanamine products with high diastereoselectivity. Even so, the authors presented a limited reaction generality due to the necessity of having an EWG group on the cyclobutene core.

In 2020, Mykhailiuk and later Salomè and co-workers in 2022 both reported a way to synthesize similar strained structures employing highly conjugated systems.[14-15] As reported in Scheme 9, in this case the products involved are distinguished by a carbon-based core obtained in very brief reaction times.

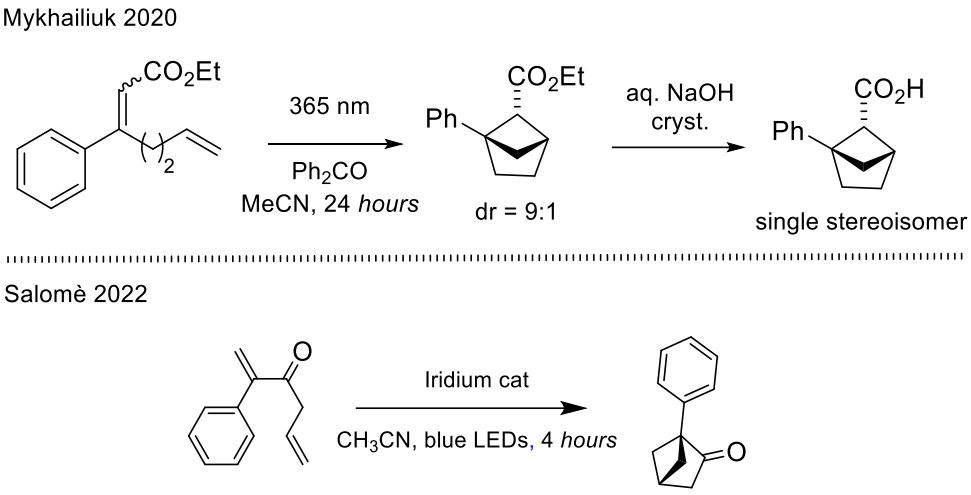

Scheme 9: Carbon-based bicycles implemented by Salomè and co-workers.

In the first case, a way to obtain saturated bio-isosteres of ortho-substituted benzenes from conjugated substrates has been validated. In the second, thanks to an iridium catalyst which acts as a sensitizer, similar systems achieved ring closure, delivering once again carbon-based products very similar to the aza-bicycles discussed before. Even if carbon-based, these highly saturated products present great potential but once again the scope is particularly limited. Instead, the complete atom economy as well as the rapidity in which the transformations occur are both peculiarities of interest and novelty.

More recently, in 2025, Jiang and co-workers expanded this chemistry, proposing an asymmetric approach to perform an intramolecular [2+2] photocycloaddition enabled by a dual catalytic system comprising 5,6-bis(5-methoxythiophen-2-yl)pyrazine-2,3-dicarbonitrile (DPZ) as a photosensitizer and a Sc(III) complex with a chiral ligand (Scheme 10).[16]

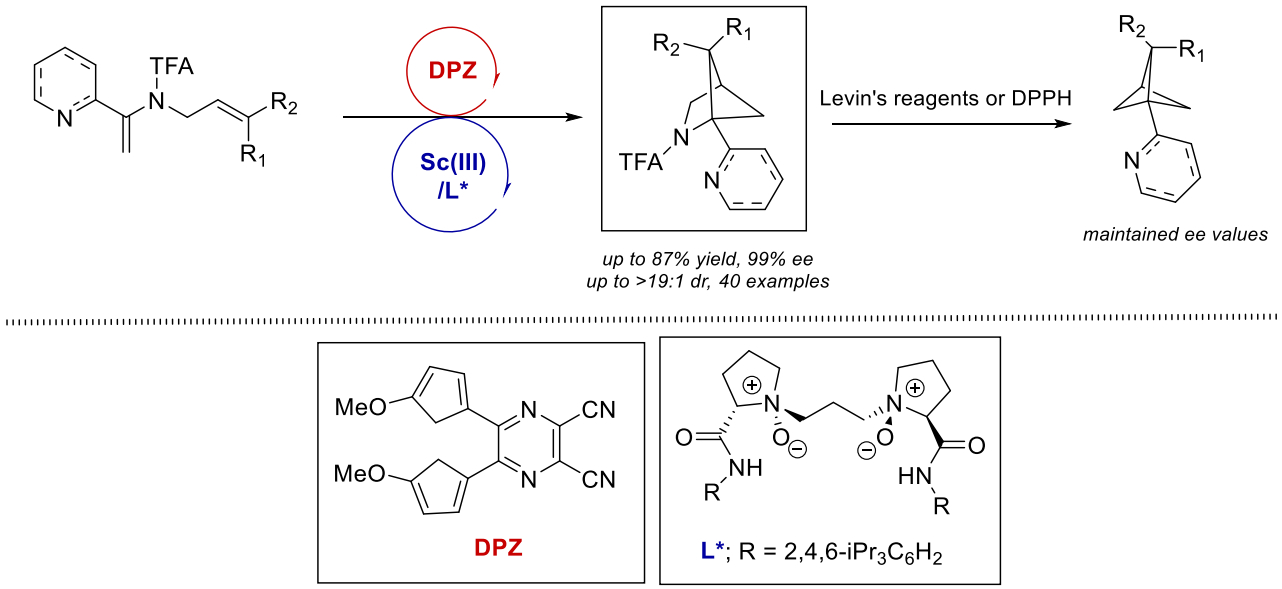

Scheme 10: Asymmetric Intramolecular [2+2] cycloaddition reaction.

This strategy facilitates the synthesis of functionalized 2-azabicyclo[2.2.1]hexanes (aza-BCHs) with high enantioselectivity. Additionally, preserving enantiomeric purity, the authors proposed a nitrogen-deletion skeletal editing of the aza-BCHs, enabling the formation of 2-substituted bicyclo[1.1.1]pentanes (BCPs) with modest substrate scope. Even if the reaction is limited by the necessity to have a high conjugation, the use of simple aza-arene substrates with chiral Lewis acids under asymmetric photocatalytic conditions, as well as the construction of all-carbon quaternary stereocenters, represents a significant advancement in the field.

The common feature of these transformations is the formation of highly saturated cores with great interest in the pharmaceutical field. On the other hand, another similar aspect is the limitation in achieving a broad product scope, a feature that still highlights the presence of huge constraints in current literature.

Results and discussion

In this chapter, a crossed [2+2] cycloaddition of allenamides is presented. This reaction is generally underdeveloped in literature due to the challenges in balancing the main factors that rule this transformation, such as the geometry, the length of the alkenyl arms and the steric effects of the substituents. On the other hand, this reaction results in being very interesting because of the nature of the products that can possibly be achieved. Exploiting allenamides, we triggered the formation of strained azabicyclic structures that were synthesized in high yields. In fact, in this photocatalytic sequence, we underline the importance of the role played by a binaphthyl co-catalyst, which, through a long and precise optimization, has been selected from a large library of additives efficiently synthesized in our laboratory. This additive, thanks to its redox properties and to its high E_T, does not compete with the role of the photocatalyst and does not hamper the activation of the substrate, but, on the contrary, it is responsible for the high selectivity reached and for the lower reaction time achieved (Scheme 1).

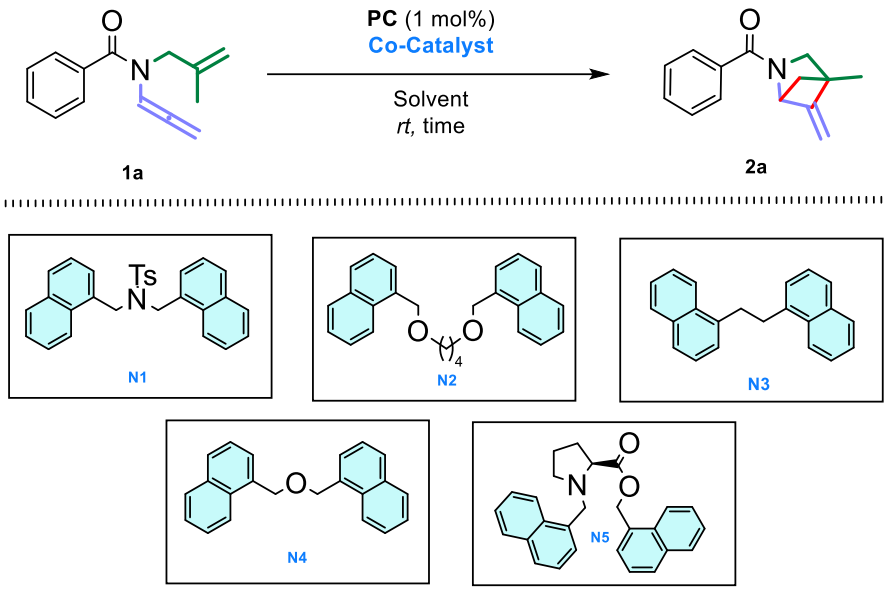

Scheme 1: General reaction for the synthesis of 2-azabicyclo[2.1.1]hexanes.

The strained heterocycles obtained through this catalytic process are known as 2-azabicyclo[2.1.1]hexanes (also abbreviated as aza-BCHs), and they are considered emerging scaffolds and bio-isosteres of pyridine and benzene in medicinal chemistry. The discovery of a visible-light-promoted reaction that occurs under mild conditions and with 100% atom economy proved to be highly appealing from a synthetic point of view. Thus we started an optimization effort (Table 1) for the model reaction reported (Scheme 1).

Entry	Catalyst (1 mol%)	Co-Catalyst	Solvent	Yield of **2a** [%][b]	Deviation time in respect to [a]
1	PC1	-	MeCN	30	10 days
2	PC1	N1	MeCN	35	14 hours
3	PC1	N1	THF	30	10 hours
4	PC1	N1	Toluene	41	12 hours
5	PC1	N2	Toluene	40	12 hours
6	PC1	N3	Toluene	32	12 hours
7	PC1	N4	Toluene	31	12 hours
8	PC1	N5	Toluene	34	12 hours
9[c]	PC5	N1	Toluene	44	10 hours
10[c]	PC4	N1	Toluene	44	10 hours
11	PC2	N1	Toluene	37	/
12	PC3	N1	Toluene	47	/
13[e]	PC3	N1	Toluene	48	/
14[e] [f]	PC3	N1	Toluene	49	/
15[e] [f]	PC3	N3	Toluene	55	/
16[e] [f]	PC3	N2	Toluene	74	/
17[d], [e] [f]	PC3	N2	Toluene	63	/

Table 1: [a] Reaction conditions: 0.1 mmol of **1a** (0.1 M), 30 mol% of BiNP additive, 1 mol % of sensitizer, reaction irradiated for a total of **8 hours** with blue LEDS at 25°C; [b] ^{1}H-NMR yield calculated using 1,3,5-trimethoxybenzene as internal standard, [c] Irradiated with purple LEDs at 30°C; [d] without performing freeze pump of the reaction, [e] 0.05M of Toluene, [f] 15 mol% of BiNP additive. **PC1** = $[Ir(ppy)_3]$, PC2 = $Ir(p\text{-}CF_3\text{-}ppy)_3$, **PC3** = $Ir(p\text{-}F\text{-}ppy)_3$, **PC4** = $[Ir\{dFCF_3ppy\}_2(dtbbpy)]PF_6$, **PC5** = $[Ir[dF(CF_3)ppy]_2(Me_4phen)]BF_4$**.**

In Table 1 are reported just a few of the most important examples regarding the transformation. The investigation was initiated by an experiment conducted in a 0.1 M MeCN solution of **1a** and 1 mol% of $Ir(ppy)_3$ (**PC1**) that were charged into a 5-mm NMR tube and efficiently degassed by freeze−pump−thaw. These are the same conditions used for the intermolecular dearomatization of naphthalene shown in Chapter 1. The reaction system was then irradiated with a household blue LED strip, and after 10 days of irradiation, 30% yield of product **2a** was identified by ^{1}H-NMR with an internal standard. At the beginning, we studied different solvents, as reported by entries 2-4, but none outperformed toluene, even if different polarities, hydrogen bonding, as well as better solubility of the substrate were exploited. Then, in a previous paper[17], it was demonstrated that the use of a binaphthyl co-catalyst efficiently stabilizes the biradical intermediate, formed after the excitation of the allenamide, through dispersion interactions. This allows the employed co-catalyst to act as a triplet-state mediator, enhancing substrate excitation without competing with the photocatalyst. In this framework, the use of tethered naphthyl units enables the use of catalytic amounts of the additive while suppressing undesired dearomatization pathways that could arise using stochiometric quantities of

naphthalene derivatives instead. Additionally, owing to its favorable redox properties and high triplet energy, the additive preserves the primary role of the photocatalyst while ultimately enabling higher selectivity and significantly reducing reaction times. Thus, after having introduced the importance of employing a co-catalyst characterized by tethering two or more naphthyl units, also for this reaction, we decided to utilize one of them. So, we tested a variety of them to analyze how the reaction changes with respect to its nature, and as reported in Scheme 1, co-catalysts bearing different electronic and structural properties, as well as different steric hindrances, were tested. In Table 1, just a few of the most important results are reported, but as already seen with the solvents, it was difficult once again to improve the reaction yields. Then, the nature of the sensitizer involved was analyzed. Different Ir-based catalysts were tried under blue and purple LEDs irradiation. The described activity was observed always combining the best performing binaphthyl unit, in this case N1, with either a homoleptic or a heteroleptic iridium complex. Nevertheless, as reported by entries 9-12, once again no linear correlation between a single photophysical property of the **PC** (Scheme 2) and the outcome of the reaction was observed.

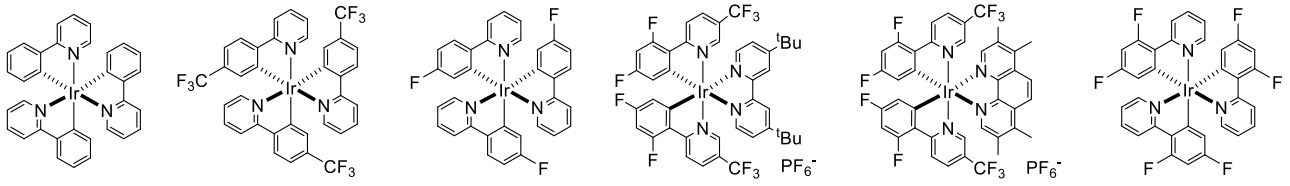

PC1 = Ir(ppy)$_3$, *58.1 kcal/mol*, 1.9 μsec

PC2 = Ir(p-CF$_3$-ppy)$_3$, *56.4 kcal/mol*, 2.2 μsec

PC3 = Ir(p-F-ppy)$_3$, *58.6 kcal/mol*, 2.0 μsec

PC4 = [Ir{dFCF$_3$ppy}$_2$(dtbbpy)]PF$_6$, *61.8 kcal/mol*, 2.3 μsec

PC5 = [Ir{dFCF$_3$ppy}$_2$(Me$_4$phen)]PF$_6$, *63.0 kcal/mol*, 3.8 μsec

PC6 = Ir(dFppy)$_3$, *63.5 kcal/mol*, 1.6 μsec

Scheme 2: Photophysical properties of the PC used.

Other key factors were then tested, such as the concentration of the mixture and the co-catalyst loading. The dilution of the reaction from 0.1 M to a 0.05 M reaction media brought to a slight improvement in reaction yields (entry 13). Instead, an increased yield to a 50% range to a satisfying 74% ^{1}H-NMR yield, as reported by entry 16, was achieved in 8 hours' time, lowering the co-catalyst loading to 15 mol% and performing crossed experiments. It is important to emphasize that high yields are obtained only with a specific combination of photocatalyst and co-catalyst, as both components must be finely matched to operate efficiently within the catalytic cycle. The best results were achieved combining N2 (15 mol%) with **PC3** (1 mol%) using toluene (0.05 M) as the solvent. The reaction then resulted to be sensitive to traces of dioxygen, a powerful triplet quencher, so this constrained us to foresee freeze-pump-thaw cycles. The degassing procedure represents an intrinsic practical limitation for a synthetic method, but it remains necessary to get improved yields (entry 17).

These experiments allowed us to finally generalize the process. The synthesis of a structurally diverse library of starting materials afforded more than 30 distinct compounds, summarized in Scheme 3.

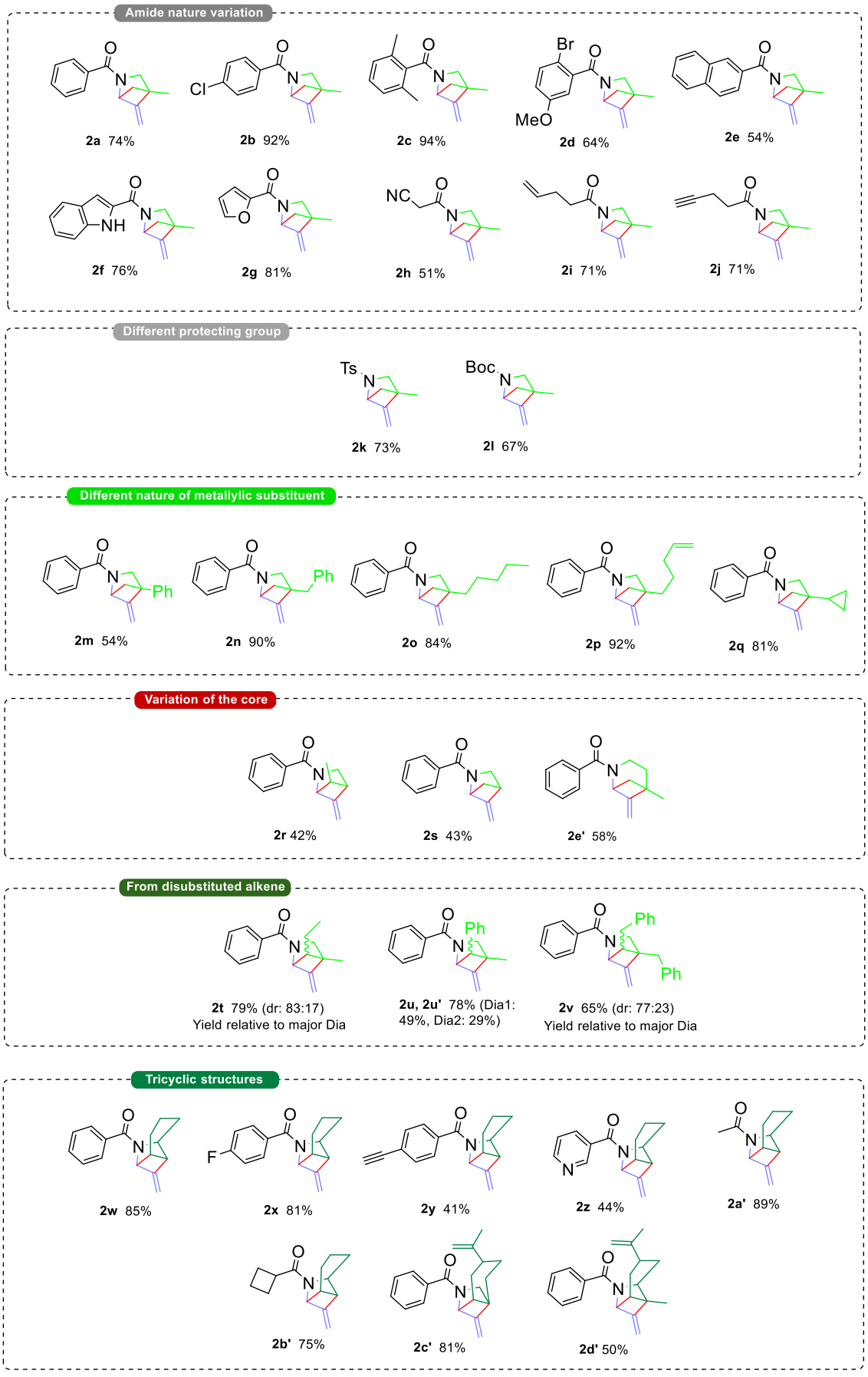

Scheme 3: Scope of 2-azabicycles[2.1.1]hexanes synthesized through crossed [2+2] cycloaddition.

After confirming that the reaction could be scaled up to 1 mmol without noticeable variations, we then undertook a detailed investigation of different substituents on the benzoyl unit, using compound **2a** as the reference substrate. We demonstrated that the presence of an electron-withdrawing group and an electron-donating group does not affect the reaction outcome; instead, the reaction benefits from this feature, achieving product yields above 90% (**2b**,**2c**). Furthermore, it has been demonstrated that heterocyclic units such as indole and furan led to the isolation of the products (**2f, 2g**). We then decided to perform the reaction in the presence of a cyano group as well as with an alkene and an alkyne fragment, with good results. Changing the protecting group for the nitrogen, with both the carbamate group and the sulfonamide group, proved to tolerate this chemistry in yields comparable to the model substrate (**2k**, **2l**). Then, we decided to vary the substituent in α-position to the double bond. Product **2m** shows the possibility to achieve crossed cycloaddition with a styrene unit in moderate yields. The method tolerates a cyclopropyl unit (**2q**) as well as a double bond without loss of efficiency (**2p**), with no polymerization or side reactions taking place. Another variation involved the study of crotyl and simple allyl moieties. These were tested and delightfully delivered the product, even if in low yields. This is probably due to a different substitution of the radical intermediate, passing from the formation of a more stable tertiary radical to a secondary one instead. However, product **2s** proved to be particularly interesting, as this compound also served as the model substrate for the dearomative para-cycloaddition described in Chapter 1. From a synthetic point of view, this indicates that the reaction outcome can be directed by adjusting the reaction conditions. Product **2e'** demonstrated that the reaction could lead to the formation of a bridged six-member ring cycle. We then tested the possibility of getting a product starting from a trisubstituted alkene. In this case, two diastereomers were obtained, as in the case of **2u** and **2u'**, or the single one, as with product **2t** or **2v**. To further broaden the scope of the reaction, we investigated its feasibility with cyclohexene as a possible substituent on the nitrogen. This approach proved to be successful, affording six distinct products in high yields. Notably, these compounds feature a tricyclic framework rather than the typical bicyclic structure. Tricyclic products **2c'** and **2d'** are particularly worthy since they derive from naturally occurring starting materials such as the enantiopure form of [S]-peryllic-alcohol and [S]-carveol.

We then analyzed the mechanism behind this transformation (Scheme 4).

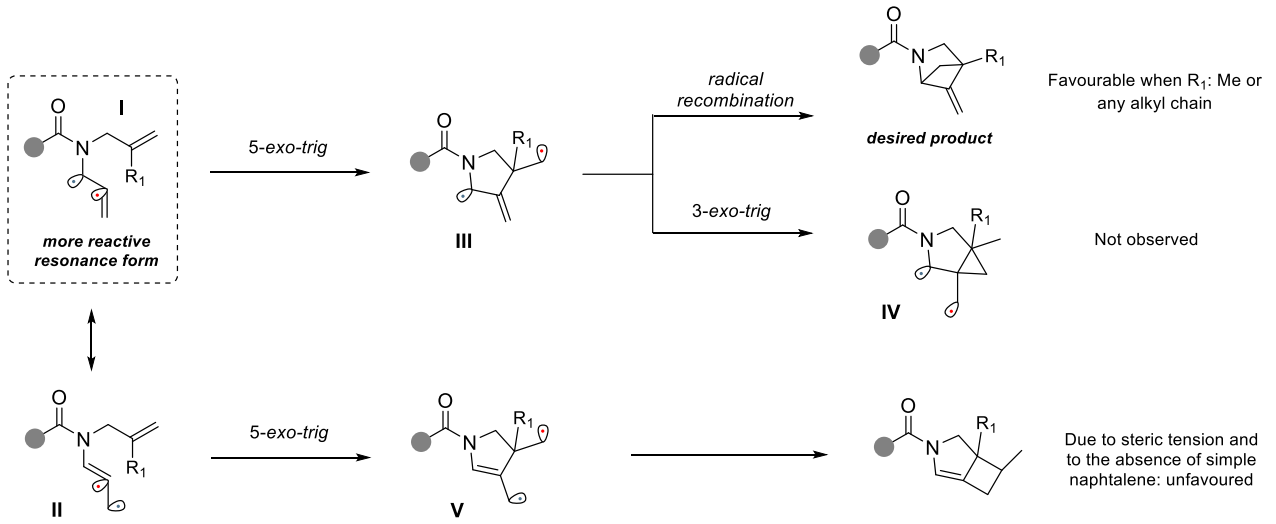

Scheme 4: Hypothesis of different reaction pathways involved.

The triplet state of the allenamide, which is a biradical represented by two resonance forms **I** and **II**, is reached thanks to the use of an Iridium-based catalyst paired with a co-catalyst. Resonance form **I** results to be the most stable, thanks to the close proximity of the nitrogen, which can stabilize the resulting radical. The vinyl radical, which is also the most unstable, attacks the tertiary carbon present in the molecule, giving intermediate **III**. Two possible pathways are then hypothesized: the first one involves the formation of the [2+2] crossed cycloaddition product through radical recombination. However, other non-negligible reactions seem to be feasible. In fact, when we have intermediate **III** still in a triplet state, another attack can occur, and this one involves a 3-exo-trig cyclization that leads to the formation of intermediate **IV**. Fortunately, any possible product derivatives have never been observed, probably because this cyclization is highly complex to happen. In Scheme 3, the possibility of achieving a 5-exo-trig cyclization, passing through intermediate **V**, is reported. However, the product deriving from radical recombination, due to the high ring tension, rapidly undergoes decomposition.

At this stage, the next step was to obtain more detailed insights into the mechanism of this photocatalytic sequence. Based on our previous findings, the co-catalyst used contributes to giving relative stabilization to the biradical involved. Fluorescence quenching experiments were performed to test the quenching of the substrate **1a** with the sensitizer and the quenching between the co-catalyst and the sensitizer. These two experiments allowed us to construct the relative Stern–Volmer plots (Scheme 5).

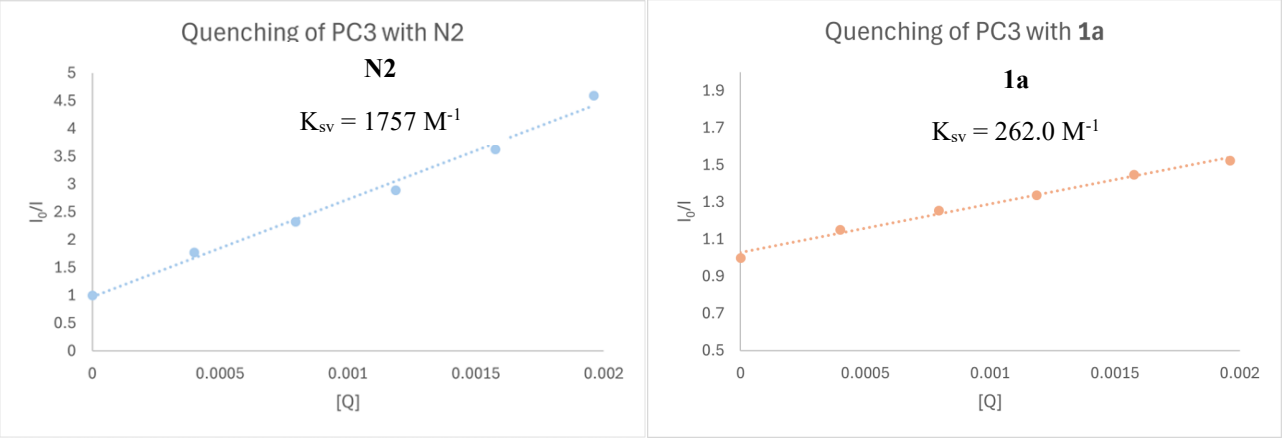

Scheme 5: Stern-Volmer analysis of the quenching between the sensitizer and the binaphthyl N2 or the sensitizer and the model substrate **1a**.

With respect to the higher Ksv observed, the iridium photocatalyst is better quenched by the co-catalyst. Successively, the co-catalyst is quenched by the substrate, which, in a triplet state, can give life to the described transformation in Scheme 6.[18]

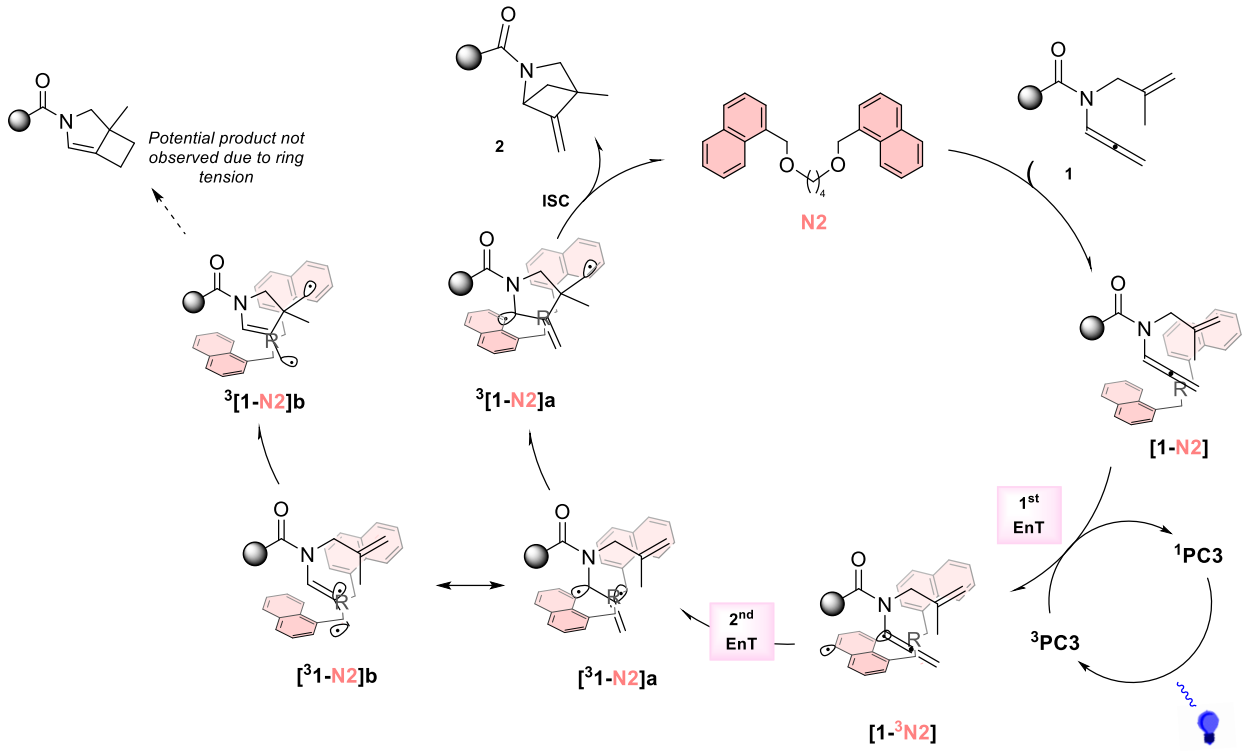

Scheme 6: Mechanistic hypothesis of the reaction involved.

Through activation of substrate **1** using **PC5** and the corresponding binaphthyl co-catalyst involved, the triplet state of the allenamide is reached. The binaphthyl contributes to giving relative stabilization of the biradical involved, resulting in increased concentration and lifetime. Then, the vinyl radical is able to attack the tertiary carbon of the metallyl moiety, delivering intermediate **^{3}[1-N2]a.** Through recombination, the release of the target product **2** is achieved, forming the aza-bicycle desired.

Kinetics studies were then performed. Through ^{1}H-NMR internal standard analysis, we conducted the reaction with and without the co-catalyst, analyzing the reaction progress over time in a toluene-*d*^{8} media (Scheme 7).

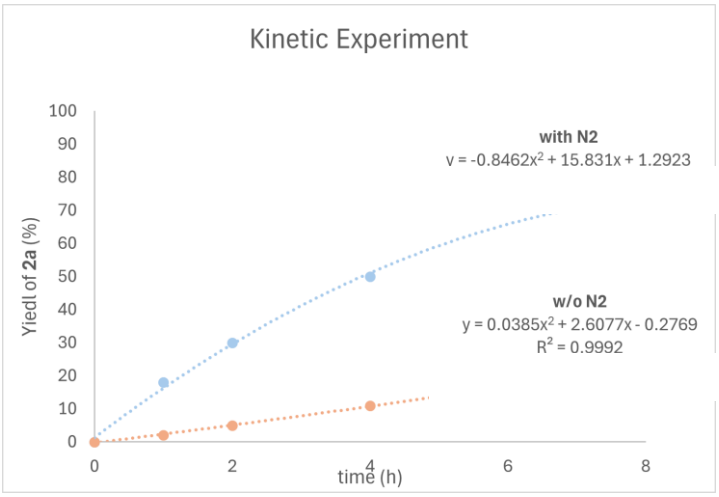

Scheme 7: Kinetic profile of the reaction with and without the presence of the co-catalyst.

What emerged with the co-catalyst present is a rapid decrease of the signals corresponding to the starting materials, while new ^{1}H-NMR peaks associated with the product emerge and intensify. Notably, after approximately 8 hours, the signals of the reactants disappear, indicating that the reaction has gone to completion. When the co-catalyst is absent, the reagent signals do not disappear. After 8 hour reaction time, the yield of the desired product was 24%, significantly lower than 74% obtained in the presence of the co-catalyst. This is an important confirmation of the benefit of having the additive.

In the end, product valorizations of the synthesized 2-azabicyclo[2.1.1]hexanes were analyzed (Scheme 8).

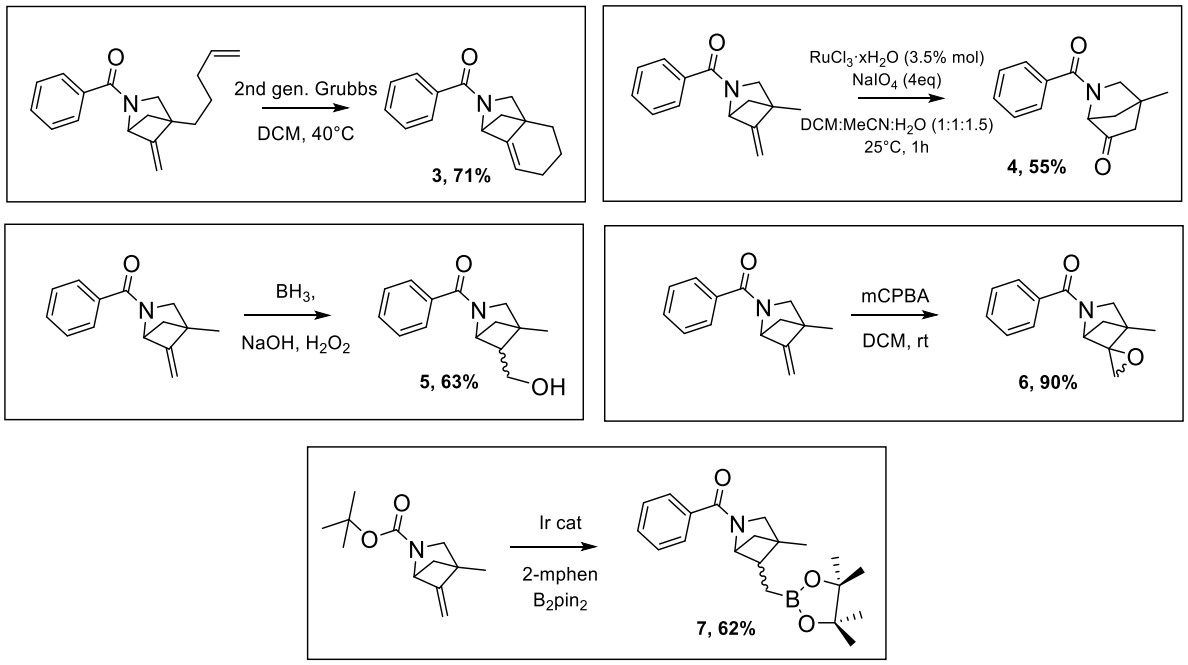

Scheme 8: Product valorization of 2-azabicyclo[2.1.1]hexanes.

With product **3,** the ring closure metathesis permitted the isolation of a more saturated product in a discrete yield. An unreported ring expansion of the cycle happened when the behavior of the model substrate **2a** with a Ru(III) catalyst and a strong oxidant, such as $NaIO_4$, was studied. Similar transformations are reported using Pd(II) in literature[19], but never using Ru(III). We hypothesize that such ring expansion happens because of the high steric tension of the system. In the case of product **5**, the transformation of the double bond was investigated, allowing the isolation of a hydroxylated derivative. A 90% yield epoxidation was reached with product **6,** giving us an interesting spiro product. In the end, the borylation of the aza-BCH containing the Boc as the protecting group gave product **7** with moderate yields.

Conclusion

With this work, we presented a simple visible-light-mediated preparation of 2-azabicyclo[2.1.1]hexanes through a notable crossed [2+2] cycloaddition through an energy transfer relay mechanism. The process, which occurs at room temperature and with broad functional group tolerance, arises from a generic allenamide structure, giving the target products with 100% atom-economy. The method combines a powerful homoleptic Ir(III) photosensitizer with a binaphthyl cocatalyst, which, as already demonstrated in previous reports, could stabilize the biradical intermediates of the sequence.

References

[1] M. Chiminelli, G. Scarica, D. Balestri, L. Marchiò, N. Della Ca', G. Maestri, *Tetrahedron Chem.,* **2023**, 8, 100053.

[2] M. Aldeghi, S. Malhotra, D. L. Selwood, A. W. E. Chan, *Chem. Biol. Drug Des.,* **2014**, 83, 450-461.

[3] A. Pantani, E. J. LaVoie, *Chem. Rev.,* **1996**, 96, 3147-3176.

[4] H. E. Diepers, J. C. L. Walker, *Beilstein J. Org. Chem.,* **2024**, 19, 859-890.

[5] S. L. Schreiber, *Science*, **2000**, 287, 1964-1969.

[6] B. Alcaide, P. Almendros, C. Arangoncillo, *Chem. Soc. Rev.,* **2010**, 39, 783-816.

[7] A. Padwa, M. A. Filipkowski, M. Meske, S. H. Watterson, Z. Ni, *J. Am. Chem. Soc.*, **1993**, 115, 3776-3777.

[8] E. M. Carreria, C. A. Hastings, M. S. Shepard, L. A. Yerkey, D. B. Millward, *J. Am. Chem. Soc.*, **1994**, 116, 6622-6630.

[9] B. T. B. Hue, J. Dijkink, S. Kuiper, S. van Schaik, J. H. van Maarseveen, H. Hiemstra , *Eur. J. Org. Chem.*, **2006**, 12, 127-137.

[10] P. Hughes, J. Clardy, *J. Org. Chem.,* **1988**, *53*, 4793-4797.

[11] C. Stevens, N. De Kimpre, *J. Org. Chem.,* **1996**, 61, 2174–2178.

[12] G. R. Krow, Y. B. Lee, W. S. Lester, H. Christian, D. A. Shaw, J. Yuan, *J. Org. Chem.* 1998, 63, 8558–8560.

[13] K. Dhake, K. J. Woelk, J. Becica, A. Un, S. E. Jenny, D. C. Leitch, *Angew. Chem. Int. Ed*., **2022**, 134, e202204719.

[14] A. Denisenko, P. Garbuz, S. V. Shishkina, N. M. Voloshchuk, P. K. Mykhailiuk, *Angew. Chem. Int. Ed.* **2020**, *59*, 20515-20521.

[15] L. Herter, I. Koutsopetras, L. Turelli, T. Fessard, C. Salomé, *Org. Biomol. Chem.*, **2022**, 20, 9108-9111.

[16] D. Tian, Y. Pan, X. Zaho, Y. Yin, Z. Jiang, *J. Am. Chem. Soc.,* **2025**, 147, 12410–12417.

[17] A. Cerveri, G. Scarica, S. Sparascio, M. Hoch, M. Chiminelli, M. Tegoni, S. Protti, G. Maestri, *Chem. Eur. J.*, **2024**, 30, e202304010.

[18] S. Sparascio, G. Scarica, A. Cerveri, G. Russo, D. Spataro, L. Marchiò, M. Lanzi, G. Maestri, *ACS Catalysis*, **2025** *15*, 13799-13809.

[19] X. Q. Shen, X. W. Yan, X. G. Zhang, *Chem. Commun.,* **2021**, 57, 10234-10237.

Experimental section

General remarks

All the chemicals whereby the syntheses are not reported here after were purchased from commercial sources and used as received. Solvents were dried passing through alumina columns using an Inert® system and were stored under nitrogen. Chromatographic purifications were performed under gradient using a Combiflash® system and prepacked disposable silica cartridges or through isocratic flash chromatography using commercial 60 Å silica gel. All reactions that required heating were performed with the use of high-vacuum grade silicon oil.

Present visible light promoted reactions require the use of dry solvents as the presence of molecular oxygen exerts a negative effect on their rate. Reactions promoted by visible light were performed into standard 5 mm NMR tubes, which were placed inside a 500 mL glass beaker equipped with a commercial strip of 300 RGB household LEDs (12V, 14W) on its internal surface. The temperature of the tubes was carefully checked with a thermometer. Cooling was ensured by two fans recovered by outdated PCs to avoid overheating due to LEDs emission.

^{1}H and ^{13}C NMR spectra were recorded at 300 K on a Bruker 400 MHz or a JEOL 600 MHz spectrometer using residual non-deuterated solvents as internal standards (7.26 ppm for ^{1}H NMR and 77.00 ppm for ^{13}C-NMR for $CDCl_3$. ^{19}F-NMR spectra were recorded in $CDCl_3$ at 298 K on a Jeol 600 spectrometer fitted with a BBFO probe head at 565 MHz. The terms m, s, d, t, q and quint represent multiplet, singlet, doublet, triplet, quadruplet and quintuplet respectively, and the term br and h mean respectively a broad signal and a heptuplet. Reported assignments were based on decoupling, COSY, NOESY, HSQC and HMBC correlation experiments.

Mass analyses were recorded on an Infusion Water Acquity Ultra Performance LC HO6UPS-823M instrument equipped with a SQ detector (Electrospray source); high-resolution mass analyses were recorded on a LTQ ORBITRAP XL Thermo Mass Spectrometer (Electrospray source).

Single crystal Data were collected with a Bruker D8 diffractometer equipped with Photon II area detector, using a CuKα or a MoKα microfocus 4 radiation source. The data collection strategy covered the sphere of reciprocal space. Absorption corrections were applied using the program SADABS. The structure was solved with the SHELXT code. Fourier analysis and refinement were performed by the full-matrix least-squares methods based on F2 using SHELXL-2014 as implemented in Olex2. All the non-H atoms were refined with anisotropic displacement parameters.

Optimization experiments

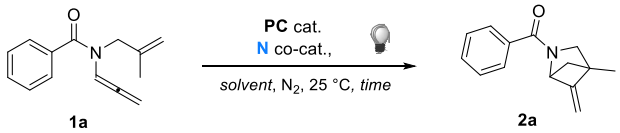

1a **2a**

---

variation of the Ir(III) photocatalyst (E_T, ^{3}PC lifetime)

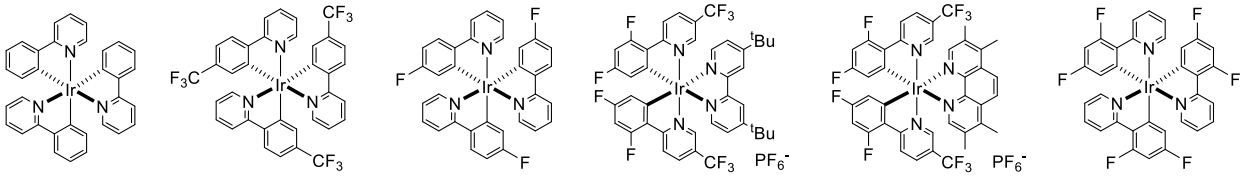

PC1 = $Ir(ppy)_3$, *58.1 kcal/mol*, 1.9 μsec

PC2 = $Ir(p\text{-}CF_3\text{-}ppy)_3$, *56.4 kcal/mol*, 2.2 μsec

PC3 = $Ir(p\text{-}F\text{-}ppy)_3$, *58.6 kcal/mol*, 2.0 μsec

PC4 = $[Ir\{dFCF_3ppy\}_2(dtbbpy)]PF_6$, *61.8 kcal/mol*, 2.3 μsec

PC5 = $[Ir\{dFCF_3ppy\}_2(Me_4phen)]PF_6$, *63.0 kcal/mol*, 3.8 μsec

PC6 = $Ir(dFppy)_3$, *63.5 kcal/mol*, 1.6 μsec

variation of the tether between the 1-naphthyl unit

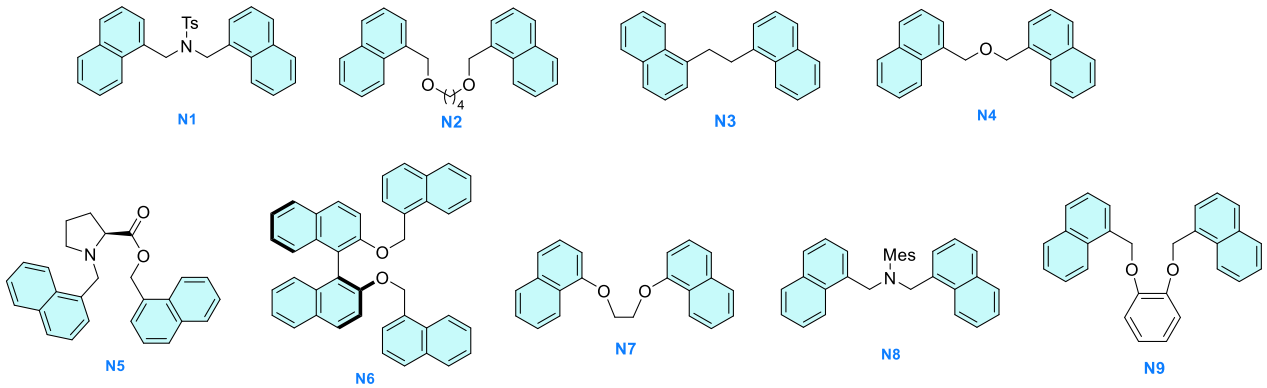

N1 **N2** **N3** **N4**

N5 **N6** **N7** **N8** **N9**

A vial was charged with allene (21.3 mg, 0.1 mmol, 1.0 equiv.), the desired iridium catalyst (1 mol%), and the desired additive. The mixture was dissolved in the freshly distilled desired solvent. The solution was then transferred into an NMR tube capped with a rubber septum and directly irradiated. Once full conversion of SM was achieved, monitored by TLC analysis, the solvent was removed. 1,3,5-Trimethoxybenzene (5.65 mg, 0.033 mmol) was added as an internal standard, and the **^{1}H NMR** of the crude was measured.

Preliminary experiments on the role of N1 on rate

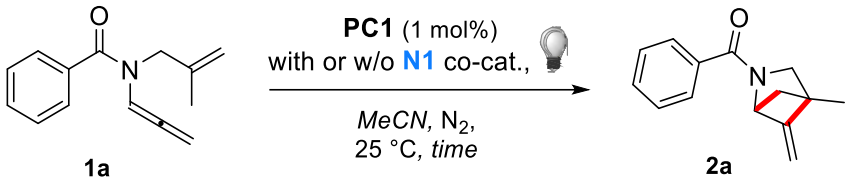

Entry	N co-cat.	Time (h)	Conversion of **1a** [%][a]	Yield of **2a** [%][a]
1	--	240	>99	30
2	**N1** (30 mol%)	16	>99	35

Table S1a. [a] by ^{1}H NMR using 1,3,5-Trimethoxybenzene as internal standard. Best result was highlighted in pale orange.

The two parallel reactions using blue LEDs irradiation showed a significantly faster conversion of **1a**, and a slight but still higher yield of **2a**, in the presence of 30 mol% of **N1** as a potential additive for the reaction system. However, the conversion was achieved fifteen times faster with respect to entry 1, performed without using any additive loading. As a starting point, the type of co-catalyst and the loading of **N1** were kept for the following steps of the optimization.

Blank experiments

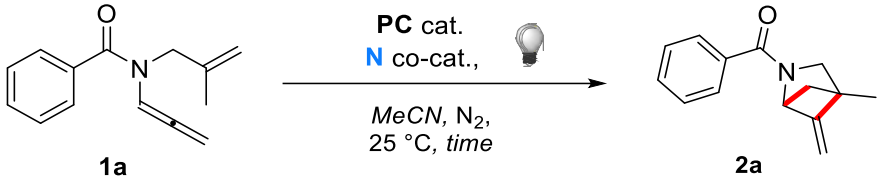

Entry	Variation	N co-cat.	Time (h)	Conversion of **1a**[a] [%]	Yield of **2a**[a] [%]
3	No **PC**	**N1** (30 mol%)	42	--	--
4	No light	**N1** (30 mol%)	42	--	--

Table S1b. [a] by ^{1}H NMR using 1,3,5-Trimethoxybenzene as internal standard.

The reaction was tested first without the photocatalyst and then without light. In both cases, no product formation was observed. This confirms that both components are essential for the reaction to proceed. The lack of reactivity is consistent with the proposed photocatalytic mechanism.

Initial evaluation of the effect of the solvent

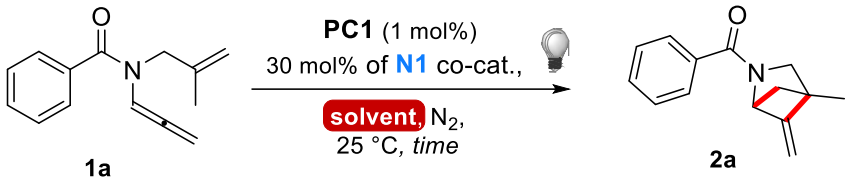

Entry	Solvent (0.1 M)	Time (h)	Conversion of **1a** [%][a]	Yield of **2a** [%][a]
2	CH_3CN	16	>99	35
5	CH_2Cl_2	20	>99	18
6	DMF	16	>99	22
7	Toluene	16	>99	41
8	Acetone	16	>99	25
9	THF	8	>99	30
10	Toluene:DCM 8:2	20	>99	41

Table S1c. [a] by ^1H NMR using 1,3,5-Trimethoxybenzene as internal standard. Best result was highlighted in pale orange.

Several different solvents characterized by different nature in terms of polarity and dielectric constant were tested and presented in **Table S1c**. Overall, the polarity of the medium and the rate of conversion of **1a** and the yield of **2a**, show a small but not negligible correlation. However, this series of results showed that a moderate increase in the yield of 2-azabicyclo[2.1.1]hexane**, 2a** could be achieved by performing the reaction in toluene media. Particularly interesting is the case of THF, where we observed a faster conversion with respect to the other entries reported, but coupled with a lower yield. Because of that, we decided to keep toluene as the solvent for the rest of the optimization effort, because in this initial part, we were more interested in reaching higher yields rather than lower reaction rate time.

Evaluation of the effect of the different N co-catalysts N1-N6

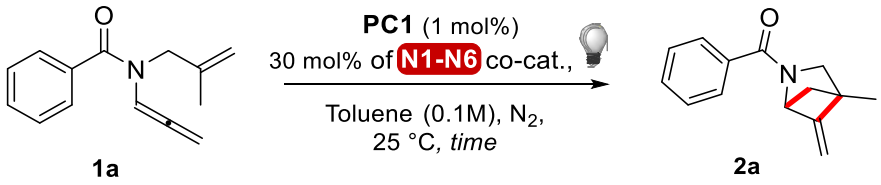

	N Co-cat.	Time (h)	Conversion of **1a**[a] [%]	Yield of **2a**[a] [%]
7	**N1**	16	>99	41
11	**N2**	14	>99	40
12	**N3**	16	>99	32
13	**N4**	14	>99	31
14	**N5**	14	>99	34
15	**N6**	14	60	11

16	**N3 + Naphtalene (1 equiv.)**	8	>99	38

Table S1d. [a] by ^{1}H NMR using 1,3,5-Trimethoxybenzene as internal standard. Best result was highlighted in pale orange.

In this case, six different poly-naphthyl derivatives were tested, varying principally the length and the rigidity of the tether between the two naphthyl arms, because this structural feature proved to be crucial in a recent study on alkene-alkene [2+2] photocycloadditions (see *Photochem. Photobio. Sci.* **2024**, *23*, 1543). Among all of the tested **N** species, **N1**, which was also the first binaphthyl chosen for the initial part of the optimization, proved to be the additive associated to the highest yield. This derivative was thus adopted for the following iteration of the optimization process.

Comparison of different Ir(III) PCs

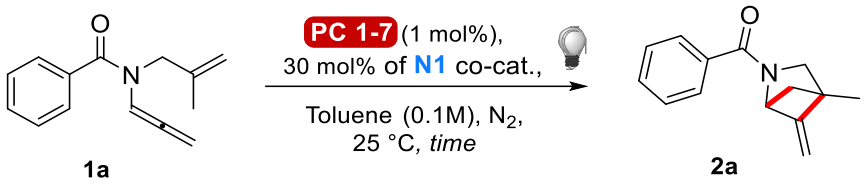

1a **2a**

Entry	**PC** cat. (1 mol %)	Time (h)	Conversion of **1a** [%][a]	Yield of **2a** [%][a]
7	**PC1**, $Ir(ppy)_3$	16	>99	41
17	**PC2**, $Ir(p\text{-}CF_3\text{-}ppy)_3$	8	>99	37
18	**PC3**, $Ir(p\text{-}F\text{-}ppy)_3$	8	>99	47
19	**PC4**, $[Ir\{dFCF_3ppy\}_2(dtbbpy)]PF_6$	12	>99	30
20[b]	**PC4**, $[Ir\{dFCF_3ppy\}_2(dtbbpy)]PF_6$	14	>99	40
21	**PC4**, $[Ir\{dFCF_3ppy\}_2(dtbbpy)]PF_6$	8	>99	44
22	**PC5**, $[Ir[dF(CF_3)ppy]_2(Me_4phen)]PF_6$	8	>99	44
23	**PC6**, $[Ir\{dFCF_3ppy\}_2(bpy)]PF_6$	14	>99	28
24[b]	**PC6**, $[Ir\{dFCF_3ppy\}_2(bpy)]PF_6$	14	>99	30
25	**PC7**, $Ru(bpy)_3(PF_6)_2$	8	/	/
26	Thioxantone (20 mol%)	8	41	11

Table S1e. [a] by ^{1}H NMR using 1,3,5-Trimethoxybenzene as internal standard. [b] with bigger crystallizer as the reaction media. Best result was highlighted in pale orange.

Different Ir(III) photocatalysts were initially tested using blue and purple LEDs irradiation in function of their properties. The comparison of results showed that **PC1-3** were competent species for the activation of **1a** in combination with **N1**. Particularly interesting is entry 18, which demonstrated to be the best one, where we achieved a yield near 50% for the first time in a slower reaction time. Even if we were more interested in performing the reaction with Blue LEDs, we decided in entries 19 to 24 to test also other classes of specific photocatalyst synthesized in our lab, which present the highest peak of absorption in the purple region. However, even if in other works this change turned out to be the right choice, this time the yield of **2a** was

sometimes slightly worse or the reaction time wasn't as slow as the one observed in entry 18. Probably, the yield of **2a** did not increase because using such high wavelengths it is possible to favor the formation of byproducts of dearomatization due to an intermolecular para-cycloaddition of the allene on one of the naphthyl arms (see *Tetrahedron Chem* **2023**, *8*, 100053). Finally, under these conditions, traces of **2a** were observed performing the reaction using thioxanthone as photosensitizer, which suggested us to exclude the use of this photosensitizer, as well as a Ruthenium catalyst, reported in entry 25, where no reaction was even observed. These results let us maintain the conditions of entry 18 and switch to the evaluation of other effects.

Evaluation of the diluition of the solvent

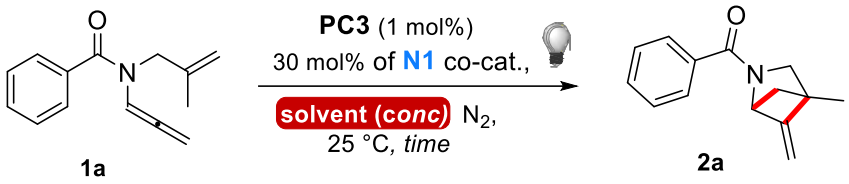

Entry	Solvent	Conc.	Time (h)	Conversion of **1a** [%][a]	Yield of **2a** [%][a]
18	Toluene	0.1 M	8	>99	47
27	Toluene	0.2 M	8	>99	47
28	Toluene	0.05 M	8	>99	48
29	THF	0.05 M	8	>99	39
30	Tol:DCM 8:2	0.05 M	16	>99	37

Table S1f. [a] by ^{1}H NMR using 1,3,5-Trimethoxybenzene as internal standard. [b] with bigger crystallizer. Best result was highlighted in pale orange.

Three different solvent concentrations were tested and presented in **Table S1f**. Although at the same rate of conversion of **1a**, the yield of **2a**, shows a tiny improvement for a diluted media of Toluene (0.05M). Therefore, we kept this concentration of toluene for the rest of the optimization effort.

Evaluation of the loading of the N1 co-catalyst

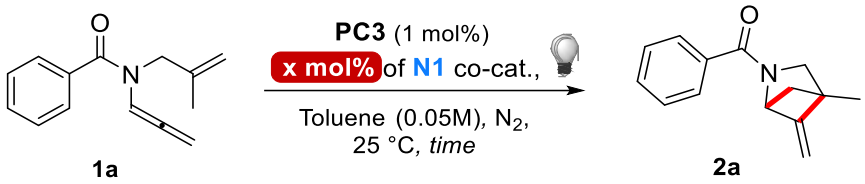

Entry	Co-Cat loading	Time (h)	Conversion of **1a** [%][a]	Yield of **2a** [%][a]
28	30 mol%	8	>99	48
31	15 mol%	8	>99	58
32[b]	15 mol%	8	>99	49
33[c]	15 mol%	8	>99	45
34	60 mol%	8	>99	46
35	10 mol%	16	>99	53
36	5 mol%	16	>99	50

Table S1g. [a] by ^{1}H NMR using 1,3,5-Trimethoxybenzene as internal standard. [b] 2 mol% **PC3**. [c] No freeze pump performed for the reaction. Best result was highlighted in pale orange.

We then subsequently investigated the influence of the co-catalyst loading on the reaction outcome, to this end, a series of reactions were carried out in which the amount of the binaphthyl co-catalyst was systematically varied, while all other parameters were kept constant. Performing the experiments, it became evident that the co-catalyst loading plays a crucial role in the transformation involved. Lowering the concentrations as in entry 31, an important effect was detected, suggesting us that a higher loading of the binaphtyl favours the arising of potential side reactions. This trend is once again confirmed by entry 34 where going towards a stochiometric quantity led us to a decreased outcome. In conclusion, even if lowering once more the co-catalyst loading brought to better results in respect to the ones observed in entry 28, this time a decrease in the reaction rate was noted, doubling the reaction time. Based on this analysis, an optimal concentration window of the additive was identified with 15 mol% in respect to the starting material and then adopted for the subsequent optimization steps.

Evaluation of the effect of other potential stereochemical factors on the N co-catalysts N7-N9 coupled with crossed experiments.

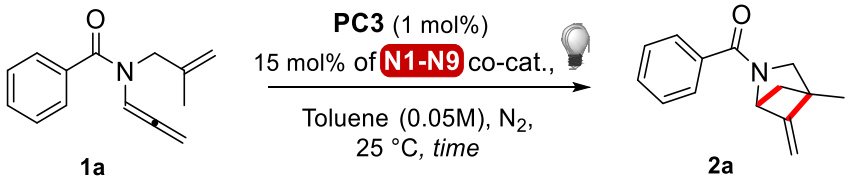

	N Co-cat.	Time (h)	Conversion of **1a**[a] [%]	Yield of **2a**[a] [%]
31	**N1**	8	>99	58
37	**N2**	8	>99	74

38[b]	**N2**	8	>99	63
39	None	60	>99	55
40	**N3**	14	>99	31
41	**N7**	14	>99	50
42	**N8**	14	>99	50
43	**N9**	8	>99	49
44[b]	**N9**	8	>99	42

Table S1h. [a] by ^{1}H NMR using 1,3,5-Trimethoxybenzene as internal standard. [b] No freeze pump performed for the reaction. Best result was highlighted in pale green this time.

Before reaching the end of the optimization, three other different poly-naphthyl derivatives were tested, this time lingering on carefully modifying the spacing and the substituents of the binaphtyl N1 to N3, which have demonstrated to perform the reaction with higher yields. Surprisingly, all the new binaphthyls involved proved to achieve worse performances but when it came to test old binaphthyls in the new optimized conditions, something interesting appeared. In fact, crossing different parameters of the reaction have permitted us to isolate higher yields, such as the one reported in entry 37. Satisfied with this one, we evaluated to stop with further optimization studies and the conditions reported in entry 37 were also the reaction conditions used for the entire scope presented.

Stern-Volmer quenching studies

The measurements of fluorescence emissions were carried out with a FLS1000 Edinburgh fluorometer, equipped with automatic polarizers. Emissions have been collected by exciting the sample with a Xenon lamp at 376 nm and the luminescence was measured at 480 nm. Fluorescence spectra are corrected for the excitation intensity and detector sensitivity. Stern–Vollmer quenching studies were carried out using a 5*10-5 M solution of Ir(p-F-ppy)$_3$ [**PC3**] in toluene and variable concentrations of both **1a** and **N2** from 0 to 2 mM. 2.5 mL of PC3's solution was transferred in a 3.5 mL quartz cuvette and degassed twice for 5 minutes (with a 30-second break in between) before collecting the first spectra. Then, after each addition of quenching, the samples were degassed for 2 minutes, and spectra were quickly recorded.

Note: Ir(p-F-ppy)$_3$ emission is highly sensitive to the presence of oxygen, more than other common photocatalysts due to the homolectic nature of the photocatalyst itself.

A linear Stern–Volmer plot was obtained at varying concentrations of both **1a** and **N2**, and K_{SV} constants were extracted according to the equation $I_0/I = 1 + K_{SV}[Q]$. There are slight differences between the values of the two constants, which are consistent with previous data collected in our group with similar allenamides. However, these values are sufficient to explain such a large difference in reaction rate, which is more reasonably imputable to the energy transfer relay mechanism, which has already been studied for a similar reaction in literature where briefly the **N2** and the general allenamide can form an adduct thanks to stabilizing π−π and C−H−π interactions. Then two sequential EnTs would follow. The first one has an intermolecular nature, and it involves the photoexcited form of PC5 and **N2**, giving a special adduct. While the second one has an intramolecular nature, and it occurs between N2 and 1, which is characterized by a delocalized allylic monooccupied molecular orbital and a reactive vinyl radical one. We hypothesize that this intermediate can efficiently start the catalytic cycle involved. The [2+2] crossed cycloaddition is then completed by a final radical recombination, allowing **N2** to turn over.

Comprehensive table of Stern–Volmer constants

QUENCHER	K_{SV}	R^2
1a	262,0 M^{-1}	0.99
N2	1757 M^{-1}	0.99

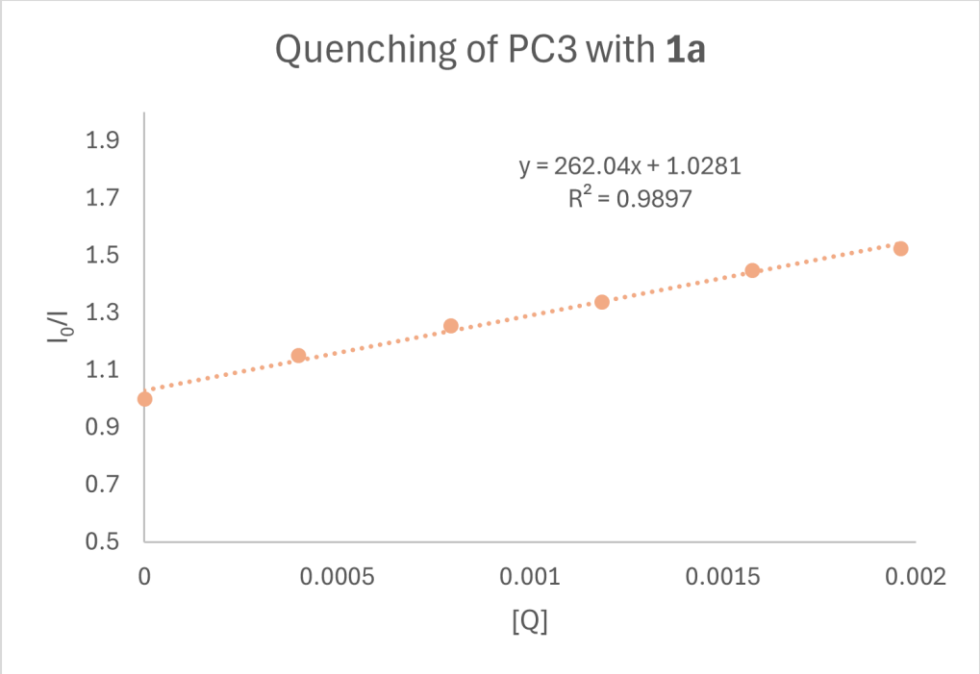

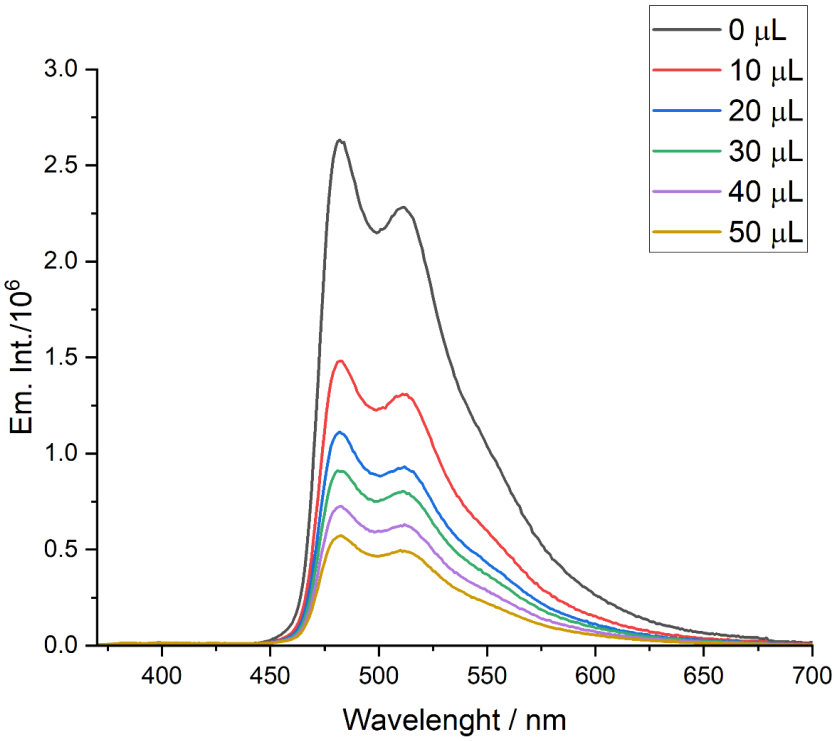

Figure 1: Measured emissions for quench of **PC3** with **1a**.

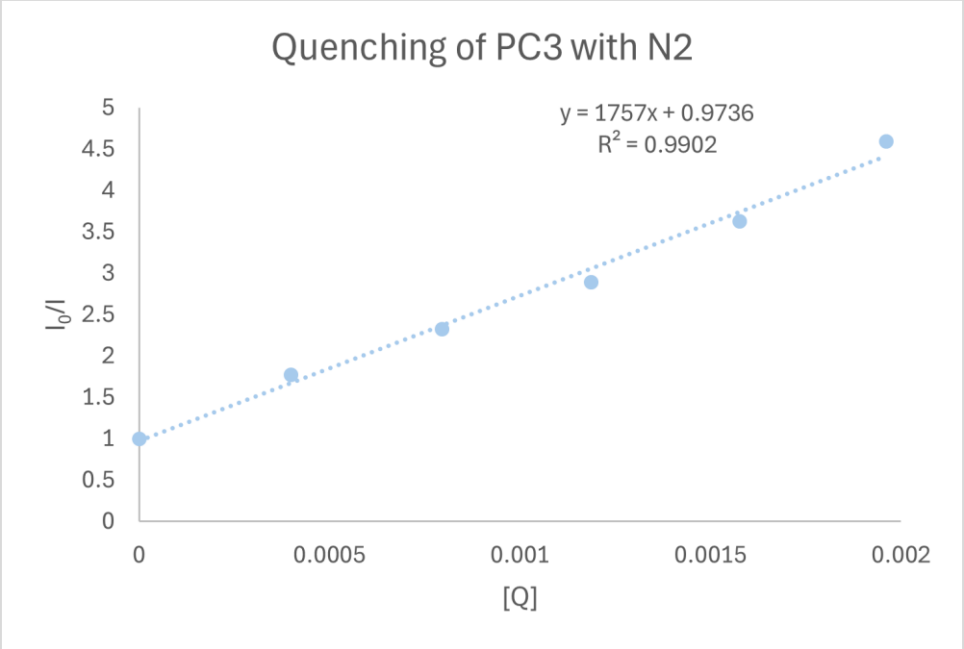

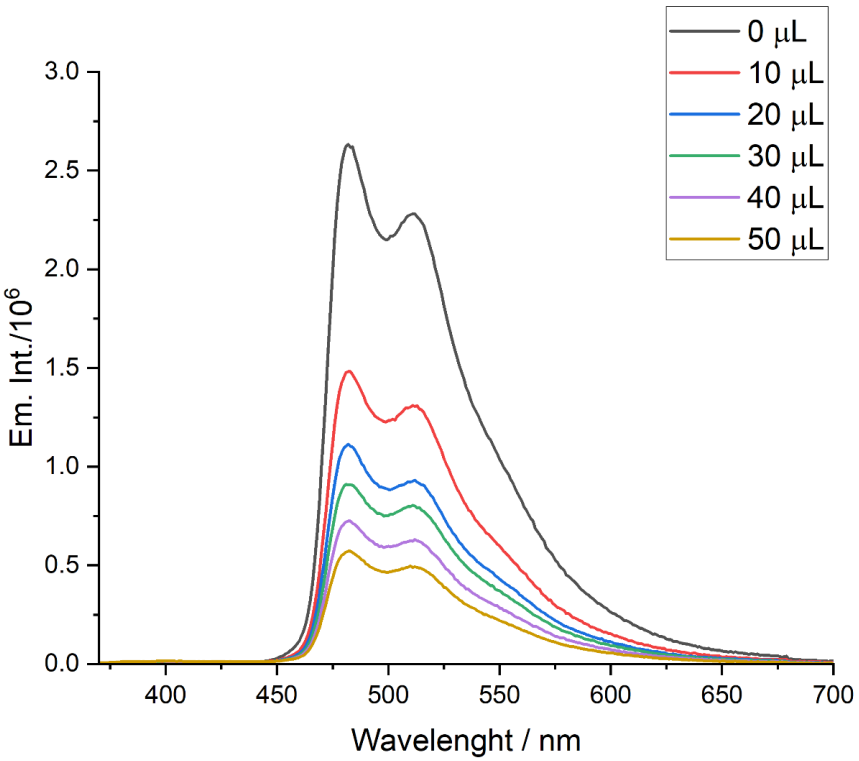

Figure 2: Measured emissions for quench of **PC3** with **N2**.

Unsuccessful substrates

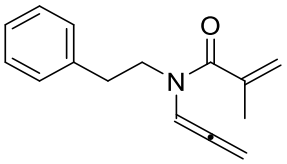

Traces + maj DEC

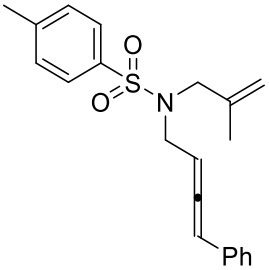

RSM

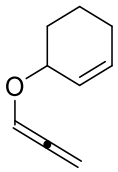

Traces + SR

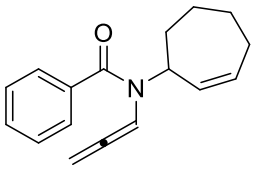

DEC

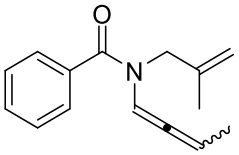

DEC

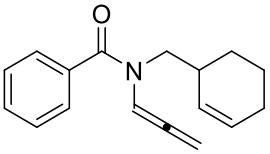

Traces + SR

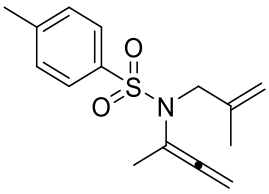

RSM + maj DEC

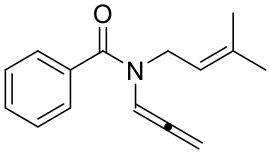

DEC

RSM: Recovery of starting material
DEC: Decomposition
SR: Side reaction

Synthesis of the substrates

General procedure B1:

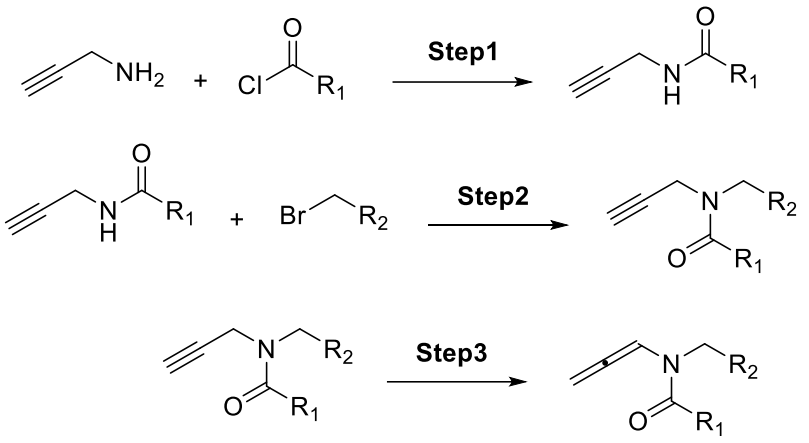

Step 1: In a round bottom flask equipped with a magnetic stirring bar, primary amine (1 equiv.), DMAP (0.02 equiv.) and DIPEA (1 equiv.) were dissolved in dry DCM (0.25 M). The solution was cooled to 0 °C and the acyl chloride (1 equiv.) was then added dropwise. The mixture was stirred at room temperature until completion, monitoring the process by TLC. The solution was then quenched with saturated NH_4Cl aqueous solution and diluted with DCM. The organic phase was then washed with brine, dried over Na_2SO_4 and concentrated under reduced pressure. The crude was finally purified by chromatography on silica gel (*n*-hexane/EtOAc gradient) to afford the desired product.

Step 2: To a solution of primary amide/carbamate (1 equiv.) in dry DMF (0.6 M), NaH (60% in paraffine oil, 1.3 equiv.) was slowly added at 0°C and the mixture was stirred for 1 h at the same temperature. The desired alkyl halide (1.3 equiv.) was then slowly added, and the reaction was stirred at room temperature for 18 h. After complete conversion as monitored by TLC, the mixture was quenched with a saturated NH_4Cl aqueous solution and extracted with EtOAc (3 times). The combined organic layers were washed with brine (3 times), dried over Na_2SO_4 and concentrated under reduced pressure. The crude was purified by chromatography on silica gel (*n*-hexane/EtOAc gradient) to afford the desired products.

Step 3: The desired propargyl amide (1 equiv.) was dissolved in dry THF (0.20 M) in a round-bottom two-necked flask equipped with a magnetic stirring bar. Then under N_2 atmosphere, *t*-BuOK (0.3 equiv.) was added at 0°C, and the resulting mixture was stirred at room temperature for 5 minutes. After complete conversion as monitored by TLC, 5 ml of saturated NH_4Cl aqueous solution was added. The mixture was sequentially extracted with EtOAc (3 x 15 ml), the organic layers separated and dried over Na_2SO_4. The solution was concentrated under reduced pressure and the crude purified by chromatography on silica gel (*n*-hexane/EtOAc gradient) to afford the corresponding allenamide.

General procedure B2:

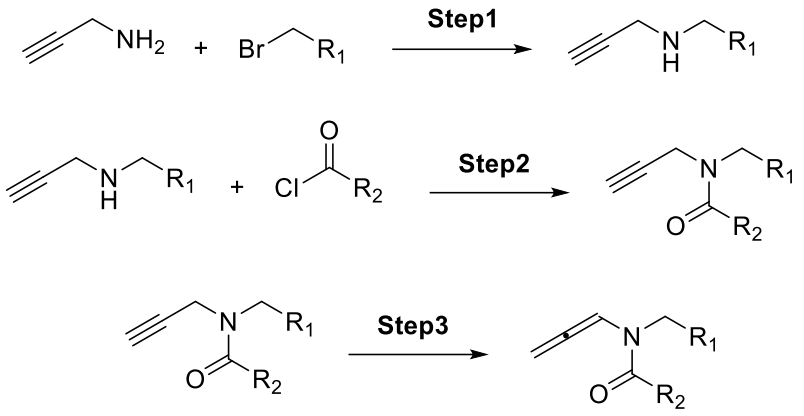

Step 1: In a round bottom flask equipped with a magnetic stirring bar, the correspondent bromide (1 equiv.) was added at 0 °C to a general primary propargyl amine (6 equiv.) and the resulting solution was stirred for 4 h at room temperature. After complete conversion as monitored by TLC, the mixture was quenched with a saturated $NaHCO_3$ aqueous solution and extracted with EtOAc (3 times). The combined organic phase was washed with brine, dried over Na_2SO_4 and concentrated under reduced pressure. The crude was finally purified by chromatography on silica gel (*n*-hexane/EtOAc gradient) to afford the desired product.

Step 2: In a round bottom flask equipped with a magnetic stirring bar, secondary amine (1 equiv.), DMAP (0.02 equiv.) and DIPEA (1 equiv.) were dissolved in dry DCM (0.25 M). The solution was cooled to 0 °C and the acyl chloride (1 equiv.) was then added dropwise. The mixture was stirred at room temperature until completion, monitoring the process by TLC. The solution was then quenched with saturated NH_4Cl aqueous solution and diluted with DCM. The organic phase was then washed with brine, dried over Na_2SO_4 and concentrated under reduced pressure. The crude was finally purified by chromatography on silica gel (*n*-hexane/EtOAc gradient) to afford the desired product.

Step 3: The desired propargyl amide (1 equiv.) was dissolved in dry THF (0.20 M) in a round-bottom two-necked flask equipped with a magnetic stirring bar. Then under N_2 atmosphere, *t*-BuOK (0.3 equiv.) was added at 0°C, and the resulting mixture was stirred at room temperature for 5 minutes. After complete conversion as monitored by TLC, 5 ml of saturated NH_4Cl aqueous solution was added. The mixture was sequentially extracted with EtOAc (3 x 15 ml), the organic layers separated and dried over Na_2SO_4. The solution was concentrated under reduced pressure and the crude purified by chromatography on silica gel (*n*-hexane/EtOAc gradient) to afford the corresponding allenamide.

If not available in our inventory, we achieved the formation of the correspondent bromide through a reported synthesis of that one. After that we followed one of the two correspondent general procedures.

Synthesis of (3-bromoprop-1-en-2-yl)benzene

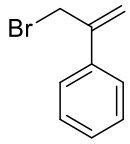

Prepared by adapting the reported procedure by L. Horner, H. Hoffmann, G. Klahre, V. G. Toscano, H. Ertel, *Chemische Berichte*, **1961**, 94, 1987-1996.

General Procedure for the Chemoselective Reduction of α,β-Unsaturated Aldehydes to Allylic Alcohols Using $NaBH_4$

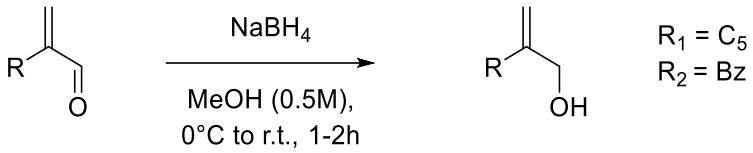

To a stirred solution of the α,β-unsaturated aldehyde (1.0 equiv.) in methanol (0.5 M) at 0 °C was added sodium borohydride (1.2 equiv.) portion-wise. The reaction mixture was stirred at 0 °C to room temperature for 1–2 h, and progress was monitored by TLC.

Upon completion, the reaction was quenched by the slow addition of saturated aqueous ammonium chloride solution. The mixture was extracted with ethyl acetate (3×20mL), and the combined organic layer were washed with brine, dried over anhydrous Na_2SO_4, filtered, and concentrated under reduced pressure.

The crude allylic alcohol was purified by flash column chromatography (eluent: hexane/ethyl acetate gradient) to afford the desired product.

Procedure for the synthesis of 2-benzylacrylaldehyde

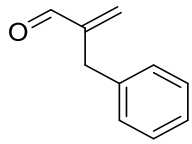

Prepared by adapting the reported procedure by G. Peng, N. Ullah, S. Streiff, K. De Oliveira Vigier, M. Pera-Titus, R. Wischert, F. Jérôme, *Chem. Eur. J.*, **2024**, 30, e202400601.

Procedure for the synthesis of 2-methylenehept-6-en-1-ol

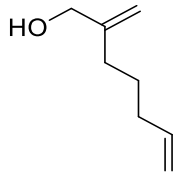

Prepared, adapting the reported procedure by S. G. Davies, G. D. Smyth, *Chem. Inform.,* **1997**, 7, 1005-1006.

General Procedure for the Bromination of Alcohols using PBr_3

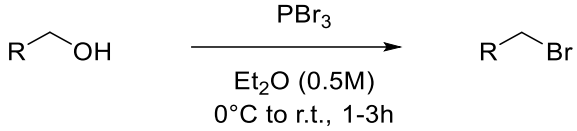

Under an inert atmosphere of nitrogen, a flame-dried flask was charged with the corresponding alcohol (1.0 equiv) dissolved in dry diethyl ether (Et_2O, 0.5 M). The solution was cooled to 0 °C, and phosphorus tribromide (PBr_3, 3.0 equiv) was added dropwise via syringe. The reaction mixture was allowed to warm to room temperature and stirred for 1–3 hours, or until complete conversion of the starting material (monitored by TLC). Upon completion, the reaction was carefully quenched by the slow addition of saturated aqueous sodium bicarbonate solution at 0 °C. The organic layer was separated, and the aqueous phase was extracted with diethyl ether (3×10mL). The combined organic layers were washed with brine, dried over anhydrous Na_2SO_4, filtered, and concentrated under reduced pressure. The crude alkyl bromide was either used directly in the next step or purified by quick filtration through a short silica gel plug using pentane as eluent.

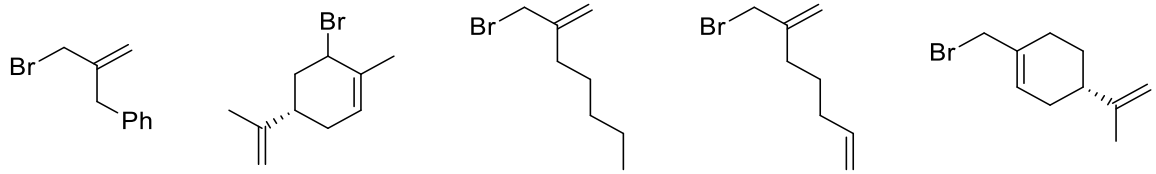

Synthesis of N-(2-Cyclopropylallyl)-N-(prop-2-yn-1-yl)benzamide

To a flame-dried round-bottom flask equipped with a magnetic stirring bar, triphenylphosphine (2.0 equiv.) was dissolved in dry tetrahydrofuran (THF, 0.3 M) under a nitrogen atmosphere and cooled to 0 °C. *n*-Butyllithium (2.7 equiv., 1.6 M in hexanes) was added dropwise, and the resulting mixture was stirred at 0 °C for 30 minutes to allow for complete formation of the phosphonium ylide.

To this solution was added N-(2-cyclopropyl-2-oxoethyl)-N-(prop-2-yn-1-yl)benzamide (1.0 equiv.) dissolved in THF. The mixture was stirred at 0 °C for 30 minutes, and the reaction was then quenched by the slow addition of water.

The aqueous phase was extracted with ethyl acetate (3×20mL), and the combined organic layers were washed with brine, dried over anhydrous Na_2SO_4, filtered, and concentrated under reduced pressure. The crude residue was triturated with saturated brine to induce precipitation, filtered, and concentrated on a rotary evaporator.

The product was purified by flash column chromatography on silica gel (eluent: n-hexane/ethyl acetate gradient) to afford N-(2-cyclopropylallyl)-N-(prop-2-yn-1-yl)benzamide as a pure compound.

General Procedure for the Aldolic Condensation

The aldehyde (1.0 equiv) was added dropwise over 1 h to a 1 M aqueous solution of sodium hydroxide containing 0.2 equiv of NaOH, maintained at 50 °C. The reaction mixture was further stirred for 1 h at 50 °C and, after cooling to room temperature, was extracted with diethyl ether (3×20mL). The combined organic layers were dried over anhydrous magnesium sulfate and concentrated in vacuo to yield the condensed aldehyde, which was used in the next step without further purification.

General Procedure for the Reductive Amination

To a stirred solution of the carbonyl compound (1.0 equiv) and propargylamine (1.2 equiv) in dry dichloromethane (DCM, 0.5 M) was added acetic acid (1.8 equiv) at room temperature. The mixture was stirred for 1–2 hours to allow imine formation. Sodium triacetoxyborohydride (2.0 equiv) was then added portionwise, and the reaction mixture was stirred at room temperature until complete consumption of the carbonyl compound (monitored by TLC). Upon completion, the reaction was quenched by the addition of saturated aqueous sodium bicarbonate. The mixture was extracted with DCM (3×20mL), and the combined organic layers were washed with brine, dried over anhydrous Na_2SO_4, filtered, and concentrated under reduced pressure. The crude product was purified by silica gel column chromatography using a gradient of hexane/ethyl acetate to afford the desired secondary amine.

Procedure for the Mesylation of 3-methylbut-3-en-1-ol

To a stirred solution of 3-methylbut-3-en-1-ol (1.0 equiv.) and triethylamine (3.0 equiv.) in dry dichloromethane (0.5 M) under nitrogen atmosphere at 0 °C was added methanesulfonyl chloride (1.2 equiv.) dropwise. The reaction mixture was allowed to warm to room temperature and stirred for 1–2 h, until complete consumption of the starting alcohol was confirmed by TLC.

Upon completion, the reaction was quenched with saturated aqueous sodium bicarbonate. The organic layer was separated, and the aqueous phase was extracted with DCM (3×). The combined organic extracts were washed with brine, dried over anhydrous Na_2SO_4, filtered, and concentrated under reduced pressure.

The crude 3-methylbut-3-en-1-yl methanesulfonate was used directly in the next synthetic step.

Procedure for synthesis of N-(3-Methylbut-3-en-1-yl)-N-(prop-2-yn-1-yl)amine

Neat propargylamine (4.0 equiv.) under a nitrogen atmosphere was added dropwise 3-methylbut-3-en-1-yl methanesulfonate (1.0 equiv.). The reaction mixture was stirred at 80 °C for 0.5–2 h, until complete consumption of the mesylate was confirmed by TLC.

After completion, the mixture was cooled to room temperature and quenched with a saturated aqueous solution of sodium bicarbonate. The aqueous phase was extracted with dichloromethane (3×), and the combined organic layers were washed with brine, dried over anhydrous Na_2SO_4, filtered, and concentrated under reduced pressure.

The crude N-alkylated amine was used directly in the next step without further purification for the amidic coupling using **GP2**.

Characterization of substrates

N-(2-methylallyl)-N-(propa-1,2-dien-1-yl)benzamide

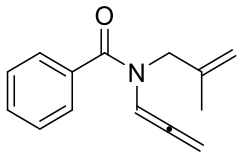

Allene **1a** was prepared following general procedure **GP-2** from the corresponding propargyl amide (213 mg, 1 mmol). Light yellow oil (175 mg, 82% yield). Two rotamers were observed due to the dynamic amide group (64:36 mixture of rotamers). **^{1}H NMR** (400 MHz, $CDCl_3$) δ 7.65 (s, 1H RotB), 7.52 – 7.50 (m, 2H RotA, 2H RotB), 7.44 – 7.38 (m, 3H RotA, 3H RotB), 6.67 (t, *J* = 6.6 Hz, 1H RotA), 5.30 (br, 2H RotA, 2H RotB), 4.92 (s, 1H RotA; 1H RotB), 4.84 (s, 1H RotA, 1H RotB), 4.24 (br, 2H RotA), 3.86 (br, 2H RotB), 1.77 (s, 3H RotA), 1.57 (s, 3H RotB). ^{13}C NMR (101 MHz, $CDCl_3$) δ 203.00 (RotB), 200.53 (RotA), 170.14 (RotB), 169.31 (RotA), 139.99 (RotA, RotB), 135.42 (RotB), 135.08 (RotA), 130.34 (2C RotA, 2C RotB), 128.56 (2C RotA, 2C RotB), 128.00 (RotA), 126.81 (RotB), 111.13 (RotA, RotB), 102.41 (RotA), 98.87 (RotB), 86.95 (RotA, RotB), 53.17 (RotB), 49.52 (RotA), 20.31 (RotA, RotB). **^{13}C NMR** (151 MHz, $CDCl_3$) δ 202.83 (RotB), 200.63 (RotA), 168.89 (RotB), 168.07 (RotA), 139.79 (RotA, RotB), 136.42 (RotA RotB), 133.70 (RotB), 133.39 (RotA), 129.50 (2C RotA, 2C RotB), 128.74 (2C RotA), 128.34 (2C RotB), 111.28 (RotA, RotB), 102.05 (RotA), 98.81 (RotB), 87.02 (RotA, RotB), 53.06 (RotB), 49.67 (RotA), 20.18 (RotA, RotB). **ESI-HRMS** calcd for $C_{14}H_{15}NNaO$ $[M+Na]^+$ 236.1051, found 236.1054.

4-chloro-N-(2-methylallyl)-N-(propa-1,2-dien-1-yl)benzamide

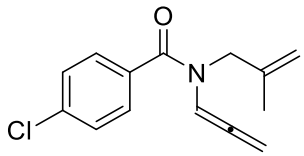

Allene **1b** was prepared following general procedure **GP-2** from the corresponding propargyl amide (247 mg, 1 mmol). Light yellow oil (188 mg, 76% yield). Two rotamers were observed due to the dynamic amide group (61:39 mixture of rotamers). **^{1}H NMR** (600 MHz, $CDCl_3$) δ 7.59 (br, 1H RotB), 7.46 – 7.44 (m, 2H RotA, 2H RotB), 7.39 – 7.32 (m, 2H RotA, 2H RotB), 6.58 (br, 1H RotA), 5.30 – 5.24 (m, 2H RotA, 2H RotB), 4.91 – 4.89 (m, 1H RotA, 1H RotB), 4.82 – 4.80 (m, 1H RotA, 1H RotB), 4.20 (s, 2H RotA), 3.81 (s, 2H RotB), 1.73 (s, 3H RotA), 1.55 (s, 3H RotB). **^{13}C NMR** (151 MHz, $CDCl_3$) δ 202.83 (RotB), 200.63 (RotA), 168.89 (RotB), 168.07 (RotA), 139.79 (RotA, RotB), 136.42 (RotA, RotB), 133.70 (RotB), 133.39 (RotA), 129.50 (2C RotA), 128.74 (2C RotA, 2C RotB), 128.34 (2C RotB), 111.28 (RotA, RotB), 102.05 (RotA), 98.81 (RotB), 87.02 (RotA, RotB), 53.06 (RotB), 49.67 (RotA), 20.18 (RotA, RotB). **ESI-HRMS** calcd for $C_{14}H_{14}NNaO$ $[M+Na]^+$ 270.0662, found 270.0668.

2,6-dimethyl-N-(2-methylallyl)-N-(propa-1,2-dien-1-yl)benzamide

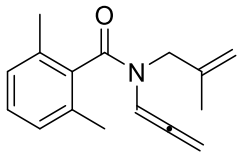

Allene **1c** was prepared following general procedure **GP-2** from the corresponding propargyl amide (241 mg, 1 mmol). Light yellow oil (166 mg, 69% yield). Two rotamers were observed due to the dynamic amide group (84:16 mixture of rotamers). **^{1}H NMR** (600 MHz, $CDCl_3$) δ 7.73 (t, *J* = 6.5 Hz, 1H RotB), 7.17 (t, *J* = 7.6 Hz, 1H RotB), 7.13 (t, *J* = 7.6 Hz, 1H RotA), 7.03 (d, *J* = 7.6 Hz, 2H RotA), 7.00 (d, *J* = 7.6 Hz, 2H RotB), 6.32 (t, *J* = 6.3 Hz, 1H RotA), 5.34 (d, *J* = 6.5 Hz, 2H RotB), 5.26 (d, *J* = 6.3 Hz, 2H RotA), 4.92 – 4.91 (m, 1H RotA), 4.89 (s, 1H RotA), 4.77 – 4.76 (m, 1H RotB), 4.58 (s, 1H RotB), 4.27 (s, 2H RotA), 3.73 (s, 2H RotB), 2.26 (s, 6H RotA), 2.23 (s, 6H RotB), 1.80 (s, 3H RotA), 1.53 (s, 3H RotB). **^{13}C NMR** (151 MHz, $CDCl_3$) δ 203.07 (RotB), 200.82 (RotA), 170.03 (RotB), 169.32 (RotA), 140.05 (RotA), 139.49 (RotB), 135.32 (RotA), 134.32 (RotB), 134.12 (RotA, RotB), 128.96 (RotB), 128.72 (RotA), 127.74 (RotA), 127.68 (RotB), 112.20 (RotB), 111.93 (RotA), 100.53 (RotA), 98.16 (RotB), 87.03 (RotB), 86.92 (RotA), 52.16 (RotB), 48.38 (RotA), 20.64 (RotA), 20.29 (RotB), 19.35 (RotB), 19.25 (RotA). **ESI-HRMS** calcd for $C_{16}H_{20}NO$ $[M+H]^+$ 242.1545, found 242.1543.

2-bromo-5-methoxy-N-(2-methylallyl)-N-(propa-1,2-dien-1-yl)benzamide

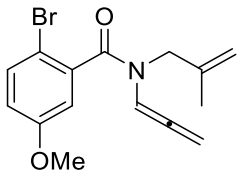

Allene **1d** was prepared following general procedure **GP-2** from the corresponding propargyl amide (322 mg, 1 mmol). Light yellow oil (315 mg, 98% yield). Two rotamers were observed due to the dynamic amide group (66:34 mixture of rotamers). **^{1}H NMR** (600 MHz, $CDCl_3$) δ 7.61 (t, *J* = 6.5 Hz, 1H RotB), 7.45 (dd, *J* = 8.5, 0.7 Hz, 1H RotA), 7.41 (dd, *J* = 8.2, 0.9 Hz, 1H RotB), 6.83 – 6.78 (m, 2H RotA, 2H RotB), 6.36 (t, *J* = 6.3 Hz, 1H RotA), 5.35 (d, *J* = 6.5 Hz, 2H RotB), 5.29 – 5.26 (m, 2H RotA), 4.92 – 4.91 (m, 2H RotA), 4.84 – 4.83 (m, 1H RotB), 4.73 (s, 1H RotB), 4.30 (d, *J* = 15.5 Hz, 1H RotA), 4.16 (d, *J* = 15.3 Hz, 1H RotA), 3.78 (s, 3H RotA, 1H RotB), 3.73 (s, 4H RotB), 1.79 (s, 3H RotA), 1.53 (s, 3H RotB). **^{13}C NMR** (151 MHz, $CDCl_3$) δ 202.96 (RotB), 200.82 (RotA), 167.41 (RotB), 166.87 (RotA), 159.23 (RotA), 158.82 (RotB), 139.77 (RotB), 139.57 (RotA), 137.92 (RotA), 137.84 (RotB), 133.94 (RotA), 133.59 (RotB), 117.07 (RotA), 117.04 (RotB), 113.69 (RotA), 113.38 (RotB), 111.95 (RotA), 111.42 (RotB), 109.55 (RotA), 109.47 (RotB), 101.08 (RotA), 98.09 (RotB), 87.29 (RotB), 87.17 (RotA), 55.73 (RotA), 55.66 (RotB), 52.42 (RotB), 48.98 (RotA), 20.49 (RotA), 20.16 (RotB). **ESI-HRMS** calcd for $C_{15}H_{16}BrNNaO_2$ $[M+Na]^+$ 344.0262, found 344.0264.

N-(2-methylallyl)-N-(propa-1,2-dien-1-yl)-2-naphthamide

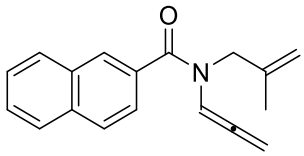

Allene **1e** was prepared following general procedure **GP-2** from the corresponding propargyl amide (263 mg, 1 mmol). Light yellow oil (160 mg, 61% yield). Two rotamers were observed due to the dynamic amide group (65:35 mixture of rotamers). **^{1}H NMR** (600 MHz, $CDCl_3$) δ 7.92 – 7.83 (m, 3H RotA, 4H RotB), 7.57 – 7.43 (m, 4H RotA, 4H RotB), 6.40 (t, *J* = 6.3 Hz, 1H RotA), 5.38 (d, *J* = 6.5 Hz, 2H RotB), 5.24 (d, *J* = 6.3 Hz, 2H RotA), 4.98 (s, 1H RotA), 4.95 (s, 1H RotA), 4.83 (s, 1H RotB), 4.79 (s, 1H RotB), 4.40 (br, 2H RotA), 3.76 – 3.69 (m, 2H RotB), 1.88 (s, 3H RotA), 1.45 (s, 3H RotB). **^{13}C NMR** (151 MHz, $CDCl_3$) δ 203.09 (RotB), 200.47 (RotA), 169.53 (RotB), 168.85 (RotA), 139.95 (RotA, RotB), 133.70 (RotA), 133.52 (RotB), 133.29 (RotB), 133.21 (RotA), 129.88 (RotA), 129.83 (RotB), 129.74 (RotB), 129.68 (RotA), 128.52 (RotA), 127.36 (RotB), 127.26 (RotA), 126.68 (RotB), 126.58 (RotA), 125.15 (RotB), 125.13 (RotA), 125.05 (RotA), 124.98 (RotA), 124.92 (RotB), 123.98 (RotB), 111.52 (RotB), 111.34 (RotA), 101.88 (RotB), 98.35 (RotA), 87.11 (RotB), 86.98 (RotA), 52.84 (RotB), 49.00 (RotA), 20.55 (RotA), 20.05 (RotB). **ESI-HRMS** calcd for $C_{18}H_{17}NNaO$ $[M+Na]^+$ 286.1208, found 286.1215.

N-(2-methylallyl)-N-(propa-1,2-dien-1-yl)-1H-indole-2-carboxamide

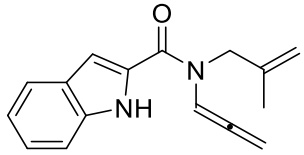

Allene **1f** was prepared following general procedure **GP-2** from the corresponding propargyl amide (252 mg, 1 mmol). Colorless oil (159 mg, 63% yield). Two rotamers were observed due to the dynamic amide group but due to the broad signals, it's impossible to calculate the ratio between them. **^{1}H NMR** (600 MHz, $CDCl_3$) δ 9.70 (s, 1H RotA, RotB), 7.74 (br, 1H RotB), 7.71 (d, *J* = 7.7 Hz, 1H RotB), 7.67 (d, *J* = 8.1 Hz, 1H RotA), 7.45 (d, *J* = 8.3 Hz, 1H RotA, RotB), 7.32 – 7.29 (m, 1H RotA, RotB), 7.16 – 7.08 (m, 2H RotA, 2H RotB), 6.92 (br, 1H RotA), 5.43 (d, *J* = 6.3 Hz, 2H RotA, 2H RotB), 4.95 (br, 2H RotA, 2H RotB), 4.34 (s, 2H RotA, 2H RotB), 1.82 (s, 3H RotA, 3H RotB). **^{13}C NMR** (151 MHz, $CDCl_3$) δ 202.86 (RotB), 202.38 (RotA), 161.69 (RotA, RotB), 139.55 (RotA, RotB), 136.27 (RotA, RotB), 128.81 (RotB), 127.75 (RotA), 125.05 (RotA, RotB), 122.36 (RotA, RotB), 120.78 (RotA, RotB), 112.00 (RotA, RotB), 111.28 (RotA, RotB), 107.99 (RotA, RotB), 106.06 (RotA, RotB), 102.12 (RotA, RotB), 100.04 (RotA, RotB), 87.29 (RotA, RotB), 52.78 (RotA), 51.30 (RotA), 20.29 (RotA, RotB). **ESI-HRMS** calcd for $C_{16}H_{16}N_2NaO$ $[M+Na]^+$ 275.1160, found 275.1164.

N-(2-methylallyl)-N-(propa-1,2-dien-1-yl)furan-2-carboxamide

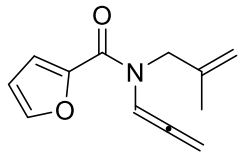

Allene **1g** was prepared following general procedure **GP-2** from the corresponding propargyl amide (203 mg, 1 mmol). Yellow oil (173 mg, 85% yield). Two rotamers were observed due to the dynamic amide group (Due to broadness of signal, impossible to determine rotameric ratio). **^{1}H NMR** (600 MHz, $CDCl_3$) δ 7.51 (br, 1H RotA, 1H RotB), 7.33 (br, 1H RotA, 1H RotB), 7.06 (br, 1H RotA, 1H RotB), 6.46 (br, 1H RotA, 1H RotB), 5.33 (d, *J* = 6.4 Hz, 2H RotA, 2H RotB), 4.86 (s, 1H RotA, 1H RotB), 4.77 (s, 1H RotA, 1H RotB), 4.20 (s, 2H RotA, 2H RotB), 1.70 (s, 3H RotA, 3H RotB). **^{13}C NMR** (151 MHz, $CDCl_3$) δ 202.69 (RotB), 201.71 (RotA), 158.12 (RotA, RotB), 147.00 (RotA, RotB), 144.79 (RotA, RotB), 139.90 (RotA, RotB), 117.54 (RotA), 116.98 (RotB), 111.47 (RotA, RotB), 111.12 (RotA), 110.60 (RotB), 101.18 (RotA), 99.77 (RotB), 87.07 (RotA, RotB), 51.90 (RotB), 50.41 (RotA), 20.10 (RotA, RotB). **ESI-HRMS** calcd for $C_{12}H_{13}NNaO_2$ $[M+Na]^+$ 226.0844, found 226.0848.

2-cyano-N-(2-methylallyl)-N-(propa-1,2-dien-1-yl)acetamide

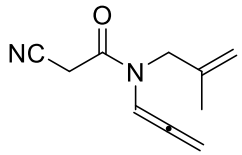

Allene **1h** was prepared following general procedure **GP-2** from the corresponding propargyl amide (176 mg, 1 mmol). Yellow oil (81 mg, 46% yield). Two rotamers were observed due to the dynamic amide group (62:38 mixture of rotamers). **^{1}H NMR** (600 MHz, $CDCl_3$) δ 7.45 (t, *J* = 6.5 Hz, 1H RotA), 6.41 (t, *J* = 6.2 Hz, 1H RotB), 5.40 (d, *J* = 6.5 Hz, 2H RotA), 5.39 (d, *J* = 6.3 Hz, 2H RotB), 4.96 (s, 1H RotA), 4.89 (s, 1H RotB), 4.77 (s, 1H RotA), 4.74 (s, 1H RotB), 4.09 (s, 2H RotB), 3.91 (s, 2H RotA), 3.64 (s, 2H RotB), 3.55 (s, 2H RotA), 1.73 (s, 3H RotA), 1.68 (s, 3H RotB). **^{13}C NMR** (151 MHz, $CDCl_3$) δ 203.21 (RotB), 201.96 (RotA), 160.53 (RotA), 160.23 (RotB), 139.18 (RotB), 138.88 (RotA), 113.62 (RotA), 113.59 (RotB), 112.57 (RotB), 111.74 (RotA), 99.33 (RotA), 98.97 (RotB), 88.45 (RotA), 87.03 (RotB), 51.52 (RotA), 51.21 (RotB), 25.56 (RotB), 25.39 (RotA), 20.12 (RotB), 19.94 (RotA). **ESI-HRMS** calcd for $C_{10}H_{12}N_2NaO$ $[M+Na]^+$ 199.0847, found 199.0842.

N-(2-methylallyl)-N-(propa-1,2-dien-1-yl)pent-4-enamide

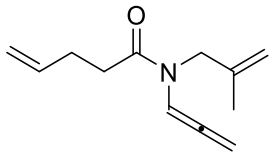

Allene **1i** was prepared following general procedure **GP-2** from the corresponding propargyl amide (191 mg, 1 mmol). Yellow oil (170 mg, 89% yield). Two rotamers were observed due to the dynamic amide group (60:40 mixture of rotamers). **^{1}H NMR** (600 MHz, $CDCl_3$) δ 7.57 (t, *J* = 6.4 Hz, 1H RotA), 6.73 (t, *J* = 6.2 Hz, 1H RotB), 5.90 – 5.80 (m, 2H), 5.31 (d, *J* = 6.4 Hz, 2H RotA, 2H RotB), 5.09 – 4.97 (m, 2H RotA, 2H RotB), 4.87 (br, 1H RotA), 4.82 (br, 1H RotB), 4.72 (s, 1H RotA), 4.67 (s, 1H RotB), 4.06 (s, 2H RotB), 3.91 (s, 2H RotA), 2.57 – 2.55 (m, 4H RotB), 2.46 – 2.39 (m, 4H RotA), 1.70 (s, 3H RotA), 1.67 (s, 3H RotB). **^{13}C NMR** (151 MHz, $CDCl_3$) δ 202.40 (RotA), 201.79 (RotB), 171.09 (RotA), 170.30 (RotB), 140.24 (RotB), 139.69 (RotA), 137.44 (RotA), 137.32 (RotB), 115.55 (RotB), 115.45 (RotA), 111.01 (RotB), 110.69 (RotA), 100.15 (RotB), 99.27 (RotA), 87.14 (RotA), 86.58 (RotB), 51.04 (RotA), 49.46 (RotB), 32.97 (RotB), 32.78 (RotA), 29.14 (RotB), 29.09 (RotA), 20.25 (RotB), 20.11 (RotA). **ESI-HRMS** calcd for $C_{12}H_{18}NO$ $[M+H]^+$ 192.1388, found 192.1385.

N-(2-methylallyl)-N-(propa-1,2-dien-1-yl)pent-4-ynamide

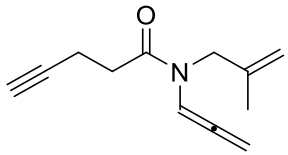

Allene **1j** was prepared following general procedure **GP-2** from the corresponding propargyl amide (189 mg, 1 mmol). Yellow oil (98 mg, 52% yield). Two rotamers were observed due to the dynamic amide group (63:37 mixture of rotamers). **^{1}H NMR** (600 MHz, $CDCl_3$) δ 7.55 (t, *J* = 6.5 Hz, 1H RotA), 6.70 (t, *J* = 6.2 Hz, 1H RotB), 5.33 (d, *J* = 6.4 Hz, 2H RotA, 2H RotB), 4.89 (s, 1H RotA), 4.83 (s, 1H RotB), 4.73 (s, 1H RotA), 4.69 (s, 1H RotB), 4.07 (s, 2H RotB), 3.91 (s, 2H RotA), 2.74 – 2.71 (m, 2H RotB), 2.61 – 2.54 (m, 4H RotA, 2H RotB), 1.98 (t, *J* = 2.7 Hz, 1H RotB), 1.96 (t, *J* = 2.6 Hz, 1H RotA), 1.72 (s, 3H RotA), 1.67 (s, 3H RotB). **^{13}C NMR** (151 MHz, $CDCl_3$) δ 202.33 (RotA), 201.94 (RotB), 169.74 (RotA), 169.00 (RotB), 140.08 (RotB), 139.41 (RotA), 111.24 (RotB), 110.78 (RotA), 99.83 (RotB), 99.22 (RotA), 87.35 (RotA), 86.70 (RotB), 83.38 (RotA), 83.31 (RotB), 69.06 (RotB), 68.94 (RotA), 50.93 (RotA), 49.71 (RotB), 32.79 (RotB), 32.63 (RotA), 20.24 (RotB), 20.12 (RotA), 14.55 (RotB), 14.49 (RotA). **ESI-HRMS** calcd for $C_{12}H_{16}NO$ $[M+H]^+$ 190.1232, found 190.1236.

4-methyl-N-(2-methylallyl)-N-(propa-1,2-dien-1-yl)benzenesulfonamide

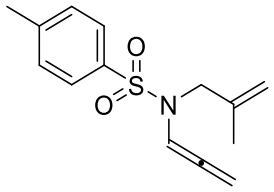

Allene **1k** was prepared following general procedure **GP-1** from the corresponding propargyl amide (209 mg, 1 mmol). Light yellow solid (178 mg, 85% yield). **^{1}H NMR** (600 MHz, $CDCl_3$) δ 7.69 (d, *J* = 8.3 Hz, 2H), 7.31 (d, *J* = 8.0 Hz, 2H), 6.78 (t, *J* = 6.2 Hz, 1H), 5.22 (d, *J* = 6.3 Hz, 2H), 4.89 – 4.87 (m, 2H), 3.65 (s, 2H), 2.43 (s, 3H), 1.71 (s, 3H). **^{13}C NMR** (151 MHz, $CDCl_3$) δ 202.43, 143.82, 139.69, 135.47, 129.82 (2C), 127.34 (2C), 113.47, 100.01, 87.85, 52.27, 21.68, 19.92. **ESI-HRMS** calcd for $C_{14}H_{17}NNaO_2S$ $[M+Na]^+$ 286.0878, found 286.0876.

tert-butyl (2-methylallyl)(propa-1,2-dien-1-yl)carbamate

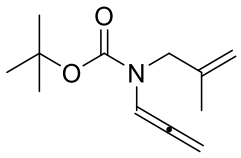

Allene **1l** was prepared following general procedure **GP-1** from the corresponding propargyl amide (209 mg, 1 mmol). Light yellow oil (178 mg, 85% yield). Two rotamers were observed due to the dynamic amide group (54:46 mixture of rotamers). **^{1}H NMR** (600 MHz, $CDCl_3$) δ 7.18 (br, 1H RotA), 7.00 (br, 1H RotB), 5.30 – 5.27 (m, 2H RotA, 2H RotB), 4.81 (s, 1H RotA, 1H RotB), 4.71 (s, 1H RotA, 1H RotB), 3.90 – 3.84 (m, 2H RotA, 2H RotB), 1.67 (s, 3H RotA, 3H RotB), 1.49 (s, 9H RotB), 1.46 (m, 9H RotA). **^{13}C NMR** (151 MHz, $CDCl_3$) δ 202.08 (RotA), 201.00 (RotB), 153.10 (RotA), 152.91 (RotB), 140.85 (RotA), 140.52 (RotB), 110.76 (RotA), 110.51 (RotB), 100.60 (RotA, RotB), 87.21 (RotA), 86.57 (RotB), 81.19 (RotB), 81.03 (RotA), 50.56 (RotA), 49.90 (RotB), 28.35 (RotA, RotB), 20.09 (RotA, RotB). **ESI-HRMS** calcd for $C_{12}H_{20}NO_2$ $[M+H]^+$ 210.1494, found 210.1497.

N-(2-phenylallyl)-N-(propa-1,2-dien-1-yl)benzamide

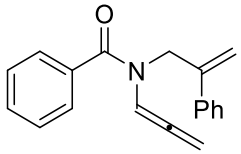

Allene **1m** was prepared following general procedure **GP-1** from the corresponding propargyl amide (275 mg, 1 mmol). Yellow oil (171 mg, 62% yield). Two rotamers were observed due to the dynamic amide group (64:36 mixture of rotamers). **^{1}H NMR** (400 MHz, $CDCl_3$) δ 7.74 (br, 1H RotB), 7.63 – 7.29 (m, 10H RotA, 10H RotB), 6.64 (br, 1H RotA), 5.48 – 5.17 (m, 4H RotA, 4H RotB), 4.74 (br, 2H RotA), 4.34 (br, 2H RotB). **^{13}C NMR** (101

MHz, $CDCl_3$) δ 202.93 (RotB), 200.70 (RotA), 170.24 (RotB), 169.49 (RotA), 143.27 (RotA, RotB), 139.48 (RotA, RotB), 135.02 (RotA, RotB), 130.44 (2C RotA, 2C RotB), 128.59 (2C RotA), 128.46 (2C RotB), 127.97 (2C RotA, 2C RotB), 126.63 (RotA), 126.19 (RotB), 112.81 (RotA, RotB), 102.26 (RotA), 98.89 (RotB), 87.16 (RotA, RotB), 51.74 (RotB), 47.80 (RotA). **ESI-HRMS** calcd for $C_{19}H_{17}NNaO$ $[M+Na]^+$ 298.1208, found 298.1214.

***N*-(2-benzylallyl)-N-(propa-1,2-dien-1-yl)benzamide**

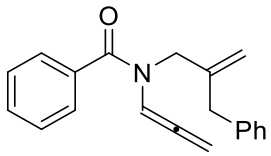

Allene **1n** was prepared following general procedure **GP-1** from the corresponding propargyl amide (289 mg, 1 mmol). Yellow oil (176 mg, 62% yield). Two rotamers were observed due to the dynamic amide group (63:37 mixture of rotamers). **^{1}H NMR** (600 MHz, $CDCl_3$) δ 7.67 (br, 1H RotB), 7.57 (br, 1H RotA), 7.47 – 7.43 (m, 3H RotA, 3H RotB), 7.36 – 7.29 (m, 3H RotA, 3H RotB), 7.23 – 7.17 (m, 3H RotA, 3H RotB), 7.03 (br, 1H RotA), 6.63 (br, 1H RotB), 5.34 – 5.18 (m, 2H RotA, 2H RotB), 5.04 – 4.95 (m, 2H RotA, 2H RotB), 4.27 (s, 2H RotA), 3.87 (s, 2H RotB), 3.45 (s, 2H RotA), 3.21 (s, 2H RotB). **^{13}C NMR** (151 MHz, $CDCl_3$) δ 202.69 (RotB), 200.27 (RotA), 170.19 (RotB), 169.28 (RotA), 143.08 (RotB), 142.75 (RotA), 138.90 (RotA), 138.15 (RotB), 135.15 (RotA), 135.01 (RotB), 130.34 (RotA), 130.15 (RotB), 129.16 (RotA, RotB), 128.90 (RotA, RotB), 128.55 (4C RotB), 128.41 (4C RotA), 128.22 (RotA, RotB), 128.00 (RotA, RotB), 126.65 (RotB), 126.37 (RotA), 112.13 (RotA), 111.98 (RotB), 102.46 (RotA), 98.90 (RotB), 87.00 (RotA), 86.85 (RotB), 51.91 (RotB), 48.53 (RotA), 41.10 (RotA), 35.95 (RotB). **ESI-HRMS** calcd for $C_{20}H_{19}NNaO$ $[M+Na]^+$ 312.1364, found 312.1366.

N-(2-methyleneheptyl)-N-(propa-1,2-dien-1-yl)benzamide

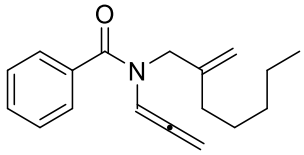

Allene **1o** was prepared following general procedure **GP-1** from the corresponding propargyl amide (269 mg, 1 mmol). Colorless oil (215 mg, 80% yield). Two rotamers were observed due to the dynamic amide group (62:38 mixture of rotamers). **^{1}H NMR** (600 MHz, $CDCl_3$) δ 7.66 (br, 1H RotB), 7.51 (br, 2H RotA, 2H RotB), 7.42 – 7.36 (m, 3H RotA, 3H RotB), 6.68 (t, *J* = 6.5 Hz, 1H RotA), 5.32 – 5.26 (m, 2H RotA, 2H RotB), 4.94 – 4.84 (m, 2H RotA, 2H RotB), 4.25 (s, 2H RotA), 3.88 (s, 2H RotB), 2.06 (t, *J* = 7.2 Hz, 2H RotA), 1.84 (br, 2H RotB), 1.52 – 1.49 (m, 2H RotA), 1.35 – 1.16 (m, 4H RotA, 6H RotB), 0.91 – 0.83 (m, 3H RotA, 3H RotB). **^{13}C NMR** (151 MHz, $CDCl_3$) δ 203.09 (RotB), 200.62 (RotA), 170.23 (RotB), 169.33 (RotA), 143.93 (RotB), 143.83 (RotA), 135.50 (RotB), 135.20 (RotA), 130.33 (RotA, RotB), 128.60 (RotA), 128.42 (RotB), 128.03 (RotA RotB), 126.83 (RotA, RotB), 109.86 (RotB), 109.53 (RotA), 102.57 (RotA), 98.99 (RotB), 86.92 (RotA, RotB), 52.33

(RotB), 48.70 (RotA), 34.16 (RotA, RotB), 31.70 (RotA), 31.49 (RotB), 27.46 (RotA), 27.31 (RotB), 22.63 (RotA, RotB), 14.15 (RotA, RotB). **ESI-HRMS** calcd for $C_{18}H_{23}NNaO$ $[M+Na]^+$ 292.1677, found 292.1674.

N-(2-methylenehept-6-en-1-yl)-N-(propa-1,2-dien-1-yl)benzamide

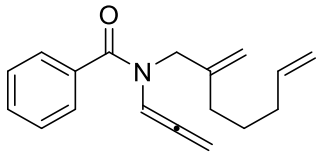

Allene **1p** was prepared following general procedure **GP-1** from the corresponding propargyl amide (267 mg, 1 mmol). Light yellow oil (222 mg, 73% yield). Two rotamers were observed due to the dynamic amide group (60:40 mixture of rotamers). **^{1}H NMR** (600 MHz, $CDCl_3$) δ 7.66 (br, 1H RotB), 7.51 (br, 2H RotA, 2H RotB), 7.43 – 7.37 (m, 3H RotA, 3H RotB), 6.68 (br, 1H RotA), 5.84 – 5.78 (m, 1H RotA), 5.75 – 5.70 (m, 1H RotB), 5.31 – 5.27 (m, 2H RotA, 2H RotB), 5.03 – 4.86 (m, 4H RotA, 4H RotB), 4.25 (s, 2H RotA), 3.88 (s, 2H RotB), 2.09 (br, 2H RotA, 2H RotB), 1.96 (br, 1H RotA, 1H RotB), 1.86 (br, 1H RotA, 1H RotB), 1.63 – 1.60 (m, 1H RotA, 1H RotB), 1.37 (br, 1H RotA, 1H RotB). **^{13}C NMR** (151 MHz, $CDCl_3$) δ 203.04 (RotB), 200.57 (RotA), 170.19 (RotB), 169.29 (RotA), 143.59 (RotB), 143.42 (RotA), 138.69 (RotA), 138.36 (RotB), 135.45 (RotB), 135.13 (RotA), 130.33 (RotA, RotB), 128.58 (2C RotA), 128.43 (2C RotB), 127.99 (2C RotA), 126.78 (2C RotB), 114.83 (RotA RotB), 110.16 (RotB), 109.93 (RotA), 102.52 (RotA), 98.93 (RotB), 86.95 (RotA, RotB), 52.28 (RotB), 48.62 (RotA), 33.47 (2C RotA), 33.28 (2C RotB), 26.92 (RotA), 26.75 (RotB). **ESI-HRMS** calcd for $C_{18}H_{22}NO$ $[M+H]^+$ 268.1701, found 268.1698.

***N*-(2-cyclopropylallyl)-N-(propa-1,2-dien-1-yl)benzamide**

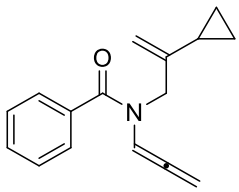

Allene **1q** was prepared following the general procedure **GP-1** from the corresponding propargyl amide (239 mg, 1 mmol). Light yellow oil (155.4 mg, 63% yield). Two rotamers were observed due to the dynamic rotations of the amide group (59:41 mixture of rotamers). **^{1}H NMR** (600 MHz, $CDCl_3$) δ 7.66 (s, 1H RotB), 7.51 – 7.37 (m, 5H RotA, 5H RotB), 6.68 (s, 1H RotA), 5.34 – 5.27 (m, 2H RotA, 2H RotB), 4.86 – 4.77 (m, 2H RotA, 2H RotB), 4.34 (s, 2H RotA), 3.96 (s, 2H RotB), 1.37 (br, 1H RotA), 1.05 (br, 1H RotB), 0.65 (s, 2H RotA), 0.55 (s, 2H RotB), 0.51 (m, 2H RotA), 0.32 (m, 2H RotB). **^{13}C NMR** (151 MHz, $CDCl_3$) δ 203.1 (RotB), 200.6 (RotA), 170.2 (RotB), 169.3 (RotA), 145.2 (RotA, RotB), 135.4 (RotB), 135.2 (RotA), 130.3 (2C RotA, 2C RotB),128.61 (2C RotA), 128.00 (2C RotB),127.0 (RotA) 126.9 (RotB), 107.8 (RotB), 107.5 (RotA), 102.62 (RotA), 99.01 (RotB), 86.97 (RotA, RotB), 52.41 (RotB), 48.86 (RotA), 14.3 (RotA),14.2 (RotB), 5.66 (2C RotA), 5.38 (2C RotB). **ESI-HRMS** calcd for $C_{16}H_{17}NNaO$ $[M+Na]^+$ 262.1208, found 262.1212.

(E)-N-(but-2-en-1-yl)-N-(propa-1,2-dien-1-yl)benzamide

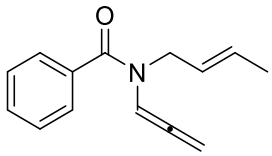

Allene **1r** was prepared following general procedure **GP-1** from the corresponding propargyl amide (267 mg, 1 mmol). Light yellow oil (222 mg, 73% yield). Reported spectra and characterization in *'The visible-light-promoted intermolecular para-cycloadditions of allenamides on naphthalene'*, Chiminelli, Maurizio et al., Tetrahedron Chem, Volume 8, 100053.

N-allyl-N-(propa-1,2-dien-1-yl)benzamide

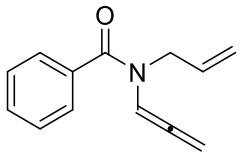

Allene **1s** was prepared following general procedure **GP-1** from the corresponding propargyl amide (267 mg, 1 mmol). Light yellow oil (222 mg, 73% yield). Reported spectra and characterization in *'The visible-light-promoted intermolecular para-cycloadditions of allenamides on naphthalene'*, Chiminelli, Maurizio et al., Tetrahedron Chem, Volume 8, 100053.

***(E)*-N-(2-methylpent-2-en-1-yl)-N-(propa-1,2-dien-1-yl)benzamide**

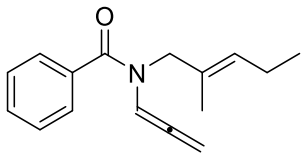

Allene **1t** was prepared following general procedure **GP-2** from the corresponding propargyl amide (241 mg, 1 mmol). Yellow oil (186 mg, 77% yield). Two rotamers were observed due to the dynamic amide group (61:39 mixture of rotamers). **^{1}H NMR** (600 MHz, $CDCl_3$) δ 7.61 (br, 1H RotB), 7.47 – 7.33 (m, 5H RotA, 5H RotB), 6.59 (br, 1H RotA), 5.29 – 5.14 (m, 4H RotA, 4H RotB), 4.21 (br, 2H RotA), 3.84 (br, 2H RotB), 2.01 (s, 2H RotA, 2H RotB), 1.61 (s, 3H RotA), 1.40 (s, 3H RotB), 0.92 (t, *J* = 7.6 Hz, 3H RotA, 3H RotB). **^{13}C NMR** (151 MHz, $CDCl_3$) δ 203.19 (RotB), 200.88 (RotA), 170.07 (RotB), 169.28 (RotA), 135.32 (RotA, RotB), 130.06 (RotA, RotB), 128.74 (RotA, RotB), 128.34 (2C RotA, 2C RotB), 127.82 (2C RotA), 126.78 (2C RotB), 102.06 (RotA), 98.75 (RotB), 86.49 (RotA, RotB), 54.16 (RotB), 50.87 (RotA), 20.92 (RotA, RotB), 13.99 (2C RotA), 13.85 (2C RotB). **ESI-HRMS** calcd for $C_{16}H_{19}NNaO$ $[M+Na]^+$ 264.1364, found 264.1368.

***(E)*-N-(2-methyl-3-phenylallyl)-N-(propa-1,2-dien-1-yl)benzamide**

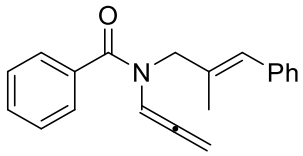

Allene **1u** was prepared following general procedure **GP-1** from the corresponding propargyl amide (289 mg, 1 mmol). Yellow oil (130 mg, 45% yield). Two rotamers were observed due to the dynamic amide group (63:37 mixture of rotamers). **^{1}H NMR** (600 MHz, $CDCl_3$) δ 7.71 (s, 1H RotB), 7.56 – 7.51 (m, 2H RotA, 2H RotB), 7.46 – 7.40 (m, 4H RotA, 4H RotB), 7.34 (t, *J* = 7.6 Hz, 2H RotA, 2H RotB), 7.25 – 7.21 (m, 2H RotA, 2H RotB), 6.70 (s, 1H RotA), 6.39 (s, 1H RotA), 6.32 (s, 1H RotB), 5.34 – 5.31 (m, 2H RotA, 2H RotB), 4.44 (s, 1H RotA), 4.06 (s, 1H RotB), 1.89 (s, 3H RotA), 1.70 (s, 3H RotB). **^{13}C NMR** (151 MHz, $CDCl_3$) δ 203.25 (RotB), 201.00 (RotA), 169.64 (RotA, RotB), 137.82 (RotA, RotB), 135.22 (RotA, RotB), 133.23 (RotA, RotB), 130.43 (RotA, RotB), 128.97 (2C RotA, 2C RotB), 128.64 (2C RotA, 2C RotB), 128.29 (4C RotA), 128.09 (4C RotB), 126.56 (RotA, RotB), 102.32 (RotA), 99.10 (RotB), 86.89 (RotA, RotB), 51.48 (RotA, RotB), 15.82 (RotA, RotB). **ESI-HRMS** calcd for $C_{20}H_{19}NNaO$ $[M+Na]^+$ 312.1364, found 312.1360.

***N*-(2-benzyl-5-phenylpent-2-en-1-yl)-*N*-(propa-1,2-dien-1-yl)benzamide**

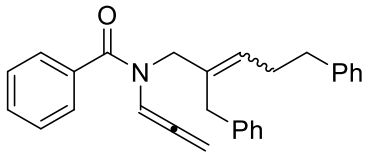

Allene **1v** was prepared following the general procedure **GP-2** from the corresponding propargyl amide (393.5 mg, 1 mmol). Light yellow oil (306.9 mg, 78% yield). Two rotamers were observed due to the dynamic rotations of the amide group (60:40 mixture of rotamers). **^{1}H NMR** (600 MHz, $CDCl_3$) δ 7.62 (s, 1H RotB), 7.49 – 7.12 (m, 15H RotA, 13H RotB), 6.85 (s, 2H RotB), 6.50 (s, 1H RotA), 5.52 (s, 1H RotA, 1H RotB), 5.11 (m, 2H RotA, 2H RotB), 4.21 (br, 2H RotA), 3.81 (br, 2H RotB), 3.46 (br, 2H RotA), 3.21 (br, 2H RotB), 2.75 (t, *J* = 7.6 Hz, 2H RotA, 2H RotB), 2.56 – 2.49 (m, 2H RotA, 2H RotB). **^{13}C NMR** (151 MHz, $CDCl_3$) δ 202.80 (RotB), 200.42 (RotA), 170.39 (RotB), 169.36 (RotA), 164.19 (RotB) 141.83 (RotA), 139.37 (RotB),138.6 (RotB), 135.20 (RotA), 134.44 (RotB),132.33 (RotB), 132.14 (RotA), 130.18 (RotA, RotB), 129.08 (RotA, RotB), 128.84 (RotB), 128.79 (RotB), 128.69 (2C RotA), 128.65 (RotA, RotB), 128.50 (2C RotA, RotB), 128.43 (2C RotA, RotB), 128.37 (RotB), 128.32 (RotB),127.94 (2C RotA, RotB), 127.16 (RotA, RotB), 126.74 (RotA, RotB), 126.12 (2C RotA, RotB), 126.01 (RotA), 125.99 (RotA, RotB), 125.7 (RotB), 102.60 (RotA), 98.97 (RotB), 86.88 (RotA, RotB), 52.48 (RotB), 49.74 (RotA), 35.99 (RotA, RotB), 35.19 (RotA, RotB), 29.91 (RotA, RotB). **ESI-HRMS** calcd for $C_{28}H_{27}NNaO$ $[M+Na]^+$ 416.1990, found 416.1994.

***N*-(cyclohex-2-en-1-yl)-N-(propa-1,2-dien-1-yl)benzamide**

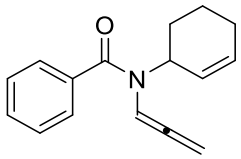

Allene **1w** was prepared following the general procedure **GP-2** from the corresponding propargyl amide (239.3 mg, 1 mmol). Colorless oil (165.1 mg, 69% yield). Two rotamers were observed due to the dynamic rotations of the amide group (73:27 mixture of rotamers). **^{1}H NMR** (600 MHz, $CDCl_3$) δ 7.58 – 7.55 (m, 1H RotB), 7.49 – 7.44 (m, 2H RotA, 2H RotB), 7.42 – 7.37 (m, 3H RotA, 2H RotB), 6.36 (br, 1H RotA, 1H RotB), 5.83 (br, 1H RotA, 1H RotB), 5.60 (d, *J* = 9.05 Hz, 1H RotA, 1H RotB), 5.39 – 4.93 (m, 3H RotA, 3H RotB), 2.22 – 1.83 (m, 6H RotA, 6H RotB). **^{13}C NMR** (151 MHz, $CDCl_3$) δ 204.11 (RotA, RotB), 170.39 (RotA, RotB), 138.02 (RotA, RotB), 136.26 (RotA, RotB), 130.83 (RotA, RotB), 129.98 (RotA, RotB), 129.18 (RotA, RotB), 128.43 (RotA, RotB), 128.37 (RotA, RotB), 128.27 (RotA, RotB), 125.44 (RotA, RotB), 84.59 (RotA, RotB), 39.40 (RotA, RotB), 26.39 (RotB), 24.65 (RotA), 22.04 (RotA, RotB), 21.60 (RotA, RotB). **ESI-HRMS** calcd for $C_{16}H_{17}NNaO$ $[M+Na]^+$ 262.1208 found 262.1213.

***N*-(cyclohex-2-en-1-yl)-4-fluoro-N-(propa-1,2-dien-1-yl)benzamide**

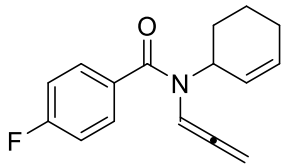

Allene **1x** was prepared following the general procedure **GP-2** from the corresponding propargyl amide (257 mg, 1 mmol). Light yellow oil (185 mg, 72% yield). Two rotamers were observed due to the dynamic rotations of the amide group (Due to broadness of signal, impossible to determine rotameric ratio). **^{1}H NMR** (600 MHz, $CDCl_3$) δ 7.50 – 7.48 (m, 2H RotA, 2H RotB), 7.06 (t, *J* = 8.7 Hz, 2H RotA, 2H RotB), 6.37 (br, 1H RotA, 1H RotB), 5.86 – 5.83 (m, 1H RotA, 1H RotB), 5.60 – 5.57 (m, 1H RotA, 1H RotB), 5.13 – 4.87 (m, 3H RotA, 3H RotB), 2.03 – 1.90 (m, 4H RotA, 4H RotB), 1.86 – 1.82 (m, 1H RotA, 1H RotB), 1.67 – 1.57 (m, 1H RotA, 1H RotB). **^{13}C NMR** (151 MHz, $CDCl_3$) δ 204.50 (RotA, RotB), 169.38 (RotA, RotB), 163.60 (d, *J* = 250.2 Hz, RotA, RotB), 132.28 (d, *J* = 3.5 Hz, RotA, RotB), 131.05 (2C RotA, 2C RotB), 130.27 (RotA, RotB), 127.99 (2C RotA, 2C RotB), 115.41 (d, *J* = 21.8 Hz, RotA, RotB), 98.05 (RotA, RotB), 84.48 (RotA, RotB), 52.80 (RotA, RotB), 26.44 (RotA, RotB), 24.60 (RotA, RotB), 21.88 (RotA, RotB). **^{19}F NMR** (565 MHz, $CDCl_3$) δ -109.82 – -109.85 (m). **ESI-HRMS** calcd for $C_{16}H_{16}FNNaO$ $[M+Na]^+$ 280.1114, found 280.1119.

***N*-(cyclohex-2-en-1-yl)-4-ethynyl-N-(propa-1,2-dien-1-yl)benzamide**

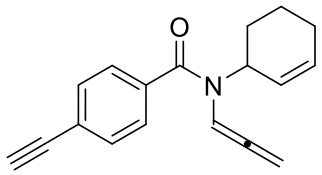

Allene **1y** was prepared following the general procedure **GP-2** from the corresponding propargyl amide (263.3 mg, 1 mmol). Light yellow oil (168.5 mg, 64% yield). **^{1}H NMR** (600 MHz, $CDCl_3$) δ 7.50 (d, *J* = 8.2 Hz, 2H), 7.43 (d, *J* = 7.8 Hz, 2H), 6.26 (br, 1H), 5.85 (br, 1H), 5.58 (dd, *J* = 10.2, 2.3 Hz, 1H), 5.29 – 4.94 (m, 3H), 3.15 (s, 1H), 2.03 – 1.82 (m, 5H), 1.73 – 1.52 (m, 1H). **^{13}C NMR** (151 MHz, $CDCl_3$) δ 204.7, 169.6, 136.5, 132.1, 131.2 (2C), 127.9 (3C), 123.8, 98.2, 84.5, 83.1, 78.9, 52.16, 26.5, 24.6, 21.9. **ESI-HRMS** calcd for $C_{18}H_{17}NNaO$ $[M+Na]^+$ 286.1208, found 286.1208.

***N*-(cyclohex-2-en-1-yl)-N-(propa-1,2-dien-1-yl)nicotinamide**

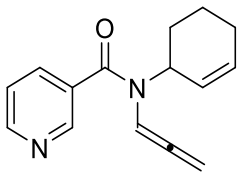

Allene **1z** was prepared following the general procedure **GP-2** from the corresponding propargyl amide (240.3 mg, 1 mmol). Light yellow oil (108.1 mg, 45% yield). **^{1}H NMR** (600 MHz, $CDCl_3$) δ 8.73 (s, 1H), 8.64 (s, 1H), 7.81 (d, *J* = 7.7 Hz, 1H), 7.35 – 7.33 (m, 1H), 6.22 (br, 1H), 5.91 (s, 1H), 5.60 (d, *J* = 10.1 Hz, 1H), 5.25 (br, 1H), 4.93 – 4.81 (m, 2H), 2.04 – 1.85 (m, 4H), 1.69 (s, 2H). **^{13}C NMR** (151 MHz, $CDCl_3$) δ 205.8, 168.0, 150.8, 149.1, 135.7, 134.9, 132.4, 131.7, 127.5, 123.3, 97.9, 84.4, 26.7, 24.6, 21.7. **ESI-HRMS** calcd for $C_{15}H_{16}N_2NaO$ $[M+Na]^+$ 263.1160, found 263.1168.

***N*-(cyclohex-2-en-1-yl)-N-(propa-1,2-dien-1-yl)acetamide**

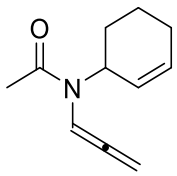

Allene **1a'** was prepared following the general procedure **GP-2** from the corresponding propargyl amide (177 mg, 1 mmol). Colorless oil (119 mg, 70% yield). Two rotamers were observed due to the dynamic rotations of the amide group (77:23 mixture of rotamers). **^{1}H NMR** (600 MHz, $CDCl_3$) δ 7.15 (t, *J* = 7.0 Hz, 1H RotB), 6.21 (t, *J* = 6.4 Hz, 1H RotA), 5.83 – 5.76 (m, 1H RotA, 1H RotB), 5.57 (d, *J* = 10.2 Hz, 1H RotB), 5.43 (d, *J* = 10.3 Hz, 1H RotA), 5.25 – 5.17 (m, 2H RotA, 1H RotB), 5.13 – 5.10 (m, 1H RotA. 1H RotB), 4.45 (br, 1H RotB), 2.17 (s, 3H RotB), 2.14 (s, 3H RotA), 2.00 – 1.95 (m, 3H RotA, 2H RotB), 1.88 – 1.76 (m, 1H RotA,

2H RotB), 1.74 – 1.70 (m, 1H RotA, 1H RotB), 1.66 – 1.60 (m, 1H RotA, 1H RotB). **^{13}C NMR** (151 MHz, $CDCl_3$) δ 205.7 (RotA), 203.2 (RotB), 169.9 (RotA), 169.1 (RotB), 130.8 (RotA), 130.3 (RotB), 128.6 (RotB), 128.2 (RotA), 96.9 (RotA), 95.9 (RotB), 85.2 (RotB), 83.7 (RotA), 55.5 (RotB), 51.1 (RotA), 27.2 (RotB), 26.6 (RotA), 24.6 (RotA), 24.4 (RotB), 23.2 (RotA), 22.8 (RotB), 22.2 (RotB), 21.7 (RotA). **ESI-HRMS** calcd for $C_{11}H_{15}NNaO$ $[M+Na]^+$ 200.1051, found 200.1045.

***N*-(cyclohex-2-en-1-yl)-N-(propa-1,2-dien-1-yl)cyclobutanecarboxamide**

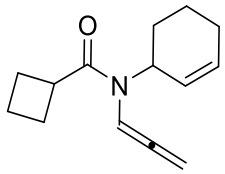

Allene **1b'** was prepared following the general procedure **GP-2** from the corresponding propargyl amide (217.1 mg, 1 mmol). Colorless oil (104.2 mg, 48% yield). Two rotamers were observed due to the dynamic rotations of the amide group (72:28 mixture of rotamers). **^{1}H NMR** (600 MHz, $CDCl_3$) δ 7.06 (br, 1H RotB), 6.20 (t, *J* = 6.4 Hz, 1H RotA), 5.79 – 5.76 (m, 1H RotA, 1H RotB), 5.51 (d, *J* = 10.3 Hz, 1H RotB), 5.45 (d, *J* = 10.1Hz, 1H RotA), 5.23 – 5.18 (m, 1H RotA, 1H RotB), 5.15 – 5.11 (m, 2H RotA), 5.09 – 5.06 (m, 1H RotB), 4.37 (br, 1H RotB), 3.41 – 3.31 (m, 1H RotA, 1H RotB), 2.42 – 2.29 (m, 2H RotA, 2H RotB), 2.20 – 2.09 (m, 2H RotA, 2H RotB), 2.05 – 1.74 (m, 6H RotA, 7H RotB), 1.69 – 1.43 (m, 2H RotA, 1H RotB). **^{13}C NMR** (151 MHz, $CDCl_3$) δ 204.6 (RotA), 203.8 (RotB), 173.9 (RotA), 173.3 (RotB), 130.5 (RotB), 130.1 (RotA), 128.7 (RotA, RotB), 96.5 (RotA), 95.2 (RotB), 84.4 (RotB), 84.0 (RotA), 54.2 (RotB), 51.8 (RotA), 38.3 (RotA), 38.2 (RotB), 27.4 (RotB), 26.4 (RotA), 25.7 (RotB), 25.5 (RotB), 25.4 (RotA), 25.3 (RotA), 24.7 (RotA), 24.5 (RotB), 22.4 (RotB), 21.9 (RotA), 18.1 (RotB), 17.9 (RotA). **ESI-HRMS** calcd for $C_{14}H_{19}NNaO$ $[M+Na]^+$ 240.1364 found 264.1361.

***N*-(((4S)-4-(prop-1-en-2-yl)cyclohex-2-en-1-yl)methyl)-N-(propa-1,2-dien-1-yl)benzamide**

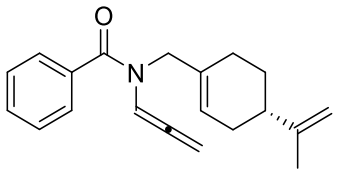

Allene **1c'** was prepared following the general procedure **GP-2** from the corresponding propargyl amide (293.1 mg, 1 mmol). Colorless oil (211.0 mg, 72% yield). Two rotamers were observed due to the dynamic rotations of the amide group (65:35 mixture of rotamers). **^{1}H NMR** (600 MHz, $CDCl_3$) δ 7.61 (s, 1H RotB), 7.48 – 7.45 (m, 2H RotA, 2H RotB), 7.39 – 7.37 (m, 3H RotA, 3H RotB), 6.61 (s, 1H RotA), 5.55 (br, 1H RotA), 5.48 (br, 1H RotB), 5.30 – 5.25 (m, 2H RotA, 2H RotB), 4.69 (d, *J* = 9.5 Hz, 2H RotA, 2H RotB), 4.20 (s, 2H RotA), 3.83 (s, 2H RotB), 2.15 – 2.11 (m, 3H RotA, 3H RotB), 1.96 – 1.91 (m, 1H RotA, 1H RotB), 1.81 – 1.76 (m, 2H RotA, 2H RotB), 1.71 (s, 3H RotA, 3H RotB), 1.47 – 1.40 (m, 1H RotA, 1H RotB). **^{13}C NMR** (151 MHz, $CDCl_3$) δ 203.1 (RotB), 200.7 (RotA), 170.0 (RotB), 169.3 (RotA), 149.6 (RotA, RotB),135.5

(RotA, RotB) 135.2 (RotA, RotB), 132.0 (2C RotA, 2C RotB), 130.1 (2C RotB), 128.4 (2C RotA), 127.9 (RotA), 126.8 (RotB), 122.6 (RotA), 122.3 (RotB), 108.7 (RotA, RotB), 102.3 (RotA), 98.9 (RotB), 86.5 (RotA, RotB), 52.9 (RotB), 49.3 (RotA), 40.9 (RotA, RotB), 30.5 (RotA, RotB), 27.4 (RotA, RotB), 26.7 (RotA, RotB), 20.8 (RotA, RotB). **ESI-HRMS** calcd for $C_{20}H_{24}NO$ $[M+H]^+$ 294.1858, found 294.1863.

N-((5R)-2-methyl-5-(prop-1-en-2-yl)cyclohex-2-en-1-yl)-N-(propa-1,2-dien-1-yl)benzamide

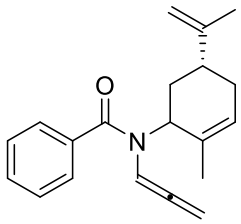

Allene **1d'** was prepared following general procedure **GP-2** from the corresponding propargyl amide (293 mg, 1 mmol). Orange oil (120 mg, 41% yield). Two rotamers were observed due to the dynamic amide group (57:43 mixture of rotamers). **^{1}H NMR** (600 MHz, $CDCl_3$) δ 7.50 – 7.36 (m, 5H RotA, 6H RotB), 6.28 (br, 1H RotB), 5.71 (br, 1H RotA, 1H RotB), 5.00 – 4.57 (m, 5H RotA, 5H RotB), 2.76 – 2.51 (m, 1H RotA, 1H RotB), 2.21 (t, *J* = 20.2 Hz, 2H RotA, 2H RotB), 2.02 – 1.87 (m, 2H RotA, 2H RotB), 1.72 (s, 6H RotA, 6H RotB). **^{13}C NMR** (151 MHz, $CDCl_3$) δ 205.62 (RotA, RotB), 170.93 (RotA, RotB), 148.04 (RotA, RotB), 136.76 (RotA, RotB), 131.04 (RotA, RotB), 129.82 (2C RotA, 2C RotB), 128.32 (2C RotA, 2C RotB), 127.99 (RotA, RotB), 127.26 (RotA, RotB), 109.55 (RotA, RotB), 99.31 (RotA, RotB), 83.64 (RotA, RotB), 53.64 (RotA, RotB), 37.53 (RotA, RotB), 32.35 (RotA, RotB), 30.02 (RotA, RotB), 21.36 (2C RotA), 20.67 (2C RotB). **ESI-HRMS** calcd for $C_{20}H_{24}NO$ $[M+H]^+$ 294.1858, found 294.1858.

N-(3-methylbut-3-en-1-yl)-N-(propa-1,2-dien-1-yl)benzamide

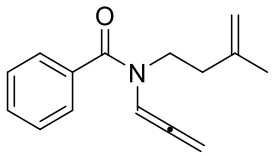

Allene **1e'** was prepared following general procedure **GP-2** from the corresponding propargyl amide (227 mg, 1 mmol). Colorless oil (134 mg, 59% yield). Two rotamers were observed due to the dynamic amide group (80:20 mixture of rotamers). **^{1}H NMR** (600 MHz, $CDCl_3$) δ 7.48 – 7.40 (m, 5H RotA, 6H RotB), 6.65 (t, *J* = 6.4 Hz, 1H RotA), 5.41 – 5.35 (d, *J* = 6.3 Hz, 2H RotA, 2H RotB), 4.78 (d, *J* = 20.5 Hz, 2H RotA), 4.68 (br, 1H RotB), 4.55 (br, 1H RotB), 3.79 (br, 2H RotA), 3.47 (br, 2H RotB), 2.37 (br, 1H RotA), 2.24 (br, 1H RotB), 1.82 (s, 3H RotA), 1.45 (s, 3H RotB). **^{13}C NMR** (151 MHz, $CDCl_3$) δ 200.02 (RotA, RotB), 169.32 (RotA), 168.21 (RotB), 143.10 (RotA, RotB), 135.82 (RotB), 135.31 (RotA), 130.30 (RotA, RotB), 128.58 (2C RotA, 2C RotB), 128.05 (2C RotA), 126.96 (2C RotB), 112.71 (RotB), 112.13 (RotA), 102.45 (RotA), 98.38 (RotB), 86.84 (RotA, RotB), 46.62 (RotB), 43.00 (RotA), 36.48 (Rotb), 35.43 (RotA), 22.60 (RotA, RotB). **ESI-HRMS** calcd for $C_{15}H_{17}NNaO$ $[M+Na]^+$ 250.1208, found 250.1216.

Synthesis and characterization of products:

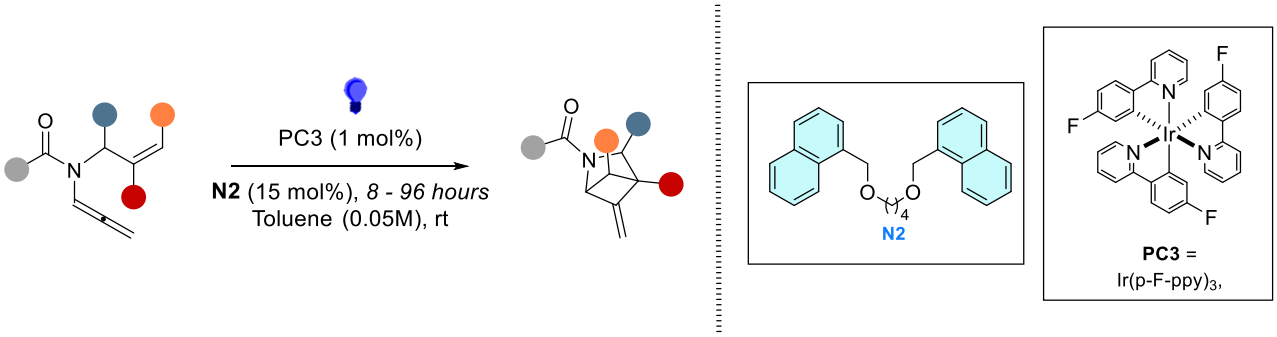

A vial was charged with allene (1 equiv., 0.1 mmol), the Iridium catalyst **PC3** (0.7 mg, 1 umol, 1 mol%), and the corresponding binaphthyl additive **N2** (5.7 mg, 0.015 mmol, 15 mol%). The mixture was dissolved in freshly distilled Toluene (2 ml, 0.05 M). The solution was transferred into an NMR tube capped with a rubber septum, degassed by freeze-pump-thaw (3 times), and afterwards irradiated with a purple LED strip for 8-96 hours at room temperature. At complete conversion of the starting material, as determined by TLC, the mixture was then concentrated in vacuo. The residue was purified by chromatography on silica gel (*n*-hexane/EtOAc gradient) to afford the desired product.

(4-methyl-5-methylene-2-azabicyclo[2.1.1]hexan-2-yl)(phenyl)methanone

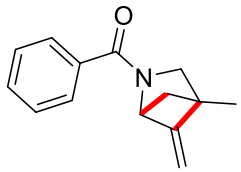

Product **2a** was prepared following general procedure **GP-1** from the corresponding allene (21.3 mg, 0.1 mmol). Only one diasteroisomer was isolated from the mixture as a light-yellow oil (15.8 mg, 74% yield). Two rotamers were observed due to the dynamic amide group (59:41 mixture of rotamers). **^{1}H NMR** (400 MHz, $CDCl_3$) δ 7.60 – 7.58 (m, 2H RotB), 7.51 – 7.49 (m, 2H RotA), 7.45 – 7.37 (m, 3H RotA, 3H RotB), 5.15 (s, 1H RotB), 4.64 (s, 1H RotB), 4.54 (s, 1H RotA), 4.51 (s, 1H RotA), 4.46 (s, 1H RotA, 1H RotB), 3.54 (d, *J* = 9.3 Hz, 1H RotA), 3.42 (s, 1H RotA), 3.32 (d, *J* = 7.7 Hz, 1H RotB), 3.26 (d, *J* = 7.8 Hz, 1H RotB), 1.82 (d, *J* = 7.0 Hz, 1H RotA), 1.76 – 1.69 (m, 1H RotA, 2H RotB), 1.39 (s, 3H RotA), 1.30 (s, 3H RotB). **^{13}C NMR** (101 MHz, $CDCl_3$) δ 170.49 (RotB), 168.28 (RotA), 152.97 (RotA), 152.62 (RotB), 136.03 (RotA), 135.61 (RotB), 130.52 (RotB), 130.24 (RotA), 128.49 (2C RotA, 2C RotB), 127.56 (2C RotA, 2C RotB), 91.13 (RotB), 90.82 (RotA), 66.06 (RotA), 62.39 (RotB), 57.26 (RotB), 53.34 (RotB), 53.23 (RotA), 52.54 (RotA), 43.52 (RotA), 42.35 (RotB), 12.95 (RotA), 12.73 (RotB). **ESI-HRMS** calcd for $C_{14}H_{15}KNO$ $[M+K]^+$ 252.0791, found 252.0794.

(4-chlorophenyl)(4-methyl-5-methylene-2-azabicyclo[2.1.1]hexan-2-yl)methanone

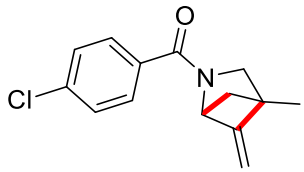

Product **2b** was prepared following general procedure **GP-1** from the corresponding allene (24.8 mg, 0.1 mmol). Only one diasteroisomer was isolated from the mixture as a colorless oil (22.7 mg, 92% yield). Two rotamers were observed due to the dynamic amide group (59:41 mixture of rotamers). **^{1}H NMR** (600 MHz, $CDCl_3$) δ 7.56 (d, *J* = 8.0 Hz, 2H RotB), 7.45 (d, *J* = 8.0 Hz, 2H RotA), 7.40 – 7.37 (m, 2H RotA, 2H RotB), 5.13 (s, 1H RotB), 4.65 (s, 1H RotB), 4.51 (s, 1H RotA), 4.50 (s, 1H RotA), 4.47 (s, 1H RotA, 1H RotB), 3.52 (d, *J* = 9.3 Hz, 1H RotA), 3.40 (d, *J* = 9.4 Hz, 1H RotA), 3.31 (d, *J* = 7.6 Hz, 1H RotB), 3.25 (d, *J* = 7.7 Hz, 1H RotB), 1.81 (d, *J* = 7.0 Hz, 2H RotB), 1.77 – 1.70 (m, 2H RotA), 1.40 (s, 3H RotA), 1.31 (s, 3H RotB). **^{13}C NMR** (151 MHz, $CDCl_3$) δ 169.48 (RotB), 167.37 (RotA), 153.06 (RotA), 152.67 (RotB), 136.68 (RotB), 136.30 (RotA), 134.68 (RotA), 134.18 (RotB), 129.29 (2C RotB), 129.13 (2C RotA), 128.82 (2C RotA), 128.75 (2C RotB), 91.25 (RotB), 90.89 (RotA), 66.20 (RotA), 62.63 (RotB), 57.45 (RotB), 53.44 (RotA), 52.67 (RotA, RotB), 43.67 (RotA), 42.46 (RotB), 12.89 (RotA), 12.67 (RotB). **ESI-HRMS** calcd for $C_{14}H_{14}ClKNO$ $[M+K]^+$ 286.0402, found 286.0405.

(2,6-dimethylphenyl)(4-methyl-5-methylene-2-azabicyclo[2.1.1]hexan-2-yl)methanone

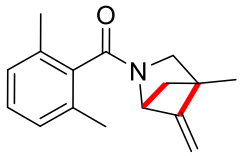

Product **2c** was prepared following general procedure **GP-1** from the corresponding allene (24.1 mg, 0.1 mmol). Only one diastereoisomer was isolated from the mixture as a light red oil (22.7 mg, 94% yield). Two rotamers were observed due to the dynamic rotations of the amide group (63:37 mixture of rotamers). **^{1}H NMR** (600 MHz, $CDCl_3$) δ 7.16 – 7.13 (m, 1H RotA, 1H RotB), 7.03 – 7.01 (m, 2H RotA, 2H RotB), 5.26 (s, 1H RotB), 4.65 (s, 1H RotB), 4.47 – 4.45 (m, 2H RotA, 1H RotB), 3.93 (s, 1H RotA), 3.55 (d, *J* = 9.3 Hz, 1H RotA), 3.45 (d, *J* = 9.4, 1H RotA), 2.90 (d, *J* = 8.0 Hz, 1H RotB), 2.77 (d, *J* = 8.1 Hz, 1H RotB), 2.30 (s, 3H RotB), 2.29 (s, 3H RotA), 2.23 (s, 3H RotA), 2.22 (s, 3H RotB), 1.83 – 1.81 (m, 1H RotB), 1.75 – 1.70 (m, 2H RotA, 1H RotB), 1.39 (s, 3H RotA), 1.27 (s, 3H RotB). **^{13}C NMR** (151 MHz, $CDCl_3$) δ 168.7 (RotB), 167.6 (RotA), 153.6 (RotA), 152.8 (RotB), 136.9 (RotA), 136.3 (RotB), 134.3 (RotA), 134.0 (RotA), 133.9 (RotB), 133.4 (RotB), 128.7 (RotB), 128.6 (RotA), 127.7 (RotB), 127.63 (RotB), 127.59 (RotA), 127.56(RotA), 91.3 (RotB), 90.9 (RotA), 65.2 (RotA), 61.6 (RotB), 54.8 (RotA), 53.1 (RotB), 52.9 (RotB), 52.6 (RotA), 44.1 (RotA), 42.7 (RotB), 19.3 (RotA),19.3 (RotA) 19.1 (RotB), 18.9 (RotB), 13.0 (RotA), 12.7 (RotB). **ESI-HRMS** calcd for $C_{16}H_{19}NNaO$ $[M+Na]^+$ 264.1364 found 264.1366.

(2-bromo-5-methoxyphenyl)(4-methyl-5-methylene-2-azabicyclo[2.1.1]hexan-2-yl)methanone

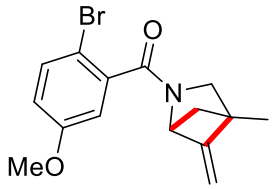

Product **2d** was prepared following general procedure **GP-1** from the corresponding allene (32.2 mg, 0.1 mmol). Only one diasteroisomer was isolated from the mixture as a light-yellow oil (20.6 mg, 64% yield). Two rotamers were observed due to the dynamic amide group (58:42 mixture of rotamers). **^{1}H NMR** (600 MHz, $CDCl_3$) δ 7.45 – 7.43 (m, 1H RotA, 1H RotB), 6.86 (d, *J* = 3.0 Hz, 1H RotA), 6.83 (d, *J* = 3.0 Hz, 1H RotB), 6.82 – 6.79 (m, 1H RotA, 1H RotB), 5.20 (s, 1H RotB), 4.64 (s, 1H RotB), 4.48 (s, 1H RotA), 4.47 (s, 1H RotA), 4.10 (s, 1H RotA), 3.79 (s, 3H RotA), 3.79 (s, 4H RotB), 3.53 (d, *J* = 9.4 Hz, 1H RotA), 3.41 (d, *J* = 9.3 Hz, 1H RotA), 3.11 (d, *J* = 7.8 Hz, 1H RotB), 2.99 (d, *J* = 7.8, 1H RotB), 1.82 (d, *J* = 7.1 Hz, 1H RotA), 1.79 – 1.77 (m, 1H RotA), 1.72 – 1.71 (m, 2H RotB), 1.39 (s, 3H RotA), 1.29 (s, 3H RotB). **^{13}C NMR** (151 MHz, $CDCl_3$) δ 166.49 (RotB), 165.41 (RotA), 159.31 (RotB), 159.19 (RotA), 153.02 (RotA), 152.46 (RotB), 139.24 (RotA), 138.95 (RotB), 133.85 (RotB), 133.78 (RotA), 116.96 (RotB), 116.83 (RotA), 113.71 (RotA), 113.26 (RotB), 109.73 (RotA), 109.38 (RotB), 91.35 (RotA, RotB), 65.75 (RotA), 62.14 (RotB), 55.78 (RotA, RotB), 55.16 (RotA), 53.22 (RotB), 53.08 (RotA), 52.59 (RotB), 43.90 (RotB), 42.51 (RotA), 12.87 (RotA), 12.65 (RotB). **ESI-HRMS** calcd for $C_{15}H_{16}BrKNO_2$ $[M+K]^+$ 360.0001, found 360.0005.

(4-methyl-5-methylene-2-azabicyclo[2.1.1]hexan-2-yl)(naphthalen-2-yl)methanone

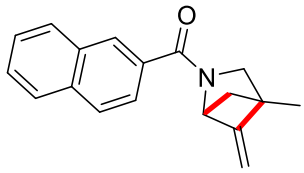

Product **2e** was prepared following general procedure **GP-1** from the corresponding allene (26.3 mg, 0.1 mmol). Only one diasteroisomer was isolated from the mixture as a light-orange solid (14.5 mg, 55% yield). **^{1}H NMR** (600 MHz, $CDCl_3$) δ 7.31 – 7.30 (m, 1H), 7.27 – 7.25 (m, 2H), 7.17 – 7.12 (m, 2H), 6.69 – 6.66 (m, 1H), 6.60 – 6.58 (m, 1H), 6.03 (t, *J* = 2.1 Hz, 1H), 4.88 (s, 1H), 4.81 (s, 1H), 4.28 – 4.26 (m, 1H), 4.21 (d, *J* = 15.5 Hz, 1H), 3.98 (d, *J* = 15.5 Hz, 1H), 2.46 (dt, *J* = 15.5, 2.5 Hz, 1H), 2.35 (dt, *J* = 15.5, 2.4 Hz, 1H), 1.72 (s, 3H). **^{13}C NMR** (151 MHz, $CDCl_3$) δ 175.76, 142.33, 140.96, 139.02, 136.18, 132.02, 126.12, 125.99, 123.56, 123.30, 121.31, 120.70, 112.87, 61.59, 48.07, 42.92, 30.01, 20.06. **ESI-HRMS** calcd for $C_{18}H_{18}NO$ $[M+H]^+$ 264.1388, found 264.1388.

(1H-indol-2-yl)(4-methyl-5-methylene-2-azabicyclo[2.1.1]hexan-2-yl)methanone

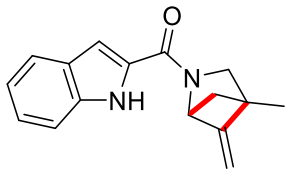

Product **2f** was prepared following general procedure **GP-1** from the corresponding allene (25.3 mg, 0.1 mmol). Only one diasteroisomer was isolated from the mixture as a white solid (19.2 mg, 76% yield). Two rotamers were observed due to the dynamic amide group (87:13 mixture of rotamers). **^{1}H NMR** (600 MHz, $CDCl_3$) δ 9.44 (br, 1H RotA), 9.35 (br, 1H RotB), 7.66 (d, *J* = 8.0 Hz, 1H RotA, 1H RotB), 7.44 (d, *J* = 8.3 Hz, 1H RotA, 1H RotB), 7.30 – 7.28 (m, 1H RotA, 1H RotB), 7.14 (t, *J* = 7.5 Hz, 1H RotA, 1H RotB), 6.89 (s, 1H RotA, 1H RotB), 5.33 (s, 1H RotB), 5.28 (s, 1H RotA), 4.66 (s, 1H RotA), 4.61 (s, 1H RotB), 3.81 (d, *J* = 7.4 Hz, 1H RotA), 3.70 (d, *J* = 7.3 Hz, 1H RotA), 3.59 (br, 1H RotB), 3.48 (br, 1H RotB), 1.83 – 1.79 (m, 2H RotA, 2H RotB), 1.44 (s, 3H RotA, 3H RotB). **^{13}C NMR** (151 MHz, $CDCl_3$) δ 160.67 (RotA), 160.50 (RotB) 153.03 (RotA, RotB), 135.57 (RotA, RotB), 131.76 (RotA, RotB), 130.22 (RotA, RotB), 128.38 (RotA, RotB), 124.65 (RotA, RotB), 122.20 (RotA, RotB), 120.61 (RotA, RotB), 111.89 (RotA, RotB), 104.53 (RotA, RotB), 91.35 (RotA, RotB), 62.76 (RotA, RotB), 56.89 (RotA, RotB), 53.51 (RotA, RotB), 42.89 (RotA, RotB), 12.84 (RotA, RotB). **ESI-HRMS** calcd for $C_{16}H_{17}N_2O$ $[M+H]^+$ 253.1341, found 253.1338.

Furan-2-yl(4-methyl-5-methylene-2-azabicyclo[2.1.1]hexan-2-yl)methanone

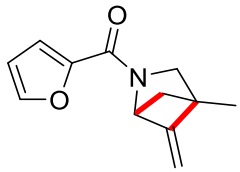

Product **2g** was prepared following general procedure **GP-1** from the corresponding allene (20.3 mg, 0.1 mmol). Only one diasteroisomer was isolated from the mixture as a light-yellow oil (16.4 mg, 81% yield). Two rotamers were observed due to the dynamic amide group (63:37 mixture of rotamers). **^{1}H NMR** (600 MHz, $CDCl_3$) δ 7.49 (d, *J* = 0.8 Hz, 1H RotA, 1H RotB), 7.10 (s, 1H RotA, 1H RotB), 6.49 (d, *J* = 1.7 Hz, 1H RotA, 1H RotB), 5.48 (s, 1H RotB), 5.19 (s, 1H RotA), 4.61 (s, 1H RotA), 4.58 (s, 1H RotB), 4.47 (s, 1H RotA, 1H RotB), 3.75 (d, *J* = 8.2 Hz, 1H RotA), 3.66 (d, *J* = 8.2 Hz, 1H RotA), 3.52 (br, 1H RotB), 3.39 (br, 1H RotB), 1.79 – 1.72 (m, 2H RotA, 2H RotB), 1.38 (s, 3H RotA, 3H RotB). **^{13}C NMR** (151 MHz, $CDCl_3$) δ 153.01 (RotA, RotB), 148.85 (RotA, RotB), 144.19 (2C RotA, 2C RotB), 116.14 (RotB), 115.84 (RotA), 111.61 (RotA RotB), 91.08 (RotA), 90.78 (RotB), 65.14 (RotB), 62.32 (RotA), 56.47 (RotA), 53.92 (RotB), 43.91 (RotB), 42.44 (RotA), 35.13 (RotA, RotB), 12.77 (RotA, RotB). **ESI-HRMS** calcd for $C_{12}H_{13}NNaO_2$ $[M+Na]^+$ 226.0844, found 226.0848.

3-(4-methyl-5-methylene-2-azabicyclo[2.1.1]hexan-2-yl)-3-oxopropanenitrile

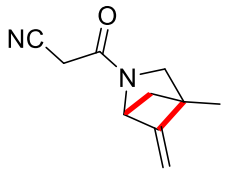

Product **2h** was prepared following general procedure **GP-1** from the corresponding allene (17.7 mg, 0.1 mmol). Only one diasteroisomer was isolated from the mixture as a colorless oil (8.8 mg, 64% yield). Two rotamers were observed due to the dynamic amide group (54:46 mixture of rotamers). **^{1}H NMR** (600 MHz, $CDCl_3$) δ 5.04 (d, *J* = 1.2 Hz, 1H RotA), 4.63 (s, 1H RotB), 4.62 (s, 1H RotA), 4.55 (d, *J* = 1.0 Hz, 1H RotB), 4.51 (s, 1H RotB), 4.50 (s, 1H RotA), 3.45 – 3.44 (m, 2H RotA, 1H RotB), 3.39 (d, *J* = 9.2 Hz, 1H RotA), 3.35 (s, 1H RotA, 1H RotB), 3.31 (dd, *J* = 7.1, 1.5 Hz, 1H RotB), 3.27 (dd, *J* = 9.3, 1.7 Hz, 1H RotB), 1.84 – 1.82 (m, 1H RotB), 1.79 – 1.77 (m, 1H RotA, 1H RotB), 1.70 – 1.69 (m, 1H RotA), 1.39 – 1.38 (m, 3H RotA, 3H RotB). **^{13}C NMR** (151 MHz, $CDCl_3$) δ 158.76 (RotA), 158.33 (RotB), 152.15 (RotA), 151.88 (RotB), 113.97 (RotB), 113.92 (RotA), 92.09 (RotA), 91.92 (RotB), 65.07 (RotB), 62.61 (RotA), 54.74 (RotA), 53.83 (RotB), 53.51 (RotA), 52.76 (RotB), 43.77 (RotB), 42.75 (RotA), 25.22 (RotB), 24.86 (RotA), 12.73 (RotB), 12.65 (RotA). **ESI-HRMS** calcd for $C_{10}H_{12}N_2NaO$ $[M+Na]^+$ 199.0847, found 199.0842.

1-(4-methyl-5-methylene-2-azabicyclo[2.1.1]hexan-2-yl)pent-4-en-1-one

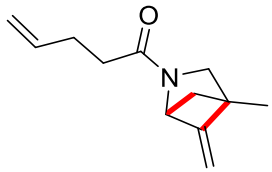

Product **2i** was prepared following general procedure **GP-1** from the corresponding allene (24.4 mg, 0.1 mmol). Only one diasteroisomer was isolated from the mixture as a light yellow oil (17.4 mg, 71% yield). Two rotamers were observed due to the dynamic amide group (52:48 mixture of rotamers). **^{1}H NMR** (600 MHz, $CDCl_3$) δ 5.85 (tdd, *J* = 16.7, 8.2, 5.6 Hz, 1H RotA, 1H RotB), 5.06 (s, 1H RotA), 5.03 (m, 1H RotA, 1H RotB), 4.99 – 4.96 (m, 1H RotA, 1H RotB), 4.53 (s, 1H RotB), 4.51 (d, *J* = 9.1 Hz, 1H RotA, 1H RotB), 4.41 (d, *J* = 6.4 Hz, 1H RotA, 1H RotB), 3.34 – 3.32 (m, 1H RotA, 1H RotB), 3.22 – 3.19 (m, 1H RotA, 1H RotB), 2.42 – 2.39 (m, 4H RotA, 2H RotB), 2.28 – 2.25 (m, 2H RotB), 1.73 – 1.71 (m, 1H RotB), 1.69 – 1.68 (m, 1H RotA, 1H RotB), 1.61 (d, *J* = 7.0 Hz, 1H RotA), 1.33 (s, 3H RotA, 3H RotB). **^{13}C NMR** (151 MHz, $CDCl_3$) δ 169.98 (RotA), 169.81 (RotB), 153.45 (RotB), 153.10 (RotA), 137.59 (RotA), 137.54 (RotB), 115.30 (RotA, RotB), 90.67 (RotA), 90.39 (RotB), 64.37 (RotB), 61.60 (RotA), 54.47 (RotA), 53.23 (RotB), 53.10 (RotA), 52.65 (RotB), 43.70 (RotB), 42.79 (RotA), 33.62 (RotB), 32.96 (RotA), 29.42 (RotB), 29.17 (RotA), 12.87 (RotB), 12.78 (RotA). **ESI-HRMS** calcd for $C_{12}H_{18}NO$ $[M+H]^+$ 192.1388, found 192.1391.

1-(4-methyl-5-methylene-2-azabicyclo[2.1.1]hexan-2-yl)pent-4-yn-1-one

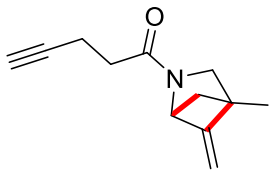

Product **2j** was prepared following general procedure **GP-1** from the corresponding allene (19.1 mg, 0.1 mmol). Only one diasteroisomer was isolated from the mixture as a light yellow oil (13.6 mg, 71% yield). Two rotamers were observed due to the dynamic amide group (57:43 mixture of rotamers). **^{1}H NMR** (600 MHz, $CDCl_3$) δ 5.04 (d, *J* = 1.8 Hz, 1H RotA), 4.56 – 4.55 (m, 1H RotA, 1H RotB), 4.52 (s, 1H RotB), 4.44 – 4.43 (m, 1H RotA, 1H RotB), 3.38 (d, *J* = 7.3 Hz, 1H RotA), 3.35 (d, *J* = 9.1 Hz, 1H RotB), 3.25 (d, *J* = 5.8 Hz, 1H RotA), 3.22 (d, *J* = 9.1 Hz, 1H RotB), 2.58 – 2.54 (m, 4H RotA, 2H RotB), 2.46 – 2.39 (m, 2H RotB), 1.96 – 1.94 (m, 1H RotA, 1H RotB), 1.75 – 1.63 (m, 2H RotA, 2H RotB), 1.35 (s, 3H RotA, 3H RotB). **^{13}C NMR** (151 MHz, $CDCl_3$) δ 168.51 (RotA), 168.34 (RotB), 153.29 (RotB), 152.97 (RotA), 90.86 (RotA), 90.61 (RotB), 83.56 (RotA, RotB), 68.86 (RotA, RotB), 64.34 (RotB), 61.77 (RotA), 54.42 (RotA), 53.26 (RotB), 53.18 (RotA), 52.63 (RotB), 43.76 (RotB), 42.86 (RotA), 33.16 (RotB), 32.55 (RotA), 14.60 (RotB), 14.46 (RotA), 12.86 (RotB), 12.79 RotA). **ESI-HRMS** calcd for $C_{12}H_{15}KNO$ $[M+K]^+$ 228.0791, found 228.0794.

4-methyl-5-methylene-2-tosyl-2-azabicyclo[2.1.1]hexane

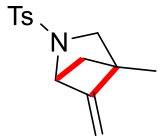

Product **2k** was prepared following general procedure **GP-1** from the corresponding allene (26.3 mg, 0.1 mmol). Only one diasteroisomer was isolated from the mixture as a colorless oil (19.5 mg, 74% yield). **^{1}H NMR** (600MHz, $CDCl_3$) δ 7.68 (d, *J* = 8.3 Hz, 2H), 7.27 (d, *J* = 8.0 Hz, 2H), 4.42 (d, *J* = 1.1 Hz, 1H), 4.15 (s, 1H), 4.12 (s, 1H), 3.24 (d, *J* = 7.9 Hz, 1H), 2.95 (dd, *J* = 8.0, 1.6 Hz, 1H), 2.41 (s, 3H), 1.60 (dt, *J* = 7.2, 1.3 Hz, 1H), 1.53 (dt, *J* = 7.2, 1.8 Hz, 1H), 1.19 (s, 3H). **^{13}C NMR** (151 MHz, $CDCl_3$) δ 151.17, 143.60, 134.80, 129.61 (2C), 128.44 (2C), 91.86, 65.46, 54.71, 53.22, 41.74, 21.67, 12.56. **ESI-HRMS** calcd for $C_{14}H_{17}KNO_2S$ $[M+K]^+$ 302.0617, found 302.0612.

tert-butyl 4-methyl-5-methylene-2-azabicyclo[2.1.1]hexane-2-carboxylate

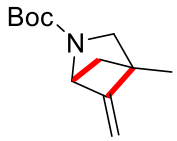

Product **2l** was prepared following general procedure **GP-1** from the corresponding allene (20.9 mg, 0.1 mmol). Only one diasteroisomer was isolated from the mixture as a colorless oil (14.0 mg, 67% yield). **^{1}H NMR** (400 MHz, $CDCl_3$) δ 4.54 (s, 1H), 4.51 (s, 1H), 4.38 (s, 1H), 3.23 (d, *J* = 8.1 Hz, 1H), 3.10 (d, *J* = 8.1 Hz, 1H), 1.66 – 1.63 (m, 2H), 1.46 (s, 9H), 1.31 (s, 3H). **^{13}C NMR** (101 MHz, $CDCl_3$) δ 154.20, 110.39, 89.95, 79.50, 53.08, 43.08, 31.15, 28.66, 18.38, 12.84. **ESI-HRMS** calcd for $C_{12}H_{19}NNaO_2$ $[M+Na]^+$ 232.1313, found 232.1315.

(5-methylene-4-phenyl-2-azabicyclo[2.1.1]hexan-2-yl)(phenyl)methanone

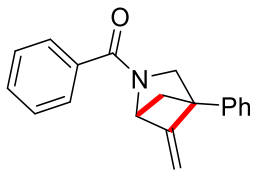

Product **2m** was prepared following general procedure **GP-1** from the corresponding allene (27.4 mg, 0.1 mmol). Only one diasteroisomer was isolated from the mixture as a colorless oil (14.8 mg, 54% yield). Two rotamers were observed due to the dynamic amide group (62:38 mixture of rotamers). **^{1}H NMR** (600 MHz, $CDCl_3$) δ 7.65 (d, *J* = 7.5 Hz, 2H RotB), 7.57 (d, *J* = 5.8 Hz, 2H RotA), 7.48 – 7.41 (m, 5H RotA, 5H RotB), 7.36 – 7.30 (m, 3H RotA, 3H RotB), 5.30 (s, 1H RotB), 4.79 (s, 1H RotB), 4.70 (s, 1H RotA), 4.65 (s, 1H RotA), 4.52 (s, 1H RotB), 4.49 (s, 1H RotA), 3.96 – 3.91 (m, 2H RotA), 3.74 (d, *J* = 7.8 Hz, 1H RotB), 3.68 (d, *J* = 7.7 Hz, 1H RotB), 2.31 – 2.27 (m, 2H RotA), 2.16 (d, *J* = 6.9 Hz, 1H RotA), 2.09 (d, *J* = 7.0 Hz, 1H RotA). **^{13}C NMR** (151 MHz, $CDCl_3$) δ 173.04 (RotB), 170.89 (RotA), 152.71 (RotA), 152.13 (RotB), 140.65 (RotA, RotB), 135.70

(RotA, RotB), 130.40 (RotA, RotB), 128.91 (2C RotA), 128.84 (2C RotB), 128.62 (2C RotA), 128.55 (2C RotB), 127.84 (2C RotA, 2C RotB), 127.70 (2C RotA, 2C RotB), 127.20 (RotA), 127.01 (RotB), 93.01 (RotB), 92.60 (RotA), 65.77 (RotA), 62.13 (RotB), 59.30 (RotA, RotB), 56.79 (RotB), 52.38 (RotA), 43.34 (RotA), 41.75 (RotB). **ESI-HRMS** calcd for $C_{19}H_{17}NNaO$ $[M+Na]^+$ 298.1208, found 298.1205.

(4-benzyl-5-methylene-2-azabicyclo[2.1.1]hexan-2-yl)(phenyl)methanone

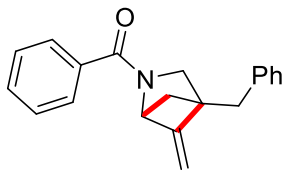

Product **2n** was prepared following general procedure **GP-1** from the corresponding allene (28.9 mg, 0.1 mmol). Only one diasteroisomer was isolated from the mixture as a colorless oil (26.0 mg, 90% yield). Two rotamers were observed due to the dynamic amide group (68:32 mixture of rotamers). **^{1}H NMR** (600 MHz, $CDCl_3$) δ 7.55 (d, *J* = 7.4 Hz, 2H RotB), 7.47 – 7.46 (m, 2H RotA), 7.44 – 7.36 (m, 3H RotA, 3H RotB), 7.32 – 7.28 (m, 2H RotA, 2H RotB), 7.25 – 7.22 (m, 1H RotA, 1H RotB), 7.19 (d, *J* = 7.4 Hz, 2H RotA), 7.11 (d, *J* = 7.5 Hz, 2H RotB), 5.14 (s, 1H RotB), 4.71 (s, 1H RotB), 4.59 – 4.58 (m, 2H RotA, 1H RotB), 4.53 (s, 1H RotA), 3.45 (s, 1H RotA, 1H RotB), 3.32 (d, *J* = 7.9 Hz, 1H RotB), 3.23 (d, *J* = 7.8 Hz, 1H RotB), 3.13 – 3.08 (m, 2H RotA, 1H RotB), 2.97 (d, *J* = 14.5 Hz, 1H RotA), 1.87 (d, *J* = 7.4 Hz, 1H RotB), 1.81 (d, *J* = 7.0 Hz, 1H RotA), 1.72 (d, *J* = 6.9 Hz, 1H RotA), 1.65 (d, *J* = 7.3 Hz, 1H RotB). **^{13}C NMR** (151 MHz, $CDCl_3$) δ 170.54 (RotB), 168.42 (RotA), 152.33 (RotA), 151.99 (RotB), 137.14 (RotB), 137.08 (RotA), 136.20 (RotA), 135.67 (RotB), 130.57 (RotB), 130.24 (RotA), 129.34 (RotA), 129.27 (RotB), 128.70 (4C RotA, 4C RotB), 128.53 (RotA), 128.47 (RotB), 127.79 (RotB), 127.58 (RotA), 126.74 (RotA, RotB), 92.21 (RotB), 91.81 (RotA), 65.41 (RotA), 61.74 (RotB), 57.57 (RotB), 56.81 (RotA), 55.45 (RotB), 51.56 (RotA), 42.16 (RotA), 40.86 (RotB), 35.12 (RotA), 34.90m (RotB). **ESI-HRMS** calcd for $C_{20}H_{19}NNaO$ $[M+Na]^+$ 312.1364, found 312.1359.

(5-methylene-4-pentyl-2-azabicyclo[2.1.1]hexan-2-yl)(phenyl)methanone

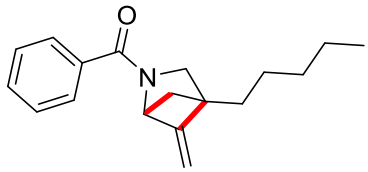

Product **2o** was prepared following general procedure **GP-1** from the corresponding allene (26.9 mg, 0.1 mmol). Only one diasteroisomer was isolated from the mixture as a light-yellow oil (22.5 mg, 84% yield). Two rotamers were observed due to the dynamic amide group (63:37 mixture of rotamers). **^{1}H NMR** (600 MHz, $CDCl_3$) δ 7.60 (d, *J* = 7.4 Hz, 2H RotB), 7.51 – 7.49 (m, 2H RotA), 7.45 – 7.39 (m, 3H RotA, 3H RotB), 5.13 (s, 1H RotB), 4.66 (s, 1H RotB), 4.53 (s, 2H RotA), 4.47 (s, 1H RotA, 1H RotB), 3.59 (d, *J* = 9.3 Hz, 1H RotA), 3.43 (d, *J* = 9.3 Hz, 1H RotA), 3.35 (d, *J* = 7.8 Hz, 1H RotB), 3.28 (d, *J* = 7.8 Hz, 1H RotB), 1.79 – 1.66 (m, 4H RotA, 4H RotB), 1.44 – 1.25 (m, 6H RotA, 6H RotB), 0.92 – 0.86 (m, 3H RotA, 3H RotB). **^{13}C NMR** (151 MHz,

$CDCl_3$) δ 170.60 (RotB), 168.48 (RotA), 152.64 (RotA), 152.26 (RotB), 136.35 (RotA), 135.89 (RotB), 130.49 (RotB), 130.18 (RotA), 128.50 (2C RotA), 128.44 (2C RotB), 127.76 (2C RotB), 127.60 (2C RotA), 91.71 (RotB), 91.34 (RotA), 65.83 (RotA), 62.16 (RotB), 57.66 (RotB), 56.80 (RotA), 55.90 (RotB), 51.83 (RotA), 41.82 (RotA), 40.55 (RotB), 32.41 (RotA, RotB), 27.92 (RotA), 27.80 (RotB), 25.13 (RotA, RotB), 22.64 (RotA), 22.61 (RotB), 14.11 (RotA, RotB). **ESI-HRMS** calcd for $C_{18}H_{23}NNaO$ $[M+Na]^+$ 292.1677, found 292.1673.

(5-methylene-4-(pent-4-en-1-yl)-2-azabicyclo[2.1.1]hexan-2-yl)(phenyl)methanone

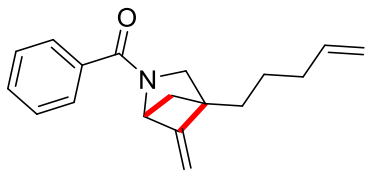

Product **2p** was prepared following general procedure **GP-1** from the corresponding allene (26.7 mg, 0.1 mmol). Only one diasteroisomer was isolated from the mixture as a light-yellow oil (24.6 mg, 92% yield). Two rotamers were observed due to the dynamic amide group (72:28 mixture of rotamers). **^{1}H NMR** (400 MHz, $CDCl_3$) δ 7.59 (br, 2H RotB), 7.52 – 7.48 (m, 2H RotA), 7.46 – 7.39 (m, 3H RotA, 3H RotB), 5.86 – 5.77 (m, 1H RotA, 1H RotB), 5.14 (s, 1H RotB), 5.05 – 4.97 (m, 2H RotA, 1H RotB), 4.66 (s, 1H RotB), 4.53 (s, 1H RotA, 1H RotB), 4.47 (s, 1H RotA), 4.17 (d, *J* = 12.9 Hz, 1H RotB), 3.98 (dd, *J* = 7.6, 5.9 Hz, 1H RotB), 3.59 (d, *J* = 9.1 Hz, 1H RotA), 3.45 – 3.43 (m, 1H RotB), 3.37 (d, *J* = 12.9 Hz, 2H RotA), 2.28 – 2.21 (m, 1H RotA), 2.14 – 1.63 (m, 5H RotA, 6H RotB), 1.54 – 1.48 (m, 2H RotA, 2H RotB). **^{13}C NMR** (101 MHz, $CDCl_3$) δ 169.25 (RotA), 168.51 (RotB), 152.41 (RotA), 152.18 (RotB), 138.28 (RotA), 137.22 (RotB), 136.28 (RotA, RotB), 130.17 (RotB), 129.89 (RotA), 128.49 (2C RotA), 128.27 (2C RotB), 127.65 (2C RotB), 127.23 (2C RotA), 115.17 (RotA, RotB), 91.71 (RotB), 91.51 (RotA), 65.83 (RotB), 61.91 (RotA), 56.62 (RotB), 54.71 (RotA), 51.82 (RotB), 51.48 (RotA), 43.18 (RotB), 34.17 (RotA), 29.35 (RotA), 28.39 (RotB), 28.05 (RotA), 27.32 (RotB), 24.72 (RotA), 22.76 (RotB). **ESI-HRMS** calcd for $C_{18}H_{21}NNaO$ $[M+Na]^+$ 290.1521, found 290.1525.

(4-cyclopropyl-5-methylene-2-azabicyclo[2.1.1]hexan-2-yl)(phenyl)methanone

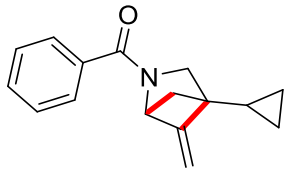

Product **2q** was prepared following general procedure **GP-1** from the corresponding allene (23.9 mg, 0.1 mmol). Only one diasteroisomer was isolated from the mixture as a light-yellow oil (19.4 mg, 81% yield). Two rotamers were observed due to the dynamic amide group (61:39 mixture of rotamers). **^{1}H NMR** (600 MHz, $CDCl_3$) δ 7.60 (d, *J* = 7.3 Hz, 1H RotA), 7.49 (d, *J* = 7.0 Hz, 2H RotA), 7.45 – 7.39 (m, 2H RotA, 5H RotB), 5.08 (s, 1H RotB), 4.67 (s, 1H RotB), 4.58 (s, 1H RotA, 1H RotB), 4.54 (s, 1H RotA), 4.47 (s, 1H RotA), 3.51 (d, *J* = 9.3 Hz, 1H RotA), 3.45 (d, *J* = 9.3 Hz, 1H RotA), 3.36 – 3.32 (m, 2H RotB), 1.65 – 1.60 (m, 2H RotA, RotB), 1.51 – 1.50 (d, *J* = 8.0 Hz, 1H RotB), 1.10 (br, 1H RotA), 0.98 (s, 1H RotB), 0.58 – 0.48 (m, 2H RotA,

2H RotB), 0.37 – 0.28 (m, 2H RotA, 2H RotB). **^{13}C NMR** (151 MHz, $CDCl_3$) δ 170.60 (RotB), 168.49 (RotA), 152.26 (RotA), 151.80 (RotB), 136.28 (RotA), 135.83 (RotB), 130.54 (RotB), 130.23 (RotA), 128.52 (2C RotA, 2C RotB), 127.78 (2C RotB), 127.62 (2C RotA), 92.13 (RotB), 91.69 (RotA), 65.03 (RotA), 61.23 (RotB), 58.76 (RotB), 57.81 (RotA), 56.02 (RotB), 51.55 (RotA), 40.50 (RotA), 38.90 (RotB), 8.17 (RotA), 7.88 (RotB), 1.65 (RotB), 1.53 (RotA), 1.28 (RotA), 1.14 (RotB). **ESI-HRMS** calcd for $C_{16}H_{17}KNO$ $[M+K]^+$ 278.0947, found 278.0950.

(5-methyl-6-methylene-2-azabicyclo[2.1.1]hexan-2-yl)(phenyl)methanone

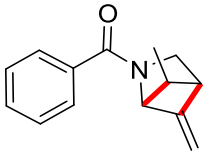

Product **2r** was prepared following general procedure **GP-1** from the corresponding allene (21.3 mg, 0.1 mmol). Only one diastereoisomer was isolated from the mixture as a light-red oil (8.9 mg, 42% yield). Two rotamers were observed due to the dynamic rotations of the amide group (65:35 mixture of rotamers). **^{1}H NMR** (600 MHz, $CDCl_3$) δ 7.61 (d, *J* = 6.8 Hz, 1H RotB), 7.47 – 7.39 (m, 5H RotA, 4H RotB), 4.99 (d, *J* = 6.9 Hz, 1H RotB), 4.68 (s, 1H RotB), 4.56 – 4.54 (m, 2H RotA, 1H RotB), 4.33 (d, *J* = 6.4 Hz, 1H RotA), 3.61 (d, *J* = 9.9 Hz, 1H RotA), 3.52 (d, *J* = 9.9 Hz, 1H RotA), 3.40 (d, *J* = 8.3 Hz, 1H RotB), 3.28 (d, *J* = 8.3 Hz, 1H RotB), 3.05 – 3.03 (m, 1H RotA), 2.94 – 2.92 (m, 1H RotB), 2.27 – 2.22 (m, 1H RotA, 1H RotB), 0.93 (d, *J* = 6.4 Hz, 3H RotA), 0.85 (d, *J* = 6.3 Hz, 3H RotB). **^{13}C NMR** (151 MHz, $CDCl_3$) δ 169.7 (RotA, RotB), 148.1 (RotA), 147.7 (RotB), 136.7 (RotA), 136.0 (RotB), 130.5 (RotB), 130.1 (RotA), 128.6 (2C RotA), 128.5 (2C RotB), 127.6 (2C RotA, 2C RotB), 94.1 (RotB), 93.7 (RotA), 69.2 (RotA), 65.7 (RotB), 48.9 (RotB), 48.4 (RotB), 47.6 (RotA), 44.9 (RotA), 41.4 (RotA), 39.7 (RotB), 9.4 (RotB), 9.2 (RotA). **ESI-HRMS** calcd for $C_{14}H_{15}NNaO$ $[M+Na]^+$ 236.1051, found 236.1055.

(5-methylene-2-azabicyclo[2.1.1]hexan-2-yl)(phenyl)methanone

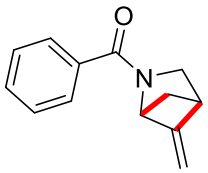

Product **2s** was prepared following general procedure **GP-1** from the corresponding allene (19.9 mg, 0.1 mmol). Only one diasteroisomer was isolated from the mixture as a light-yellow oil (8.6 mg, 43% yield). Two rotamers were observed due to the dynamic amide group (65:35 mixture of rotamers). **^{1}H NMR** (600 MHz, $CDCl_3$) δ 7.61 (d, *J* = 7.3 Hz, 1H RotB), 7.51 (d, *J* = 7.1 Hz, 1H RotA), 7.45 – 7.39 (m, 4H RotA, 4H RotB), 5.17 (d, *J* = 7.1 Hz, 1H RotB), 4.67 (s, 1H RotB), 4.56 – 4.54 (m, 2H RotA, 1 RotB), 3.68 (d, *J* = 9.5 Hz, 1H RotA), 3.62 (d, *J* = 9.5 Hz, 1H RotA), 3.47 – 3.46 (m, 2H RotB), 3.34 – 3.33 (m, 1H RotA), 3.23 (br, 1H RotB), 2.01 – 2.00 (m, 1H RotB), 1.98 – 1.96 (m, 1H RotA), 1.73 (d, *J* = 7.1 Hz, 1H RotA), 1.63 (d, *J* = 7.1 Hz, 1H

RotB). **^{13}C NMR** (151 MHz, $CDCl_3$) δ 171.01 (RotB), 168.73 (RotA), 149.53 (RotA), 149.17 (RotB), 136.58 (RotA), 135.88 (RotB), 130.53 (RotB), 130.22 (RotA), 128.52 (2C RotA), 127.76 (2C RotB), 127.58 (2C RotA), 127.31 (2C RotB), 93.73 (RotB), 93.34 (RotA), 67.44 (RotA), 63.77 (RotB), 52.81 (RotB), 48.89 (RotA), 46.60 (RotB), 45.76 (RotA), 38.81 (RotA), 37.60 (RotB). **ESI-HRMS** calcd for $C_{13}H_{13}NNaO$ $[M+Na]^+$ 222.0895, found 222.0899.

(5-ethyl-4-methyl-6-methylene-2-azabicyclo[2.1.1]hexan-2-yl)(phenyl)methanone

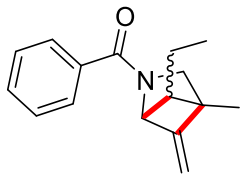

Product **2t** was prepared following general procedure **GP-1** from the corresponding allene (24.1 mg, 0.1 mmol). A mixture of diasteroisomers were obtained in ratio 83:17 and only one diasteroisomer was isolated from the mixture as a colorless oil (19.0 mg, 79% yield). Two rotamers were observed due to the dynamic amide group (68:32 mixture of rotamers). **^{1}H NMR** (600 MHz, $CDCl_3$) δ 7.58 (d, *J* = 7.1 Hz, 2H RotB), 7.47 – 7.45 (m, 2H RotA), 7.44 – 7.39 (m, 3H RotA, 3H RotB), 5.06 (s, 1H RotB), 4.65 (s, 1H RotB), 4.53 (s, 1H RotA), 4.47 (s, 1H RotA, 1H RotB), 4.38 (s, 1H RotA), 3.45 (d, *J* = 9.7 Hz, 1H RotA), 3.28 (d, *J* = 9.8 Hz, 1H RotA), 3.16 (d, *J* = 8.5 Hz, 1H RotB), 3.11 (d, *J* = 8.0 Hz, 1H RotB), 1.74 (t, *J* = 7.1 Hz, 1H RotB), 1.68 (t, *J* = 7.1 Hz, 1H RotA), 1.63 – 1.60 (m, 1H RotA, 1H RotB), 1.29 (s, 3H RotA, 2H RotB), 1.26 (br, 2H RotB), 1.19 (s, 3H RotB), 0.94 (t, *J* = 7.5 Hz, 3H RotB), 0.85 (t, *J* = 7.5 Hz, 3H RotA). **^{13}C NMR** (151 MHz, $CDCl_3$) δ 169.46 (RotA, RotB), 152.34 (RotA), 152.00 (RotB), 136.53 (RotA, RotB), 130.40 (RotB), 130.08 (RotA), 128.54 (2C RotA), 128.46 (2C RotB), 127.58 (2C RotB), 127.55 (2C RotA), 91.07 (RotB), 90.73 (RotA), 67.46 (RotA), 63.91 (RotB), 54.13 (RotB), 53.82 (RotA), 53.26 (RotA), 53.23 (RotB), 51.67 (RotB), 49.68 (RotA), 16.55 (RotB), 16.34 (RotA), 12.25 (RotA), 12.20 (RotB), 12.00 (RotA), 11.72 (RotB). **ESI-HRMS** calcd for $C_{16}H_{20}NO$ $[M+H]^+$ 242.1545, found 242.1549.

(4-methyl-5-methylene-6-phenyl-2-azabicyclo[2.1.1]hexan-2-yl)(phenyl)methanone

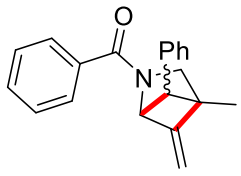

Products **2u** and **2u'** were prepared following general procedure **GP-1**, from the corresponding allene (28.9 mg, 0.1 mmol). Light-yellow oil (22.6 mg, 78% yield). Two diasteroisomers were observed with a ratio of 63:37 and sequentially separated by chromatography column (nHex:EtOAc 8:2).

Product **2u**, two rotamers were observed due to the dynamic amide group (67:33 mixture of rotamers). Colorless oil (14.3 mg, 49% yield). **^{1}H NMR** (600 MHz, $CDCl_3$) δ 7.51 – 7.43 (m, 3H RotA, 2H RotB), 7.36 –

7.27 (m, 4H RotA, 5H RotB), 7.25 – 7.24 (m, 1H RotA, 1H RotB), 7.18 (d, *J* = 7.2 Hz, 2H RotA), 7.01 (d, *J* = 7.5 Hz, 2H RotB), 5.57 (m, 1H RotA), 4.86 (s, 1H RotB), 4.83 (s, 1H RotA), 4.74 (s, 1H RotB), 4.65 (s, 1H RotB), 4.63 (s, 1H RotA), 3.30 (d, *J* = 9.6 Hz, 1H RotB), 3.25 (d, *J* = 9.6 Hz, 1H RotB), 3.16 (s, 1H RotA), 3.04 (d, *J* = 8.1 Hz, 1H RotA, 1H RotB), 2.84 (d, *J* = 8.1 Hz, 1H RotA), 1.58 (s, 3H RotB), 1.47 (s, 3H RotA). **^{13}C NMR** (151 MHz, $CDCl_3$) δ 169.69 (RotA), 168.76 (RotB), 151.41 (RotB), 150.65 (RotA), 136.05 (RotB), 135.57 (RotA), 130.10 (RotB), 129.89 (RotA), 128.70 (2C RotB), 128.62 (2C RotA), 128.58 (2C RotB), 128.26 (2C RotA), 127.87 (2C RotA), 127.62 (2C RotB), 127.50 (RotA, RotB), 127.12 (2C RotB), 126.84 (2C RotA), 122.03 (RotA, RotB), 92.47 (RotA), 91.77 (RotB), 67.41 (RotB), 63.26 (RotA), 56.31 (RotA), 55.01 (RotB), 53.85 (RotB), 53.23 (RotA), 52.81 (RotA), 49.71 (RotB), 12.91 (RotB), 12.64 (RotA). **ESI-HRMS** calcd for $C_{20}H_{19}NNaO$ $[M+Na]^+$ 312.1364, found 312.1366.

Products **2u'**, two rotamers were observed due to the dynamic amide group (63:37 mixture of rotamers). Colorless oil (8.3 mg, 29% yield). **^{1}H NMR** (600 MHz, $CDCl_3$) δ 7.65 (d, *J* = 6.6 Hz, 2H RotB), 7.54 (d, *J* = 7.2 Hz, 2H RotA), 7.46 – 7.41 (m, 3H RotA, 3H RotB), 7.29 – 7.23 (m, 3H RotA, 3H RotB), 7.16 (br, 1H RotA, 1H RotB), 7.09 – 7.07 (m, 1H RotA, 1H RotB), 5.43 (s, 1H RotB), 4.90 (s, 1H RotB), 4.79 (s, 1H RotA), 4.77 (s, 1H RotA), 4.52 (s, 1H RotA, 1H RotB), 3.81 (d, *J* = 9.3 Hz, 1H RotA), 3.65 (d, *J* = 10.1 Hz, 1H RotA, 1H RotB), 3.50 (s, 1H RotB), 3.35 (s, 1H RotA), 3.26 (s, 1H RotB), 1.19 (s, 3H RotA), 1.10 (m, 3H RotB). **^{13}C NMR** (151 MHz, $CDCl_3$) δ 172.39 (RotB), 168.54 (RotA), 151.94 (RotA), 151.56 (RotB), 136.15 (RotB), 135.67 (RotA), 130.68 (RotB), 130.39 (RotA), 128.77 (3C RotB), 128.60 (3C RotA), 128.14 (4C RotA, 4C RotB), 127.81 (2C RotB), 127.65 (2C RotA), 127.00 (RotA), 126.89 (RotB), 96.16 (RotB), 95.90 (RotA), 67.94 (RotA), 64.25 (RotB), 59.74 (RotA), 57.93 (RotB), 57.68 (RotA), 57.31 (RotB), 56.50 (RotB), 55.79 (RotA), 10.56 (RotA), 10.48 (RotB). **ESI-HRMS** calcd for $C_{20}H_{19}NNaO$ $[M+Na]^+$ 312.1364, found 312.1367.

(4-benzyl-5-methylene-6-phenethyl-2-azabicyclo[2.1.1]hexan-2-yl)(phenyl)methanone

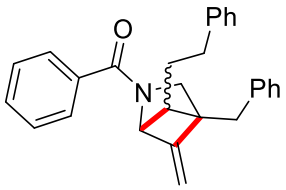

Product **2v** was prepared following general procedure **GP-1** from the corresponding allene (39.3 mg, 0.1 mmol). A mixture of diasteroisomers were obtained in ratio 77:23 and only one diasteroisomer was isolated from the mixture as a colorless oil (25.5 mg, 65% yield). Two rotamers were observed due to the dynamic amide group (65:35 mixture of rotamers). **^{1}H NMR** (600 MHz, $CDCl_3$) δ 7.56 (d, *J* = 7.4 Hz, 2H RotB), 7.44 – 7.38 (m, 5H RotA, 3H RotB), 7.30 – 7.27 (m, 2H RotA, 2H RotB), 7.24 – 7.14 (m, 5H RotA, 6H RotB), 7.06 (d, *J* = 7.5 Hz, 1H RotA, 1H RotB), 7.02 (d, *J* = 7.4 Hz, 2H RotA, 1H RotB), 5.10 (s, 1H RotB), 4.72 (s, 1H RotB), 4.60 – 4.57 (m, 2H RotA, 1H RotB), 4.28 (s, 1H RotA), 3.50 (d, *J* = 9.8 Hz, 1H RotA), 3.39 (d, *J* = 9.8 Hz, 1H RotA), 3.28 (d, *J* = 8.2 Hz, 1H RotB), 3.15 (d, *J* = 8.2 Hz, 1H RotB), 3.04 (d, *J* = 14.2 Hz, 1H RotA), 2.99 (d, *J* = 14.2 Hz, 1H RotA), 2.91 (s, 2H RotB), 2.72 – 2.67 (m, 1H RotB), 2.53 – 2.48 (m, 1H RotB), 2.41 (t, *J* = 7.7 Hz, 2H RotA), 1.94 (d, *J* = 8.2 Hz, 1H RotB), 1.85 (d, *J* = 8.3 Hz, 1H RotA), 1.44 – 1.28 (m, 2H RotA, 2H RotB). **^{13}C NMR** (151 MHz, $CDCl_3$) δ 169.49 (RotA, RotB), 151.19 (RotA, RotB), 141.29 (RotA), 140.59 (RotB), 137.07

(RotA), 136.22 (RotB), 130.56 (RotB), 130.22 (RotA), 129.65 (2C RotA), 129.54 (2C RotB), 128.63 (2C RotA, 2C RotB), 128.59 (2C RotA, 2C RotB), 128.56 (4C RotA, 4C RotB), 128.54 (2C RotA, 2C RotB), 128.37 (RotB), 127.67 (RotA), 127.57 (RotA), 126.74 (RotA), 126.68 (RotB), 126.18 (RotA), 126.05 (RotB), 92.94 (RotB), 92.47 (RotA), 67.26 (RotA), 63.54 (RotB), 58.08 (RotB), 57.23 (RotA), 52.62 (RotB), 50.00 (RotA), 48.63 (RotA), 48.08 (RotB), 34.51 (RotA), 34.32 (RotA), 34.21 (RotB), 33.96 (RotB), 25.46 (RotB), 24.53 (RotA). **ESI-HRMS** calcd for $C_{28}H_{27}NNaO$ $[M+Na]^+$ 416.1990, found 416.1993.

(9-methylene-7-azatricyclo[4.3.0.0^{2,8}]nonan-7-yl)(phenyl)methanone

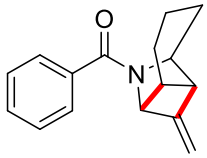

Product **2w** was prepared following general procedure **GP-1** from the corresponding allene (23.9 mg, 0.1 mmol). Only one diastereoisomer was isolated from the mixture as a white solid (20.3 mg, 85% yield). Two rotamers were observed due to the dynamic rotations of the amide group (77:23 mixture of rotamers). **^{1}H NMR** (400 MHz, $CDCl_3$) δ 7.49 – 7.47 (m, 2H RotA, 2H RotB), 7.43 – 7.38 (m, 3H RotA, 3H RotB), 5.09 (d, *J* = 7.2 Hz, 1H RotB), 4.64 (s, 1H RotB), 4.47 – 4.46 (m, 2H RotA, 1H RotB), 4.36 – 4.33 (m, 2H RotA), 4.03 (s, 1H RotB), 2.90 (br, 1H RotA), 2.82 (s, 1H RotB), 2.40 – 2.34 (m, 1H RotA), 2.33 – 2.30 (m, 1H RotA, 2H RotB), 1.80 – 1.65 (m, 3H RotA, 3H RotB), 1.63 – 1.55 (m, 1H RotA, 1H RotB), 1.43 – 1.25 (m, 1H RotA, 1H RotB). **^{13}C NMR** (101 MHz, $CDCl_3$) δ 168.3 (RotA, RotB), 148.7 (RotA, RotB), 136.9 (RotA, RotB), 130.0 (RotA, RotB), 128.5 (2C RotA, 2C RotB), 127.6 (RotA, RotB), 126.8 (RotA, RotB), 92.8 (RotA, RotB), 69.0 (RotA), 65.8 (RotB), 57.0 (RotB), 55.0 (RotA), 50.0 (RotB), 48.4 (RotA), 42.1 (RotA), 40.6 (RotB), 25.4 (RotB), 24.2 (RotA), 22.0 (RotB), 21.8 (RotA), 17.3 (RotA), 16.5 (RotB). **ESI-HRMS** calcd for $C_{16}H_{19}NNaO$ $[M+Na]^+$ 264.1364 found 264.1366. **ESI-HRMS** calcd for $C_{16}H_{17}KNO$ $[M+K]^+$ 278.0947 found 278.0941.

(4-fluorophenyl)(9-methylene-7-azatricyclo[4.3.0.0^{2,8}]nonan-7-yl)methanone

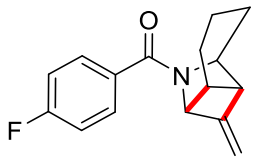

Product **2x** was prepared following general procedure **GP-1** from the corresponding allene (25.7 mg, 0.1 mmol). Only one diasteroisomer was isolated from the mixture as a colorless oil (20.8 mg, 81% yield). Two rotamers were observed due to the dynamic rotations of the amide group (79:21 mixture of rotamers). **^{1}H NMR** (600 MHz, $CDCl_3$) δ 7.50 – 7.47 (m, 2H RotA, 2H RotB), 7.09 (t, *J* = 8.5 Hz, 2H RotA, 2H RotB), 5.06 (s, 1H RotB), 4.63 (s, 1H RotB), 4.47 – 4.46 (m, 2H RotA, 1H RotB), 4.34 (s, 1H RotA), 4.32 (d, *J* = 6.8 Hz, 1H RotA), 4.02 (s, 1H RotB), 2.90 (br, 1H RotA), 2.83 (br, 1H RotB), 2.36 – 2.28 (m, 2H RotA, 2H RotB), 1.75 – 1.68 (m, 3H RotA, 2H RotB), 1.61 – 1.56 (m, 1H RotA, 1H RotB), 1.42 – 1.28 (m, 1H RotA, 2H RotB). **^{13}C NMR** (151 MHz, $CDCl_3$) δ 167.32 (RotA, RotB), 163.64 (d, *J* = 249.7 Hz, RotA, RotB), 148.52 (RotA,

RotB), 133.00 (RotA), 129.77 (d, *J* = 8.5 Hz, 2C RotA, 2C RotB), 129.08 (RotB), 115.54 (d, *J* = 21.7 Hz, 2C RotA, 2C RotB), 92.95 (RotA, RotB), 69.03 (RotA), 65.89 (RotB), 57.12 (RotB), 55.08 (RotA), 49.99 (RotB), 48.36 (RotA), 42.16 (RotA), 40.52 (RotB), 25.43 (RotB), 24.19 (RotA), 21.94 (RotB), 21.77 (RotA), 17.34 (RotA), 16.42 (RotB). **^{19}F NMR** (565 MHz, $CDCl_3$) δ -110.12 – -110.17 (m, RotA, RotB). **ESI-HRMS** calcd for $C_{16}H_{16}N_2FNNaO$ $[M+Na]^+$ 280.1114, found 280.1117.

(4-ethynylphenyl)(9-methylene-7-azatricyclo[4.3.0.0^{2,8}]nonan-7-yl)methanone

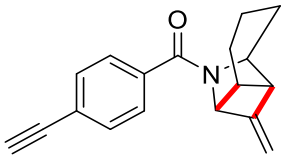

Product **2y** was prepared following general procedure **GP-1** from the corresponding allene (26.3 mg, 0.1 mmol). Only one diastereoisomer was isolated from the mixture as a light-red oil (10.7 mg, 41% yield). Two rotamers were observed due to the dynamic rotations of the amide group (80:20 mixture of rotamers). **^{1}H NMR** (600 MHz, $CDCl_3$) δ 7.53 (d, *J* = 7.9 Hz, 2H RotA, 2H RotB), 7.47 – 7.43 (m, 2H RotA, 2H RotB), 5.07 (d, *J* = 7.1 Hz, 1H RotB), 4.64 (s, 1H RotB), 4.47 (d, *J* = 9.5 Hz, 2H RotA, 1H RotB), 4.34 (s, 1H RotA), 4.29 (d, *J* = 6.6 Hz, 1H RotA), 4.01 (br, 1H RotB), 3.15 (s, 1H RotA, 1H RotB), 2.91– 2.89 (m, 1H RotA), 2.83 (br, 1H RotB), 2.37 – 2.29 (m, 2H RotA, 2H RotB), 1.75 – 1.56 (m, 3H RotA, 3H RotB), 1.46 – 1.37 (m, 1H RotA), 1.32 – 1.29 (m, 1H RotA, 2H RotB). **^{13}C NMR** (151 MHz, $CDCl_3$) δ 167.49 (RotA, RotB), 148.47 (RotA, RotB), 137.05 (RotA, RotB), 132.46 (2C RotB), 132.28 (2C RotA), 127.57 (2C RotA), 126.86 (2C RotB), 123.85 (RotA, RotB), 93.01 (RotA, RotB), 83.10 (RotA, RotB), 78.74 (RotA, RotB), 68.96 (RotA), 65.87 (RotB), 57.0 (RotB) 55.13 (RotA), 48.35 (RotA), 47.06 (RotB), 42.18 (RotA), 40.56 (RotB), 25.42 (RotB), 24.17 (RotA), 21.77 (RotA), 21.22 (RotB), 17.35 (RotA), 16.43 (RotB). **ESI-HRMS** calcd for $C_{18}H_{17}NNaO$ $[M+Na]^+$ 286.1208, found 286.1214.

(9-methylene-7-azatricyclo[4.3.0.0^{2,8}]nonan-7-yl)(pyridin-3-yl)methanone

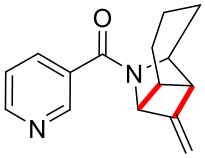

Product **2z** was prepared following general procedure **GP-1** from the corresponding allene (24.0 mg, 0.1 mmol). Only one diastereoisomer was isolated from the mixture as a light-red oil (10.6 mg, 44% yield). Two rotamers were observed due to the dynamic rotations of the amide group (77:23 mixture of rotamers). **^{1}H NMR** (600 MHz, $CDCl_3$) δ 8.76 (s, 1H RotB), 8.73 (s, 1H RotA), 8.67 (d, *J* = 4.9 Hz, 1H RotA, 1H RotB), 7.85 – 7.83 (m, 1H RotA, 1H RotB), 7.38 – 7.36 (m, 1H RotA, 1H RotB), 5.09 (d, *J* = 7.2 Hz, 1H RotB), 4.66 (s, 1H RotB), 4.50 (d, *J* = 3.1 Hz, 2H RotA, 1H RotB), 4.37 (s, 1H RotA), 4.31 (d, *J* = 6.5 Hz 1H RotA), 4.04 (s, 1H RotB), 2.92 (br, 1H RotA), 2.86 (br, 1H RotB), 2.38 – 2.29 (m, 2H RotA, 2H RotB), 1.76 – 1.58 (m, 3H RotA, 3H RotB), 1.44 – 1.38 (m, 1H RotA, 1H RotB), 1.34 (br, 1H RotA, 1H RotB). **^{13}C NMR** (151 MHz, $CDCl_3$) δ

165.7 (RotA, RotB), 151.0 (RotA, RotB), 148.5 (RotA, RotB), 148.2 (RotA), 147.9 (RotB), 135.4 (RotA), 134.6 (RotB), 133.0 (RotB), 132.7 (RotA), 123.6 (RotA), 123.5 (RotB), 93.3 (RotA, RotB), 69.1 (RotA), 66.0 (RotB), 57.1 (RotB), 55.4 (RotA), 50.0 (RotB), 48.4 (RotA), 42.3 (RotA), 40.6 (RotB), 25.5 (RotB), 24.1 (RotA), 22.0 (RotA), 21.7 (RotB), 17.3 (RotB), 16.4 (RotA). **ESI-HRMS** calcd for $C_{15}H_{16}KN_2O$ $[M+K]^+$ 279.0900, found 279.0905.

1-(9-methylene-7-azatricyclo[4.3.0.0^{2,8}]nonan-7-yl)ethan-1-one

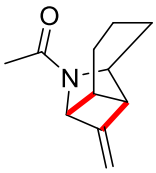

Product **2a'** was prepared following general procedure **GP-1** from the corresponding allene (17.7 mg, 0.1 mmol). Only one diasteroisomer was isolated from the mixture as a light-orange oil (15.8 mg, 89% yield). Two rotamers were observed due to the dynamic amide group (55:45 mixture of rotamers). **^{1}H NMR** (600 MHz, $CDCl_3$) δ 4.89 (d, *J* = 7.1 Hz, 1H RotB), 4.55 (s, 1H RotB), 4.51 (s, 1H RotA), 4.45 (s, 1H RotA), 4.42 (s, 1H RotB), 4.26 (d, *J* = 6.7 Hz, 1H RotA), 4.13 (br, 1H RotA), 3.95 – 3.94 (m, 1H RotB), 2.87 – 2.85 (m, 1H RotB), 2.82 – 2.81 (m, 1H RotA), 2.33 (br, 1H RotA), 2.26 (br, 1H RotB), 2.21 (dt, *J* = 13.4, 4.8 Hz, 1H RotA), 2.06 (d, 3H RotA), 2.02 (d, *J* = 1.1 Hz, 3H RotB), 2.01 – 1.97 (m, 1H RotB), 1.73 – 1.46 (m, 3H RotA, 4H RotB), 1.38 – 1.25 (m, 2H RotA, 1H RotB). **^{13}C NMR** (151 MHz, $CDCl_3$) δ 169.10 (RotB), 167.99 (RotA), 148.87 (RotB), 148.69 (RotA), 92.65 (RotB), 92.64 (RotA), 67.95 (RotA), 64.82 (RotB), 56.01 (RotB), 54.89 (RotA), 49.69 (RotB), 48.43 (RotA), 42.26 (RotA), 40.96 (RotB), 25.81 (RotB), 24.14 (RotA), 22.13 (RotB), 21.85 (RotA), 21.80 (RotB), 21.64 (RotA), 17.31 (RotA), 16.74 (RotB). **ESI-HRMS** calcd for $C_{11}H_{15}KNO$ $[M+K]^+$ 216.0791, found 216.0793.

cyclobutyl(9-methylene-7-azatricyclo[4.3.0.0^{2,8}]nonan-7-yl)methanone

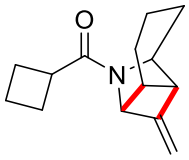

Product **2b'** was prepared following general procedure **GP-1** from the corresponding allene (21.7 mg, 0.1 mmol). Only one diastereoisomer was isolated from the mixture as a colorless oil (16.2 mg, 75% yield). Two rotamers were observed due to the dynamic rotations of the amide group (73:27 mixture of rotamers). **^{1}H NMR** (600 MHz, $CDCl_3$) δ 4.88 (d, *J* = 7.1 Hz, 1H RotB), 4.51 (s, 1H RotB), 4.43 (s, 1H RotA), 4.40 (s, 1H RotA), 4.37 (s, 1H RotB), 4.18 (d, *J* = 6.7 Hz, 1H RotA), 4.10 – 4.08 (m, 1H RotA), 3.88 (d, *J* = 4.2 Hz, 1H RotB), 3.19 (p, *J* = 8.6 Hz, 1H RotA), 3.12 (p, *J* = 8.4 Hz, 1H RotB), 2.82 – 2.80 (m, 1H RotB), 2.79 (dd, *J* = 6.7, 3.1 Hz, 1H RotA), 2.45 – 2.28 (m, 3H RotA, 3H RotB), 2.22 – 2.18 (m, 1H RotA, 1H RotB), 2.16 – 2.03 (m, 2H RotA, 2H RotB), 2.00 – 1.81 (m, 3H RotA, 3H RotB), 1.62 – 1.53 (m, 2H RotA, 2H RotB), 1.52 – 1.44

(m, 1H RotA, 1H RotB), 1.34 – 1.23 (m, 1H RotA, 1H RotB). **^{13}C NMR** (151 MHz, $CDCl_3$) δ 173.5 (RotB), 172.2 (RotA), 149.3 (RotB), 149.1 (RotA), 92.4 (RotB), 92.3 (RotA), 66.4 (RotA), 64.9 (RotB), 55.0 (RotB), 54.5 (RotA), 49.6 (RotB), 48.3 (RotA), 42.0 (RotA), 40.6 (RotB), 38.1 (RotA), 37.6 (RotB), 26.2 (RotA, RotB), 25.2 (RotB), 24.8 (RotA), 24.7 (RotB), 24.2 (RotA), 21.9 (RotB), 21.6 (RotA), 18.4 (RotB), 18.3 (RotA), 17.3 (RotA), 16.8 (RotB). **ESI-HRMS** calcd for $C_{14}H_{19}NNaO$ $[M+Na]^+$ 240.1364 found 264.1369.

((6R)-8-methylene-6-(prop-1-en-2-yl)hexahydro-1,3a-methanoisoindol-2(3H)-yl)(phenyl)methanone

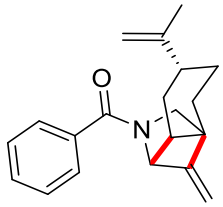

Product **2c'** was prepared following general procedure **GP-1** from the corresponding allene (29.3 mg, 0.1 mmol). Only one diastereoisomer was isolated from the mixture as a light red oil (23.7 mg, 81% yield). Two rotamers were observed due to the dynamic rotations of the amide group (60:40 mixture of rotamers). **^{1}H NMR** (600 MHz, $CDCl_3$) δ 7.59 (d, *J* = 7.6 Hz, 2H RotB), 7.50 – 7.48 (m, 2H RotA), 7.45 – 7.38 (m, 3H RotA, 3H RotB), 4.97 (s, 1H RotB), 4.93 (s, 1H RotB) 4.80 (s, 1H RotA), 4.70 – 4.68 (m, 2H RotA, 1H RotB), 4.65 (s,1H RotA, 2H RotB), 4.34 (s, 1H RotA), 3.55 (d, *J* = 9.1 Hz, 1H RotA), 3.48 (d, *J* = 9.1 Hz, 1H RotA), 3.43 (d, *J* = 7.6 Hz, 1H RotB), 3.25 (d, *J* = 7.6 Hz, 1H RotB), 2.09 – 2.04 (m, 2H RotA), 1.97 – 1.94 (m, 2H RotA), 1.90 – 1.87 (m, 1H RotB), 1.82 – 1.77 (m, 1H RotB), 1.75 – 1.67 (m, 5H RotA, 6H RotB), 1.66 – 1.58 (m, 2H RotA, 2H RotB), 1.52 – 1.42 (m, 2H RotA, 1H RotB), 1.34 (q, *J* = 12.1 Hz, 1H RotB). **^{13}C NMR** (151 MHz, $CDCl_3$) δ 170.6 (RotB), 168.5 (RotA), 151.0 (RotA), 150.6 (RotB), 149.9 (RotB), 149.8 (RotA), 136.5 (RotA), 135.9 (RotB), 130.5 (RotB), 130.2 (RotA), 128.5 (2C RotA), 128.5 (2C RotB), 127.7 (2C RotB), 127.6 (2C RotA), 109.1 (RotB), 109.1 (RotA), 97.5 (RotB), 97.1(RotA), 69.2 (RotA), 65.5 (RotB), 57.7 (RotA), 54.8 (RotB), 54.0 (RotB), 53.6 (RotA) 48.7 (RotA), 47.7 (RotB), 43.1 (RotB), 42.8 (RotA), 28.5 (RotB), 28.4 (RotA), 27.0 (RotB), 26.9 (RotA), 22.8 (RotA), 22.7 (RotB), 21.0 (RotA), 21.0 (RotB). **ESI-HRMS** calcd for $C_{20}H_{23}NNaO$ $[M+Na]^+$ 316.1677, found 316.1674.

((4S)-1-methyl-9-methylene-4-(prop-1-en-2-yl)-7-azatricyclo[4.3.0.0^{2,8}]nonan-7-yl)(phenyl)methanone

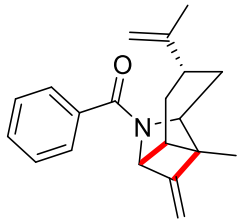

Product **2d'** was prepared following general procedure **GP-1** from the corresponding allene (29.3 mg, 0.1 mmol). Only one diasteroisomer was isolated from the mixture as a light orange oil (14.7 mg, 50% yield). Two rotamers were observed due to the dynamic amide group (68:32 mixture of rotamers). **^{1}H NMR** (600 MHz,

$CDCl_3$) δ 7.50 – 7.45 (m, 2H RotA, 2H RotB), 7.44 – 7.39 (m, 3H RotA, 3H RotB), 5.18 (s, 1H RotB), 4.74 (s, 2H RotA), 4.67 (s, 1H RotB), 4.65 (s, 1H RotB), 4.64 (s, 1H RotB), 4.49 (s, 1H RotA), 4.47 (s, 1H RotA), 4.44 (s, 1H RotB), 4.42 (s, 1H RotA), 4.11 (d, *J* = 5.3 Hz, 1H RotA), 3.71 (d, *J* = 3.9 Hz, 1H RotB), 2.69 – 2.60 (m, 1H RotA, 1H RotB), 2.51 – 2.47 (m, 1H RotA, 1H RotB), 1.99 (s, 1H RotB), 1.96 (s, 1H RotA), 1.93 – 1.89 (m, 1H RotA, 1H RotB), 1.74 (s, 3H RotA), 1.58 – 1.50 (m, 3H RotA, 3H RotB), 1.29 (s, 3H RotA), 1.23 (s, 3H RotB). **^{13}C NMR** (151 MHz, $CDCl_3$) δ 167.64 (RotA, RotB), 153.17 (RotA, RotB), 148.90 (RotA), 148.58 (RotB), 136.69 (RotA, RotB), 130.03 (RotA), 129.95 (RotB), 128.58 (2C RotB), 128.53 (2C RotA), 127.56 (2C RotA), 126.56 (2C RotB), 109.38 (RotA, RotB), 90.42 (RotB), 90.10 (RotA), 68.75 (RotA), 65.29 (RotB), 61.15 (RotB), 58.88 (RotA), 52.64 (RotA, RotB), 46.97 (RotA), 45.28 (RotB), 35.75 (RotA), 35.16 (RotB), 27.63 (RotB), 26.83 (RotA), 26.70 (RotB), 26.06 (RotA), 20.82 (RotA), 20.56 (RotB), 10.62 (RotB), 10.51 (RotA). **ESI-HRMS** calcd for $C_{20}H_{23}KNO$ $[M+K]^+$ 332.1417, found 332.1411.

(5-methyl-6-methylene-2-azabicyclo[3.1.1]heptan-2-yl)(phenyl)methanone

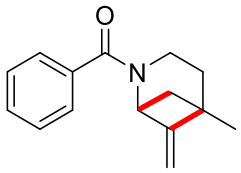

Product **2e'** was prepared following general procedure **GP-1** from the corresponding allene (22.5 mg, 0.1 mmol). Only one diasteroisomer was isolated from the mixture as a light-yellow oil (13.1 mg, 58% yield). Two rotamers were observed due to the dynamic amide group (56:44 mixture of rotamers). **^{1}H NMR** (600 MHz, $CDCl_3$) δ 7.50 – 7.48 (m, 2H RotA, 2 RotB), 7.43 – 7.37 (m, 3H RotA, 3H RotB), 5.36 (s, 1H RotB), 5.02 (d, *J* = 2.5 Hz, 1H RotB), 4.89 (s, 1H RotB), 4.84 (d, *J* = 2.2 Hz, 1H RotA), 4.60 (s, 1H RotA), 4.32 – 4.28 (m, 1H RotA), 4.25 (s, 1H RotA), 3.70 – 3.67 (m, 2H RotB), 3.62 – 3.57 (m, 1H RotA), 2.62 – 2.54 (m, 1H RotA, 1H RotB), 2.48 (d, *J* = 16.5 Hz, 1H RotB), 2.32 (d, *J* = 15.9 Hz, 1H RotA), 1.93 – 1.65 (m, 2H RotA, 2H RotB), 1.36 (s, 3H RotB), 1.28 (s, 3H RotA). **^{13}C NMR** (151 MHz, $CDCl_3$) δ 170.32 (RotA), 168.82 (RotB), 145.56 (RotB), 145.19 (RotA), 137.13 (RotA, RotB), 129.89 (RotA), 129.87 (RotB), 128.44 (2C RotA), 128.32 (2C RotB), 127.58 (2C RotA), 127.29 (2C RotB), 112.43 (RotB), 111.27 (RotA), 69.06 (RotA), 66.59 (RotB), 49.43 (RotB), 46.31 (RotA), 44.47 (RotA), 42.06 (RotB), 39.96 (RotA, RotB), 38.31 (RotB), 36.61 (RotA), 24.36 (RotA, RotB). **ESI-HRMS** calcd for $C_{15}H_{17}NNaO$ $[M+Na]^+$ 250.1208, found 250.1212.

Valorization of products

Ring closing metathesis of [2p]

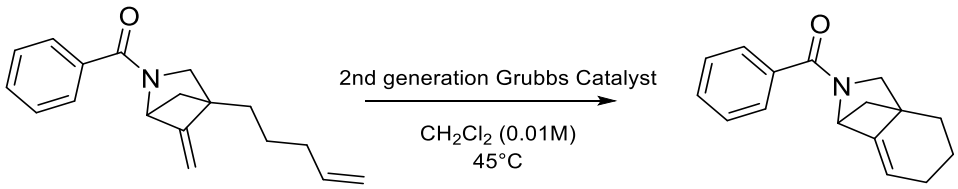

Phenyl(1,4,5,6-tetrahydro-1,3a-methanoisoindol-2(3H)-yl)methanone (3)

To a solution of **2p** (40.1 mg, 0.15 mmol, 1 equiv.) in CH_2Cl_2 (1.5 mL, 0.01 M) was added Grubbs 2nd Generation Catalyst (6.4 mg, 0.0075 mmol, 5 mol%). The resulting mixture was stirred at reflux until complete conversion of the starting material (1 hour). The mixture was allowed to warm to room temperature and the crude was directly purified through silica gel column (*n*-Hexane/AcOEt gradient *8:2 to 1:1*) to give **3** as colorless oil in 71% yield (28.5 mg).

^{1}H NMR (400 MHz, $CDCl_3$) δ 7.61 (br, 2H RotB), 7.50 (br, 2H RotA), 7.45 – 7.38 (m, 3H RotA, 3H RotB), 5.35 – 5.30 (m, 1H RotA, 1H RotB), 5.19 (s, 1H RotA), 4.68 (s, 1H RotB), 3.54 (br, 2H RotA), 3.36 (br, 2H RotB), 2.05 – 1.91 (m, 2H RotA, 2H RotB), 1.60 – 1.42 (m, 2H RotA, 2H RotB), 0.98 – 0.76 (m, 4H RotA, 4H RotB). **^{13}C NMR** (101 MHz, $CDCl_3$) δ 168.93 (RotA, RotB), 141.87 (RotA, RotB), 136.37 (RotA, RotB), 130.26 (RotA, RotB), 128.47 (2C RotA, 2C RotB), 127.68 (2C RotA, 2C RotB), 103.78 (RotA, RotB), 67.11 (RotA, RotB), 50.81 (RotA, RotB), 44.88 (RotA), 37.07 (RotB), 32.07 (RotA), 29.51 (RotB), 24.27 (RotA), 23.93 (RotA, RotB), 22.84 (RotB), 20.53 (RotA), 14.27 (RotB). **ESI-HRMS** calcd for $C_{16}H_{17}NNaO$ $[M+Na]^+$ 262.1208, found 262.1212.

Oxidative Ring Expansion of terminal alkene [2a]

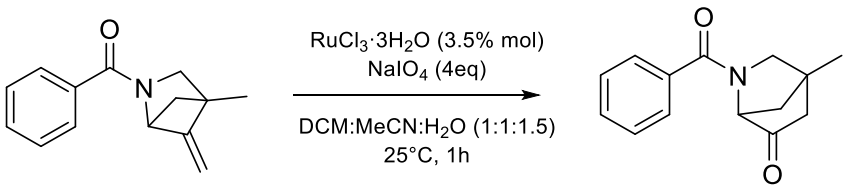

2-benzoyl-4-methyl-2-azabicyclo[2.2.1]heptan-6-one (4)

In a flame-dried Schlenk tube under nitrogen atmosphere, 21.3 mg (0.10 mmol, 1.0 equiv) of alkene **2a** was dissolved in a 1:1 mixture of CH_2Cl_2 (0.60 mL, 0.15 M) and MeCN (0.60 mL, 0.15 M). Separately, sodium periodate ($NaIO_4$, 85.6 mg, 0.40 mmol, 4.0 equiv.) was dissolved in 0.90 mL of Milli-Q water and added to the reaction mixture. Subsequently, in a separate vial, ruthenium(III) chloride hydrate ($RuCl_3 \cdot 3H_2O$, 1.0 mg, ~0.0035 mmol, 3.5 mol%) was dissolved in 0.50 mL of Milli-Q water and added dropwise to the reaction mixture and a dark brown suspension formed immediately. The reaction was stirred at room temperature for 1 hour,

and monitored by TLC (*n*-Hexane/Ethyl Acetate 6:4). Upon completion, the reaction mixture was transferred to a round-bottom flask, concentrated under reduced pressure, and purified directly by preparative thin-layer chromatography (pTLC) using *n*-Hexane/Ethyl Acetate 7:3 as eluent, affording the desired product **4** as a colorless solid (13.1 mg, 57% yield).

^{1}H NMR (600 MHz, $CDCl_3$) δ 7.81 (d, *J* = 7.5 Hz, 2H), 7.51 (t, *J* = 7.5 Hz, 1H), 7.44 (t, *J* = 7.5 Hz, 2H), 5.53 (br, 1H), 4.37 (d, *J* = 17.3 Hz, 1H), 4.28 (d, *J* = 17.3 Hz, 1H), 3.72 (d, *J* = 12.4 Hz, 1H), 3.64 (d, *J* = 12.4 Hz, 1H), 2.25 (d, *J* = 12.5 Hz, 1H), 2.10 (dd, *J* = 12.5, 3.4 Hz, 1H), 1.34 (s, 3H). **^{13}C NMR** (151 MHz, $CDCl_3$) δ 207.5, 170.6, 134.7, 131.5, 128.6 (2C), 128.4 (2C), 85.3, 68.5, 55.3, 49.7, 42.4, 16.0. **ESI-HRMS** calcd for $C_{14}H_{15}KNO_2$ $[M+K]^+$ 268.0749, found 268.1472.

Oxidative hydroboration of [2a]

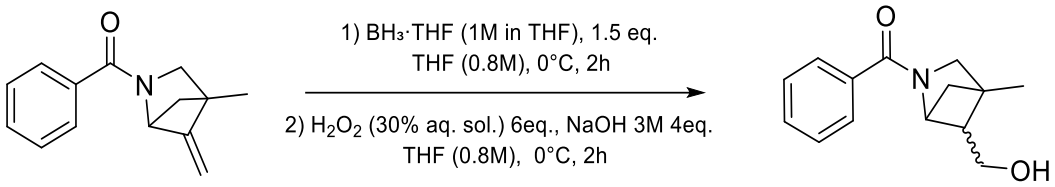

(5-(hydroxymethyl)-4-methyl-2-azabicyclo[2.1.1]hexan-2-yl)(phenyl)methanone (5)

In a flame-dried Schlenk tube under a nitrogen atmosphere, 21.3 mg (0.10 mmol, 1.0 equiv) of alkene **2a** was dissolved in THF (0.8 mL, 0.8 M) and cooled to 0 °C thanks to the use of an ice bath. Then, borane–tetrahydrofuran complex (BH_3·THF, 1.5 equiv) was carefully added dropwise and the reaction mixture was stirred at 0 °C for 2 hours. Subsequently, while maintaining the temperature at 0 °C, hydrogen peroxide (6.0 equiv, H_2O_2 in 30% aqueous solution) was added dropwise, followed by sodium hydroxide (NaOH, 4.0 equiv, 3M aqueous solution). The mixture then was stirred for additional 2 hours at 0 °C. Upon completion of the reaction, monitoreted by TLC, the reaction was quenched with H_2O (5 mL) and extracted with Ethyl Acetate (3 × 5 mL). The combined organic layers were dried over anhydrous Na_2SO_4, filtered, and concentrated under reduced pressure. The crude product was purified by flash column chromatography on silica gel using (*n*-Hexane/Ethyl Acetate 65:35) as eluent, affording the hydroboration–oxidation product **5** as a mixture of diastereomers (*dr* = 61:39) as a colorless oil (13.4 mg, 63% yield).

^{1}H NMR (600 MHz, $CDCl_3$) δ 7.62 (d, *J* = 6.8 Hz, 2H Dia2), 7.48 (d, *J* = 6.8 Hz, 2H Dia1), 7.45 – 7.37 (m, 3H Dia1, 3H Dia2), 4.79 (s, 1H Dia2), 4.24 (s, 1H Dia1), 3.92 – 3.89 (m, 2H Dia1), 3.78 (m, 2H Dia2), 3.51 – 3.47 (m, 2H Dia1), 3.32 (d, *J* = 8.1 Hz, 1H Dia2), 3.29 (d, *J* = 8.1 Hz, 1H Dia2), 2.24 (d, *J* = 8.5 Hz, 1H Dia2), 2.22 – 2.18 (m, 2H Dia1), 2.10 – 2.06 (m, 1H Dia2), 1.80 (br, 1H Dia1, 1H Dia2), 1.68 (t, *J* = 7.8 Hz, 1H Dia1), 1.58 (t, *J* = 7.9 Hz, 1H Dia2), 1.27 (s, 3H Dia1), 1.18 (s, 3H Dia2). **^{13}C NMR** (151 MHz, $CDCl_3$) δ 170.8 (Dia2), 168.4 (Dia1), 136.3 (Dia1), 136.0 (Dia2), 130.6 (Dia2), 130.2 (Dia1), 128.5 (2C Dia1, 2C Dia2), 127.8 (Dia1), 127.7 (Dia2), 127.6 (Dia1), 127.2 (Dia2), 62.6 (Dia1), 60.1 (Dia2), 60.0 (Dia1), 59.8 (Dia2), 58.9 (Dia2), 58.4 (Dia1), 57.5 (Dia2), 55.7 (Dia1), 48.5 (Dia2), 47.2 (Dia1), 42.4 (Dia1), 41.3 (Dia2), 14.4 (Dia1), 14.3 (Dia2). **ESI-HRMS** calcd for $C_{14}H_{17}NNaO_2$ $[M+Na]^+$ 254,1164, found 254.4142.

Epoxidation of [2a]

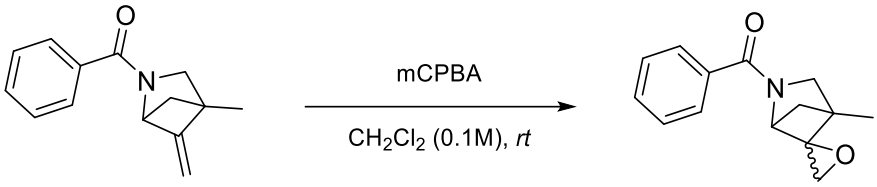

Phenyl(2-azaspiro[bicyclo[2.1.1]hexane-5,2'-oxiran]-2-yl)methanone (6)

To a solution of product **2a** (21.3 mg, 0.1 mmol, 1 equiv.) in CH_2Cl_2 (1 mL, 0.1 M) *m-CPBA* (70% pure, 73.7 mg, 0.3 mmol, 3 equiv.) was added, and the reaction was stirred at rt for 2h. After complete conversion, as monitored by TLC, the solution was concentrated and directly purified by preparative thin layer chromatography (*n-Hexane/EtOAc 8:2*) to afford the desired product **6** as a mixture of two diasteroisomers in ratio 54:46. Colorless oil (19.2 mg, 90%).

^{1}H NMR (600 MHz, $CDCl_3$) δ 7.66 – 7.65 (m, 1H RotA, 1H RotB), 7.47 – 7.36 (m, 4H RotA, 4H RotB), 4.86 (s, 1H RotB), 4.22 (s, 1H RotA), 3.62 (d, *J* = 9.6 Hz, 1H RotA), 3.57 (d, *J* = 9.6 Hz, 1H RotA), 3.48 (d, *J* = 8.2 Hz, 1H RotB), 3.32 (d, *J* = 8.1 Hz, 1H RotB), 3.19 (d, *J* = 4.4 Hz, 1H RotB), 3.09 – 3.07 (m, 2H RotA, 1H RotB), 1.74 – 1.71 (m, 2H RotA), 1.67 (d, *J* = 7.9 Hz, 2H RotB), 1.20 (s, 3H RotA), 1.09 (s, 3H RotB). **^{13}C NMR** (151 MHz, $CDCl_3$) δ 169.27 (Dia1), 166.89 (Dia2), 136.21 (Dia1), 135.79 (Dia2), 130.66 (Dia2), 130.17 (Dia1), 128.48 (2C Dia1, 2C Dia2), 127.86 (2C Dia2), 127.73 (2C Dia1), 69.25 (Dia1), 68.50 (Dia2), 65.38 (Dia1), 61.72 (Dia2), 55.49 (Dia2), 51.51 (Dia1), 49.37 (Dia2), 48.55 (Dia1), 47.92 (Dia2), 47.71 (Dia1), 37.55 (Dia1), 36.22 (Dia2), 11.70 (Dia1), 11.42 (Dia2). **ESI-HRMS** calcd for $C_{14}H_{15}NNaO_2$ $[M+Na]^+$ 252.1000 found 252.1004.

Double bond borylation of [2l]

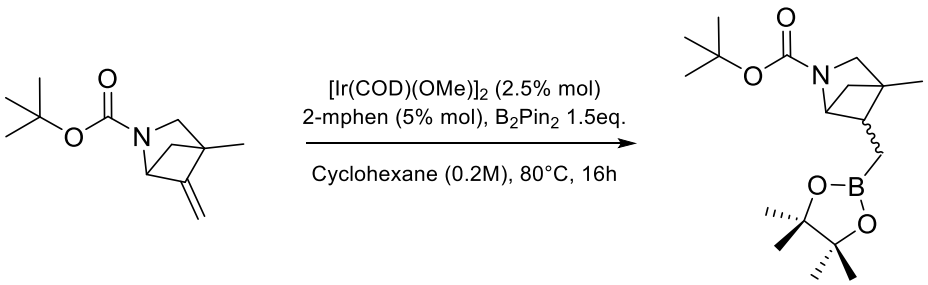

***tert-butyl*-4-methyl-5-((4,4,5,5-tetramethyl-1,3,2-dioxaborolan-2-yl)methyl)-2-azabicyclo[2.1.1]hexane-2-carboxylate (7)**

In a flame-dried Schlenk tube under a nitrogen atmosphere, 2-mphen (2.43 mg, 12.5 *μ*mol, 5.0 mol%), $[Ir(COD)(OMe)]_2$ (3.84 mg, 6.25 μmol, 2.5 mol%), B_2pin_2 (95.2 mg, 0.375 mmol, 1.5 equiv), and alkene **2n** (52.3 mg, 0.250 mmol, 1.0 equiv) were sequentially added. To the reaction mixture, anhydrous cyclohexane (0.5 mL) was added, and the mixture was then stirred at 80 °C in an oil bath for 16 hours. After cooling to room temperature, $CDCl_3$ and CH_2Br_2 were added to the crude mixture, and a sample was taken and analyzed by

^{1}H NMR spectroscopy to determine conversion and yield. The reaction mixture was then co-evaporated with methanol (3 × 5 mL) at 45 °C. The crude product was purified by preparative thin-layer chromatography (pTLC) using (*n*-Hexane/Ethyl Acetate 85:15) as eluent, affording the borylated compound **7** as a mixture of diastereomers (*dr* = 59:41) in the form of a colorless oil (21.6 mg, 62% yield). Yield determined via ^{1}H NMR with CH_2Br_2 as internal standard.

^{1}H NMR (600 MHz, $CDCl_3$) δ 4.82 (s, 1H Dia1), 4.44 (s, 1H Dia2), 3.05 – 3.01 (m, 2H Dia2), 2.97 – 2.91 (m, 2H Dia1), 1.87 – 1.82 (m, 1H Dia1, 1H Dia2), 1.45 – 1.44 (m, 2H Dia1, 2H Dia2), 1.43 (s, 9H Dia1, 9H Dia2), 1.25 (d, *J* = 2.8 Hz, 12H Dia1, 12H Dia2), 0.93 (d, *J* = 6.7 Hz, 3H Dia1, 3H Dia2), 0.83 (d, *J* = 6.5 Hz, 1H Dia2), 0.80 (d, *J* = 6.4 Hz, 1H Dia1), 0.70 (d, *J* = 7.4 Hz, 1H Dia1), 0.68 (d, *J* = 7.6 Hz, 1H Dia2). **^{13}C NMR** (151 MHz, $CDCl_3$) δ 156.2 (Dia1, Dia2), 83.3 (2C Dia1, 2C Dia2), 79.0 (Dia1, Dia2), 48.7 (Dia1), 47.7 (Dia2), 41.0 (Dia1, Dia2), 33.5 (Dia1, Dia2), 28.7 (Dia1), 28.7 (Dia2), 28.6 (3C Dia1, 3C Dia2), 25.1 (2C Dia1, 2C Dia2), 25.02 (Dia1, Dia2), 24.98 (Dia1), 24.96 (Dia2), 24.94 (2C Dia1, 2C Dia2), 20.6 (Dia1), 15.5 (Dia2). **^{11}B NMR** (193 MHz, $CDCl_3$) δ 32.95. **ESI-HRMS** calcd for $C_{18}H_{32}BNNaO_4$ $[M+Na]^+$ 360.2324 found 360.0564.

Chapter 3:

'Synthesis of β-lactams from Allenamides via Energy-Transfer Relay'

From this chapter:

G. Scarica, S. Sparascio, A. Cerveri, G. Russo, D. Spataro, L. Marchiò, M. Lanzi, G. Maestri., Synthesis of Vinyl Azetidines and β-Lactams from Allenamides via Energy Transfer Relay, ACS Catal., **2025**, 15, 13799−13809. DOI:10.1021/acscatal.5c04424.

Introduction

Small ring cycles containing nitrogen have received significant attention from scientists during the last few years, and growing efforts have been directed toward developing methods for their synthesis. In fact, they have a vital role in the production of many useful compounds, from the pharmaceutical field to the agrochemical one.[1-3] Nevertheless, the examples present several limitations, ranging from the necessity to use toxic reagents to the use of harsh conditions or complicated setups.[4]

Over the past year, our group has developed a more general and robust synthetic approach to strained heterocycles. By employing versatile substrates such as allenamides, this method enabled access to densely functionalized monocyclic derivatives. Given the well-established use of allenamides in a wide range of photocatalytic transformations within our group,[5–6] we sought to extend this reactivity toward the synthesis of strained nitrogen-containing heterocycles.

Specifically, as 4-membered ring cycles are concerned, the most important strained heterocycles are azetidines and β-lactams. The latter is arguably among the most important classes of compounds regarding pharmaceutical chemistry, as demonstrated by its presence in important molecules such as penicillin antibiotics, as well as in the other compounds reported in Scheme 1.[7]

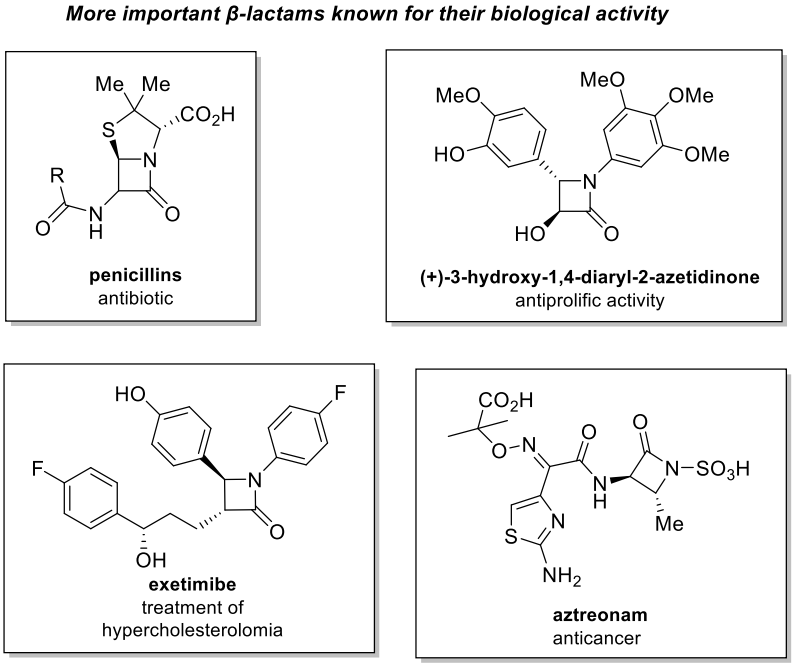

Scheme 1: Class of pharmaceutical compounds with a β-lactam scaffold.

Additionally, this class of compounds proves to be very interesting from a synthetic point of view because the reduction of their carbonyl group readily leads to the formation of azetidines. This feature is important because, in literature [8], this reaction can be performed on sensitive substrates with high selectivity.

As a result, there is considerable interest in developing efficient approaches for synthesizing β-lactams. Few techniques have already been established over time, but many of these methods rely on highly reactive starting materials such as ketenes and nitrones, which can restrict their applicability in certain contexts.[9] Therefore, exploring whether β-lactams could be generated from more accessible and less hazardous precursors by leveraging visible-light-induced energy transfer processes is something that caught interest.

Direct functionalization of C–H bonds represents one of the most powerful and transformative strategies in modern synthetic chemistry, particularly when applied to the modification of inactivated aliphatic C(sp^3)–H bonds. These transformations offer the potential to perform synthetic transformations by skipping the need for pre-functionalized starting materials.

In this context, hydrogen atom transfer (HAT) strategies have emerged as highly promising. HAT processes offer a fundamentally different and complementary approach to the most common C–H bond activation. Rather than relying on coordination to a metal center, these reactions proceed just via homolytic cleavage of C–H bonds through radical intermediates, preferably under mild conditions. A particularly attractive subclass of HAT-based methods involves Norrish–Yang-type photocyclization reactions. These transformations can be carried out under relatively mild conditions and do not require an initiator.

Specifically, the first reports on the synthesis of β-lactam using this methodology can be found already around the 80s with the works of Aoyama (1978) and Wehrli (1980).[10-11] These works were inspired by a previous study by Hasegawa and co-workers who reported a β-lactam synthesis via a rare C-to-C 1,5-HAT in 1977 (Scheme 2).[12] However, all these reported studies require the use of a high-power UV light source, which is usually associated with some limits in the reaction scope and on the product yields, as these powerful wavelengths usually present less selectivity.

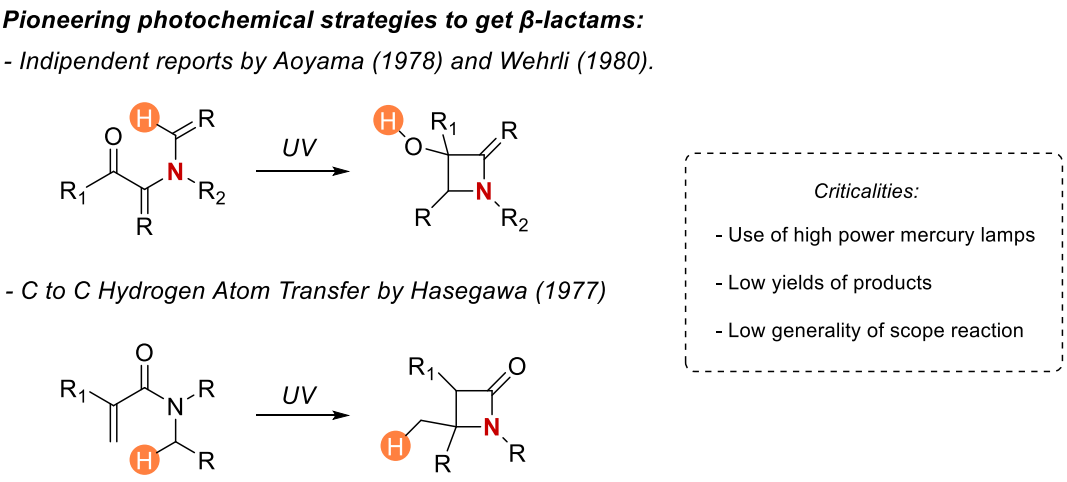

Scheme 2: Pioneering works involving the formation of β-lactams through UV.

Related methods for the synthesis of β-lactams or direct azetidines synthesis emerged from other groups, but again, the use of a powerful UV light source to form the excited triplet states seemed to be essential to perform the reaction.[13]

To the best of our knowledge, the first published report to make β-lactam through a different methodology was described by Sarpong and co-workers, which focuses on a Norrish-Yang cyclization of a keto-amide under blue light irradiation.[14] A more notable variation using visible light was disclosed instead when Koert and co-workers reported for the very first time a carbon-to-carbon 1,5-HAT, rather than the carbon-to-oxygen 1,5-HAT typical of Sarpong's work through an EnT-mediated olefin sensitization (Scheme 3).[15] The method brings to the formation of cyclobutene structures in this case.

First visible-light processes to achieve β-lactams:

- Visible-light Norrish-Yang cyclization by Sarpong's group (2020)

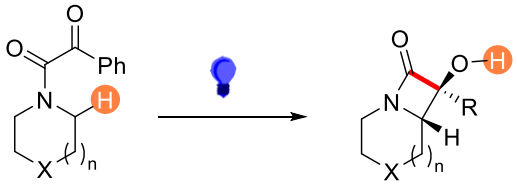

- Visible-light C to C HAT by Koert's group (2020)

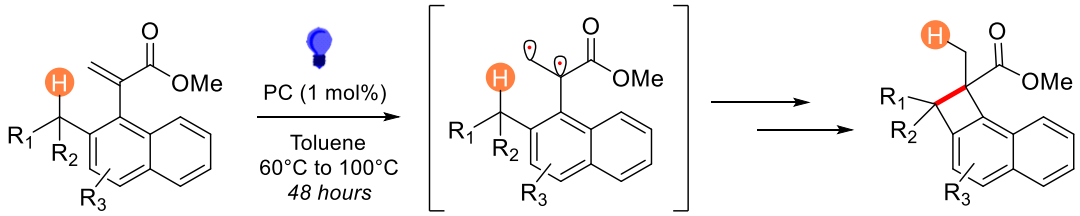

Scheme 3: First visible-light approaches to achieve the formation of β-lactams.

Hydrogen atom transfer (HAT) processes involving carbon-to-carbon hydrogen shift remain nowadays a relatively underexplored area of synthetic chemistry. A particularly notable recent contribution to this area came from Bach and co-workers, who reported a novel β-lactam-forming transformation.[16] Their work describes the synthesis of β-spirocyclic azetidine-3,3'-indolines through a triplet energy transfer mechanism. In this reaction, excitation of indole precursors via a triplet sensitizer under visible light enables intramolecular cyclization, providing spirocyclic frameworks. Building on these advances, Petersen's group recognized a key opportunity to further expand the synthetic potential of EnT catalysis.[17] By harnessing visible-light-mediated energy transfer, they have been able to develop a novel and efficient method for synthesizing β-lactams under metal-free and room-temperature conditions. This transformation utilizes simple, bench-stable acrylamide precursors and proceeds via a highly unusual carbon-to-carbon hydrogen atom transfer (Scheme 4).

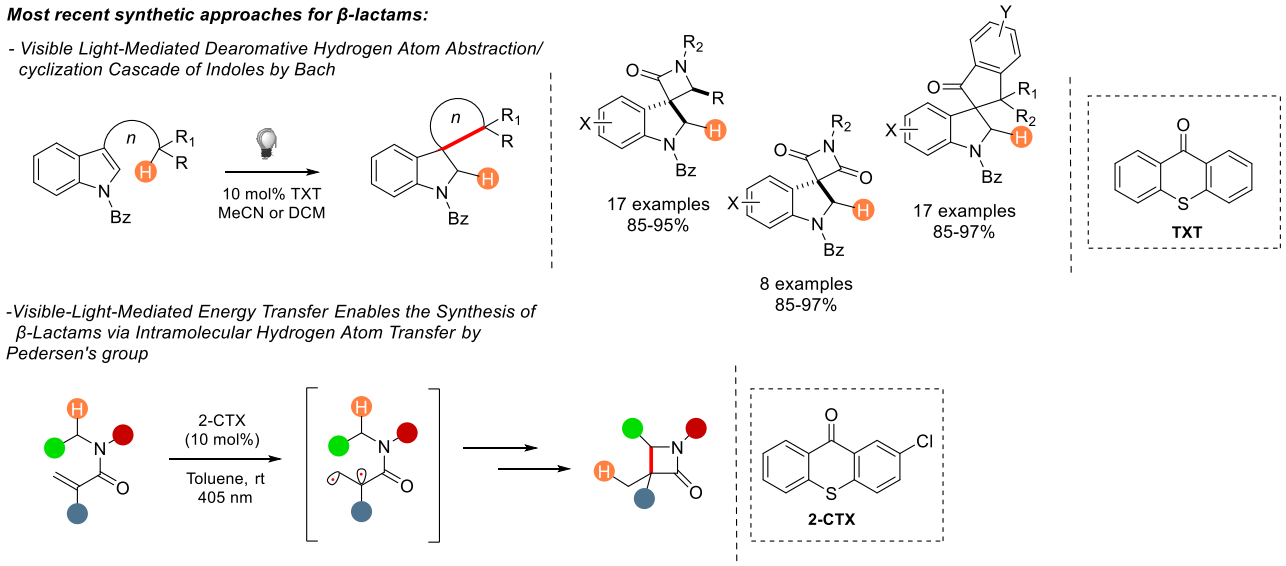

Scheme 4: Most recent approaches for the synthesis of β-lactams.

What sets this approach apart from its simplicity, functional group tolerance, and mechanistic novelty with respect to the previous ones is that the reaction avoids the need for harsh conditions but instead relies on visible light to mediate the EnT process that initiates the C(sp³)–H bond functionalization. Furthermore, the hydrogen atom donor component of the substrate was shown to be highly tunable, accommodating a broad range of aromatic, heteroaromatic, and non-aromatic groups.

Inspired by the latest, allenamides were exploited as potential starting materials, targeting a fascinating cumulated π-system. A few reports show that EnT activation of an allene can form species with a vinyl-radical site, and this one can be a useful platform for the formation of multiple products. In 2024, we reported that bis-aryl allenamides can afford δ-lactams via 1,5-HAT in the presence of a sensitizer and a molar excess of naphthalene.[18] Unfortunately, even if the reaction was interesting and gave life to a discrete series of stable compounds bearing a 6-member ring cycle, that chemistry was highly limited to conjugated trisubstituted allenes, which brought back once again to the problem of having a low generality on the scope (Scheme 5).

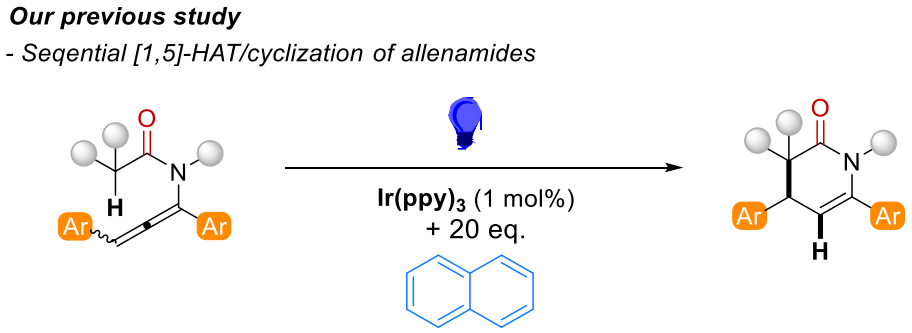

Scheme 5: Our previous study on sequential 1,5 HAT to obtain δ-lactams.

To prevent this problem, we also tested terminal allenamides but proved completely unreactive. This is likely attributable to the reduced conjugation of the system and, more importantly, to the presence of naphthalene, which exhibits higher reactivity towards dearomatization.

However, this outline is challenging because the use of monosubstituted allenamides in EnT methods has few precedents, and none involve a HAT step.

Results and discussions

In this chapter, the construction of monocyclic β-lactams derived from unbiased allenyl substrates is reported. (Scheme 1).

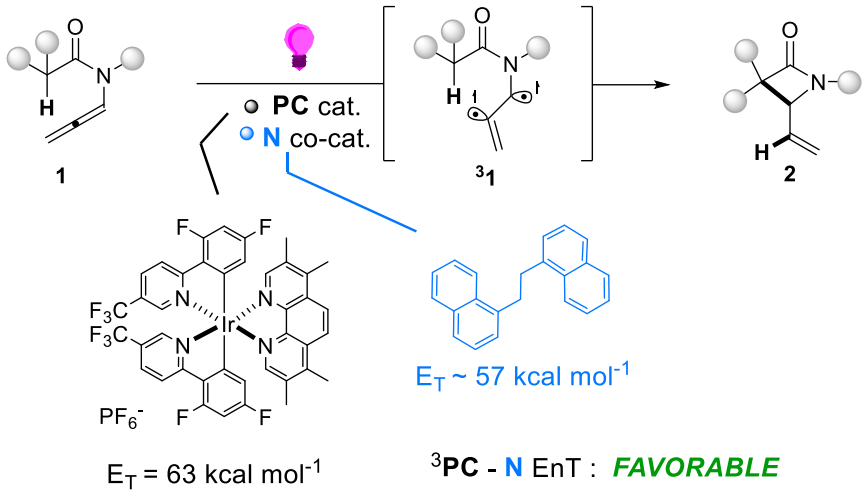

Scheme 1: Recent approach for treating terminal allenamides in the HAT process to deliver monocyclic β-lactams.

The reactivity demonstrates wide compatibility with various functional groups and furnishes products featuring a quaternary carbon center alongside an exocyclic vinyl moiety. The strategy utilizes a custom-designed Iridium (III) photocatalyst with elevated triplet energy (E_T), paired with a binaphthyl cocatalyst that fulfills a dual function. This one not only stabilizes the biradical reactive intermediate through dispersion forces, an aspect recognized in catalysis for closed-shell systems,[19] but serves as a triplet-state mediator as well, enhancing the efficiency of substrate activation (Scheme 2).[20]

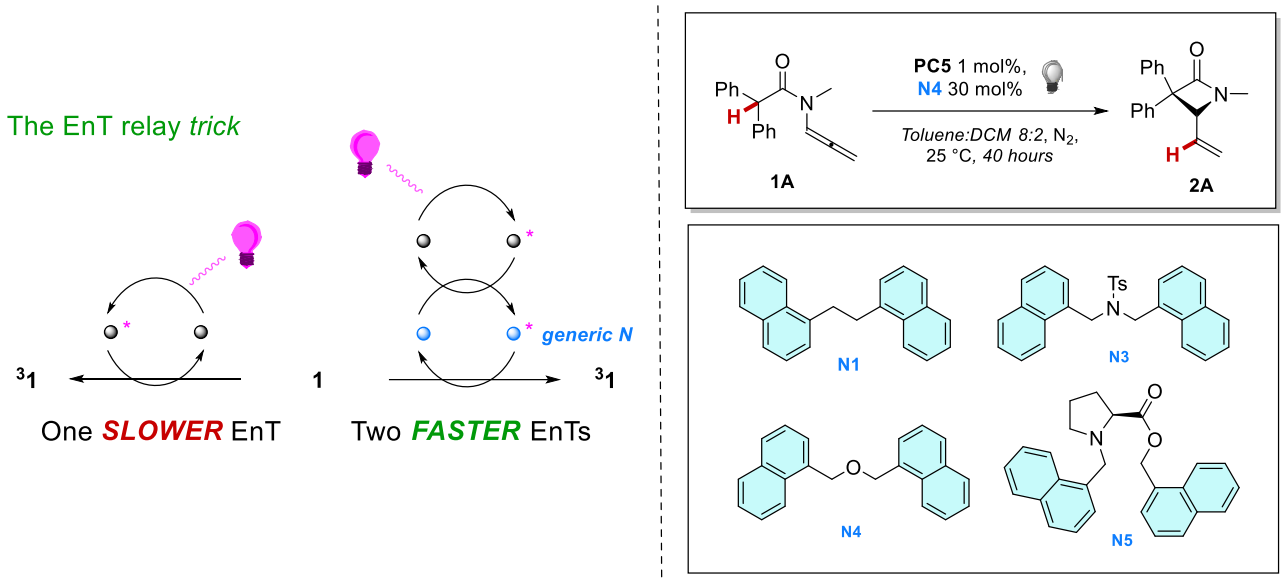

Scheme 2: Represented advantage of an energy transfer relay process.

Therefore, we started an optimization effort, which is summarized in Table 1.

Entry	Deviation from optimal[a]	**Time (h)**	**4a** conversion [%][b]	**4a** yield [%][b]
1	-	40	>99	61
2	with 20 equiv. of Np	24	>99	39
3	with 5 equiv. of Np	48	>99	48
4	with **N3**	216	86	44
5	with **N4**	120	79	50
6	with **N5**	120	75	47
7	with 1 equiv. of **N1**	48	84	48
8	With **PC4**	48	>99	61
9	With **PC5**	40	>99	61
10	With **PC6**	40	>99	65
11	With **PC6** w/o freeze-pump	48	>99	59
12	With Toluene	48	75	46
13	With DMF	48	54	29

Table 1: [a] Reaction conditions: 0.15 mmol of **1A** (0.1 M in Toluene: DCM 8:2), 30 mol% of **N1**, 1 mol % of **PC5**, reaction irradiated for a total of 20 hours with blue LEDS at 25°C; [b] ^{1}H-NMR yield calculated using 1,3,5-trimethoxybenzene as internal standard. **PC4** = $[Ir\{dFCF_3ppy\}_2(dtbbpy)]PF_6$, **PC5** = $[Ir[dF(CF_3)ppy]_2(Me_4phen)]BF_4$, **PC6** = $Ir(d\text{-}F\text{-}ppy)_3$.

Initial hits on the synthesis of product **2A** were observed when performing the reactions in the presence of a molar excess of naphthalene. The reaction ensured the full consumption of the substrate **1A** upon 24 hours of

irradiation, but the yield of **2A** remained low because of the formation of dearomatization products. Initially, the concentration of naphthalene was reduced (entry 3), but this modification led to longer reaction times and lower selectivity. These preliminary experiments suggested the use of binaphthyl derivatives, which, unlike naphthalene, could be used in catalytic amounts. These additives have already been used in other works.[20-21] During this stage of the optimization, six different poly-naphthyl derivatives were tested, varying the length and the rigidity of the tether between the two naphthyl groups. Among the tested **N** species, entry 5 was the one in which the best conversion of the starting material was reported, while entry 1 provided the highest yield of **2A**. Therefore, the latter derivative was adopted for the following iteration of the optimization process. Different loadings of **N1** were tested in combination with **PC1**. Reactions in which a higher amount of the binaphthyl derivative was used led to faster conversion of the starting material **1A**. However, the yield of the desired product **2A** did not improve, as demonstrated by entry 7. At this point, a study performing the reaction with different Iridium-based photocatalysts was necessary. Among this series, good results were achieved using both the homoleptic complex **PC4** and the heteroleptic complex **PC5** (entries 8-9). With the latter, a yield of **2A** up to 61% was achieved. Additionally, as reported by entry 1, using **PC5,** no differences were found if the mixture was not thoroughly degassed by freeze-pump-thaw. We also tested **PC6** complex. The use of the latter allowed one to achieve a higher yield of **2A** (65%, entry 10). However, the use of **PC6** required the freeze-pump-thaw technique to achieve the best outcome (entry 11). This part of the optimization study showed that the highest yield of **2A** was achieved using **PC6**. However, the use of **PC5** retains a significant advantage in terms of practical viability because these reactions do not suffer from the presence of traces of dioxygen. A final comparison was made using different reaction media, with solvents of different polarity. Entries 12-13 demonstrate that the best result was obtained by maintaining an 8:2 toluene/DCM mixture. Toluene and DMF brought to a slower conversion of **1A** or afforded **2A** in reduced yields. We next examined the scope of these reactions.

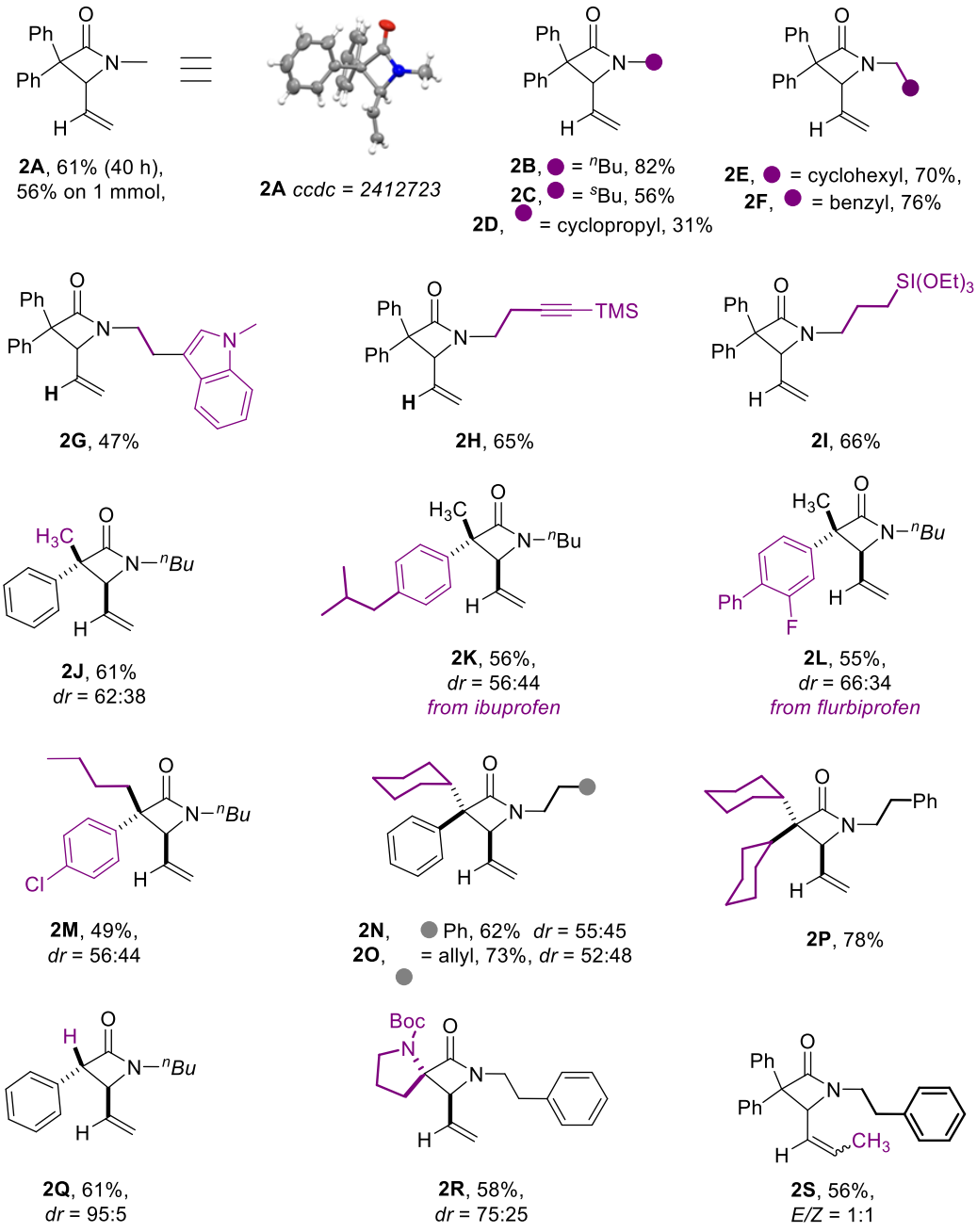

Scheme 3: Scope of β-lactams synthesized from allenamides.

A variety of substrates were easily prepared with sequential synthesis of the secondary amine, acylation, and isomerization. Alternatively, a first step of acylation took place, delivering a secondary amide. This one was then alkylated and isomerized to deliver the allenamide. A large panel of β-lactams could thus become accessible by combining these different building blocks. The scope presented in Scheme 3 shows how substrates with different N-substituents afforded β-lactams in up to 82% yield (**2A−F**). Best results were obtained with substituents on nitrogen that bear steric hindrance but are sufficiently far from the reactive site. This feature relates to the possibility of switching off the potential reaction of dearomatization, which could still happen, to a minor extent, even under optimized reaction conditions. Nevertheless, products bearing a sec-butyl or cyclopropyl fragment (**2C−D**) were synthesized, with lower yields. Substrates with N-aryl moieties were

also tried, but these ones performed poorly. On the contrary, β-lactams featuring an indole, an alkyne, or a silyloxy pendant were smoothly accessed (**2G−I**). Substituted C(sp^3)−H groups could be functionalized, leading to the formation of the β-lactams in generally good yields and moderate diastereocontrol (**2J-O**). This series included bulky cyclohexyl fragments and poly-substituted aryls, such as those derived from two commercial drugs. Since the reaction is favored by the stabilization of the radical formed after hydrogen abstraction from the vinyl radical of the activated allenamide, we initially hypothesized that the presence of at least one aryl substituent could be crucial for the reaction to occur. However, product **2P** demonstrates that the presence of the aryl groups is not necessary. Of greater importance is example **2Q,** where the functionalization of a secondary C(sp^3)−H group, which had a relatively higher BDE, occurred diastereoselectively and with moderate yields. To conclude, the spirocycle **2R** bears high relevance, showing that the method can be applied to amino acid derivatives as well. Finally, disubstituted allenes could be employed (**2S**), showing that modifications on the allylamine fragment, which is a vaunted structural feature, are well tolerated.

Three additional substrates were investigated, each designed to enable access to four-membered ring systems that could give rise to either β-lactam or azetidine frameworks, as depicted in Scheme 4.

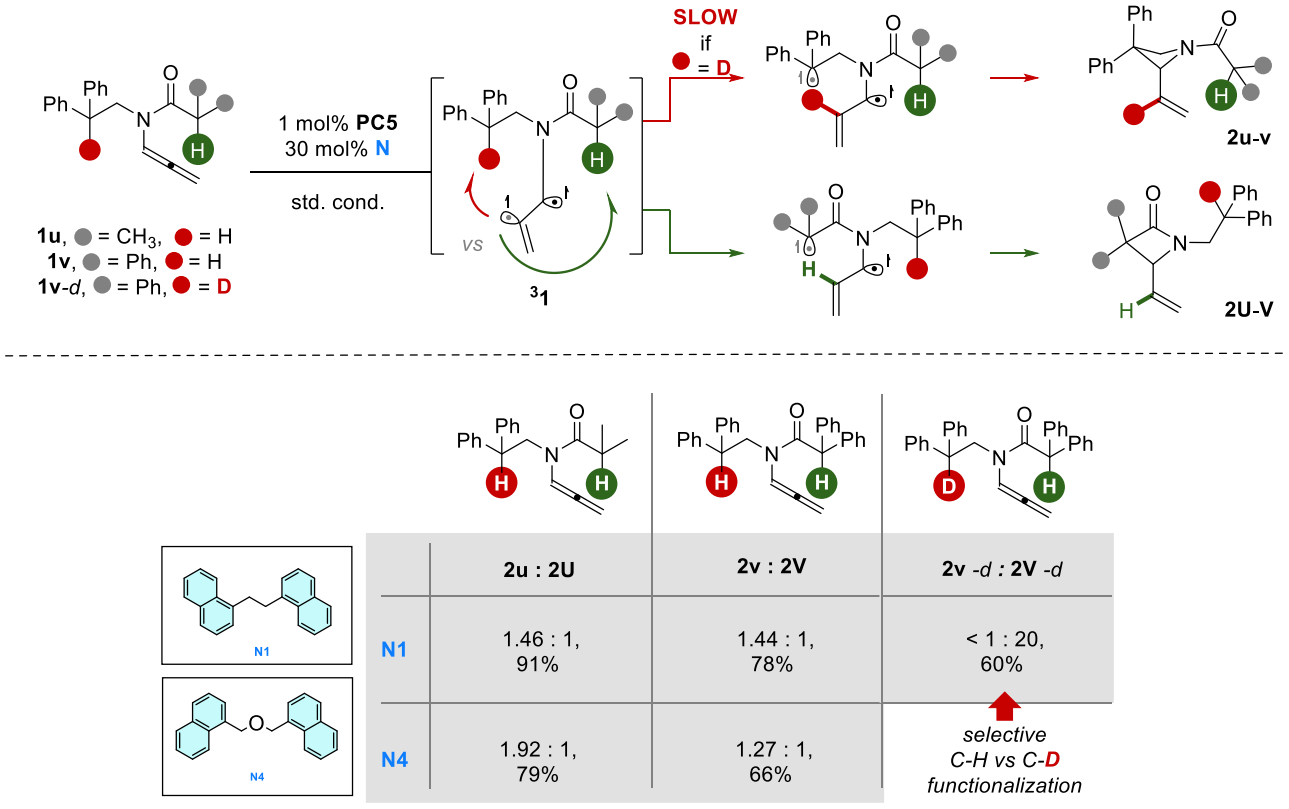

Scheme 4: Reaction that involves the possibility of both azetidine and β-lactam frameworks.

The reaction of **1u** afforded a 1.46:1 mixture of azetidine **2u** and β-lactam **2U**. The ratio was slightly altered by varying the co-catalyst involved, reaching up to 1.92:1. The same trend was observed using compound **1v**. Both substrates had two competing C(sp^3)−H groups (green vs red −H in Scheme 4), able to deliver either azetidine or β-lactam derivatives. Lastly, the reaction was performed with **1v**-*d*. The *d*-labeled β-lactam was

accessed by steering the selectivity of the C−H vs C−D functionalization, which is often challenging.[22] The result is particularly striking since it is evident that this step presents a large primary kinetic isotope affording exclusively product **2V**-*d*.

The catalytic role of **N1** was then established by monitoring two parallel reactions through time by ^{1}H-NMR in which the rate of formation of **2A** was sharply lower without **N1**. This effect can be explained by the mechanism of formation of the β-lactam presented in Scheme 5. The **N1** and generic allenamide **1** can form the [**1:N1**] adduct thanks to stabilizing π−π and C−H−π interactions. Two sequential EnTs would follow. The first one is intermolecular, and it involves the photoexcited **PC5** and **N1**, giving [**1:**^{3}**N4**]. The second EnT is intramolecular, and it occurs between ^{3}**N4** and **1**, affording [^{3}**1:N4**] that has a delocalized allylic monooccupied molecular orbital and a reactive vinyl-radical one. This intermediate can deliver ^{3}**[I:N4]**, which has a more stable tertiary benzylic radical site, via 1,5-HAT. The final ring closure is established upon intersystem crossing via radical recombination, allowing **N4** to turn over and to finally start another catalytic cycle. This rationale is supported by experimental and computational evidence.

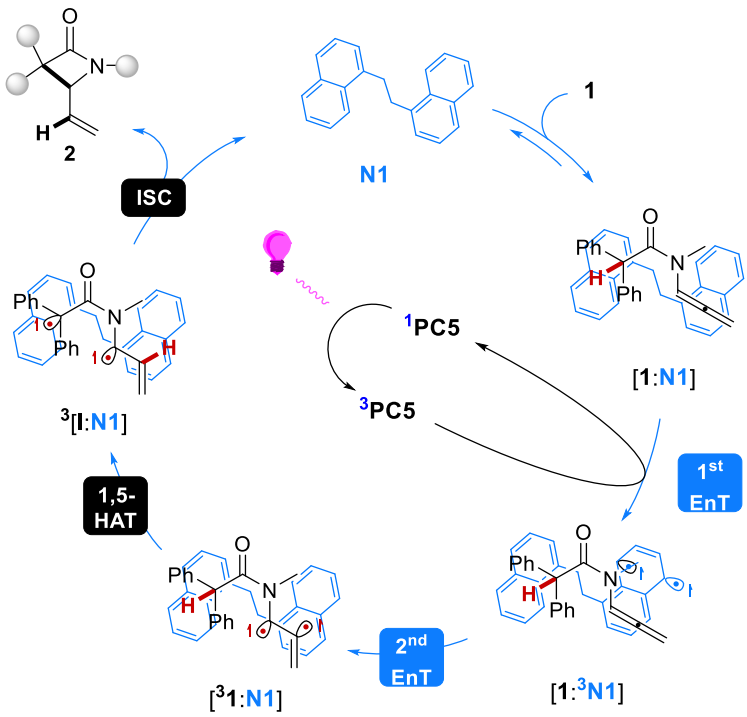

Scheme 5: Hypothesis of the two sequential EnT involved in the reaction.

To better explain, initially, the **N1** quenches ^{3}**PC5** much more efficiently than **1** (K_{SV} = 5120 vs 346 M^{-1}). The lifetime (τ) of ^{3}**PC5** in an 8:2 toluene/DCM solution at room temperature is 1.8 μs. Therefore, the **PC5-1** bimolecular quenching constant Kq is significantly smaller than the **PC5-N1** one. These results suggest that the initial EnT occurs between the ^{3}**PC5** and the cocatalyst **N1**. According to the DFT modeling data, this step is exergonic by 5.3 kcal mol^{-1}. These results strengthen the case for an initial EnT between the excited photosensitizer and the N cocatalyst, rather than the allenyl substrate, in the present reaction. The ^{3}**N1** and **1**

can then undergo a second EnT, delivering a sensitized substrate. This relay mechanism ensures the efficient activation of challenging substrates, such as terminal allenamides. The scenario resembles the concept of polarity reversal catalysis in HAT reactions, in which a hydrogen abstraction step that has a poor rate is offset by two kinetically fast ones.[23-24] Although extended aromatics have been used as triplet-state reservoirs[25], we are unaware of reports proving that the cooperation of two distinct EnT cycles increases the kinetics of substrate sensitization. The **^{3}N1−1** EnT can occur through an encounter complex between **^{3}N1** and the substrate, taking advantage of the long lifetime of the former. Alternatively, a supramolecular adduct can form at the ground state and then engage in two sequential EnT: the first one is an intermolecular event, while the second becomes an intramolecular one, bypassing concentration issues. However, both cases would lead, in the end, to the formation of the key intermediate. According to DFT modeling data, the sensitization of the adduct between the sensitized substrate and the co-catalyst seems more likely because the latter is more stable than the corresponding separate species taken alone. This feature has also been confirmed by NMR titration in an experiment conducted with allene W that led to the formation of an azetidine, as reported in Scheme 6.

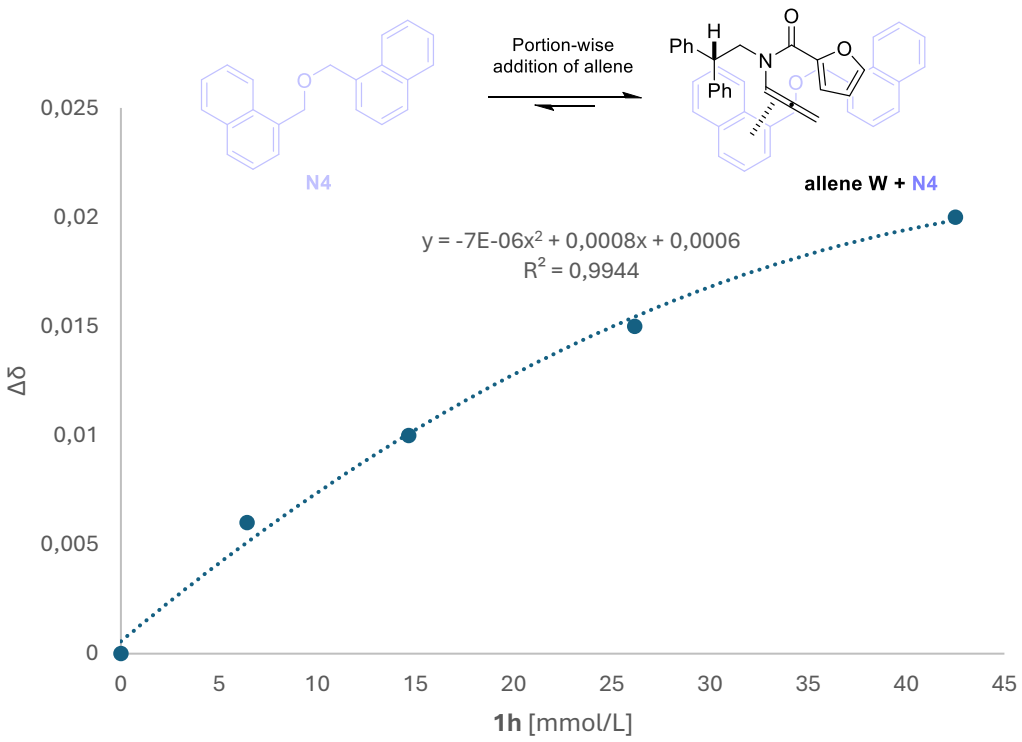

Scheme 6: NMR titration of the complex between N4 and the allene.

Various shifts in lower or higher fields were observed both for **N4** and for the reported allene W in different regions of the spectrum. The shifts were proportional to the *p*-interaction between the two species, so they are more evident in the allenylic and aromatic protons, while the aliphatic protons were generally less shifted. It has been assumed that the same process happens with the formation of β-lactams as well.

In the end, we proposed a derivatization of β-vinyl β-lactams. The extension of the chemical space through these substrates led to a series of potentially useful products (Scheme 7).

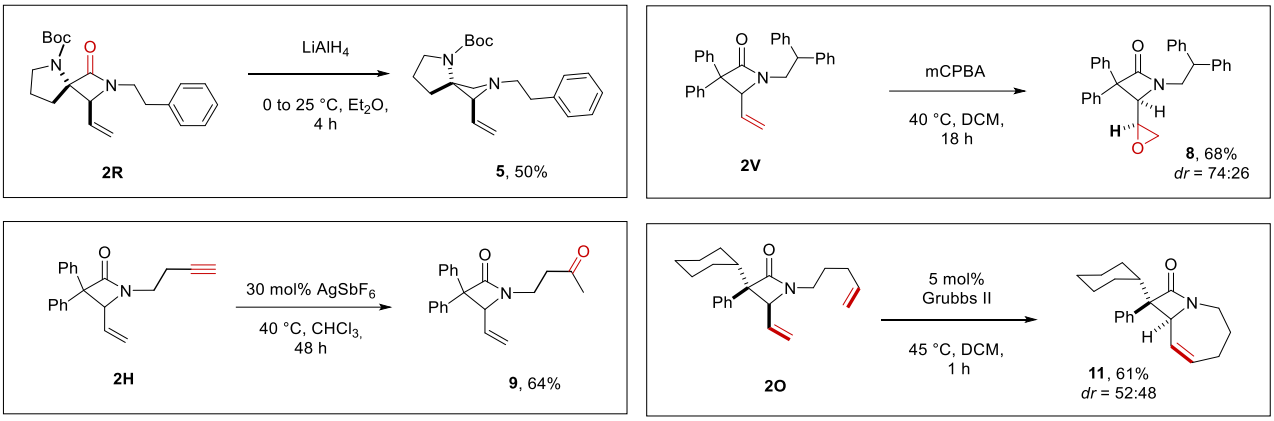

Scheme 7: Product valorization of β-vinyl β-lactams.

The most relevant post-functionalization achieved is the reduction of **2R,** which delivered the spirocyclic azetidine **5**. The vinyl group can then be treated with a peracid, delivering epoxide **8** with good diastereocontrol. We efficiently tested a mild alkyne hydration that leaves the heterocyclic core untouched (**9**). In the end, a possible application of the double bond was tested, performing a ring-closing metathesis. In this case, a fused bicyclic product, **11**, was easily synthesized and characterized, increasing the architectural complexity of the derived product.

Conclusions

With this work, a visible-light-mediated preparation of densely functionalized β-lactams, bearing a valuable allylamine unit, from interesting substrates such as allenamides was presented. A dual EnT process allows the synthesis of these challenging heterocycles at room temperature with broad functional group tolerance. The original HAT sequence involves a vinyl radical site, which has been generated in an atom-economical fashion. The method combines a powerful Ir(III) photosensitizer, which was not previously exploited in EnT reactions, with a binaphthyl cocatalyst, which can stabilize the intermediates of the sequence. Moreover, it ensures efficient substrate activation by relaying two EnT cycles. We anticipate the broad application of the relay concept for the synthesis of elaborate molecular architectures.

References

[1] H. Mughal, M. Szostak, *Organic & Biomolecular Chemistry*, **2021**, 19, 3274–3286.

[2] D. Antermite, L. Degennaro, R. Luisi, *Organic & Biomolecular Chemistry*, **2017**, 15, 34-50.

[3] A. Brandi, S. Cicchi, F. M. Cordero, A. Goti, *Chem. Rev.,* **2014**, 114, 7317–7420.

[4] C. R. Pitts, T. Lectka, Chem. Rev. **2014**, 114, 7930−7953.

[5] A. Serafino, D. Balestri, L. Marchiò, M. Malacria, E. Derat, G. Maestri, *Org. Lett.,* **2020**, 22, 6354–6359.

[6] M, Chiminelli, G. Scarica, A. Serafino, L. Marchiò, R. Viscardi, G. Maestri, *Molecules*, **2024**, 29, 595-596.

[7] S. Hosseyni, A. Jarrahpour, *Organic & Biomolecular Chemistry*, **2018**, 16, 6840−6852.

[8] B. Alcaide, P. Almendros, C. Aragoncillo, G. Gómez-Campillos, *Adv. Synt. & Catal.,* **2013**, 355, 2089-2094.

[9] J. H. Ye, P. Bellotti, T. O. Paulisch, C. G. Daniliuc, F. Glorius, *Angew. Chem. Int. Ed.,* **2021**, 60, 13671-13676.

[10] H. Aoyama, T. Hasegawa, M. Watabe, H. Shiraishi, Y. Omote, *J. Org. Chem*., **1978**, 43, 419–422.

[11] H. Wehrli, *Helv. Chim. Acta*, **1980**, 63, 1915–1919.

[12] T. Hasegawa, M. Watabe, H. Aoyama, Y. Omote, *Tetrahedron*, **1977**, 33, 485–488.

[13] J. B. Roque, Y. Kuroda, J. Jurczyk, L. P. Xu, J. S. Ham, L. T. Göttemann, C. A. Roberts, D. Adpressa, J.Saurí, L. A. Joyce, D. G. Musaev, C. S. Yeung, R. Sarpong, *ACS Catal.,* **2020**, 10, 2929–2941.

[14] M. Sakamoto, S. Watanabe, T. Fujita, M. Tohnishi, H. Aoyama, Y. Omote, *J. Chem. Soc., Perkin Trans. 1*, **1988**, 2203-2207.

[15] T. Peez, V. Schmalz, K. Harms, U. Koert, *Org. Lett.,* **2019**, 21, 4365–4369.

[16] Y. Xiong, J. Großkopf, C. Jandl, T. Bach, *Angew. Chem. Int. Ed.,* **2022**, 61, e202200555.

[17] M. J. Oddy, D. A. Kusza, R. G. Epton, J. M. Lynam, W. P. Unsworth, W. F. Petersen, *Angew. Chem. Int. Ed.,* **2022**, 61, e202213086.

[18] A. Cerveri, G. Scarica, S. Sparascio, M. Hoch, M. Chiminelli, M. Tegoni, S. Protti, G. Maestri, *Chem. Eur. J.,* **2024**, 30, e202304010.

[19] B. Li, H. Xu, Y. Dang, K. N. Houk, *J. Am. Chem. Soc.*, **2022**, 144, 1971–1985.

[20] M. Hoch, S. Sparascio, A. Cerveri, F. Bigi, R. Maggi, R. Viscardi, G. Maestri, *Photochem. Photobiol. Sci.* **2024**, 23, 1543−1563.

[21] M. Chiminelli, C. Galbardi, R. Maggi, F. Bigi, L. Capaldo, N. Della Cà, R. Viscardi, L. Marchiò, G. Maestri, M. Lanzi, *Org. Lett.*, **2025**, 27, 8909–8914.

[22] M. Miyashita, M. Sesaki, I. Hattori, M. Sekai, K. Tanino, *Science*, **2004**, 305, 495-499.

[23] B. P. Roberts, *Chem. Soc. Rev.,* **1999**, 28, 25-35.

[24] X. Pan, E. Lacote, J. Lalevèe, D. P. Curran, *J. Am. Chem. Soc.*, **2012**, 134, 5669–5674.

[25] C. Wang, F. Reichenauer, W. R. Kitzmann, C. Kerzig, K. Heinze, U. Resch-Genger, *Angew. Chem. Int. Ed.,* **2022**, 61, e202202238.

Experimental section

General remarks

All the chemicals whereby the syntheses are not reported here after were purchased from commercial sources and used as received. Solvents were dried by passing through alumina columns using an Inert® system and were stored under nitrogen. Chromatographic purifications were performed under gradient using a Combiflash® system and prepacked disposable silica cartridges or through isocratic flash chromatography using commercial 60 Å silica gel. All reactions that required heating were performed with the use of high-vacuum grade silicon oil.

Present visible light-promoted reactions require the use of dry solvents as the presence of molecular oxygen exerts a negative effect on their rate. Reactions promoted by visible light were performed into standard 5 mm NMR tubes, which were placed inside a 500 mL glass beaker equipped with a commercial strip of 300 RGB household LEDs (12V, 14W) on its internal surface. The temperature of the tubes was carefully checked with a thermometer. Cooling was ensured by two fans recovered by outdated PCs to avoid overheating due to LEDs emission.

^{1}H and ^{13}C NMR spectra were recorded at 300 K on a Bruker 400 MHz or a Jeol 600 MHz spectrometers using residual non-deuterated solvents as internal standards (7.26 ppm for ^{1}H NMR and 77.00 ppm for ^{13}C-NMR for $CDCl_3$, 2.05 ppm for ^{1}H NMR and 29.84 ppm for ^{13}C NMR for acetone-d6). ^{19}F-NMR spectra were recorded in $CDCl_3$ at 298 K on a Jeol 600 spectrometer fitted with a BBFO probe head at 565 MHz. The terms m, s, d, t, q and quint represent multiplet, singlet, doublet, triplet, quadruplet and quintuplet respectively, and the term br and h mean respectively a broad signal and a heptuplet. Reported assignments were based on decoupling, COSY, NOESY, HSQC and HMBC correlation experiments.

Mass analyses were recorded on an Infusion Water Acquity Ultra Performance LC HO6UPS-823M instrument equipped with a SQ detector (Electrospray source); high-resolution mass analyses were recorded on a LTQ ORBITRAP XL Thermo Mass Spectrometer (Electrospray source).

Single crystal Data were collected with a Bruker D8 diffractometer equipped with PhotonII area detector, using a CuKα or a MoKα microfocus 4 radiation source. The data collection strategy covered the sphere of reciprocal space. Absorption corrections were applied using the program SADABS. The structure was solved with the SHELXT code. Fourier analysis and refinement were performed by the full-matrix least-squares methods based on F2 using SHELXL-2014 as implemented in Olex2. All the nonH atoms were refined with anisotropic displacement parameters.

CCDC 2412723 contains supplementary crystallographic data for compound **2A**.

Optimization experiments

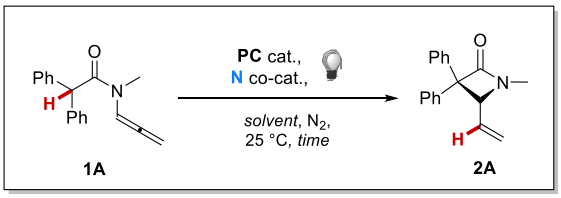

variation of the Ir(III) photocatalyst (E_T, ^{3}PC lifetime)

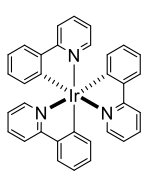

PC1 = Ir(ppy)$_3$, *58.1 kcal/mol*, 1.9 μsec

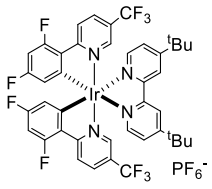

PC4 = [Ir{dFCF$_3$ppy}$_2$(dtbbpy)]PF$_6$, *61.8 kcal/mol*, 2.3 μsec

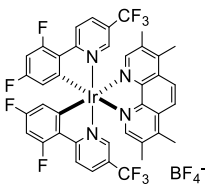

PC5 = [Ir{dFCF$_3$ppy}$_2$(Me$_4$phen)]BF$_4$, *63.0 kcal/mol*, **3.8 μsec**

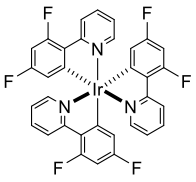

PC6 = Ir(dFppy)$_3$, *63.5 kcal/mol*, 1.6 μsec

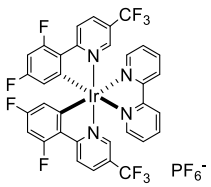

PC8 = [Ir{dFCF3ppy}2(bpy)]PF$_6$, *61.6 kcal/mol*, 2.3 μsec

variation of the tether between the 1-naphthyl unit

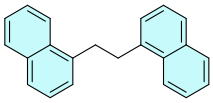

N1

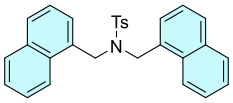

N2

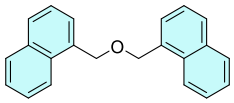

N3

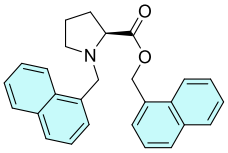

N4

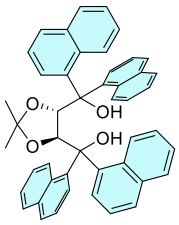

N5

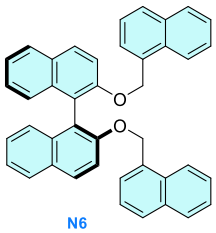

N6

A vial was charged with the allene **1A** (53 mg, 0.2 mmol, 1 equiv.), the desired photocatalyst (1 mol%), and the co-catalyst **N**. A freshly spilled dry solvent was added, and the solution was transferred into an NMR tube capped with a rubber septum. The mixture was directly irradiated with either blue or purple LEDs. The reaction was monitored by TLC; once the conversion reached a plateau, the tube was recovered, the solvent removed under vacuum and 1,3,5-Trimethoxybenzene (11.2 mg, 0.067 mmol) was added as internal standard. A **^{1}H NMR** was eventually collected to quantify the conversion **1A** and the yield of **2A**.

Preliminary experiments on the role of naphthalene on rate

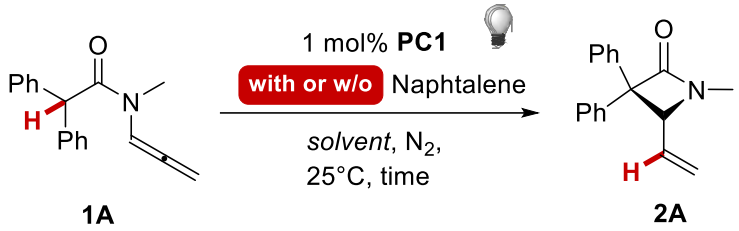

1A **2A**

	Conc. of Naphtalene	Solvent (0.1M)	Time (h)	Conversion of **1A**[a] [%]	Yield of **3A**[a] [%]
1	20 equiv.	MeCN	24	>99	39
2	20 equiv.	Tol:DCM 8:2	24	>99	41
3	10 equiv.	Tol:DCM 8:2	48	>99	50
4	5 equiv.	Tol:DCM 8:2	48	>99	48
5	1 equiv.	Tol:DCM 8:2	120	88	57
6	--	Tol:DCM 8:2	120	39	17

Table S1a. [a] by ^{1}H NMR using 1,3,5-Trimethoxybenzene as internal standard.

Initial hits on the synthesis of product **3A** were observed performing the reactions in the presence of a molar excess of naphthalene, which proved to be an efficient additive in allene-arene [4+2] dearomative cycloadditions that were initiated via EnT. Reactions performed with a large excess ensured the full consumption of the substrate **1A** upon 24 hours of irradiation. However, the yield of **2A** remained low because of the concomitant formation of side products derived from the intermolecular dearomatization seen in chapter 1. The rate of this undesired side-reaction could be reduced by reducing the concentration of naphthalene (entries 3-5). However, a progressively longer irradiation time was required to ensure the consumption of the starting material. The best result was observed using 1 equiv. of naphthalene, and the corresponding reaction afforded **2A** in 57% yield. Nonetheless, 5 days of irradiation were required in this case. Finally, a much slower conversion of the starting material and a low yield of the desired product were observed when performing the reaction without any additive (entry 6). These preliminary experiments suggested us to consider the use of **N** derivatives, which could be used in catalytic amounts, because they allow the formation of adducts with substrates, driven by dispersion interactions, which have a lower entropic penalty compared to those formed using naphthalene. The use of a lower loading of **N**, compared to naphthalene, should have thus minimized the efficiency of the undesired dearomative side-reaction, and thus hopefully led to a higher yield of the product **2A**.

Blank experiments.

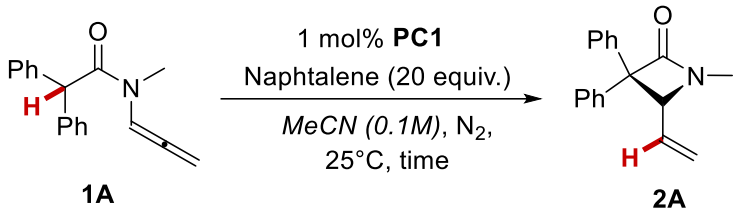

	Variation	Time (h)	Conversion of **1A**[a] [%]	Yield of **3A**[a] [%]
7	No PC	24	--	--
8	No light	24	--	--

Table S1b. [a] by ^{1}H NMR using 1,3,5-Trimethoxybenzene as internal standard.

Blank experiments confirmed that no reaction occurred without either the **PC** or the visible light source.

Evaluation of the effect of the different N co-catalysts (N1-N8).

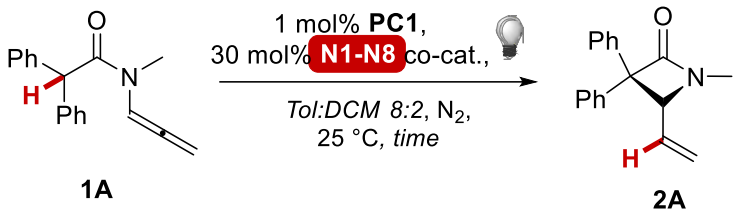

	N Co-cat. (30 mol%)	Time (h)	Conversion of **1A**[a] [%]	Yield of **3A**[a] [%]
6	**--**	120	39	17
9	**N1**	120	77	54
10	**N2**	216	86	44
11	**N3**	120	79	50
12	**N4**	120	75	47
13	**N5**	120	63	36
14	**N6**	120	75	42

Table S1c. [a] by ^{1}H NMR using 1,3,5-Trimethoxybenzene as internal standard. Best result was highlighted in pale orange.

During this stage of the optimization, six different poly-naphthyl derivatives were tested, varying the length and/or the rigidity of the tether between the two naphthyl groups, because this structural feature proved to be crucial in a recent. In all of these cases, the rate of conversion of **1A** was significantly higher (entries 9-14) than that observed without the co-catalyst (entry 6). Among the tested **N** species, the reaction performed in the presence of **N3** gave the better conversion of the starting material (entry 11), while the use of **N1** provided the highest yield of **2A** (entry 9). Therefore, the latter derivative was adopted for the following iteration of the optimization process.

Effect of different concentration of N1 as a co-catalyst.

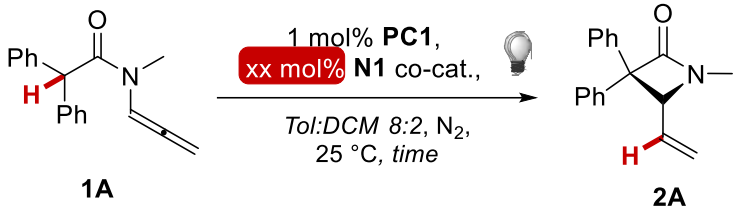

	N1 co-cat.loading	Time (h)	Conversion of **1A**[a] [%]	Yield of **3A**[a] [%]
9	**30 mol%**	120	77	54
15[b]	**30 mol%**	120	78	52
15	**70 mol%**	48	76	44
16	**1 equiv.**	48	84	48

Table S1d. [a] by ^{1}H NMR using 1,3,5-Trimethoxybenzene as internal standard. [b] 10 mol% of PC1, Best result highlighted in pale orange.

Different loadings of **N1** were tested in combination with **PC1**. Reactions in which a higher amount of the derivative was used led to faster conversion of the starting material **1A**. However, the yield of the desired product **2A** did not improve because of the formation of the above-mentioned side products between the allenyl substrate and the **N** derivative. Similarly, a higher loading of the photocatalyst proved futile (entry 15).

Comparison of different Ir(III) PCs.

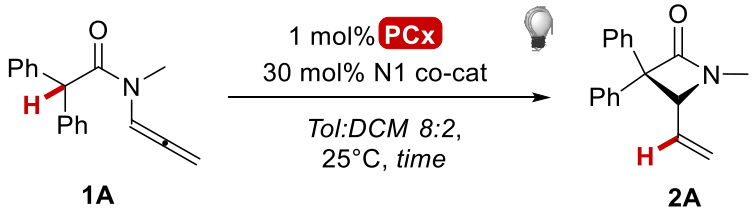

	PC cat. (1 mol%)	Co-cat. (30 mol%)	Time (h)	Conversion of **1A**[a] [%]	Yield of **3A**[a] [%]
9	**PC1,** $Ir(ppy)_3$	**N1**	120	77	54
18	**PC4**, $[Ir\{dFCF_3ppy\}_2(dtbbpy)]PF_6$	**N1**	48	>99	61
19[b]	**PC4**, $[Ir\{dFCF_3ppy\}_2(dtbbpy)]PF_6$	**N1**	48	>99	59
20	**PC5**, $[Ir[dF(CF_3)ppy]_2(Me_4phen)]BF_4$	**N1**	40	>99	61
21[b]	**PC5**, $[Ir[dF(CF_3)ppy]_2(Me_4phen)]BF_4$	**N1**	40	>99	61
22	**PC6**, $Ir(d\text{-}F\text{-}ppy)_3$	**N1**	40	>99	65
23[b]	**PC6**, $Ir(d\text{-}F\text{-}ppy)_3$	**N1**	48	>99	59
24	**PC8**, $[Ir\{dFCF_3ppy\}_2(bpy)]PF_6$	**N1**	48	68	49

Table S1e. [a] by ^{1}H NMR using 1,3,5-trimethoxybenzene as internal standard, [b] reactions performed without degassing the mixture via freeze-pump-thaw (3 times). Best results were highlighted in pale orange. Reactions performed with purple LEDs for **PC5-8**, with blue LEDs for **PC1**.

Four additional Iridium (III) photocatalysts were tested under the most promising experimental conditions previously developed. Among this series, good results were achieved using both the homoleptic complex **PC4** and the heteroleptic complex **PC5** (entries 18-21). In particular, a yield of **2A** up to 61% was achieved. However, a slightly worse result was displayed in the presence of **PC4** if the mixture was not thoroughly degassed by freeze-pump-thaw (entries 18-19). On the contrary, no differences were found between the two protocols using **PC5**. During the revision of the present work, we also tested the **PC6** complex, out of a brilliant suggestion by one of the reviewers, which we warmly thank. The use of **PC6** allowed one to achieve a higher yield of **2A** (65%, entry 22). Additionally, as observed in the case of **PC4**, the use of **PC6** required the freeze-pump-thaw technique to achieve the best outcome (entries 22-23). EnT reactions are usually very sensitive to the presence of dioxygen, which is a well-known quencher of the photoexcited Iridium (III) complexes. As a possible rationale for the outcome of this series of experiments, a series of bimolecular quenching constansts k_q, referred to the reaction between dioxygen and a photoexcited Ir(III) complex, were reported by Tobita (see J. Photochem. Photobio. A Chem, **2016**, 324, 134). In this series, all of the measured k_q were close to diffusional rates (k_q > 109 mol^{-1} sec^{-1}), but those of homoleptic Ir(III) species were always higher than those of heteroleptic ones, by a factor between 1.5 and 4. According to our luminescence quenching studies, all of the four bimolecular k_{qs} between **PC5,6** and **N1,3** are similarly close to diffusional rates (k_q > 109 mol^{-1} sec^{-1}). We thus speculate that the heteroleptic complex **PC5** might be intrinsically less sensitive to the presence of traces of dioxygen, while a certain competition between the latter and the N co-catalyst might take place using homoleptic complex **PC6**. This part of the optimization study showed that the highest yield of **2A** was achieved using **PC6**; however, the use of **PC5** retains a significant advantage in terms of practical viability because these reactions do not suffer from the presence of traces of oxygen, and it could thus allow one to skip the rather tedious freeze-pump-thaw cycle.

Experiments confirming the co-catalytic role of N1.

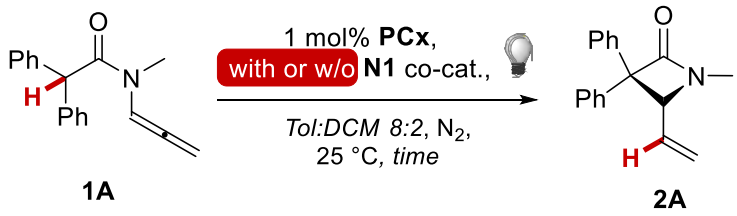

1A **2A**

	PC cat. (1 mol%)	Co-cat. (30 mol%)	Time (h)	Conversion of **1A**[a] [%]	Yield of **3A**[a] [%]
18	**PC4**, $[Ir\{dFCF_3ppy\}_2(dtbbpy)]PF_6$	**N1**	48	>99	61
25	**PC4**, $[Ir\{dFCF_3ppy\}_2(dtbbpy)]PF_6$	**--**	48	43	17
21[b]	**PC5**, $[Ir[dF(CF_3)ppy]_2(Me_4phen)]BF_4$	**N1**	40	>99	61
26	**PC5**, $[Ir[dF(CF_3)ppy]_2(Me_4phen)]BF_4$	--	40	45	16
22	**PC6**, $Ir(d\text{-}F\text{-}ppy)_3$	**N1**	40	>99	65
27	**PC6**, $Ir(d\text{-}F\text{-}ppy)_3$	--	40	64	42

Table S1f. [a] by ^{1}H NMR using 1,3,5-trimethoxybenzene as internal standard; [b] reactions performed without degassing the mixture via freeze-pump-thaw (3 times). Best results were highlighted in pale orange. Reactions performed with purple LEDs.

Three couples of experiments were performed to confirm the beneficial role of **N1**. Table S1f presents the outcome of parallel experiments using the three photosensitizers that gave the best results (**PC4- 6**), in the presence and in the absence of **N1**. In all cases, a significantly faster conversion of substrate **1A** was observed in the presence of the co-catalyst. On the contrary, the yield of **2A** and the conversion of the starting material was invariably lower in the absence of **N1** (entries 25-27).

Evaluation of the effect of the solvent in optimized purple LEDs conditions.

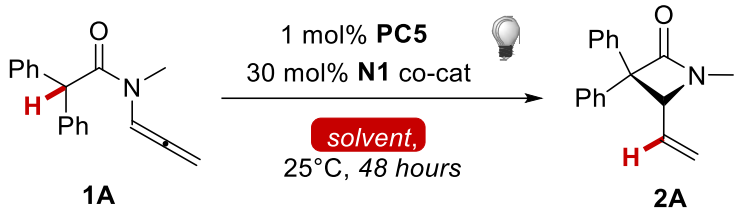

1A **2A**

	Solvent (0.1 M)	Conversion of **1A** [%][a]	Yield of **3A** [%][a]
21	Tol:DCM	>99	61
28	DMF	54	29
29	CH_3CN:DCM 8:2	90	57
30	Toluene	75	46
31	DCM	88	56
32	DCE	69	43
33	Chloroform	>99	14

Table S1g. [a] by ^{1}H NMR using 1,3,5-Trimethoxybenzene as internal standard. Best result was highlighted in pale orange.

A final comparison of different reaction media, using solvents of different polarity and combination thereof, was tested. The best result was obtained using a 8:2 toluene/DCM mixture, as observed for the synthesis of azetidines, while all the different tests provided worst, either because of a slower conversion of **1A** or by affording **3A** in reduced yields.

Stern-Volmer quenching studies

The measurements were carried out with a FLS1000 Edinburgh Fluorometer, equipped with automatic polarizers. Emissions have been collected by exciting samples with a Xenon lamp at 293 nm and the luminescence was measured at 412 nm. Luminescence spectra are corrected for the excitation intensity and detector sensitivity.

Stern – Volmer quenching studies were carried out using a 10^{-5} M solution of **PC5** in Toluene/DCM 8:2 and variable concentrations of **1A** and **N1** from 0 to 9.1 mM. 2.5 mL or 2 mL of **PC5** solution was transferred into a 3.5 mL quartz cuvette and degassed twice for 5 minutes (with a 30-second break in between) before collecting the first spectra. Then, after each addition of quencher, the samples were degassed for 2 minutes and spectras were extemporaneously recorded.

Linear Stern – Volmer plots were obtained at varying concentrations of the three substrates, and K_{SV} constants were extracted according to the equation $I_0/I = 1 + K_{SV}[Q]$. **1A** clearly quench **PC5**. K_q constants were obtained according to the equation $K_q = Ksv/\tau_0$.

Comprehensive table of Stern – Volmer constants and Kinetic constants:

QUENCHER	**K_{SV}**	**R^2**	**K_q [$mol^{-1} \cdot L \cdot sec^{-1}$] x 10^8**
1A	384	0.99	1.01
N1	4442	0.97	11.69

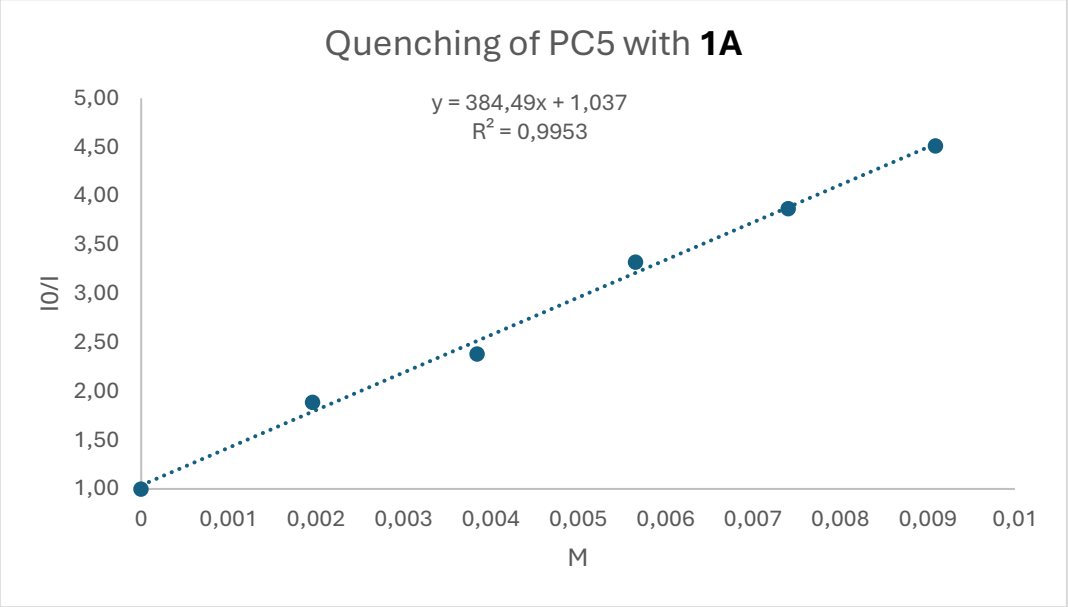

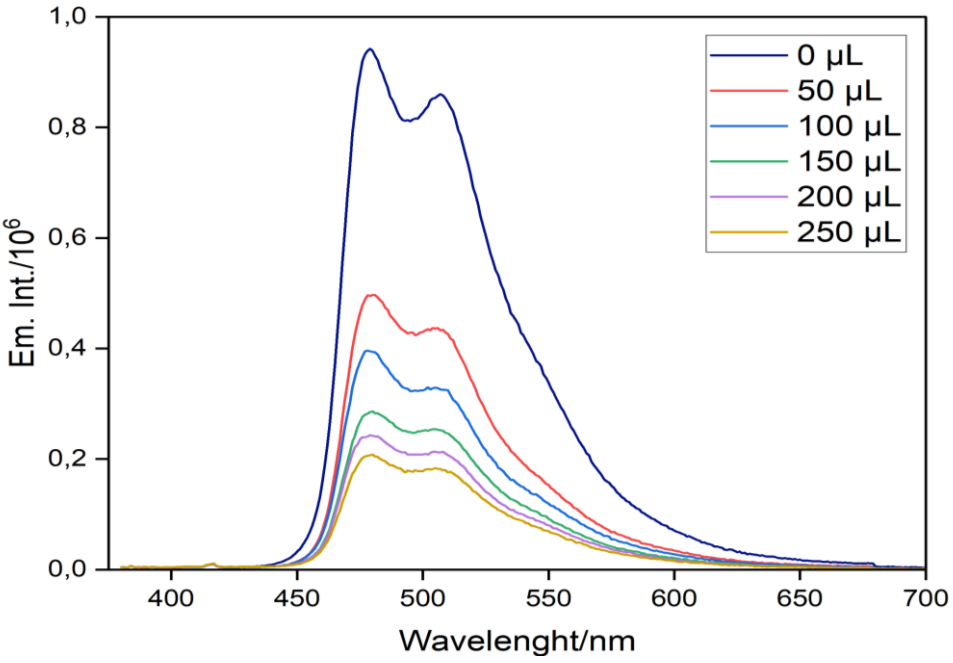

Figure 1: Measured emissions for quench of PC5 with 50µL, 100µL, 150µL, 200µL, and 250µL of **1A**

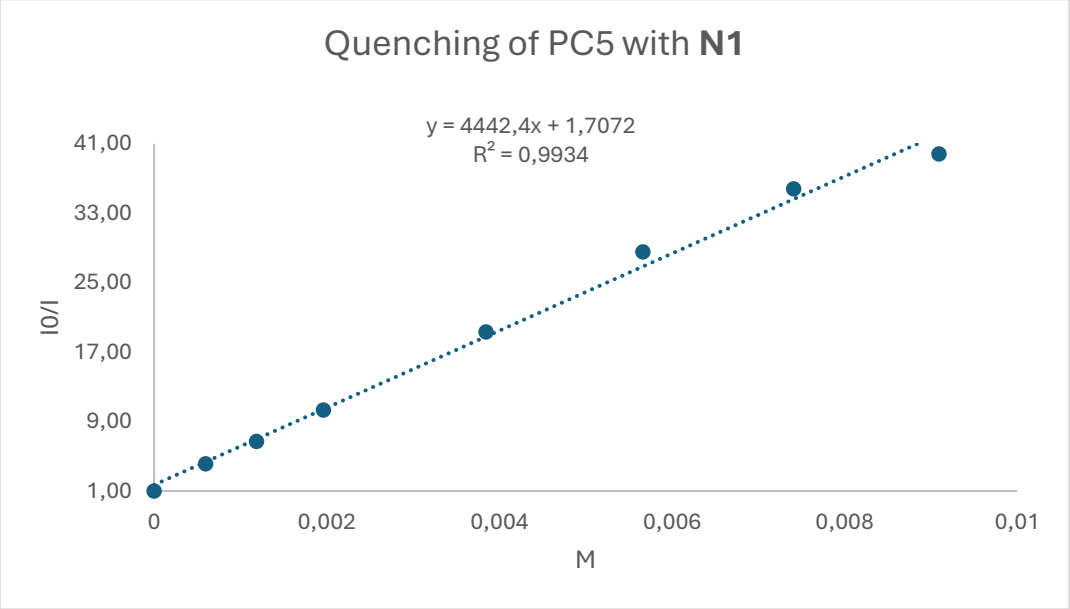

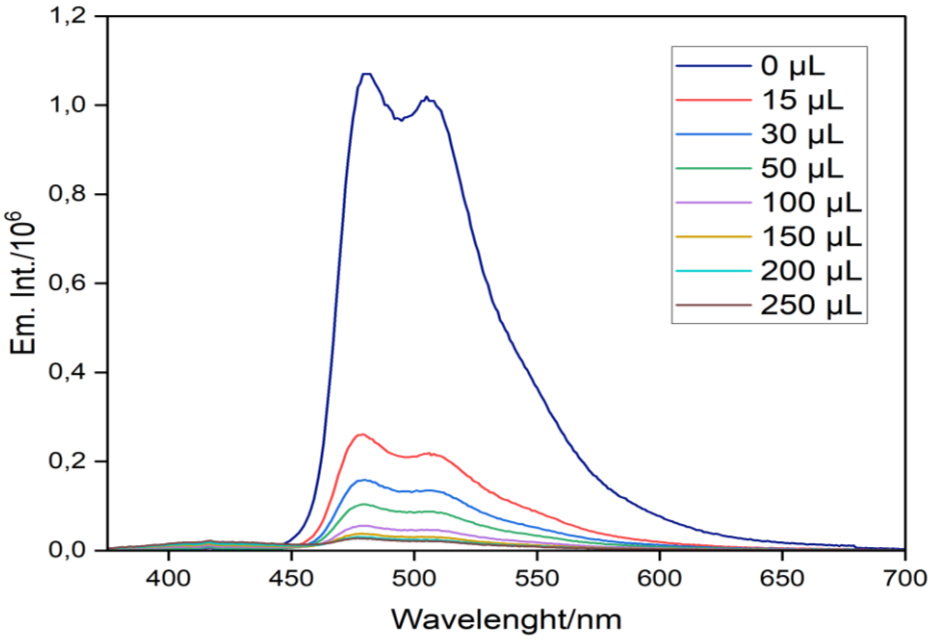

Figure 2: Measured emissions for quench of PC5 with 15 µL, 30 µL,50µL, 100µL , 150µL, 200µL, and 250µL of **N1**

Unsuccessful substrates

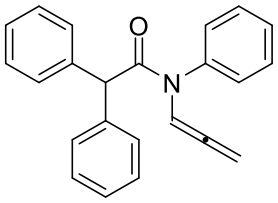

Traces + RSM

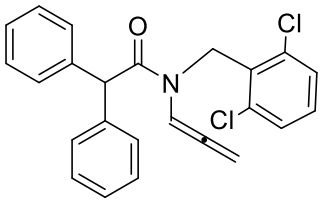

Traces + RSM

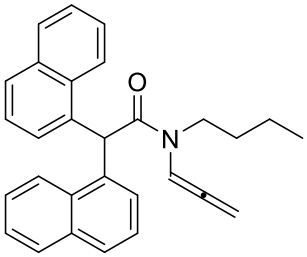

SR

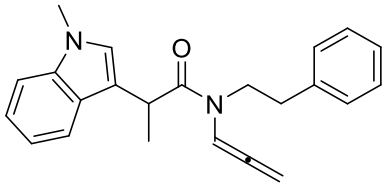

SR + DEC: deallenation

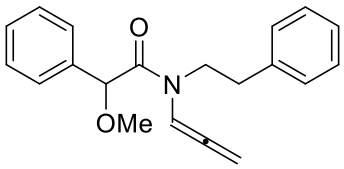

RSM

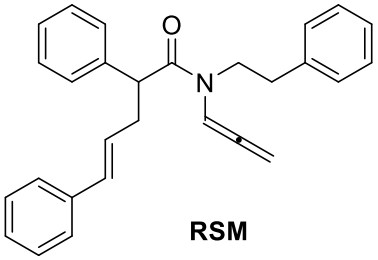

RSM

RSM: Recovery of starting material
DEC: Decomposition
SR: Side reaction

Synthesis of substrates

General procedure B1:

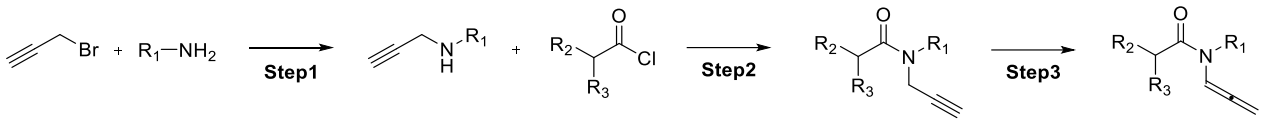

Step 1: In a round-bottom flask equipped with a magnetic stirring bar, propargyl bromide (1 equiv.) was added at 0 °C to a general primary amine (6 equiv.), and the resulting solution was stirred for 18 h at room temperature. After complete conversion as monitored by TLC, the mixture was quenched with a saturated $NaHCO_3$ aqueous solution and extracted with Et_2O (3 times). The combined organic phase was washed with brine, dried over Na_2SO_4 and concentrated under reduced pressure. The crude was finally purified by chromatography on silica gel (*n*-hexane/EtOAc gradient) to afford the desired product.

Step 2: In a round-bottom flask equipped with a magnetic stirring bar, secondary amine (1 equiv.), DMAP (0.02 equiv.) and DIPEA (1 equiv.) were dissolved in dry DCM (0.25 M). The solution was cooled to 0 °C and the acyl chloride (1 equiv.) was then added dropwise. The mixture was stirred at room temperature until completion, monitoring the process by TLC. The solution was then quenched with saturated NH_4Cl aqueous solution and diluted with DCM. The organic phase was then washed with brine, dried over Na_2SO_4 and concentrated under reduced pressure. The crude was finally purified by chromatography on silica gel (*n*-hexane/EtOAc gradient) to afford the desired product.

Step 3: The desired propargyl amide (1 equiv.) was dissolved in dry toluene (0.20 M) in a round-bottom two-necked flask equipped with a magnetic stirring bar. Then under N_2 atmosphere, *t*-BuOK (0.3 equiv.) was added at 0°C, and the resulting mixture was stirred at room temperature for 5 minutes. After complete conversion as monitored by TLC, 5 ml of saturated NH_4Cl aqueous solution was added. The mixture was sequentially extracted with EtOAc (3 x 15 ml), the organic layers separated and dried over Na_2SO_4. The solution was concentrated under reduced pressure and the crude purified by chromatography on silica gel (*n*-hexane/EtOAc gradient) to afford the corresponding allenamide.

General procedure B2:

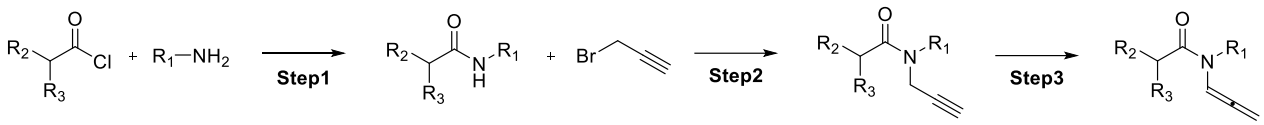

Step 1: In a round bottom flask equipped with a magnetic stirring bar, primary amine (1 equiv.), DMAP (0.02 equiv.) and DIPEA (1 equiv.) were dissolved in dry DCM (0.25 M). The solution was cooled to 0 °C and the acyl chloride (1 equiv.) was then added dropwise. The mixture was stirred at room temperature until completion, monitoring the process by TLC. The solution was then quenched with saturated NH_4Cl aqueous solution and diluted with DCM. The organic phase was then washed with brine, dried over Na_2SO_4 and concentrated under reduced pressure. The crude product was used without further purification.

Step 2: To a solution of primary amide/carbamate (1 equiv.) in dry DMF (0.6 M), NaH (60% in paraffine oil, 1.3 equiv.) was slowly added at 0°C and the mixture was stirred for 1 h at the same temperature. The desired alkyl halide (1.3 equiv.) was then slowly added, and the reaction was stirred at room temperature for 18 h. After complete conversion as monitored by TLC, the mixture was quenched with a saturated NH_4Cl aqueous solution and extracted with EtOAc (3 times). The combined organic layers were washed with brine (3 times), dried over Na_2SO_4 and concentrated under reduced pressure. The crude was purified by chromatography on silica gel (*n*-hexane/EtOAc gradient) to afford the desired products.

Step 3: The desired propargyl amide (1 equiv.) was dissolved in dry toluene (0.20 M) in a round-bottom two-necked flask equipped with a magnetic stirring bar. Then under N_2 atmosphere, *t*-BuOK (0.3 equiv.) was added at 0°C, and the resulting mixture was stirred at room temperature for 5 minutes. After complete conversion as monitored by TLC, 5 ml of saturated NH_4Cl aqueous solution was added. The mixture was sequentially extracted with EtOAc (3 x 15 ml), the organic layers separated and dried over Na_2SO_4. The solution was concentrated under reduced pressure and the crude was purified by chromatography on silica gel (*n*-hexane/EtOAc gradient) to afford the corresponding allenamide.

Characterization of substrates for β-lactams

N-methyl-2,2-diphenyl-N-(propa-1,2-dien-1-yl)acetamide

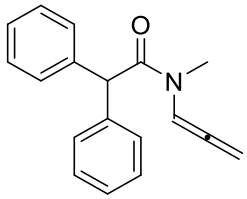

Allene **1A** was prepared following general procedure **GP-B2** from the corresponding propargyl amide (263 mg, 1 mmol). White solid (210 mg, 80% yield). Two rotamers were observed due to the dynamic amide group (54:46 mixture of rotamers).

^{1}H NMR (400 MHz, $CDCl_3$) δ 7.66 (t, *J* = 6.4 Hz, 1H RotA), 7.36 – 7.24 (m, 10H RotA, 10H RotB), 6.89 (t, *J* = 6.1 Hz, 1H RotB), 5.40 – 5.29 (m, 3H RotA, 3H RotB), 3.08 (s, 3H RotB), 3.03 (s, 3H RotA). **^{13}C NMR** (101 MHz, $CDCl_3$) δ 202.6 (RotA), 201.3 (RotB), 170.2 (RotA), 170.1 (RotB), 139.2 (2C RotB), 139.0 (2C RotA), 129.1 (4C RotA, 4C RotB), 128.8 (4C RotA, 4C RotB), 127.3 (2C RotA, 2C RotB), 101.4 (RotB), 100.3 (RotA), 87.4 (RotA), 86.7 (RotB), 55.8 (RotA), 55.2 (RotB), 33.4 (RotA), 31.9 (RotB). **ESI-HRMS** calcd for $C_{18}H_{18}NO$ $[M+H]^+$ 264.1388, found 264.1393.

N-butyl-2,2-diphenyl-N-(propa-1,2-dien-1-yl)acetamide

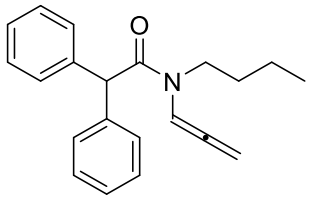

Allene **1B** was prepared following general procedure **GP-B2** from the corresponding propargyl amide (306 mg, 1 mmol). Light-yellow oil (165 mg, 54% yield). Two rotamers were observed due to the dynamic amide group (53:47 mixture of rotamers).

^{1}H NMR (400 MHz, $CDCl_3$) δ 7.58 (t, *J* = 6.5 Hz, 1H RotB), 7.36 – 7.31 (m, 4H RotA, 4H RotB), 7.29 – 7.24 (m, 6H RotA, 6H RotB), 6.76 (t, *J* = 6.2 Hz, 1H RotA), 5.36 (d, *J* = 6.5 Hz, 1H RotA, 1H RotB), 5.37 – 5.27 (m, 2H RotA, 2H RotB), 3.59 – 3.55 (m, 1H RotA, 1H RotB), 3.43 – 3.39 (m, 1H RotA, 1H RotB), 1.60 – 1.52 (m, 2H RotA, 2H RotB), 1.32 (dt, *J* = 14.8, 7.4 Hz, 2H RotA, 2H RotB), 0.92 (td, *J* = 7.4, 3.4 Hz, 3H RotA, 3H RotB). **^{13}C NMR** (101 MHz, $CDCl_3$) δ 202.5 (RotB), 201.5 (RotA), 169.9 (RotB), 169.7 (RotA), 139.3 (2C RotA), 139.2 (2C RotB), 129.1 (4C RotA), 129.1 (4C RotB), 128.8 (4C RotA, 4C RotB), 127.34 (2C RotB), 127.26 (2C RotA), 100.3 (RotA), 99.0 (RotB), 86.8 (RotB), 86.1 (RotA), 55.3 (RotA), 55.2 (RotB), 46.0 (RotB), 44.9 (RotA), 31.0 (RotB), 29.4 (RotA), 20.2 (RotA), 20.1 (RotB), 14.0 (RotA RotB). **ESI-HRMS** calcd for $C_{21}H_{24}NO$ $[M+H]^+$ 306.1858, found 306.1864.

N-(sec-butyl)-2,2-diphenyl-N-(propa-1,2-dien-1-yl)acetamide

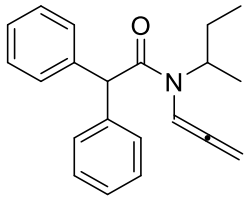

Allene **1C** was prepared following general procedure **GP-B1** from the corresponding propargyl amide (306 mg, 1 mmol). Light-orange oil (95 mg, 31% yield).

^{1}H NMR (400 MHz, $CDCl_3$) δ 7.35 – 7.22 (m, 10H), 6.14 (t, *J* = 6.3 Hz, 1H), 5.42 (s, 1H), 4.99 (d, *J* = 6.2 Hz, 2H), 4.62 (dt, *J* = 9.1, 6.6 Hz, 1H), 1.70 – 1.63 (m, 1H), 1.55 – 1.46 (m, 1H), 1.18 (d, *J* = 6.8 Hz, 3H), 0.84 (t, *J* = 7.4 Hz, 3H). **^{13}C NMR** (101 MHz, $CDCl_3$) δ 207.4, 171.2, 139.7 (2C), 129.23 (2C), 129.20 (2C), 128.6 (2C), 128.5 (2C), 127.0 (2C), 95.1, 82.3, 56.2, 53.0, 27.1, 18.3, 11.2. **ESI-HRMS** calcd for $C_{21}H_{24}NO$ $[M+H]^+$ 306.1858, found 306.1867.

N-cyclopropyl-2,2-diphenyl-N-(propa-1,2-dien-1-yl)acetamide

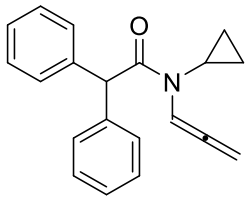

Allene **1D** was prepared following general procedure **GP-B1** from the corresponding propargyl amide (291 mg, 1 mmol). Orange oil (67 mg, 23% yield).

^{1}H NMR (400 MHz, $CDCl_3$) δ 7.38 (t, *J* = 6.5 Hz, 1H), 7.35 – 7.23 (m, 10H), 5.92 (s, 1H), 5.29 (d, *J* = 6.5 Hz, 2H), 2.54 (tt, *J* = 7.0, 4.0 Hz, 1H), 0.99 – 0.96 (m, 2H), 0.92 – 0.89 (m, 2H). **^{13}C NMR** (101 MHz, $CDCl_3$) δ 203.4, 172.9, 139.4 (2C), 129.1 (4C), 128.7 (4C), 127.2 (2C), 99.7, 85.6, 54.8, 28.8, 10.6 (2C). **ESI-HRMS** calcd for $C_{20}H_{20}NO$ $[M+H]^+$ 290.1545, found 290.1549.

N-(cyclohexylmethyl)-2,2-diphenyl-N-(propa-1,2-dien-1-yl)acetamide

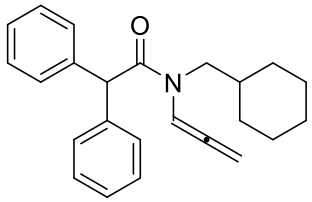

Allene **1E** was prepared following general procedure **GP-B1** from the corresponding propargyl amide (345 mg, 1 mmol). Light-yellow oil (145 mg, 42% yield). Two rotamers were observed due to the dynamic amide group (61:39 mixture of rotamers).

^{1}H NMR (400 MHz, $CDCl_3$) δ 7.63 (t, *J* = 6.4 Hz, 1H RotB), 7.35 – 7.31 (m, 4H RotA, 4H RotB), 7.28 – 7.25 (m, 6H RotA, 6H RotB), 6.78 (t, *J* = 6.2 Hz, 1H RotA), 5.34 (t, *J* = 5.9 Hz, 2H RotA, 2H RotB), 5.28 (d, *J* = 6.2 Hz, 1H RotA, 1H RotB), 3.43 (d, *J* = 7.2 Hz, 2H RotA), 3.27 (d, *J* = 6.9 Hz, 2H RotB), 1.80 – 1.60 (m, 6H RotA, 6H RotB), 1.28 – 1.12 (m, 3H RotA, 3H RotB), 1.03 – 0.90 (m, 2H RotA, 2H RotB). **^{13}C NMR** (101 MHz, $CDCl_3$) δ 202.9 (RotB), 201.8 (RotA), 170.4 (RotB), 170.1 (RotA), 139.3 (2C RotA, 2C RotB), 129.11 (4C RotA), 129.05 (4C RotB), 128.7 (4C RotA, 4C RotB), 127.29 (2C RotB), 127.26 (2C RotA), 100.9 (RotA), 99.7 (RotB), 86.9 (RotB), 86.2 (RotA), 55.5 (RotA), 54.9 (RotB), 52.0 (RotB), 51.0 (RotA), 37.9 (RotB), 36.2 (RotA), 31.1 (RotB), 30.9 (RotA), 26.5 (2C RotA), 26.4 (2C RotB), 26.2 (2C RotB), 26.0 (2C RotA). **ESI-HRMS** calcd for $C_{24}H_{28}NO$ $[M+H]^+$ 346.2171, found 346.2173.

N-phenethyl-2,2-diphenyl-N-(propa-1,2-dien-1-yl)acetamide

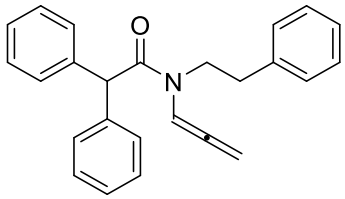

Allene **1F** was prepared following general procedure **GP-B1** from the corresponding propargyl amide (353 mg, 1 mmol). Light-orange oil (208 mg, 59% yield). Two rotamers were observed due to the dynamic amide group (51:49 mixture of rotamers).

^{1}H NMR (400 MHz, $CDCl_3$) δ 7.70 (t, *J* = 6.5 Hz, 1H RotB), 7.41 – 7.23 (m, 12H RotA, 12 RotB), 7.19 (d, *J* = 6.6 Hz, 1H RotA, 1H RotB), 7.13 (d, *J* = 6.9 Hz, 2H RotA, 2H RotB), 6.79 (t, *J* = 6.2 Hz, 1H RotA), 5.49 (d, *J* = 6.5 Hz, 1H RotA, 1H RotB), 5.37 (d, *J* = 6.2 Hz, 1H RotA, 1H RotB), 5.35 (s, 1H RotA), 4.99 (s, 1H RotB), 3.86 – 3.82 (m, 1H RotA, 1H RotB), 3.68 (t, *J* = 7.4 Hz, 1H RotA, 1H RotB), 2.94 – 2.90 (m, 1H RotA, 1H RotB), 2.82 (t, *J* = 7.4 Hz, 1H RotA, 1H RotB). **^{13}C NMR** (101 MHz, $CDCl_3$) δ 202.6 (RotB), 201.4 (RotA), 170.0 (RotB), 169.7 (RotA), 139.1 (2C RotB), 139.01 (2C RotA), 138.98 (RotA), 138.5 (RotB), 129.1 (4C RotA, 4C RotB), 129.0 (4C RotA, 4C RotB), 128.8 (2C RotA), 128.7 (2C RotB), 128.5 (RotA, RotB), 127.3 (2C RotA, 2C RotB), 127.0 (2C RotA), 126.4 (2C RotB), 100.2 (RotA), 98.6 (RotB), 87.0 (RotB), 86.5 (RotA), 55.5 (RotB), 55.3 (RotA), 47.7 (RotB), 46.6 (RotA), 34.5 (RotB), 33.5 (RotA). **ESI-HRMS** calcd for $C_{25}H_{23}NNaO$ $[M+Na]^+$ 376.1677, found 376.1685.

N-(2-(1-methyl-1H-indol-3-yl)ethyl)-2,2-diphenyl-N-(propa-1,2-dien-1-yl)acetamide

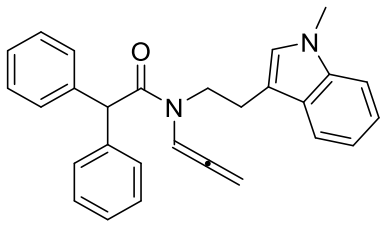

Allene **1G** was prepared following general procedure **GP-B1** from the corresponding propargyl amide (406 mg, 1 mmol). Yellow oil (102 mg, 25% yield). Two rotamers were observed due to the dynamic amide group (60:40 mixture of rotamers).

^{1}H NMR (400 MHz, $CDCl_3$) δ 7.68 – 7.62 (m, 1H RotA, 1H RotB), 7.61 (d, *J* = 7.9 Hz, 1H RotA), 7.38 – 7.27 (m, 5H RotA, 5H RotB), 7.24 – 7.17 (m, 6H RotA, 6H RotB), 6.83 – 6.81 (m, 3H RotA, 3H RotB), 6.76 (t, *J* = 6.2 Hz, 1H RotB), 5.45 (d, *J* = 6.5 Hz, 2H RotA), 5.32 (s, 1H RotB), 5.30 (d, *J* = 6.2 Hz, 2H RotB), 4.67 (s, 1H RotA), 3.86 – 3.82 (m, 1H RotA, 1H RotB), 3.73 – 3.66 (m, 4H RotA, 4H RotB), 3.03 – 3.97 (m, 2H RotA, 2H RotB). **^{13}C NMR** (101 MHz, $CDCl_3$) δ 202.7 (RotA), 201.5 (RotB), 170.4 (RotA), 169.8 (RotB), 139.3 (2C RotA, 2C RotB), 137.4 (RotA, RotB), 137.1 (RotA, RotB), 129.2 (4C RotB), 128.83 (4C RotA), 128.81 (4C RotB), 128.5 (4C RotA), 127.8 (RotB), 127.7 (RotA), 127.3 (RotB), 127.1 (RotA), 122.3 (2C RotA), 121.6 (2C RotB), 119.5 (RotA), 119.4 (RotB), 118.9 (RotB), 118.7 (RotA), 111.7 (RotB), 110.8 (RotA), 109.7 (RotA), 109.2 (RotB), 100.4 (RotB), 98.5 (RotA), 86.9 (RotA), 86.4 (RotB), 55.4 (RotB), 54.9 (RotA), 46.6 (RotA), 46.2 (RotB), 32.8 (RotA), 32.7 (RotB), 23.9 (RotA), 23.1 (RotB). **ESI-HRMS** calcd for $C_{28}H_{26}N_2NaO$ $[M+Na]^+$ 429.1943, found 429.1947.

2,2-diphenyl-N-(propa-1,2-dien-1-yl)-N-(4-(trimethylsilyl)but-3-yn-1-yl)acetamide

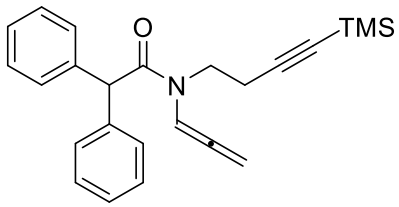

Allene **1H** was prepared following general procedure **GP-B1** from the corresponding propargyl amide (374 mg, 1 mmol). White solid (318 mg, 85% yield). Two rotamers were observed due to the dynamic amide group (56:44 mixture of rotamers).

^{1}H NMR (600 MHz, $CDCl_3$) δ 7.58 (t, *J* = 6.5 Hz, 1H RotB), 7.36 – 7.32 (m, 4H RotA, 4H RotB), 7.29 – 7.25 (m, 6H RotA, 6H RotB), 6.75 (t, *J* = 6.2 Hz, 1H RotA), 5.56 (s, 1H RotB), 5.39 (d, *J* = 6.5 Hz, 2H RotB), 5.33 (d, *J* = 6.2 Hz, 2H RotA), 5.32 (s, 1H RotA), 3.76 – 3.73 (m, 2H RotA), 3.60 (t, *J* = 6.9 Hz, 2H RotB), 2.55 – 2.53 (m, 2H RotA), 2.48 (t, *J* = 6.9 Hz, 2H RotB), 0.18 (s, 9H RotB), 0.13 (s, 9H RotA). **^{13}C NMR** (151 MHz, $CDCl_3$) δ 201.9 (RotA), 201.4 (RotB), 170.2 (RotB), 169.8 (RotA), 139.03 (2C RotA), 139.00 (2C RotB), 129.10 (4C RotB), 129.08 (4C RotA), 128.8 (4C RotA, 4C RotB), 127.4 (2C RotB), 127.3 (2C RotA), 103.9 (RotA),

103.2 (RotB), 100.4 (RotA), 98.5 (RotB), 87.5 (RotB), 87.4 (RotA), 86.8 (RotA), 85.9 (RotB), 55.3 (RotA), 55.2 (RotB), 44.6 (RotB), 44.1 (RotA), 19.9 (RotB), 18.6 (RotA), 0.2 (3C RotA), 0.1 (3C RotB). **ESI-HRMS** calcd for $C_{24}H_{28}NOSi$ $[M+H]^+$ 374.1940, found 374.1945.

2,2-diphenyl-N-(propa-1,2-dien-1-yl)-N-(3-(triethoxysilyl)propyl)acetamide (1l)

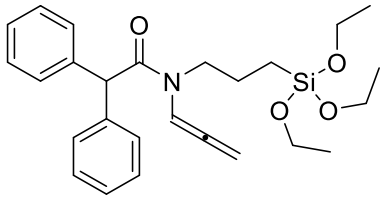

Allene **1l** was prepared following general procedure **GP-B1** from the corresponding propargyl amide (453 mg, 1 mmol). Light-yellow oil (172 mg, 38% yield). Two rotamers were observed due to the dynamic amide group (52:48 mixture of rotamers).

^{1}H NMR (600 MHz, Acetone-d_6) δ 7.53 (t, *J* = 6.5 Hz, 1H RotA), 7.37 – 7.30 (m, 8H RotA, 8H RotB), 7.27 – 7.23 (m, 2H RotA, 2H RotB), 7.10 (t, *J* = 6.2 Hz, 1H RotB), 5.65 (s, 1H RotB), 5.56 (s, 1H RotA), 5.40 (d, *J* = 6.5 Hz, 2H RotA), 5.33 (d, *J* = 6.2 Hz, 2H RotB), 3.81 – 3.77 (m, 6H RotA, 6H RotB), 3.56 – 3.52 (m, 2H RotA, 2H RotB), 1.72 – 1.61 (m, 2H RotA, 2H RotB), 1.20 – 1.16 (m, 9H RotA, 9H RotB), 0.60 – 0.58 (m, 1H RotA, 1H RotB), 0.55 – 0.52 (m, 1H RotA, 1H RotB). **^{13}C NMR** (151 MHz, Acetone-d_6) δ 203.18 (RotA), 202.05 (RotB), 170.36 (RotA), 170.08 (RotB), 140.88 (2C RotB), 140.80 (2C RotA), 129.97 (4C RotB), 129.91 (4C RotA), 129.21 (4C RotA), 129.19 (4C RotB), 127.81 (2C RotA), 127.70 (2C RotB), 101.18 (RotB), 99.14 (RotA), 87.03 (RotA), 86.27 (RotB), 58.90 (3C RotA), 58.80 (3C RotB), 54.95 (RotB), 54.92 (RotA), 49.07 (RotA), 47.65 (RotB), 23.19 (RotA), 21.48 (RotB), 18.71 (3C RotA, 3C RotB), 8.25 (RotB), 7.94 (RotA). **ESI-HRMS** calcd for $C_{26}H_{36}NO_4Si$ $[M+H]^+$ 454.2414, found 454.2410.

N-butyl-2-phenyl-N-(propa-1,2-dien-1-yl)propanamide

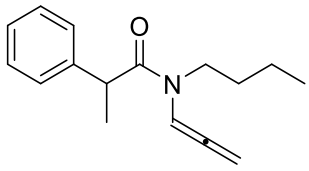

Allene **1J** was prepared following general procedure **GP-B1** from the corresponding propargyl amide (244 mg, 1 mmol). White solid (173 mg, 71% yield). Two rotamers were observed due to the dynamic amide group (53:47 mixture of rotamers).

^{1}H NMR (400 MHz, Acetone-d^6) δ 7.54 (t, *J* = 6.5 Hz, 1H RotB), 7.35 – 7.31 (m, 4H RotA, 4H RotB), 7.27 – 7.22 (m, 1H RotA, 1H RotB), 6.99 (t, *J* = 6.2 Hz, 1H RotB), 5.40 – 5.24 (m, 2H RotA, 2H RotB), 4.21 (q, *J* = 6.8 Hz, 1H RotA), 4.13 (q, *J* = 6.8 Hz, 1H RotB), 3.60 – 3.53 (m, 1H RotA), 3.46 – 3.29 (m, 1H RotA, 2H RotB), 1.56 – 1.37 (m, 5H RotA, 5H RotB), 1.29 – 1.13 (m, 2H RotA, 2H RotB), 0.90 – 0.82 (m, 3H RotA, 3H RotB). **^{13}C NMR** (101 MHz, Acetone-d^6) δ 203.1 (RotB), 201.6 (RotA), 172.0 (RotB), 171.7 (RotA), 142.9 (RotA, RotB),

129.6 (2C RotA, 2C RotB), 128.12 (2C RotB), 128.06 (2C RotA), 127.7 (RotB), 127.6 (RotA), 100.9 (RotA), 99.1 (RotB), 86.8 (RotB), 86.2 (RotA), 45.9 (RotB), 44.3 (RotA), 44.0 (RotB), 43.5 (RotA), 31.0 (RotB), 30.0 (RotA), 21.6 (RotB), 21.3 (RotA), 20.6 (RotA), 20.5 (RotB), 14.13 (RotA), 14.06 (RotB). **ESI-HRMS** calcd for $C_{16}H_{21}NNaO$ $[M+Na]^+$ 266.1521, found 266.1535.

N-butyl-2-(4-isobutylphenyl)-N-(propa-1,2-dien-1-yl)propanamide

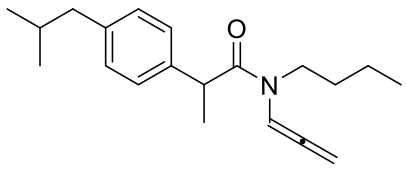

Allene **1K** was prepared following general procedure **GP-B1** from the corresponding propargyl amide (300 mg, 1 mmol). Light-yellow oil (198 mg, 66% yield). Two rotamers were observed due to the dynamic amide group (52:48 mixture of rotamers).

^{1}H NMR (600 MHz, $CDCl_3$) δ 7.54 (t, *J* = 6.5 Hz, 1H RotB), 7.17 – 7.13 (m, 2H RotA, 2H RotB), 7.09 – 7.08 (m, 2H RotA, 2H RotB), 6.73 (t, *J* = 6.2 Hz, 1H RotA), 5.34 – 5.21 (m, 2H RotA, 2H RotB), 3.93 (q, *J* = 6.8 Hz, 1H RotA), 3.88 (q, *J* = 6.8 Hz, 1H RotB), 3.58 – 3.53 (m, 1H RotA), 3.46 – 3.41 (m, 1H RotA), 3.39 – 3.34 (m, 1H RotB), 3.26 – 3.22 (m, 1H RotB), 2.44 (d, *J* = 7.2 Hz, 2H RotA, 2H RotB), 1.86 – 1.82 (m, 1H RotA, 1H RotB), 1.52 – 1.43 (m, 4H RotA, 4H RotB), 1.27 (p, *J* = 7.5 Hz, 3H RotB), 1.23 – 1.18 (m, 3H RotA), 0.90 – 0.88 (m, 6H RotA, 9H RotB), 0.85 (t, *J* = 7.1 Hz, 3H RotA). **^{13}C NMR** (151 MHz, $CDCl_3$) δ 202.6 (RotA), 201.3 (RotB), 172.1 (RotB), 171.8 (RotA), 140.6 (RotB), 140.5 (RotA), 138.9 (RotB), 138.8 (RotA), 129.8 (2C RotA), 129.8 (2C RotB), 127.1 (2C RotB), 127.0 (2C RotA), 100.3 (RotA), 98.9 (RotB), 86.5 (RotB), 85.9 (RotA), 45.7 (RotB), 45.19 (RotA), 45.16 (RotB), 44.5 (RotA), 43.6 (RotB), 43.4 (RotA), 30.5 (RotB), 30.32 (RotB), 30.30 (RotA), 29.5 (RotA), 22.52 (2C RotA), 22.50 (2C RotB), 21.2 (RotB), 20.9 (RotA), 20.2 (RotA), 20.1 (RotB), 14.0 (RotA), 13.9 (RotB). **ESI-HRMS** calcd for $C_{20}H_{30}NO$ $[M+H]^+$ 300.2327, found 300.2335.

N-butyl-2-(2-fluoro-[1,1'-biphenyl]-4-yl)-N-(propa-1,2-dien-1-yl)propanamide

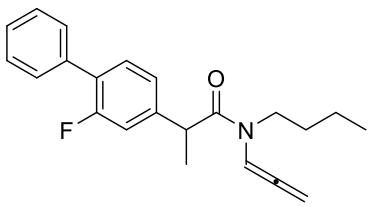

Allene **1L** was prepared following general procedure **GP-B1** from the corresponding propargyl amide (339 mg, 1 mmol). Colorless oil (155 mg, 46% yield). Two rotamers were observed due to the dynamic amide group (51:49 mixture of rotamers).

^{1}H NMR (600 MHz, $CDCl_3$) δ 7.57 – 7.52 (m, 2H RotA, 3H RotB), 7.45 – 7.35 (m, 4H RotA, 4H RotB), 7.15 – 7.08 (m, 2H RotA, 2H RotB), 6.74 (t, *J* = 6.2 Hz, 1H RotA), 5.38 – 5.27 (m, 2H RotA, 2H RotB), 4.02 (q, *J* = 6.8 Hz, 1H RotA), 3.97 (q, *J* = 6.8 Hz, 1H RotB), 3.62 – 3.57 (m, 1H RotA), 3.50 – 3.41 (m, 1H RotA, 1H RotB),

3.30 (ddd, *J* = 15.1, 10.5, 4.9 Hz, 1H RotB), 1.53 – 1.50 (m, 4H RotA, 3H RotB), 1.39 – 1.27 (m, 3H RotA, 4H RotB), 0.93 – 0.89 (m, 3H RotA, 3H RotB). **^{13}C NMR** (151 MHz, $CDCl_3$) δ 202.5 (RotB), 201.4 (RotA), 171.3 (RotB), 171.0 (RotA), 160.8 (d, *J* = 6.5 Hz, RotA), 159.2 (d, *J* = 6.7 Hz, RotB), 143.0 (RotB), 142.9 (RotA), 135.6 (RotA, RotB), 131.3 (d, *J* = 3.9 Hz, RotA), 131.2 (d, *J* = 4.0 Hz, RotB), 129.1 (2C RotB), 129.0 (2C RotA), 128.57 (2C RotB), 128.55 (2C RotA), 127.9 (d, *J* = 13.5 Hz, RotB), 127.8 – 127.7 (m, 2RotA, RotB), 123.43 (d, *J* = 3.3 Hz, RotB), 123.38 (d, *J* = 3.0 Hz, RotA), 115.2 (d, *J* = 10.4 Hz, RotB), 115.1 (d, *J* = 10.4 Hz, RotA), 100.0 (RotA), 98.9 (RotB), 86.7 (RotB), 86.2 (RotA), 45.7 (RotB), 44.7 (RotA), 43.2 (RotB), 43.1 (RotA), 30.8 (RotB), 29.4 (RotA), 20.9 (RotB), 20.6 (RotA), 20.2 (RotA), 20.1 (RotB), 14.0 (RotA, RotB). **^{19}F NMR** (565 MHz, $CDCl_3$) δ -117.0 (q, *J* = 10.2 Hz). **ESI-HRMS** calcd for $C_{22}H_{25}FNO$ $[M+H]^+$ 338.1920, found 338.1925.

N-butyl-2-phenyl-N-(propa-1,2-dien-1-yl)hexanamide

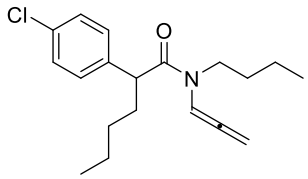

Allene **1M** was prepared following general procedure **GP-B1** from the corresponding propargyl amide (319 mg, 1 mmol). Yellow oil (214 mg, 67% yield). Two rotamers were observed due to the dynamic amide group (53:47 mixture of rotamers).

^{1}H NMR (400 MHz, $CDCl_3$) δ 7.50 (t, *J* = 6.6 Hz, 1H RotB), 7.30 – 7.20 (m, 4H RotA, 4H RotB), 6.71 (t, *J* = 6.2 Hz, 1H RotA), 5.37 – 5.24 (m, 2H RotA, 2H RotB), 3.76 (t, *J* = 7.3 Hz, 1H RotA), 3.69 (t, *J* = 7.3 Hz, 1H RotB), 3.56 – 3.35 (m, 2H RotA, 1H RotB), 3.24 (ddd, *J* = 15.1, 10.4, 4.9 Hz, 1H RotB), 2.12 – 2.03 (m, 1H RotA, 1H RotB), 1.74 – 1.64 (m, 1H RotA, 1H RotB), 1.59 – 1.57 (m, 2H RotA, 2H RotB), 1.48 – 1.38 (m, 2H RotA, 2H RotB), 1.33 – 1.22 (m, 4H RotA, 4H RotB), 1.18 – 1.12 (m, 1H RotA, 1H RotB), 0.95 – 0.79 (m, 5H RotA, 5H RotB). **^{13}C NMR** (101 MHz, $CDCl_3$) δ 202.5 (RotB), 201.4 (RotA), 171.0 (RotB), 170.8 (RotA), 138.64 (RotB), 138.61 (RotA), 133.0 (RotB), 132.9 (RotA), 129.33 (2C RotB), 129.29 (2C RotA), 129.1 (2C RotA), 128.1 (2C RotB), 99.9 (RotA), 98.8 (RotB), 86.7 (RotB), 86.2 (RotA), 49.0 (RotB), 48.7 (RotA), 45.6 (RotB), 44.6 (RotA), 35.4 (RotB), 35.0 (RotA), 30.9 (RotB), 30.1 (RotA), 30.0 (RotA), 29.4 (RotB), 22.8 (RotB), 22.7 (RotA), 20.1 (RotA, RotB), 14.08 (RotA), 14.07 (RotB), 13.97 (RotA, RotB). **ESI-HRMS** calcd for $C_{19}H_{27}ClNO$ $[M+H]^+$ 320.1781, found 320.1786.

2-cyclohexyl-N-phenethyl-2-phenyl-N-(propa-1,2-dien-1-yl)acetamide

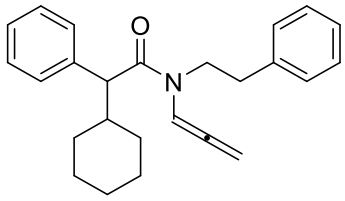

Allene **1N** was prepared following general procedure **GP-B1** from the corresponding propargyl amide (359 mg, 1 mmol). Light-yellow oil (334 mg, 93% yield). Two rotamers were observed due to the dynamic amide group (53:47 mixture of rotamers).

^{1}H NMR (600 MHz, $CDCl_3$) δ 7.63 (t, *J* = 6.5 Hz, 1H RotB), 7.37 – 7.32 (m, 5H RotA, 5H RotB), 7.29 – 7.15 (m, 5H RotA, 5H RotB), 6.90 (t, *J* = 6.2 Hz, 1H RotB), 5.45 – 5.42 (m, 1H RotB), 5.39 – 5.32 (m, 1H RotA, 1H RotB), 5.29 – 5.26 (m, 1H RotA), 3.78 – 3.68 (m, 2H RotA, 1H RotB), 3.60 – 3.55 (m, 1H RotB), 3.52 (d, *J* = 9.9 Hz, 1H RotA), 3.39 (d, *J* = 9.9 Hz, 1H RotB), 2.86 (ddd, *J* = 13.2, 10.5, 6.2 Hz, 1H RotA), 2.79 (t, *J* = 7.8 Hz, 1H RotA, 1H RotB), 2.65 (ddd, *J* = 13.2, 10.3, 5.1 Hz, 1H RotB), 2.21 – 2.15 (m, 1H RotA, 1H RotB), 1.90 – 1.86 (m, 1H RotA, 1H RotB), 1.73 – 1.62 (m, 3H RotA, 3H RotB), 1.37 – 1.23 (m, 2H RotA, 2H RotB), 1.18 – 1.10 (m, 2H RotA, 2H RotB), 0.98 – 0.91 (m, 1H RotA), 0.84 – 0.71 (m, 2H RotA, 1H RotB). **^{13}C NMR** (151 MHz, $CDCl_3$) δ 202.6 (RotA), 201.4 (RotB), 171.1 (RotB), 171.0 (RotA), 139.1 (RotA), 138.4 (RotB), 138.1 (RotB), 138.0 (RotA), 129.1 (RotA), 129.0 (RotA, RotB), 128.82 (RotA, RotB), 128.79 (2C RotA, 2C RotB), 128.75 (RotA), 128.72 (RotB), 128.69 (RotA), 128.6 (RotB), 128.4 (RotA, RotB), 128.3 (RotB), 127.2 (RotB), 127.1 (RotA), 126.8 (RotB), 126.2 (RotA), 100.2 (RotA), 98.7 (RotB), 86.8 (RotB), 86.2 (RotA), 56.4 (RotA), 55.6 (RotB), 47.4 (RotB), 46.4 (RotA), 41.8 (RotB), 41.6 (RotA), 34.9 (RotB), 33.6 (RotA), 32.9 (RotB), 32.7 (RotA), 30.73 (RotB), 30.68 (RotA), 26.59 (RotA), 26.55 (RotB), 26.28 (RotB), 26.26 (RotA), 26.2 (RotA, RotB). **ESI-HRMS** calcd for $C_{25}H_{30}NO$ $[M+H]^+$ 360.2327, found 360.2334.

2-cyclohexyl-N-(pent-4-en-1-yl)-2-phenyl-N-(propa-1,2-dien-1-yl)acetamide

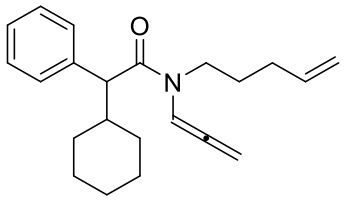

Allene **1O** was prepared following general procedure **GP-B1** from the corresponding propargyl amide (324 mg, 1 mmol). Light-yellow oil (178 mg, 55% yield). Two rotamers were observed due to the dynamic amide group (51:49 mixture of rotamers).

^{1}H NMR (400 MHz, $CDCl_3$) δ 7.57 (t, *J* = 6.5 Hz, 1H RotB), 7.37 – 7.24 (m, 5H RotA, 5H RotB), 6.92 (t, *J* = 6.2 Hz, 1H RotA), 5.89 – 5.76 (m, 1H RotA, 1H RotB), 5.39 – 5.27 (m, 2H RotA, 2H RotB), 5.12 – 4.94 (m, 2H RotA, 2H RotB), 3.59 – 3.48 (m, 2H RotA, 2H RotB), 3.41 (d, *J* = 10.1 Hz, 1H RotA), 3.31 (ddd, *J* = 15.3, 10.5, 5.5 Hz, 1H RotB), 2.22 – 1.92 (m, 4H RotA, 4H RotB), 1.76 – 1.56 (m, 4H RotA, 4H RotB), 1.39 – 1.14 (m, 5H RotA, 5H RotB), 1.00 – 0.77 (m, 2H RotA, 2H RotB). **^{13}C NMR** (101 MHz, $CDCl_3$) δ 202.4 (RotB), 201.4 (RotA),

171.2 (RotB), 171.1 (RotA), 138.2 (RotB), 138.13 (RotA), 138.11 (RotA), 137.4 (2C RotB), 128.7 (2C RotA, 2C RotB), 128.64 (RotA), 128.61 (RotB), 128.3 (RotA), 127.2 (RotB), 127.1 (RotA), 115.7 (RotB), 114.8 (RotA), 100.2 (RotA), 98.8 (RotB), 86.6 (RotB), 86.0 (RotA), 56.2 (RotA), 55.7 (RotB), 45.2 (RotB), 44.4 (RotA), 41.9 (RotB), 41.6 (RotA), 33.0 (RotB), 32.7 (RotA), 31.1 (RotA), 30.9 (RotB), 30.8 (RotB), 30.7 (RotA), 29.8 (RotB), 27.8 (RotA), 26.58 (RotA), 26.57 (RotB), 26.5 (RotA, RotB), 26.3 (RotA), 26.2 (RotB). **ESI-HRMS** calcd for $C_{22}H_{29}NNaO$ $[M+Na]^+$ 338.2484, found 338.2489.

2,2-dicyclohexyl-N-phenethyl-N-(propa-1,2-dien-1-yl)acetamide

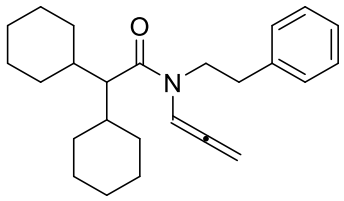

Allene **1P** was prepared following general procedure **GP-B1** from the corresponding propargyl amide (366 mg, 1 mmol). White solid (329 mg, 90% yield). Two rotamers were observed due to the dynamic amide group (73:27 mixture of rotamers).

^{1}H NMR (600 MHz, $CDCl_3$) δ 7.64 (t, *J* = 6.5 Hz, 1H RotB), 7.34 – 7.31 (m, 2H RotB), 7.28 – 7.24 (m, 3H RotA, 3H RotB), 7.21 – 7.17 (m, 2H RotA), 6.97 (t, *J* = 6.2 Hz, 1H RotA), 5.44 (d, *J* = 6.5 Hz, 2H RotB), 5.39 (d, *J* = 6.2 Hz, 2H RotA), 3.77 – 3.74 (m, 2H RotA), 3.71 – 3.69 (m, 2H RotB), 2.90 – 2.87 (m, 2H RotB), 2.85 – 2.82 (m, 2H RotB), 2.53 (t, *J* = 7.3 Hz, 1H RotA), 2.49 (t, *J* = 7.3 Hz, 1H RotB), 1.83 – 1.61 (m, 11H RotA, 11H RotB), 1.27 – 1.05 (m, 9H RotA, 9H RotB), 0.99 – 0.89 (m, 2H RotA, 2H RotB). **^{13}C NMR** (151 MHz, $CDCl_3$) δ 202.9 (RotB), 201.3 (RotA), 173.1 (RotA, RotB), 139.4 (RotA), 138.6 (RotB), 129.1 (2C RotA), 128.84 (2C RotB), 128.75 (2C RotB), 128.5 (2C RotA), 126.8 (RotB), 126.4 (RotA), 101.0 (RotB), 98.4 (RotA), 86.6 (RotA), 86.3 (RotB), 52.8 (2C RotB), 51.8 (2C RotA), 48.2 (RotB), 46.0 (RotA), 38.3 (2C RotB), 37.9 (2C RotA), 35.2 (RotB), 33.8 (RotA), 31.6 (RotB), 31.5 (RotA), 30.5 (2C RotB), 29.8 (2C RotA), 26.9 (2C RotB), 26.8 (2C RotA), 26.7 (2C RotA, 2C RotB), 26.63 (2C RotA), 26.61 (2C RotB). **ESI-HRMS** calcd for $C_{25}H_{36}NO$ $[M+H]^+$ 366.2797, found 366.2800.

N-butyl-2-phenyl-N-(propa-1,2-dien-1-yl)acetamide

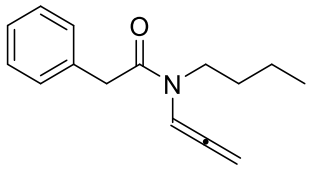

Allene **1Q** was prepared following general procedure **GP-B2** from the corresponding propargyl amide (229 mg, 1 mmol). White solid (167 mg, 73% yield). Two rotamers were observed due to the dynamic amide group (54:46 mixture of rotamers).

^{1}H NMR (400 MHz, $CDCl_3$) δ 7.52 (t, *J* = 6.5 Hz, 1H RotB), 7.34 – 7.30 (m, 2H RotA, 2H RotB), 7.27 – 7.23 (m, 3H RotA, 3H RotB), 6.74 (t, *J* = 6.2 Hz, 1H RotA), 5.34 (d, *J* = 6.5 Hz, 2H RotA), 5.32 (d, *J* = 6.2 Hz, 2H RotB), 3.80 (d, *J* = 7.4 Hz, 2H RotA, 2H RotB), 3.53 – 3.49 (m, 2H RotA), 3.40 – 3.36 (m, 2H RotB), 1.53 – 1.46 (m, 2H RotA, 2H RotB), 1.29 (h, *J* = 7.3 Hz, 2H RotA, 2H RotB), 0.90 (t, *J* = 7.4 Hz, 3H RotA, 3H RotB). **^{13}C NMR** (101 MHz, $CDCl_3$) δ 202.4 (RotB), 201.1 (RotA), 169.0 (RotB), 168.7 (RotA), 134.70 (RotB), 134.66 (RotA), 128.9 (2C RotA, 2C RotB), 128.8 (2C RotA, 2C RotB), 127.05 (RotB), 126.99 (RotA), 100.6 (RotA), 98.6 (RotB), 86.7 (RotB), 86.3 (RotA), 46.2 (RotB), 44.2 (RotA), 41.2 (RotA, RotB), 30.5 (RotB), 29.4 (RotA), 20.1 (RotA), 20.1 (RotB), 14.0 (RotA), 13.9 (RotB). **ESI-HRMS** calcd for $C_{15}H_{20}NO$ $[M+H]^+$ 230.1545, found 230.1549.

tert-butyl 2-(phenethyl(propa-1,2-dien-1-yl)carbamoyl)pyrrolidine-1-carboxylate

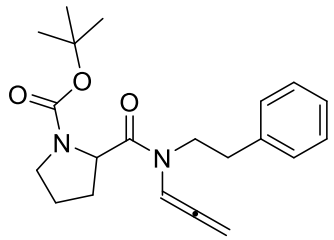

Allene **1R** was prepared following general procedure **GP-B1** from the corresponding propargyl amide (356 mg, 1 mmol). Orange oil (342 mg, 96% yield). Two rotamers were observed due to the dynamic amide group (58:42 mixture of rotamers).

^{1}H NMR (600 MHz, $CDCl_3$) δ 7.50 (dt, *J* = 25.2, 6.4 Hz, 1H RotB), 7.31 – 7.30 (m, 1H RotA, RotB), 7.25 – 7.14 (m, 4H RotA, 4H RotB), 6.77 (dt, *J* = 37.2, 6.2 Hz, 1H RotB), 5.49 – 5.45 (m, 1H RotB), 5.41 – 5.40 (m, 1H RotA, 1H RotB), 5.35 (d, *J* = 6.2 Hz, 1H RotA), 4.72 – 4.54 (m, 1H RotA, 1H RotB), 3.94 – 3.36 (m, 4H RotA, 4H RotB), 2.99 – 2.79 (m, 2H RotA, 2H RotB), 2.19 – 1.71 (m, 3H RotA, 3H RotB), 1.44 (d, *J* = 2.2 Hz, 9H RotB), 1.39 (d, *J* = 10.1 Hz, 9H RotA). **^{13}C NMR** (151 MHz, $CDCl_3$) δ 202.4 (d, *J* = 32.7 Hz, RotA), 201.5 (d, *J* = 7.4 Hz, RotB), 171.0 (d, *J* = 34.3 Hz, RotB), 170.5 (d, *J* = 62.1 Hz, RotA), 154.4 (d, *J* = 8.4 Hz, RotB), 153.7 (d, *J* = 9.2 Hz, RotA), 138.9 (d, *J* = 35.0 Hz, RotA), 138.2 (d, *J* = 66.6 Hz, RotB), 129.0 (d, *J* = 13.9 Hz, 2C RotA), 128.9 (d, *J* = 4.5 Hz, 2C RotB), 128.7 (d, *J* = 2.3 Hz, 2C RotA), 128.4 (d, *J* = 19.4 Hz, RotB), 126.8 (d, *J* = 41.2 Hz, RotB), 126.3 (d, *J* = 26.4 Hz, RotA), 99.7 (d, *J* = 39.2 Hz, RotA), 98.7 (d, *J* = 31.8 Hz, RotB), 87.2 (d, *J* = 47.7 Hz, RotB), 86.5 (d, *J* = 31.0 Hz, RotA), 79.8 (d, *J* = 61.7 Hz, RotB), 79.6 (RotA, RotB), 57.0 (d, *J* = 12.0 Hz, RotA), 56.8 (d, *J* = 32.8 Hz, RotB), 47.4 (d, *J* = 5.0 Hz, RotA), 46.9 (d, *J* = 16.0 Hz, RotB), 46.6 (d, *J* = 26.1 Hz, RotA), 46.4 (d, *J* = 23.3 Hz, RotB), 34.8 (d, *J* = 40.8 Hz, RotB), 33.6 (d, *J* = 32.3 Hz, RotA), 30.9 (d, *J* = 82.8 Hz, RotA), 29.9 (d, *J* = 60.3 Hz, RotB), 28.53 (d, *J* = 2.1 Hz, 3C RotA), 28.45 (d, *J* = 16.5 Hz, 3C RotB), 24.2 (d, *J* = 32.9 Hz, RotB), 23.5 (d, *J* = 8.8 Hz, RotA). **ESI-HRMS** calcd for $C_{21}H_{29}N_2O_3$ $[M+H]^+$ 357.2178, found 357.2185.

N-(buta-1,2-dien-1-yl)-N-phenethyl-2,2-diphenylacetamide

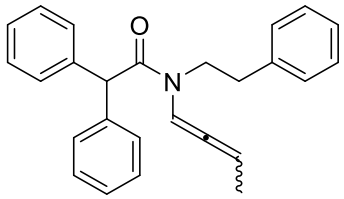

Allene **1S** was prepared following general procedure **GP-B1** from the corresponding propargyl amide (368 mg, 1 mmol). Light-yellow oil (151 mg, 41% yield). Two rotamers were observed due to the dynamic amide group (56:44 mixture of rotamers).

^{1}H NMR (400 MHz, $CDCl_3$) δ 7.58 (dq, *J* = 6.0, 2.9 Hz, 1H RotB), 7.40 – 7.22 (m, 13H RotA, 13H RotB), 7.17 – 7.12 (m, 2H RotA, 2H RotB), 6.70 (dq, *J* = 5.5, 2.7 Hz, 1H RotA), 5.84 (p, *J* = 6.8 Hz, 1H RotB), 5.74 (m, 1H RotA), 5.36 (s, 1H RotA), 5.02 (s, 1H RotB), 3.88 – 3.74 (m, 2H RotA), 3.65 (t, *J* = 7.5 Hz, 2H RotB), 2.90 (t, *J* = 8.0 Hz, 2H RotA), 2.79 (td, *J* = 7.3, 3.1 Hz, 2H RotB), 1.86 (dd, *J* = 7.0, 2.9 Hz, 3H RotB), 1.79 (dd, *J* = 7.0, 2.7 Hz, 3H RotA). **^{13}C NMR** (101 MHz, $CDCl_3$) δ 197.0 (RotB), 196.2 (RotA), 170.1 (RotB), 169.8 (RotA), 139.3 (RotA), 139.22 (RotB), 139.16 (RotB), 139.1 (RotA, RotB), 138.6 (RotA), 129.1 (4C RotA, 4C RotB), 129.04 (4C RotA), 129.01 (2C RotA), 128.73 (4C RotB), 128.71 (2C RotB), 128.67 (2C RotB), 128.5 (2C RotA), 127.3 (2C RotB), 127.2 (2C RotA), 126.9 (RotB), 126.4 (RotA), 99.4 (RotA, RotB), 98.0 (RotA), 97.5 (RotB), 55.6 (RotB), 55.3 (RotA), 47.8 (RotB), 46.6 (RotA), 34.3 (RotB), 33.4 (RotA), 16.2 (RotB), 15.9 (RotA). **ESI-HRMS** calcd for $C_{26}H_{26}NO$ $[M+H]^+$ 368.2014, found 368.2019.

Synthesis and characterization of products:

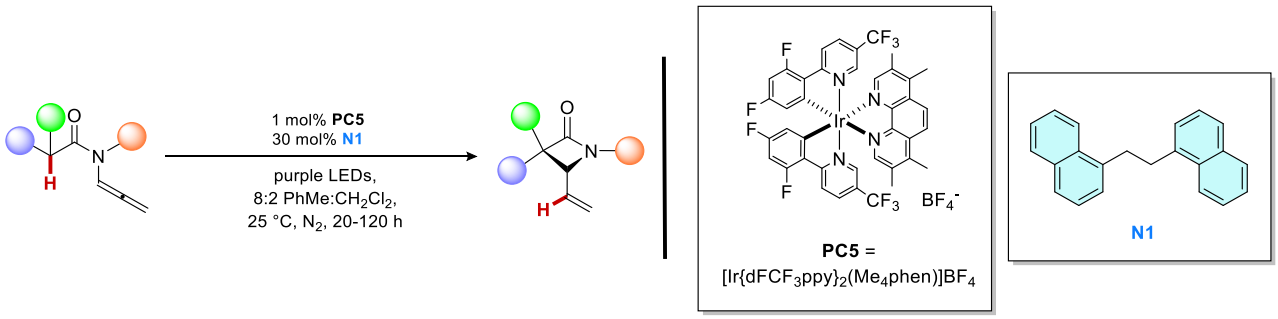

A vial was charged with allene **1** (1 equiv., 0.2 mmol), the iridium catalyst **PC5** (2 mg, 2 umol, 1 mol%), and the correspondent bi-naphthyl additive **N1** (17 mg, 0.06 mmol, 30 mol%). The mixture was dissolved in a freshly distilled PhMe and CH_2Cl_2 8:2 (0.1 M). The solution was transferred into an NMR tube capped with a rubber septum and directly irradiated with a purple LED strip for 20 – 120 hours at 25°C. After total conversion of the starting material, as monitored by TLC, the mixture was then concentrated in vacuo. The residue was purified by chromatography on silica gel (*n*-hexane/EtOAc gradient) to afford the desired product.

1-methyl-3,3-diphenyl-4-vinylazetidin-2-one

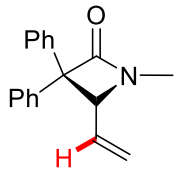

Product **2A** was prepared following general procedure **GP-2** in 48 hours, from the corresponding allene (52.7 mg, 0.2 mmol). White solid (32.0 mg, 61% yield).

^{1}H NMR (600 MHz, $CDCl_3$) δ 7.51 – 7.49 (m, 2H), 7.36 – 7.20 (m, 8H), 5.47 – 5.44 (m, 1H), 5.35 – 5.29 (m, 1H), 5.26 – 5.25 (m, 1H), 4.59 (d, *J* = 8.8 Hz, 1H), 2.84 (s, 3H). **^{13}C NMR** (151 MHz, $CDCl_3$) δ 169.3, 140.9, 138.1, 134.7, 128.8 (2C), 128.5 (2C), 128.4, 127.5 (2C), 127.4 (2C), 127.3, 121.2, 71.4, 67.9, 26.9. **ESI-HRMS** calcd for $C_{18}H_{18}NO$ $[M+H]^+$ 264.1388, found 264.1391.

1-butyl-3,3-diphenyl-4-vinylazetidin-2-one

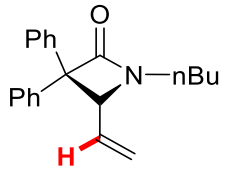

Product **2B** was prepared following general procedure **GP-2** in 40 hours, from the corresponding allene (61.1 mg, 0.2 mmol). Light-yellow oil (50.1 mg, 82% yield).

^{1}H NMR (400 MHz, $CDCl_3$) δ 7.50 – 7.48 (m, 2H), 7.37 – 7.20 (m, 8H), 5.46 (dd, *J* = 16.8, 1.9 Hz, 1H), 5.36 – 5.27 (m, 1H), 5.23 (dd, *J* = 9.9, 1.9 Hz, 1H), 4.64 (d, *J* = 8.9 Hz, 1H), 3.41 – 3.34 (m, 1H), 3.13 – 3.06 (m, 1H), 1.59 – 1.50 (m, 2H), 1.36 – 1.26 (m, 2H), 0.90 (t, *J* = 7.3 Hz, 3H). **^{13}C NMR** (101 MHz, $CDCl_3$) δ 169.1, 140.9, 138.2, 135.5, 128.7 (2C), 128.5 (4C), 127.4, 127.3 (2C), 127.2, 120.9, 70.6, 66.8, 40.6, 30.2, 20.3, 13.8. **ESI-HRMS** calcd for $C_{21}H_{24}NO$ $[M+H]^+$ 306.1858, found 306.1862.

1-(sec-butyl)-3,3-diphenyl-4-vinylazetidin-2-one

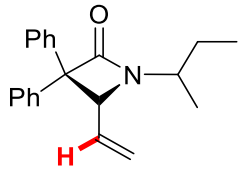

Product **2C** was prepared following general procedure **GP-2** in 60 hours, from the corresponding allene (61.1 mg, 0.2 mmol). Light-yellow oil (34.2 mg, 56% yield). Two diasteroisomers were observed with ratio 53:47.

^{1}H NMR (600 MHz, $CDCl_3$) δ 7.50 (t, *J* = 7.7 Hz, 2H Dia1, 2H Dia2), 7.36 – 7.21 (m, 8H Dia1, 8H Dia2), 5.48 – 5.44 (m, 1H Dia1, 1H Dia2), 5.41 – 5.30 (m, 1H Dia1, 1H Dia2), 5.19 – 5.17 (m, 1H Dia1, 1H Dia2), 4.72 –

4.68 (m, 1H Dia1, 1H Dia2), 3.69 (dq, *J* = 20.1, 7.4 Hz, 1H Dia1, 1H Dia2), 1.75 – 1.70 (m, 1H Dia2), 1.61 – 1.52 (m, 1H Dia1, 1H Dia2), 1.49 – 1.44 (m, 1H Dia1), 1.25 (d, *J* = 6.5 Hz, 3H Dia1), 1.19 (d, *J* = 6.8 Hz, 3H Dia2), 0.94 (t, *J* = 7.4 Hz, 3H Dia2), 0.88 – 0.85 (m, 3H Dia1). **^{13}C NMR** (101 MHz, $CDCl_3$) δ 168.9 (Dia2), 168.8 (Dia1), 140.9 (Dia1), 140.9 (Dia2), 138.4 (Dia1, Dia2), 137.1 (Dia1), 136.8 (Dia2), 129.0 (2C Dia2), 128.9 (2C Dia1), 128.7 (2C Dia1), 128.51 (2C Dia2), 128.46 (2C Dia2), 128.4 (2C Dia1), 127.4 (2C Dia1, 2C Dia2), 127.3 (2C Dia1), 127.2 (2C Dia2), 120.12 (Dia2), 120.05 (Dia1), 69.7 (Dia1), 69.6 (Dia2), 65.7 (Dia2), 65.4 (Dia1), 50.4 (Dia1), 50.3 (Dia2), 29.0 (Dia2), 27.4 (Dia1), 19.9 (Dia1), 18.1 (Dia2), 11.3 (Dia1), 11.2 (Dia2). **ESI-HRMS** calcd for $C_{21}H_{23}NNaO$ $[M+H]^+$ 328.1677, found 328.1684.

1-cyclopropyl-3,3-diphenyl-4-vinylazetidin-2-one

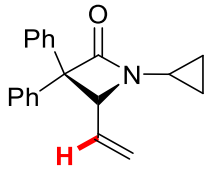

Product **2D** was prepared following general procedure **GP-2** in 60 hours, from the corresponding allene (57.9 mg, 0.2 mmol). Light-yellow oil (17.9 mg, 31% yield). Two rotamers were observed due to the dynamic amide group (66:34 mixture of rotamers).

^{1}H NMR (400 MHz, $CDCl_3$) δ 7.35 – 7.24 (m, 10H RotA, 10H RotB), 6.93 – 6.92 (m, 1H RotB), 6.51 – 6.47 (m, 1H RotA, 1H RotB), 6.42 (s, 1H RotA), 6.34 (d, *J* = 5.6 Hz, 1H RotA), 6.25 (d, *J* = 5.6 Hz, 1H RotB), 5.18 – 5.16 (m, 1H RotA, 1H RotB), 5.14 (s, 1H RotA), 5.05 (s, 1H RotB), 4.45 (d, *J* = 14.4 Hz, 1H RotA), 4.23 (d, *J* = 12.4 Hz, 1H RotB), 4.10 (d, *J* = 14.5 Hz, 1H RotA), 4.05 (d, *J* = 12.4 Hz, 1H RotB), 2.70 – 2.59 (m, 1H RotA, 1H RotB), 1.93 – 1.84 (m, 1H RotA, 1H RotB). **^{13}C NMR** (101 MHz, $CDCl_3$) δ 167.6 (RotA), 167.4 (RotB), 139.2 (RotA, RotB), 138.8 (RotA), 138.6 (RotB), 137.52 (RotA), 137.49 (RotB), 134.4 (RotA), 134.1 (RotB), 129.2 (RotA, RotB), 129.1 (RotA, RotB), 129.0 (RotA, RotB), 128.9 (2C RotA, 2C RotB), 128.8 (RotA, RotB), 128.6 (RotA, RotB), 127.4 (RotA), 127.3 (RotB), 127.2 (RotA), 124.9 (RotB), 121.3 (RotB), 120.4 (RotA), 96.5 (RotB), 94.5 (RotA), 82.0 (RotB), 81.9 (RotA), 56.5 (RotB), 56.3 (RotA), 49.2 (RotB), 48.8 (RotA), 28.8 (RotA), 28.7 (RotB). **ESI-HRMS** calcd for $C_{20}H_{20}NO$ $[M+H]^+$ 290.3860, found 290.3851.

1-(cyclohexylmethyl)-3,3-diphenyl-4-vinylazetidin-2-one

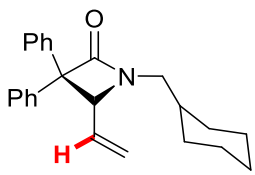

Product **2E** was prepared following general procedure **GP-2** in 40 hours, from the corresponding allene (69.1 mg, 0.2 mmol). Light-yellow oil (48.4 mg, 70% yield).

^{1}H NMR (400 MHz, $CDCl_3$) δ 7.51 – 7.49 (m, 2H), 7.36 – 7.20 (m, 8H), 5.48 – 5.44 (m, 1H), 5.34 – 5.22 (m, 2H), 4.64 (d, *J* = 8.6 Hz, 1H), 3.19 (dd, *J* = 14.0, 7.3 Hz, 1H), 2.91 (dd, *J* = 14.0, 6.7 Hz, 1H), 1.72 – 1.57 (m, 6H), 1.21 – 1.10 (m, 3H), 0.99 – 0.85 (m, 2H). **^{13}C NMR** (101 MHz, $CDCl_3$) δ 169.4, 141.1, 138.3, 135.4, 128.7 (2C), 128.46 (2C), 128.45, 127.4 (2C), 127.3 (2C), 127.2, 121.1, 70.6, 67.5, 47.3, 36.8, 31.2, 31.1, 26.4, 25.8, 25.8. **ESI-HRMS** calcd for $C_{24}H_{27}NNaO$ $[M+H]^+$ 368.1990, found 368.1997.

1-phenethyl-3,3-diphenyl-4-vinylazetidin-2-one

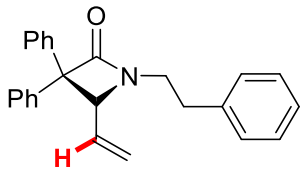

Product **2F** was prepared following general procedure **GP-2** in 40 hours, from the corresponding allene (70.9 mg, 0.2 mmol). Light-yellow oil (53.7 mg, 76% yield).

^{1}H NMR (400 MHz, $CDCl_3$) δ 7.38 – 7.14 (m, 15H), 5.33 – 5.16 (m, 3H), 4.39 (d, *J* = 7.2 Hz, 1H), 3.71 (dt, *J* = 14.1, 7.0 Hz, 1H), 3.31 (dt, *J* = 14.4, 7.4 Hz, 1H), 2.91 (q, *J* = 6.7 Hz, 2H). **^{13}C NMR** (101 MHz, $CDCl_3$) δ 169.0, 140.7, 138.5, 138.0, 135.0, 128.9 (2C), 128.7 (2C), 128.6 (2C), 128.43, 128.39 (2C), 127.4 (2C), 127.3 (2C), 127.2, 126.7, 121.1, 70.6, 67.1, 41.9, 34.5. **ESI-HRMS** calcd for $C_{25}H_{23}KNO$ $[M+K]^+$ 392.1417, found 392.1411.

1-(2-(1-methyl-1H-indol-3-yl)ethyl)-3,3-diphenyl-4-vinylazetidin-2-one

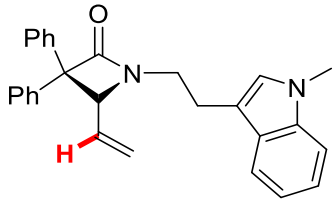

Product **2G** was prepared following general procedure **GP-2** in 48 hours, from the corresponding allene (81.3 mg, 0.2 mmol). Yellow oil (38.2 mg, 47% yield).

^{1}H NMR (400 MHz, $CDCl_3$) δ 7.43 (d, *J* = 7.8 Hz, 1H), 7.37 – 7.27 (m, 8H), 7.24 – 7.19 (m, 4H), 7.17 – 7.08 (m, 2H), 6.43 (d, *J* = 5.3 Hz, 1H), 6.07 (ddd, *J* = 17.3, 10.1, 5.3 Hz, 1H), 5.36 (d, *J* = 10.0 Hz, 1H), 4.98 (d, *J* = 17.2 Hz, 1H), 4.08 (dd, *J* = 14.1, 5.4 Hz, 1H), 3.59 (s, 3H), 3.40 – 3.33 (m, 1H), 2.66 (dd, *J* = 15.2, 4.1 Hz, 1H), 2.54 – 2.46 (m, 1H). **^{13}C NMR** (101 MHz, $CDCl_3$) δ 170.6, 139.8, 139.4, 137.4, 134.6, 132.7, 129.2 (2C), 129.1 (2C), 128.8 (2C), 128.7 (2C), 127.3, 127.2, 126.3, 121.7, 119.7, 119.2, 118.2, 109.1, 108.1, 55.5, 50.5, 40.1, 29.9, 22.1. **ESI-HRMS** calcd for $C_{28}H_{26}N_2NaO$ $[M+Na]^+$ 429.1943, found 429.1950.

3,3-diphenyl-1-(4-(trimethylsilyl)but-3-yn-1-yl)-4-vinylazetidin-2-one

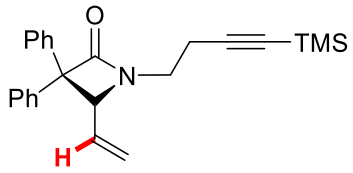

Product **2H** was prepared following general procedure **GP-2** in 48 hours, from the corresponding allene (74.7 mg, 0.2 mmol). Pale yellow oil (48.6 mg, 65% yield).

^{1}H NMR (600 MHz, $CDCl_3$) δ 7.49 (dd, *J* = 8.4, 1.3 Hz, 2H), 7.36 – 7.27 (m, 6H), 7.25 – 7.21 (m, 2H), 5.47 (dd, *J* = 16.9, 1.6 Hz, 1H), 5.36 – 5.30 (m, 1H), 5.25 (dd, *J* = 10.1, 1.6 Hz, 1H), 4.82 (d, *J* = 9.1 Hz, 1H), 3.55 (dt, *J* = 13.9, 6.5 Hz, 1H), 3.28 – 3.23 (m, 1H), 2.63 – 2.40 (m, 2H), 0.10 (s, 9H). **^{13}C NMR** (151 MHz, $CDCl_3$) δ 169.1, 140.7, 138.0, 135.2, 129.2, 129.0, 128.8 (2C), 128.5 (2C), 128.5, 127.5 (2C), 127.3, 121.4, 103.7, 86.8, 71.0, 67.3, 39.6, 20.0, 0.1 (3C). **ESI-HRMS** calcd for $C_{24}H_{28}NOSi$ $[M+H]^+$ 374.1940, found 374.1929.

3,3-diphenyl-1-(3-(triethoxysilyl)propyl)-4-vinylazetidin-2-one

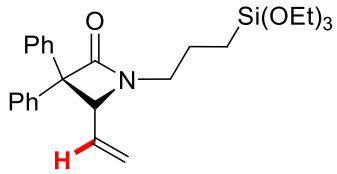

Product **2I** was prepared following general procedure **GP-2** in 40 hours, from the corresponding allene (90.6 mg, 0.2 mmol). Colorless oil (60.0 mg, 66% yield).

^{1}H NMR (400 MHz, $CDCl_3$) δ 7.51 – 7.48 (m, 2H), 7.35 – 7.19 (m, 8H), 5.45 (dd, *J* = 16.8, 1.8 Hz, 1H), 5.37 – 5.27 (m, 1H), 5.22 (dd, *J* = 9.9, 1.8 Hz, 1H), 4.65 (d, *J* = 8.9 Hz, 1H), 3.79 – 3.69 (m, 6H), 3.41 – 3.33 (m, 1H), 3.14 – 3.07 (m, 1H), 1.69 – 1.61 (m, 2H), 1.27 – 1.17 (m, 9H), 0.58 (dd, *J* = 9.3, 7.6 Hz, 2H). **^{13}C NMR** (101 MHz, $CDCl_3$) δ 169.1, 140.9, 138.2, 135.4, 129.1, 128.9, 128.7, 128.4 (2C), 127.4, 127.3, 127.2, 120.9, 70.6, 66.7, 58.5 (3C), 43.4, 31.4, 21.7, 18.6, 18.4 (3C), 7.9. **ESI-HRMS** calcd for $C_{26}H_{36}NO_4Si$ $[M+H]^+$ 454.2414, found 454.2419.

1-butyl-3-methyl-3-phenyl-4-vinylazetidin-2-one

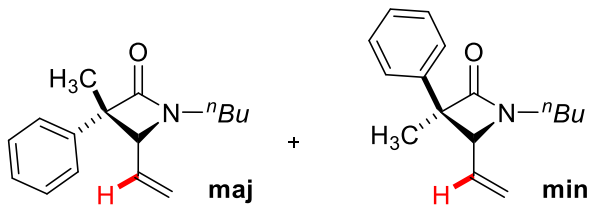

Product **2J** was prepared following general procedure **GP-2** in 72 hours, from the corresponding allene (48.7 mg, 0.2 mmol). Light-orange oil (29.7 mg, 61% yield). Two diasteroisomers were observed with ratio 62:38.

^{1}H NMR (400 MHz, $CDCl_3$) δ 7.40 – 7.23 (m, 5H Dia1, 5H Dia2), 5.97 – 5.88 (m, 1H Dia1), 5.48 – 5.42 (m, 2H Dia1), 5.32 – 5.26 (m, 1H Dia2), 5.19 – 5.10 (m, 2H Dia2), 4.10 (d, *J* = 8.7 Hz, 1H Dia1), 3.92 (d, *J* = 8.4 Hz, 1H Dia2), 3.43 – 3.33 (m, 1H Dia1, 1H Dia2), 3.06 – 2.98 (m, 1H Dia1, 1H Dia2), 1.71 (s, 3H Dia2), 1.55 – 1.45 (m, 5H Dia1, 2H Dia2), 1.39 – 1.26 (m, 2H Dia1, 2H Dia2), 0.95 – 0.87 (m, 3H Dia1, 3H Dia2). **^{13}C NMR** (101 MHz, $CDCl_3$) δ 171.5 (Dia1), 171.3 (Dia2), 142.5 (Dia1), 138.5 (Dia2), 135.8 (Dia2), 134.1 (Dia1), 128.8 (2C Dia1), 128.5 (2C Dia2), 127.4 (Dia1, Dia2), 127.1 (Dia1), 127.1 (Dia2), 125.9 (Dia1, Dia2), 121.3 (Dia1), 120.3 (Dia2), 68.1 (Dia2), 66.7 (Dia1), 62.9 (Dia2), 61.9 (Dia1), 40.2 (Dia1), 40.2 (Dia2), 30.2 (Dia1), 30.1 (Dia2), 23.8 (Dia1, Dia2), 20.3 (Dia1), 19.8 (Dia2), 13.8 (Dia2), 13.8 (Dia1). **ESI-HRMS** calcd for $C_{16}H_{21}NNaO$ $[M+Na]^+$ 266.1521, found 266.1527.

1-butyl-3-(4-isobutylphenyl)-3-methyl-4-vinylazetidin-2-one

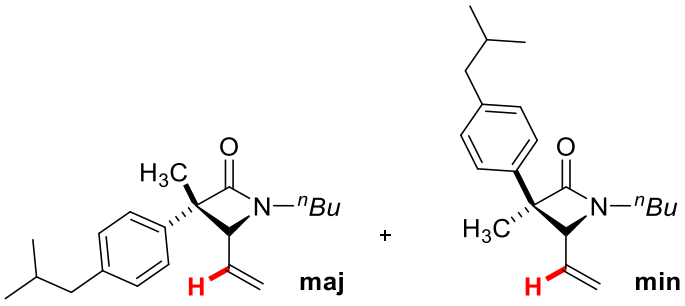

Product **2K** was prepared following general procedure **GP-2** in 72 hours, from the corresponding allene (59.8 mg, 0.2 mmol). Colorless oil (38.9 mg, 56% yield). Two diasteroisomers were observed with ratio 56:44.

^{1}H NMR (600 MHz, $CDCl_3$) δ 7.35 – 7.21 (m, 7H Dia1, 7H Dia 2), 7.15 – 7.10 (m, 2H Dia1, 2H Dia2), 7.03 – 7.01 (m, 1H Dia1, 1H Dia2), 5.93 – 5.87 (m, 1H Dia1), 5.39 – 5.35 (m, 1H Dia1, 1H Dia2), 5.23 – 5.18 (m, 1H Dia2), 5.14 – 5.11 (m, 1H Dia1, 1H Dia2), 3.95 (d, *J* = 9.0 Hz, 1H Dia1), 3.91 (d, *J* = 8.4 Hz, 1H Dia2), 3.73 – 3.68 (m, 1H Dia2), 3.57 – 3.52 (m, 1H Dia1), 3.17 – 3.12 (m, 1H Dia1, 1H Dia2), 2.90 – 2.85 (m, 1H Dia1, 1H Dia2), 2.82 – 2.76 (m, 1H Dia1, 1H Dia2), 2.30 (d, *J* = 13.0 Hz, 1H Dia1), 1.95 – 1.93 (m, 1H Dia2), 1.87 (tt, *J* = 11.9, 2.8 Hz, 1H Dia1), 1.72 – 1.64 (m, 2H Dia1, 2H Dia2), 1.60 – 1.52 (m, 2H Dia1, 2H Dia2) 1.38 (d, *J* = 11.2 Hz, 1H Dia2), 1.27 – 1.03 (m, 3H Dia1, 3H Dia2), 0.92 – 0.82 (m, 1H Dia1, 2H Dia2), 0.64 – 0.57 (m, 1H Dia1). **^{13}C NMR** (151 MHz, $CDCl_3$) δ 170.9 (Dia1), 170.2 (Dia2), 138.7 (Dia1), 138.4 (Dia1), 136.4 (Dia2), 136.2 (Dia2), 134.0 (Dia1, Dia2), 128.9 (Dia1), 128.8 (Dia2), 128.7 (Dia2), 128.5 (Dia1), 127.8 (Dia2), 127.6 (Dia1), 126.9 (Dia1), 126.8 (Dia2), 126.7 (Dia2), 126.5 (Dia1), 121.3 (Dia1), 120.1 (Dia2), 70.5 (Dia2), 69.5 (Dia1), 66.9 (Dia1), 64.0 (Dia2), 44.8 (Dia2), 41.7 (Dia1), 41.2 (Dia1), 40.9 (Dia2), 34.5 (Dia2), 34.4 (Dia1), 29.2 (Dia2), 28.6 (Dia1), 28.4 (Dia1), 28.4 (Dia2), 26.8 (Dia2), 26.53 (Dia1), 26.49 (Dia2), 26.4 (Dia1), 26.3 (Dia2), 26.3 (Dia1). **ESI-HRMS** calcd for $C_{20}H_{30}NO$ $[M+H]^+$ 300.2327, found 300.2336.

1-butyl-3-(2-fluoro-[1,1'-biphenyl]-4-yl)-3-methyl-4-vinylazetidin-2-one

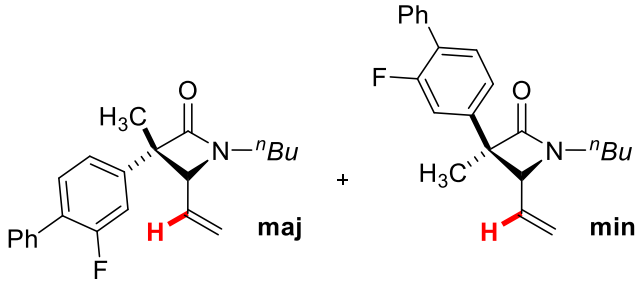

Product **2L** was prepared following general procedure **GP-2** in 72 hours, from the corresponding allene (67.7 mg, 0.2 mmol). Light-yellow oil (37.1 mg, 55% yield). Two diasteroisomers were observed with ratio 66:34.

^{1}H NMR (600 MHz, $CDCl_3$) δ 7.55 – 7.53 (m, 2H Dia1, 2H Dia2), 7.45 – 7.35 (m, 4H Dia1, 4H Dia2), 7.24 (dd, *J* = 8.0, 1.8 Hz, 1H Dia1), 7.19 – 7.16 (m, 1H Dia1, 1H Dia2), 7.11 (dd, *J* = 11.9, 1.8 Hz, 1H Dia2), 5.96 – 5.90 (m, 1H Dia1), 5.51 – 5.46 (m, 1H Dia1, 2H Dia2), 5.35 (dd, *J* = 16.5, 2.1 Hz, 1H Dia2), 5.27 – 5.18 (m, 1H Dia1), 4.12 (d, *J* = 8.7 Hz, 1H Dia1), 3.96 (d, *J* = 8.6 Hz, 1H Dia2), 3.40 (tt, *J* = 14.7, 7.5 Hz, 1H Dia1, 1H Dia2), 3.06 – 3.01 (m, 1H Dia1, 1H Dia2), 1.73 (s, 3H Dia2), 1.56 – 1.51 (m, 5H Dia1, 2H Dia2), 1.39 – 1.29 (m, 2H Dia1, 2H Dia2), 0.96 – 0.90 (m, 3H Dia1, 3H Dia2). **^{13}C NMR** (151 MHz, $CDCl_3$) δ 170.9 (Dia1), 170.7 (Dia2), 159.9 (d, *J* = 248.9 Hz, Dia1, Dia2), 143.7 (d, *J* = 7.5 Hz, Dia2), 140.0 (d, *J* = 7.9 Hz, Dia1), 135.63 (Dia2), 135.60 (Dia1), 135.4 (Dia2), 133.7 (Dia1), 131.1 (d, *J* = 3.9 Hz, Dia1), 130.7 (d, *J* = 3.8 Hz, Dia2), 129.10 (2C Dia1, 2C Dia2), 129.09 (Dia1, Dia2), 128.61 (Dia1), 128.58 (Dia2), 127.84 (Dia1), 127.80 (Dia2), 123.4 (d, *J* = 3.5 Hz, Dia2), 121.9 (d, *J* = 3.4 Hz, Dia1), 121.7 (Dia1), 120.9 (Dia2), 115.2 (d, *J* = 23.9 Hz, Dia2), 113.9 (d, *J* = 23.8 Hz, Dia1), 68.0 (Dia2), 66.6 (Dia1), 62.4 (Dia2), 61.5 (Dia1), 40.4 (Dia1, Dia2), 30.2 (Dia1), 30.1 (Dia2), 23.7 (Dia2), 20.4 (Dia1), 20.3 (Dia2), 19.5 (Dia1, Dia2), 13.80 (Dia2), 13.76 (Dia1). **^{19}F NMR** (565 MHz, $CDCl_3$) δ -117.0 (dd, *J* = 11.6, 8.2 Hz), -117.4 (dd, *J* = 11.8, 8.3 Hz). **ESI-HRMS** calcd for $C_{22}H_{25}FNO$ $[M+H]^+$ 338.1920, found 338.1923.

1,3-dibutyl-3-(4-chlorophenyl)-4-vinylazetidin-2-one

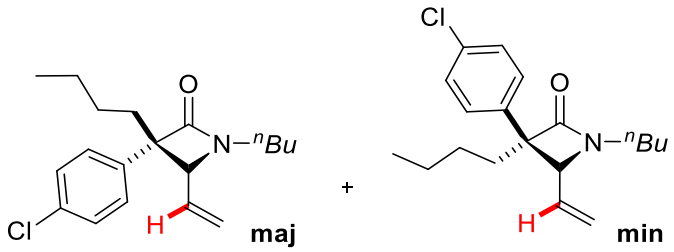

Product **2M** was prepared following general procedure **GP-2** in 60 hours, from the corresponding allene (64.0 mg, 0.2 mmol). Orange oil (31.2 mg, 49% yield). Two diasteroisomers were observed with ratio 56:44.

^{1}H NMR (600 MHz, $CDCl_3$) δ 7.33 – 7.30 (m, 2H Dia1, 2H Dia2), 7.28 – 7.24 (m, 2H Dia1, 2H Dia2), 6.00 – 5.94 (m, 1H Dia1), 5.49 – 5.43 (m, 1H Dia1, 1H Dia2), 5.32 – 5.29 (m, 1H Dia2), 5.17 – 5.10 (m, 1H Dia1, 1H Dia2), 4.03 (d, *J* = 8.8 Hz, 1H Dia1), 3.95 (d, *J* = 8.7 Hz, 1H Dia2), 3.38 – 3.32 (m, 1H Dia1, 1H Dia2), 3.01 – 2.94 (m, 1H Dia1, 1H Dia2), 2.00 – 1.95 (m, 1H Dia1, 1H Dia2), 1.87 (ddd, *J* = 13.6, 12.3, 4.5 Hz, 1H Dia1),

1.72 (ddd, *J* = 13.6, 12.4, 4.4 Hz, 1H Dia1), 1.54 – 1.42 (m, 2H Dia1, 4H Dia2), 1.37 – 1.13 (m, 4H Dia1, 5H Dia2), 1.02 – 0.96 (m, 1H Dia1), 0.92 (t, *J* = 7.4 Hz, 3H Dia2), 0.88 – 0.84 (m, 3H Dia1, 3H Dia2), 0.79 (t, *J* = 7.4 Hz, 3H Dia1). **^{13}C NMR** (151 MHz, $CDCl_3$) δ 170.7 (Dia1), 170.2 (Dia2), 139.5 (Dia1, Dia2), 136.3 (Dia2), 135.8 (Dia1), 133.9 (Dia1), 132.9 (Dia2), 129.2 (Dia1, Dia2), 128.7 (Dia1, Dia2), 128.5 (Dia1, Dia2), 128.1 (Dia1, Dia2), 121.4 (Dia1), 120.6 (Dia2), 66.4 (Dia1), 66.3 (Dia2), 66.1 (Dia1), 65.2 (Dia2), 40.2 (Dia1), 40.1 (Dia2), 38.1 (Dia2), 34.1 (Dia1), 30.1 (Dia2), 30.0 (Dia1), 27.0 (Dia2), 26.8 (Dia1), 23.2 (Dia1), 23.1 (Dia2), 20.4 (Dia2), 20.2 (Dia1), 14.0 (Dia2), 13.9 (Dia1), 13.8 (Dia2), 13.7 (Dia1). **ESI-HRMS** calcd for $C_{19}H_{27}ClNO$ $[M+H]^+$ 320.1781, found 320.1775.

3-cyclohexyl-1-phenethyl-3-phenyl-4-vinylazetidin-2-one

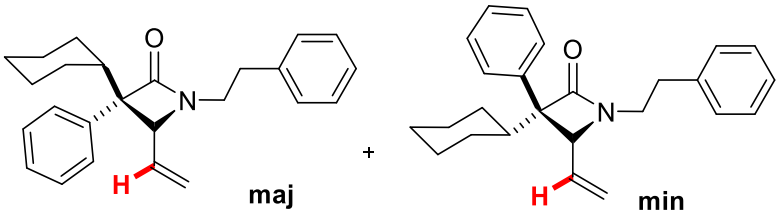

Product **2N** was prepared following general procedure **GP-2** in 60 hours, from the corresponding allene (72.1 mg, 0.2 mmol). Pale yellow oil (44.6 mg, 62% yield). Two diasteroisomers were observed with ratio 55:45.

^{1}H NMR (600 MHz, $CDCl_3$) δ 7.37 – 7.12 (m, 9H Dia1, 9H Dia2), 7.04 – 7.02 (m, 1H Dia1, 1H Dia2), 5.91 (ddd, *J* = 16.9, 10.3, 8.9 Hz, 1H Dia1), 5.40 – 5.36 (m, 1H Dia1, 1H Dia2), 5.23 – 5.20 (m, 1H Dia2), 5.15 – 5.12 (m, 1H Dia1, 1H Dia2), 3.96 (d, *J* = 8.9 Hz, 1H Dia1), 3.92 (d, *J* = 8.3 Hz, 1H Dia2), 3.71 (ddd, *J* = 14.5, 8.0, 6.9 Hz, 1H Dia2), 3.55 (ddd, *J* = 14.3, 8.0, 6.5 Hz, 1H Dia1), 3.18 – 3.13 (m, 1H Dia1, 1H Dia2), 2.90 – 2.87 (m, 2H Dia2), 2.82 – 2.78 (m, 2H Dia1), 2.33 – 2.30 (m, 1H Dia1), 1.97 – 1.94 (m, 1H Dia2), 1.90 – 1.86 (m, 1H Dia1), 1.73 – 1.66 (m, 2H Dia1, 2H Dia2), 1.61 – 1.53 (m, 2H Dia1, 3H Dia2), 1.40 – 1.38 (m, 1H Dia1), 1.28 – 1.04 (m, 1H Dia1, 4H Dia2), 0.91 – 0.83 (m, 2H Dia1, 1H Dia2), 0.66 – 0.59 (m, 1H Dia1). **^{13}C NMR** (151 MHz, $CDCl_3$) δ 170.9 (Dia1), 170.2 (Dia2), 138.7 (Dia1, Dia2), 138.4 (Dia1), 136.4 (Dia2), 136.2 (Dia2), 133.9 (Dia1), 128.9 (Dia1, Dia2), 128.9 (Dia1, Dia2), 128.8 (2C Dia2), 128.7 (2C Dia2), 128.6 (2C Dia1), 128.5 (2C Dia1), 127.8 (Dia2), 127.6 (Dia1), 126.9 (2C Dia1), 126.7 (2C Dia2), 126.7 (Dia2), 126.5 (Dia1), 121.2 (Dia1), 120.1 (Dia2), 70.5 (Dia2), 69.5 (Dia1), 66.8 (Dia1), 64.0 (Dia2), 44.8 (Dia2), 41.7 (Dia1), 41.2 (Dia1), 40.9 (Dia2), 34.5 (Dia2), 34.4 (Dia1), 29.2 (Dia2), 28.6 (Dia1), 28.4 (Dia1), 28.4 (Dia2), 26.8 (Dia2), 26.5 (Dia1), 26.5 (Dia2), 26.3 (Dia1), 26.3 (Dia2), 26.4 (Dia1). **ESI-HRMS** calcd for $C_{25}H_{30}NO$ $[M+H]^+$ 360.2327, found 360.2331.

3-cyclohexyl-1-(pent-4-en-1-yl)-3-phenyl-4-vinylazetidin-2-one

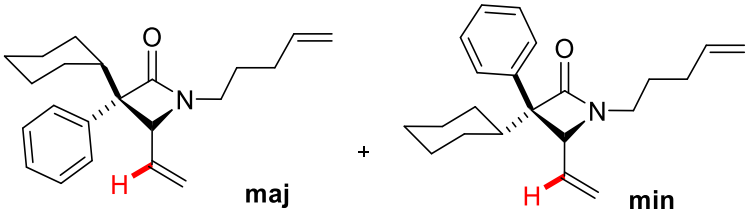

Product **2O** was prepared following general procedure **GP-2** in 60 hours, from the corresponding allene (64.7 mg, 0.2 mmol). Pale-orange oil (47.1 mg, 73% yield). Two diasteroisomers were observed with ratio 52:48.

^{1}H NMR (400 MHz, $CDCl_3$) δ 7.43 – 7.40 (m, 1H Dia1, 1H Dia2), 7.35 – 7.22 (m, 4H Dia1, 4H Dia2), 6.14 – 6.05 (m, 1H Dia1), 5.84 – 5.66 (m, 1H Dia1, 1H Dia2), 5.54 (dd, *J* = 17.2, 1.4 Hz, 1H Dia1), 5.46 (dd, *J* = 10.1, 1.4 Hz, 1H Dia2), 5.36 – 5.29 (m, 1H Dia2), 5.26 – 5.15 (m, 1H Dia1, 1H Dia2), 5.06 – 4.89 (m, 2H Dia1, 2H Dia2), 4.21 (d, *J* = 8.9 Hz, 1H Dia1), 4.11 (d, *J* = 8.5 Hz, 1H Dia2), 3.39 – 3.25 (m, 1H Dia1, 1H Dia2), 3.02 – 2.90 (m, 1H Dia1, 1H Dia2), 2.31 (dd, *J* = 12.9, 3.4 Hz, 1H Dia1), 2.11 – 2.05 (m, 2H Dia1, 1H Dia2), 1.99 – 1.94 (m, 1H Dia1, 2H Dia2), 1.93 – 1.75 (m, 1H Dia1, 2H Dia2), 1.71 – 1.44 (m, 5H Dia1, 4H Dia2), 1.29 – 0.85 (m, 4H Dia1, 4H Dia2), 0.67 – 0.63 (m, 1H Dia2). **^{13}C NMR** (101 MHz, $CDCl_3$) δ 171.0 (Dia1), 170.1 (Dia2), 138.5 (Dia1), 137.6 (Dia2), 137.5 (Dia1), 136.7 (Dia1, Dia2), 136.4 (Dia2), 134.3 (Dia1, Dia2), 128.8 (Dia2), 128.6 (Dia1), 127.8 (Dia2), 127.6 (Dia1), 126.9 (2C Dia1), 126.8 (2C Dia2), 121.2 (Dia1), 120.0 (Dia2), 115.5 (Dia2), 115.4 (Dia1), 70.5 (Dia2), 69.5 (Dia1), 66.5 (Dia1), 63.7 (Dia2), 44.8 (Dia2), 41.3 (Dia1), 39.8 (Dia1), 39.6 (Dia2), 31.3 (Dia2), 31.1 (Dia1), 29.2 (Dia2), 28.6 (Dia1), 28.49 (Dia1), 28.48 (Dia2), 27.4 (Dia2), 27.1 (Dia1), 26.8 (Dia2), 26.53 (Dia2), 26.51 (Dia1), 26.4 (Dia1), 26.32 (Dia1), 26.3 (Dia2). **ESI-HRMS** calcd for $C_{22}H_{29}NNaO$ $[M+H]^+$ 346.2147, found 346.2152.

3,3-dicyclohexyl-1-phenethyl-4-vinylazetidin-2-one

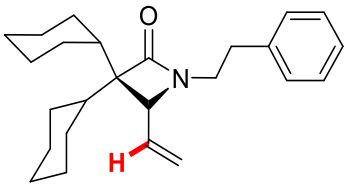

Product **2P** was prepared following general procedure **GP-2** in 48 hours, from the corresponding allene (73.1 mg, 0.2 mmol). Colorless oil (49.1 mg, 78% yield).

^{1}H NMR (400 MHz, $CDCl_3$) δ 7.30 – 7.27 (m, 2H), 7.22 – 7.19 (m, 3H), 5.92 – 5.83 (m, 1H), 5.28 – 5.21 (m, 2H), 3.88 (d, *J* = 8.2 Hz, 1H), 3.63 – 3.54 (m, 1H), 3.27 – 3.20 (m, 1H), 2.84 (t, *J* = 7.6 Hz, 2H), 1.76 – 1.56 (m, 11H), 1.27 – 1.08 (m, 9H), 0.95 – 0.85 (m, 2H). **^{13}C NMR** (101 MHz, $CDCl_3$) δ 172.1, 138.7, 134.5, 128.8 (2C), 128.6 (2C), 126.6, 120.2, 69.6, 60.5, 41.1, 38.6, 37.3, 34.4, 29.6, 29.3, 28.8 (2C), 27.4, 26.8, 26.8, 26.63, 26.61, 26.60. **ESI-HRMS** calcd for $C_{25}H_{36}NO$ $[M+H]^+$ 366.2797, found 366.2801.

1-butyl-3-phenyl-4-vinylazetidin-2-one

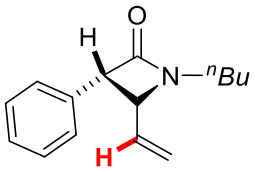

Product **2Q** was prepared following general procedure **GP-2** in 120 hours, from the corresponding allene (45.8 mg, 0.2 mmol). Light-yellow oil (27.8 mg, 61% yield). Only one diasteroisomer was isolated.

^{1}H NMR (400 MHz, $CDCl_3$) δ 7.37 – 7.33 (m, 2H), 7.30 – 7.26 (m, 3H), 5.98 – 5.89 (m, 1H), 5.42 – 5.30 (m, 2H), 4.02 (d, *J* = 2.2 Hz, 1H), 3.95 (dd, *J* = 8.6, 2.2 Hz, 1H), 3.46 (dt, *J* = 14.0, 7.6 Hz, 1H), 3.04 (dt, *J* = 13.9, 6.9 Hz, 1H), 1.60 – 1.52 (m, 2H), 1.38 (h, *J* = 7.6 Hz, 2H), 0.94 (t, *J* = 7.3 Hz, 3H). **^{13}C NMR** (101 MHz, $CDCl_3$) δ 167.77, 136.10, 135.26, 129.02 (2C), 127.69, 127.51 (2C), 120.05, 63.39, 61.85, 40.52, 30.23, 20.39, 13.79. **ESI-HRMS** calcd for $C_{15}H_{20}NO$ $[M+H]^+$ 230.1545, found 230.1550.

tert-butyl 1-oxo-2-phenethyl-3-vinyl-2,5-diazaspiro[3.4]octane-5-carboxylate

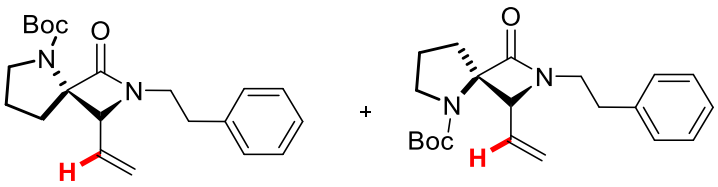

3R **3R'**

Products **2R** and **2R'** were prepared following general procedure **GP-2** in 96 hours, from the corresponding allene (71.2 mg, 0.2 mmol). Light-yellow oil (41.3 mg, 58% yield). Two diasteroisomers were observed with ratio 75:25 and sequentially separated by chromatography column (nHex:EtOAc 6:4).

Products **2R**, two rotamers were observed due to the dynamic amide group (54:46 mixture of rotamers). Light-yellow oil (32.8 mg, 46% yield).

^{1}H NMR (600 MHz, $CDCl_3$) δ 7.30 (t, *J* = 7.4 Hz, 2H RotA, 2H RotB), 7.24 – 7.17 (m, 3H RotA, 3H RotB), 5.54 – 5.48 (m, 1H RotB), 5.46 – 5.40 (m, 1H RotA), 5.32 – 5.19 (m, 2H RotA, 2H RotB), 4.36 (d, *J* = 8.5 Hz, 1H RotB), 4.15 (d, *J* = 8.8 Hz, 1H RotA), 3.66 – 3.61 (m, 1H RotA), 3.54 – 3.46 (m, 1H RotA, 1H RotB), 3.44 – 3.35 (m, 2H RotA, 2H RotB), 3.16 – 3.11 (m, 1H RotA), 3.02 – 2.85 (m, 2H RotA, 2H RotB), 2.08 – 2.03 (m, 2H RotB), 2.02 – 1.98 (m, 2H RotA), 1.85 – 1.79 (m, 1H RotA, 1H RotB), 1.60 – 1.58 (m, 1H RotA, 1H RotB), 1.48 (s, 9H RotA), 1.48 (s, 9H RotB). **^{13}C NMR** (151 MHz, $CDCl_3$) δ 170.2 (RotB), 170.0 (RotA), 153.7 (RotA), 153.4 (RotB), 139.3 (RotB), 138.7 (RotA), 133.2 (RotB), 133.1 (RotA), 129.1 (2C RotB), 128.9 (2C RotA), 128.7 (2C RotA), 128.5 (2C RotB), 126.7 (RotA), 126.4 (RotB), 121.4 (RotA), 120.9 (RotB), 81.1 (RotA), 80.1 (RotB), 76.7 (RotB), 76.3 (RotA), 67.1 (RotA), 64.6 (RotB), 47.7 (RotB), 47.6 (RotA), 43.5 (RotA), 42.8 (RotB), 34.8 (RotA), 34.3 (RotB), 30.5 (RotA), 29.3 (RotB), 28.6 (3C RotA, 3C RotB), 22.9 (RotB), 22.0 (RotA). **ESI-HRMS** calcd for $C_{21}H_{29}N_2O_3$ $[M+H]^+$ 357.2178, found 357.2183.

Products **2R'**, two rotamers were observed due to the dynamic amide group (58:42 mixture of rotamers). Light-yellow oil (8.5 mg, 12% yield).

^{1}H NMR (400 MHz, $CDCl_3$) δ 7.33 – 7.27 (m, 2H RotA, 2H RotB), 7.25 – 7.18 (m, 3H RotA, 3H RotB), 6.12 – 5.94 (m, 1H RotA, 1H RotB), 5.28 – 5.10 (m, 2H RotA, 2H RotB), 3.83 – 3.74 (m, 1H RotA, 1H RotB), 3.58 – 3.55 (m, 1H RotA, 1H RotB), 3.41 – 3.11 (m, 3H RotA, 3H RotB), 3.00 – 2.78 (m, 2H RotA, 2H RotB), 2.32 – 2.16 (m, 1H RotA, 1H RotB), 1.94 – 1.81 (m, 2H RotA, 2H RotB), 1.71 – 1.59 (m, 1H RotA, 1H RotB), 1.47 (s, 9H RotA), 1.44 (s, 9H RotB). **^{13}C NMR** (101 MHz, $CDCl_3$) δ 168.4 (RotA, RotB), 153.7 (RotA, RotB), 138.9 (RotB), 138.5 (RotA), 134.8 (RotB), 133.9 (RotA), 128.9 (2C RotB), 128.8 (2C RotA), 128.8 (2C RotA), 128.7 (2C RotB), 126.8 (RotA), 126.6 (RotB), 121.9 (RotA), 120.9 (RotB), 81.2 (RotA), 80.0 (RotB), 71.4 (RotB), 70.9 (RotA), 48.1 (RotB), 47.9 (RotA), 41.5 (RotB), 41.3 (RotA), 35.7 (RotA, RotB), 34.8 (RotB), 34.3 (RotA), 29.9 (3C RotA, 3C RotB), 28.5 (RotB), 28.3 (RotA), 23.0 (RotB), 22.3 (RotA). **ESI-HRMS** calcd for $C_{21}H_{29}N_2O_3$ $[M+H]^+$ 357.2178, found 357.2183.

1-phenethyl-3,3-diphenyl-4-(prop-1-en-1-yl)azetidin-2-one

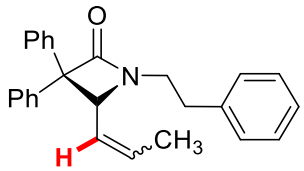

Product **2S** was prepared following general procedure **GP-2** in 96 hours, from the corresponding allene (73.7 mg, 0.2 mmol). Light-yellow oil (29.3 mg, 40% yield). The two isomer *E*/*Z* are observed with ratio 1:1.

^{1}H NMR (400 MHz, $CDCl_3$) δ 7.36 – 7.28 (m, 5H), 7.25 – 7.19 (m, 6H), 7.14 – 7.11 (m, 3H), 5.74 – 5.63 (m, 1H), 4.81 – 4.72 (m, 1H Iso1, 1H Iso2), 4.35 (d, *J* = 9.6 Hz, 1H Iso1), 3.75 – 3.62 (m, 1H), 3.33 – 3.19 (m, 1H), 2.92 – 2.81 (m, 2H), 1.70 (d, *J* = 7.7 Hz, 3H Iso1), 1.59 (d, *J* = 5.8 Hz, 3H Iso2). **^{13}C NMR** (151 MHz, $CDCl_3$) δ 169.3, 169.2, 162.7, 141.04, 140.99, 138.70, 138.66, 138.2, 137.5, 132.6, 131.2, 129.18 (2C), 129.16, 129.0 (2C), 128.8, 128.72, 128.67 (2C), 128.64 (2C), 128.59, 128.5, 128.4, 128.34 (2C), 128.28, 128.0, 127.5, 127.4, 127.21, 127.15, 127.1, 127.0, 126.7, 126.6, 70.9, 70.4, 66.9, 60.0, 41.9, 41.7, 34.7, 34.5, 18.0, 13.4. **ESI-HRMS** calcd for $C_{26}H_{26}NO$ $[M+H]^+$ 368.2014, found 368.2020.

1-(2,2-diphenylethyl)-3,3-dimethyl-4-vinylazetidin-2-one

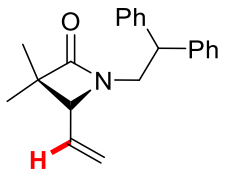

Product **2U** was prepared following general procedure **GP-1** in 24 hours, as a mixture with the correspondent product **2u**, from the corresponding allene (61.1 mg, 0.2 mmol). Light-yellow oil (22.6 mg, 37% yield).

^{1}H NMR (600 MHz, $CDCl_3$) δ 7.28 – 7.17 (m, 10H), 5.57 – 5.51 (m, 1H), 5.24 (d, *J* = 10.3 Hz, 1H), 5.16 (d, *J* = 17.1 Hz, 1H), 4.29 (td, *J* = 8.5, 2.3 Hz, 1H), 4.05 (ddd, *J* = 14.3, 8.7, 2.3 Hz, 1H), 3.41 (ddd, *J* = 14.2, 8.2, 2.3 Hz, 1H), 3.17 (dd, *J* = 8.4, 2.3 Hz, 1H), 0.94 (s, 3H), 0.89 (s, 3H). **^{13}C NMR** (151 MHz, $CDCl_3$) δ 173.8, 142.0, 141.4, 134.2, 128.79 (2C), 128.76 (2C), 128.3, 128.1 (2C), 127.03 (2C), 126.98, 120.5, 66.2, 54.6, 49.7, 44.5, 22.0, 17.6. **ESI-HRMS** calcd for $C_{21}H_{24}NO$ $[M+H]^+$ 306.1858, found 306.1866.

1-(2,2-diphenylethyl)-3,3-diphenyl-4-vinylazetidin-2-one

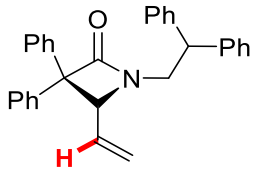

Product **2V** was prepared following general procedure **GP-2** in 24 hours, as a mixture with the correspondent product **2v**, from the corresponding allene (85.8 mg, 0.2 mmol). Light-yellow oil (27.5 mg, 32% yield).

^{1}H NMR (400 MHz, $CDCl_3$) δ 7.28 – 7.18 (m, 15H), 7.11 – 7.09 (m, 5H), 5.28 (dd, *J* = 15.5, 3.3 Hz, 1H), 5.19 – 5.09 (m,2H), 4.39 (t, *J* = 8.4 Hz, 1H), 4.17 (d, *J* = 8.5 Hz, 1H), 4.07 (dd, *J* = 14.1, 7.8 Hz, 1H), 3.66 (dd, *J* = 14.1, 9.1 Hz, 1H). **^{13}C NMR** (101 MHz, $CDCl_3$) δ 169.2, 141.8, 141.4, 140.3, 137.6, 135.0, 128.84 (2C), 128.81 (2C), 128.6 (2C), 128.5 (2C), 128.4 (2C), 128.3 (2C), 128.0 (2C), 127.4, 127.2, 127.04 (2C), 127.00 (2C), 121.3, 70.7, 67.5, 49.7, 45.4. **ESI-HRMS** calcd for $C_{31}H_{28}NO$ $[M+H]^+$ 430.2093, found 430.2097.

Valorization of products

β-lactam reduction toward bicyclic azetidine:

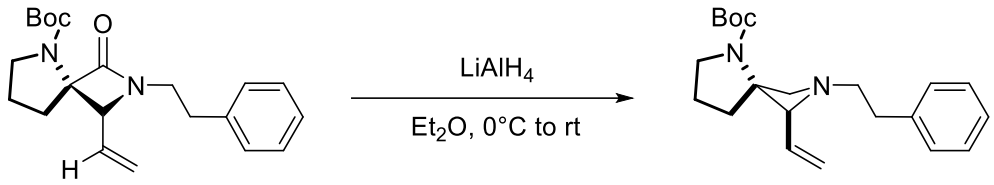

***tert*-butyl-2-phenethyl-1-vinyl-2,5-diazaspiro[3.4]octane-5-carboxylate (5)**

To a solution of **2R** (35 mg, 0.1 mmol, 1 equiv.) in dry Et_2O (0.1 mL, 1.0 M), $LiAlH_4$ (6 mg, 0.15 mmol, 1.5 equiv.) was added portion wise at 0 °C. The resulting solution was allowed to warm to room temperature and stirred for 4 hours. After complete conversion as determined by TLC, the solvent was removed under reduced pressure, and the crude was directly purified through preparative TLC to provide **5** in 50% yield (17 mg, 0.05 mmol, 50%).

^{1}H NMR (600 MHz, Acetone-d_6) δ 7.27 (t, *J* = 7.4 Hz, 2H), 7.22 (d, *J* = 7.5 Hz, 2H), 7.17 (t, *J* = 7.3 Hz, 1H), 5.62 (dt, *J* = 17.9, 9.3 Hz, 1H), 5.19 (d, *J* = 18.3 Hz, 2H), 3.68 (dd, *J* = 31.7, 9.7 Hz, 2H), 3.53 (d, *J* = 11.0 Hz, 1H), 3.46 (d, *J* = 8.7 Hz, 1H), 3.23 – 3.18 (m, 1H), 2.92 – 2.89 (m, 1H), 2.57 – 2.55 (m, 1H), 2.08 – 2.06 (m, 2H), 1.73 – 1.72 (m, 2H), 1.42 – 1.41 (m, 9H). **^{13}C NMR** (151 MHz, Acetone-d_6) δ 163.03, 138.58, 135.50, 130.77, 129.57 (2C), 129.41, 129.14 (2C), 126.74, 98.04, 64.20, 57.47, 50.34, 49.67, 30.59, 30.34, 28.63 (3C), 23.09. **ESI-HRMS** calcd for $C_{21}H_{31}N_2O_2$ $[M+H]^+$ 342.2307, found 342.2300.

Epoxidation of 2V:

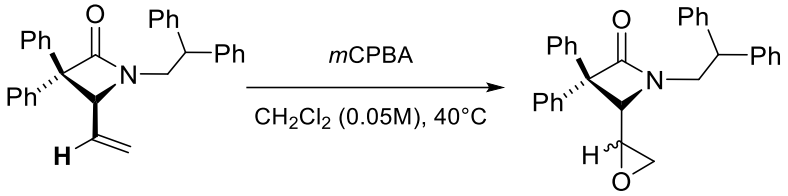

1-(2,2-diphenylethyl)-4-(oxiran-2-yl)-3,3-diphenylazetidin-2-one (8)

To a solution of product **2V** (27.5 mg, 0.064 mmol, 1 equiv.) in CH_2Cl_2 (1.3 mL, 0.05 M) *m-CPBA* (70% pure, 48.3 mg, 0.28 mmol, 3 equiv.) was added, and the reaction was stirred at 40 °C for 18 h. After complete conversion, as monitored by TLC, the solution was concentrated and directly purified by preparative thin layer chromatography (*n-Hexane/EtOAc 8:2*) to afford the desired product **9** as a mixture of two diasteroisomers in ratio 74:26. Pale yellow oil (19.5 mg, 68%).

^{1}H NMR (600 MHz, $CDCl_3$) δ 7.34 – 7.27 (m, 5H Dia1, 5H Dia2), 7.25 – 7.14 (m, 13H Dia1, 13H Dia2), 7.08 – 7.06 (m, 1H Dia1, 1H Dia2), 7.02 – 7.00 (m, 1H Dia1, 1H Dia2), 4.59 (t, *J* = 8.7 Hz, 1H Dia1), 4.40 (t, *J* = 8.4 Hz, 1H Dia2), 4.06 – 4.02 (m, 2H Dia1), 3.77 – 3.73 (m, 1H Dia2), 3.53 (d, *J* = 7.1 Hz, 1H Dia2), 3.42 (d, *J* = 8.7 Hz, 1H Dia1), 2.64 (t, *J* = 4.3 Hz, 1H Dia1), 2.60 – 2.59 (m, 1H Dia1, 1H Dia2), 2.49 (dd, *J* = 5.0, 2.6 Hz, 1H Dia2), 2.42 – 2.39 (m, 1H Dia2), 2.30 – 2.28 (m, 1H Dia1). **^{13}C NMR** (151 MHz, $CDCl_3$) δ 169.4 (Dia2), 168.8 (Dia1), 141.5 (Dia1, Dia2), 141.3 (Dia1, Dia2), 139.1 (Dia1, Dia2), 137.5 (Dia1, Dia2), 128.92 (4C Dia2), 128.85 (4C Dia1), 128.8 (2C Dia1, 2C Dia2), 128.7 (2C Dia1), 128.61 (2C Dia1), 128.57 (2C Dia2), 128.5 (2C Dia1), 128.3 (2C Dia2), 128.20 (2C Dia2), 128.17 (Dia1), 128.1 (Dia1), 128.0 (2C Dia2), 127.6 (2C Dia1), 127.5 (Dia2), 127.40 (Dia2), 127.36 (2C Dia1), 127.3 (2C Dia2), 127.2 (Dia2), 127.1 (Dia2), 127.01 (Dia1), 126.97 (Dia1), 69.0 (Dia1, Dia2), 66.3 (Dia1), 64.8 (Dia2), 52.0 (Dia1), 50.3 (Dia2), 49.8 (Dia2), 49.3 (Dia1), 46.5 (Dia2), 46.11 (Dia2), 46.07 (Dia1), 45.2 (Dia1). **ESI-HRMS** calcd for $C_{31}H_{28}NO_2$ $[M+H]^+$ 446.2120, found 446.2126.

Synthesis of ketone:

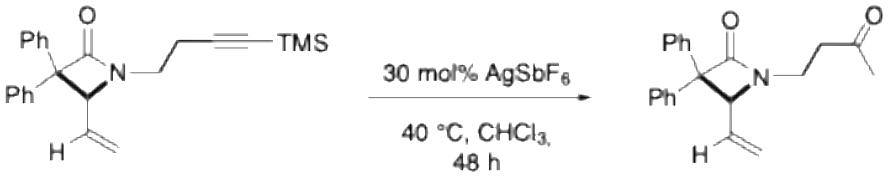

1-(3-oxobutyl)-3,3-diphenyl-4-vinylazetidin-2-one (9)

To a solution of **2H** (19 mg, 0.05 mmol, 1 equiv.) in MeOH (0.1 mL, 0.5 M) K_2CO_3 (5 mg, mmol, 0.5 equiv.) was added, and the resulting suspension was stirred for 2 hours at room temperature. After complete conversion as determined by TLC, the solution was dried over Na_2SO_4 and purified through a chromatography column to provide a quantitative yield of the deprotected product.

To a solution of the deprotected product (0.05 mmol, 1 equiv.) in dry $CHCl_3$ (1.7 mL, 0.03 M), $AgSbF_6$ (4 mg, 0.015 mmol, 30 mol%) was added, and the resulting solution was stirred at 40 °C for 48 hours. After complete conversion as determined by TLC, the solution was dried over Na_2SO_4 and purified through preparative TLC to provide **9**, as a pale-yellow oil (10 mg, 0.031 mmol, 63%).

^{1}H NMR (600 MHz, $CDCl_3$) δ 7.46 – 7.44 (m, 2H), 7.34 (t, *J* = 7.8 Hz, 2H), 7.28 (d, *J* = 4.7 Hz, 4H), 7.45 – 7.21 (m, 2H), 5.50 – 5.47 (m, 1H), 5.35 – 5.24 (m, 2H), 4.65 (d, *J* = 8.7 Hz, 1H), 3.57 – 3.52 (m, 1H), 3.40 – 3.35 (m, 1H), 2.89 – 2.84 (m, 1H), 2.80 – 2.75 (m, 1H), 2.14 (s, 3H). **^{13}C NMR** (151 MHz, $CDCl_3$) δ 206.3, 169.3, 140.6, 138.0, 135.0, 128.8 (2C), 128.5 (2C), 128.4, 127.4 (4C), 127.3, 121.5, 70.8, 67.3, 41.7, 36.1, 30.1. **ESI-HRMS** calcd for $C_{21}H_{22}NO_2$ $[M+H]^+$ 320.1651, found 320.1649.

Ring closing metathesis of 2N:

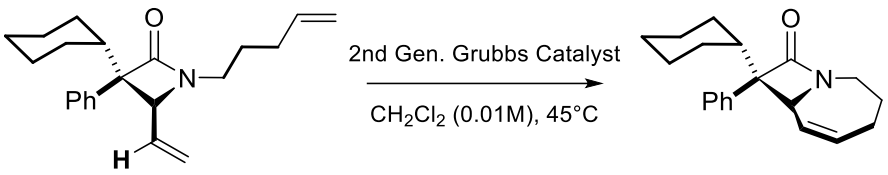

8-cyclohexyl-8-phenyl-1-azabicyclo[5.2.0]non-5-en-9-one (11)

To a solution of product **2O** (36 mg, 0.120 mmol) in dry CH_2Cl_2 (12 mL, 0.01 M), a 2nd Generation Grubbs Catalyst (5 mg, 0.006mmol, 5 mol%) was added at 45 °C. The reaction was refluxed until complete conversion (45 minutes). The resulting mixture was then concentrated under reduced pressure and the pure product was obtained through silica gel column purification (n-*Hexane/EtOAc gradient 9:1 to 8:2*) as a mixture of two diasteroisomers in a 53:47 ratio. Pale yellow oil (20.5 mg, 61%).

^{1}H NMR (400 MHz, $CDCl_3$) δ 7.43 – 7.40 (m, 1H Dia1, 1H Dia2), 7.33 – 7.21 (m, 4H Dia1, 4H Dia2), 5.97 – 5.91 (m, 1H Dia1, 1H Dia2), 5.48 – 5.43 (m, 1H Dia2), 5.26 (dd, *J* = 11.6, 1.6 Hz, 1H Dia1), 4.49 (br, 1H Dia1), 4.42 (t, *J* = 2.2 Hz, 1H Dia2), 3.91 – 3.79 (m, 1H Dia1, 1H Dia2), 3.14 (dt, *J* = 13.3, 4.9 Hz, 1H Dia2), 3.04 (dt, *J* = 13.3, 4.9 Hz, 1H Dia1), 2.42 – 2.24 (m, 2H Dia1, 2H Dia2), 2.16 – 2.08 (m, 1H Dia1, 1H Dia2), 2.01 – 1.47 (m, 7H Dia1, 7H Dia2), 1.24 – 0.73 (m, 5H Dia1, 5H Dia2). **^{13}C NMR** (101 MHz, $CDCl_3$) δ 169.8 (Dia1), 169.6 (Dia2), 139.3 (Dia1), 137.2 (Dia2), 132.4 (Dia1), 130.6 (Dia2), 128.31 (Dia1, Dia2), 128.29 (Dia1, Dia2), 128.23 (Dia2), 128.18 (Dia1), 127.9 (Dia1, Dia2), 127.0 (Dia1, Dia2), 126.9 (Dia1), 126.8 (Dia2), 71.7 (Dia2), 69.9 (Dia1), 64.6 (Dia1), 60.1 (Dia2), 43.3 (Dia2), 42.1 (Dia1), 41.6 (Dia2), 41.3 (Dia1), 31.7 (Dia2), 30.0 (Dia1), 29.4 (Dia2), 28.7 (Dia1), 28.5 (Dia2), 28.2 (Dia1), 27.7 (Dia2), 26.9 (Dia1), 26.8 (Dia1), 26.6 (Dia2), 26.6 (Dia1), 26.5 (Dia2), 26.3 (Dia2), 26.2 (Dia1). **ESI-HRMS** calcd for $C_{20}H_{26}NO$ $[M+H]^+$ 296.2014, found 296.2019.

Synthesis of deuterated substrate

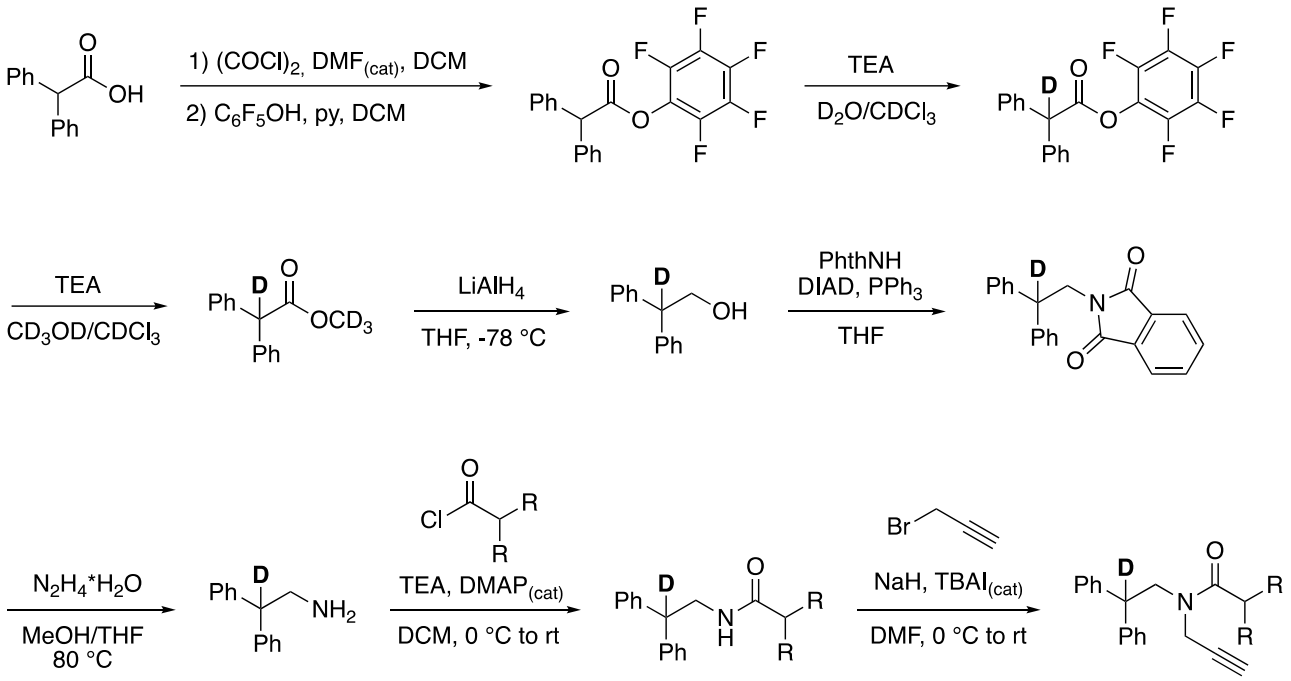

Highly deuterated precursors **[D]-1v** has been prepared adapting the reported procedure by M. Peng, H. Li, Z. Qin, J. Li, Y. Sun, X. Zhang, L. Jiang, H. Do, J. An, *Adv. Synth. Catal.* **2022**, *364*, 2184.

To a solution of diphenylacetic acid (2.12 g, 10 mmol, 1 equiv.) in DCM (30 mL) a few drops of DMF and $(COCL)_2$ (1.11 mL, 13 mmol, 1.3 equiv.) were added at 0°C. The reaction was stirred at rt for 2 hours, and then a solution of pentafluorophenol (2.02 g, 11 mmol, 1.1 equiv.) and pyridine (0.89 mL, 11 mmol, 1.1 equiv.) in DCM (10 mL) were slowly added. The reaction was stirred overnight and then quenched with a saturated NH_4Cl aqueous solution (20 mL) and extracted with DCM (3x20 mL). The combined organic layers were washed with brine, dried over sodium sulfate, and concentrated under reduced pressure. The crude was purified by chromatography on silica gel (*n-h*exane/EtOAc 30:1), affording perfluorophenyl 2,2-diphenylacetate as a white solid (3.77 g, 99% yield).

The pentafluorophenyl ester obtained was subjected to deuteration by vigorously stirring in a solution of D_2O (5 mL) and $CDCl_3$ (3.5 mL) in the presence of TEA (0.28 mL, 2 mmol, 0.2 equiv.). After 24 hours the organic layer was separated, and the aqueous phase was extracted with DCM (2x20 mL). The combined organic layers were washed with brine, dried over sodium sulfate, and concentrated under reduced pressure. The crude was purified by chromatography on silica gel (*n-h*exane/EtOAc 30:1), affording perfluorophenyl 2,2-diphenylacetate-*d* as a white solid (3.45 g, 91% yield, 95% D).

The deuterated pentafluorophenyl ester was then transesterificated by vigorously stirring in a solution of CD_3OD (6 mL) and $CDCl_3$ (4 mL) in the presence of TEA (1.27 mL, 9.1 mmol, 1 equiv.). After 24 hours the solvent was evaporated. The crude was purified by chromatography on silica gel (*n-h*exane/EtOAc 20:1), affording methyl-d_3 2,2-diphenylacetate-*d* as a white solid (3.17 g, 92% yield, 95% D).

The deuterated methyl ester (1.15 g, 5 mmol, 1 equiv.) was dissolved in THF (23 mL) and the solution was added dropwise to a solution of $LiAlH_4$ (0.57 g, 15 mmol, 3 equiv.) in THF (15 mL), under a nitrogen atmosphere at -78 °C. The reaction was stirred at the same temperature for 1 hour, then allowed to warm to rt and quenched by the addition of a saturated aqueous solution of sodium/potassium tartrate. The mixture was extracted with EtOAc (3x20 mL) and the combined organic layers were washed with brine, dried over sodium sulfate, and concentrated under reduced pressure. The crude was purified by chromatography on silica gel (*n-h*exane/EtOAc 4:1), affording 2,2-diphenylethan-2-*d*-1-ol as a white solid (0.99 g, 99% yield, >90% D).

To a solution of deuterated alcohol (0.99 g, 5 mmol, 1 equiv.), phthalimide (1.84 g, 12.5 mmol, 2.5 equiv.) and PPh_3 (3.27 g, 12.5 mmol, 2.5 equiv.) in THF (50 mL), DIAD (2.46 mL, 12.5 mmol, 2.5 equiv.) was added dropwise at 0°C under a nitrogen atmosphere, and the reaction mixture was stirred at rt overnight. The reaction was quenched with water (40 mL), extracted with EtOAc (3x20 mL), and the combined organic layers were washed with brine, dried over sodium sulfate, and concentrated under reduced pressure. The crude was purified by chromatography on silica gel (*n-h*exane/EtOAc 6:1), affording 2-(2,2-diphenylethyl-2-*d*)isoindoline-1,3-dione as a white solid (1.38 g, 84% yield, >95% D).

The phthalimide was removed by refluxing the deuterated imide (1.2 g, 3.66 mmol, 1 equiv.) in a solution of THF (20 mL) and MeOH (30 mL) in the presence of hydrazine hydrated (1.1 mL, 21.96 mmol, 6 equiv.) for 2 hours. The resulting mixture was filtered on a celite pad, the solution obtained was concentrated under reduced pressure, washed with a saturated $NaHCO_3$ aqueous solution and extracted with DCM (3x20 mL), affording the crude primary amine which was used in the following step without further purification.

To a solution of crude 2,2-diphenylethan-2-*d*-1-amine (356 mg, 1.8 mmol, 1 equiv.), TEA (0.5 mL, 3.6 mmol 2 equiv.) and a catalytic amount of DMAP in DCM (9 mL), the desired acyl chloride (2.7 mmol, 1.5 equiv.)was added at 0°C, and the reaction was stirred at rt for 1 hour. The reaction was quenched by the addition of water and extracted with DCM (3x10 mL). The combined organic layers were washed with brine, dried over sodium sulfate, and concentrated under reduced pressure. The crude was purified by chromatography on silica gel (*n-h*exane/EtOAc), affording the deuterated secondary amide.

To a solution of the desired amide (1.3 mmol, 1 equiv.) in DMF (6 mL) a catalytic amount of TBAI and NaH (60% dispersion, 63 mg, 1.6 mmol, 1.2 equiv.) were added at 0°C under a nitrogen atmosphere. After stirring at the same temperature for 30 min, propargyl bromide (80% in toluene, 0.18 mL, 1.7 mmol, 1.3 equiv.) was added dropwise, and the reaction was allowed to stir at rt overnight. The reaction was quenched by the addition of water and extracted with EtOAc (3x10 mL). The combined organic layers were washed with brine, dried over sodium sulfate, and concentrated under reduced pressure. The crude was purified by chromatography on silica gel (*n-h*exane/EtOAc), affording the deuterated propargyl amide.

N-(2,2-diphenylethyl-2-d)-2,2-diphenyl-N-(2l5-propa-1,2-dien-1-yl)acetamide

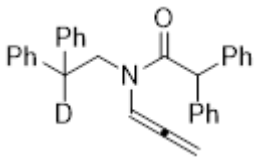

Allene **[D]-1v** was prepared following general procedure **GP-A** from the corresponding propargyl amide (430 mg, 1 mmol). Light-yellow oil (275 mg, 64% yield). Two rotamers were observed due to the dynamic amide group (70:30 mixture of rotamers). Deuterated 99%.

^{1}H NMR (600 MHz, $CDCl_3$) δ 7.66 (t, *J* = 6.5 Hz, 1H RotB), 7.37 – 7.34 (m, 2H RotA, 1H RotB), 7.31 – 7.21 (s, 12H RotA, 12H RotB), 6.95 – 6.93 (m, 4H RotA), 6.86 – 6.85 (m, 4H RotB), 6.52 (t, *J* = 6.2 Hz, 1H RotA), 5.31 – 5.30 (m, 2H RotA, 2H RotB), 5.19 (s, 1H RotA), 4.53 (s, 1H RotB), 4.28 (s, 2H RotA), 3.95 (s, 2H RotB). **^{13}C NMR** (151 MHz, $CDCl_3$) δ 202.4 (RotB), 202.2 (RotA), 170.5 (RotB), 170.3 (RotA), 141.9 (2C RotB), 141.7 (2C RotA), 139.04 (2C RotA), 138.97 (2C RotB), 129.1 (2C RotA), 129.02 (RotB), 128.97 (4C RotB), 128.67 (4C RotA), 128.65 (RotB), 128.63 (2C RotA, 2C RotB), 128.52 (4C RotA), 128.49 (4C RotB), 127.3 (4C RotB), 127.2 (4C RotB), 127.1 (4C RotA), 126.8 (4CRotA), 100.0 (RotA), 98.8 (RotB), 87.3 (RotB), 86.3 (RotA), 55.5 (RotA), 55.4 (RotB), 51.1 (RotB), 48.8 (RotA), 48.5 – 48.3 (m, RotA, RotB). **ESI-HRMS** calcd for $C_{31}H_{26}DNNaO$ $[M+Na]^+$ 453.2053, found 453.2050.

1-(2,2-diphenylethyl-2-d)-3,3-diphenyl-4-vinylazetidin-2-one

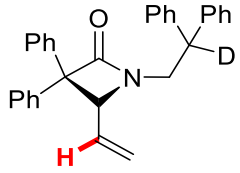

Product **[D]-3V** was prepared following general procedure **GP-2** from the corresponding allene (86.2 mg, 0.2 mmol). Light-yellow oil (51.6 mg, 60% yield).

^{1}H NMR (600 MHz, $CDCl_3$) δ 7.29 – 7.17 (m, 16H), 7.11 – 7.10 (m, 4H), 5.30 – 5.27 (m, 1H), 5.20 – 5.11 (m, 2H), 4.17 (d, *J* = 9.0 Hz, 1H), 4.07 (d, *J* = 14.1 Hz, 1H), 3.66 (d, *J* = 14.1 Hz, 1H). **^{13}C NMR** (151 MHz, $CDCl_3$) δ 169.2, 141.7, 141.3, 140.3, 137.7, 135.0, 128.84 (4C), 128.81 (4C), 128.6 (8C), 128.5 (2C), 128.4 (8C), 128.3 (4C), 128.0 (4C), 127.4 (8C), 127.2 (2C), 127.03 (2C), 127.00 (4C), 121.2 (2C), 70.7, 67.4, 49.4 – 49.2 (m), 45.32. **ESI-HRMS** calcd for $C_{31}H_{27}DNO$ $[M+H]^+$ 431.2234, found 431.2228.

Chapter 4:

‘Remote enantioselective ε-Amination of trienecarbamates enabled by Chiral Phosphoric Acid catalysts in conjugated π-systems’

From this chapter:

Manuscript in preparation

Introduction

The incorporation of functional groups in an enantioselective way at distant positions with respect to the site of coordination of the chiral catalyst represents a powerful and challenging operation for conjugated π-systems.[1] This strategy has proven to be particularly effective in the context of α,β-unsaturated carbonyl compounds and their conjugated analogs bearing a more extended structure. With the latter, chiral amine-based organocatalysis plays a pivotal role. In these transformations, chiral dienamines are generated in situ through the condensation of α,β-unsaturated carbonyls with chiral amines, facilitating highly regio- and enantioselective additions, most commonly at the α and γ positions.[2-4]

Expanding this concept, these intermediates, which are demonstrated to originate from the chiral amine, have emerged as valuable tools for enantioselective synthesis, while their application in remote functionalization remained, for a long time, comparatively less explored than their well-established utility in cycloadditions.[5] However, recent investigations have demonstrated the ability to form bonds selectively at the ε-position.[6]

A notable example comes from Albrecht and co-workers, who reported the first asymmetric ε-functionalization of furfural derivatives via this trienamine activation (intermediate TS-A, Scheme 1), employing nitroolefins as electrophiles.[7] This transformation yielded moderate to good levels of diastereo- and enantioselectivity, with moderate enantiomeric excesses reaching up to 63% (Scheme 1).

- Organocatalytic Non-Classical Trienamine Activation in the Remote Alkylation of Furan Derivatives

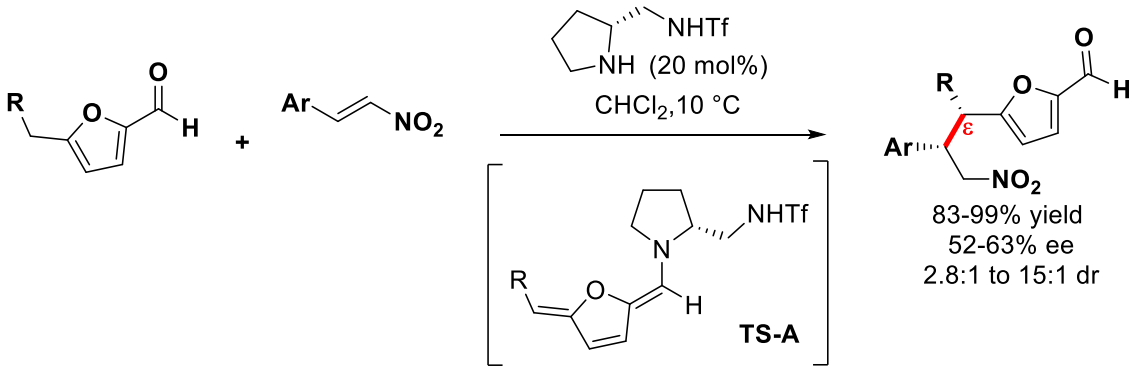

Scheme 1: First asymmetric remote ε-functionalization.

Building on this, Miura and colleagues later improved the enantioselectivity and achieved moderate to high diastereoselectivity using an effective dual aminocatalyst (Scheme 2).[8]

- Expansion of the later work and improvement in diasteroselectivity and enantioselectivity

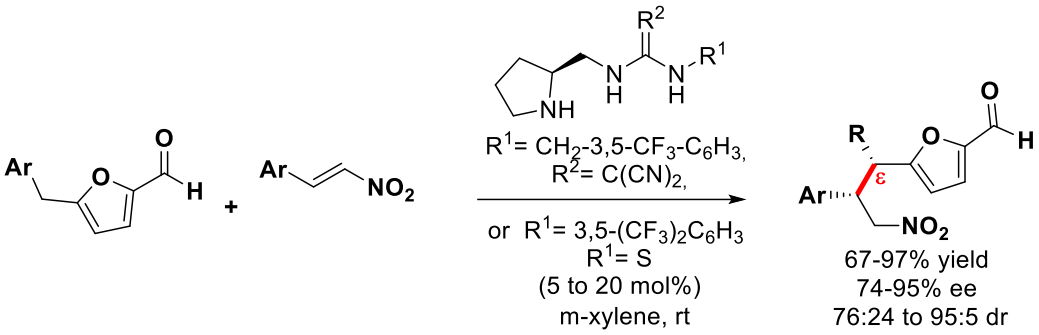

Scheme 2: Work expansion with improvement in diastereoselectivity and enantioselectivity.

These two examples reported the use of nitroolefins as potential electrophiles, but with time, the ε-functionalization was subsequently expanded, including a broader range of other partners, such as α,α-dicyanoalkenes, β-trifluoromethyl enones, β,γ-unsaturated α-ketoesters, and even palladium complexes.[9-11]

However, continuing this trend, Chen group demonstrated that this trienamine catalysis could be extended beyond the furfural cores to other furan-derived substrates.[12] Their enantioselective ε-functionalization of β-allyl-2-cyclohexenone afforded α,α-dicyanodiene derivatives with high enantiomeric excess, as reported in Scheme 3.

- Enantioselective ε-functionalization of β-allyl-2-cyclohexenone by Chen's group

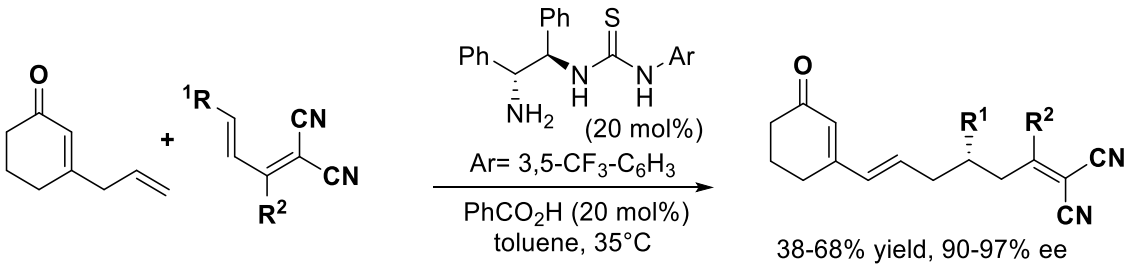

Scheme 3: α,α-dicyanodiene derivatives obtained with high enantiomeric excess by Chen group.

A year later, the Melchiorre group introduced a photo-organocatalytic ε-alkylation of linear dienals using bromomalonates, achieving full ε-selectivity, although with no stereocontrol (Scheme 4).[13]

- Melchiorre's photo-organocatalytic ε-alkylation of linear dienals using bromomalonates

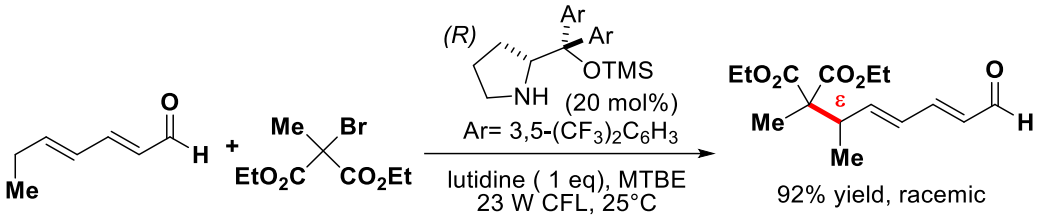

Scheme 4: ε-selectivity strategy performed by Melchiorre group.

Nevertheless, most recently, Kudo and co-workers reported a milestone achievement.[14] In fact, they reported the first catalytic enantioselective ε-alkylation of acyclic γ-branched 2,4-dienals using a peptide-based catalyst, delivering moderate to good enantioselectivities (Scheme 5). This peptide-based strategy is something particularly interesting associated with these reactions due to their tunable nature and to the potential to perform a milder and eventually aqueous-media reaction.

- Most recent catalytic enantioselective ε-alkylation of acyclic γ-branched 2,4-dienals using a peptide-based catalyst

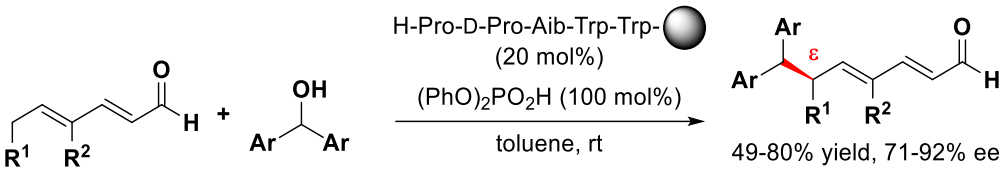

Scheme 5: First catalytic enantioselective ε-alkylation using a peptide-based catalyst.

All these works highlight the significant interest and extensive investigation into the ε-functionalization position of these substrates. Nonetheless, the utility of trienamine catalysis extends beyond ε-functionalization. In fact, this type of chemistry has also enabled regioselective modifications at different positions, such as the β- and γ-positions, as reported in 2012 by Jørgensen and co-workers.[15] In this work, they have disclosed an enantioselective γ-alkylation of cyclic dienones via in situ generated trienamines and olefinic bis-sulfones, achieving complete regioselectivity, high enantioselectivity, and good diastereocontrol (Scheme 6).

- Jørgensen's enantioselective γ-alkylation of cyclic dienones

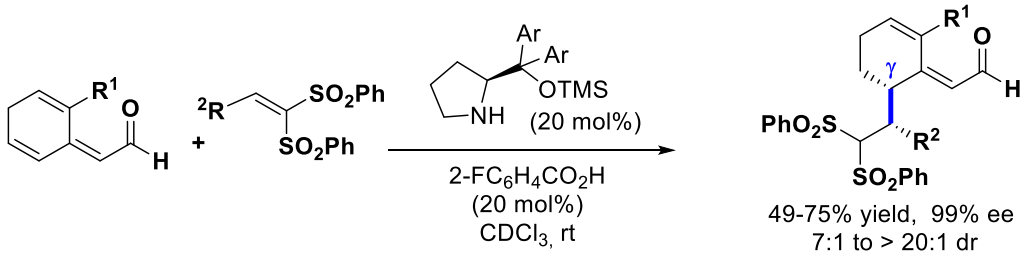

Scheme 6: Jørgensen enantioselective approach.

Later, in 2019, Appayee further expanded the synthetic potential of trienamines by developing an α-alkylation of unsaturated aldehydes using diarylcarbinols in the presence of pyrrolidine.[16] This transformation selectively furnished α-alkylated products in moderate to good yields (Scheme 7).

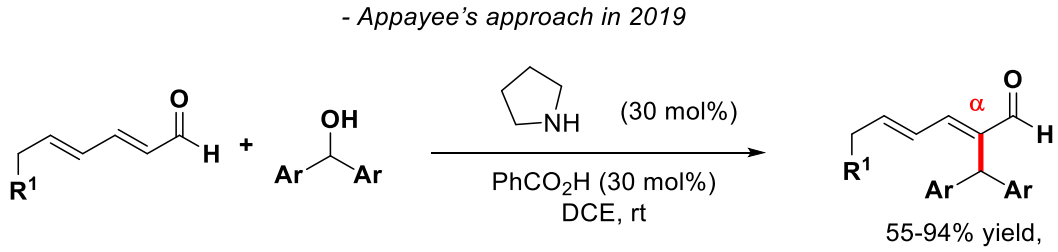

Scheme 7: Appayee non-enantioselective α-alkylation on unsaturated aldehydes.

Taken together, these progressive advancements highlight a clear evolution in the field from early γ- and ε-selective reactions to increasingly sophisticated, catalyst-controlled processes targeting multiple remote positions. This culminates in the most recent contributions, which not only achieve regio- and enantioselectivity but also broaden the landscape of accessible molecular architectures.

Although structurally related to trienamines, trienamides have seen limited exploration in organic synthesis and, to date, they have never been employed as nucleophiles in single-bond-forming additions to electrophiles, as happened instead with trienamines. However, unlike these, trienamides are stable and isolable, thanks to the presence of electron-withdrawing groups (simple amides or carbamates) on the nitrogen atom. On the other hand, the conjugated system presents a reduced electron density, resulting in lower nucleophilicity compared to trienamines. This feature has never been tested for the reactions encountered before. Additionally, the presence of three potentially reactive sites (β, δ, and ε) along the conjugated backbone could inevitably complicate the regioselectivity.

One method that introduces their use is reported in an interesting [4+2] cycloaddition between 2-benzothiazolimines and dienecarbamates.[17] Dienecarbamates have been considered since a long time a valuable building block in organic synthesis. In fact, after being introduced by Overman in 1978, they have been considered units that enable the synthesis of several natural products with surprisingly high regioselectivity and enantioselectivity.[18] In particular, the reaction involved is performed with 4-substituted dienes, producing interesting benzothiazolopyrimidines as the major product in high yields, as a single diastereoisomer and with an ee between 93 and 99%, as shown in Scheme 8.

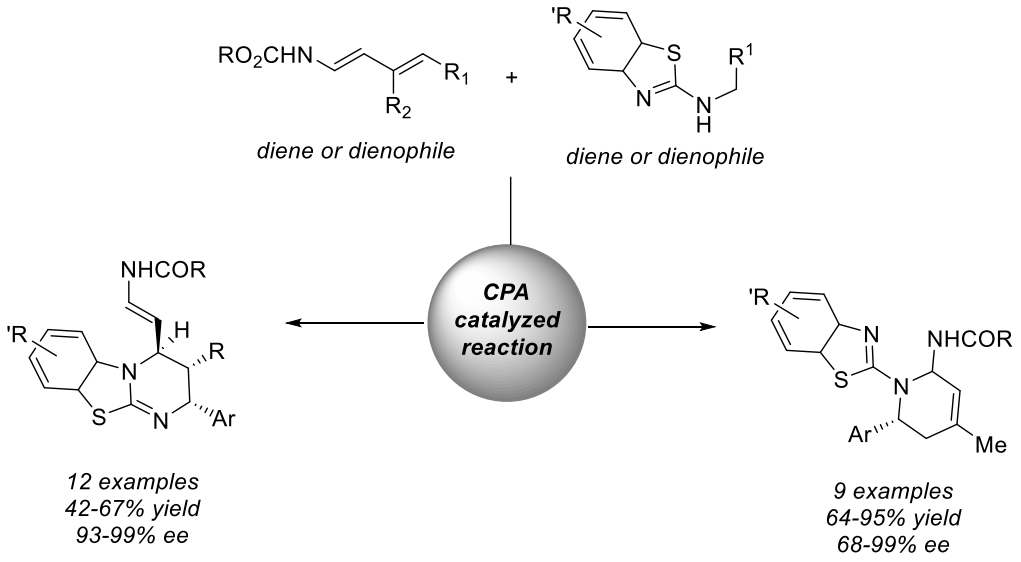

Scheme 8: Chiral Phosphoric Acid-catalyzed enantioselective formal [4+2] cycloaddition using dienecarbamates.

Interestingly, the same reaction performed this time with 3-substituted dienes instead gave highly enantioenriched tetrahydropyridine as major products, even if with moderate diastereoselectivities and enantioselectivities.

More recently, an enantio- and diastereoselective process has been reported, in which *N*H-triene-carbamates are involved. The substrates can lead to three different interesting dihydro oxazine regioisomers with excellent diastereoselectivities and high enantioselectivities, thanks to the careful modeling of the reaction conditions (Scheme 9).[19]

Enantioselective and Regiodivergent Synthesis of Dihydro-1,2-oxazines from Triene-Carbamates via Chiral Phosphoric Acid-Catalysis

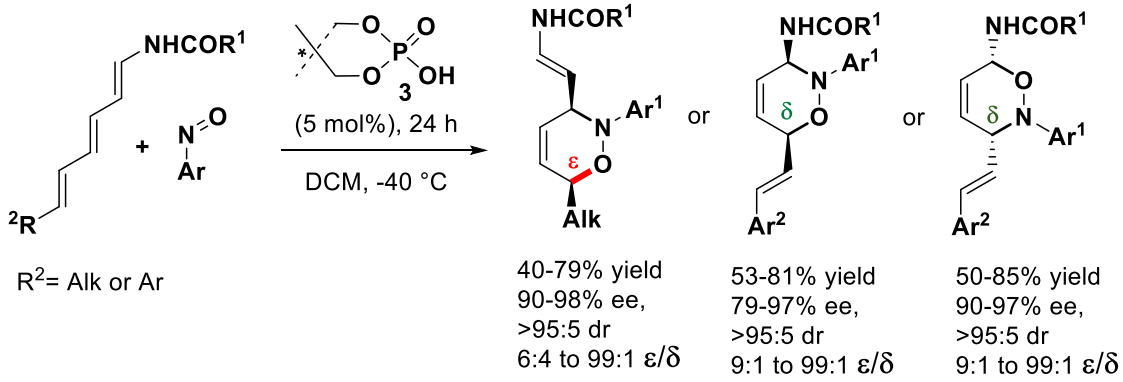

Scheme 9: Recent works with trienamides by Masson and coworkers.

Apart from this work, nowadays, limited success has been achieved in the field of trienamides functionalization due to the challenging control of regioselectivity as well as the difficulties in isolating the starting material to perform the reaction in different conditions.

Results and discussions

In this chapter, the main focus is on the selective remote chiral phosphoric acid-catalyzed enantioselective functionalization at the ε position of trienecarbamate species.

In the introduction, the importance of performing reactions with trienecarbamates as substrates for the enantioselective formation of products featuring stereocenters in a remote ε-position, far from the chiral catalyst's coordination, has been described. Drawing inspiration from earlier works on enamides, it has been hypothesized that a general chiral phosphoric acid catalyst could effectively mediate the enantioselective addition of trienecarbamates to nitrogen-based electrophiles guided by a well-organized hydrogen-bonding environment. This transformation was expected to deliver enantioenriched ε-aminated imine intermediates, which, upon hydrolysis, would yield ε-aminated α,β-dienals, which are known as synthetically versatile building blocks with potential relevance in the preparation of biologically active compounds.[20]

Regarding the partner that triggers this complex reactivity, previous studies employed an azodicarboxylate as the nitrogen electrophile. However, these species are generally good electron donors, and because of that, some complications could arise when applying them to trienecarbamates, due to their possible reactivity as dienophiles.[21]

To overcome this limitation and identify a more suitable electrophilic nitrogen partner, attention focused on *p*-benzoquinone diimines. In fact, numerous examples collectively underscore the broad potential of *p*-benzoquinone diimines as versatile nitrogen electrophiles in enantioselective phosphoric acid-catalysis.[22-23] Motivated by these advances, we set out to explore their compatibility with trienecarbamates. Based on previous results with related systems such as dienecarbamates, which did not undergo cycloaddition with *p*-benzoquinone diimines, a similar behavior was anticipated in this case. Nonetheless, the extended conjugation of trienecarbamates was expected to increase the risk of an undesired cycloaddition pathway, even though the reaction partner had changed.[24]

To test this hypothesis, a model reaction between ((1E,3E,5E)-hepta-1,3,5-trien-1-yl)carbamate (**1a**) and N, N'-tosyl-p-benzoquinone diimine (**2a**) in dichloromethane (DCM), via chiral phosphoric acid (CPA) catalysis, has been examined, as described by Scheme 1.

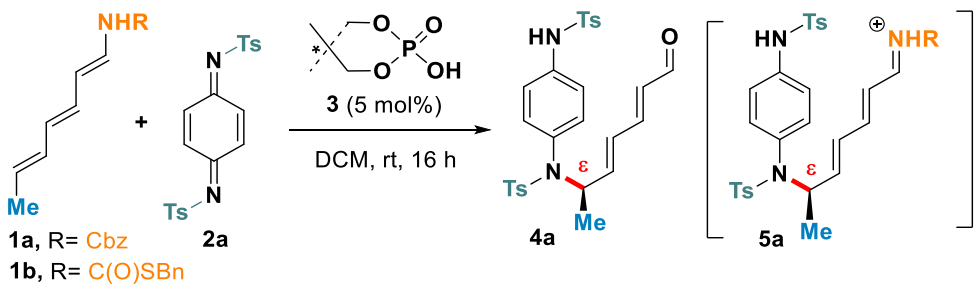

Scheme 1: Examination of reaction model.

The reaction has been conducted at room temperature with 5 mol% of (S)-TRIP (**3a,** Scheme 2), a BINOL-derived CPA, which led to the formation of the desired ε-N-alkylated α,β-unsaturated aldehyde **4a**, generated through in situ hydrolysis of the corresponding iminium intermediate **5a**, reported in Scheme 1. The product was obtained in 61% yield as a single regioisomer, with both olefins in the E configuration, and exhibited a promising 44% enantiomeric excess.

A complex optimization effort started. For this one, a great variety of chiral phosphoric acid catalysts have been taken into consideration, as reported in Scheme 2.

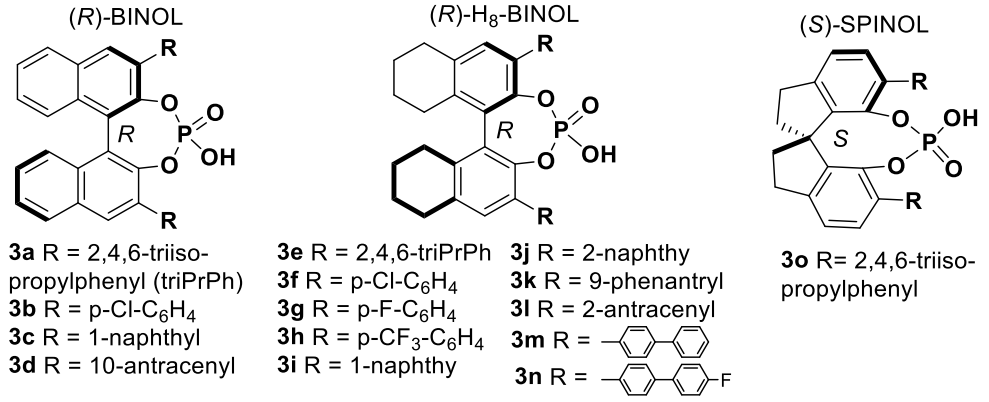

Scheme 2: Class of chiral phosphoric acid catalyst used for the optimization effort.

Entry	Catalyst	SM 1	Temperature	**4a** yield [%][b]	**4a** ee [%][c]
1	(*R*)-**3a**	1a	rt	61	44
2	(*R*)-**3b**	1a	rt	31	41
3	(*R*)-**3c**	1a	rt	69	47
4	(*R*)-**3d**	1a	rt	30	42
5	(*R*)-**3e**	1a	rt	52	60
6	(*R*)-**3f**	1a	rt	80	67
7	(*R*)-**3g**	1a	rt	69	78
8	(*R*)-**3h**	1a	rt	75	53
9	(*R*)-**3i**	1a	rt	78	63
10	(*R*)-**3j**	1a	rt	74	71
11	(*R*)-**3k**	1a	rt	85	55
12	(*R*)-**3l**	1a	rt	42	44
13	(*S*)-**3o**	1a	rt	75	18
14	(*R*)-**3m**	1a	-20°C	40	78
15	(*R*)-**3m**	1a	-20°C	61	80
16	(*R*)-**3 m**	1b	-20°C	63	82
17[d]	(*R*)-**3 m**	1b	-20°C	52	86

18[d]	(*R*)-**3n**	1b	-20°C	61	90

Table 1: [a] Reaction conditions: 0.1 mmol of **1a** (0.1 M), 5 mol% of CPA catalyst additive, reaction run for a total of 24 hours; [b] Isolated yield after preparative column chromatography, [c] Determined by HPLC analysis on a chiral stationary phase vs the racemic. [d] Triene added as a solution already at -20°C.

This reaction and its corresponding enantioselectivity are highly influenced by the chiral phosphoric acid involved. It is well known in literature that these are recognized as efficient organocatalysts for a variety of enantioselective transformations to achieve high enantiomeric excesses, especially for reactions involving carbon–carbon and carbon–heteroatom bond formation.[25-26] Nowadays, these are easily built with different skeletons and with different functional groups. In entry 13, CPAs based on the SPINOL framework are reported, and this kind of skeleton is demonstrated to be associated with low enantioselectivity. In contrast, catalysts derived from the H_8-BINOL backbone consistently demonstrated superior asymmetric induction relative to their classical BINOL-derived counterparts. Usually, to introduce a variation on these catalysts, the positions which are subject of interest are the C3 and C3′. Comparing catalysts with the same variations and with a hydrogenated skeleton or not demonstrated to give different results (entries 1–4 vs. 5–12). This feature is probably justified by the fact that a larger dihedral angle of hydrogenated BINOL-derived phosphoric acid catalysts creates a more three-dimensional and sterically confined chiral environment. Additionally, an optimization of hydrogen-bonding and ion-pairing interactions and a major stabilization of a more selectively organized transition state contribute decisively to the enhanced reactivity and stereocontrol observed.

Incorporation of 4-chlorophenyl substituents at the C3 and C3′ positions of the H_8-BINOL catalyst improved the ε-aminated product **4a** yield to 80% with 67% ee (entry 6). Then, the chlorine substituent has been substituted with a slightly more electronegative 4-fluorophenyl group (entry 7). The result was a lower yield (69%) but a significant improvement in the enantioselectivity (78% ee). This feature led us to further increase the electron-withdrawing character by testing 4-trifluoromethylphenyl groups (entry 8). Unfortunately, this functional group turned out to be particularly disappointing due to a drastic drop in enantioselectivity (53% ee).

Then attention has been focused on catalyst **3j**, bearing a 2-naphthyl substituent, but this attempt delivered product **4a** in 74% yield with 71% ee (entry 10). When bulkier aromatic groups such as 9-phenanthryl or 2-anthracenyl were introduced, a decrease in enantioselectivity was observed, with ee values dropping to 55% and 44%, respectively (entries 11 and 12).

However, this study shows that modifications of the catalyst structure, such as altering the C3 and C3′ positions with bulky groups, electron-withdrawing substituents, or motifs that promote π–π interactions, failed to deliver significant improvement in achieving better enantiomeric excesses. These findings highlight the limitations of empirical approaches in identifying an optimal CPA for this transformation and motivate a shift toward a data-driven strategy, using machine learning.[27-28] This powerful tool led to a selection of different CPAs to form a chemically diverse Universal Training Set (UTS), designed to explore a broad range of enantioselectivities and maximize the model training potential. In addition, a separate set of CPAs was prepared to constitute a test set (TS), enabling a preliminary evaluation of the model's capacity to extrapolate beyond the training data. The

catalytic performance of each CPA in the UTS and TS was then evaluated in the ε-amination on the model reaction and enantiomeric excesses, as well as the corresponding yields, were determined. The experimental results were then used to initiate model training and the analysis initially indicated that [H_8]-BINOL-derived CPA bearing 4-phenylphenyl substituents **3m** could deliver the highest enantioselectivity.

Indeed, other modifications that emerged to be effective in other works[21] were tried with the goal of increasing the enantiomeric excesses. For example, we tested the optimized catalyst at –20 °C, obtaining the ε-aminated product **4a** with 80% ee (entry 15). The use of thiocarbamate substitution (**1b**) enhanced the stereoselectivity of the reaction. These substrates are more difficult to prepare because of their cumbersome isolation, but enantioselectivity has been improved, affording **4a** with 82% ee (entry 16). At this point, different solvents were also evaluated, but none outperformed DCM in terms of enantioselectivity. Pleasingly, the slow addition of the trienethiocarbamate **1b** solution to a mixture of quinone and CPA at –20 °C further improved the enantioselectivity to 86% ee (entry 17).

In the end, previous observations showed that fluorine substituents enhanced catalyst performance, leading us to prepare and evaluate a 4-fluorophenylphenyl-derived CPA (**3n**). As a result, we finally achieved a superior enantiomeric excess of 90% ee.

This extensive optimization successfully established the best-performing conditions for the ε-amination reaction: 4-fluorophenylphenyl [H_8]-BINOL CPA **3n** as catalyst, triene bearing thiocarbamate as substrate and DCM solvent at –20 °C. The reaction has been generalized (Scheme 3).

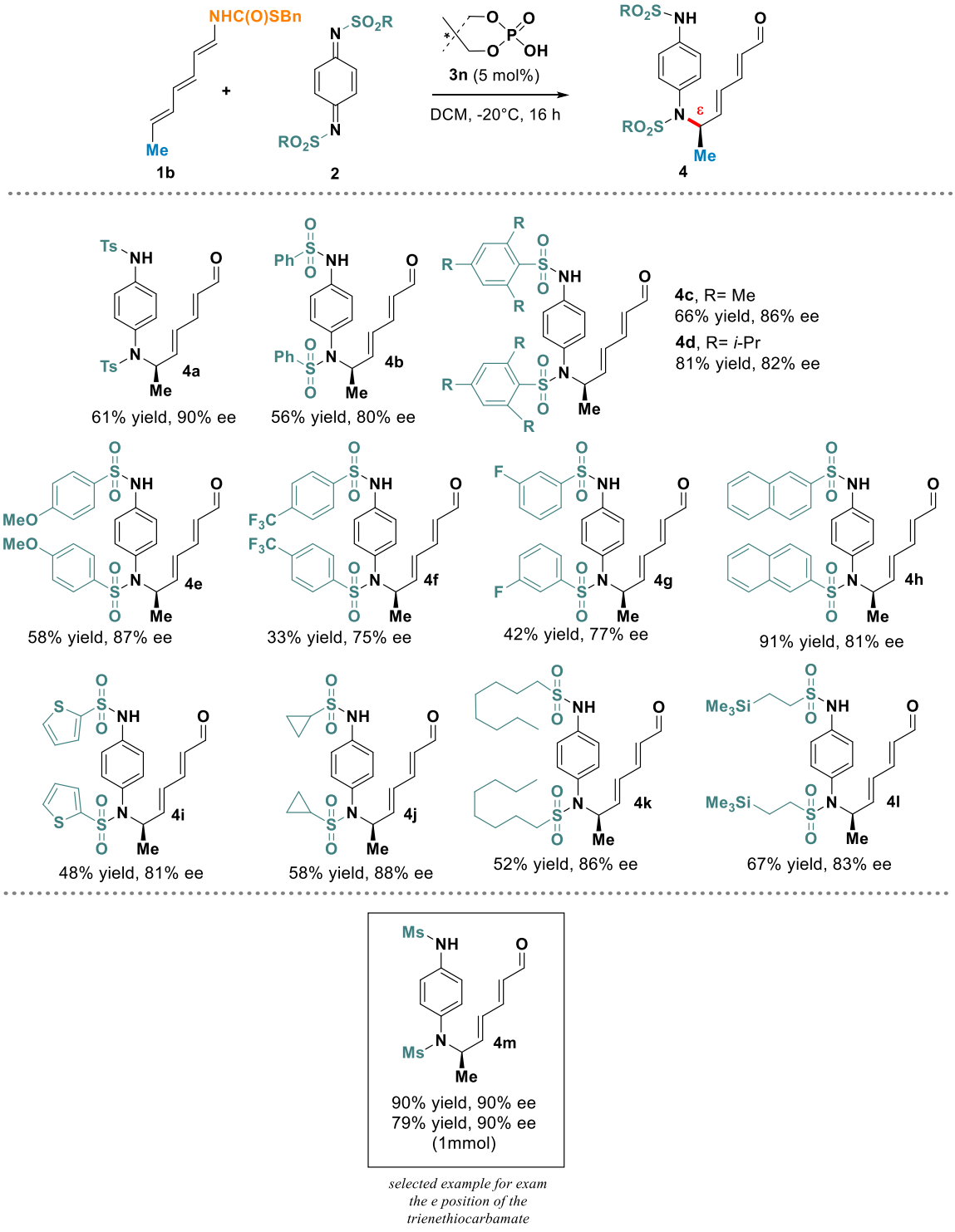

Scheme 3: Scope of enantioselective synthesis of ε-aminated dienals

First we subjected model trienethiocarbamate **1b** to the reaction with a variety of p-benzoquinone diimines. Interestingly, we observed that modifications to the sulfonyl group influenced both the yields and enantioselectivities but never the regioselectivity, allowing us to isolate different interesting products. For instance, substituting the *p*-tolyl group with a phenyl group led to **4b** with a 10% decrease in enantioselectivity.

Both bulky 2,4,6-trimethylphenyl and *p*-methoxyphenyl groups formed products **4c** and **4d** with enantioselectivities slightly lower than 90% ee. While the more sterically hindered 2,4,6-triisopropylphenyl group resulted in diminished enantioselectivity, it surprisingly resulted in the formation of **4d** in slightly improved yield (82%). The presence of electron-withdrawing groups on the aryl ring, such as 4-CF_3 (**4f**) or 3-F (**4g**), consistently reduced both the yield and enantioselectivity. Heteroaromatic and naphthyl derivatives were also tolerated, giving us the possibility to isolate products **4h** and **4l** with 81% ee and 91% ee, respectively and both with 48% yields. Also, aliphatic sulfonyl groups, including cyclopropyl, octenyl, and 2-(trimethylsilyl)ethyl, proved to be compatible, providing the corresponding ε-aminated aldehydes (**4j-4l**) in satisfactory yields and good enantioselectivities ranging from 83% to 88% ee. The use of di-mesylated *p*-benzoquinone diamine, **2m** proved to be one of the most relevant examples, obtaining product **4m** with 90% ee, with a notably enhanced yield (90%). The scalability of the protocol was further demonstrated by a 1 mmol synthesis of compound **4m**, which afforded the desired product in slightly reduced yield while maintaining the same level of enantioselectivity.

Encouraged by these initial results, we proceeded to examine the influence of ε-substitution on the reactivity of trienethiocarbamates, using *p*-benzoquinone diimine **2m** as the electrophilic nitrogen source (Scheme 4).

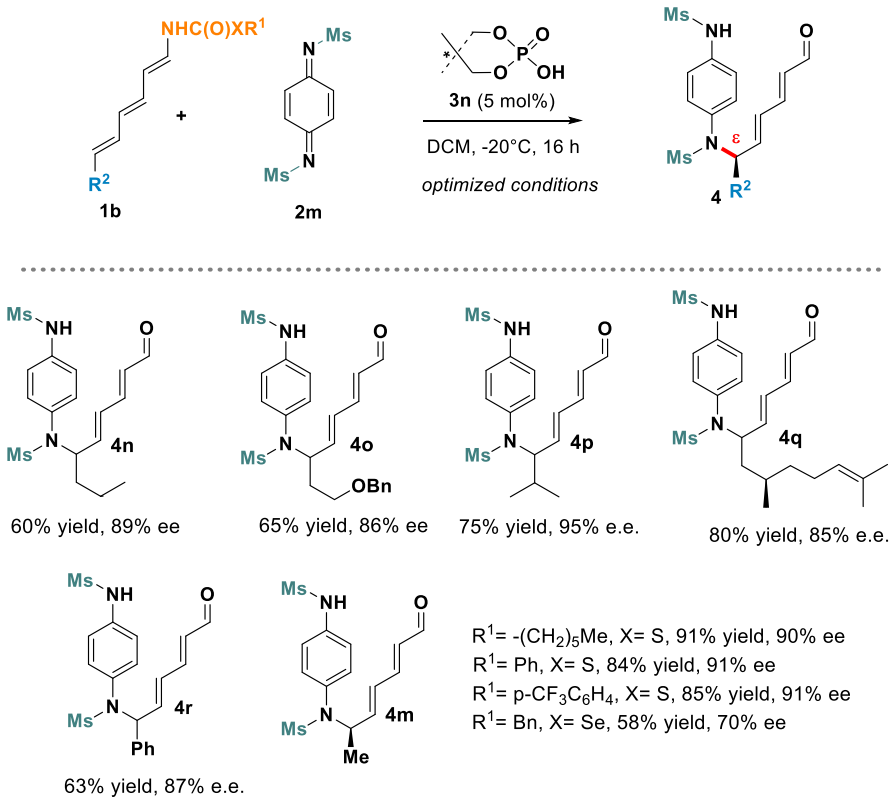

Scheme 4: Scope of ε-aminated dienals differently ε-substituted.

Fortunately, trienethiocarbamates bearing various linear alkyl chains were readily converted into the corresponding ε-aminated aldehydes (**4n** and **4o**), each obtained with good levels of enantioselectivity.

Remarkably, we also found that a branched alkyl group such as isopropyl could be successfully incorporated at the ε-position, delivering product **4p** in 95% enantiomeric excess. Notably, the substrate derived from (S)-citronellol underwent smooth conversion to give **4q** as a single diastereomer, in excellent yield and with 85% ee. In contrast to our previous findings in the nitroso-Diels–Alder reaction,[29] the triene substrate featuring a phenyl substituent at the ε-position cleanly produced the corresponding ε-aminated product **4r** in 83% yield and 87% ee, without evidence of competing reactivity. Further investigations into the role of the thiocarbamate moiety revealed that variations in its substitution pattern had minimal impact on enantioselectivity. Both alkyl- and aryl-substituted thiocarbamates, including those bearing electron-withdrawing groups designed to enhance the acidity of the NH proton, consistently afforded products **4m** with excellent enantioselectivities (90–91% ee). However, when a selenium-containing trienecarbamate has been tested, a marked drop in enantioselectivity was observed.

To better understand the mechanism, the outcomes of some control experiments have been analyzed (Scheme 5).

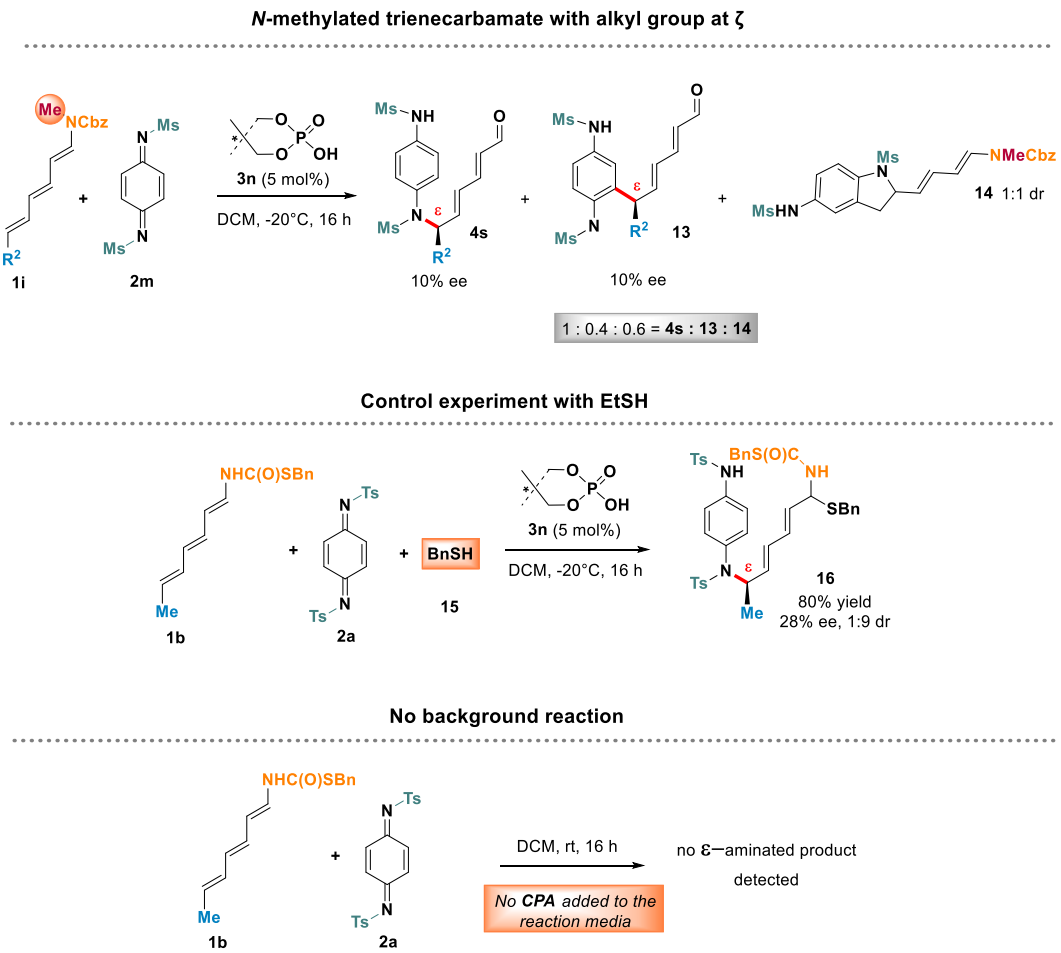

Scheme 5: Control experiments for the transformation.

Having a free NH group has a great importance in secondary trienethiocarbamates during the chiral phosphoric acid (CPA)-catalyzed enantioselective ε-amination. In fact, when a tertiary N-methylated derivative has been

tested (**1i**) with *p*-benzoquinone diimine (**2m**) under the standard reaction conditions, the desired ε-aminated product **4s** was obtained, but enantioselectivity dropped drastically to only 10% ee (Scheme 5). In addition, the reaction gave rise to a C-alkylated byproduct **13**, also with poor stereocontrol, as well as an indoline derivative **14**, formed via a (3+2) cycloaddition involving the terminal alkene of **1i** and the azodiene. These outcomes strongly suggest that the NH group in secondary trienethiocarbamates plays a crucial role. To further investigate this hypothesis, another control experiment has been performed by introducing benzyl mercaptan (**15**) as an additive. Its protic character was expected to interfere with the catalyst's hydrogen-bonding network, perturbing the asymmetric induction involved in the catalytic cycle. Under these conditions, the reaction led to the formation of α-amido-sulfone diene **16** through electrophilic ε-amination. While the product was obtained in good yield and with high diastereoselectivity (9:1 dr), enantioselectivity was significantly reduced (28% ee). Moreover, the ε-amination of **1i** failed to proceed in the absence of the CPA catalyst, indicating that phosphoric acid is essential not only for activating the electrophile (**2m**) but also for engaging the trienethiocarbamate nucleophile.

Taken together, these findings support a mechanistic model in which the chiral phosphoric acid catalyst initially forms a hydrogen bond with the *p*-benzoquinone diimine (**2**), while the NH moiety of the trienethiocarbamate simultaneously coordinates with the phosphoryl oxygen of the catalyst. This dual interaction aligns the two substrates in a well-defined chiral pocket, facilitating a stereoselective approach of the nucleophile to the electrophilic nitrogen in the transition state. A key step in this pathway involves a proton transfer within the catalyst complex, leading to the formation of the iminium intermediate (**5**), which is subsequently hydrolyzed to yield the final ε-aminated dienal product (**4**). An early in situ ^{1}H-NMR monitoring revealed early formation of the aldehyde product, despite the use of rigorously dried solvents and glassware. This suggests that hydrolysis of the iminium intermediate occurs earlier than anticipated, and it is likely promoted by trace water weakly coordinated to the CPA catalyst, which may be sufficient to trigger the transformation.

However, to further corroborate the mechanism described, further DFT calculations will be carried out.

Conclusions

In this work, the first enantioselective electrophilic ε-amination of trienecarbamates via phosphoric acid catalysis is described. This transformation provides direct access to ε-aminated α,β-conjugated dienals with high enantioselectivity and broad substrate scope. Optimization guided by both catalyst structure activity studies and machine learning identified an [H_8]-BINOL-derived CPA as the most efficient catalyst. Control experiments established the essential role of the NH group in both enantio- and regioselectivity, and NMR studies revealed that iminium hydrolysis occurs early in the reaction, probably due to the presence of traces of water coordinated to the catalyst. The ε-aminated dienals obtained were shown to be versatile scaffolds for possible product valorizations.

References

[1] M. Oiarbide, C. Palomo, *Chem. Eur. J.,* **2021**, 27, 10226–10236.

[2] C. Curti, L. Battistini, A. Sartori, F. Zanardi*, Chem. Rev*., **2020**, 120, 2448–2612.

[3] H. Jiang, L. Albrecht, K. A. Jørgensen, *Chem. Sci.,* **2013**, 4, 2287–2300.

[4] C. J. F. Cole, L. Fuentes, S. A. Snyder, *Chem. Sci.,* **2020**, 11, 2175–2180.

[5] S. Li, X. Li, H. Yao, M. Tan, D. Xu, N. Huang, N. Wang, *Org. Chem. Front.*, **2024**,11, 236-253.

[6] S. Muthusamy, V. Kesavan, *Eur. J. Org. Chem.,* **2019**, 4046–4055.

[7] M. Dyguda, A. Przydacz, A. Krzemińska, L. Albrecht, *Org. Biomol. Chem.,* **2019**, 17, 6025–6031.

[8] H. Akutsu, K. Nakashima, Y. Kanetsuna, M. Kawada, S. I. Hirashima, T. Miura, *Synthesis*, **2020**, 52, 3874-3880.

[9] G. J. Yang, W. Du, Y. C. Chen, *J. Org. Chem.,* **2016**, 81, 10056–10061.

[10] M. H. Xu, Y. H. Yuan, D. D. Liang, X. M. Zhang, F. M. Zhang, Y. Q. Tu, A. J. Ma, K. Zhang, J. P. Peng, *Org. Chem. Front.,* **2021**, 8, 3292–3297.

[11] Y. L. Su, Z. Y. Han, Y. H. Li, L. Z. Gong, *ACS Catal.,* **2017**, 7, 7917–7922.

[12] X. Feng, Z. Zhou, X. Yin, R. Li, Y. C. Chen, *Eur. J. Org. Chem.,* **2014**, 5906–5909.

[13] M. Silvi, E. Arceo, I. D. Jurberg, C. Cassani, P. Melchiorre, J. Am. Chem. Soc., **2015**, 137, 6120–6123.

[14] Q. Liu, K. Akagawa, K. Kudo, Chem. Commun., **2025**, 61, 5467–5470.

[15] K. S. Halskov, T. K. Johansen, R. L. Davis, M. Steurer, F. Jensen, K. A. Jørgensen, *J. Am. Chem. Soc.,* **2012**, 134, 12943–12946.

[16] V. M. D. Padmaja, S. Jangra, C. Appayee, *Org. Biomol. Chem.,* **2019**, 17, 1714–1717.

[17] W. Y. Ma, E. Montinho-Inacio, B. I. Iorga, P. Retailleau, X. Moreau, L. Neuville, G. Masson, *Adv. Synth. Catal.,* **2022**, 364, 1708-1715.

[18] L. E. Overman, G. F. Taylor, C. B. Petty, P. J. Jessup, *Journal of Organic Chemistry*, **1978**, 43, 2164-2167.

[19] E. Naulin, M. Lombard, V. Gandon, P. Retailleau, E. V. Elslande, L. Neuville, G. Masson, *J. Am. Chem. Soc.,* **2023**, 145, 26504–26515.

[20] T. Farghaly, A. M. Abo Alnaja, M. R. Shaaban, *Curr Org Synth.,* **2021**, 7, 639-684.

[21] T. Varlet, G. Levitre, P. Ratailleau, G. Masson, *Bioorganic and Medicinal Chemistry*, **2019**, 27, 2438-2443.

[22] Y. Nishiyama, Y. Ikagami, S. Seto, *Bull. Chem. Soc. Jpn.* **1965**, 38, 72–76.

[23] J. Qin, T. Zhou, T.-P. Zhou, L. Tang, H. Zuo, H. Yu, G. Wu, Y. Wu, R.-Z. Liao, F. Zhong, *Angew. Chem. Int. Ed.* **2022**, *61*, e202205159.

[24] W. Y. Ma, C. Gelis, D. Bouchet, P. Retailleau, X. Moreau, L. Neuville, G. Masson, *Org. Lett.* **2021**, 23, 442–448.

[25] A. G. Woldegiorgis, X. Lin, *Beilstein J. Org. Chem.,* **2021**, 17, 2729-2764.

[26] F. Zhou, H. Yamamoto, *Angew. Chem. Int. Ed.* **2016**, 55, 8970-8974.

[27] A. F. Zahrt, J. J. Henle, B. T. Rose, Y. Wang, W. T. Darrow, S. E. Denmark, *Science*, **2019**, 363, eaau5631.

[28] J. J. Henle, A. F. Zahrt, B. T. Rose, W. T. Darrow, Y. Wang, S. E. Denmark, *J. Am. Chem. Soc.,* **2020**, *142*, 11578–11592.

[29] A. Dumoulin, G. Masson, *J. Org. Chem.,* **2016**, 81, 10154–10159.

Experimental section

General remarks

All reactions were carried out in oven-dried glassware with magnetic stirring. Reagents were obtained from commercial suppliers and used without further purification unless otherwise noted. Syntheses of trienecarbamates, thio-trienecarbamates as well as the quinone diimides were synthesized following known procedure and for those already reported the spectral data fully matched with the literature data.

Phosphoric acid catalysts were synthesized according to reported literature procedures. Analytical thin layer chromatography (TLC) was purchased from Merck KGaA (silica gel 60 F254). Visualization was accomplished by irradiation with a UV light at 254 nm. Flash column chromatography was performed using silica gel 60 (0.040-0.063 mm) (Merck). Analytical thin layer chromatography (TLC) was performed using silica gel 60 F254. ^{1}H NMR and ^{13}C spectra were recorded with Bruker 500 MHz and 300 MHz instruments. Proton chemical shifts are reported in ppm (δ) relative to tetramethylsilane (TMS) with the solvent resonance employed as the internal standard ($CDCl_3$, δ 7.26 ppm). Data are reported as follows: chemical shift, multiplicity (s = singlet, br s = broad singlet, d = doublet, t = triplet, q = quartet, qt = quintuplet, h = hexuplet, ht = heptuplet, m = multiplet), coupling constants (Hz) and integration. ^{13}C chemical shifts are reported in ppm from tetramethylsilane (TMS) with the solvent resonance as the internal standard ($CDCl_3$, 77.2 ppm). Infrared spectra were recorded on neat samples, with a Perkin Elmer Spectrum BX FT-IR spectrometer and the characteristic IR absorption frequencies are reported in cm^{-1}. UPLC-MS analysis was run using an Acquity Waters UPLC equipped with a Waters LCT Premier XE (ESI ionization) and a Waters Acquity PDA detector, using a column BEH C18 1.7 µm, 2.1 mm × 50 mm. Gradients were run using water and acetonitrile (1:1) with 0.1% of acetic acid. Temperature: 40°C. UV detection from 210 to 410 nm. ESI+ detection in the 80−1500 m/z range. Chiral HPLC analysis was performed on Hitachi LaChrom-Elite apparatus equipped with diode array UV detector (UV detection monitored at 254 nm or 214 nm), using Daicel Chiralcel OD-H, IA, IB and IC columns. The enantiomeric excesses were determined by HPLC analysis employing the chiral stationary phase column specified in the individual experiment, by comparing the samples with the appropriate racemic mixtures. Optical rotations were performed on a Jasco P-1010 polarimeter (589 nm) using a 700- µL cell with a path length of 1 dm.

Synthesis of substrates

Synthesis of trienecarbamates

Note: The triene-carbamates, thiotriene-carbamates and selenotriene-carbamate are not very stable at r.t.and should be stored under an inert atmosphere in the freezer (-20°C). Moreover, it seems important to remove the thiol correctly from the last step, which seems to favour degradation more rapidly.

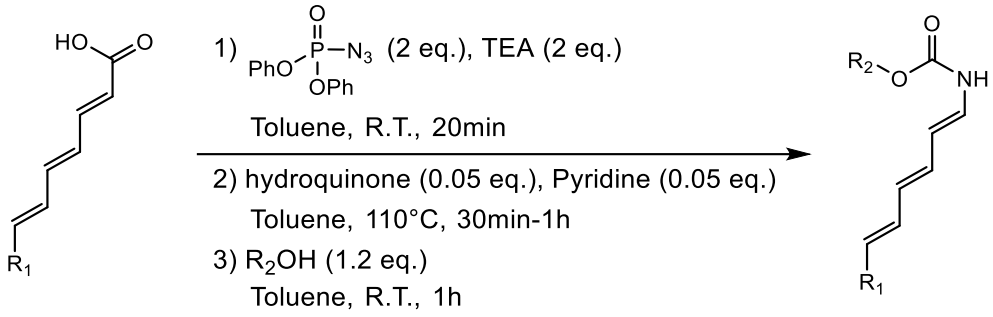

Step 1: To a solution of trienoic acid (1.0 equiv.) in distilled toluene (0.15 M), Et_3N (2.0 eq) was added, and then diphenylphosphoryl azide (DPPA, 2.0 eq.) was added dropwise. The mixture was stirred 20min at room temperature until completion. Then, the limpid brown solution was diluted with brine, and the layers were separated. The yellow organic layer was dried over Na_2SO_4 and concentrated by 2/3 under reduced pressure (not to dryness, the azide can be explosive!). Then, the crude acyl azide was purified by column chromatography on silica gel (PET/EtOAc) and fraction were concentrated by 2/3 under reduced pressure. Toluene was added and concentration by 2/3 was repeated (not to dryness again).

Step 2: The acyl-azide solution was added dropwise (10 min) to a mixture of hydroquinone and pyridine already at 110°C. After the addition, the corresponding alcohol was injected dropwise, and the solution was stirred for an additional 50 min (around 1h in total). The mixture was concentrated under reduced pressure, and the crude product was dissolved in a minimum amount of DCM, n-Heptane was then added. DCM was removed under reduced pressure, and the mixture was filtered. Finally, the recovered solid was dried under high vacuum to afford the corresponding thiotrienecarbamate.

Synthesis of thiotrienecarbamates

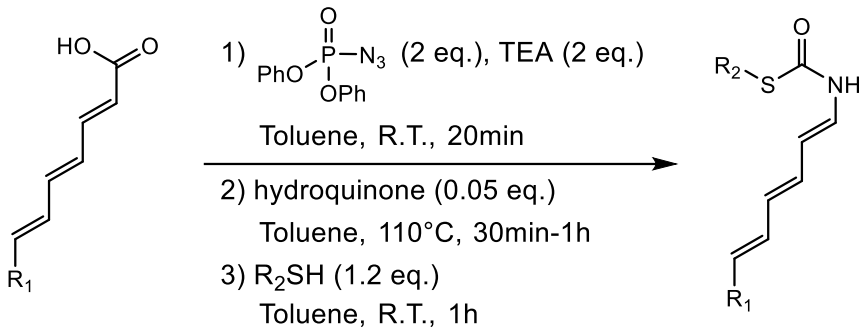

Step 1: To a solution of trienoic acid (1.0 equiv.) suspended in distilled toluene (0.15 M), Et_3N (2.0 eq.) was added. Then, diphenylphosphoryl azide (DPPA, 2.0 eq.) was added dropwise. The mixture was stirred at room temperature until completion (20 min). Then, the limpid brown solution was diluted with brine, and the layers were separated. The yellow organic layer was dried over Na_2SO_4 and concentrated by 2/3 under reduced pressure (not to dryness, the azide can be explosive!). Then, the crude acyl azide was purified by column chromatography on silica gel (PET/EtOAc) and the fraction was concentrated by 2/3 under reduced pressure. Toluene was added and the concentration by 2/3 was repeated (not to dryness again).

Step 2: The acyl-azide solution was then added very dropwise (10 min) into a solution of hydroquinone at 110°C, the mixture is stirred until no more bubbles were observed (30min to 1h). The mixture is then cooled to R.T. and the corresponding thiol is injected dropwise; the solution is stirred for an additional 50 min. The mixture was concentrated under reduced pressure, and the crude product was dissolved in a minimum amount of DCM, n-Heptane was then added. DCM was removed under reduced pressure, and the mixture was filtered. Finally, the recovered solid was dried under high vacuum to afford the corresponding thiotriene-carbamate.

Synthesis of quinone-di-imines

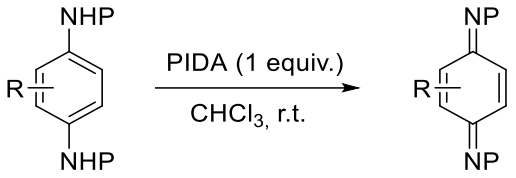

To a stirred solution of the corresponding amine (1mmol) in $CHCl_3$ (7mL/mmol), was added PIDA (1 equiv). The mixture was stirred overnight at room temperature. The reaction was then diluted with water and quenched with a saturated solution of aqueous $NaHCO_3$ (0.1 M). Aqueous layer was extracted three times with DCM, the combined organic layers were dried over Na_2SO_4 and concentrated in vacuo. The crude product was rapidly filtered through a plug of silica with DCM as eluent to afford the desired product.

Characterization of substrates

Trienes

_S_-benzyl ((1E,3E,5E)-hepta-1,3,5-trien-1-yl)carbamothioate

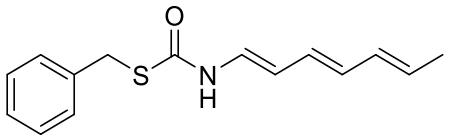

Prepared according to general procedure to provide the title compound **1a** as pale-yellow solid. (400 mg, 78% yield).

^{1}H NMR (300 MHz, $CDCl_3$) δ 7.38 – 7.27 (m, 5H), 7.08 – 6.75 (m, 2H), 6.16 – 5.96 (m, 3H), 5.79 – 5.57 (m, 2H), 4.20 (s, 2H), 1.76 (d, *J* = 5.8 Hz, 3H).

^{13}C NMR (75 MHz, $CDCl_3$) δ 131.86, 131.26, 129.01, 128.81, 127.57, 127.33, 124.45, 116.37, 113.73, 34.52, 18.36.

HRMS (ESI-TOF) m/z: $[M + H]^+$ Calcd for $C_{15}H_{18}NOS$ 260.1104, found 260.1109.

IR (neat) *v* (cm^{-1}): 3281, 3015, 2909, 1655, 1638, 1630, 1601, 1507, 1492, 1448, 1267, 1227, 1204, 1109, 982, 913, 856, 708, 691.

S-benzyl ((1E,3E,5E)-7-ethylepta-1,3,5-trien-1-yl)carbamothioate

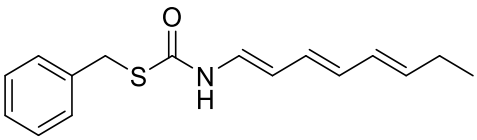

Prepared according to general procedure to provide the title compound **1n** as pale-yellow solid. (311 mg, 57% yield).

^{1}H NMR (300 MHz, $CDCl_3$) δ 7.40 – 7.27 (m, 4H), 7.04 – 6.74 (m, 2H), 6.16 – 5.95 (m, 3H), 5.80 – 5.69 (m, 1H), 5.63 (dd, *J* = 14.8, 6.8 Hz, 1H), 4.20 (s, 2H), 2.34 (h, *J* = 6.7 Hz, 1H), 1.00 (d, *J* = 6.7 Hz, 6H).

^{13}C NMR (75 MHz, $CDCl_3$) δ 159.81, 141.65, 131.53, 129.01, 128.80, 127.57, 124.41, 113.74, 112.05, 102.23, 68.17, 34.53, 31.37, 22.49.

HRMS (ESI-TOF) m/z: $[M + H]^+$ Calcd for $C_{17}H_{22}NOS$ 288.1417, found 288.1422.

IR (neat) *v* (cm^{-1}): 3294, 2965, 2932, 1648, 1495, 1454, 1366, 1187, 988, 834, 698.

S-benzyl ((1E,3E,5E)-8-((tert-butyldiphenylsilyl)oxy)octa-1,3,5-trien-1-yl)carbamothioate

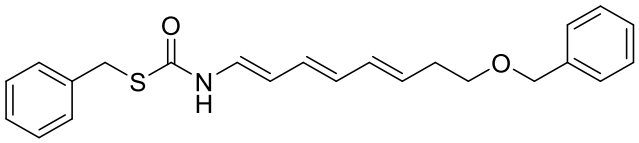

Prepared according to general procedure to provide the title compound **1o** as pale-yellow solid. (267 mg, 43% yield).

^{1}H NMR (300 MHz, $CDCl_3$) δ 7.44 – 7.27 (m, 11H), 7.11 – 6.77 (m, 2H), 6.20 – 6.00 (m, 3H), 5.80 – 5.59 (m, 2H), 4.52 (s, 2H), 4.20 (s, 2H), 3.52 (t, *J* = 6.7 Hz, 2H), 2.41 (q, *J* = 7.1 Hz, 2H).

^{13}C NMR (75 MHz, $CDCl_3$) δ 138.62, 132.29, 131.01, 130.17, 129.01, 128.81, 128.52, 128.33, 127.82, 127.71, 127.57, 124.82, 120.41, 120.35, 113.57, 73.10, 69.96, 34.52, 33.40.

HRMS (ESI-TOF) m/z: $[M + H]^+$ Calcd for $C_{23}H_{26}NO_2S$ 380.1679, found 380.1684.

IR (neat) *v* (cm^{-1}): 3277, 3017, 2860, 2171, 1651, 1629, 1600, 1505, 1494, 1453, 1228, 1210, 1076, 982, 874, 747, 693.

S-benzyl ((1E,3E,5E)-8-methylnona-1,3,5-trien-1-yl)carbamothioate

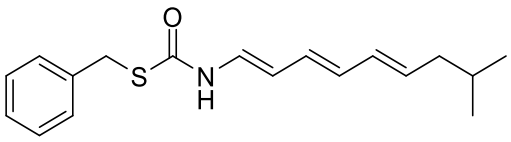

Prepared according to general procedure to provide the title compound **1p** as pale-yellow solid. (311 mg, 59% yield).

^{1}H NMR (300 MHz, $CDCl_3$) δ 7.41 – 7.27 (m, 4H), 7.04 – 6.77 (m, 2H), 6.16 – 5.97 (m, 3H), 5.83 – 5.56 (m, 2H), 4.20 (s, 2H), 1.97 (t, *J* = 6.9 Hz, 2H), 1.62 (hept, 4H), 0.88 (d, *J* = 6.5 Hz, 6H).

^{13}C NMR (75 MHz, $CDCl_3$) δ 137.88, 133.45, 131.58, 131.41, 129.02, 128.82, 127.58, 124.46, 116.38, 113.77, 63.88, 42.36, 34.52, 28.76, 22.47.

HRMS (ESI-TOF) m/z: $[M + H]^+$ Calcd for $C_{18}H_{24}NOS$ 302.1573, found 302.1576.

IR (neat) *v* (cm^{-1}): 3287, 3012, 2955, 2869, 1654, 1638, 1630, 1601, 1503, 1467, 1234, 1211, 984, 836, 691.

S-benzyl ((S,1E,3E,5E)-8,13-dimethyltetradeca-1,3,5,12-tetraen-1-yl)carbamothioate

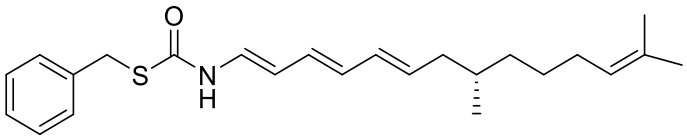

Prepared according to general procedure to provide the title compound **1q** as pale-yellow solid. (360 mg, 70% yield).

^{1}H NMR (300 MHz, $CDCl_3$) δ 7.48 – 7.20 (m, 5H), 7.08 – 6.78 (m, 2H), 6.20 – 5.99 (m, 3H), 5.85 – 5.57 (m, 2H), 5.11 (t, *J* = 6.9 Hz, 1H), 4.23 (s, 2H), 2.20 – 1.87 (m, 4H), 1.70 (s, 3H), 1.62 (s, 3H), 1.53 (h, *J* = 6.6 Hz, 1H), 1.43 – 1.28 (m, 1H), 1.24 – 1.07 (m, 1H), 0.89 (d, *J* = 6.6 Hz, 3H).

^{13}C NMR (75 MHz, $CDCl_3$) δ 149.72, 133.24, 131.71, 131.42, 131.30, 129.02, 128.82, 127.58, 124.99, 124.47, 120.45, 116.39, 113.78, 40.45, 36.87, 34.54, 33.14, 25.84, 25.78, 19.64, 17.78.

HRMS (ESI-TOF) m/z: $[M + Na]^+$ (Need to be performed).

IR (neat) *v* (cm^{-1}): (Need to be performed).

S-benzyl ((1E,3E,5E)-7-phenylhepta-1,3,5-trien-1-yl)carbamothioate

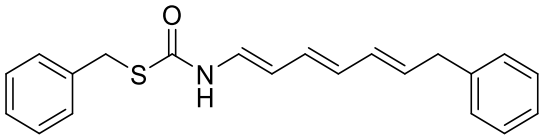

Prepared according to general procedure to provide the title compound **1r** as pale-yellow solid. (327 mg, 67% yield).

^{1}H NMR (Need to be performed)

^{13}C NMR (Need to be performed)

HRMS (ESI-TOF) m/z: $[M + H]^+$ Calcd for $C_{21}H_{22}NOS$ 336.1417, found 336.1415.

IR (neat) *v* (cm^{-1}): 3282, 3017, 1655, 1631, 1601, 1507, 1492, 1451, 1230, 1207, 983, 691.

***S*-hexyl ((1E,3E,5E)-hepta-1,3,5-trien-1-yl)carbamothioate**

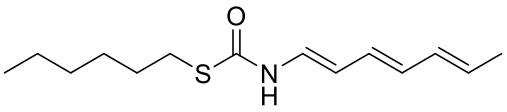

Prepared according to general procedure to provide the title compound **4m'** as pale-yellow solid. (350 mg, 69% yield).

^{1}H NMR (300 MHz, $CDCl_3$) δ 7.01 – 6.77 (m, 2H), 6.14 – 6.00 (m, 3H), 5.78 – 5.59 (m, 2H), 2.95 (t, *J* = 7.3 Hz, 2H), 1.81 – 1.72 (m, 3H), 1.68 – 1.59 (m, 2H), 1.40 – 1.22 (m, 6H).

^{13}C NMR (75 MHz, $CDCl_3$) δ 131.91, 131.01, 128.82, 127.49, 124.61, 116.38, 113.26, 31.44, 30.36, 30.26, 28.53, 22.65, 18.36, 14.12.

HRMS (ESI-TOF) m/z: $[M + H]^+$ Calcd for $C_{14}H_{24}NOS$ 254.1573, found 254.1579.

IR (neat) *v* (cm^{-1}): 3281, 2958, 2924, 2860, 1655, 1638, 1625, 1604, 1514, 1273, 1234, 1201, 1108, 986, 920, 684.

***S*-phenyl ((1E,3E,5E)-hepta-1,3,5-trien-1-yl)carbamothioate**

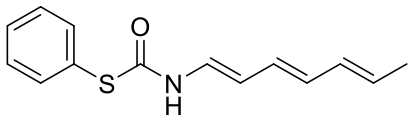

Prepared according to general procedure to provide the title compound **4m''** as pale-yellow solid. (352 mg, 70% yield).

^{1}H NMR (300 MHz, $CDCl_3$) δ 7.61 – 7.50 (m, 2H), 7.50 – 7.38 (m, 3H), 7.02 – 6.88 (m, 1H), 6.86 – 6.74 (m, 1H), 6.14 – 5.95 (m, 3H), 5.76 – 5.57 (m, 2H), 1.76 (d, *J* = 5.8 Hz, 3H).

^{13}C NMR (75 MHz, $CDCl_3$) δ 135.63, 131.85, 131.49, 130.18, 129.76, 129.15, 127.23, 124.33, 114.18, 64.82, 29.85, 18.34.

HRMS (ESI-TOF) m/z: $[M + H]^+$ Calcd for $C_{14}H_{16}NOS$ 246.0947, found 246.0952.

IR (neat) *v* (cm^{-1}): 3279, 3014, 1647, 1504, 1476, 1439, 1227, 1202, 985, 745, 685.

S-(4-(trifluoromethyl)phenyl) ((1E,3E,5E)-hepta-1,3,5-trien-1-yl)carbamothioate

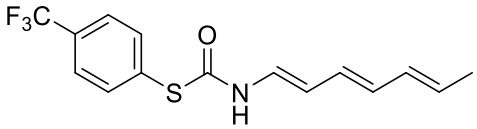

Prepared according to general procedure to provide the title compound **4m'''** as pale-yellow solid. (252 mg, 53% yield).

^{1}H NMR (300 MHz, $CDCl_3$) δ 7.66 (s, 4H), 7.05 (d, *J* = 10.5 Hz, 1H), 6.79 (t, *J* = 12.2 Hz, 1H), 6.19 – 5.97 (m, 3H), 5.88 – 5.60 (m, 2H), 1.77 (d, *J* = 6.6 Hz, 3H).

^{13}C NMR (75 MHz, $CDCl_3$) δ 135.25, 131.97, 131.78, 129.53, 126.97, 126.25, 126.20, 124.00, 114.90, 72.95, 60.32, 18.36.

^{19}F NMR (282 MHz, $CDCl_3$) δ -62.94.

HRMS (ESI-TOF) m/z: $[M + H]^+$ Calcd for $C_{15}H_{15}F_3NOS$ 314.0821, found 314.0826.

IR (neat) *v* (cm^{-1}): 3276, 3014, 1681,1659,1646,1638, 1601, 1508, 1445, 1323, 1225, 1170, 1114, 988, 837, 707.

***Se*-benzyl ((1E,3E,5E)-hepta-1,3,5-trien-1-yl)carbamoselenoate**

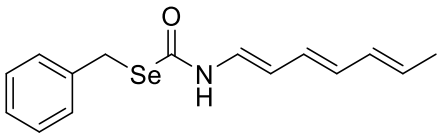

Prepared according to general procedure to provide the title compound **4m'''** as pale-yellow solid.

^{1}H NMR (300 MHz, $CDCl_3$) δ 7.36 – 7.27 (m, 5H), 7.12 – 6.77 (m, 2H), 6.14 – 5.99 (m, 3H), 5.82 – 5.59 (m, 2H), 4.25 (s, 2H), 1.76 (d, *J* = 6.2 Hz, 3H).

^{13}C NMR (Need to be performed)

HRMS (ESI-TOF) m/z: $[M + H]^+$ Calcd for $C_{15}H_{18}NOSe$ 308.0553, found 308.0538.

IR (neat) *v* (cm^{-1}): 3224, 2977, 1655, 1639, 1452, 1408, 3174, 1335, 1196, 1171, 1094, 1052, 984, 695.

Quinones

Note: The quinone diimides reported are the new ones, the others are already reported in literature.

N,N'-(cyclohexa-2,5-diene-1,4-diylidene)bis(2,4,6-trimethylbenzenesulfonamide)

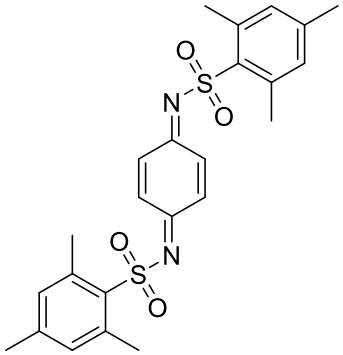

Prepared according to general procedure to provide the title compound **2c** as a yellow solid.

^{1}H NMR (300 MHz, $CDCl_3$) δ 8.11 – 8.07 (m, 2H), 7.00 (s, 4H), 6.94 – 6.89 (m, 2H), 2.64 (s, 12H), 2.33 (s, 6H).

^{13}C NMR (75 MHz, $CDCl_3$) δ 162.36, 162.21, 143.43, 139.49, 139.23, 139.10, 131.88, 129.91, 129.16, 22.74, 21.03.

HRMS (ESI-TOF) m/z: $[M + Na]^+$ Calcd for $C_{24}H_{26}N_2NaO_4S_2$ 493.1232, found 493.1227.

IR (neat) *v* (cm^{-1}): 2978, 2939, 1576, 1552, 1315, 1147, 1109, 1055, 857, 716, 683.

N,N'-(cyclohexa-2,5-diene-1,4-diylidene)bis(3-fluorobenzenesulfonamide)

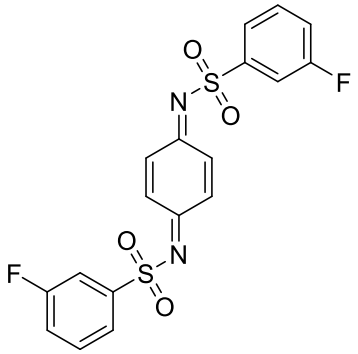

Prepared according to general procedure to provide the title compound **2g** as a yellow solid. (277 mg, 62% yield, rotamers).

^{1}H NMR (300 MHz, $CDCl_3$) δ 8.10 – 8.05 (m, 2H), 7.82 (dt, *J* = 7.9, 1.3 Hz, 2H), 7.72 (dt, *J* = 8.0, 2.1 Hz, 2H), 7.58 (td, *J* = 8.1, 5.2 Hz, 2H), 7.37 (td, *J* = 8.1, 2.5 Hz, 2H), 6.98 – 6.93 (m, 2H).

^{13}C NMR (75 MHz, $CDCl_3$) δ 164.05, 162.75, 162.67, 160.71, 139.54, 139.22, 131.04, 130.93, 130.06, 129.60, 123.42, 123.38, 121.01 (d, *J* = 21.3 Hz), 115.10 (d, *J* = 24.6 Hz).

^{19}F NMR (282 MHz, $CDCl_3$) δ -109.16.

HRMS (ESI-TOF) m/z: [M + Na]$^+$ Calcd for $C_{18}H_{12}F_2N_2NaO_4S_2$ 445.0104, found 445.0107.

IR (neat) *v* (cm^{-1}): 3071, 2850, 1578, 1557, 1473, 1435, 1326, 1303, 1226, 1145, 1082, 954, 897, 854, 786.

N-4-((thiophen-2-ylsulfonyl)imino)cyclohexa-2,5-dien-1-ylidene)thiophene-2-sulfonamide

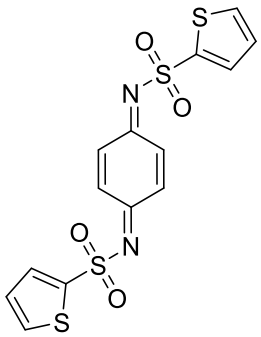

Prepared according to general procedure to provide the title compound **2i** as an orange solid.

^{1}H NMR (300 MHz, $CDCl_3$) δ 8.10 – 8.06 (m, 2H), 7.82 – 7.74 (m, 4H), 7.16 (t, *J* = 4.4 Hz, 2H), 6.98 – 6.95 (m, 2H).

^{13}C NMR (75 MHz, $CDCl_3$) δ 139.66, 139.33, 134.17, 134.06, 129.68, 129.19, 127.55.

HRMS (ESI-TOF) m/z: [M + Na]$^+$ Calcd for $C_{14}H_{10}N_2NaO_4S_4$ 420.9421, found 420.9415.

IR (neat) *v* (cm^{-1}): 3092, 3076, 1566, 1403, 1302, 1147, 1087, 1015, 954, 877, 846, 736, 708.

N,N'-(cyclohexa-2,5-diene-1,4-diylidene)dicyclopropanesulfonamide

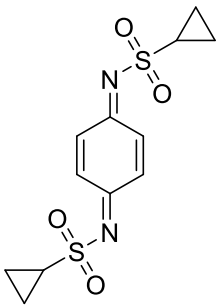

Prepared according to general procedure to provide the title compound **2j** as a pale-yellow solid.

^{1}H NMR (500 MHz, $CDCl_3$) δ 7.91 – 7.85 (m, 2H), 6.99 – 6.92 (m, 2H), 2.80 (td, *J* = 8.1, 4.0 Hz, 2H), 1.34 – 1.30 (m, 4H), 1.18 – 1.15 (m, 4H).

^{13}C NMR (75 MHz, $CDCl_3$) δ 162.63, 162.52, 139.05, 138.99, 130.01, 129.32, 32.04, 6.06.

HRMS (ESI-TOF) m/z: [M + Na]$^+$ Calcd for $C_{12}H_{14}N_2NaO_4S_2$ 337.0293, found 337.0285.

IR (neat) *v* (cm^{-1}): 3091, 1584, 1557, 1314, 1294, 1133, 1118, 1039, 860, 828, 710.

N,N'-(cyclohexa-2,5-diene-1,4-diylidene)bis(octane-1-sulfonamide)

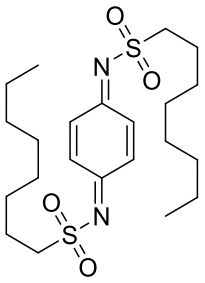

Prepared according to general procedure to provide the title compound **2k** as a yellow solid.

^{1}H NMR (300 MHz, $CDCl_3$) δ 7.92 – 7.88 (m, 2H), 6.96 – 6.88 (m, 2H), 3.32 – 3.27 (m, 4H), 1.93 (p, *J* = 7.8 Hz, 4H), 1.52 – 1.45 (m, 4H), 1.34 – 1.26 (m, 12H), 0.90 – 0.82 (m, 10H).

^{13}C NMR (75 MHz, $CDCl_3$) δ 163.11, 163.01, 138.88, 130.11, 129.40, 55.03, 31.68, 28.96, 28.90, 28.20, 23.17, 22.55, 13.99.

HRMS (ESI-TOF) m/z: $[M + Na]^+$ Calcd for $C_{22}H_{38}N_2NaO_4S_2$ 481.2171, found 481.2163.

IR (neat) *v* (cm^{-1}): 2917, 2847, 1580, 1570, 1563, 1321, 1296, 1281, 1134, 1103, 869, 778, 673.

N,N'-(cyclohexa-2,5-diene-1,4-diylidene)bis(2-(trimethylsilyl)ethane-1-sulfonamide)

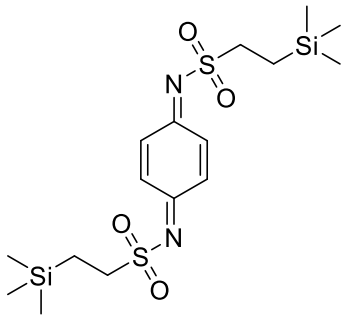

Prepared according to general procedure to provide the title compound **2l** as a pale orange solid.

^{1}H NMR (300 MHz, $CDCl_3$) δ 7.92 – 7.86 (m, 2H), 6.95 – 6.87 (m, 2H), 3.25 – 3.19 (m, 4H), 1.16 – 1.10 (m, 4H), 0.00 (s, 18H).

^{13}C NMR (75 MHz, $CDCl_3$) δ 165.40, 165.29, 140.82, 132.09, 131.40, 53.54, 11.81, 0.00.

HRMS (ESI-TOF) m/z: $[M + Na]^+$ Calcd for $C_{16}H_{30}N_2NaO_4S_2Si_2$ 457.1083, found 457.1076.

IR (neat) *v* (cm^{-1}): 2954, 2936, 1576, 1560, 1317, 1251, 1134, 1112, 857, 742, 699.

Synthesis and characterization of products:

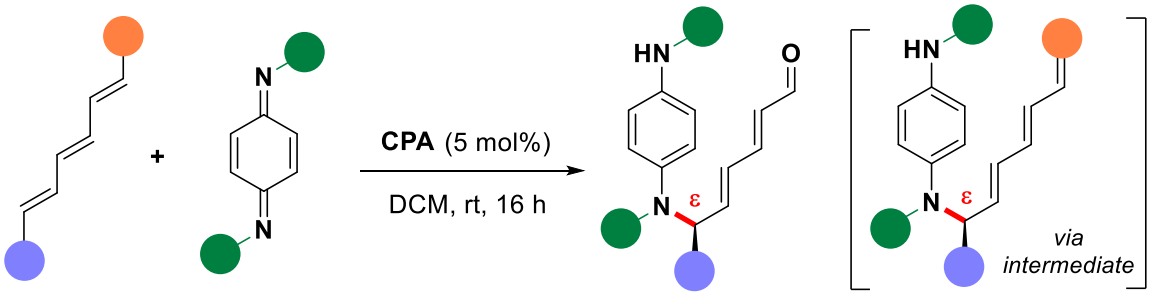

The quinone (0.05 mmol, 2.0 equiv.) and the CPA catalyst (0.0125 µmol, 0.05 equiv.) are dissolved in freshly distilled CH_2Cl_2 (0.25 mL) in a flame-dried tube. The tube is then placed in a thermostated bath at -20°C. Then, after 10 minutes, the thio-trienecarbamate (0.025 mmol, 1 equiv.) is dissolved in 0.25 mL of CH_2Cl_2 and added dropwise into the test tube. The resulting solution is stirred at -20°C for 16 hours. Upon completion of the reaction, the mixture is directly purified by preparative thin layer chromatography (*PET:EtOAc*) and then repurified again to get clean desired product with another preparative thin layer chromatography (*DCM:Acetone*).

4-methyl-N-(4-((4-methylphenyl)sulfonamido)phenyl)-N-((3E,5E)-7-oxohepta-3,5-dien-2-yl)benzenesulfonamide

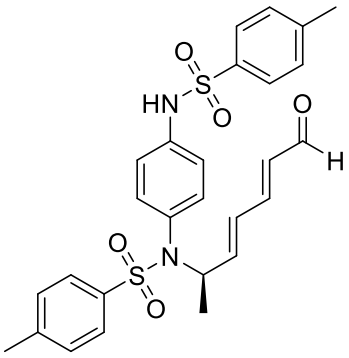

Prepared according to general procedure to provide the title compound **4a** as a vanilla solid. (8.0 mg, 61% yield).

^{1}H NMR (300 MHz, $CDCl_3$) δ 9.54 (d, *J* = 7.8 Hz, 1H), 7.68 (d, *J* = 8.1 Hz, 2H), 7.51 (d, *J* = 8.1 Hz, 2H), 7.27 – 7.21 (m, 4H), 7.01 – 6.95 (m, 3H), 6.92 – 6.85 (m, 3H), 6.29 – 6.20 (m, 1H), 6.13 – 6.01 (m, 2H), 5.05 (p, *J* = 6.8 Hz, 1H), 2.42 (s, 3H), 2.41 (s, 3H), 1.15 (d, *J* = 6.9 Hz, 3H).

^{13}C NMR (75 MHz, $CDCl_3$) δ 150.28, 144.26, 143.59, 143.50, 137.65, 137.29, 136.16, 133.08, 132.45, 131.92, 129.73, 129.48, 127.49, 127.25, 120.77, 55.95, 21.53, 18.91.

HRMS (ESI-TOF) m/z: $[M + Na]^+$ Calcd for $C_{27}H_{28}N_2O_5S_2Na$ 547.1337, found 547.1332.

IR (neat) ν (cm^{-1}): 3240, 3063, 3032, 2925, 2854, 1669, 1641, 1597, 1506, 1454, 1329, 1169, 1090, 919, 812, 706, 660.

HPLC analysis (Daicel Chiralpak IC, Heptane/EtOH = 80/20, flow rate 1.0 mL/min, 254 nm): t_R = 90 min, t_R = 120 min.

Enantiomeric excess: 90%. **$[\alpha]_D^{22}$** ([c] = 1 g/L, CH_2Cl_2) -9.0°.

N-((3E,5E)-7-oxohepta-3,5-dien-2-yl)-N-(4-(phenylsulfonamido)phenyl)benzenesulfonamide

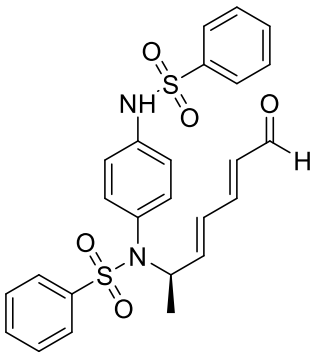

Prepared according to general procedure to provide the title compound **4b** as a brown solid. (6.9 mg, 56% yield).

^{1}H NMR (300 MHz, $CDCl_3$) δ 9.54 (d, *J* = 7.8 Hz, 1H), 7.81 – 7.77 (m, 2H), 7.67 – 7.54 (m, 4H), 7.51 – 7.41 (m, 4H), 7.02 – 6.86 (m, 4H), 6.64 (s, 1H), 6.29 – 6.20 (m, 1H), 6.13 – 5.99 (m , 2H), 5.08 (p, *J* = 6.7 Hz, 1H), 1.16 (d, *J* = 6.9 Hz, 3H).

^{13}C NMR (75 MHz, $CDCl_3$) δ 193.23, 150.07, 143.21, 140.53, 139.07, 137.16, 133.30, 133.12, 132.76, 132.56, 132.01, 129.60, 129.13, 128.88, 127.44, 127.20, 120.95, 56.02, 18.93.

HRMS (ESI-TOF) m/z: $[M + Na]^+$ Calcd for $C_{25}H_{24}N_2O_5S_2Na$ 519.1019, found 519.1013.

IR (neat) *v* (cm^{-1}): 3239, 3064, 2922, 2851, 1669, 1639, 1605, 1505, 1446, 1395, 1327, 1162, 1088, 916, 723, 686.

HPLC analysis (Daicel Chiralpak IC, Hexane/EtOH = 80/20, flow rate 1.0 mL/min, 254 nm): t_R = 63 min, t_R = 79 min.

Enantiomeric excess: 80%. **$[\alpha]_D^{22}$** ([c] = 1 g/L, CH_2Cl_2) -33.0°.

2,4,6-trimethyl-N-((3E,5E)-7-oxohepta-3,5-dien-2-yl)-N-(4-((2,4,6-trimethylphenyl)sulfonamido)phenyl)benzenesulfonamide

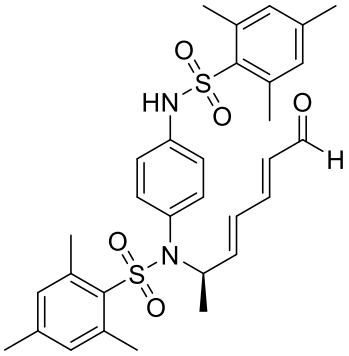

Prepared according to general procedure to provide the title compound **4c** as a pale-yellow solid. (7.6 mg, 66% yield).

^{1}H NMR (500 MHz, $CDCl_3$) δ 9.55 (d, *J* = 7.8 Hz, 1H), 7.03 (dd, *J* = 15.4, 10.0 Hz, 1H), 6.92 (s, 2H), 6.86 – 6.78 (m, 6H), 6.66 (s, 1H), 6.32 – 6.21 (m, 2H), 6.11 (dd, *J* = 15.4, 7.8 Hz, 1H), 5.16 (p, *J* = 6.8 Hz, 1H), 2.56 (s, 6H), 2.30 – 2.26 (m, 12H), 1.21 (d, *J* = 6.8 Hz, 3H).

^{13}C NMR (75 MHz, $CDCl_3$) δ 193.25, 150.41, 143.92, 142.88, 142.59, 140.14, 139.29, 137.05, 133.44, 132.48, 132.08, 131.73, 131.61, 129.53, 121.10, 54.66, 22.92, 22.56, 20.94, 18.56.

HRMS (ESI-TOF) m/z: $[M + Na]^+$ Calcd for $C_{31}H_{36}N_2O_5S_2Na$ 603.1993, found 603.1198.

IR (neat) *v* (cm^{-1}): 3347, 3257, 3192, 3091, 2923, 2852, 1663, 1636, 1605, 1507, 1447, 1331, 1170, 1123, 1102, 990, 922, 759, 732.

HPLC analysis (Daicel Chiralpak IA, Hexane/iPrOH = 90/10, flow rate 1.0 mL/min, 254 nm): t_R = 74 min, t_R = 81 min.

Enantiomeric excess: 86%. **$[\alpha]_D^{22}$** ([c] = 1 g/L, CH_2Cl_2) -25°.

2,4,6-triisopropyl-N-((3E,5E)-7-oxohepta-3,5-dien-2-yl)-N-(4-((2,4,6-triisopropylphenyl)sulfonamido)phenyl)benzenesulfonamide

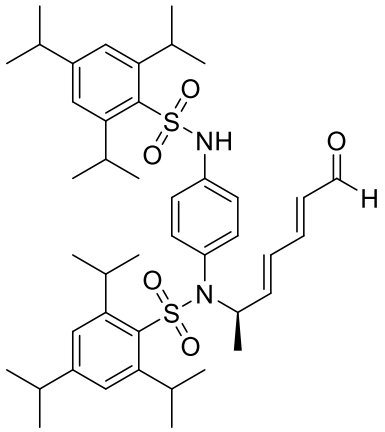

Prepared according to general procedure to provide the title compound **4d** as a vanilla solid. (15.4 mg, 82% yield).

^{1}H NMR (300 MHz, $CDCl_3$) δ 9.55 (d, *J* = 7.9 Hz, 1H), 7.14 (s, 2H), 7.06 – 6.89 (m, 7H), 6.53 (s, 1H), 6.35 – 6.24 (m, 2H), 6.11 (dd, *J* = 15.4, 7.8 Hz, 1H), 5.22 – 5.17 (m, 1H), 4.11 (p, *J* = 6.8 Hz, 2H), 3.72 (p, *J* = 6.8 Hz, 2H), 2.94 – 2.79 (m, 2H), 1.26 – 1.17 (m, 27H), 1.06 (d, *J* = 6.7 Hz, 6H), 0.94 (d, *J* = 6.8 Hz, 6H).

^{13}C NMR (75 MHz, $CDCl_3$) δ 193.29, 153.48, 153.17, 151.14, 150.52, 150.47, 144.00, 137.52, 133.88, 132.49, 132.17, 131.89, 131.34, 129.64, 124.09, 123.64, 120.82, 54.58, 34.12, 34.04, 29.76, 29.42, 24.74, 24.64, 24.59, 23.47, 18.62.

HRMS (ESI-TOF) m/z: $[M + Na]^+$ Calcd for $C_{43}H_{60}N_2O_5S_2$ 771.3836, found 771.3820.

IR (neat) *v* (cm^{-1}): 3290, 3050, 2958, 2927, 2868, 1683, 1644, 1601, 1504, 1305, 1294, 1257, 1162, 1153, 1105, 1058, 997, 908, 883.

HPLC analysis (Daicel Chiralpak IC, Hexane/EtOH = 95/15, flow rate 1.0 mL/min, 254 nm): t_R = 27 min, t_R = 33 min.

Enantiomeric excess: 81%. **$[\alpha]_D^{22}$** ([c] = 1 g/L, CH_2Cl_2) -29.0°.

4-methoxy-N-(4-((4-methoxyphenyl)sulfonamido)phenyl)-N-((3E,5E)-7-oxohepta-3,5-dien-2-yl)benzenesulfonamide

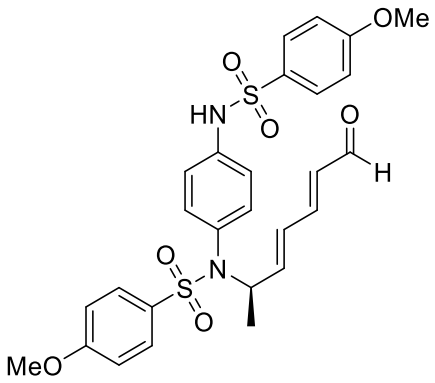

Prepared according to general procedure to provide the title compound **4e** as a yellowish oil. (8.0 mg, 58% yield).

^{1}H NMR (500 MHz, $CDCl_3$) δ 9.55 (d, *J* = 7.8 Hz, 1H), 7.72 (d, *J* = 8.5 Hz, 2H), 7.55 (d, *J* = 8.4 Hz, 2H), 6.99 – 6.86 (m, 9H), 6.74 (s, 1H), 6.28 – 6.23 (m, 1H), 6.13 – 6.04 (m, 2H), 5.05 (t, *J* = 6.9 Hz, 1H), 3.87 (s, 4H), 3.85 (s, 5H), 1.15 (d, *J* = 6.9 Hz, 3H).

^{13}C NMR (75 MHz, $CDCl_3$) δ 193.24, 163.40, 162.97, 150.23, 143.56, 137.26, 133.12, 132.46, 132.15, 132.10, 130.59, 129.61, 129.46, 120.85, 114.28, 113.98, 55.86, 55.65, 55.60, 18.94.

HRMS (ESI-TOF) m/z: $[M + Na]^+$ Calcd for $C_{27}H_{28}N_2O_7S_2Na$ 579.1236, found 579.1230.

IR (neat) *v* (cm^{-1}): 3245, 3106, 3063, 2929, 2843, 1673, 1641, 1594, 1578, 1497, 1461, 1331, 1258, 1178, 1091, 1013, 914, 832, 727, 665.

HPLC analysis (Daicel Chiralpak OD-H, Hexane/EtOH = 80/20, flow rate 1.0 mL/min, 254 nm): t_R = 36 min, t_R = 48 min.

Enantiomeric excess: 87%. **$[\alpha]_D^{22}$** ([c] = 1 g/L, CH_2Cl_2) -36.0°.

N-((3E,5E)-7-oxohepta-3,5-dien-2-yl)-4-(trifluoromethyl)-N-(4-((4-(trifluoromethyl)phenyl)sulfonamido)phenyl)benzenesulfonamide

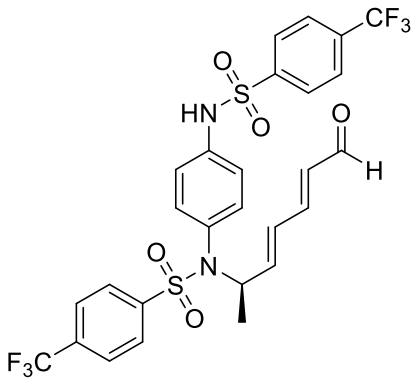

Prepared according to general procedure to provide the title compound **4f** as a white solid. (5.2 mg, 33% yield).

^{1}H NMR (300 MHz, $CDCl_3$) δ 9.55 (d, *J* = 7.7 Hz, 1H), 7.96 – 7.93 (m, 2H), 7.77 – 7.69 (m, 5H), 7.07 – 6.81 (m, 4H), 6.81 (s, 1H), 6.34 – 6.25 (m 1H), 6.17 – 5.99 (m, 2H), 5.18 – 4.96 (m, 1H), 1.18 (d, *J* = 6.9 Hz, 3H).

^{13}C NMR (75 MHz, $CDCl_3$) δ 193.02, 149.46, 142.34, 136.88, 133.18, 132.91, 130.00, 127.86, 127.76, 126.35 (q, *J* = 3.3 Hz), 126.09 (q, *J* = 3.2 Hz), 121.17, 56.50, 19.04.

^{19}F NMR (282 MHz, $CDCl_3$) δ -63.10, -63.22.

HRMS (ESI-TOF) m/z: $[M + Na]^+$ Calcd for $C_{27}H_{22}F_6N_2NaO_5S_2$ 655.0772, found 655.0765.

IR (neat) *v* (cm^{-1}): 3497, 3238, 2921, 2851, 1661, 1642, 1607, 1505, 1452, 1404, 1320, 1163, 1126, 1107, 1092, 1011, 989, 923, 837, 712.

HPLC analysis (Daicel Chiralpak IC, Hexane/EtOH = 90/10, flow rate 1.0 mL/min, 254 nm): t_R = 36 min, t_R = 52 min.

Enantiomeric excess: 75%. **$[\alpha]_D^{22}$** ([c] = 1 g/L, CH_2Cl_2) -52.0.

3-fluoro-N-(4-((3-fluorophenyl)sulfonamido)phenyl)-N-((3E,5E)-7-oxohepta-3,5-dien-2-yl)benzenesulfonamide

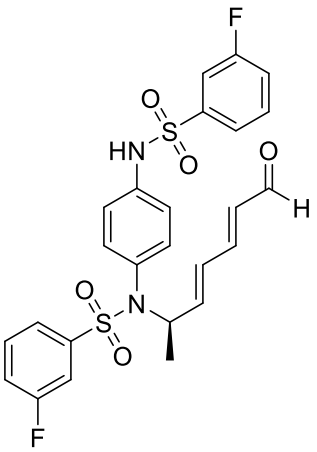

Prepared according to general procedure to provide the title compound **4g** as a white solid. (5.6 mg, 42% yield).

^{1}H NMR (300 MHz, $CDCl_3$) δ 9.55 (d, *J* = 7.8 Hz, 1H), 7.60 (dt, *J* = 7.9, 1.2 Hz, 1H), 7.51 – 7.42 (m, 4H), 7.34 – 7.26 (m, 3H), 7.05 – 6.89 (m, 5H), 6.76 (s, 1H), 6.33 – 6.24 (m, 1H), 6.16 – 6.00 (m, 2H), 5.09 (p, *J* = 6.7 Hz, 1H), 1.18 (d, *J* = 6.9 Hz, 3H).

^{13}C NMR (75 MHz, $CDCl_3$) δ 193.17, 149.74, 142.63, 136.95, 133.17, 132.79, 131.03 (d, *J* = 7.4 Hz), 130.70 (d, *J* = 7.5 Hz), 129.88, 123.16 (d, *J* = 3.6 Hz), 122.93 (d, *J* = 3.4 Hz), 121.35, 120.63 (d, *J* = 21.0 Hz), 120.01 (d, *J* = 21.3 Hz), 114.88 (d, *J* = 16.6 Hz), 114.56 (d, *J* = 17.1 Hz), 56.33, 18.98.

^{19}F NMR (282 MHz, $CDCl_3$) δ -109.08, -109.36.

HRMS (ESI-TOF) m/z: $[M + Na]^+$ Calcd for $C_{25}H_{22}F_2N_2NaO_5S_2$ 555.0836, found 555.0826.

IR (neat) ν (cm^{-1}): 3158, 3107, 3067, 2932, 2886, 1656, 1634, 1591, 1508, 1476, 1343, 1223, 1173, 1086, 987, 928, 884, 787, 693.

HPLC analysis (Daicel Chiralpak IC, Hexane/EtOH = 90/10, flow rate 1.0 mL/min, 254 nm): t_R = 37 min, t_R = 54 min.

Enantiomeric excess: 77%. **$[\alpha]_D^{22}$** ([c] = 1 g/L, CH_2Cl_2) -58.0.

N-(4-(naphthalene-2-sulfonamido)phenyl)-N-((3E,5E)-7-oxohepta-3,5-dien-2-yl)naphthalene-2-sulfonamide

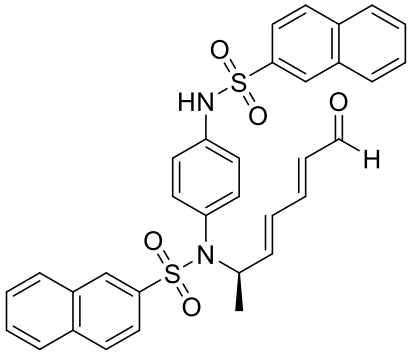

Prepared according to general procedure to provide the title compound **4h** as a white solid. (11.1 mg, 91% yield).

^{1}H NMR (300 MHz, $CDCl_3$) δ 9.47 (d, *J* = 7.8 Hz, 1H), 8.37 (d, *J* = 1.9 Hz, 1H), 8.14 (d, *J* = 1.9 Hz, 1H), 7.93 – 7.85 (m, 4H), 7.80 – 7.73 (m, 3H), 7.70 – 7.53 (m, 5H), 7.03 – 7.00 (m, 2H), 6.90 – 6.81 (m, 3H), 6.26 – 6.17 (m, 1H), 6.05 – 5.94 (m, 2H), 5.11 (p, *J* = 6.8 Hz, 1H), 1.12 (d, *J* = 6.9 Hz, 3H).

^{13}C NMR (75 MHz, $CDCl_3$) δ 193.19, 150.06, 143.13, 137.31, 137.18, 135.90, 135.05, 134.74, 133.19, 132.51, 132.01, 129.63, 129.54, 129.29, 129.23, 129.15, 129.09, 128.92, 128.83, 127.97, 127.87, 127.80, 127.61, 122.62, 122.11, 121.04, 56.16, 19.01.

HRMS (ESI-TOF) m/z: $[M + Na]^+$ Calcd for $C_{33}H_{28}N_2O_5S_2Na$ 619.1337, found 619.1332.

IR (neat) *v* (cm^{-1}): 3239, 3056, 2920, 2851, 1673, 1640, 1604, 1505, 1330, 1154, 1130, 1073, 1011, 919, 813, 747, 695.

HPLC analysis (Daicel Chiralpak OD-H, Hexane/EtOH = 80/20, flow rate 1.0 mL/min, 254 nm): t_R = 31 min, t_R = 42 min.

Enantiomeric excess: 81%. **$[\alpha]_D^{22}$** ([c] = 1 g/L, CH_2Cl_2) -10.0°.

N-((3E,5E)-7-oxohepta-3,5-dien-2-yl)-N-(4-(thiophene-2-sulfonamido)phenyl)thiophene-2-sulfonamide

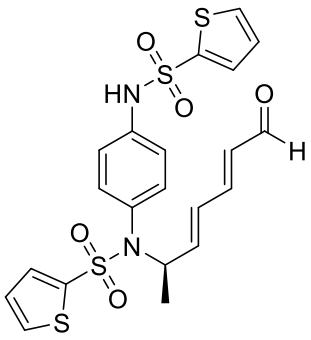

Prepared according to general procedure to provide the title compound **4i** as a grey solid. (6.1 mg, 48% yield).

^{1}H NMR (500 MHz, $CDCl_3$) δ 9.56 (d, *J* = 7.9 Hz, 1H), 7.60 – 7.57 (m, 2H), 7.54 (d, *J* = 3.7 Hz, 1H), 7.39 (d, *J* = 3.7 Hz, 1H), 7.10 (d, *J* = 8.3 Hz, 2H), 7.05 – 6.96 (m, 5H), 6.75 (s, 1H), 6.32 – 6.27 (m, 1H), 6.11 (td, *J* = 14.9, 7.4 Hz, 2H), 5.09 (p, *J* = 6.9 Hz, 1H), 1.21 (d, *J* = 6.9 Hz, 3H).

^{13}C NMR (75 MHz, $CDCl_3$) δ 193.23, 150.02, 142.85, 141.35, 139.49, 137.02, 133.03, 132.91, 132.75, 132.67, 132.24, 132.12, 129.83, 127.36, 127.18, 121.31, 56.41, 18.96.

HRMS (ESI-TOF) m/z: $[M + Na]^+$ Calcd for $C_{21}H_{20}N_2O_5S_4Na$ 531.0153, found 531.0147.

IR (neat) *v* (cm^{-1}): 3233, 3112, 3053, 2926, 2872, 1662, 1637, 1609, 1507, 1402, 1343, 1225, 1156, 1111, 1014, 991, 923, 723, 660.

HPLC analysis (Daicel Chiralpak IC, Hexane/EtOH = 80/20, flow rate 1.0 mL/min, 254 nm): t_R = 67 min, t_R = 83 min.

Enantiomeric excess: 81%. **$[\alpha]_D^{22}$** ([c] = 1 g/L, CH_2Cl_2) -11.0°.

N-(4-(cyclopropanesulfonamido)phenyl)-N-((3E,5E)-7-oxohepta-3,5-dien-2-yl)cyclopropanesulfonamide

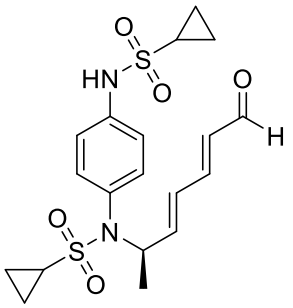

Prepared according to general procedure to provide the title compound **4j** as a brown solid. (6.1 mg, 58% yield).

^{1}H NMR (300 MHz, $CDCl_3$) δ 9.59 (d, *J* = 7.8 Hz, 1H), 7.27 (s, 4H), 7.09 (dd, *J* = 15.4, 10.3 Hz, 1H), 6.53 (s, 1H), 6.44 – 6.13 (m, 3H), 5.03 (p, *J* = 6.7 Hz, 1H), 2.53 (ddd, *J* = 12.8, 8.2, 4.8 Hz, 1H), 2.41 (td, *J* = 7.9, 3.9 Hz, 1H), 1.32 (d, *J* = 6.9 Hz, 3H), 1.28 – 1.15 (m, 2H), 1.10 – 0.96 (m, 6H).

^{13}C NMR (75 MHz, $CDCl_3$) δ 193.21, 150.12, 143.80, 137.56, 133.35, 132.67, 132.47, 129.61, 121.01, 56.07, 30.85, 30.39, 19.32, 5.85, 5.80.

HRMS (ESI-TOF) m/z: $[M + Na]^+$ Calcd for $C_{19}H_{24}N_2O_5S_2$ 447,1024, found 447.1019.

IR (neat) *v* (cm^{-1}): 3250, 3051, 2926, 2851, 1673, 1641, 1605, 1507, 1329, 1296, 1159, 1113, 1012, 922, 886, 713.

HPLC analysis (Daicel Chiralpak IA, Hexane/EtOH = 80/20, flow rate 1.0 mL/min, 254 nm): t_R = 57 min, t_R = 85 min.

Enantiomeric excess: 88%. **$[\alpha]_D^{22}$** ([c] = 1 g/L, CH_2Cl_2) -31.0°.

N-(4-(octylsulfonamido)phenyl)-N-((3E,5E)-7-oxohepta-3,5-dien-2-yl)octane-1-sulfonamide

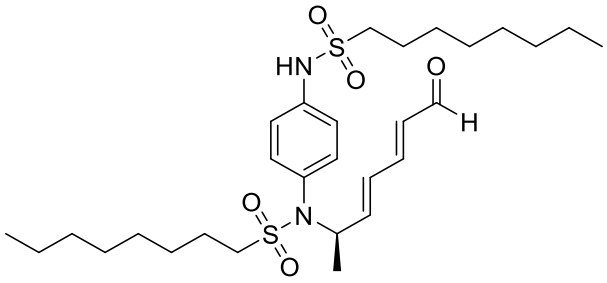

Prepared according to general procedure to provide the title compound **4k** as a pale-yellow oil. (7.4 mg, 52% yield).

^{1}H NMR (300 MHz, $CDCl_3$) δ 9.58 (d, *J* = 7.8 Hz, 1H), 7.20 (s, 4H), 7.07 (dd, *J* = 15.4, 10.5 Hz, 1H), 6.58 (s, 1H), 6.43 – 6.34 (m, 1H), 6.25 – 6.13 (m, 2H), 4.99 (p, *J* = 6.8 Hz, 1H), 3.17 – 3.11 (m, 2H), 3.02 – 2.96 (m, 2H), 1.89 – 1.77 (m, 4H), 1.40 – 1.26 (m, 23H), 0.90 – 0.85 (m, 6H).

^{13}C NMR (75 MHz, $CDCl_3$) δ 193.19, 150.06, 143.57, 137.70, 133.37, 132.75, 131.68, 129.72, 119.85, 55.92, 52.95, 52.56, 31.66, 29.07, 28.98, 28.91, 28.86, 28.31, 28.13, 23.64, 23.55, 22.66, 22.55, 19.51, 19.43, 14.05, 14.00.

HRMS (ESI-TOF) m/z: $[M + Na]^+$ Calcd for $C_{29}H_{48}N_2O_5S_2Na$ 591.2902, found 591.2893.

IR (neat) *v* (cm^{-1}): 3250, 3037, 2924, 2855, 1678, 1642, 1605, 1507, 1464, 1398, 1330, 1296, 1148, 1112, 1011, 990, 923, 725.

HPLC analysis (Daicel Chiralpak IA, Hexane/EtOH = 95/5, flow rate 1.0 mL/min, 254 nm): t_R = 102 min, t_R = 117 min.

Enantiomeric excess: 86%. **$[\alpha]_D^{22}$** ([c] = 1 g/L, CH_2Cl_2) -65.0°.

N-((3E,5E)-7-oxohepta-3,5-dien-2-yl)-2-(trimethylsilyl)-N-(4-((2-(trimethylsilyl)ethyl)sulfonamido)phenyl)ethane-1-sulfonamide

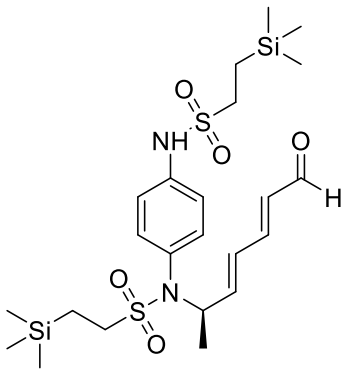

Prepared according to general procedure to provide the title compound **4l** as a slight yellow solid. (9.1 mg, 67% yield).

^{1}H NMR (500 MHz, $CDCl_3$) δ 9.58 (d, *J* = 7.8 Hz, 1H), 7.20 (s, 4H), 7.10 – 7.04 (m, 1H), 6.60 (s, 1H), 6.39 – 6.34 (m, 1H), 6.25 – 6.12 (m, 2H), 4.99 (p, *J* = 6.9 Hz, 1H), 3.08 – 3.04 (m, 2H), 2.91 (t, *J* = 8.7 Hz, 2H), 1.29 (d, *J* = 6.8 Hz, 3H), 1.08 – 1.02 (m, 4H), 0.03 (s, 9H), 0.00 (s, 9H).

^{13}C NMR (75 MHz, $CDCl_3$) δ 195.27, 152.16, 145.79, 139.92, 135.46, 134.82, 133.79, 131.80, 121.93, 58.00, 50.96, 50.71, 21.45, 12.70, 0.10, 0.00.

HRMS (ESI-TOF) m/z: $[M + Na]^+$ Calcd for $C_{23}H_{40}N_2O_5S_2Si_2$ 567.1815, found 567.1809.

IR (neat) *v* (cm^{-1}): 3255, 3037, 2953, 2927, 2852, 1679, 1642, 1606, 1507, 1328, 1250, 1166, 1143, 1109, 1012, 924, 858, 739.

HPLC analysis (Daicel Chiralpak IC, Heptane/EtOH = 80/20, flow rate 1.0 mL/min, 254 nm): t_R = 31 min, t_R = 79 min.

Enantiomeric excess: 83%. **$[\alpha]_D^{22}$** ([c] = 1 g/L, CH_2Cl_2) -91.0°.

N-(4-(methylsulfonamido)phenyl)-N-((3E,5E)-7-oxohepta-3,5-dien-2-yl)methanesulfonamide

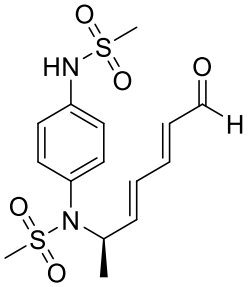

Prepared according to general procedure to provide the title compound **4m** as a pale brown solid. (7.4 mg, 79% yield).

^{1}H NMR (300 MHz, $CDCl_3$) δ 9.59 (d, *J* = 7.7 Hz, 1H), 7.24 (s, 4H), 7.08 (dd, *J* = 15.4, 10.5 Hz, 1H), 6.79 (s, 1H), 6.42 (dd, *J* = 15.3, 10.7 Hz, 1H), 6.26 – 6.14 (m, 2H), 5.05 – 5.01 (m, 1H), 3.08 (s, 3H), 2.96 (s, 3H), 1.30 (d, *J* = 6.9 Hz, 3H).

^{13}C NMR (75 MHz, $CDCl_3$) δ 193.19, 149.87, 143.01, 137.66, 133.14, 132.91, 132.06, 129.97, 120.19, 56.10, 40.57, 40.12, 19.33.

HRMS (ESI-TOF) m/z: $[M + Na]^+$ Calcd for $C_{15}H_{20}N_2O_5S_2Na$ 395.0711, found 395,0706.

IR (neat) *v* (cm^{-1}): 3260, 3020, 2980, 2933, 1672, 1641, 1606, 1507, 1319, 1171, 1114, 1013, 962, 912, 764, 727.

HPLC analysis (Daicel Chiralpak IA, Hexane/EtOH = 80/20, flow rate 1.0 mL/min, 254 nm): t_R = 51 min, t_R = 61 min.

Enantiomeric excess: 90%. **$[\alpha]_D^{22}$** ([c] = 1 g/L, CH_2Cl_2) -42.0°.

N-(4-(methylsulfonamido)phenyl)-N-((R,4E,6E)-8-oxoocta-4,6-dien-3-yl)methanesulfonamide

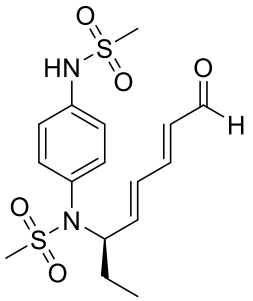

Prepared according to general procedure to provide the title compound **4n** as a white powder. (6 mg, 86% yield).

^{1}H NMR (400 MHz, $CDCl_3$) δ 9.60 (d, *J* = 7.8 Hz, 1H), 7.24 (s, 4H), 7.10 (dd, *J* = 15.4, 10.8 Hz, 1H), 6.87 (s, 1H), 6.53 (dd, *J* = 15.3, 10.8 Hz, 1H), 6.22 (dd, *J* = 15.4, 7.8 Hz, 1H), 6.10 (dd, *J* = 15.3, 8.8 Hz, 1H), 4.67 (q, *J* = 7.9 Hz, 1H), 3.08 (s, 3H), 2.94 (s, 3H), 1.68 – 1.61 (m, 1H), 1.52 – 1.40 (m, 1H), 0.98 (t, *J* = 7.3 Hz, 3H).

^{13}C NMR (101 MHz, $CDCl_3$) δ 193.53, 150.13, 141.89, 137.81, 133.18, 133.13, 132.28, 131.45, 120.31, 62.96, 40.51, 40.23, 26.46, 11.08.

HRMS (ESI-TOF) m/z: $[M - H]^+$ Calcd for $C_{23}H_{27}N_2O_6S_2$ (Need to be performed).

IR (neat) *v* (cm^{-1}): (Need to be performed)

HPLC analysis (Daicel Chiralpak IA, Hexane/EtOH = 80/20, flow rate 1.0 mL/min, 254 nm): t_R = 37 min, t_R = 69 min.

Enantiomeric excess: 94%. **$[\alpha]_D^{22}$** ([c] = 1 g/L, CH_2Cl_2) +103°.

N-((2E,4E)-1-(benzyloxy)-6-oxohexa-2,4-dien-1-yl)-N-(4-(methylsulfonamido)phenyl)methanesulfonamide

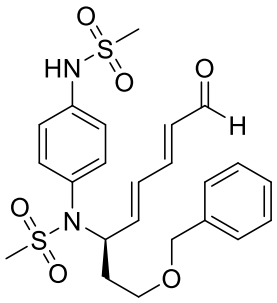

Prepared according to general procedure to provide the title compound **4o** as a white powder. (6 mg, 86% yield).

^{1}H NMR (300 MHz, $CDCl_3$) δ 9.58 (d, *J* = 7.7 Hz, 1H), 7.37 – 7.27 (m, 5H), 7.21 (s, 4H), 7.06 (dd, *J* = 15.4, 10.7 Hz, 1H), 6.90 (s, 1H), 6.47 (dd, *J* = 15.3, 10.8 Hz, 1H), 6.25 – 6.08 (m, 2H), 4.97 (q, *J* = 7.7 Hz, 1H), 4.47 (q, 2H), 3.64 – 3.41 (m, 2H), 3.06 (s, 3H), 2.92 (s, 3H), 2.00 – 1.88 (m, 1H), 1.81 – 1.68 (m, 1H).

^{13}C NMR (75 MHz, $CDCl_3$) δ 193.35, 149.92, 141.49, 138.06, 137.80, 133.23, 133.00, 132.77, 131.43, 128.65, 128.06, 120.43, 73.44, 66.22, 58.87, 40.61, 40.28, 33.73, 29.84.

HRMS (ESI-TOF) m/z: $[M - H]^+$ Calcd for $C_{23}H_{27}N_2O_6S_2$ 491.1305, found 491.1297.

IR (neat) *v* (cm^{-1}): 3269, 2918, 2849, 1660, 1507, 1495, 1454, 1324, 1146, 967, 698.

HPLC analysis (Daicel Chiralpak IA, Hexane/EtOH = 80/20, flow rate 1.0 mL/min, 254 nm): t_R = 37 min, t_R = 69 min.

Enantiomeric excess: 86%. **$[\alpha]_D^{22}$** ([c] = 1 g/L, CH_2Cl_2) +103°.

N-((4E,6E)-2-methyl-8-oxoocta-4,6-dien-3-yl)-N-(4-(methylsulfonamido)phenyl)methanesulfonamide

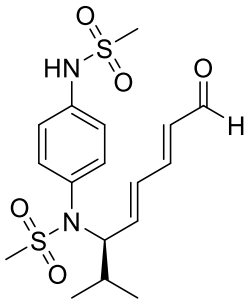

Prepared according to general procedure to provide the title compound **4p** as a white solid. (7 mg, 66% yield).

^{1}H NMR (300 MHz, $CDCl_3$) δ 9.61 (d, *J* = 7.7 Hz, 1H), 7.42 – 7.27 (m, 3H), 7.25 – 7.21 (m, 1H), 7.12 (dd, *J* = 15.4, 10.8 Hz, 1H), 6.91 (s, 1H), 6.59 (dd, *J* = 15.2, 10.8 Hz, 1H), 6.25 (dd, *J* = 15.4, 7.7 Hz, 1H), 6.10 (dd, *J* = 15.2, 10.1 Hz, 1H), 4.31 (t, *J* = 10.2 Hz, 1H), 3.09 (s, 3H), 2.89 (s, 3H), 1.71 – 1.59 (m, 1H), 1.19 (d, *J* = 6.5 Hz, 3H), 0.79 (d, *J* = 6.7 Hz, 3H).

^{13}C NMR (75 MHz, $CDCl_3$) δ 193.12, 149.55, 141.44, 137.57, 133.01, 132.89, 131.89, 120.25, 68.62, 40.18, 39.99, 30.36, 20.41, 19.67.

HRMS (ESI-TOF) m/z: $[M - H]^+$ Calcd for $C_{17}H_{23}N_2O_5S_2$ 399.1043, found 399.1036.

IR (neat) *v* (cm^{-1}): 3247, 2918, 2849, 1675, 1507, 1323, 1147, 968, 756.

HPLC analysis (Daicel Chiralpak IC, Heptane/EtOH = 80/20, flow rate 1.0 mL/min, 254 nm): t_R = 136 min, t_R = 147 min.

Enantiomeric excess: 95%. **$[\alpha]_D^{22}$** ([c] = 1 g/L, CH_2Cl_2) -157°.

N-((2E,4E,8S)-8,12-dimethyl-1-oxotrideca-2,4,11-trien-6-yl)-N-(4-(methylsulfonamido)phenyl)methanesulfonamide

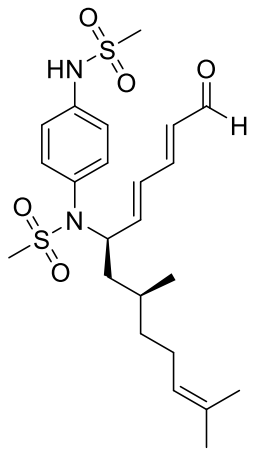

Prepared according to general procedure to provide the title compound **4q** as a yellow solid. (10 mg, 80% yield).

^{1}H NMR (300 MHz, $CDCl_3$) δ 9.60 (d, *J* = 7.8 Hz, 1H), 7.24 (s, 4H), 7.10 (dd, *J* = 15.4, 10.8 Hz, 1H), 6.78 (s, 1H), 6.53 (dd, *J* = 15.2, 10.8 Hz, 1H), 6.26 – 6.10 (m, 2H), 5.06 (t, *J* = 7.3 Hz, 1H), 4.93 (q, *J* = 8.4 Hz, 1H), 3.08 (s, 3H), 2.91 (s, 3H), 1.95 (p, *J* = 7.8 Hz, 2H), 1.69 (s, 3H), 1.59 – 1.49 (m, 5H), 1.31 – 1.18 (s, 2H), 0.97 (d, *J* = 6.4 Hz, 3H), 0.93 – 0.82 (m, 2H).

^{13}C NMR (75 MHz, $CDCl_3$) δ 193.12, 149.78, 142.33, 137.64, 133.09, 132.99, 132.20, 131.81, 130.81, 124.27, 120.11, 59.06, 40.45, 40.28, 40.13, 36.83, 29.67, 28.71, 25.68, 25.15, 19.35, 17.67.

HRMS (ESI-TOF) m/z: $[M - H]^+$ Calcd for $C_{23}H_{33}N_2O_5S_2$ 481.1825, found 481.1843.

IR (neat) *v* (cm^{-1}): 3246, 2918, 2850, 1675, 1508, 1323, 1146, 968, 764.

HPLC analysis (Daicel Chiralpak IC, Hexane/EtOH = 90/10, flow rate 1.0 mL/min, 254 nm): t_R = 40 min, t_R = 43 min.

Enantiomeric excess: 85%. **$[\alpha]_D^{22}$** ([c] = 1 g/L, CH_2Cl_2) -5°.

N-(4-(methylsulfonamido)phenyl)-N-((2E,4E)-6-oxo-1-phenylhexa-2,4-dien-1-yl)methanesulfonamide

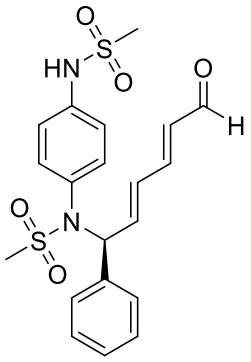

Prepared according to general procedure to provide the title compound **4r** as a white solid. (6.7 mg, 62% yield).

^{1}H NMR (300 MHz, $CDCl_3$) δ 9.60 (d, *J* = 7.7 Hz, 1H), 7.34 – 7.30 (m, 3H), 7.21 – 7.17 (m, 2H), 7.13 – 7.08 (m, 2H), 7.00 – 6.94 (m, 2H), 6.81 (s, 1H), 6.69 – 6.47 (m, 2H), 6.21 (dd, *J* = 15.4, 7.8 Hz, 1H), 6.05 (d, *J* = 7.6 Hz, 1H), 3.03 (s, 3H), 2.91 (s, 3H).

^{13}C NMR (75 MHz, $CDCl_3$) δ 193.15, 149.62, 139.86, 137.61, 137.56, 133.50, 133.30, 133.15, 132.61, 131.70, 128.78, 128.65, 119.87, 64.70, 40.77, 39.96.

HRMS (ESI-TOF) m/z: $[M + Na]^+$ Calcd for $C_{20}H_{22}N_2NaO_5S_2$ 457.0868, found 457.0859.

IR (neat) *v* (cm^{-1}): 3250, 3030, 2930, 2852, 1672, 1638, 1605, 1507, 1320, 1170, 1015, 965, 916, 759, 700.

HPLC analysis (Daicel Chiralpak IC, Hexane/EtOH = 90/10, flow rate 1.0 mL/min, 254 nm): t_R = 34 min, t_R = 43 min.

Enantiomeric excess: 87%. **$[\alpha]_D^{22}$** ([c] = 1 g/L, CH_2Cl_2) -58°.

Dottorati di Ricerca – Ph.D. Positions (DM 351)

Ente finanziatore: progetto finanziato dall'Unione Europea - NextGenerationEU – Piano Nazionale Ripresa e Resilienza (PNRR) - Missione 4 Componente 1 Investimento 3.4 Didattica e competenze universitarie avanzate" e Investimento 4.1 "Estensione del numero di dottorati di ricerca e dottorati innovativi per la pubblica amministrazione e il patrimonio culturale" – Avviso N. 351 del 09/04/2022 del Ministero dell'Università e della Ricerca;

Funder: Project funded under the National Recovery and Resilience Plan (NRRP), Mission 4 Component 1 Investment 3.4 and 4.1 - Call for tender No. 351 of 09/04/2022 of Italian Ministry of University and Research funded by the European Union – NextGenerationEU